IMPACT OF SYSTEM BIOLOGY AND MOLECULAR MEDICINE ON THE MANAGEMENT OF COMPLEX IMMUNE MEDIATED RESPIRATORY DISEASES

EDITED BY: Blanca Cárdaba and Girolamo Pelaia

PUBLISHED IN: Frontiers in Immunology and Frontiers in Medicine

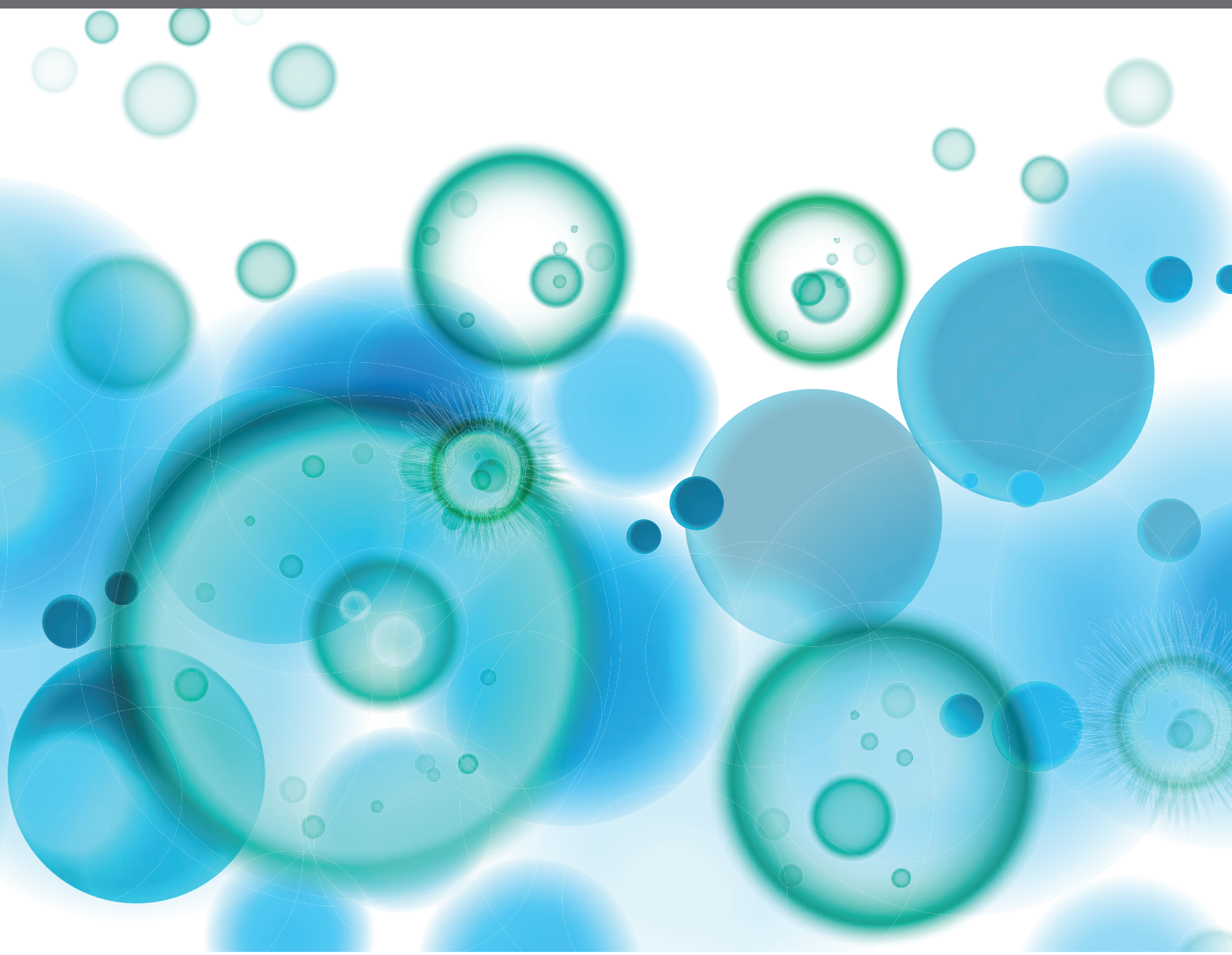

frontiers Research Topics

frontiers

Frontiers eBook Copyright Statement

The copyright in the text of individual articles in this eBook is the property of their respective authors or their respective institutions or funders. The copyright in graphics and images within each article may be subject to copyright of other parties. In both cases this is subject to a license granted to Frontiers.

The compilation of articles constituting this eBook is the property of Frontiers.

Each article within this eBook, and the eBook itself, are published under the most recent version of the Creative Commons CC-BY licence. The version current at the date of publication of this eBook is CC-BY 4.0. If the CC-BY licence is updated, the licence granted by Frontiers is automatically updated to the new version.

When exercising any right under the CC-BY licence, Frontiers must be attributed as the original publisher of the article or eBook, as applicable.

Authors have the responsibility of ensuring that any graphics or other materials which are the property of others may be included in the CC-BY licence, but this should be checked before relying on the CC-BY licence to reproduce those materials. Any copyright notices relating to those materials must be complied with.

Copyright and source acknowledgement notices may not be removed and must be displayed in any copy, derivative work or partial copy which includes the elements in question.

All copyright, and all rights therein, are protected by national and international copyright laws. The above represents a summary only. For further information please read Frontiers' Conditions for Website Use and Copyright Statement, and the applicable CC-BY licence.

ISSN 1664-8714
ISBN 978-2-88971-544-2
DOI 10.3389/978-2-88971-544-2

About Frontiers

Frontiers is more than just an open-access publisher of scholarly articles: it is a pioneering approach to the world of academia, radically improving the way scholarly research is managed. The grand vision of Frontiers is a world where all people have an equal opportunity to seek, share and generate knowledge. Frontiers provides immediate and permanent online open access to all its publications, but this alone is not enough to realize our grand goals.

Frontiers Journal Series

The Frontiers Journal Series is a multi-tier and interdisciplinary set of open-access, online journals, promising a paradigm shift from the current review, selection and dissemination processes in academic publishing. All Frontiers journals are driven by researchers for researchers; therefore, they constitute a service to the scholarly community. At the same time, the Frontiers Journal Series operates on a revolutionary invention, the tiered publishing system, initially addressing specific communities of scholars, and gradually climbing up to broader public understanding, thus serving the interests of the lay society, too.

Dedication to Quality

Each Frontiers article is a landmark of the highest quality, thanks to genuinely collaborative interactions between authors and review editors, who include some of the world's best academicians. Research must be certified by peers before entering a stream of knowledge that may eventually reach the public - and shape society; therefore, Frontiers only applies the most rigorous and unbiased reviews.
Frontiers revolutionizes research publishing by freely delivering the most outstanding research, evaluated with no bias from both the academic and social point of view. By applying the most advanced information technologies, Frontiers is catapulting scholarly publishing into a new generation.

What are Frontiers Research Topics?

Frontiers Research Topics are very popular trademarks of the Frontiers Journals Series: they are collections of at least ten articles, all centered on a particular subject. With their unique mix of varied contributions from Original Research to Review Articles, Frontiers Research Topics unify the most influential researchers, the latest key findings and historical advances in a hot research area! Find out more on how to host your own Frontiers Research Topic or contribute to one as an author by contacting the Frontiers Editorial Office: frontiersin.org/about/contact

IMPACT OF SYSTEM BIOLOGY AND MOLECULAR MEDICINE ON THE MANAGEMENT OF COMPLEX IMMUNE MEDIATED RESPIRATORY DISEASES

Topic Editors:
Blanca Cárdaba, Health Research Institute Foundation Jimenez Diaz (IIS-FJD), Spain
Girolamo Pelaia, University of Catanzaro, Italy

Citation: Cárdaba, B., Pelaia, G., eds. (2021). Impact of System Biology and Molecular Medicine on the Management of Complex Immune Mediated Respiratory Diseases. Lausanne: Frontiers Media SA.
doi: 10.3389/978-2-88971-544-2

Table of Contents

frontiers in Medicine

EDITORIAL
published: 08 September 2021
doi: 10.3389/fmed.2021.745739

Editorial: Impact of System Biology and Molecular Medicine on the Management of Complex Immune Mediated Respiratory Diseases

Blanca Cárdaba[1,2]* *and Girolamo Pelaia*[3]

[1] Immunology Department, Instituto de Investigación Sanitaria-Fundación Jiménez Díaz, Universidad Autónoma de Madrid (UAM), Madrid, Spain, [2] Center for Biomedical Network of Respiratory Diseases (CIBERES), Instituto de Salud Carlos III, Madrid, Spain, [3] Department of Health Sciences, University "Magna Græcia" of Catanzaro, Catanzaro, Italy

Keywords: asthma, chronic obstructive pulmonary disease, COPD, respiratory inflammation, systems biology, biological therapies

Editorial on the Research Topic

Impact of System Biology and Molecular Medicine on the Management of Complex Immune Mediated Respiratory Diseases

Chronic respiratory disorders, including bronchial asthma and chronic obstructive pulmonary disease (COPD), are common, highly complex and heterogeneous inflammatory diseases that include a broad clinical spectrum. These disorders could be caused by numerous genetic, pharmacologic, physiologic, biological, and/or immunologic mechanisms, giving rise to subclasses of phenotypes and endotypes. This great heterogeneity is reflected in the absence of a good therapeutic option for a substantial percentage of patients and is behind extensive studies aimed at applying precision or personalized medicine, which requires different diagnostic and therapeutic approaches, in the field. In this Research Topic we aim to provide an overview of the latest advances in the search for new approaches to discover and validate new tools related with diagnosis, prognosis, exacerbations, and treatment monitoring as well as molecular targets for new biological therapies.

Twelve articles have been published, summarizing different aspects related mainly with asthma and COPD. Seven report the results of human studies and five are examples of the relevance of animal models in the knowledge base on respiratory disorders.

Starting with studies in humans, Zhang et al. prove the efficacy of single allergen (*Dermatophagoides farinae*) sublingual immunotherapy (SLIT) in polysensitized patients allergic to *D. farinae* with allergic asthma. They describe a 3-year longitudinal case-control study with three kinds of cases: the single-allergen group [only sensitized to house dust mite (HDM)], the 1–2 allergen group (HDM combined with 1–2 other allergens), and the 3 or more allergens group (HDM combined with 3 or more other allergens). Their results show an improvement in patients sensitized to HDM with and without other allergens after 3 years of SLIT, but with a slower recovery of symptoms in patients with 3 or more allergen sensitizations.

Pelaia et al. provide an exhaustive overview of asthma complexity, focusing on new molecular therapeutics options according to the pathobiological mechanisms underlying the various cellular and molecular phenotypes of severe asthma. They underscore the relevant improvement in the management of patients with severe, allergic, or non-allergic eosinophilic T2-high asthma, especially in that their susceptibility to suffer from frequent and often serious disease exacerbations is lessened due to the new drugs approved, anti-IgE, anti-IL-5, anti-IL-5 receptor,

OPEN ACCESS

Edited and reviewed by:
Bo Li,
Chongqing Normal University, China

***Correspondence:**
Blanca Cárdaba
bcardaba@fjd.es

Specialty section:
This article was submitted to Pulmonary Medicine, a section of the journal Frontiers in Medicine

Received: *22 July 2021*
Accepted: *13 August 2021*
Published: *08 September 2021*

Citation:
Cárdaba B and Pelaia G (2021) Editorial: Impact of System Biology and Molecular Medicine on the Management of Complex Immune Mediated Respiratory Diseases. Front. Med. 8:745739. doi: 10.3389/fmed.2021.745739

and anti-IL-4/IL-13, all receptor monoclonal antibodies, and the promising new monoclonal antibodies, mainly targeting the innate cytokines known as alarmins, which are in development stage. However, they highlight the need to increase the search for new molecular targets for patients with severe T2-low asthma (neutrophilic or paucigranulocytic asthma) who currently are largely excluded from the therapeutic benefits achievable for people who experience T2-high severe disease.

Ragnoli et al. focus on other prevalent respiratory diseases, obstructive sleep apnea syndrome (OSAS), which is currently underdiagnosed. They review the model that proposes a bidirectional correlation between severe asthma (SA) and OSAS, with a mutual negative effect in terms of disease severity. These two diseases share common risk factors, such as obesity, rhinitis, and gastroesophageal reflux (GER). Also, it has been proposed that OSAS and asthma patients may be more susceptible to SA attacks induced by systemic inflammation. In their review, the authors describe the published evidence on the interrelationship between OSAS and SA, from endo-phenotype to clinical aspects, highlighting possible implications for clinical practice and future research directions, remarking that OSAS treatment can also improve lung function tests in adult asthmatic patients and that assessing the coexistence of OSAS and SA could help in the management of both diseases.

The next 4 articles (Cremades-Jimeno et al.; Kim et al.; Ricciardi et al.; Cañas et al.) are examples of how the new bioinformatic tools and systems biology approaches are helping to describe new molecular biomarkers or molecular motifs of diseases and new gene regulatory networks or specific regulatory elements (RNA-binding proteins or RBPs, Micro-RNAS, or miRNAs), which are opening up new fields to better understand and manage these complex diseases.

Cremades-Jimeno et al. used systems biology approaches to define molecular motifs of three diseases, allergic asthma (AA), non-allergic asthma (NA), and respiratory allergy (RA) and categorize the relevance of molecular biomarkers previously defined experimentally in peripheral blood mononuclear cells (PBMCs) in order to prioritize them according to their relationship to specific molecular motifs or to disease. The study provides new information on potential biomarkers with a mechanistic implication, opening a new focus with which to find diagnostic and therapeutic tools for these types of diseases.

Kim et al. assess gene regulatory networks (how the transcription factors (TFs) regulate gene expression to determine the responsiveness to anti-asthma therapy) of adult patients with asthma who showed good or poor lung function improvements in response to inhaled corticosteroids (ICSs). Their results indicated that responses between good and poor responders to a certain drug is not necessarily derived from differential gene expression networks but may instead be from regulatory gene expression networks. They identified TFs that showed different gene connections and enrichment in distinct biological pathways, remarking TGF-β signaling, cell cycle related, and IL-4 and IL-13 signaling pathways that could be important in determining responses to ICSs in patients with asthma.

Regarding severe asthma and COPD, Ricciardi et al. describe an interesting *in silico* analysis of posttranscriptional gene regulation using a curated list of mRNA-binding RNA Binding Proteins (mRBPs) in selected Gene Expression Omnibus (GEO) transcriptomic databases of airway epithelium isolated from chronic obstructive pulmonary disease (COPD), severe asthma (SA), and matched control subjects. This study identifies an overall downregulation of RBP expression that was shared by a subset of smoker control subjects; changes in mRBP expression impacted several biological pathways also involved in several aspects of COPD pathogenesis; finally, at least five groups of coregulated RBPs were identified. Importantly, airway epithelial mRBP expression was found to be much less regulated in patients with SA. Overall, the COPD-related mRBP profile found in this study suggests post-transcriptional control of epithelial gene expression as substantial, yet understudied process possibly contributing to key pathogenic mechanisms in COPD.

RNA-binding proteins exert their function as part of ribonucleoprotein (mRNP) complexes, constituted by proteins and non-coding RNAs such as microRNAs (miRNAs). In this Research Topic, Cañas et al. contribute an elegant review of the current knowledge and promising roles of miRNAs (small non-coding RNAs) in pathophysiology, diagnosis, and treatment of asthma and COPD. This paper exhaustively surveys recent descriptions of differential expression of miRNAs in peripheral and target-derived samples of asthma and COPD patients focusing on the growth potential of these regulatory elements in relation to key aspects of those diseases and how their complexity could be better understood with a systems biology approach to compile and elucidate the complex miRNA regulatory system to define their usefulness in the management of these diseases.

Finally, five articles describe relevant aspects of respiratory disorders by experimental animal models.

Foray et al. describe a new house dust mite-induced asthma model to elucidate allergic dysimmune mechanisms involving Th2 and Th17 responses that could better mimic some asthmatic endoytpes. In this study, non-obese diabetic (NOD) mice, which spontaneously develop autoimmune diabetes, undergo more severe allergic asthma airway inflammation and airway hyperresponsiveness (AHR) than pro-Th2 BALB/c mice upon house dust mite (HDM) sensitization and challenge. The use of IL-4-deficient NOD mice and the *in vivo* neutralization of IL-17 demonstrated that both IL-4 and IL-17 are responsible for the exacerbated airway inflammation and AHR observed in NOD mice. Although further studies are required to better determine whether Th2 and Th17 responses act together or independently to induce vast airway inflammation and AHR in NOD mice, this could represent a unique model to better understand the key mechanisms implicated in the association between allergic airway inflammation and autoimmune diabetes, as well as to understand several asthmatic phenotypes with mixed Th2 and Th17 inflammation.

Lertnimitphun et al. analyze the effectiveness of Safranal—one of the active compounds from *Crocus sativus*, known in Chinese herbal medicine to have many anti-inflammatory properties—in two allergic murine models: ovalbumin (OVA)-induced asthma and passive systemic anaphylaxis (PSA) models. This paper demonstrates that Safranal has potential to stabilize mast cells and inhibit cytokine production through the inhibition of the

MAPKs and NF-κB pathways, being a potential candidate to treat allergic diseases such as systemic anaphylaxis and asthma.

Finally, three interesting articles study new therapies for acute lung injury (ALI)/acute respiratory distress syndrome (ARDS), a serious illness characterized by severe pulmonary edema and a profound inflammatory response in the lung. Life-threatening acute lung inflammation can be induced by diverse ischemia/reperfusion (IR) injury conditions, including resuscitation for cardiac arrest, cardiopulmonary bypass, hemorrhagic shock, pulmonary embolism, and lung transplantation. Here, three articles describe animal models to test new treatments using different ALI inductors.

Liao et al. using a perfused rat lung model (ischemia/reperfusion (IR)-induced acute lung inflammation), analyze the effect of a potent-anti-inflammatory agent, 2-Methoxyestradiol (2ME), a natural 17-β estradiol metabolite. Also, its correlation with Annexin A1, a glucocorticoid-regulated protein that reduces vascular inflammatory responses associated with IR injury, was analyzed. Their results show that 2ME ameliorates IR-induced acute lung inflammation by upregulating the expression of endogenous AnxA1 in the lungs, alveolar epithelial cells, and neutrophils.

Pao et al. analyzed the influence of endoplasmic reticulum (ER) stress inhibitor, 4-phenyl butyric acid (4-PBA), a chemical chaperone, in mice with hyperoxia-induced acute lung injury (HALI). Also, its correlation with claudin-4 protein (a member of integral membrane proteins that are essential components in the tight junction (TJ) formation and function) was analyzed. In this study, 4-PBA effectively reduced oxidative and ER stress, the level of proinflammatory cytokines, and apoptosis, but increased claudin 4 protein expression in HALI. 4-PBA significantly improved multiple indices of HALI, such as prolonging survival, and decreasing AFC, lung edema, and disruption of tight junction proteins, production of pro-inflammatory cytokines, oxidative stress, the pulmonary neutrophil influx, and lung tissue damage. Consistent with *in vivo* findings, 4-PBA treatment had a similar advantageous effect on *in vitro* epithelial cells exposed to hyperoxia, however, these protective effects of 4-PBA were abolished when claudin-4 was knocked down. These experiments indicate that 4-PBA may have potential benefits as adjuvant therapy for HALI and the protective mechanism was *via* enhancing claudin-4 expression.

Tai et al. analyzed a new treatment, tanshinone IIA (TIIA), the main active ingredient in *Salvia miltiorrhiza* Bge, combined with cyclosporine A (CsA) in a model of obese rats with induced renal ischemia-reperfusion (IR). The authors analyze lung apoptosis led by renal IR and evaluate whether this combination could alleviate lung apoptosis by regulating mitochondrial function through the PI3K/Akt/Bad pathway in obese rats. Their results demonstrate that lung mitochondrial dysfunction was induced in the process of renal IR, especially in obese rats, with dynamics altered and biogenesis inhibited. TIIA+CsA were protective agent, which can attenuate lung apoptosis via modulating mitochondrial function by activating the PI3K/Akt/Bad pathway in obese rats. These results may be a promising protective strategy for managing obesity-related acute kidney injury and acute lung injury. However, this application needs further large-scale experimental and clinical studies.

Globally, these 12 articles show a brushstroke on the multiple not yet well-defined aspects, related to the molecular bases underlying to these complex respiratory diseases, which need to be validated in more extensive clinical studies to be clinically translated in a near future. In summary, this Research Topic reflects the high complexity of respiratory diseases and the many efforts, from different points of view, that are needed to improve the management of these disorders, which affect a high number of subjects around the world. Thank you to the authors and researchers who have contributed to this topic and we hope that this issue helps readers understand the extent to which efforts in this field are needed to offer best quality of life to patients.

AUTHOR CONTRIBUTIONS

BC and GP wrote and reviewed the manuscript. Both authors contributed to the article and approved the submitted version.

FUNDING

This work was supported by research grant PI20/00903 cofunded by FEDER, CIBERES (ISCIII, 0013), and RETIC (RD09/0076/00101) from the *Fondo de Investigación Sanitaria* (*Ministerio de Sanidad y Consumo*, Spain) and in part by the research grant *Ayudas de la Sociedad Española de Alergia e Inmunología Clínica* (SEAIC 2018).

ACKNOWLEDGMENTS

The authors want to thank Dr. Oliver Shaw for English editorial work.

Conflict of Interest: The authors declare that the research was conducted in the absence of any commercial or financial relationships that could be construed as a potential conflict of interest.

Publisher's Note: All claims expressed in this article are solely those of the authors and do not necessarily represent those of their affiliated organizations, or those of the publisher, the editors and the reviewers. Any product that may be evaluated in this article, or claim that may be made by its manufacturer, is not guaranteed or endorsed by the publisher.

Copyright © 2021 Cárdaba and Pelaia. This is an open-access article distributed under the terms of the Creative Commons Attribution License (CC BY). The use, distribution or reproduction in other forums is permitted, provided the original author(s) and the copyright owner(s) are credited and that the original publication in this journal is cited, in accordance with accepted academic practice. No use, distribution or reproduction is permitted which does not comply with these terms.

frontiers in Immunology

ORIGINAL RESEARCH
published: 16 October 2020
doi: 10.3389/fimmu.2020.579889

Posttranscriptional Gene Regulatory Networks in Chronic Airway Inflammatory Diseases: *In silico* Mapping of RNA-Binding Protein Expression in Airway Epithelium

*Luca Ricciardi[1], Giorgio Giurato[1], Domenico Memoli[1], Mariagrazia Pietrafesa[1], Jessica Dal Col[1], Ilaria Salvato[2], Annunziata Nigro[1], Alessandro Vatrella[1], Gaetano Caramori[2], Vincenzo Casolaro[1,3] and Cristiana Stellato[1,3]**

[1] Department of Medicine, Surgery and Dentistry Scuola Medica Salernitana, University of Salerno, Salerno, Italy, [2] Pulmonology, Department of Biomedical Sciences, Dentistry and Morphological and Functional Imaging (BIOMORF), University of Messina, Messina, Italy, [3] Department of Medicine, Johns Hopkins University School of Medicine, Baltimore, MD, United States

OPEN ACCESS

Edited by:
Girolamo Pelaia,
University of Catanzaro, Italy

Reviewed by:
Hartmut Kleinert,
Johannes Gutenberg University Mainz, Germany
Kenta Shinoda,
National Institutes of Health (NIH), United States

***Correspondence:**
Cristiana Stellato
cstellato@unisa.it

Specialty section:
This article was submitted to Inflammation, a section of the journal Frontiers in Immunology

Received: 03 July 2020
Accepted: 19 August 2020
Published: 16 October 2020

Citation:
Ricciardi L, Giurato G, Memoli D, Pietrafesa M, Dal Col J, Salvato I, Nigro A, Vatrella A, Caramori G, Casolaro V and Stellato C (2020) Posttranscriptional Gene Regulatory Networks in Chronic Airway Inflammatory Diseases: In silico Mapping of RNA-Binding Protein Expression in Airway Epithelium. Front. Immunol. 11:579889. doi: 10.3389/fimmu.2020.579889

Background: Posttranscriptional gene regulation (PTGR) contributes to inflammation through alterations in messenger RNA (mRNA) turnover and translation rates. RNA-binding proteins (RBPs) coordinate these processes but their role in lung inflammatory diseases is ill-defined. We evaluated the expression of a curated list of mRNA-binding RBPs (mRBPs) in selected Gene Expression Omnibus (GEO) transcriptomic databases of airway epithelium isolated from chronic obstructive pulmonary disease (COPD), severe asthma (SA) and matched control subjects, hypothesizing that global changes in mRBPs expression could be used to infer their pathogenetic roles and identify novel disease-related regulatory networks.

Methods: A published list of 692 mRBPs [Nat Rev Genet 2014] was searched in GEO datasets originated from bronchial brushings of stable COPD patients (C), smokers (S), non-smokers (NS) controls with normal lung function (n = 6/12/12) (GEO ID: GSE5058) and of (SA) and healthy control (HC) (n = 6/12) (GSE63142). Fluorescence intensity data were extracted and normalized on the medians for fold change (FC) comparisons. FCs were set at $\geq |1.5|$ with a false discovery rate (FDR) of ≤ 0.05. Pearson correlation maps and heatmaps were generated using tMEV tools v4_9_0.45. DNA sequence motifs were searched using PScan-ChIP. Gene Ontology (GO) was performed with Ingenuity Pathway Analysis (IPA) tool.

Results: Significant mRBP expression changes were detected for S/NS, COPD/NS and COPD/S (n = 41, 391, 382, respectively). Of those, 32% of genes changed by FC $\geq |1.5|$ in S/NS but more than 60% in COPD/NS and COPD/S (n = 13, 267, 257, respectively). Genes were predominantly downregulated in COPD/NS (n = 194, 73%) and COPD/S (n = 202, 79%), less so in S/NS (n = 4, 31%). Unsupervised cluster analysis identified in 4 out of 12 S the same mRBP pattern seen in C, postulating subclinical COPD. Significant DNA motifs enrichment for transcriptional regulation

was found for downregulated RBPs. Correlation analysis identified five clusters of co-expressed mRBPs. GO analysis revealed significant enrichments in canonical pathways both specific and shared among comparisons. Unexpectedly, no significant mRBPs modulation was found in SA compared to controls.

Conclusions: Airway epithelial mRBPs profiling reveals a COPD-specific global downregulation of RBPs shared by a subset of control smokers, the potential of functional cooperation by coexpressed RBPs and significant impact on relevant pathogenetic pathways in COPD. Elucidation of PTGR in COPD could identify disease biomarkers or pathways for therapeutic targeting.

Keywords: airway epithelium, chronic inflammation, COPD, posttranscriptional gene regulation, RNA binding proteins, severe asthma

INTRODUCTION

RNA-binding proteins (RBPs) are key regulatory factors in post-transcriptional gene regulation (PTGR) involved in the maturation, stability, transport and degradation of cellular RNAs. RBP convey PTGR by binding to conserved regulatory elements shared by subsets of transcripts and by directing the bound targets toward cytoplasmic sites of translation or decay (1). Importantly, RBPs exert their function as part of ribonucleoprotein (mRNP) complexes, constituted by proteins and non-coding RNAs, such as microRNAs (2). Through stimulus-dependent cues, changes in mRBP composition ultimately determine the rate of target mRNA stability and translation. Therefore, understanding RBP function in disease models requires a larger evaluation of co-expression and regulatory scenarios, shaped by disease-driven triggers and signaling.

For human cancer the occurrence of aberrant RBP expression, along with altered RNA turnover and translation rates have been characterized in preclinical models, identified in human disease and further probed with *in silico* approaches (3, 4) leading to the identification of this class of regulators as novel disease biomarkers and as targets for small molecule-based therapeutics (5–7). Similar studies in human chronic inflammatory diseases are lagging behind, despite ample knowledge of deregulated PTGR in inflammatory responses by *in vitro* studies and the strong inflammatory phenotypes obtained in some of the knock-out animal models (8, 9). This knowledge chasm is also present for lung diseases, despite the strong link between chronic inflammatory diseases such as Chronic Obstructive Pulmonary Disease (COPD) and some lung cancer types (10) and the extensive overlap of RBP-regulated genes contributing to both disease process (11).

Airway epithelium is a major driver in the pathogenesis of inflammatory lung diseases such as asthma and COPD. Deregulated epithelial responses are a main therapeutic target of inhaled corticosteroids (ICS), the mainstay anti-inflammatory drug class for asthma symptom control (www.ginasthma.org) and for treating exacerbations in COPD (www.goldcopd.org). Involvement of RBPs in airway epithelial responses to inflammatory stimuli and glucocorticoid treatment has been well-characterized *in vitro* (12–15) but awaits evidence from patient-based studies. To this end, in a previous characterization of ARE-binding proteins expression in COPD (16) we identified a selective loss of the RBP AU-binding Factor (AUF)−1 in bronchial biopsies in stable COPD patients vs. smoker controls. Besides replicating this finding *in vitro* upon challenge of the epithelial cell line BEAS-2B with inflammatory cytokines and cigarette smoke extract, we confirmed this loss in primary epithelium, by interrogating a transcriptome database generated from bronchial brushings of COPD patients vs. normal smokers and non-smokers controls (17).

On these basis, we hypothesized that changes in mRNA-binding RBPs (mRBP) expression may occur on a larger scale in chronic inflammatory airways diseases, such as COPD and severe asthma (SA) and that identification of these changes can be used to infer their putative pathogenetic roles as disease-related regulatory networks, as in cancer (18). We therefore set out to evaluate the expression profile of a curated gene list of mRBPs in selected public Gene Expression Omnibus (GEO) transcriptomic databases derived from airway epithelium isolated from bronchial brushings of phenotyped patients affected by COPD, SA and relative control populations, enrolled in relevant translational studies on disease pathophysiology. In particular, we employed for COPD the same database (17) in which we found loss of AUF-1 in COPD samples vs. controls, as observed *ex vivo* in COPD airway biopsies (16) and a GEO database from SA and healthy controls (HC) enrolled in the Severe Asthma Research Program (SARP) study (19). The list of mRBPs we utilized for this study has been created by annotation of proteins as RBPs generated by domain search, considering known RNA binding domains [among 800 domains extracted from the protein family (Pfam) database], or including proteins known as validated partners of RNP complex (20). The mRBP expression profiles we obtained were then evaluated through gene ontology analysis to evaluate their potential relevance to disease pathogenesis; moreover, we searched for coregulated RBP expression indicative of common participation to regulatory pathways.

In airway epithelial samples from COPD patients, this approach identified a global downregulation of RBP expression that was shared by a subset of smoker control subjects; changes in mRBP expression impacted several biological pathways also

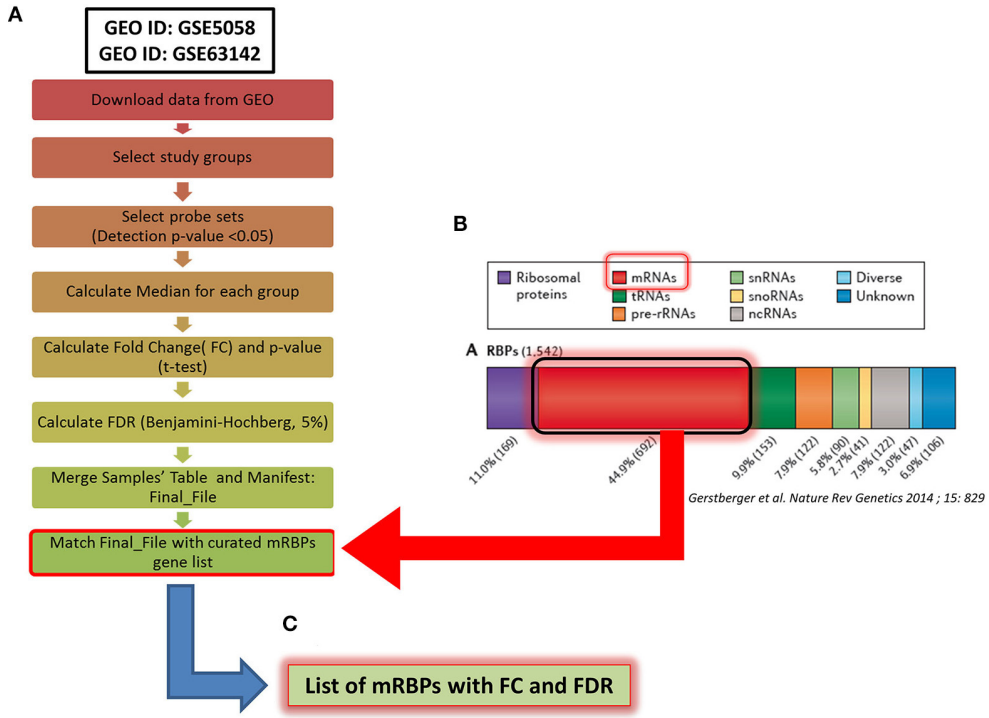

FIGURE 1 | Methodological flowchart of the study for expression profiling of mRNA-binding proteins (mRBPs) in airway epithelium transcriptomic studies in COPD and severe asthma (SA). **(A)** Flowchart for data analysis of the trascriptomic datasets obtained in the Gene Expression Omnibus (GEO) public database (see Methods). Briefly, fluorescence intensity data (raw data) from the chosen datasets (NS, S, stable COPD for GSE5058; SA and HC for GSE63142) were extracted and processed to calculate the probes fluorescence compared to the background. Probes with at least one detection $p < 0.05$ in all three groups were considered for further analysis. Data were then normalized by the median to calculate fold change (FC) expression among groups (S/NS, COPD/NS, COPD/S; SA/HC); only those showing a False Discovery Rate (FDR) ≤ 0.05 in each comparison were considered, forming a Final File for each GSE. Concurrently, a curated gene list of 692 RBPs binding to mRNA (mRBPs) was downloaded from a published census of RNA-binding proteins (20) **(B)** and searched in the Final File, producing a dataset of mRBPs with statistically significant fold changes in disease state vs. controls **(C)**.

involved in several aspects of COPD pathogenesis; finally, at least five groups of coregulated RBPs were identified. Importantly, airway epithelial mRBP expression was found to be much less regulated in patients with SA.

MATERIALS AND METHODS

Sample Selection and Data Processing

We selected the following two trascriptomic databases generated from human airway epithelial cells obtained by bronchial brushings, downloaded from the GEO public repository of high-throughput gene expression data (**Figure 1A**):

- **GEO ID: GSE5058**. COPD patients (C), Smokers (S) and Non-Smokers (NS) as controls with normal al lung function (NLF) ($n = 6/12/12$, respectively) (17);
- **GEO ID: GSE63142**. Patients with severe Asthma (SA), healthy control subjects (HC) ($n = 6/12$, respectively, randomly selected from databes to match number of cases considered in GSE5058) (19).
- **GEO ID: GSE8545**. Patients with stable COPD (C), Smokers (S) and Non-Smokers (NS) as controls with normal lung function (NLF) ($n = 18/18/18$, respectively) (21). This dataset has been utilized to validate the RBP expression profile in COPD/S identified in GSE5058 (**Figure 8**).

The Affymetrix Human Genome U133 Plus 2.0 Array platform was used for both COPD studies while the SA study was performed using Agilent-014850 Whole Human Genome Microarray 4x44K G4112F. Fluorescence intensity data from individual datasets (raw data) were extracted and processed applying the standard Affimetrix MAS5 algorithm to calculate the fluorescence of the single probes compared to the background. Probes with at least one detected $p < 0.05$ in all three groups were considered for further analysis. Data were then normalized by the median to calculate fold change (FC) expression among groups; only those showing a False Discovery Rate (FDR) ≤ 0.05 in each comparison were considered. As genes are represented on the array platforms by multiple probes spanning different transcript portions, only genes with consistency across probes $\geq 67\%$ were considered for final analysis. The curated gene list of 692 RBPs binding to mRNA (mRBPs) published in a general census of RNA-binding proteins was downloaded from the original file (https://www.nature.com/articles/nrg3813#MOESM25, Supplemetary Information S3) (20) and searched in the final FC files (**Figure 1B**), producing a list of mRBPs

regulated in disease state vs. controls (**Figure 1C**). The analysis first identified statistically significant genes regardless of fold change value, which were denominated Differentially Expressed Genes (DEG). Then, FCs threshold was set at $\geq |1.5|$ for identification of genes denominated Significant FC/Differentially Expressed Genes (SDEG) as in standard array analysis.

For the validation analysis, COPD and S data ($n = 18/18$) were extracted from GSE8545 dataset. The GEO2R tool was used for FC data analysis (22).

Generation of Venn diagram analysis for overlapping/unique gene lists was performed using Venny 2.1 (23). Pearson correlation matrix generation was produced using R version 3.6.2. Pearson correlation maps for mRBPs expression changes and heatmaps were generated using tMEV tools v4_9_0.45 (24, 25).

Enrichment for DNA sequence motifs for transcription factors binding sites, according to motif descriptors in the JASPAR database, was identified using PScanChIP (26) with the following parameters: "Organism: Homo Sapiens," "Assembly: hg38," "Background: Promoters," "Descriptors: Jaspar 2018 NR." Promoter regions have been calculated as the range from +1,500 bp upstream to −500 bp downstream of the transcription start site (TSS) of all the submitted gene list. Only over-represented motifs with $p \leq 0.05$ were considered.

Gene Ontology (GO)

GO analysis was performed with Ingenuity Pathway Analysis (IPA) software on microarray probes of RBPs identified as DEG. The significance values for the canonical pathways is calculated by Fisher's exact test right-tailed. The prediction of activation or inhibition of Canonical Pathways was calculated by z-score (27) as follows:

$$z - score = \frac{\sum (Upregulated) - \sum (Downregulated)}{\sqrt{Ntot}}$$

Statistical Analysis

Statistical analysis was performed using GraphPad Prism 5 (*GraphPad Software Inc.*).

A

GEO ID: GSE5058

HG-U133 Plus 2.0 array			
	Small airways		
	Normal nonsmokers	Normal smokers	Established COPD smokers
n	12	12	6
Sex (male/female)	10/2	9/3	5/1
Age (y)	42±8	45±4	49±6
Race (B/W/H)	6/4/2	7/5/0	2/4/0
Smoking history (pack-years)	0	26±9	26±13
Urine nicotine (ng/mL)	negative	648±265	347±155
Urine cotinine (ng/mL)	negative	1,263±212	835±374
Venous CO-Hb	1.7±0.7	3.3±0.9	1.4±0.6
Pulmonary function variables (% predicted)			
FVC	105±9	103±12	106±11
FEV1	105±7	100±14	87±25
FEV1/FVC	99±7	97±7	66±14
TLC	97±8	96±15	107±20
DLCO	95±12	94±10	82±19
Epithealial cells			
Total number recovered x 10^6	5.3±1.7	6.8±2.2	5.7±0.5
% epithelial	99±1	99±1	96±1
% inflammatory	1±1	1±1	4±1
Differential epithelial cell count			
Ciliated	78±7	75±10	71±4
Secretory	7±3	7±3	9±4
Basal	7±2	9±4	2±1
Undifferentiated	8±4	9±4	2±1

Abbreviations: B=black, DLCO=diffusing capacity of the lung for carbon monoxide, FEV1/FVC=Tiffeneau-Pinelli index, FEV1=forced expiratory volume in 1 second, FVC= forced vital capacity, H=hispanic, TLC=total lung capacity, Venous CO-Hb = venous carboxyhemoglobin, W=White (Caucasian). *(Modified from Carolan et al, Cancer Res 2006;66:10729, with permission)*

B

n= DEG FDR ≤ 0.05					
S/NS		COPD/NS		COPD/S	
Probes	Genes	Probes	Genes	Probes	Genes
44	41	653	391	644	382

C

n= SDEG FDR ≤ 0.05; FC ≥ |1.5|					
S/NS		COPD/NS		COPD/S	
Probes	Genes	**Probes**	Genes	**Probes**	Genes
16	13	**393**	267	**390**	257
Up	Down	Up	Down	Up	Down
11	5	93	300	63	327

FIGURE 2 | Regulated mRBP expression in Small Airway Epithelial Transcriptomics in stable COPD. **(A)** Clinical and spirometric phenotyping of COPD smoker patients (COPD), non-smokers (NS), and smokers (S) with normal lung function (NLF) as control cohorts providing small airway epithelial cells by bronchial brushings for trascriptomic analysis reported in GEO GSE5058 [modified from (17) with permission] utilized in this study for mRBP expression analysis. **(B,C)** For each gene, multiple probes spanning different gene regions are represented on array platforms. Panels show the numbers of mRBP probes and corresponding genes obtained after FDR filtering (see **Figure 1A**). **(B)** Statistically significant, Differentially Expressed mRBP Genes, regardless of fold change value (DEG) and **(C)**. Statistically Significant/Differential Expressed mRBP Genes with differential expression set at $\geq |1.5)$ (SDEG) obtained comparing datasets from S vs. NS, COPD vs. S and vs. NS. Number of Up- or down-regulated SDEG probes are shown below.

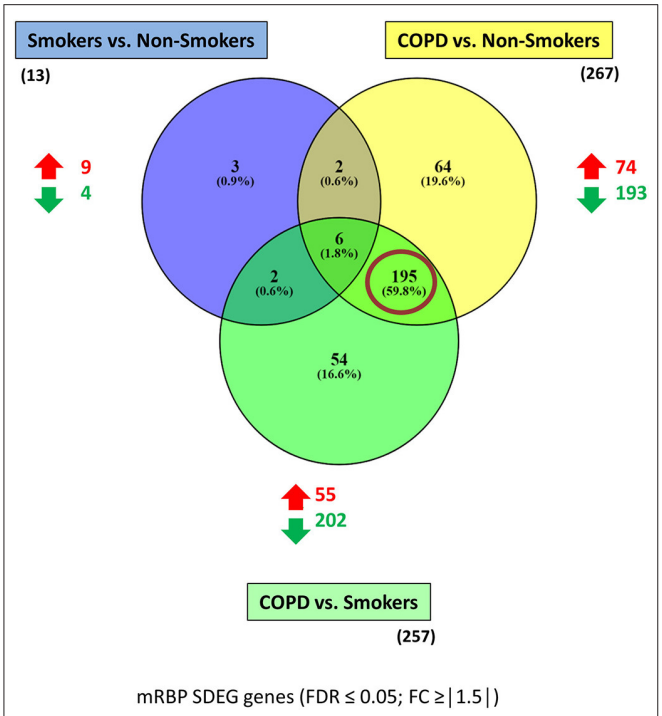

FIGURE 3 | mRBP SDEG genes in small airway epithelium of stable COPD patients vs. non-smoking and smoking control subjects: unique and overlapping regulated expression. Venn diagram generated with Venny 2.1 (23), showing selective and shared mRBPs SDEG genes (FDR ≤ 0.05; FC ≥ |1.5|) among the three comparisons. The number of up-and down-regulated mRBPs for each comparison are shown by red/green arrows; the total number is indicated in parenthesis. Red circle highlights the predominant number of SDEG differentially expressed in COPD, regardless the smoking status of controls.

RESULTS

Expression Profile of mRBPs in Airway Epithelial Transcriptomic Database of Patients With Stable COPD Compared to Non-smoker and Smoker Control Subjects

The mRBPs gene list was searched in the GSE5058 dataset to identify disease-dependent mRBP gene expression in patients with established COPD compared to control groups, clinically phenotyped as shown (**Figure 2A**). Comparisons of expression levels for the smoking control group vs. non-smoking control group dataset (S/NS) and of COPD patients vs. both NS and S group datasets (COPD/NS, COPD/S) were performed. The number of regulated mRBP genes is reported along with corresponding array probes, which detect different fragments of each gene sequence and generate the fluorescence intensity raw data. We first calculated regulated genes with statistically significant changes regardless of fold change (FC) value, defined as Differentially Expressed Genes (DEG) (**Figure 2B**). These data revealed an overall greater expression of mRBPs in COPD patients vs. both NS and S control groups, about 9-fold higher than that triggered by smoke exposure alone. The mRBP genes displaying a statistically significant FC value ≥|1.5|, denominated Significant FC/Differentially Expressed Genes (SDEG) were further selected (**Figure 2C**). Approximately 70% of the mRBP DEG genes were included in this category when COPD samples were compared to both control samples (COPD/NS, COPD/S), while only 30% of S/NS DEG genes were upregulated over this threshold. A small number of genes were excluded from further computing for probe discordance ≥ 67% (n = 30/267, 11% for COPD/NS; 10/257 for COPD/S, 3%). The SDEG profiles indicate that the majority of mRBP genes in COPD were downregulated compared to both controls (n = 194/267, 73% for COPD/NS; n = 202/257, 79% for COPD vs. S) while in S/NS only 30% (n = 4/13) were downregulated (**Figure 3**). **Table 1** lists the main functions, published or described in GeneCards (80) for mRBP SDEG with the highest numerical FC value in COPD vs. both control groups.

The three gene groups (NS/S, COPD/NS, COPD/S) were intersected to identify both unique and overlapping mRBP expression profiles. As shown in the Venn's diagram (**Figure 3**), 195 SDEG genes are shared between the COPD patients vs. both NS and S groups, pointing at a distinctive mRBP signature driven by COPD beyond the active exposure to cigarette smoke.

Using the larger DEG lists, the three gene sets were then analyzed by IPA software probing changes in the categories of canonical pathways and intersected, (**Figure 4**) as done for the SDEG gene groups. Five out of eight canonical pathways impacted by COPD were shared by comparisons to NS and S groups (**Figure 4A**). Calculation of the z-score parameter yielded a predictive assessment of the downstream effect - activation or inactivation - exerted by the identified RBP profile on the metabolic pathways (**Figure 4B**). **Table 2** lists the regulated mRBPs impacting upon the canonical pathways shown in **Figure 4B**.

We then selected the gene set obtained for the comparison COPD/S (n = 409 SDEG probes) to perform an unsupervised clustering analysis of each subject's mRBP expression profile for the three groups (NS, S, COPD), using Pearson's hierarchical clusters/complete linkage method. Results were represented in a heatmap generated with the T-MeV software (**Figure 5**) (24, 25). As expected, the heatmap clearly showed how the expression of mRBPs appears predominantly diminished compared to NS and most of S subjects; interestingly, it also identified in the S group a subset of four subjects displaying an expression profile highly homologous to the one identified in COPD patients (**Figure 5A**). This similarity was confirmed by performing unsupervised cluster analysis for both genes and subjects using an Euclidean distance metrics (**Figure 5B**). This analysis confirmed that the RBP expression profile of this S subgroup indeed clustered with the samples from COPD patients.

To initiate mechanistic understanding of predominant RBP downregulation in subjects with stable COPD and in selected smokers with normal lung function, we conducted for the RBP gene set obtained for COPD/S a search for transcription factor (TF) binding motif within promoter regions. Significant binding site enrichment for several TFs (**Figure 6**, listed in **Supplementary Table 1**) was exclusively found for the genes downregulated in their expression.

TABLE 1 | Regulated RBPs in COPD vs. normal non-smokers and smokers: selected list with known functions.

Gene	Complete name	$FC_{COPD\ vs.\ S}$	$FC_{COPD\ vs.\ NS}$	Main functions	References
FUS	FUS RNA binding protein	−34.63	−37.5	Involved in pre-mRNA splicing and the export of fully processed mRNA to the cytoplasm	(28)
				Maintenance of genomic integrity and mRNA/microRNA processing	(29)
THRAP3	Thyroid hormon receptor associated protein 3	−33.54	−31.58	Enhances the transcriptional activation mediated by PPARG cooperatively with HELZ2	(30)
				Acts as a coactivator of the CLOCK-ARNTL heterodimer	(31)
				Involved in response to DNA damage	(30)
DDX17	DEAD-Box helicase 17	−31.04	−46.27	RNA helicase	(32)
				pre-mRNA splicing, alternative splicing, ribosomal RNA processing and miRNA processing, transcription regulation	(33–36)
				Splicing of mediators of steroid hormone signaling pathway	(37)
				Synergizes with TP53 in the activation of the MDM2 promoter; may also coactivate MDM2 transcription through a TP53-independent pathway	(38–40)
				Coregulates SMAD-dependent transcriptional activity during epithelial-to-mesenchymal transition	(35)
				Plays a role in estrogen and testosterone signaling pathway	(37, 39–41)
				Promotes mRNA degradation mediated by the antiviral zinc-finger protein ZC3HAV1	(42)
SCAF11	SR-Related CTD associated factor 11	−14.4	−12.7	Plays a role in pre-mRNA alternative splicing by regulating spliceosome assembly	(43)
STRAP	Serine/threonine kinase receptor associated protein	−10.8	−8.22	Plays a catalyst role in the assembly of small nuclear ribonucleoproteins (snRNPs), the building blocks of the spliceosome	(44)
				Negatively regulates TGFβ signaling	(44)
				Positively regulates the PDPK1 kinase activity	(44)
RBM14	RNA binding motif protein 14	−7.36	−6.31	General nuclear coactivator, and an RNA splicing modulator. Isoform 1 may function as a nuclear receptor coactivator. Isoform 2, functions as a transcriptional repressor	(45)
				Plays a role in the regulation of DNA virus-mediated innate immune response by assembling into the HDP-RNP complex, a complex that serves as a platform for IRF3 phosphorylation	(46)
BCLAF1	Bcl-2-associated transcription factor 1	−7.32	−4.13	Regulation of apoptosis interacting with BCL2 proteins	(47)
ILF3	Interleukin enhancer binding factor 3	−6.33	−4.61	Forms a heterodimer with ILF2, required for T-cell expression of IL-2	(44)
				Post transcriptional regulation of mRNA binding to poly-U elements and AU-rich elements (AREs) in the 3′-UTR of target mRNA	(48)
				Participates in the innate antiviral response	(49, 50)
				Plays an essential role in the biogenesis of circRNAs	(50)
SFSWAP	Splicing factor SWAP	−5.81	−3.34	Regulates the splicing of fibronectin and CD45 genes	(51)
RBM25	RNA binding motif protein 25	−5.7	−4.16	Regulator of alternative pre-mRNA splicing	(52)
				Involved in apoptotic cell death through the regulation of the apoptotic factor BCL2L1 (proapoptotic isoform S, antiapoptotic isoform L)	(52)
DHX36	DEAH-Box helicase 36	−4.96	−5.31	Enhance the deadenylation and decay of mRNAs with 3′-UTR AU-rich elements (ARE-mRNA)	(53)
				Multifunctional ATP-dependent helicase that unwinds G-quadruplex (G4) structures	(54–57)
				Plays a role in genomic integrity. Converts the G4-RNA structure present in TREC into a double-stranded RNA	(56, 58–62)
				Plays a role in the regulation of cytoplasmic mRNA translation and mRNA stability	(63, 64)

(Continued)

TABLE 1 | Continued

Gene	Complete name	$FC_{COPD\ vs.\ S}$	$FC_{COPD\ vs.\ NS}$	Main functions	References
				Plays a role in transcriptional regulation and post-transcriptional regulation	(54, 65, 66)
HNRNPA2B1	Heterogeneous nuclear ribonucleoprotein A2/B1	−4.91	−4.63	Associates with nascent pre-mRNAs, packaging them into hnRNP particles and drive them into transcription, pre-mRNA processing, RNA nuclear export, subcellular location, mRNA translation and stability of mature mRNAs.	(67)
				Involved in transport of specific mRNAs to the cytoplasm in oligodendrocytes and neurons recognizing binding the A2RE or the A2RE11 sequence motifs present on some mRNAs.	(68)
				Specifically binds single-stranded telomeric DNA sequences, protecting telomeric DNA repeat against endonuclease digestion	(69)
				Involved in the transport of HIV-1 genomic RNA out of the nucleus, to the MTOC, and then from the MTOC to the cytoplasm: acts by specifically recognizing and binding the A2RE sequence motifs present on HIV-1 genomic RNA.	(69)
CCAR1	Cell division cycle and apoptosis regulator 1	−2.79	−2.93	Plays a role in cell cycle progression and/or cell proliferation	(70, 71)
				p53 coactivator	(72)
NR0B1	Nuclear receptor subfamily 0 Group B member 1	1.57	3.31	Acts as a dominant-negative regulator of transcription which is mediated by the retinoic acid receptor	(73)
				Functions as an anti-testis gene by acting antagonistically to Sry	(73)
				Plays a role in the development of the embryo and in the maintenance of embryonic stem cell pluripotency	(73)
RBPMS	RNA-Binding protein with multiple splicing	1.77	1.4	pre-mRNA maturation (binds to poly(A) RNA)	(74, 75)
				Required to increase TGFB1/Smad-mediated transactivation	(75)
HDLBP	High density lipoprotein binding protein	1.91	2.53	Regulates excess cholesterol levels in cells	(76)
				Induces heterochromatin formation	(76)
MATR3	Matrin 3	2	3.3	Plays a role in the regulation of DNA virus-mediated innate immune response by assembling into the HDP-RNP complex, a complex that serves as a platform for IRF3	(46)
DHX30	DExH-Box helicase 30	2.18	2.45	Assembly of the mitochondrial large ribosomal subunit	(77, 78)
				Required for optimal function of the zinc-finger antiviral protein ZC3HAV1	(79)
				Involved in nervous system development differentiation	(79)

A2RE, 21 nucleotide hnRNP A2 response element; A2RE11, 11-nucleotide subsegment of the A2RE; ARE, AU Rich Elements; ARNTL, Aryl Hydrocarbon Receptor Nuclear Translocator Like; circRNA, circular RNA; CLOCK, Circadian Locomoter Output Cycles Protein Kaput; HELZ2, Helicase With Zinc Finger 2; hnRNP, heteronuclear ribonucleoprotein; IL-2, Interleukin2; IRF3, Interferon Regulatory Factor 3; MDM2, Proto-oncogene MDM2; miRNA, micro RNA; MTOC, microtubule organizing center; NONO, Non-POU Domain Containing Octamer Binding; PDPK1, 3-Phosphoinositide Dependent Protein Kinase 1; rRNA, ribosomal RNA; SMAD, small mother against decantaplegic; TGFβ, Transforming Growth Factor β; TP53, Tumor Protein 53; TREC, telomerase RNA template component; ZC3HAV1, Zinc Finger CCCH-Type Containing Antiviral 1.

As mRBPs exert their function by dinamically assembling in RNP complexes, the same gene dataset (SDEG in COPD/S) was then searched for RBPs with correlated expression, which may indicate disease-driven, coordinated target regulation (20). Pearson correlation map showed at least five highly correlated mRBP clusters ($r \geq 0.70$) (**Figure 7A**). Clusters of RBP gene lists and their FC values between COPD and both S/NS control populations are listed in **Supplementary Table 2**. Canonical pathway analysis indicated that RBP genes in clusters commonly impacted upon RAN signaling and Telomere Extension by Telomerase, along with more cluster- restricted influence on other pathways, such as inhibition of ARE-mediated mRNA degradation and IL-15 expression (**Table 3**). In particular, cluster 3 included 40 genes, among which was included *HNRNPD*, coding for the RBP AUF-1 that we previously identified as repressed in small airway epithelium in airway biopsies of an independent subject cohort of COPD patients compared to smoker controls (16). For cluster 3, IPA analysis identified enrichment of genes involved in RAN signaling, telomere extension, IL-15 expression (**Figure 7B**). **Figure 7C** shows normalized fold changes across the three groups for eight representative mRBPs, including *HNRNPD*, contained in cluster 3.

We then submitted the mRBP profile obtained in the COPS/S, used also to identify gene clusters, to validation in an independent transcriptomic dataset of small airway epithelium obtained from bronchial brushing of NS, S and COPD (GOLD stages I or II) [$n = 18$ each cohort, deposited in public GEO repository

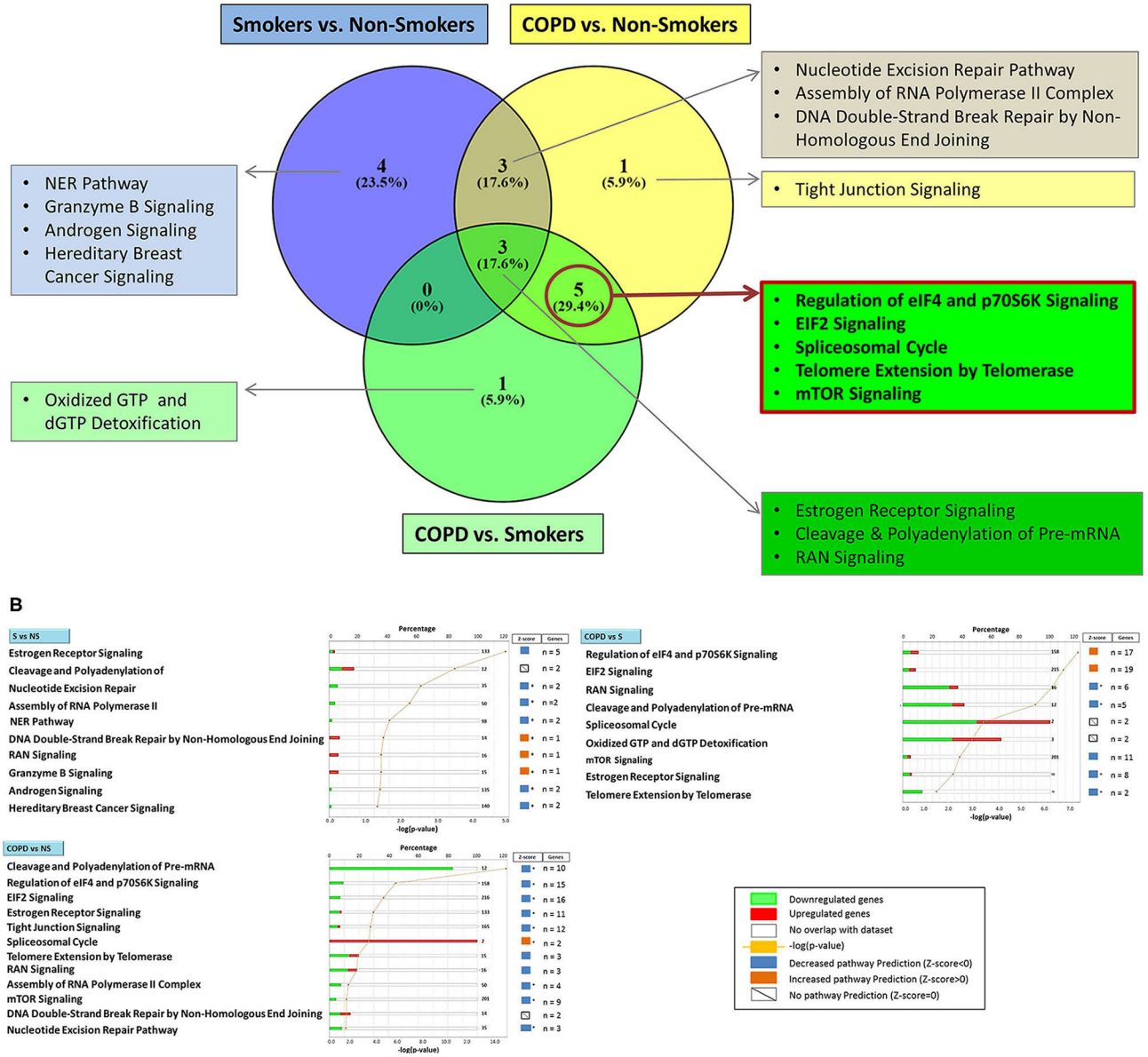

FIGURE 4 | Genome Ontology analysis of mRBPs expression in small airway epithelium of stable COPD patients vs. non-smoking and smoking control subjects: involvement in established COPD pathogenic pathways. Ingenuity Pathway Analysis (IPA) of mRBP in COPD GSE5058 Dataset. **(A)** Venn diagram showing selective and shared canonical pathways among the group comparisons, calculated by Ingenuity Pathway Analysis (IPA) on DEGs for increased statistical power and listed as in **Figure 3**. In evidence (red lined rectangle) the pathways enriched in COPD vs. both NS and S control groups. **(B)** List of canonical pathways identified for each group comparisons. For each pathway, bargraphs indicate the number of RBP genes associated with the pathway (total number listed at the end of the bar) that were found up (red)- or down (green)-regulated in the dataset; z-score (on the right) predicts pathway repression (blue) or activation (orange) given by the expression profile (see Methods); far right: genes n = indicates number of regulated mRBP genes involved for each pathway (also listed in **Table 2**). * z-score ≥ |1|.

as GSE 8545 (21). Analysis of COPD/S in GSE 8545 largely confirmed the global downregulation of RBP in COPD/S, with 56% of probe sets downregulated with an FC ≤ - 1.5 (217/390) vs. 80% (327/390) downregulated in GSE5058. Importantly, the comparison reproduced differential expression for all RBP cluster genes (listed in **Table 3**) identified by IPA as having significant impact on canonical pathways (**Figure 8**).

Expression Profile of mRBPs in Bronchial Epithelium of Patients With Severe Asthma Compared to Control Subjects

Transcriptomic data in airway epithelium from bronchial brushing of patients with severe asthma (SA) and healthy controls (HCs) were searched for mRBP expression using the

TABLE 2 | GO analysis by IPA indicating canonical pathways in which RBP enrichment is significant for each comparison, with predicted functional outcome indicated by z-score (See Methods for details), and RBP molecules involved.

2A. S/NS				
Ingenuity canonical pathways	***p*-value**	**z-score**	**Prediction**	**Molecules**
Estrogen receptor signaling	1.38E-05	−0.44	Inhibition	PRKDC,NR0B1,SPEN,POLR2H, POLR2L
Cleavage and polyadenylation of Pre-mRNA	3.47E-04	0	0	CPSF2,CPSF6
Nucleotide excision repair pathway	3.02E-03	−1.41	Inhibition	POLR2H,POLR2L
Assembly of RNA polymerase II complex	6.03E-03	−1.41	Inhibition	POLR2H,POLR2L
NER pathway	2.19E-02	−1.41	Inhibition	POLR2H,POLR2L
DNA double-strand break repair by non-homologous end joining	3.24E-02	1	Activation	PRKDC
RAN signaling	3.63E-02	1	Activation	TNPO1
Granzyme B signaling	3.63E-02	1	Activation	PRKDC
Androgen signaling	3.98E-02	−1.41	Inhibition	POLR2H,POLR2L
Hereditary breast cancer signaling	4.68E-02	−1.41	Inhibition	POLR2H,POLR2L
2B. COPD/NS				
Cleavage and polyadenylation of pre-mRNA	2E-15	−3.16	Inhibition	PAPOLA,CPSF2,CPSF6,CSTF1,NUDT21,CPSF1,CSTF2,CPSF3, CSTF3,CPSF4
Regulation of eIF4 and p70S6K signaling	2.88E-06	−3.87	Inhibition	EIF2B4,PAIP2,EIF3E,EIF4G1,EIF2B2,EIF4E,EIF3M,EIF3G,EIF1, EIF3B,EIF3A,EIF2B1, EIF3L,EIF1AX,EIF3K
EIF2 signaling	3.02E-05	−4	Inhibition	EIF2B4,EIF3E,EIF4G1,EIF2B2,EIF4E,EIF3,EIF3G,PTBP1,EIF1,EIF3, HNRNPA1,EIF2B,EIF3A,EIF3L,EIF1AX,EIF3K
Estrogen receptor signaling	0.000209	−2.11	Inhibition	PRKDC,DDX5,THRAP3,SPEN,NR0B1,POLR2H,GTF2F1,HNRNPD, RBFOX2,POLR2K,POLR2L
Tight junction signaling	0.000363	−1.73	Inhibition	CPSF2,CPSF6,CSTF1,NUDT21,CPSF1,CSTF2,YBX3,CPSF3, SYMPK,SAFB,CSTF3,CPSF4
Spliceosomal cycle	0.000501	1.41	Activation	U2AF1/U2AF1L5,U2AF2
Telomere extension by telomerase	0.004169	−0.57	Inhibition	HNRNPA1,XRCC6,HNRNPA2B1
RAN signaling	0.005129	−0.57	Inhibition	KPNB1,RANBP2,TNPO1
Assembly of RNA polymerase II complex	0.025704	−2	Inhibition	POLR2H,GTF2F1,POLR2K,POLR2L
mTOR signaling	0.038019	−3	Inhibition	EIF3G,EIF3B,EIF3A,EIF3E,EIF4G1,EIF4E,EIF3L,EIF3M,EIF3K
2C. COPD/S				
Regulation of eIF4 and p70S6K signaling	5.75E-08	0.24	Activation	EIF2B4,EIF4G3,PAIP2,EIF3E,EIF4G1,EIF2B2,EIF4E,EIF3M,EIF3G, EIF1,EIF3B,PAIP1,EIF3A,EIF2B5,EIF1AX,EIF3L,EIF3K
EIF2 signaling	2.24E-07	0.22	Activation	EIF2B4,EIF4G3,EIF3E,EIF4G1,EIF2B2,EIF4E,EIF3M,EIF3G,PTBP1, EIF1,EIF3B,HNRNPA1,EIF5,PAIP1,EIF3A,EIF2B5,EIF1AX,EIF3,EIF3K
RAN signaling	6.46E-07	−1.63	Inhibition	KPNB1,RANBP2,TNPO1,RAN,XPO1,IPO5
Cleavage and polyadenylation of pre-mRNA	3.16E-06	−1.34	Inhibition	PAPOLA,CPSF2,CSTF1,NUDT21,CSTF3
Spliceosomal cycle	0.000468	0	0	U2AF1/U2AF1L5,U2AF2
Oxidized GTP and dGTP detoxification	0.00138	0	0	DDX6,RUVBL2
mTOR signaling	0.004365	−0.30	Inhibition	EIF3G,EIF3B,EIF3A,EIF4G3,EIF3,EIF4G1,EIF3L,EIF4E,EIF3M, EIF4B,EIF3K
Estrogen receptor signaling	0.008318	−1.41	Inhibition	PRKDC,THRAP3,NR0B1,SPEN,HNRNPD,GTF2F1,POLR2K,POLR2
Telomere extension by telomerase	0.040738	−1.41	Inhibition	HNRNPA1,HNRNPA2B1

In bold are the pathways associated with COPD vs. both controls.

same methodology (**Figure 1**). Clinical characteristics of the original study, from which we extracted GEO data only for SA and HC groups, are shown in **Supplementary Table 3**. We randomly extracted from the GSE63142 dataset (19) the same number of patients of the GSE5058 COPD dataset ($n = 6$ SA, $n = 12$ HCs). Only 30 probes (corresponding to 29 genes) were differentially expressed (DEG) in SA vs. HCs, but none of the DEG genes changed by at least 50% compared with HCs, thus none was categorized as SDEG (FDR ≤ 0.05; FC $\geq |1.5|$). We then extended the search to the entire number of subjects of the

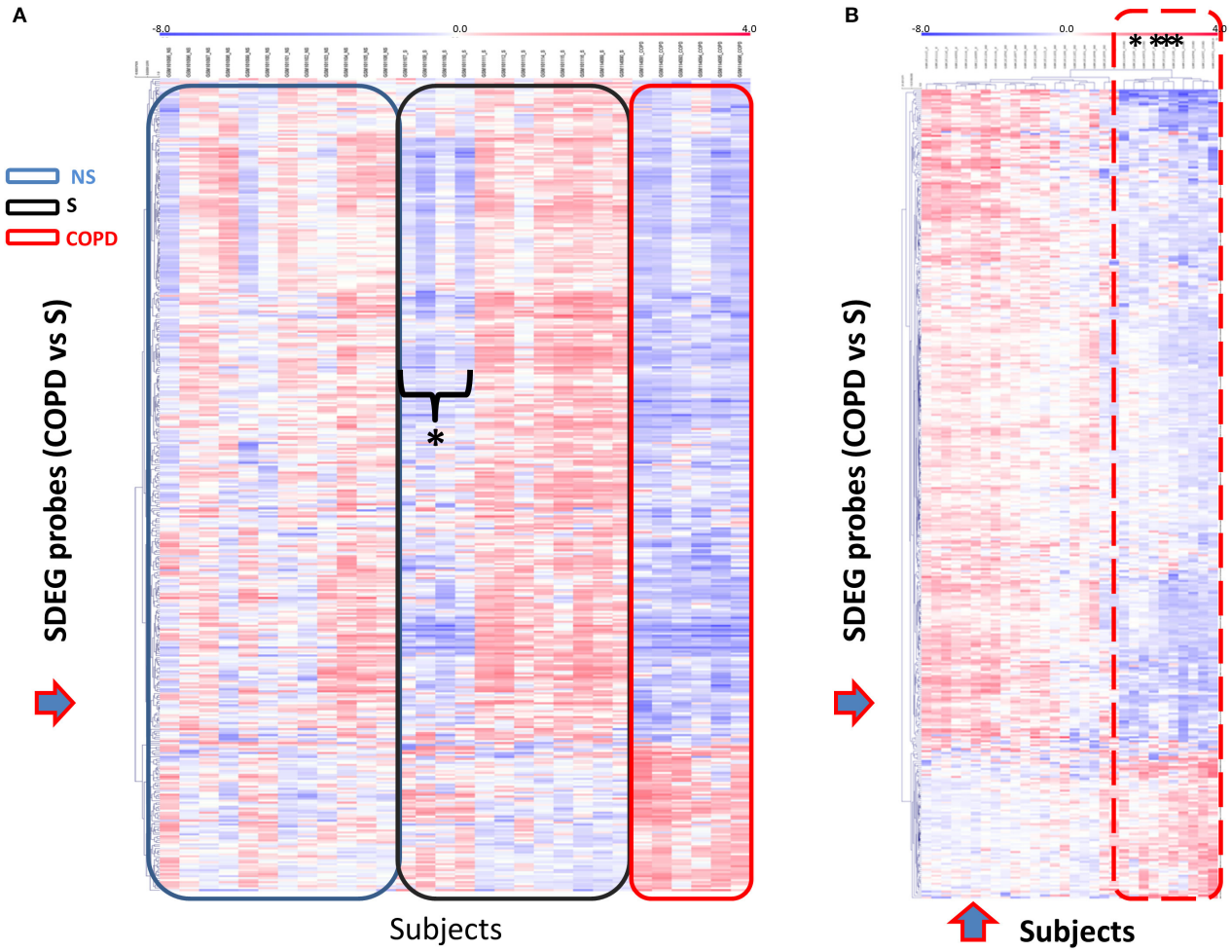

FIGURE 5 | Unsupervised gene cluster analysis across the individual samples from GSE5058 dataset identifies selective global mRBPs repression in COPD patients shared by a subset of smoker controls. **(A)** Unsupervised clustering analysis applied to (blue arrow) SDEG probe list identified in COPD/S ($n = 409$). Heatmap shows SDEG probes' fluorescence intensity value (blue < 0, reduced: red > 0, increased). The data were normalized on the median and $\log_2$-trasformed for relative fold changes (See Methods). **(B)** Unsupervised clustering analysis applied to both SDEG probe list and individual samples (blue arrows). Asterisks indicate the SDEG profiles of four smokers with NLF, clustering with those of COPD patients indicated by the dotted line.

datasets ($n = 56$ SA and 27 HCs) and identified as DEG 68 gene probes corresponding to 62 genes; as for the previous analysis, none of the DEG was categorizable as SDEG (genes listed in **Supplementary Table 4**).

DISCUSSION

In the present study, global changes in mRBP gene expression in human airway epithelium were evaluated, for the first time, using public gene array databases derived from bronchial brushings of patients affected by two major chronic lung inflammatory diseases, COPD and severe asthma, and their relative control subjects. We report that significant changes were largely exclusive to samples from COPD and that they were mostly due to downregulated mRBP expression, a feature that was found also in a subset of control smokers. These changes were associated with the occurrence of several clusters of co-regulated mRBPs, and they impacted relevant pathways deemed pathogenic for COPD.

We recently identified in a GEO database of airway epithelial cells from stable COPD patients a significant loss of the RBP AUF-1 compared to smoker controls, matching the loss we identified at protein level in airway samples of patients with stable COPD compared to normal smokers (16). The present study was undertaken on this basis as a broader investigation of epithelial RBP patterns comparing two lung diseases characterized by chronic inflammation and oxidative stress – COPD and SA - since preclinical studies clearly identified the role of this class of posttranscriptional regulators in these pathological processes (14, 81, 82), yet they are scarcely described in human disease driven by them. This proof-of concept study could serve as springboard for studies focused on specific PTGR pathways and molecular species exploitable as phenotype/endotype disease biomarker or for therapeutic targetability.

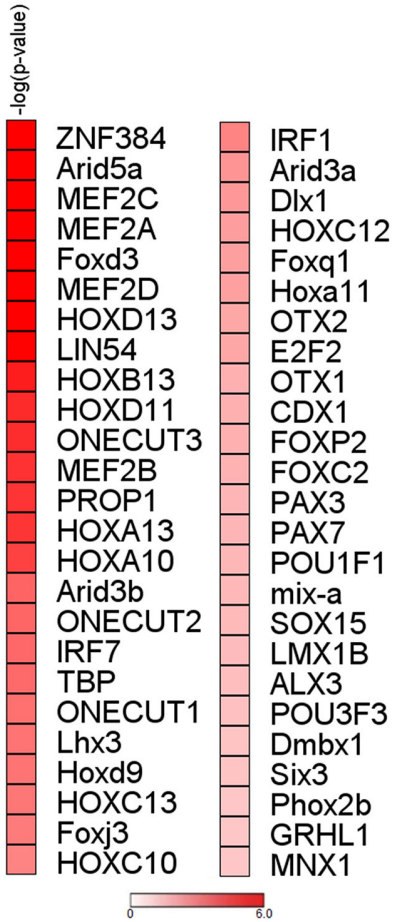

FIGURE 6 | Analysis of upstream regions of mRBP genes regulated in COPD/S identifies enrichment of transcription factors binding sites for downregulated genes. Enrichment analysis of transcription factor binding sites for COPD/S SDEG gene list ($n = 257$) within the promoter regions orderd by -log(p-value). Promoter regions have been calculated as the range from +1,500 bp upstream to −500 bp downstream of the gene transcription start site (TSS). Only over-represented motifs with $p \leq 0.05$ were considered.

To generate the list of mRBPs we used for this study, Gerstberger et al. (20) searched the human genome for protein-coding genes bearing RBDs using specific statistical probability models and futher manual curation, which led to a final census of 1,542 RBPs. Strikingly, the biological functions of a third of these proteins is unknown or minimally defined, at least in human disease; some of these - such as DEAD/DEAH box helicases – were found to be significantly regulated in airway epithelium of COPD patients by our analysis.

In our study the DEAD-box RNA helicase, DDX17 was in fact among the top downregulated mRBP in COPD; its role is not yet defined in this disease. DDX17 is a nucleocytoplasmic shuttling factor that functions as RNA helicase and is involved in transcription, splicing and miRNA processing. Several studies indicate its involvement in antiviral responses: in a recent study, a significant decrease in DDX17 was found in transcriptional signature to vaccination to H1N1 influenza virus in human subjects, which correlated with antibody titter and IFN-γ production by T-cells (83). Upregulated DDX17 expression has been reported to be associated with resistance to the tyrosine kinase inhibitor drug, gefitinib in non-small cell lung cancer (NSCLC) cells (84). We also found as significantly downregulated the 3′-5′ DEAH-box helicase DHX36, also known as RHAU (RNA helicase associated with AU-rich element) (58). In addition to regulating the transport and half-life of ARE-bearing mRNAs, it has a role in the mechanisms of preservation of genome integrity and in the maintenance of telomeres. In particular, DHX36 assists the activity of the TERT (Telomerase Reverse Transcriptase) enzyme (54, 58–62). As helicase, DHX36 unwinds parallel G-quadruplex structures formed in DNA and RNA. Interestingly, a recent study indicates that ablation of DHX36 results in increased SG formation and protein kinase R (PKR/EIF2AK2) phosphorylation, indicating that DHX36 is involved in resolution of cellular stress at the level of SG (85). Moreover, in rat alveolar epithelial cells DHX36 downregulates epithelial sodium channel (ENaC) mRNA stability by binding with T-cell internal antigen-1 related protein (TIAR-1) to the transcript 3′-UTR (86).

The results from the study in COPD revealed for the first time a significant, global downregulation of mRBPs in cells from COPD patients compared to controls; interestingly, a pattern very similar was found in samples from four out of 12 smoker controls with normal lung function, as confirmed by cluster analysis. This data suggest that this expression profile could indicate subjects at higher risk related to smoke, or with disease at preclinical stage. It would be important to understand, upon validation on larger datasets, the specific mechanisms and epithelial responses affected by this mRBP profile, and whether it leads to molecular changes underpinning a specific clinical disease phenotype.

To this end, a search for common transcriptional control and global pathway analysis may assist in directing further studies on a scale larger than single-gene analysis, in particular when exploring relatively uncharted pathways.

Of note, significant enrichment for TF binding motifs in COPD/S-regulated genes was found only for downregulated RBP, further supporting a biological relevance of this global change, possibly representing a coordinated shift in response to pathogenic triggers. Overall, the TFs putatively binding to the DNA motifs identified with highest enrichment, such as the MEF2 TF family, have pleiotropic functions in cell cycle, cell differentiation, proliferation, apoptosis (87); Interestingly, ARID5A acts both as TF and as RBP according to nuclear or cytoplasmic localization (88); FoxD3 acts as tumor suppressor in lung cancer (89) while HOX genes are overexpressed in non-small cell lung cancer and postulated to act as oncogenes (90).

In our genome ontology analysis (**Table 2**), some of the pathways significantly affected by the changes in mRBPs are already recognized as impacted by the pathogenetic process in COPD, such as the expression/activity of the telomerase enzyme and the signaling coordinated by the kinase mTOR (Mammalian Target Of Rapamycin) (91–94); others may indicate so far under recognized disease determinants.

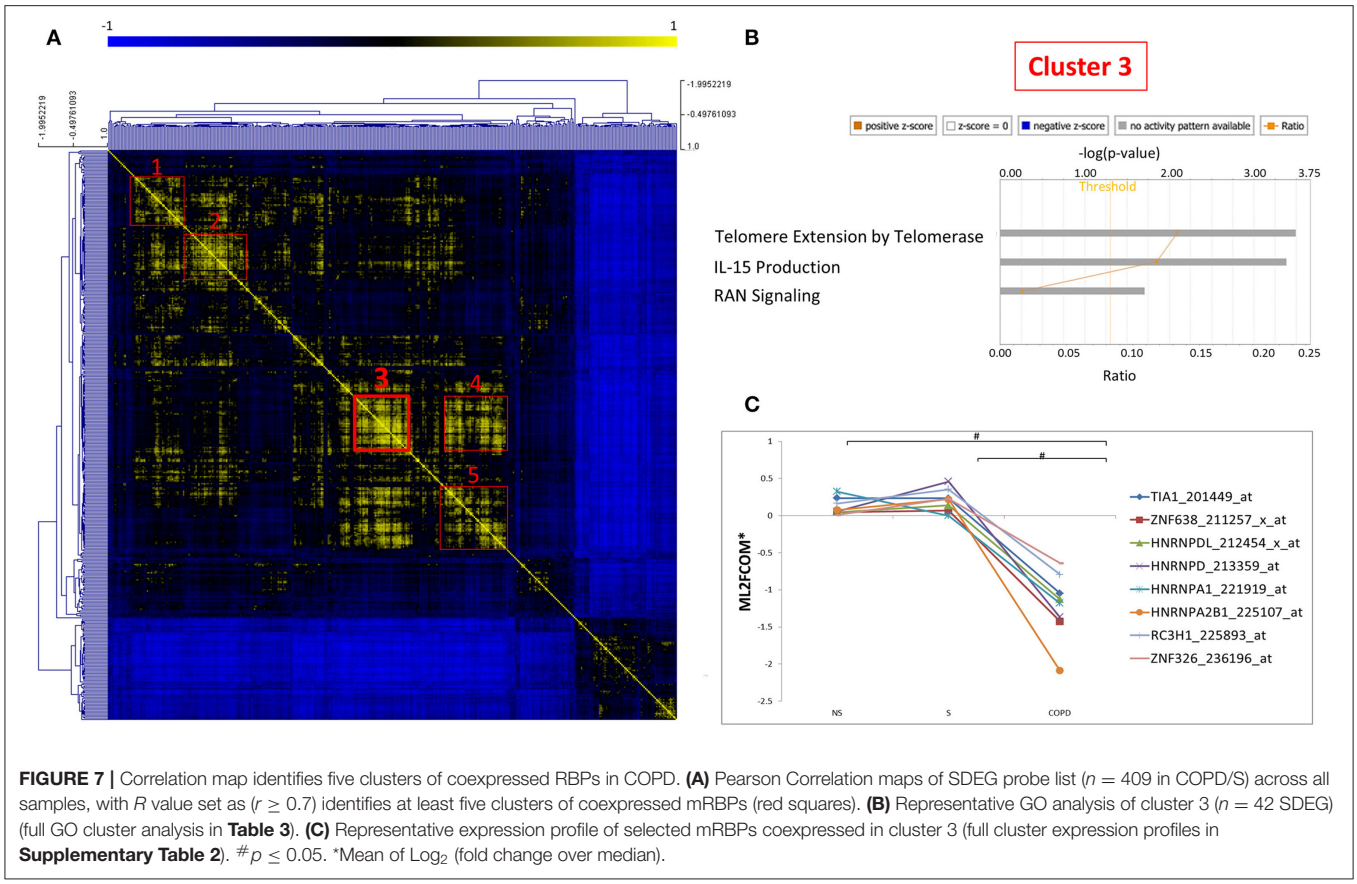

FIGURE 7 | Correlation map identifies five clusters of coexpressed RBPs in COPD. **(A)** Pearson Correlation maps of SDEG probe list ($n = 409$ in COPD/S) across all samples, with R value set as ($r \geq 0.7$) identifies at least five clusters of coexpressed mRBPs (red squares). **(B)** Representative GO analysis of cluster 3 ($n = 42$ SDEG) (full GO cluster analysis in **Table 3**). **(C)** Representative expression profile of selected mRBPs coexpressed in cluster 3 (full cluster expression profiles in **Supplementary Table 2**). $^{\#}p \leq 0.05$. *Mean of Log_2 (fold change over median).

Telomerase is an enzyme complex that reverse-transcribes an integral RNA template in order to add short DNA repeats at the 3′-ends of telomeres. In our study, the mRBPs HnRNPA1 and HnRNPA2B were found as downregulated SDEG in COPD and this profile was predicted by IPA to inhibit telomere extension by telomerase. Early studies established that hnRNP-A1, hnRNP-A2, and hnRNP-B1 proteins can interact with telomeres and are products of two different genes (*HNRNPA1* and *HNRNPA2B1*) but display similar structures (two RRMs and four RGG motifs in each)(95). The mRBP hnRNP A1 is the best characterized and found to be associated with human telomeres *in vivo* (96); depletion of hnRNP A/B proteins in human embryonic kidney 293 cell extracts greatly reduced telomerase activity, which was rescued by addition of recombinant hnRNP A1 (96). Recently, a large study conducted in a group of 576 patient with moderate-to-severe COPD found a significant relationship of absolute telomere length, measured by PCR in DNA from peripheral blood samples, with several clinical parameters such as quality of life, number of exacerbations, and mortality (97). These evidence suggest that shorter leukocyte telomere lengths could be evaluated as a biomarker for clinical outcomes in COPD. Furthermore, these two RBPs were coexpressed in cluster 3 (**Figure 7**), along with another known TERT-regulating factor, AUF-1 (98), which we initially documented as downregulated in COPD patients vs. controls by immunohistochemistry (16). AUF-1 positively regulates TERT1 at promoter level, but its loss may impact cellular senescence also by concomitant lack of its destabilization function for cell-cycle checkpoint mRNAs (98). Coexpression is often found among RBPs that participate to common posttranscriptional pathways; therefore, the novel mRBP clusters we identified (**Figure 7** and **Supplementary Table 2**) can be used as starting point to infer mRBP putative regulatory roles and identify coordinated expression of targets (20). Taken together, depletion in COPD of RBPs that are crucial for telomere length, as suggested by our findings, may have a role in shaping several COPD clinical outcomes by impacting this function also in airway epithelium.

In our pathway analysis, signaling of eukariotic initiation factors (eIF) was negatively impacted by downregulation of several eIFs, an effect which was also linked to a negative influence on mTOR signaling. The expression and functions of eukariotic initiation factors (eIF) are generally regulated in aging, transformation, and growth arrest and are critically hampered in cancer and during pathogenic stress conditions (99). Acceleration of cellular aging driven by oxidative stress in COPD lung is characterized by activation of PI3K (phosphoinositide-3-kinase) and mTOR signaling, through oxidation of tyrosine phosphatases such as and SHIP-1 (SH2-containing inositol-59-phosphatase-1) and PTEN (phosphatase tensin homolog) (100). The activity of eIF4E-binding protein(BP)1/eIF4E pathway is required for mTOR-dependent G1-phase progression (101), in particular it mediates mTORC1-dependent increased expression of cyclin D1

TABLE 3 | Canonical Pathways identified by IPA analysis of mRBPs clusters 1 to 5 as shown in **Figure 7**.

Ingenuity canonical pathways		
Cluster 1	***p*-value**	**Molecules**
RAN signaling	2.24E-02	TNPO1
Apelin muscle signaling pathway	2.51E-02	TFAM
Cluster 2	***p*-value**	**Molecules**
RAN Signaling	1.20E-02	RANBP2
Pyrimidine ribonucleotides interconversion	2.95E-02	DDX3X
Pyrimidine ribonucleotides *de novo* biosynthesis	3.09E-02	DDX3X
Cluster 3	***p*-value**	**Molecules**
Telomere extension by telomerase	3.24E-04	HNRNPA1,HNRNPA2B1
RAN signaling	4.17E-04	RANBP2,TNPO1
IL-15 production	2.00E-02	CLK1,CLK4
Cluster 4	***p*-value**	**Molecules**
RAN signaling	1.48E-05	RANBP2,TNPO1,XPO1
Telomere extension by telomerase	8.32E-04	HNRNPA1,HNRNPA2B1
Cleavage and polyadenylation of pre-mRNA	3.39E-02	NUDT21
IL-15 production	4.68E-02	CLK1,CLK4
Inhibition of ARE-Mediated mRNA degradation pathway	4.79E-02	DCP2,TIA1
Cluster 5	***p*-value**	**Molecules**
Telomere extension by telomerase	3.31E-04	HNRNPA1,HNRNPA2B1
Ran signaling	4.27E-04	RANBP2,XPO1
Inhibition of ARE-mediated mRNA degradation pathway	2.04E-02	DCP2,TIA1
Cleavage and polyadenylation of pre-mRNA	2.14E-02	NUDT21

(102). In cancer cells, decreased expression and functions of eIFs leads to inhibition of global translation and enhancement of translation of subsets of mRNAs by alternative mechanisms (99). Therefore, pathway analysis of COPD-related mRBP patterns strongly suggests a key role for altered translational regulation as a pathogenic mechanism by which oxidative stress alters specific protein levels and cellular functions. A more specific understanding of dysregulation of mRNA translation could uncover new strategies to diagnose and treat at least some forms of chronic inflammation and possibly indicate mechanisms linking COPD to lung cancer development.

Cytokines, chemokines and proinflammatory molecules secreted by senescent cells are collectively described as the senescence-associated secretory phenotype (SASP) (103). Multiple RBPs, such as Human antigen (Hu)R, AUF-1, tristetraprolin (TTP) have been shown to regulate several of the inflammatory transcripts that take also part to the SARP phenotype (12, 81, 104). In particular, CCL2, CXCL1 and IL-6 were identified among others as HuR-associated and regulated transcripts in human airway epithelial BEAS-2B cells stimulated with TNFα plus IFNγ. However, levels of TTP expression appear unchanged in airway samples from COPD patients and smoker controls as well as in epithelial *in vitro* models of cigarette smoke challenge, and there are conflicting evidence regarding airway epithelial HuR expression in COPD (16, 105, 106). The documented loss of epithelial AUF-1 may contribute also to SASP, besides impacting on cellular senescence, through loss of its mRNA decay-promoting function for several of its factors, such as IL-1β, TNFα, IL-6, CXCL1, VEGF (104). It is noteworthy that in our correlation analysis of COPD-regulated mRBPs, expression of T-cell intracellular antigen (TIA)-1, a critical translational repressor of TNFα (107), clusters with that of AUF-1 (**Figure 7C**).

Lastly, the pathway impacted by COPD-associated RBP expression in all clusters is Ras-related nuclear protein (Ran) signaling. Ran controls nucleo-cytoplasmic protein transport through the nuclear pore complex and regulates cell cycle progression (108, 109). As regulators of RNA throughout their lifespan, numerous RBPs undertake regulated nucleocytoplasmic shuttling in complex with their targets; key RBPs, such as HuR and HNRNPA1, are known to bind to transportin-1 (110). Conversely, several factors involved in Ran-mediated nucleo-cytoplasmic transport system, including transportin 1, are controlled by RBPs such as HuR (111) and by posttranscriptional control at large. As disruption of Ran expression and function is linked to most cancers, including NSCLC (112, 113), this data suggest that the impact of RBP expression changes on Ran pathway may contribute to increased risk of cancer development in a subset of COPD patients.

Unexpectedly, no significant differential mRBP expression was found when applying the mRBP list search to the database derived from bronchial brushings of SA patients vs. healthy controls. Triggers and inflammatory features of bronchial asthma have distinct features from those of COPD, however in severe asthma the inflammatory pattern is less divergent: increased oxidative stress and a poor response to corticosteroids are SA features common to COPD, especially in SA subjects who are smokers (114). Moreover, global alterations in airway epithelial-derived miRNA and polysome-bound mRNAs have been reported in other smaller SA patient cohorts compared to HC, indicating the occurrence of alteration in posttranscriptional pathways (115). Furthermore, a recent study reports that in primary airway epithelial cells harvested by bronchial brushing in SA patients, IL-17A in combination with TNFα prevents the cytoplasmic translocation of the RBP TIAR. Nuclear sequestration of TIAR halted the cytoplasmic binding and translational repression of its targets, IL-6 and CXCL8 mRNAs and correlated with corticosteroid insensitivity, *in vivo* neutrophilic inflammation and the post-bronchodilator FEV1 of SA patients (116). Posttranscriptional changes in asthma could be driven by a more diverse pattern of molecular species and mechanisms and changes in mRBPs localization and binding, rather that expression, may be predominant. This underscores the need to implement studies probing RBP posttranslational modifications in human airway samples or cell lines and to characterize the RBP interactome and understand its regulation of disease-related epithelial responses. More studies will be necessary to validate this significant negative finding in SA also using additional airway epithelial databases from patients

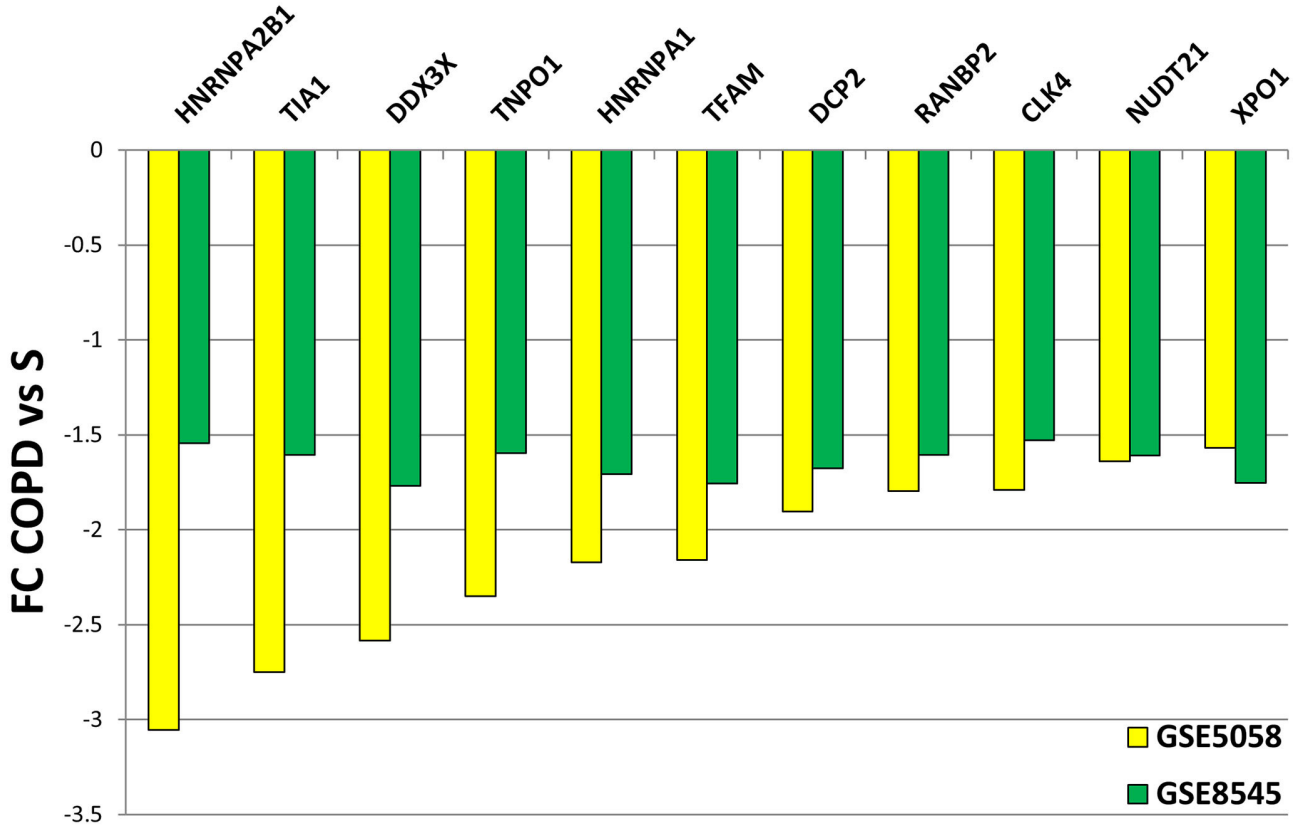

FIGURE 8 | Validation of differential expression for RBP genes in GSE8545 COPD/S dataset. Comparison of FC values for COPD/S mRBP genes between GSE5058 (test dataset) and GSE8545 (validation dataset; See Methods) for the RBP cluster genes (listed in **Table 3**) identified by IPA as having significant impact on canonical pathways.

with defined eosinophilic T2 phenotypes and neutrophilic or pauci-granulocytic non-T2 phenotypes (117). Moreover, evaluation of datasets derived from patients with milder asthma could add relevant information, for example to confirm a potential role of RBP modulation by glucocorticoid therapy, so far identified in human airway epithelium *in vitro* (12).

There are several limitations also to the results obtained for the COPD database, the main one being the small number of subjects included. In support of our findings, however, this patient and control cohort did have statistical power to support the findings of the original study. We were able to validate our main finding of global downregulation of mRBPs in COPD/S in an independent small airway epithelial cell transcriptomic study (21), in particular for coexpressed mRBP genes whose changes were deemed by IPA analys to have a significant impact on several canonical pathways. It is nevertheless essential to evaluate other independent databases with larger number of COPD subjects and controls, possibly with detailed clinical phenotyping including alpha-1-antitrypsin deficiency status, length of smoking history or time from smoking cessation as well as history of exacerbation. However, a rate-limiting factor for this validation lies in the fact that few studies have focused on transcriptomic of small airway epithelium in large number of patients. While correlation network analysis is being conducted on the transcriptome of larger COPD case/control cohorts for which lung tissue samples are available (118), other systems-biology approaches using single-cell sequencing of small airway epithelial cells are concurrently uncovering relevant biological features using brushing samples isolated in a number of COPD and control subjects equal to, or smaller than that of the study we evaluated (119, 120).

Moreover, we searched epithelial GEO databases for a list of RBPs selected on the basis of canonical RBDs (20). It remains to be probed the profile of other RBPs that do not contain conventional RBDs (121), which have been increasingly identified in human RNA interactome studies. These RBPs also have RNA binding activity but hold several other functions, such enzymatic activity in metabolic pathways or in RNA modification; their role in human epithelial biology is largely unknown.

Overall, the COPD-related mRBP profile found in our study suggests post-transcriptional control of epithelial gene expression as substantial, yet understudied process possibly contributing to key pathogenic mechanisms in COPD. In-depth characterization of proteins dynamically interacting with mRNAs is necessary to understand how PTGR participates to the disease process – and

whether it can be targeted therapeutically. Therefore, creating a map of RBP expression is a necessary first step to then analyze epithelial mRNA-bound proteome and potential changes in disease. Focused functional analysis and validating proteomic experiments will be needed to validate the coexpression of mRBPs and to address whether expression of mRBP targets, when known, in the COPD epithelial transcriptome database would show alterations consistent with – and dependent from - the documented changes of mRBPs expression.

DATA AVAILABILITY STATEMENT

The datasets presented in this study can be found in online repositories. The names of the repository/repositories and accession number(s) can be found in the article/ **Supplementary Material**.

AUTHOR CONTRIBUTIONS

LR implemented all analyses, generated figures, and assisted in manuscript preparation. GG and DM bioinformatic and statistical analysis. JD, IS, and AN data extraction from GEO databases and analysis of specific datasets. MP generation of Tables and referencing. AV, GC, and VC selection of databases, data mining, and manuscript editing. CS study design and manuscript preparation. All authors contributed to the article and approved the submitted version.

FUNDING

Fondazione con il Sud (Grant: Brains2South 2015 PDR-0224 to JD), Regione Campania, POR FESR 2014/20 RarePlatNet Project (Az. 1.2, CUP B63D18000380007) (to VC), POR Campania FESR 2007–2013–RETE DELLE BIOTECNOLOGIE IN CAMPANIA – Project Terapie Innovative di Malattie Infiammatorie croniche, metaboliche, Neoplastiche e Geriatriche – TIMING (University of Salerno, CS); FARB 2018/19 (University of Salerno, VC, and CS).

ACKNOWLEDGMENTS

The authors wish to thank Prof. Ian M. Adcock for critical discussions on data.

SUPPLEMENTARY MATERIAL

The Supplementary Material for this article can be found online at: https://www.frontiersin.org/articles/10.3389/fimmu.2020.579889/full#supplementary-material

REFERENCES

1. Keene JD. RNA regulons: coordination of post-transcriptional events. *Nat Rev Genet.* (2007) 8:533–43. doi: 10.1038/nrg2111
2. Gehring NH, Wahle E, Fischer U. Deciphering the mRNP code: RNA-bound determinants of post-transcriptional gene regulation. *Trends Biochem Sci.* (2017) 42:369–82. doi: 10.1016/j.tibs.2017.02.004
3. Hitti E, Bakheet T, Al-Souhibani N, Moghrabi W, Al-Yahya S, Al-Ghamdi M, et al. Systematic analysis of AU-rich element expression in cancer reveals common functional clusters regulated by key RNA-binding proteins. *Cancer Res.* (2016) 76:4068–80. doi: 10.1158/0008-5472.CAN-15-3110
4. Pereira B, Billaud M, Almeida R. RNA-binding proteins in cancer: old players and new actors. *Trends Cancer.* (2017) 3:506–28. doi: 10.1016/j.trecan.2017.05.003
5. Wang Z, Bhattacharya A, Ivanov DN. Identification of small-molecule inhibitors of the HuR/RNA interaction using a fluorescence polarization screening assay followed by NMR validation. *PLoS ONE.* (2015) 10:e0138780. doi: 10.1371/journal.pone.0138780
6. Hong S. RNA binding protein as an emerging therapeutic target for cancer prevention and treatment. *J Cancer Prev.* (2017) 22:203–10. doi: 10.15430/JCP.2017.22.4.203
7. Patial S, Blackshear PJ. Tristetraprolin as a therapeutic target in inflammatory disease. *Trends Pharmacol Sci.* (2016) 37:811–21. doi: 10.1016/j.tips.2016.07.002
8. Taylor GA, Carballo E, Lee DM, Lai WS, Thompson MJ, Patel DD, et al. A pathogenetic role for tnfα in the syndrome of cachexia, arthritis, and autoimmunity resulting from tristetraprolin (TTP) deficiency. *Immunity.* (1996) 4:445–54. doi: 10.1016/S1074-7613(00)80411-2
9. Lu J-Y, Sadri N, Schneider RJ. Endotoxic shock in AUF1 knockout mice mediated by failure to degrade proinflammatory cytokine mRNAs. *Genes Dev.* (2006) 20:3174–84. doi: 10.1101/gad.1467606
10. Durham AL, Adcock IM. The relationship between COPD and lung cancer. *Lung Cancer.* (2015) 90:121–7. doi: 10.1016/j.lungcan.2015.08.017
11. Khabar KSA. Post-transcriptional control during chronic inflammation and cancer: a focus on AU-rich elements. *Cell Mol Life Sci.* (2010) 67:2937–55. doi: 10.1007/s00018-010-0383-x
12. Ishmael FT, Fang X, Galdiero MR, Atasoy U, Rigby WFC, Gorospe M, et al. Role of the RNA-binding protein tristetraprolin in glucocorticoid-mediated gene regulation. *J Immunol.* (2008) 180:8342. doi: 10.4049/jimmunol.180.12.8342
13. Ishmael FT, Fang X, Houser KR, Pearce K, Abdelmohsen K, Zhan M, et al. The human glucocorticoid receptor as an RNA-binding protein: global analysis of glucocorticoid receptor-associated transcripts and identification of a target RNA motif. *J Immunol.* (2011) 186:1189–98. doi: 10.4049/jimmunol.1001794
14. Fan J, Ishmael FT, Fang X, Myers A, Cheadle C, Huang SK, et al. Chemokine transcripts as targets of the RNA-binding protein HuR in human airway epithelium. *J Immunol.* (2011) 186:2482–94. doi: 10.4049/jimmunol.0903634
15. Stellato C. Glucocorticoid actions on airway epithelial responses in immunity: functional outcomes and molecular targets. *J Allergy Clin Immunol.* (2007) 120:1247–63. doi: 10.1016/j.jaci.2007.10.041
16. Ricciardi L, Col JD, Casolari P, Memoli D, Conti V, Vatrella A, et al. Differential expression of RNA-binding proteins in bronchial epithelium of stable COPD patients. *Int J Chron Obstruct Pulmon Dis.* (2018) 13:3173–90. doi: 10.2147/COPD.S166284
17. Carolan BJ, Heguy A, Harvey BG, Leopold PL, Ferris B, Crystal RG. Up-regulation of expression of the ubiquitin carboxyl-terminal hydrolase L1 gene in human airway epithelium of cigarette smokers. *Cancer Res.* (2006) 66:10729–40. doi: 10.1158/0008-5472.CAN-06-2224
18. Kechavarzi B, Janga SC. Dissecting the expression landscape of RNA-binding proteins in human cancers. *Genome Biol.* (2014) 15:R14. doi: 10.1186/gb-2014-15-1-r14
19. Modena BD, Tedrow JR, Milosevic J, Bleecker ER, Meyers DA, Wu W, et al. Gene expression in relation to exhaled nitric oxide identifies novel asthma phenotypes with unique biomolecular pathways. *Am J Respir Crit Care Med.* (2014) 190:1363–72. doi: 10.1164/rccm.201406-1099OC
20. Gerstberger S, Hafner M, Tuschl T. A census of human RNA-binding proteins. *Nat Rev Genetics.* (2014) 15:829. doi: 10.1038/nrg3813

21. Ammous Z, Hackett NR, Butler MW, Raman T, Dolgalev I, O'Connor TP, et al. Variability in small airway epithelial gene expression among normal smokers. *Chest.* (2008) 133:1344–53. doi: 10.1378/chest.07-2245
22. Barrett T, Wilhite SE, Ledoux P, Evangelista C, Kim IF, Tomashevsky M, et al. NCBI GEO: archive for functional genomics data sets—update. *Nucleic Acids Res.* (2012) 41:D991–5. doi: 10.1093/nar/gks1193
23. Oliveros JC. *VENNY. An Interactive Tool for Comparing Lists With Venn Diagrams*. (2007–2015) Available online at: http://bioinfogp.cnb.csic.es/tools/venny/index.html
24. Howe E, Holton K, Nair S, Schlauch D, Sinha R, Quackenbush J. MeV: MultiExperiment viewer. In: Ochs MF, Casagrande JT, Davuluri RV, editors. *Biomedical Informatics for Cancer Research*. Boston, MA: Springer US. (2010). p. 267–77. doi: 10.1007/978-1-4419-5714-6_15
25. Saeed AI, Sharov V, White J, Li J, Liang W, Bhagabati N, et al. TM4: a free, open-source system for microarray data management and analysis. *BioTechniques.* (2003) 34:374–8. doi: 10.2144/03342mt01
26. Zambelli F, Pesole G, Pavesi G. PscanChIP: finding over-represented transcription factor-binding site motifs and their correlations in sequences from ChIP-Seq experiments. *Nucleic Acids Res.* (2013) 41:W535–43. doi: 10.1093/nar/gkt448
27. Walter W, Sánchez-Cabo F, Ricote M. GOplot: an R package for visually combining expression data with functional analysis. *Bioinformatics.* (2015) 31:2912–4. doi: 10.1093/bioinformatics/btv300
28. Yamaguchi A, Takanashi K. FUS interacts with nuclear matrix-associated protein SAFB1 as well as Matrin3 to regulate splicing and ligand-mediated transcription. *Sci Rep.* (2016) 6:35195. doi: 10.1038/srep35195
29. Baechtold H, Kuroda M, Sok J, Ron D, Lopez BS, Akhmedov AT. Human 75-kDa DNA-pairing protein is identical to the pro-oncoprotein TLS/FUS and is able to promote D-loop formation. *J Biol Chem.* (1999) 274:34337–42. doi: 10.1074/jbc.274.48.34337
30. Crucs S, Chatterjee S, Gavis ER. Overlapping but distinct RNA elements control repression and activation of nanos translation. *Mol Cell.* (2000) 5:457–67. doi: 10.1016/S1097-2765(00)80440-2
31. Lande-Diner L, Boyault C, Kim JY, Weitz CJ. A positive feedback loop links circadian clock factor CLOCK-BMAL1 to the basic transcriptional machinery. *Proc Natl Acad Sci USA.* (2013) 110:16021. doi: 10.1073/pnas.1305980110
32. Mukhopadhyay R, Jia J, Arif A, Ray PS, Fox PL. The GAIT system: a gatekeeper of inflammatory gene expression. *Trends Biochem Sci.* (2009) 34:324–31. doi: 10.1016/j.tibs.2009.03.004
33. Hönig A, Auboeuf D, Parker MM, Malley BW, Berget SM. Regulation of alternative splicing by the ATP-dependent DEAD-Box RNA helicase p72. *Mol Cell Biol.* (2002) 22:5698. doi: 10.1128/MCB.22.16.5698-5707.2002
34. Dardenne E, Pierredon S, Driouch K, Gratadou L, Lacroix-Triki M, Espinoza MP, et al. Splicing switch of an epigenetic regulator by RNA helicases promotes tumor-cell invasiveness. *Nat Struct Mol Biol.* (2012) 19:1139–46. doi: 10.1038/nsmb.2390
35. Dardenne E, Polay Espinoza M, Fattet L, Germann S, Lambert M-P, Neil H, et al. RNA helicases DDX5 and DDX17 dynamically orchestrate transcription, miRNA, and splicing programs in cell differentiation. *Cell Rep.* (2014) 7:1900–13. doi: 10.1016/j.celrep.2014.05.010
36. Germann S, Gratadou L, Zonta E, Dardenne E, Gaudineau B, Fougère M, et al. Dual role of the ddx5/ddx17 RNA helicases in the control of the pro-migratory NFAT5 transcription factor. *Oncogene.* (2012) 31:4536–49. doi: 10.1038/onc.2011.618
37. Samaan S, Tranchevent L-C, Dardenne E, Polay Espinoza M, Zonta E, Germann S, et al. The Ddx5 and Ddx17 RNA helicases are cornerstones in the complex regulatory array of steroid hormone-signaling pathways. *Nucleic Acids Res.* (2013) 42:2197–207. doi: 10.1093/nar/gkt1216
38. Shin S, Janknecht R. Concerted activation of the Mdm2 promoter by p72 RNA helicase and the coactivators p300 and P/CAF. *J Cell Biochem.* (2007) 101:1252–65. doi: 10.1002/jcb.21250
39. Mooney SM, Grande JP, Salisbury JL, Janknecht R. Sumoylation of p68 and p72 RNA helicases affects protein stability and transactivation potential. *Biochemistry.* (2010) 49:1–10. doi: 10.1021/bi901263m
40. Mooney SM, Goel A, D'Assoro AB, Salisbury JL, Janknecht R. Pleiotropic effects of p300-mediated acetylation on p68 and p72 RNA helicase. *J Biol Chem.* (2010) 285:30443–52. doi: 10.1074/jbc.M110.143792
41. Dutertre M, Gratadou L, Dardenne E, Germann S, Samaan S, Lidereau R, et al. Estrogen regulation and physiopathologic significance of alternative promoters in breast cancer. *Cancer Res.* (2010) 70:3760. doi: 10.1158/0008-5472.CAN-09-3988
42. Chen G, Guo X, Lv F, Xu Y, Gao G. p72 DEAD box RNA helicase is required for optimal function of the zinc-finger antiviral protein. *Proc Natl Acad Sci USA.* (2008) 105:4352. doi: 10.1073/pnas.0712276105
43. Sampath P, Mazumder B, Seshadri V, Fox PL. Transcript-selective translational silencing by gamma interferon is directed by a novel structural element in the ceruloplasmin mRNA 3′ untranslated region. *Mol Cell Biol.* (2003) 23:1509–19. doi: 10.1128/MCB.23.5.1509-1519.2003
44. Mazumder B, Seshadri V, Imataka H, Sonenberg N, Fox PL. Translational silencing of ceruloplasmin requires the essential elements of mRNA circularization: poly(A) tail, poly(A)-binding protein, and eukaryotic translation initiation factor 4G. *Mol Cell Biol.* (2001) 21:6440–9. doi: 10.1128/MCB.21.19.6440-6449.2001
45. Iwasaki T, Chin WW, Ko L. Identification and characterization of RRM-containing Coactivator Activator (CoAA) as TRBP-interacting protein, and its splice variant as a Coactivator Modulator (CoAM). *J Biol Chem.* (2001) 276:33375–83. doi: 10.1074/jbc.M101517200
46. Morchikh M, Cribier A, Raffel R, Amraoui S, Cau J, Severac D, et al. HEXIM1 and NEAT1 long non-coding RNA form a multi-subunit complex that regulates DNA-mediated innate immune response. *Mol Cell.* (2017) 67:387–99.e5. doi: 10.1016/j.molcel.2017.06.020
47. Kapasi P, Chaudhuri S, Vyas K, Baus D, Komar AA, Fox PL, et al. L13a blocks 48S assembly: role of a general initiation factor in mRNA-specific translational control. *Mol Cell.* (2007) 25:113–26. doi: 10.1016/j.molcel.2006.11.028
48. Tran H, Schilling M, Wirbelauer C, Hess D, Nagamine Y. Facilitation of mRNA deadenylation and decay by the exosome-bound, DExH protein RHAU. *Mol Cell.* (2004) 13:101–11. doi: 10.1016/S1097-2765(03)00481-7
49. Harashima A, Guettouche T, Barber GN. Phosphorylation of the NFAR proteins by the dsRNA-dependent protein kinase PKR constitutes a novel mechanism of translational regulation and cellular defense. *Genes Dev.* (2010) 24:2640–53. doi: 10.1101/gad.1965010
50. Li X, Liu C-X, Xue W, Zhang Y, Jiang S, Yin Q-F, et al. Coordinated circRNA biogenesis and function with NF90/NF110 in viral infection. *Mol Cell.* (2017) 67:214–27.e7. doi: 10.1016/j.molcel.2017.05.023
51. Arif A, Jia J, Mukhopadhyay R, Willard B, Kinter M, Fox PL. Two-site phosphorylation of EPRS coordinates multimodal regulation of noncanonical translational control activity. *Mol Cell.* (2009) 35:164–80. doi: 10.1016/j.molcel.2009.05.028
52. Rahman MA, Masuda A, Ohe K, Ito M, Hutchinson DO, Mayeda A, et al. HnRNP L and hnRNP LL antagonistically modulate PTB-mediated splicing suppression of CHRNA1 pre-mRNA. *Sci Rep.* (2013) 3:2931. doi: 10.1038/srep02931
53. Damianov A, Ying Y, Lin C-H, Lee J-A, Tran D, Vashisht Ajay A, et al. Rbfox proteins regulate splicing as part of a large multiprotein complex LASR. *Cell.* (2016) 165:606–19. doi: 10.1016/j.cell.2016.03.040
54. Giri B, Smaldino PJ, Thys RG, Creacy SD, Routh ED, Hantgan RR, et al. G4 resolvase 1 tightly binds and unwinds unimolecular G4-DNA. *Nucleic Acids Res.* (2011) 39:7161–78. doi: 10.1093/nar/gkr234
55. Vaughn JP, Creacy SD, Routh ED, Joyner-Butt C, Jenkins GS, Pauli S, et al. The DEXH protein product of the DHX36 gene is the major source of tetramolecular quadruplex G4-DNA resolving activity in HeLa cell lysates. *J Biol Chem.* (2005) 280:38117–20. doi: 10.1074/jbc.C500348200
56. Chalupníková K, Lattmann S, Selak N, Iwamoto F, Fujiki Y, Nagamine Y. Recruitment of the RNA helicase RHAU to stress granules via a unique RNA-binding domain. *J Biol Chem.* (2008) 283:35186–98. doi: 10.1074/jbc.M804857200
57. Lattmann S, Giri B, Vaughn JP, Akman SA, Nagamine Y. Role of the amino terminal RHAU-specific motif in the recognition and resolution of guanine quadruplex-RNA by the DEAH-box RNA helicase RHAU. *Nucleic Acids Res.* (2010) 38:6219–33. doi: 10.1093/nar/gkq372

58. Meier M, Patel TR, Booy EP, Marushchak O, Okun N, Deo S, et al. Binding of G-quadruplexes to the N-terminal recognition domain of the RNA helicase associated with AU-rich element (RHAU). *J Biol Chem.* (2013) 288:35014–27. doi: 10.1074/jbc.M113.512970
59. Lattmann S, Stadler MB, Vaughn JP, Akman SA, Nagamine Y. The DEAH-box RNA helicase RHAU binds an intramolecular RNA G-quadruplex in TERC and associates with telomerase holoenzyme. *Nucleic Acids Res.* (2011) 39:9390–404. doi: 10.1093/nar/gkr630
60. Booy EP, Meier M, Okun N, Novakowski SK, Xiong S, Stetefeld J, et al. The RNA helicase RHAU (DHX36) unwinds a G4-quadruplex in human telomerase RNA and promotes the formation of the P1 helix template boundary. *Nucleic Acids Res.* (2012) 40:4110–24. doi: 10.1093/nar/gkr1306
61. Booy EP, McRae EKS, McKenna SA. Biochemical characterization of G4 quadruplex telomerase RNA unwinding by the RNA helicase RHAU. In: Boudvillain M, editor. *RNA Remodeling Proteins: Methods and Protocols*. New York, NY: Springer. (2015). p. 125–35. doi: 10.1007/978-1-4939-2214-7_9
62. Sexton AN, Collins K. The 5′ guanosine tracts of human telomerase RNA are recognized by the G-quadruplex binding domain of the RNA helicase DHX36 and function to increase RNA accumulation. *Mol Cell Biol.* (2011) 31:736. doi: 10.1128/MCB.01033-10
63. Booy EP, Howard R, Marushchak O, Ariyo EO, Meier M, Novakowski SK, et al. The RNA helicase RHAU (DHX36) suppresses expression of the transcription factor PITX1. *Nucleic Acids Res.* (2013) 42:3346–61. doi: 10.1093/nar/gkt1340
64. Nie J, Jiang M, Zhang X, Tang H, Jin H, Huang X, et al. Post-transcriptional regulation of Nkx2-5 by RHAU in heart development. *Cell Rep.* (2015) 13:723–32. doi: 10.1016/j.celrep.2015.09.043
65. Huang W, Smaldino PJ, Zhang Q, Miller LD, Cao P, Stadelman K, et al. Yin Yang 1 contains G-quadruplex structures in its promoter and 5′-UTR and its expression is modulated by G4 resolvase 1. *Nucleic Acids Res.* (2011) 40:1033–49. doi: 10.1093/nar/gkr849
66. Newman M, Sfaxi R, Saha A, Monchaud D, Teulade-Fichou M-P, Vagner S. The G-quadruplex-specific RNA helicase DHX36 regulates p53 pre-mRNA 3′-end processing following UV-induced DNA damage. *J Mol Biol.* (2017) 429:3121–31. doi: 10.1016/j.jmb.2016.11.033
67. He Y, Smith R. Nuclear functions of heterogeneous nuclear ribonucleoproteins A/B. *Cell Mol Life Sci.* (2009) 66:1239–56. doi: 10.1007/s00018-008-8532-1
68. Munro TP, Magee RJ, Kidd GJ, Carson JH, Barbarese E, Smith LM, et al. Mutational analysis of a heterogeneous nuclear ribonucleoprotein A2 response element for rna trafficking. *J Biol Chem.* (1999) 274:34389–95. doi: 10.1074/jbc.274.48.34389
69. Coelho MB, Attig J, Bellora N, König J, Hallegger M, Kayikci M, et al. Nuclear matrix protein Matrin3 regulates alternative splicing and forms overlapping regulatory networks with PTB. *EMBO J.* (2015) 34:653–68. doi: 10.15252/embj.201489852
70. Rishi AK, Zhang L, Boyanapalli M, Wali A, Mohammad RM, Yu Y, et al. Identification and characterization of a cell cycle and apoptosis regulatory protein-1 as a novel mediator of apoptosis signaling by retinoid CD437. *J Biol Chem.* (2003) 278:33422–35. doi: 10.1074/jbc.M303173200
71. Seo W-Y, Jeong BC, Yu EJ, Kim HJ, Kim S-H, Lim JE, et al. CCAR1 promotes chromatin loading of androgen receptor (AR) transcription complex by stabilizing the association between AR and GATA2. *Nucleic Acids Res.* (2013) 41:8526–36. doi: 10.1093/nar/gkt644
72. Nakamura H, Kawagishi H, Watanabe A, Sugimoto K, Maruyama M, Sugimoto M. Cooperative role of the RNA-binding proteins Hzf and HuR in p53 activation. *Mol Cell Biol.* (2011) 31:1997–2009. doi: 10.1128/MCB.01424-10
73. Cho SJ, Zhang J, Chen X. RNPC1 modulates the RNA-binding activity of, and cooperates with, HuR to regulate p21 mRNA stability. *Nucleic Acids Res.* (2010) 38:2256–67. doi: 10.1093/nar/gkp1229
74. Sun Y, Ding L, Zhang H, Han J, Yang X, Yan J, et al. Potentiation of smad-mediated transcriptional activation by the RNA-binding protein RBPMS. *Nucleic Acids Res.* (2006) 34:6314–26. doi: 10.1093/nar/gkl914
75. Teplova M, Farazi TA, Tuschl T, Patel DJ. Structural basis underlying CAC RNA recognition by the RRM domain of dimeric RNA-binding protein RBPMS. *Q Rev Biophys.* (2016) 49:e1. doi: 10.1017/S0033583515000207
76. Wang Isabel X, So E, Devlin James L, Zhao Y, Wu M, Cheung Vivian G. ADAR regulates RNA editing, transcript stability, and gene expression. *Cell Rep.* (2013) 5:849–60. doi: 10.1016/j.celrep.2013.10.002
77. Antonicka H, Shoubridge Eric A. Mitochondrial RNA granules are centers for posttranscriptional RNA processing and ribosome biogenesis. *Cell Rep.* (2015) 10:920–32. doi: 10.1016/j.celrep.2015.01.030
78. Lessel D, Schob C, Küry S, Reijnders MRF, Harel T, Eldomery MK, et al. *De novo* missense mutations in DHX30 impair global translation and cause a neurodevelopmental disorder. *Am J Hum Genet.* (2017) 101:716–24. doi: 10.1016/j.ajhg.2017.09.014
79. Anantharaman A, Gholamalamdari O, Khan A, Yoon J-H, Jantsch MF, Hartner JC, et al. RNA-editing enzymes ADAR1 and ADAR2 coordinately regulate the editing and expression of Ctn RNA. *FEBS Lett.* (2017) 591:2890–904. doi: 10.1002/1873-3468.12795
80. Stelzer G, Rosen N, Plaschkes I, Zimmerman S, Twik M, Fishilevich S, et al. The GeneCards suite: from gene data mining to disease genome sequence analyses. *Curr Protoc Bioinform.* (2016) 54:1.30.1–1.3. doi: 10.1002/cpbi.5
81. Anderson P. Post-transcriptional regulons coordinate the initiation and resolution of inflammation. *Nat Rev Immunol.* (2010) 10:24–35. doi: 10.1038/nri2685
82. Kotb A, Yuki K, Hyeon Ho K, Myriam G. Posttranscriptional gene regulation by RNA-binding proteins during oxidative stress: implications for cellular senescence. *Biol Chem.* (2008) 389:243–55. doi: 10.1515/BC.2008.022
83. Skibinski DAG, Jones LA, Zhu YO, Xue LW, Au B, Lee B, et al. Induction of human T-cell and cytokine responses following vaccination with a novel influenza vaccine. *Sci Rep.* (2018) 8:18007. doi: 10.1038/s41598-018-36703-7
84. Li K, Mo C, Gong D, Chen Y, Huang Z, Li Y, et al. DDX17 nucleocytoplasmic shuttling promotes acquired gefitinib resistance in non-small cell lung cancer cells via activation of β-catenin. *Cancer Lett.* (2017) 400:194–202. doi: 10.1016/j.canlet.2017.02.029
85. Sauer M, Juranek SA, Marks J, De Magis A, Kazemier HG, Hilbig D, et al. DHX36 prevents the accumulation of translationally inactive mRNAs with G4-structures in untranslated regions. *Nat Commun.* (2019) 10:2421. doi: 10.1038/s41467-019-10432-5
86. Migneault F, Gagnon F, Pascariu M, Laperle J, Roy A, Dagenais A, et al. Post-transcriptional modulation of aENaC mRNA in alveolar epithelial cells: involvement of its 3′ untranslated region. *Cell Physiol Biochem.* (2019) 52:984–1002. doi: 10.33594/000000068
87. Pon JR, Marra MA. MEF2 transcription factors: developmental regulators and emerging cancer genes. *Oncotarget.* (2016) 7:2297–312. doi: 10.18632/oncotarget.6223
88. Nyati KK, Zaman MM-U, Sharma P, Kishimoto T. Arid5a, an RNA-binding protein in immune regulation: RNA stability, inflammation, and autoimmunity. *Trends Immunol.* (2020) 41:255–68. doi: 10.1016/j.it.2020.01.004
89. Lin C, Song W, Bi X, Zhao J, Huang Z, Li Z, et al. Recent advances in the ARID family: focusing on roles in human cancer. *Onco Targets Ther.* (2014) 7:315–24. doi: 10.2147/OTT.S57023
90. Plowright L, Harrington KJ, Pandha HS, Morgan R. HOX transcription factors are potential therapeutic targets in non-small-cell lung cancer (targeting HOX genes in lung cancer). *Br J Cancer.* (2009) 100:470–5. doi: 10.1038/sj.bjc.6604857
91. Ito K, Barnes PJ. COPD as a disease of accelerated lung aging. *Chest.* (2009) 135:173–80. doi: 10.1378/chest.08-1419
92. Barnes PJ. Senescence in COPD and its comorbidities. *Ann Rev Physiol.* (2017) 79:517–39. doi: 10.1146/annurev-physiol-022516-034314
93. Houssaini A, Breau M, Kebe K, Abid S, Marcos E, Lipskaia L, et al. mTOR pathway activation drives lung cell senescence and emphysema. *JCI Insight.* (2018) 3:e93203. doi: 10.1172/jci.insight.93203
94. Mercado N, Ito K, Barnes PJ. Accelerated ageing of the lung in COPD: new concepts. *Thorax.* (2015) 70:482. doi: 10.1136/thoraxjnl-2014-206084
95. Shishkin SS, Kovalev LI, Pashintseva NV, Kovaleva MA, Lisitskaya K. Heterogeneous nuclear ribonucleoproteins involved in the functioning of telomeres in malignant cells. *Int J Mol Sci.* (2019) 20:745. doi: 10.3390/ijms20030745
96. Zhang Q-S, Manche L, Xu R-M, Krainer AR. hnRNP A1 associates with telomere ends and stimulates telomerase activity. *RNA.* (2006) 12:1116–28. doi: 10.1261/rna.58806

97. Jin M, Lee EC, Ra SW, Fishbane N, Tam S, Criner GJ, et al. Relationship of absolute telomere length with quality of life, exacerbations, and mortality in COPD. *Chest.* (2018) 154:266–73. doi: 10.1016/j.chest.2018.05.022
98. Pont Adam R, Sadri N, Hsiao Susan J, Smith S, Schneider Robert J. mRNA decay factor AUF1 maintains normal aging, telomere maintenance, and suppression of senescence by activation of telomerase transcription. *Mol Cell.* (2012) 47:5–15. doi: 10.1016/j.molcel.2012.04.019
99. Sharma DK, Bressler K, Patel H, Balasingam N, Thakor N. Role of eukaryotic initiation factors during cellular stress and cancer progression. *J Nucleic Acids.* (2016) 2016:8235121. doi: 10.1155/2016/8235121
100. Barnes PJ, Baker J, Donnelly LE. Cellular senescence as a mechanism and target in chronic lung diseases. *Am J Respir Crit Care Med.* (2019) 200:556–64. doi: 10.1164/rccm.201810-1975TR
101. Fingar DC, Richardson CJ, Tee AR, Cheatham L, Tsou C, Blenis J. mTOR controls cell cycle progression through its cell growth effectors S6K1 and 4E-BP1/eukaryotic translation initiation factor 4E. *Mol Cell Biol.* (2004) 24:200. doi: 10.1128/MCB.24.1.200-216.2004
102. Averous J, Fonseca BD, Proud CG. Regulation of cyclin D1 expression by mTORC1 signaling requires eukaryotic initiation factor 4E-binding protein 1. *Oncogene.* (2008) 27:1106–13. doi: 10.1038/sj.onc.1210715
103. Salama R, Sadaie M, Hoare M, Narita M. Cellular senescence and its effector programs. *Genes Dev.* (2014) 28:99–114. doi: 10.1101/gad.235184.113
104. Moore AE, Chenette DM, Larkin LC, Schneider RJ. Physiological networks and disease functions of RNA-binding protein AUF1. *Wiley Interdiscip Rev RNA.* (2014) 5:549–64. doi: 10.1002/wrna.1230
105. Hassibi S, Baker J, Donnelly L, Barnes P. The RNA binding protein HuR regulates the senescence-associated secretory phenotype under conditions of oxidative stress. *Eur Respir J.* (2019) 54(Suppl. 63):PA2374. doi: 10.1183/13993003.congress-2019.PA2374
106. Usmani OS, Lavorini F, Marshall J, Dunlop WCN, Heron L, Farrington E, et al. Critical inhaler errors in asthma and COPD: a systematic review of impact on health outcomes. *Respir Res.* (2018) 19:10. doi: 10.1186/s12931-017-0710-y
107. Piecyk M, Wax S, Beck ARP, Kedersha N, Gupta M, Maritim B, et al. TIA-1 is a translational silencer that selectively regulates the expression of TNF-α. *EMBO J.* (2000) 19:4154–63. doi: 10.1093/emboj/19.15.4154
108. Lei EP, Silver PA. Protein and RNA export from the nucleus. *Dev Cell.* (2002) 2:261–72. doi: 10.1016/S1534-5807(02)00134-X
109. Cavazza T, Vernos I. The RanGTP pathway: from nucleo-cytoplasmic transport to spindle assembly and beyond. *Front Cell Dev Biol.* (2016) 3:82. doi: 10.3389/fcell.2015.00082
110. Rebane A, Aab A, Steitz JA. Transportins 1 and 2 are redundant nuclear import factors for hnRNP A1 and HuR. *RNA.* (2004) 10:590–9. doi: 10.1261/rna.5224304
111. Zhang W, Vreeland AC, Noy N. RNA-binding protein HuR regulates nuclear import of protein. *J Cell Sci.* (2016) 129:4025. doi: 10.1242/jcs.192096
112. Ning J, Liu W, Zhang J, Lang Y, Xu S. Ran GTPase induces EMT and enhances invasion in non-small cell lung cancer cells through activation of PI3K-AKT pathway. *Oncol Res.* (2013) 21:67–72. doi: 10.3727/096504013X13747716581417
113. Boudhraa Z, Carmona E, Provencher D, Mes-Masson A-M. Ran GTPase: a key player in tumor progression and metastasis. *Front Cell Dev Biol.* (2020) 8:345. doi: 10.3389/fcell.2020.00345
114. Barnes PJ. Immunology of asthma and chronic obstructive pulmonary disease. *Nat Rev Immunol.* (2008) 8:183–92. doi: 10.1038/nri2254
115. Martinez-Nunez RT, Rupani H, Platé M, Niranjan M, Chambers RC, Howarth PH, et al. Genome-wide posttranscriptional dysregulation by MicroRNAs in human asthma as revealed by frac-seq. *J Immunol.* (2018) 201:251. doi: 10.4049/jimmunol.1701798
116. Ravi A, Chowdhury S, Dijkhuis A, Bonta PI, Sterk PJ, Lutter R. Neutrophilic inflammation in asthma and defective epithelial translational control. *Eur Respir J.* (2019) 54:1900547. doi: 10.1183/13993003.00547-2019
117. Kuo C-HS, Pavlidis S, Loza M, Baribaud F, Rowe A, Pandis I, et al. A transcriptome-driven analysis of epithelial brushings and bronchial biopsies to define asthma phenotypes in U-BIOPRED. *Am J Respir Crit Care Med.* (2016) 195:443–55. doi: 10.1164/rccm.201512-2452OC
118. Paci P, Fiscon G, Conte F, Licursi V, Morrow J, Hersh C, et al. Integrated transcriptomic correlation network analysis identifies COPD molecular determinants. *Sci Rep.* (2020) 10:3361. 10:3361. doi: 10.1038/s41598-020-60228-7
119. Duclos GE, Teixeira VH, Autissier P, Gesthalter YB, Reinders-Luinge MA, Terrano R, et al. Characterizing smoking-induced transcriptional heterogeneity in the human bronchial epithelium at single-cell resolution. *Sci Adv.* (2019) 5:eaaw3413. doi: 10.1126/sciadv.aaw3413
120. Zuo W-l, Rostami MR, Shenoy SA, LeBlanc MG, Salit J, Strulovici-Barel Y, et al. Cell-specific expression of lung disease risk-related genes in the human small airway epithelium. *Respir Res.* (2020) 21:200. 21:200. doi: 10.1186/s12931-020-01442-9
121. Hentze MW, Castello A, Schwarzl T, Preiss T. A brave new world of RNA-binding proteins. *Nat Rev Mol Cell Biol.* (2018) 19:327–41. doi: 10.1038/nrm.2017.130

Conflict of Interest: The authors declare that the research was conducted in the absence of any commercial or financial relationships that could be construed as a potential conflict of interest.

Copyright © 2020 Ricciardi, Giurato, Memoli, Pietrafesa, Dal Col, Salvato, Nigro, Vatrella, Caramori, Casolaro and Stellato. This is an open-access article distributed under the terms of the Creative Commons Attribution License (CC BY). The use, distribution or reproduction in other forums is permitted, provided the original author(s) and the copyright owner(s) are credited and that the original publication in this journal is cited, in accordance with accepted academic practice. No use, distribution or reproduction is permitted which does not comply with these terms.

frontiers in Immunology

REVIEW
published: 30 November 2020
doi: 10.3389/fimmu.2020.603312

Molecular Targets for Biological Therapies of Severe Asthma

*Corrado Pelaia[1], Claudia Crimi[2], Alessandro Vatrella[3], Caterina Tinello[4], Rosa Terracciano[5] and Girolamo Pelaia[6]**

[1] Respiratory Medicine Unit, University "Magna Græcia" of Catanzaro, Catanzaro, Italy, [2] Department of Clinical and Experimental Medicine, University of Catania, Catania, Italy, [3] Department of Medicine, Surgery and Dentistry, University of Salerno, Salerno, Italy, [4] Pediatrics Unit, Provincial Outpatient Center of Catanzaro, Catanzaro, Italy, [5] Department of Experimental and Clinical Medicine, University "Magna Græcia" of Catanzaro, Catanzaro, Italy, [6] Department of Health Sciences, University "Magna Græcia" of Catanzaro, Catanzaro, Italy

Asthma is a heterogeneous respiratory disease characterized by usually reversible bronchial obstruction, which is clinically expressed by different phenotypes driven by complex pathobiological mechanisms (endotypes). Within this context, during the last years several molecular effectors and signalling pathways have emerged as suitable targets for biological therapies of severe asthma, refractory to standard treatments. Indeed, various therapeutic antibodies currently allow to intercept at different levels the chain of pathogenic events leading to type 2 (T2) airway inflammation. In addition to pro-allergic immunoglobulin E (IgE), that chronologically represents the first molecule against which an anti-asthma monoclonal antibody (omalizumab) was developed, today other targets are successfully exploited by biological treatments of severe asthma. In particular, pro-eosinophilic interleukin 5 (IL-5) can be targeted by mepolizumab or reslizumab, whereas benralizumab is a selective blocker of IL-5 receptor. Moreover, dupilumab behaves as a dual receptor antagonist of pleiotropic interleukins 4 (IL-4) and 13 (IL-13). Besides these drugs that are already available in medical practice, other biologics are under clinical development such as those targeting innate cytokines, also including the alarmin thymic stromal lymphopoietin (TSLP), which plays a key role in the pathogenesis of type 2 asthma. Therefore, ongoing and future biological therapies are significantly changing the global scenario of severe asthma management. These new therapeutic options make it possible to implement phenotype/endotype-specific treatments, that are delineating personalized approaches precisely addressing the individual traits of asthma pathobiology. Such tailored strategies are thus allowing to successfully target the immune-inflammatory responses underlying uncontrolled T2-high asthma.

Keywords: T2-high asthma, IgE, IL-4, IL-5, IL-13, monoclonal antibodies

OPEN ACCESS

Edited by:
Robson Coutinho-Silva, Federal University of Rio de Janeiro, Brazil

Reviewed by:
Luigi Cari, University of Perugia, Italy
Rui Li, University of Pennsylvania, United States

***Correspondence:**
Girolamo Pelaia
pelaia@unicz.it

Specialty section:
This article was submitted to Inflammation, a section of the journal Frontiers in Immunology

Received: *06 September 2020*
Accepted: *03 November 2020*
Published: *30 November 2020*

Citation:
Pelaia C, Crimi C, Vatrella A, Tinello C, Terracciano R and Pelaia G (2020) Molecular Targets for Biological Therapies of Severe Asthma. Front. Immunol. 11:603312. doi: 10.3389/fimmu.2020.603312

INTRODUCTION

Asthma is a very diffuse chronic respiratory disease whose main pathologic features include airway inflammation and remodelling, which are responsible for variable airflow limitation and bronchial hyperresponsiveness (1–3). More than 300 million people currently suffer from asthma worldwide, and this number is probably destined to undergo further increases during the next years (4, 5).

In most subjects with asthma a good disease control can be achieved using standard inhaled treatments. However, about 5–10% of patients included in the global population of asthmatic individuals experience various subtypes of inadequately controlled and difficult-to-treat asthma (6). In this regard, severe asthma was jointly defined by both European Respiratory Society (ERS) and American Thoracic Society (ATS) as a condition controlled by high dosages of inhaled corticosteroids (ICS)/long-acting β_2-adrenergic agonists (LABA) combinations, which can also require the addition of other drugs (i.e. tiotropium, leukotriene modifiers, oral corticosteroids); even worse, severe asthma might remain uncontrolled despite such massive inhaled and systemic treatments (7). Hence, within the overall spectrum of subjects with asthma, severe asthmatic patients are characterized by the most urgent unmet medical needs and can be eligible to add-on biological therapies (8). The latter mainly consist of already licensed monoclonal antibodies targeting specific molecules involved in the pathobiology of type 2 (T2-high) eosinophilic, allergic and non-allergic asthma, including immunoglobulins E (IgE), interleukin-5 (IL-5) and its receptor, as well as interleukin-4 (IL-4) receptor (9–11). Other experimental biologics target upstream innate cytokines such as thymic stromal lymphopoietin (TSLP) (12, 13). Conversely, current pharmacotherapeutic pipelines are very scarce with regard to investigational drugs directed against molecular targets implicated in the pathogenesis of T2-low, mostly neutrophilic severe asthma. Therefore, a careful characterization of the biological mechanisms (endotypes) underlying the different phenotypes plays a key role in driving the clinical choice of the most appropriate add-on therapy for each individual patient with severe asthma (14, 15).

On the basis of the above considerations, the aim of this review article is to outline the cellular and molecular pathophysiology of severe asthma, in order to provide a logical premise for the subsequent discussion of the current and future biological strategies that can be used to treat the patients with uncontrolled disease.

PATHOBIOLOGY OF SEVERE ASTHMA

Asthma is a heterogeneous disease, originating from complex interactions between genetic and environmental factors, which consists of several different phenotypes sustained by cytokine-based biological mechanisms known as endotypes (16, 17). The inflammatory endotypes include eosinophilic, neutrophilic, mixed and paucigranulocitic cellular patterns (2, 18–22). In particular, T2-high eosinophilic inflammation is quite common in patients with either allergic or non-allergic asthma, and can frequently characterize severe and fatal disease (23–27).

T2-high eosinophilic allergic asthma, occurring especially in children and adolescents, develops as a consequence of an intricate cross-talk between innate and adaptive immune responses (28). In particular, allergic asthma is triggered by dust mites, tree pollen and animal dander, which within the airways are captured by dendritic cells that internalize and process these aeroallergens, and also transport them to thoracic lymph nodes. Here, dendritic cells expose on their surface the processed allergen peptides and, within the context of specific HLA class II molecules of the major histocompatibility complex (MHC class II), operate antigen presentation to the T-cell receptors of naïve $CD4^+$ T lymphocytes, thus inducing their polarization towards the T helper 2 (Th2) lineage (1). This event is driven by interleukin-4 (IL-4) produced by mast cells and basophils, and is also dependent on selective reciprocal recognition of specific co-stimulatory molecules located on the plasma membranes of dendritic cells (CD80/B7.1, CD86/B7.2, OX40 ligand, ICOS ligand) and T lymphocytes (CD28, OX40, ICOS), respectively (29, 30). As a result of such a complex process of differentiation and activation, mature Th2 cells secrete large quantities of IL-4, IL-13, and IL-5. IL-13 and especially IL-4 induce Ig class switching by stimulating B lymphocytes to synthesize allergen-specific immunoglobulins E (IgE), which bind to high-affinity (FcεRI) and low-affinity (CD23/FcεRII) receptors present on both immune/inflammatory and structural cells of the respiratory tract (31–34). These adaptive immune pathways are crucially integrated by innate immune mechanisms involving important functions of airway epithelial cells and innate lymphoid cells, as well as further contributions of dendritic cells (35, 36). Indeed, aeroallergens, respiratory viruses, cigarette smoking and airborne pollutants induce bronchial epithelial cells to produce the innate cytokines thymic stromal lymphopoietin (TSLP), interleukin-25 (IL-25) and interleukin-33 (IL-33), that in turn potentiate Th2-mediated adaptive immune responses and promote the release of IL-4, IL-13, and IL-5 from Th2 lymphocytes and group 2 innate lymphoid cells (ILC2) (37). Another relevant cellular source of IL-4 is represented by T follicular helper cells (Tfh), whose development in lung-draining lymph nodes depends on TSLP-induced activation of dendritic cells expressing OX40 ligand (38). Dendritic cells also secrete CCL17 and CCL22 chemokines, that selectively interact with CCR4 receptors expressed by mature Th2 lymphocytes, thus promoting their migration from thoracic lymph nodes to the airways (39).

In regard to the functions of Th2 cytokines, IL-4 drives IgE biosynthesis, IL-13 mainly contributes to mucus production, airway remodelling and bronchial hyperresponsiveness, and IL-5 is the key inducer of eosinophil differentiation, activation and survival (17, 40). In addition to Th2 lymphocytes, IL-5 is also produced by mast cells, natural killer T cells, eosinophils themselves and especially ILC2, the latter being the main cellular orchestrators of non-allergic eosinophilic asthma (40–42), frequently characterized by a late onset in adulthood. IL-5 is responsible for eosinophil maturation, and in asthmatic patients this eosinophilopoietic action occurs not only in the bone marrow, but also in bronchial mucosa (43–45). Indeed, IL-5 concentrations and the numbers of both mature eosinophils and eosinophil progenitors are increased in induced sputum from asthmatic subjects. High IL-5 levels can be also detected in serum, especially when obtained from patients with severe

asthma (46). Moreover, IL-5 exerts an inhibitory effect on eosinophil apoptosis, and the numbers of apoptotic eosinophils are negatively correlated with sputum IL-5 concentrations in stable asthma, as well as during disease exacerbations (47, 48). IL-5 also contributes to eosinophil recruitment within asthmatic airways, thereby cooperating with eosinophil chemoattractants such as eotaxins (49). Furthermore, in patients with T2-high asthma IL-5 stimulates the interaction of eosinophils with periostin, an extracellular matrix protein whose expression resulted to be up-regulated during eosinophil migration towards airways (50). Especially in severe asthma, IL-5-activated eosinophils also contribute to bronchial structural changes *via* the release of powerful pro-remodelling mediators such as transforming growth factor-β (TGF-β) (51, 52).

T2-low asthma is often characterized by airway neutrophilia, particularly in patients suffering from severe disease forms (53). In this regard, the Th17 subset of $CD4^+$ T lymphocytes seems to play a pivotal pathogenic role (54–56). Th17 cells produce IL-17A and IL-17F, whose expression was shown to be significantly up-regulated in bronchial biopsies from patients with severe asthma (57). Th17 cell development depends on the coordinate actions of IL-1β, IL-6, and TGF-β, which are essential for induction of differentiation of this cellular immunophenotype (58–60). In addition, IL-21 produced by Th17 cells themselves plays a key role as autocrine amplifier of Th17 response (60, 61). Mature Th17 lymphocytes also express the specific receptor of IL-23, a cytokine which is required to stabilize the Th17 phenotype and to maintain Th17 cells in a state of effective activation (60–62). Cigarette smoke and diesel exhaust particles can induce airway neutrophilia, which was shown to be associated with Th17-dependent severe asthma (63, 64). Infectious agents also seem to be able to trigger Th17-mediated severe asthma, and this effect may involve the assembly of the inflammasome, an intracellular multiprotein complex which activates caspase-1, a protease that converts pro-IL-1β in its active form, thus enabling it to induce Th17 cell differentiation (65, 66). Inflammasome activation was also shown to be implicated in obesity-associated bronchial hyperresponsiveness (67). In severe asthma, Th17 cell polarization and neutrophilic airway inflammation can also be promoted by neutrophil extracellular traps (NETs), consisting of anti-microbial complexes of extracellular DNA, histones and granular proteins extruded from neutrophils that become anuclear cells known as cytoplasts (68–70). In addition to Th17 lymphocytes, other cellular sources of IL-17 include invariant NK T cells, γδ T cells, cytotoxic T cells, and especially group 3 innate lymphoid cells (ILC3) (71, 72). High numbers of ILC3 were found in bronchoalveolar lavage fluid (BALF) from adults with severe asthma, as well as in blood of obese asthmatic children (72, 73). Once secreted from Th17 lymphocytes, ILC3 and other cell types, IL-17A and IL-17F induce bronchial epithelial cells and sub-epithelial airway fibroblasts to release potent neutrophil chemoattractants including IL-8 (CXCL8) and CXCL1/GRO-α (74–76]. IL-17-mediated neutrophilic asthma is often associated with a relevant insensitivity to the therapeutic actions of corticosteroids, which indeed exert an anti-apoptotic effect on neutrophils, thus prolonging their survival (77). In addition to Th17 lymphocytes, also IL-12-dependent Th1 cells can contribute to the pathobiology of severe neutrophilic asthma (59, 78). In fact, Th1 lymphocyte numbers and the levels of their cytokines such as interferon-γ (IFN-γ) and tumor necrosis factor-α (TNF-α) are enhanced in severe asthmatic patients (59, 79).

The mixed eosinophilic/neutrophilic inflammatory phenotype is often associated with severe asthma. In particular, circulating Th2/Th17 cell clones producing both IL-4 and IL-17A were found in asthmatic patients (80). Moreover, high numbers of dual-positive Th2/Th17 lymphocytes secreting large quantities of IL-4 and IL-17 were detected in BALF from patients with severe asthma (81). Indeed, these BALF lymphocytes were shown to concomitantly express two transcription factors such as GATA3 and RORγt (81), which are essential for differentiation of Th2 and Th17 cells, respectively. Such observations corroborated the results of previous studies performed in mice, which had demonstrated that Th2/Th17 lymphocytes were involved in the induction of severe forms of experimental asthma (82). Hence, additional studies are needed to further characterize the cellular phenotypes of dual Th2/Th17 lymphocyte subsets, and to better understand if IL-4 and IL-17 produced by these cells could eventually exert additive or synergistic effects, especially in the pathobiology of severe asthma (83).

In addition to eosinophilic, neutrophilic, and mixed granulocytic inflammatory profiles, also paucigranulocytic histopathological patterns have been found in airway biopsies from asthmatic patients (84, 85). The cellular pathophysiology of this particular asthmatic phenotype, characterized by the lack of increased counts of eosinophils or neutrophils in either sputum or blood, has not been clearly elucidated. However, it appears that paucigranulocytic asthma is featured by an uncoupling of bronchial obstruction from inflammation, possibly due to structural changes mainly resulting in non-inflammatory thickening of airway smooth muscle layer (86).

LICENSED BIOLOGICAL THERAPIES OF SEVERE ASTHMA

There are currently five approved monoclonal antibodies for add-on biologic treatment of severe asthma. They include omalizumab, mepolizumab, reslizumab, benralizumab, and dupilumab (**Figure 1**).

Omalizumab has been the first licensed biologic drug for clinical use in the management of severe asthma. This recombinant humanized monoclonal antibody, originally developed in mice, binds to the two Cε3 domains of the constant portion of IgE, thus forming IgE/anti-IgE immune complexes that prevent IgE interactions with both high-affinity FcεRI and low-affinity FcεRII/CD23 membrane receptors (87, 88). As a consequence, omalizumab inhibits all IgE-dependent cellular and molecular events involved in the immune/inflammatory cascade underlying allergic asthma. Systematic

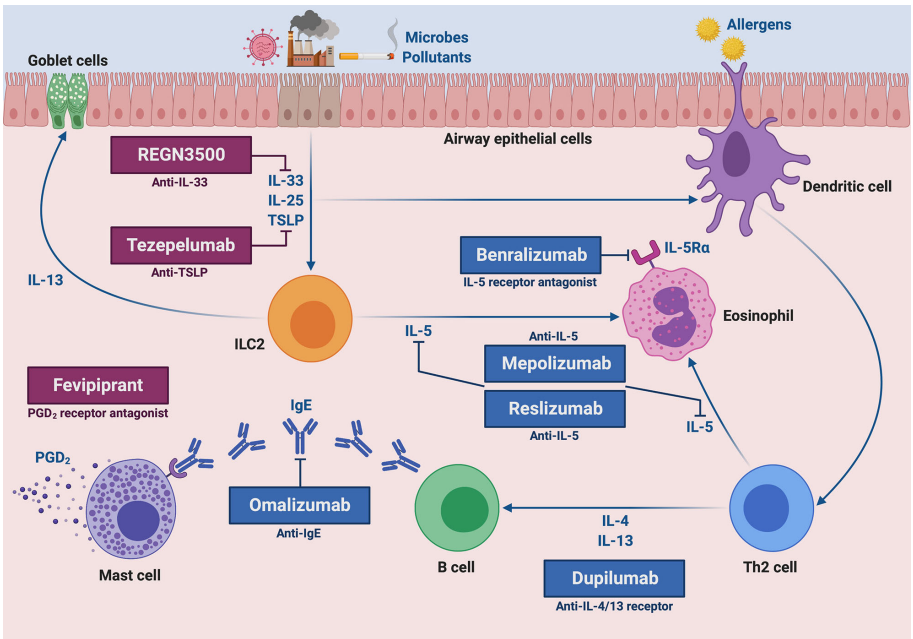

FIGURE 1 | Molecular targets of current and future biological therapies of severe type 2 asthma. The targets of approved add-on biologic treatments (highlighted in blue color) of severe asthma include IgE (omalizumab), IL-5 (mepolizumab and reslizumab), IL-5 receptor (benralizumab), and IL-4/IL-13 receptor complex (dupilumab). Moreover, experimental drugs (highlighted in dark magenta color) such as tezepelumab, REGN3500 and fevipiprant target TSLP, IL-33 and the CRTH2 receptor of PGD_2, respectively. This original figure was created by the authors using "BioRender.com".

reviews and pooled analyses of randomized controlled trials have clearly shown that omalizumab was able to significantly decrease the rate of asthma exacerbations, and this therapeutic effect was observed up to 48–60 weeks of treatment (89, 90). Such a favourable clinical outcome has been further corroborated by several worldwide real-life studies (91). In addition to confirming the positive impact of omalizumab on asthma exacerbations, emergency room accesses and hospitalizations, real-world experiences have also demonstrated relevant improvements in symptom control, quality of life, and intake of oral corticosteroids (OCS), as well as a lower loss of working and school days (91–93). Despite some discordant published data regarding the effects of omalizumab on lung function (15), many real-life studies have shown that this anti-IgE monoclonal antibody can induce significant and persistent increases in forced expiratory volume in the first second (FEV_1), lasting 5, 7, and even 9 years (94–96). Moreover, it was also recently reported that omalizumab can effectively improve both clinical manifestations and computed tomography (CT) images of nasal polyps associated with severe allergic asthma (97). All these beneficial outcomes achieved by patients undergoing add-on therapy with omalizumab explain the high degree of adherence to this biologic drug (98). The real-life therapeutic effectiveness of omalizumab coexists with a long-term, very good safety and tolerability profile (99).

Mepolizumab is a humanized IgG1/κ monoclonal antibody of murine origin which binds with high affinity to human IL-5, thus preventing its interaction with the α subunit of IL-5 receptor (IL-5Rα) (100). The efficacy of mepolizumab was firstly evidenced by Nair et al. and by Haldar et al., who showed in a few frequent exacerbators with severe eosinophilic asthma that this biologic drug significantly reduced disease exacerbations, as well as blood and sputum eosinophils (101, 102). These positive effects of mepolizumab were later confirmed by the phase IIb/III DREAM (Dose Ranging Efficacy And safety with Mepolizumab) trial, carried out by Pavord et al. in a much larger number of patients (103). Moreover, MENSA (MEpolizumab as adjunctive therapy iN patients with Severe Asthma) and SIRIUS (SteroId ReductIon with mepolizUmab Study) trials, performed by Ortega et al., and Bel et al., respectively, documented that in subjects with severe eosinophilic asthma mepolizumab lowered asthma exacerbation rate, improved quality of life and symptom control, and also slightly increased FEV_1 (104, 105). In addition, the SIRIUS study demonstrated that mepolizumab exerted an effective OCS sparing action, thereby decreasing prednisone intake by 50% (105). Furthermore, the phase IIIb MUSCA trial, carried out by Chupp et al., corroborated the significant results achieved by patients undergoing add-on mepolizumab therapy with regard to improvement of health-related quality of life (106). All these randomized controlled studies also reported a very good pattern of drug safety and tolerability. Besides such controlled trials, uncontrolled, open-label, and real-life investigations are providing further information about the therapeutic properties of mepolizumab. Indeed, some real-world data suggest that in

clinical practice mepolizumab effectiveness can be even greater than that one observed in randomized controlled trials, and these better results might be dependent on the higher numbers of baseline blood eosinophils detectable in patients enrolled in real-life experiences (107, 108). The latter have shown that mepolizumab is very effective in both non allergic and allergic patients with severe eosinophilic asthma, also in case of switching from omalizumab to mepolizumab because of an inadequate disease control provided by anti-IgE treatment (109–111). With regard to lung function, it is noteworthy that in real-life setting mepolizumab was able not only to increase FEV_1, but also to improve airflow limitation at level of small airways (112). Mepolizumab was capable of inducing beneficial therapeutic effects also in severe nasal polyposis, thus improving subjective symptoms and endoscopic nasal polyp score, as well as leading to a decreased need for surgical polypectomy (113).

Another anti-IL-5 biologic drug is reslizumab, a humanized IgG4/κ monoclonal antibody of rat origin, whose clinical and functional effects have been assessed in many randomized trials (114, 115). The first phase II trial was conducted by Kips et al., who demonstrated that reslizumab reduced both sputum and blood eosinophil counts, as well as transiently increased FEV_1 (116). A further phase II study, performed by Castro et al. in patients with severe eosinophilic asthma, showed that reslizumab induced a significant FEV_1 increase, associated with a non-significant tendency towards an improvement in asthma control, particularly in asthmatic subjects with high blood eosinophil numbers and coexistent nasal polyposis (117). Subsequently, two phase III trials carried out by Castro et al. in patients with severe asthma and blood eosinophil counts higher than 400 cells/μL, evidenced that reslizumab lowered the annual asthma exacerbation rate by more than 50%, improved asthma control and incremented FEV_1 (118). Such findings were further confirmed by Brusselle et al., especially in subjects with late-onset eosinophilic asthma (119). Moreover, Bjermer et al. observed that the positive effects of reslizumab on lung function were not limited to the large airways, as shown by FEV_1 increases, but also extended to the small airways resulting in significant enhancements of mid-expiratory flow at 25–75% of forced vital capacity (FEF_{25-75}) (120). Similar to omalizumab and mepolizumab, also reslizumab displays a more than satisfactory profile of safety and tolerability (114).

Differently from mepolizumab and reslizumab, benralizumab is characterized by a dual mechanism of action. Indeed, this humanized afucosylated IgG1/κ monoclonal antibody of murine origin binds through its Fab fragments to IL-5Rα, thereby impeding the assembly of the ternary molecular complex consisting of IL-5, IL-5Rα, and the βc subunits of IL-5 receptor (121, 122); as a consequence, IL-5 cannot exert its biological effects on target cells (eosinophils, basophils, ILC2). Moreover, *via* the constant Fc portion benralizumab interacts with the surface FcγRIIIa receptor of natural killer cells, thus triggering eosinophil apoptosis operated by antibody-dependent cell-mediated cytotoxicity (ADCC), a mechanism that is remarkably potentiated by afucosylation (121, 122). In regard to the randomized clinical trials, phase III SIROCCO and CALIMA studies have demonstrated that benralizumab significantly reduced the annual rate of severe eosinophilic asthma exacerbations, and also bettered asthma symptom control and increased FEV_1 (123, 124). Chipps et al. performed a pooled analysis of SIROCCO and CALIMA trials, thus showing that benralizumab was effective as adjunctive biological therapy in both allergic and non-allergic patients with severe eosinophilic asthma (125). The BISE trial confirmed the positive impact of benralizumab on lung function, whereas the ZONDA study showed that benralizumab significantly decreased daily OCS intake (126, 127). Furthermore, the BORA trial documented that benralizumab use was associated with long-term safety and tolerability (128). All these findings, regarding clinical and functional outcomes, have been corroborated, and even extended and amplified by recent real-life experiences. The latter are providing convincing evidence referring to the safety and efficacy of benralizumab, detected in both atopic and non-atopic subjects with eosinophilic uncontrolled asthma, with regard to relevant improvements in asthma exacerbations, OCS consumption, symptom control, airflow limitation, lung hyperinflation, and nasal polyposis (129–132).

Dupilumab is a fully human IgG4 monoclonal antibody, which specifically recognizes and occupies the α subunit of IL-4 receptor, thereby inhibiting the biological actions of both IL-4 and IL-13 (133). Indeed, these two cytokines not only exert overlapping effects related to IgE class switching, eosinophil chemotaxis and airway hyperresponsiveness, but also share common receptor mechanisms and signalling pathways, based on activation of IL-4Rα coupled to the JAK/TYK transduction machinery (10, 133). Therefore, dupilumab behaves as a dual receptor antagonist of IL-4 and IL-13 (134). In an initial phase IIa trial, Wenzel et al. randomly assigned to either dupilumab or placebo 104 patients with persistent, moderate-to-severe eosinophilic asthma, thus showing that dupilumab significantly lowered the asthma exacerbation rate by 87%, and also enhanced FEV_1 by more than 200 mL, despite ICS/LABA withdrawal (135). A subsequent larger, phase IIb study carried out in uncontrolled adult asthmatics confirmed the positive impact of dupilumab on asthma exacerbations and lung function, especially but not only in subjects with high blood eosinophil counts (136). More recently, the phase III LIBERTY ASTHMA QUEST trial showed that in asthmatic patients with blood eosinophil numbers ≥ 300 cells/μL, dupilumab was able to decrease asthma exacerbations by more than 65%, as well as to increase FEV_1 by more than 200 mL (137). Corren et al. performed a *post hoc* analysis of the LIBERTY ASTHMA QUEST study, thereby demonstrating that the above beneficial effects of dupilumab can be indifferently detected in both allergic and non-allergic asthmatics (138). Furthermore, the LIBERTY ASTHMA VENTURE trial highlighted the significant OCS-sparing action of dupilumab (139). Overall, dupilumab is quite safe and well tolerated, even if in some patients this biologic drug can induce conjunctivitis or a marked blood eosinophilia (10), which however tends to resolve spontaneously in a few months,

TABLE 1 | Licensed biological therapies for severe asthma.

Licensed biological therapies	Targets	Molecular mechanisms of action	Effects in the control of severe asthma
Omalizumab	IgE	Generation of IgE/anti-IgE immune complexes that inhibit IgE-mediated allergic cascade	↓ Exacerbations ↑ Quality of life and symptom control ↑ FEV1
Mepolizumab	IL-5	Prevention of IL-5 binding to IL-5Rα	↓ Blood and sputum eosinophils ↓ Exacerbations ↑ Quality of life and symptom control ↓ OCS intake ↑ FEV1
Reslizumab	IL-5	Prevention of IL-5 binding to IL-5Rα	↓ Blood and sputum eosinophils ↓ Exacerbations ↑ Quality of life and symptom control ↑ FEV1
Benralizumab	IL-5Rα	Blockade of IL-5Rα ADCC-induced eosinophil apoptosis	↓ Blood eosinophils ↓ Exacerbations ↑ Quality of life and symptom control ↓ OCS intake ↑ FEV1
Dupilumab	IL-4Rα	Dual receptor antagonism of IL-4/IL-13	↓ Exacerbations ↓ OCS intake ↑ FEV1

without apparent consequences in most cases. Dupilumab is also very effective for treatment of relevant asthma comorbidities such as atopic dermatitis and nasal polyposis (140, 141).

The molecular targets, mechanisms of action and therapeutic effects of the above mentioned drugs are summarized in **Table 1**.

TARGETS OF EMERGING BIOLOGICAL THERAPIES IN CLINICAL DEVELOPMENT

In addition to the currently available biological therapies of severe asthma, the recent advances in our understanding of the pathobiology of this complex disease are allowing to disclose new potential targets for future anti-asthma treatments. In particular, besides the downstream effectors of type 2 airway inflammation such as IgE, IL-5, IL-4/13 and their receptors, other very interesting pathogenic molecules include upstream activators of cellular pathways leading to T2-high asthma. Within this context, a key role is played by the innate cytokines known as alarmins, including TSLP, IL-33, and IL-25 (142). So far, the most extensively studied alarmin as suitable target for novel biological therapies of asthma has been TSLP (13, 143).

TSLP bioactivities are involved in several pathogenic aspects of type 2 asthma. Indeed, by up-regulating OX40 ligand expression, TSLP acts as a powerful inducer of dendritic cell activation (144). Upon TSLP-mediated stimulation, dendritic cells drive naïve Th lymphocytes towards differentiation into active Th2 cells producing IL-4, IL-5, and IL-13 (145). Moreover, TSLP up-regulates the expression of such cytokines at level of other cellular sources, including basophils, mast cells, and especially ILC2 (142, 146, 147). In regard to these latter cells, TSLP also promotes their survival and steroid resistance (147, 148). TSLP appears to be also implicated in T2-low asthma pathobiology. In fact, this alarmin can induce dendritic cells to drive the commitment of naïve Th cells towards a Th17 immunophenotype (149).

Tezepelumab is an anti-TSLP fully human monoclonal antibody (**Figure 1**), which prevents TSLP binding to its receptor complex (150). Tezepelumab was firstly tested in patients with mild allergic asthma by Gauvreau et al., who noted that this anti-TSLP antibody reduced allergen-induced FEV_1 decreases, as well as post-allergen increases in blood/sputum eosinophils and FeNO (151). A subsequent phase IIb trial was carried out by Corren et al., who showed that tezepelumab decreased the annualized asthma exacerbation rate by 60–70% and enhanced pre-bronchodilator FEV_1, independently of blood eosinophil numbers (152). Furthermore, tezepelumab lowered the most relevant biomarkers of T2-high asthma, including IgE serum concentrations, blood eosinophil counts and FeNO levels (152). Ongoing phase II and III trials are evaluating the safety profile of tezepelumab, as well as its eventual efficacy in decreasing airway inflammation and OCS intake (142). So far, tezepelumab has not yet been investigated in regard to its potential therapeutic effects in patients with T2-low asthma.

IL-33 cooperates with TSLP in promoting type-2 immune/inflammatory responses (153). In particular, IL-33 induces airway hyperresponsiveness by stimulating IL-13 release from ILC2 and mast cells (154, 155). Several phase II trials are underway with the aim of evaluating some biologic drugs which target IL-33 or its ST2 receptor (142). In particular, it has been shown that the anti-IL-33 monoclonal antibody REGN3500 (**Figure 1**) was able to improve the control of severe asthma, but its therapeutic effects did not result to be better than those induced by dupilumab (142). Moreover, when tested in association with this IL-4/IL-13 dual receptor antagonist, the anti-asthma actions of such two biologicals were comparable to those exerted by dupilumab alone (142).

Although IL-25 plays a relevant pathogenic role in allergic inflammation, to our knowledge no anti-IL-25 monoclonal antibody is currently in clinical development for add-on treatment of severe asthma.

Another key mediator of type-2 asthma is prostaglandin D_2 (PGD_2), mainly produced by mast cells (156). PGD_2 exerts its pro-inflammatory actions *via* stimulation of CRTH2 (chemoattractant receptor-homologous molecule expressed on Th2 cells) receptor, expressed by Th2 lymphocytes, ILC2 and eosinophils (156). Binding of PGD_2 to CRTH2 can be blocked by fevipiprant (**Figure 1**), a selective receptor antagonist which is not a monoclonal antibody, but rather a small compound used as an oral drug (156). Despite the partially promising results of some preliminary studies carried out in asthmatic patients, however fevipiprant seems to induce only a weak FEV_1 increase, similar to the functional effect of the leukotriene

TABLE 2 | New potential targets of emerging anti-asthma therapies.

New potential targets	New potential drugs	Molecular mechanisms of action	Effects in the control of severe asthma
TSLP	Tezepelumab	Prevention of TSLP binding to its receptor complex	↓ Blood eosinophils ↓ FeNO ↓ Exacerbations ↑ FEV1
IL-33	REGN3500	Prevention of IL-33 binding to ST2 receptor	↑ Quality of life and symptom control
PGD2	Fevipiprant	Selective antagonism of CRTH2 receptor	Weak FEV1 increase

receptor antagonist montelukast (157, 158). Further studies are thus needed, even if the therapeutic potential of fevipiprant for asthma therapy currently appears to be quite uncertain.

The molecular targets, mechanisms of action and therapeutic effects of the above mentioned drugs are summarized in **Table 2**.

With regard to the potential molecular targets of biological therapies for type 2-low neutrophilic asthma, the main focus of current studies is the pathogenic axis connecting IL-1β, IL-23, and IL-17. In particular, the IL-1 receptor antagonist anakinra and the anti-IL-1β monoclonal antibody canakinumab are currently under clinical investigation in phase I/II trials enrolling patients with mild asthma (159, 160). In addition, further phase II studies are evaluating, in patients with severe type 2-low asthma, the efficacy and safety of the anti-IL-23 antibody risankizumab, as well as of an anti-IL-17A monoclonal antibody (159, 160). However, a previous trial carried out in moderate-to-severe asthmatics, aimed to investigate the effects of the anti-IL-17 receptor monoclonal antibody brodalumab, did not show any improvement in asthma symptom control and lung function (161).

CONCLUSIONS

Ongoing progress in our knowledge of the pathobiological mechanisms underlying the various cellular and molecular phenotypes of severe asthma has made it possible to unveil suitable targets for add-on biological therapies. Several approved anti-IgE, anti-IL-5, anti-IL-5 receptor, and anti-IL-4/IL-13 receptor monoclonal antibodies are currently prescribed by clinicians. These drugs are helping patients with severe, allergic or non-allergic eosinophilic T2-high asthma, to significantly improve symptom control, lung function and global health status, and especially to lessen their susceptibility to suffer from frequent and often serious disease exacerbations. Moreover, new promising monoclonal antibodies, mainly targeting the innate cytokines known as alarmins, are in advanced clinical development. However, patients with severe T2-low asthma are largely excluded from the therapeutic benefits achievable by people who experience T2-high severe disease. Therefore, in the coming years strong research efforts should be finalized to develop novel biological treatments for severe neutrophilic or paucigranulocytic asthma, thus hoping that patients expressing such uncontrolled phenotypes may pursue in the near future better health conditions than the current ones.

AUTHOR CONTRIBUTIONS

All authors contributed to elaborate the text and to draw the figure. All authors contributed to the article and approved the submitted version.

REFERENCES

1. Holgate ST, Wenzel S, Postma DS, Weiss ST, Renz H, Sly PD. Asthma. *Nat Rev Dis Primers* (2015) 1:15025. doi: 10.1038/nrdp.2015.25
2. Papi A, Brightling C, Pedersen SE, Reddel HK. Asthma. *Lancet* (2018) 391:783–800. doi: 10.1016/S0140-6736(17)33311-1
3. Khalaf K, Paoletti G, Puggioni F, Racca F, De Luca E, Giorgis V, et al. Asthma from immune pathogenesis to precision medicine. *Semin Immunol* (2019) 46:101294. doi: 10.1016/j.smim.2019.101294
4. To T, Stanojevic S, Moores G, Gershon AS, Bateman ED, Cruz AA, et al. Global asthma prevalence in adults: findings from the cross-sectional world health survey. *BMC Public Health* (2012) 12:204. doi: 10.1186/1471-2458-12-204
5. Stern J, Pier J, Litonjua AA. Asthma epidemiology and risk factors. *Semin Immunopathol* (2020) 42:5–15. doi: 10.1007/s00281-020-00785-1
6. Heffler E, Blasi F, Latorre M, Menzella F, Paggiaro P, Pelaia G, et al. SANI network. The severe asthma network in Italy: findings and perspectives. *J Allergy Clin Immunol Pract* (2019) 7:1462–8. doi: 10.1016/j.jaip.2018.10.016
7. Chung KF, Wenzel SE, Brozek JL, Bush A, Castro M, Sterk PJ, et al. International ERS/ATS guidelines on definition, evaluation and treatment of severe asthma. *Eur Respir J* (2014) 43:343–73. doi: 10.1183/13993003.52020-2013
8. Siddiqui S, Denlinger LC, Fowler SJ, Akuthota P, Shaw DE, Heaney LG, et al. Unmet needs in severe asthma subtyping and precision medicine trials. Bridging clinical and patient perspectives. *Am J Respir Crit Care Med* (2019) 199:823–9. doi: 10.1164/rccm.201809-1817PP
9. Pelaia G, Vatrella A, Maselli R. The potential of biologics for the treatment of asthma. *Nat Rev Drug Discovery* (2012) 11:958–72. doi: 10.1038/nrd3792
10. Peters MC, Wenzel SE. Intersection of biology and therapeutics: type 2 targeted therapeutics for adult asthma. *Lancet* (2020) 395:371–83. doi: 10.1016/S0140-6736(19)33005-3
11. Chupp GL, Kaur R, Mainardi A. New therapies for emerging endotypes of asthma. *Annu Rev Med* (2020) 71:25.1–25.14. doi: 10.1146/annurev-med-041818-020630
12. Al-Sajee D, Oliveria JP, Sehmi R, Gauvreau GM. Antialarmins for treatment of asthma. *Curr Opin Pulm Med* (2018) 24:32–41. doi: 10.1097/MCP.0000000000000443
13. Nakajima S, Kabata H, Kabashima K, Asano K. Anti-TSLP antibodies: targeting a master regulator of type 2 immune responses. *Allergol Int* (2020) 69:197–203. doi: 10.1016/j.alit.2020.01.001
14. Pepper AN, Renz H, Casale TB, Garn H. Biologic therapy and novel molecular targets of severe asthma. *J Allergy Clin Immunol Pract* (2017) 5:909–16. doi: 10.1016/j.jaip.2017.04.038

15. Krings JG, McGregor MC, Bacharier LB, Castro M. Biologics for severe asthma: treatment-specific effects are important in choosing a specific agent. *J Allergy Clin Immunol Pract* (2019) 7:1379–92. doi: 10.1016/j.jaip.2019.03.008
16. Kuruvilla ME, Lee FE, Lee GB. Understanding asthma phenotypes, endotypes, and mechanisms of disease. *Clin Rev Allergy Immunol* (2019) 56:219–33. doi: 10.1007/s12016-018-8712-1
17. Lambrecht BN, Hammad H, Fahy JV. The cytokines of asthma. *Immunity* (2019) 50:975–91. doi: 10.1016/j.immuni.2019.03.018
18. Pelaia G, Vatrella A, Busceti MT, Gallelli L, Calabrese C, Terracciano R, et al. Cellular mechanisms underlying eosinophilic and neutrophilic airway nflammation in asthma. *Mediators Inflamm* (2015) 2015:879783. doi: 10.1155/2015/879783
19. Wenzel SE. Complex phenotypes in asthma: current definitions. *Pulm Pharmacol Ther* (2013) 26:710–15. doi: 10.1016/j.pupt.2013.07.003
20. Ray A, Oriss TB, Wenzel SE. Emerging molecular phenotypes of asthma. *Am J Physiol Lung Cell Mol Physiol* (2015) 308:L130–40. doi: 10.1152/ajplung.00070.2014
21. Schoettler N, Strek ME. Recent advances in severe asthma: from phenotypes to personalized medicine. *Chest* (2020) 157:516–28. doi: 10.1016/j.chest.2019.10.009
22. McDowell PJ, Heaney LG. Different endotypes and phenotypes drive the heterogeneity in severe asthma. *Allergy* (2020) 75:302–10. doi: 10.1111/all.13966
23. Bousquet J, Chanez P, Lacoste JY, Barnéon G, Ghavanian N, Enander I, et al. Eosinophilic inflammation in asthma. *N Engl J Med* (1990) 323:1033–9. doi: 10.1056/NEJM199010113231505
24. Schleich F, Brusselle G, Louis R, Vandenplas O, Michils A, Pilette C, et al. Heterogeneity of phenotypes in severe asthma. The Belgian severe asthma registry (BSAR). *Respir Med* (2014) 108:1723–32. doi: 10.1016/j.rmed.2014.10.007
25. Huber KL, Koessler K. The pathology of fatal asthma. *Arch Intern Med* (1922) 30:689–760. doi: 10.1001/archinte.1922.00110120002001
26. Houston JC, De Navasquez S. Trounce JR. A clinical and pathological study of fatal cases of status asthmaticus. *Thorax* (1953) 8:207–13. doi: 10.1136/thx.8.3.207
27. Nelson RK, Bush A, Stokes J, Nair P, Akuthota P. Eosinophilic asthma. *J Allergy Clin Immunol* (2020) 8:465–73. doi: 10.1016/j.jaip.2019.11.024
28. Lambrecht BN, Hammad H. The immunology of asthma. *Nat Immunol* (2015) 16:45–54. doi: 10.1038/ni.3049
29. Kaiko GE, Horvat JC, Beagley KW, Hansbro PM. Immunological decision-making: how does the immune system decide to mount a helper T-cell response? *Immunology* (2008) 123:326–38. doi: 10.1111/j.1365-2567.2007.02719.x
30. Kallinich T, Beier KC, Wahn U, Stock P, Hamelmann E. T-cell co-stimulatory molecules: their role in allergic immune reactions. *Eur Respir J* (2007) 29:1246–55. doi: 10.1183/09031936.00094306
31. Froidure A, Mouthuy J, Durham SR, Chanez P, Sibille Y, Pilette C. Asthma phenotypes and IgE responses. *Eur Respir J* (2016) 47:304–19. doi: 10.1183/13993003.01824-2014
32. Gould HJ, Sutton BJ. IgE in allergy and asthma today. *Nat Rev Immunol* (2008) 8:205–17. doi: 10.1038/nri2273
33. Hentges F, Leonard C, Arumugam K, Hilger C. Immune responses to inhalant mammalian allergens. *Front Immunol* (2014) 5:234. doi: 10.3389/fimmu.2014.00234
34. Dullaers M, De Bruyne R, Ramadani F, Gould HJ, Gevaert P, Lambrecht BN. The who, where and when of IgE in allergic airway disease. *J Allergy Clin Immunol* (2012) 129:635–45. doi: 10.1016/j.jaci.2011.10.029
35. Hammad H, Lambrecht BN. Barrier epithelial cells and the control of type 2 immunity. *Immunity* (2015) 43:29–40. doi: 10.1016/j.immuni.2015.07.007
36. Morita H, Moro K, Koyasu S. Innate lymphoid cells in allergic and non-allergic inflammation. *J Allergy Clin Immunol* (2016) 138:1253–64. doi: 10.1016/j.jaci.2016.09.011
37. Cosmi L, Annunziato F. ILC2 are the earliest recruiters of eosinophils in lungs of allergic asthmatic patients. *Am J Respir Crit Care Med* (2017) 196:666–8. doi: 10.1164/rccm.201704-0799ED
38. Pattarini L, Trichot C, Bogiatzi S, Grandclaudon M, Meller S, Keuylian Z, et al. TSLP-activated dendritic cells induce human T follicular helper cell differentiation through OX40-ligand. *J Exp Med* (2017) 214:1529–46. doi: 10.1084/jem.20150402
39. Barnes PJ. The cytokine network in asthma and chronic obstructive pulmonary disease. *J Clin Invest* (2008) 118:3546–56. doi: 10.1172/JCI36130
40. Pelaia C, Paoletti G, Puggioni F, Racca F, Pelaia G, Canonica GW, et al. Interleukin-5 in the pathophysiology of severe asthma. *Front Physiol* (2019) 10:1514. doi: 10.3389/fphys.2019.01514
41. Brusselle GG, Maes T, Bracke KR. Eosinophilic airway inflammation in non allergic asthma. *Nat Med* (2013) 19:977–9. doi: 10.1038/nm.3300
42. Walker JA, Barlow JL, McKenzie AM. Innate lymphoid cells: how did we miss them? *Nat Rev Immunol* (2013) 13:75–87. doi: 10.1038/nri3349
43. Wood LJ, Sehmi R, Dorman S, Hamid Q, Tulic MK, Watson RM, et al. Allergen-induced increases in bone marrow T lymphocytes and interleukin-5 expression in subjects with asthma. *Am J Respir Crit Care Med* (2002) 166:883–9. doi: 10.1164/rccm.2108015
44. Dorman SC, Efthimiadis A, Babirad I, Watson RM, Denburg JA, Hargreave FE, et al. Sputum CD34+ IL-5Rα+ cells increase after allergen: evidence for in situ eosinophilopoiesis. *Am J Respir Crit Care Med* (2004) 169:573–7. doi: 10.1164/rccm.200307-1004OC
45. Bhalla A, Mukherjee M, Nair P. Airway eosinophilopoietic and autoimmune mechanisms of eosinophilia in severe asthma. Immunol. *Allergy Clin N Am* (2018) 38:639–54. doi: 10.1016/j.iac.2018.06.003
46. Greenfeder S, Umland SP, Cuss FM, Chapman RW, Egan RW. Th2 cytokines and asthma. The role of interleukin-5 in allergic eosinophilic disease. *Respir Res* (2001) 2:71–9. doi: 10.1186/rr41
47. Xu J, Jiang F, Nayeri F, Zetterstrom O. Apoptotic eosinophils in sputum from asthmatic patients correlate negatively with levels of IL-5 and eotaxin. *Respir Med* (2007) 101:1447–54. doi: 10.1016/j.rmed.2007.01.026
48. Ilmarinen P, Moilanen E, Kankaanranta H. Regulation of spontaneous eosinophil apoptosis – a neglected area of importance. *J Cell Death* (2014) 7:1–9. doi: 10.4137/JCD.S13588
49. Fulkerson PC, Rothenberg ME. Targeting eosinophils in allergy, inflammation and beyond. *Nat Rev Drug Discovery* (2013) 12:117–29. doi: 10.1038/nrd3838
50. Johansson MV. Eosinophil activation status in separate compartments and association with asthma. *Front Med* (2017) 4:75. doi: 10.3389/fmed.2017.00075
51. Wenzel S. Severe asthma in adults. *Am J Respir Crit Care Med* (2005) 172:149–60. doi: 10.1164/rccm.200409-1181PP
52. Makinde T, Murphy RF, Agrawall DK. The regulatory role of TGF-β in airway remodeling in asthma. *Immunol Cell Biol* (2007) 85:348–56. doi: 10.1038/sj.icb.7100044
53. Ray A, Kolls JK. Neutrophilic inflammation in asthma and association with disease severity. *Trends Immunol* (2017) 38:942–54. doi: 10.1016/j.it.2017.07.003
54. Aujla SJ, Alcorn JF. T_H17 cells in asthma and inflammation. *Biochim Biophys Acta* (2011) 1810:1066–79. doi: 10.1016/j.bbagen.2011.02.002
55. Newcomb DC, Peebles RSJr. Th17-mediated inflammation in asthma. *Curr Opin Immunol* (2013) 25:755–60. doi: 10.1016/j.coi.2013.08.002
56. Cosmi L, Liotta F, Maggi S, Romagnani S, Annunziato F. Th17 cells: new players in asthma pathogenesis. *Allergy* (2011) 66:989–98. doi: 10.1111/j.1398-9995.2011.02576.x
57. Al-Ramli W, Prefontaine D, Chouiali F, Martin JG, Olivenstein R, Lemière C, et al. T_H17-associated cytokines (IL-17A and IL-17F) in severe asthma. *J Allergy Clin Immunol* (2009) 123:1185–7. doi: 10.1016/j.jaci.2009.02.024
58. Huang G, Wang Y, Chi H. Regulation of T_H17 cell differentiation by innate immune signals. *Cell Mol Immunol* (2012) 9:287–95. doi: 10.1038/cmi.2012.10
59. Vroman H, van den Blink B, Kool M. Mode of dendritic cell activation: the decisive hand in Th2/Th17 cell differentiation. Implications in asthma severity? *Immunobiology* (2015) 220:254–61. doi: 10.1016/j.imbio.2014.09.016
60. Zhou L, Ivanov II, Spolski R, Min R, Shenderov K, Egawa T, et al. IL-6 programs T(H)-17 cell differentiation by promoting sequential engagement of the IL-21 and IL-23 pathways. *Nat Immunol* (2007) 8:967–74. doi: 10.1038/ni1488
61. Ramakrishnan RK, Heialy SA, Hamid Q. Role of IL-17 in asthma pathogenesis and its implications for the clinic. *Expert Rev Respir Med* (2019) 13:1057–68. doi: 10.1080/17476348.2019.1666002
62. McGeachy MJ, Chen Y, Tato CM, Laurence A, Joyce-Shaikh B, Blumenschein WM, et al. The interleukin 23 receptor is essential for the terminal differentiation of interleukin 17-producing effector T helper cells in vivo. *Nat Immunol* (2009) 10:314–24. doi: 10.1038/ni.1698

63. Thomson NC, Chaudhuri R, Livingston E. Asthma and cigarette smoking. *Eur Respir J* (2004) 24:822–33. doi: 10.1183/09031936.04.00039004
64. Polosa R, Thomson NC. Smoking and asthma: dangerous liaisons. *Eur Respir J* (2013) 41:716–26. doi: 10.1183/09031936.00073312
65. Brusselle GG, Provoost S, Bracke KR, Kuchmiy A, Lamkanfi M. Inflammasomes in respiratory disease: from bench to bedside. *Chest* (2014) 145:1121–33. doi: 10.1378/chest.13-1885
66. Lee TH, Song HJ, Park CS. Role of inflammasome activation in development and exacerbation of asthma. *Asia Pac Allergy* (2014) 4:187–96. doi: 10.5415/apallergy.2014.4.4.187
67. Kim HY, Lee HJ, Chang YJ, Pichavant M, Shore SA, Fitzgerald KA, et al. Interleukin-17-producing innate lymphoid cells and the NLRP3 inflammasome facilitate obesity-associated airway hyper-reactivity. *Nat Med* (2014) 20:54–61. doi: 10.1038/nm.3423
68. Krishnamoorthy N, Douda DN, Bruggermann TR, Ricklefs I, Duvall MG, Abdulnour REE, et al. Neutrophil cytoplasts induce TH17 differentiation toward neutrophilia in severe asthma. *Sci Immunol* (2018) 3:eaao4747. doi: 10.1126/sciimmunol.aao4747
69. Uddin M, Watz H, Malmgren A, Pedersen F. NETopathic inflammation in chronic obstructive pulmonary disease and severe asthma. *Front Immunol* (2019) 10:47. doi: 10.3389/fimmu.2019.00047
70. Twaddell SH, Baines KJ, Grainge C, Gibson PG. The emerging role of neutrophil extracellular traps in respiratory disease. *Chest* (2019) 156:774–82. doi: 10.1016/j.chest.2019.06.012
71. Manni ML, Robinson KM, Alcorn JF. A tale of two cytokines: IL-17 and IL-22 in asthma and infection. *Expert Rev Respir Med* (2014) 8:25–42. doi: 10.1586/17476348.2014.854167
72. Yu S, Kim HY, Chang YJ, DeKruiff RH, Umetsu DT. Innate lymphoid cells and asthma. *J Allergy Clin Immunol* (2014) 133:943–50. doi: 10.1016/j.jaci.2014.02.015
73. Wu Y, Yue J, Wu J, Zhou W, Li D, Ding K, et al. Obesity may provide pro-ILC3 development inflammatory environment in asthmatic children. *J Immunol Res* (2018) 2018:1628620. doi: 10.1155/2018/1628620
74. Durrant DM, Metzger DW. Emerging roles of T helper subsets in the pathogenesis of asthma. *Immunol Investig* (2010) 39:526–49. doi: 10.3109/08820131003615498
75. Wang YH, Wills-Karp MS. The potential role of interleukin-17 in severe asthma. *Curr Allergy Asthma Rep* (2011) 11:388–94. doi: 10.1007/s11882-011-0210-y
76. Halwani R, Al-Muhsen S, Hamid Q. T helper 17 cells in airway diseases: from laboratory bench to bedside. *Chest* (2013) 143:494–501. doi: 10.1378/chest.12-0598
77. Saffar AS, Ashdown H, Gounni AS. The molecular mechanisms of glucocorticoids-mediated neutrophil survival. *Curr Drug Targets* (2011) 12:556–62. doi: 10.2174/138945011794751555
78. Kadowaki N. Dendritic cells: a conductor of T cell differentiation. *Allergol Int* (2007) 56:193–9. doi: 10.2332/allergolint.R-07-146
79. Berry MA, Hargadon B, Shelley M, Parker D, Shaw DE, Green RH, et al. Evidence of a role of tumor necrosis factor α in refractory asthma. *N Engl J Med* (2006) 354:697–708. doi: 10.1056/NEJMoa050580
80. Cosmi L, Maggi L, Santarlasci V, Capone M, Cardilicchia E, Frosati F, et al. Identification of a novel subset of human circulating memory $CD4^+$ T cells that produce both IL-17A and IL-4. *J Allergy Clin Immunol* (2010) 125:222–30. doi: 10.1016/j.jaci.2009.10.012
81. Irvin C, Zafar I, Good J, Rollins D, Christianson C, Gorska MM, et al. Increased frequency of dual-positive T_H2/T_H17 cells in bronchoalveolar lavage fluid characterizes a population of patients with severe asthma. *J Allergy Clin Immunol* (2014) 134:1175–86. doi: 10.1016/j.jaci.2014.05.038
82. Wang YH, Voo KS, Liu B, Chen CY, Uygungil B, Spoede W, et al. A novel subset of CD4(+) T(H)2 memory effector cells that produce inflammatory IL-17 cytokine and promote the exacerbation of chronic allergic asthma. *J Exp Med* (2010) 207:2479–91. doi: 10.1084/jem.20101376
83. Bhakta NR, Erle DJ. IL-17 and "T_H2-high" asthma: adding fuel to the fire? *J Allergy Clin Immunol* (2014) 134:1187–8. doi: 10.1016/j.jaci.2014.07.034
84. Jenkins HA, Cherniack R, Szefler SJ, Covar R, Gelfand EW, Spahn JD. A comparison of the clinical characteristics of children and adults with severe asthma. *Chest* (2003) 124:1318–24. doi: 10.1378/chest.124.4.1318
85. Wenzel SE. Asthma: defining of the persistent adult phenotypes. *Lancet* (2006) 368:804–13. doi: 10.1016/S0140-6736(06)69290-8
86. Tliba O, Panettieri RAJr. Paucigranulocytic asthma: uncoupling of airway obstruction from inflammation. *J Allergy Clin Immunol* (2019) 143:1287–94. doi: 10.1016/j.jaci.2018.06.008
87. Pelaia G, Vatrella A, Busceti MT, Gallelli L, Terracciano R, Maselli R. Anti-IgE therapy with omalizumab for severe asthma: current concepts and potential developments. *Curr Drug Targets* (2015) 16:171–8. doi: 10.2174/1389450116666141219122157
88. Pelaia G, Canonica GW, Matucci A, Paolini R, Triggiani M, Paggiaro P. Targeted therapy in severe asthma today: focus on immunoglobulin E. *Drug Des Devel Ther* (2017) 11:1979–87. doi: 10.2147/DDDT.S130743
89. Rodrigo GJ, Neffen H, Castro-Rodriguez JA. Efficacy and safety of subcutaneous omalizumab vs placebo as add-on therapy to corticosteroids for children and adults with asthma: a systematic review. *Chest* (2011) 139:28–35. doi: 10.1378/chest.10-1194
90. Normansell R, Walker S, Milan SJ, Walters EH, Nair P. Omalizumab for asthma in adults and children. *Cochrane Database Syst Rev* (2014) 1: CD003559. doi: 10.1002/14651858.CD003559.pub4
91. Pelaia C, Calabrese C, Terracciano R, de Blasio F, Vatrella A, Pelaia G. Omalizumab, the first available antibody for biological treatment of asthma: more than a decade of real life effectiveness. *Ther Adv Respir Dis* (2018) 12. 1753466618810192. doi: 10.1177/1753466618810192
92. Cabrejos S, Moreira A, Ramirez A, Quirce S, Campos GS, Davila I, et al. FENOMA study: achieving full control in patients with severe allergic asthma. *J Asthma Allergy* (2020) 13:159–66. doi: 10.2147/JAA.S246902
93. Pelaia G, Gallelli L, Romeo P, Renda T, Busceti MT, Proietto A, et al. Omalizumab decreases exacerbation frequency, oral intake of corticosteroids and peripheral blood eosinophils in atopic patients with uncontrolled asthma. *Int J Clin Pharmacol Ther* (2011) 49:713–21. doi: 10.5414/CP201586
94. Pelaia C, Calabrese C, Barbuto S, Busceti MT, Preianò M, Gallelli L, et al. Omalizumab lowers asthma exacerbations, oral corticosteroid intake and blood eosinophils: results of a 5-year single centre observational study. *Pulm Pharmacol Ther* (2019) 54:25–30. doi: 10.1016/j.pupt.2018.11.002
95. Pace E, Ferraro M, Bruno A, Chiappara G, Bousquet J, Gjomarkaj M, et al. Clinical benefits of 7 years of treatment with omalizumab in severe uncontrolled asthmatics. *J Asthma* (2011) 48:387–92. doi: 10.3109/02770903.2011.561512
96. Menzella F, Galeone C, Formisano D, Castagnetti C, Ruggiero P, Simonazzi A, et al. Real life efficacy of omalizumab after 9 years of follow-up. *Allergy Asthma Immunol Res* (2017) 9:368–72. doi: 10.4168/aair.2017.9.4.368
97. Tiotiu A, Oster JP, Roux PR, Nguyen Thi PL, Peiffer G, Bonniaud P, et al. Effectiveness of omalizumab in severe allergic asthma and nasal polyposis: a real-life study. *J Invest Allergol Clin Immunol* (2020) 30:49–57. doi: 10.18176/jiaci.0391
98. Campisi R, Crimi C, Intravaia R, Strano S, Noto A, Foschino MP, et al. Adherence to omalizumab: a multi center "real-world" study. *World Allergy Organ J* (2020) 13:100103. doi: 10.1016/j.waojou.2020.100103
99. Di Bona D, Fiorino I, Taurino M, Frisenda F, Minenna E, Pasculli C, et al. Long-term "real life" safety of omalizumab in patients with severe uncontrolled asthma: a nine-year study. *Respir Med* (2017) 130:55–60. doi: 10.1016/j.rmed.2017.07.013
100. Pelaia C, Vatrella A, Busceti MT, Gallelli L, Terracciano R, Savino R, et al. Severe eosinophilic asthma: from the pathogenic role of interleukin-5 to the therapeutic action of mepolizumab. *Drug Des Devel Ther* (2017) 11:3137–44. doi: 10.2147/DDDT.S150656
101. Haldar P, Brightling CE, Hargadon B, Gupta S, Monteiro W, Sousa A, et al. Mepolizumab and exacerbations of refractory eosinophilic asthma. *New Engl J Med* (2009) 360:973–84. doi: 10.1056/NEJMoa0808991
102. Nair P, Pizzichini MM, Kjarsgaard M, Inman MD, Efthimiadis A, Pizzichini E, et al. Mepolizumab for prednisone-dependent asthma with sputum eosinophilia. *New Engl J Med* (2009) 360:985–93. doi: 10.1056/NEJMoa0805435
103. Pavord ID, Korn S, Howarth P, Bleecker ER, Buhl R, Keene ON, et al. Mepolizumab for severe eosinophilic asthma (DREAM): a multicentre, double-blind, placebo-controlled trial. *Lancet* (2012) 380:651–9. doi: 10.1016/S0140-6736(12)60988-X

104. Ortega HG, Liu MC, Pavord ID, Brusselle GG, FitzGerald JM, Chetta A, et al. Mepolizumab treatment in patients with severe eosinophilic asthma. *N Engl J Med* (2014) 371:1198–207. doi: 10.1056/NEJMoa1403290
105. Bel EH, Wenzel SE, Thompson PJ, Prazma CM, Keene ON, Yancey SW, et al. Oral glucocorticoid-sparing effect of mepolizumab in eosinophilic asthma. *N Engl J Med* (2014) 371:1189–97. doi: 10.1056/NEJMoa1403291
106. Chupp GL, Bradford ES, Albers FC, Bratton DJ, Wang-Jairaj J, Nelsen LM, et al. Efficacy of mepolizumab add-on therapy on health-related quality of life and markers of asthma control in severe eosinophilic asthma (MUSCA): a randomized, double-blind, placebo-controlled, parallel-group, multicenter, phase 3b trial. *Lancet Respir Med* (2017) 5:390–400. doi: 10.1016/S2213-2600(17)30125-X
107. Bagnasco D, Milanese M, Rolla G, Lombardi C, Bucca C, Heffler E, et al. The North-Western Italian experience with anti IL-5 therapy and comparison with regulatory trials. *World Allergy Organ J* (2018) 11:34. doi: 10.1186/s40413-018-0210-7
108. Pelaia C, Busceti MT, Solinas S, Terracciano R, Pelaia G. Real-life evaluation of the clinical, functional, and hematological effects of mepolizumab in patients with severe eosinophilic asthma: results of a single-centre observational study. *Pulm Pharmacol Ther* (2018) 53:1–5. doi: 10.1016/j.pupt.2018.09.006
109. Pelaia C, Crimi C, Pelaia G, Nolasco S, Campisi R, Heffler E, et al. Real-life evaluation of mepolizumab efficacy in patients with severe eosinophilic asthma, according to atopic trait and allergic phenotype. *Clin Exp Allergy* (2020) 50:780–8. doi: 10.1111/cea.13613
110. Chapman KR, Albers FC, Chipps B, Munoz X, Devouassoux G, Bergna M, et al. The clinical benefit of mepolizumab replacing omalizumab in uncontrolled severe eosinophilic asthma. *Allergy* (2019) 74:1716–26. doi: 10.1111/all.13850
111. Carpagnano GE, Pelaia C, D'Amato M, Crimi N, Scichilone N, Scioscia G, et al. Switching from omalizumab to mepolizumab: real-life experience from Southern Italy. *Ther Adv Respir Dis* (2020) 14. 1753466620929231. doi: 10.1177/1753466620929231
112. Sposato B, Camiciottoli G, Bacci E, Scalese M, Carpagnano GE, Pelaia C, et al. Mepolizumab effectiveness on small airway obstruction, corticosteroid sparing and maintenance therapy step-down in real life. *Pulm Pharmacol Ther* (2020) 61:101899. doi: 10.1016/j.pupt.2020.101899
113. Bachert C, Sousa AR, Lund VJ, Scadding GK, Gevaert P, Nasser S, et al. Reduced need for surgery in severe nasal polyposis with mepolizumab: randomized trial. *J Allergy Clin Immunol* (2017) 140:1024–31. doi: 10.1016/j.jaci.2017.05.044
114. Pelaia G, Vatrella A, Busceti MT, Gallelli L, Preianò M, Lombardo N, et al. Role of biologics in severe eosinophilic asthma: focus on reslizumab. *Ther Clin Risk Manage* (2016) 12:1075–82. doi: 10.2147/TCRM.S111862
115. Varricchi G, Senna G, Loffredo S, Bagnasco D, Ferrando M, Canonica GW. Reslizumab and eosinophilic asthma: one step closer to precision medicine? *Front Immunol* (2017) 8:242. doi: 10.3389/fimmu.2017.00242
116. Kips JC, O'Connor BJ, Langley SJ, Woodcock A, Kerstjens HA, Postma DS, et al. Effects of SCH55700, a humanized anti-human interleukin-5 antibody, in severe persistent asthma: a pilot study. *Am J Respir Crit Care Med* (2003) 167:1655–9. doi: 10.1164/rccm.200206-525OC
117. Castro M, Mathur S, Hargreave F, Boulet LP, Xie F, Young J, et al. Reslizumab for poorly controlled, eosinophilic asthma: a randomized, placebo-controlled study. *Am J Respir Crit Care Med* (2011) 184:1125–32. doi: 10.1164/rccm.201103-0396OC
118. Castro M, Zangrilli J, Wechsler ME, Bateman ED, Brusselle GG, Bardin P, et al. Reslizumab for inadequately controlled asthma with elevated blood eosinophil counts: results from two multicentre, parallel, double-blind, randomised, placebo-controlled, phase 3 trials. *Lancet Respir Med* (2015) 3:355–66. doi: 10.1016/S2213-2600(15)00042-9
119. Brusselle G, Germinaro M, Weiss S, Zangrilli J. Reslizumab in patients with inadequately controlled late-onset asthma and elevated blood eosinophils. *Pulm Pharmacol Ther* (2017) 43:39–45. doi: 10.1016/j.pupt.2017.01.011
120. Bjermer L, Lemiere C, Maspero J, Weiss S, Zangrilli J, Germinaro M. Reslizumab for inadequately controlled asthma with elevated blood eosinophil levels: a randomized phase 3 study. *Chest* (2016) 150:789–98. doi: 10.1016/j.chest.2016.03.032
121. Pelaia C, Vatrella A, Bruni A, Terracciano R, Pelaia G. Benralizumab in the treatment of severe asthma: design, development and potential place in therapy. *Drug Des Devel Ther* (2018) 12:619–28. doi: 10.2147/DDDT.S155307
122. Pelaia C, Calabrese C, Vatrella A, Busceti MT, Garofalo E, Lombardo N, et al. Benralizumab: from the basic mechanism of action to the potential use in the biological therapy of severe eosinophilic asthma. *BioMed Res Int* (2018) 2018:4839230. doi: 10.1155/2018/4839230
123. Bleecker ER, FitzGerald JM, Chanez P, Papi A, Weinstein SF, Barker P, et al. Efficacy and safety of benralizumab for patients with severe asthma uncontrolled with high-dosage inhaled corticosteroids and long-acting β_2-agonists (SIROCCO): a randomized, multicentre, placebo-controlled phase 3 trial. *Lancet* (2016) 388:2115–27. doi: 10.1016/S0140-6736(16)31324-1
124. FitzGerald JM, Bleecker ER, Nair P, Korn S, Ohta K, Lommatzsch M, et al. Benralizumab, an anti-interleukin-5 receptor α monoclonal antibody, as add-on treatment for patients with severe, uncontrolled eosinophilic asthma (CALIMA): a randomised, double-blind, placebo-controlled phase 3 trial. *Lancet* (2016) 388:2128–41. doi: 10.1016/S0140-6736(16)31322-8
125. Chipps BE, Newbold P, Hirsch I, Trudo F, Goldman M. Benralizumab efficacy by atopy status and serum immunoglobulin E for patients with severe, uncontrolled asthma. *Ann Allergy Asthma Immunol* (2018) 120:504–11. doi: 10.1016/j.anai.2018.01.030
126. Ferguson GT, FitzGerald JM, Bleecker ER, Laviolette M, Bernstein D, LaForce C, et al. Benralizumab for patients with mild to moderate persistent asthma (BISE): a randomised, double-blind, placebo-controlled phase 3 trial. *Lancet Respir Med* (2017) 5:568–76. doi: 10.1016/S2213-2600(17)30190-X
127. Nair P, Wenzel S, Rabe KF, Bourdin A, Lugogo NL, Kuna P, et al. Oral glucocorticoid-sparing effect of benralizumab in severe asthma. *N Engl J Med* (2017) 376:2448–58. doi: 10.1056/NEJMoa1703501
128. Busse ER, Bleecker JM, FitzGerald GT, Ferguson GT, Barker P, Sproule S, et al. Long-term safety and efficacy of benralizumab in patients with severe, uncontrolled asthma: 1-year results from the BORA phase 3 extension trial. *Lancet Respir Med* (2019) 7:46–59. doi: 10.1016/S2213-2600(18)30406-5
129. Pelaia C, Busceti MT, Vatrella A, Rago GF, Crimi C, Terracciano R, et al. Real-life rapidity of benralizumab effects in patients with severe allergic asthma: assessment of blood eosinophils, symptom control, lung function and oral corticosteroid intake after the first drug dose. *Pulm Pharmacol Ther* (2019) 58:101830. doi: 10.1016/j.pupt.2019.101830
130. Pelaia C, Busceti MT, Crimi C, Carpagnano GE, Lombardo N, Terracciano R, et al. Real-life effects of benralizumab on exacerbation number and lung hyperinflation in atopic patients with severe eosinophilic asthma. *BioMed Pharmacother* (2020) 129:110444. doi: 10.1016/j.biopha.2020.110444
131. Pelaia C, Busceti MT, Vatrella A, Ciriolo M, Garofalo E, Crimi C, et al. Effects of the first three doses of benralizumab on symptom control, lung function, blood eosinophils, oral corticosteroid intake, and nasal polyps in a patient with severe allergic asthma. *SAGE Open Med Case Rep* (2020) 8. 2050313X20906963. doi: 10.1177/2050313X20906963
132. Lombardo N, Pelaia C, Ciriolo M, Della Corte M, Piazzetta G, Lobello N, et al. Real-life effects of benralizumab on allergic chronic rhinosinusitis and nasal polyposis associated with severe asthma. *Int J Immunopathol Pharmacol* (2020) 34. 2058738420950851. doi: 10.1177/2058738420950851
133. Pelaia C, Vatrella A, Gallelli L, Terracciano R, Navalesi P, Maselli R, et al. Dupilumab for the treatment of asthma. *Expert Opin Biol Ther* (2017) 17:1565–72. doi: 10.1080/14712598.2017.1387245
134. Harb H, Chatila TA. Mechanisms of dupilumab. *Clin Exp Allergy* (2020) 50:5–14. doi: 10.1111/cea.13491
135. Wenzel S, Ford L, Pearlman D, Spector S, Sher L, Skobieranda F, et al. Dupilumab in persistent asthma with elevated eosinophil levels. *N Engl J Med* (2013) 368:2455–66. doi: 10.1056/NEJMoa1304048
136. Wenzel S, Castro M, Corren J, Maspero J, Wang L, Zhang B, et al. Dupilumab efficacy and safety in adults with uncontrolled persistent asthma despite use of medium-to-high-dose inhaled corticosteroids plus a long-acting β_2 agonist: a randomised double-blind placebo-controlled pivotal phase 2b dose-ranging trial. *Lancet* (2016) 388:31–44. doi: 10.1016/S0140-6736(16)30307-5
137. Castro M, Corren J, Pavord ID, Maspero J, Wenzel S, Rabe K, et al. Dupilumab efficacy and safety in moderate-to-severe uncontrolled asthma. *N Engl J Med* (2018) 378:2486–96. doi: 10.1056/NEJMoa1804092

138. Corren J, Castro M, O'Riordan T, Hanania NA, Pavord ID, Quirce S, et al. Dupilumab efficacy in patients with uncontrolled, moderate-to-severe allergic asthma. *J Allergy Clin Immunol Pract* (2020) 8:516–26. doi: 10.1016/j.jaip.2019.08.050
139. Rabe KF, Nair P, Brusselle G, Maspero JF, Castro M, Sher L, et al. Efficacy and safety of dupilumab in glucocorticoid-dependent severe asthma. *N Engl J Med* (2018) 378:2475–85. doi: 10.1056/NEJMoa1804093
140. Seegraber M, Srour J, Walter A, Knop M, Wollenberg A. Dupilumab for treatment of atopic dermatitis. *Expert Rev Clin Pharmacol* (2018) 11:467–74. doi: 10.1080/17512433.2018.1449642
141. Bachert C, Hellings PW, Mullol J, Hamilos DL, Gevaert P, Naclerio RM, et al. Dupilumab improves health-related quality of life in patients with chronic rhinosinusitis with nasal polyposis. *Allergy* (2020) 75:148–57. doi: 10.1111/all.13984
142. Porsbjerg CM, Sverrild A, Lloyd CM, Menzies-Gow AN, Bel EH. Anti-alarmins in asthma: targeting the airway epithelium with next-generation biologics. *Eur Respir J* (2020) 56. doi: 10.1183/13993003.00260-2020. in press.
143. Matera MG, Rogliani P, Calzetta L, Cazzola M. TSLP inhibitors for asthma: current status and future prospects. *Drugs* (2020) 80:449–58. doi: 10.1007/s40265-020-01273-4
144. Ito T, Wang YH, Duramad O, Hori T, Delespesse GJ, Watanabe L, et al. TSLP-activated dendritic cells induce an inflammatory T helper type 2 cell response through OX40 ligand. *J Exp Med* (2005) 202:1213–23. doi: 10.1084/jem.20051135
145. Soumelis V, Reche PA, Kanzler H, Yuan W, Edward G, Homey B, et al. Human epithelial cells trigger dendritic cell mediated allergic inflammation by producing TSLP. *Nat Immunol* (2002) 3:673–80. doi: 10.1038/ni805
146. Allakhverdi Z, Comeau MR, Jessup HK, Yoon BR, Brewer A, Chartier S, et al. Thymic stromal lymphopoietin is released by human epithelial cells in response to microbes, trauma, or inflammation and potently activates mast cells. *J Exp Med* (2007) 204:253–8. doi: 10.1084/jem.20062211
147. Camelo A, Rosignoli G, Ohne Y, Stewart RA, Overed-Sayer C, Sleeman MA, et al. IL-33, IL-25, and TSLP induce a distinct phenotypic and activation profile in human type 2 innate lymphoid cells. *Blood Adv* (2017) 1:577–89. doi: 10.1182/bloodadvances.2016002352
148. Liu S, Verma M, Michalec L, Liu W, Sripada A, Rollins D, et al. Steroid resistance of airway type 2 innate lymphoid cells from patients with severe asthma: the role of thymic stromal lymphopoietin. *J Allergy Clin Immunol* (2018) 141:257–68. doi: 10.1016/j.jaci.2017.03.032
149. Tanaka J, Watanabe N, Kido M, Saga K, Akamatsu T, Nishio A, et al. and TLR3 ligands promote differentiation of Th17 cells with a central memory phenotype under Th2-polarizing conditions. *Clin Exp Allergy* (2009) 39:89–100. doi: 10.1111/j.1365-2222.2008.03151.x
150. Marone G, Spadaro G, Braile M, Poto R, Criscuolo G, Pahima H. Tezepelumab: a novel biological therapy for the treatment of severe uncontrolled asthma. *Expert Opin Invest Drugs* (2019) 28:931–40. doi: 10.1080/13543784.2019.1672657
151. Gauvreau GM, O'Byrne PM, Boulet LP, Wang Y, Cockcroft D, Bigler J, et al. Effects of an anti-TSLP antibody on allergen-induced asthmatic responses. *N Engl J Med* (2014) 370:2102–10. doi: 10.1056/NEJMoa1402895
152. Corren J, Parnes JR, Wang L, Roseti SL, Griffiths JM, van der Merwe R. Tezepelumab in adults with uncontrolled asthma. *N Engl J Med* (2017) 377:936–46. doi: 10.1056/NEJMoa1704064
153. Murakami-Satsutani N, Ito T, Nakanishi T, Inagaki N, Tanaka A, Vien PT, et al. IL-33 promotes the induction and maintenance of Th2 immune responses by enhancing the function of OX40 ligand. *Allergol Int* (2014) 63:443–55. doi: 10.2332/allergolint.13-OA-0672
154. Barlow JL, Peel S, Fox J, Panova V, Hardman CS, Camelo A, et al. IL-33 is more potent than IL-25 in provoking IL-13-producing nuocytes (type 2 innate lymphoid cells) and airway contraction. *J Allergy Clin Immunol* (2013) 132:933–41. doi: 10.1016/j.jaci.2013.05.012
155. Kaur D, Gomez E, Doe C, Berair R, Woodman L, Saunders R, et al. IL-33 drives airway hyper-responsiveness through IL-13-mediated mast cell-airway smooth muscle crosstalk. *Allergy* (2015) 70:556–67. doi: 10.1111/all.12593
156. Pelaia C, Crimi C, Vatrella A, Busceti MT, Gaudio A, Garofalo E, et al. New treatments for asthma: from the pathogenic role of prostaglandin D_2 to the therapeutic effects of fevipiprant. *Pharmacol Res* (2020) 155:104490. doi: 10.1016/j.phrs.2019.104490
157. Gonem S, Berair R, Singapuri A, Hartley R, Laurencin MFM, Bacher G, et al. Fevipiprant, a prostaglandin D_2 receptor 2 antagonist, in patients with persistent eosinophilic asthma: a single-centre, randomized, double-blind, parallel-group, placebo-controlled trial. *Lancet Respir Med* (2016) 4:699–707. doi: 10.1016/S2213-2600(16)30179-5
158. Bateman ED, Guerreros AG, Brockhaus F, Holzhauer B, Pethe A, Kay RA, et al. Fevipiprant, an oral prostaglandin DP_2 receptor (CRTh2) antagonist, in allergic asthma uncontrolled on low-dose inhaled corticosteroids. *Eur Respir J* (2017) 50:1700670. doi: 10.1183/13993003.00670-2017
159. Kalchiem-Dekel O, Yao X, Levine SJ. Meeting the challenge of identifying new treatments for type 2-low neutrophilic asthma. *Chest* (2020) 157:26–33. doi: 10.1016/j.chest.2019.08.2192
160. Nair P, Prabhavalkar KS. Neutrophilic asthma and potentially related target therapies. *Curr Drug Targets* (2020) 21:374–88. doi: 10.2174/1389450120666191011162526
161. Busse WW, Holgate S, Kerwin E, Chon Y, Feng J, Lin J, et al. Randomized, double-blind, placebo-controlled study of brodalumab, a human anti-IL-17 receptor monoclonal antibody, in moderate to severe asthma. *Am J Respir Crit Care Med* (2013) 188:1294–302. doi: 10.1164/rccm.201212-2318OC

Conflict of Interest: The authors declare that the research was conducted in the absence of any commercial or financial relationships that could be construed as a potential conflict of interest.

Copyright © 2020 Pelaia, Crimi, Vatrella, Tinello, Terracciano and Pelaia. This is an open-access article distributed under the terms of the Creative Commons Attribution License (CC BY). The use, distribution or reproduction in other forums is permitted, provided the original author(s) and the copyright owner(s) are credited and that the original publication in this journal is cited, in accordance with accepted academic practice. No use, distribution or reproduction is permitted which does not comply with these terms.

frontiers in Immunology

REVIEW
published: 08 January 2021
doi: 10.3389/fimmu.2020.608666

MicroRNAs as Potential Regulators of Immune Response Networks in Asthma and Chronic Obstructive Pulmonary Disease

José A. Cañas[1,2*], *José M. Rodrigo-Muñoz*[1,2], *Beatriz Sastre*[1,2], *Marta Gil-Martinez*[1], *Natalia Redondo*[1] *and Victoria del Pozo*[1,2*]

[1] Immunoallergy Laboratory, Immunology Department, Instituto de Investigación Sanitaria Fundación Jiménez Díaz (IIS-FJD), Madrid, Spain, [2] CIBER de Enfermedades Respiratorias (CIBERES), Madrid, Spain

OPEN ACCESS

Edited by:
Girolamo Pelaia,
University of Catanzaro, Italy

Reviewed by:
Chiaki Iwamura,
Chiba University, Japan
Kenta Shinoda,
National Institutes of Health (NIH),
United States

***Correspondence:**
Victoria del Pozo
vpozo@fjd.es
José A. Cañas
jose.canas@fjd.es

Specialty section:
This article was submitted to Inflammation, a section of the journal Frontiers in Immunology

Received: 21 September 2020
Accepted: 23 November 2020
Published: 08 January 2021

Citation:
Cañas JA, Rodrigo-Muñoz JM, Sastre B, Gil-Martinez M, Redondo N and del Pozo V (2021) MicroRNAs as Potential Regulators of Immune Response Networks in Asthma and Chronic Obstructive Pulmonary Disease. Front. Immunol. 11:608666. doi: 10.3389/fimmu.2020.608666

Chronic respiratory diseases (CRDs) are an important factor of morbidity and mortality, accounting for approximately 6% of total deaths worldwide. The main CRDs are asthma and chronic obstructive pulmonary disease (COPD). These complex diseases have different triggers including allergens, pollutants, tobacco smoke, and other risk factors. It is important to highlight that although CRDs are incurable, various forms of treatment improve shortness of breath and quality of life. The search for tools that can ensure accurate diagnosis and treatment is crucial. MicroRNAs (miRNAs) are small non-coding RNAs and have been described as promising diagnostic and therapeutic biomarkers for CRDs. They are implicated in multiple processes of asthma and COPD, regulating pathways associated with inflammation, thereby showing that miRNAs are critical regulators of the immune response. Indeed, miRNAs have been found to be deregulated in several biofluids (sputum, bronchoalveolar lavage, and serum) and in both structural lung and immune cells of patients in comparison to healthy subjects, showing their potential role as biomarkers. Also, miRNAs play a part in the development or termination of histopathological changes and comorbidities, revealing the complexity of miRNA regulation and opening up new treatment possibilities. Finally, miRNAs have been proposed as prognostic tools in response to both conventional and biologic treatments for asthma or COPD, and miRNA-based treatment has emerged as a potential approach for clinical intervention in these respiratory diseases; however, this field is still in development. The present review applies a systems biology approach to the understanding of miRNA regulatory networks in asthma and COPD, summarizing their roles in pathophysiology, diagnosis, and treatment.

Keywords: chronic respiratory diseases, systems biology, microRNAs, asthma, chronic pulmonary obstructive disease

INTRODUCTION

Chronic respiratory diseases (CRDs) like asthma and chronic obstructive pulmonary disease (COPD) are complex and heterogeneous diseases that pose a challenge for investigation and management. Multiple environmental factors and genetic predisposition modulate asthma and COPD phenotypes and severity, as well as how a patient responds to treatment. In these diseases, genomics, metabolomics, epigenomics, and transcriptomics engage in intricate interaction at the cellular level. Systems biology tries to construct models or approaches throughout the network that reveal the underlying biology and help to understand living systems. Traditionally, gene modulation and cell-signaling networks have been thought to be the main regulatory systems in cells, and RNAs have been considered molecules that only codify genetic information to protein synthesis. However, this idea is changing due to the recent advances in non-coding RNAs, such as microRNAs (miRNAs) (1). MiRNAs are 18–22 nucleotides in length and block protein translation by RNA-miRNA interaction (2). These small RNAs regulate hundreds to thousands of genes, offering a broad combinatorial possibility and constituting complicated regulatory networks. As a result, systems biology approaches are essential to understand miRNAs functions in complex diseases such as asthma and COPD, combining data from high-throughput experiments with computational models for performance of data driven modeling and model driven experimental methods (**Figure 1**).

New procedures have been applied in this topic, particularly to determine the coordinate function of miRNAs in cancer. Lai et al. used a systems biology approach to unravel the role of miRNAs therapeutics in this disease (3, 4). This approach highlights the importance of high-throughput experiments to determine from the same biological experiments the transcriptome of miRNAs and their gene targets, with further exploration by proteomic data, or immunoprecipitation-based analysis, as this is very helpful in validating the huge amount of predicted miRNA-gene interactions detected *in silico* by diverse bioinformatic tools reviewed by Gomes et al. (5). After getting this data, then it is easier to apply computational biology approaches, most of them based on previously validated data for gene-miRNA interaction determination. After this, system biology comes in, because as previously stated it helps in creating maps of miRNA-gene-pathway interactions that may have an actual function in cell physiology (6). The actual mapping can be further detailed by introducing the regulation that occurs on the controllers (miRNAs) themselves, as we have to take into account miRNA biogenesis and structure, epigenetics, epitranscriptomics, transcription factor circuits and super enhancers, all of them modulating miRNAs functions in diseases (7).

In this review, we will focus on asthma and COPD, two of the most common CRDs worldwide, providing an overview about those molecular pathology mechanisms by miRNAs. Additionally, we will explore new insights in the field of miRNAs as biomarkers of these diseases. Lastly, we will highlight altered after specific treatment for each disease and discuss clinical advances in the use of miRNAs. With this review we want to set the foundations of actual data of miRNAs as regulators and biomarkers of chronic respiratory diseases, being able to serve as a guide for future application of complex system biology approaches to determine the actual combined effects of this miRNAs in these diseases, seeing the big picture of the pathophysiology.

PATHOPHYSIOLOGY OF ASTHMA AND COPD

CRDs are an important cause of morbidity and mortality worldwide. According to the World Health Organization, the most common CRDs are asthma, COPD, lung hypertension, and occupational lung diseases (8). It is estimated that more than 300 million people worldwide have asthma and 3 million people die each year from COPD, accounting for an estimated 6% of total deaths globally (8).

The causes triggering the development of CRDs are diverse. Asthma is a multifactorial and heterogeneous disease, and a variety of risk factors have been linked to this disease such as genetics, atopy, and recurrent viral infections (9). Additionally, tobacco has been described as the main cause of COPD, though exposure to other toxic substances such as air pollution originated from biomass fuel has been also linked to COPD (10, 11). Independently of origin, CRDs are characterized by the inflammation and obstruction of the lower respiratory tract due to a hyperresponse of the immune system accompanied by cellular infiltration (12, 13). In allergic asthma, the predominant leucocytes are eosinophils, with a triggered type 2 immune response with high abundance of interleukin (IL)-4, IL-5, and IL-13 (14, 15); however, in COPD the most abundant cellular populations are neutrophils, macrophages, and T lymphocytes (11, 13).

Asthma presents with high variability among patients, thus posing a challenge for the improvement of diagnostic and therapeutic tools (16). Asthma is characterized by chronic airway inflammation, mucus hypersecretion, and bronchial hyperresponsiveness and the presence of respiratory symptoms such as wheezing, shortness of breath, chest tightness, and cough (17). Airway inflammation and structural remodeling together with reversible airflow obstruction and airway hyperreactivity are the main distinctive findings of asthmatic disease (18). In addition, asthma encompasses several disease variants, meaning that it can

Abbreviations: α-SMA, alpha-smooth muscle actin; ACO, Asthma-COPD overlapping; ASMC, airway smooth muscle cells; AUC, area under curve; BALF, bronchoalveolar lavage fluid; COPD, chronic obstructive pulmonary disease; COX-2. cyclooxygenase-2; CRDs, chronic respiratory diseases; CSE, cigarette smoke extract; FEV1, forced respiratory volume in the first second; GCs, glucocorticoids; HBECs, human bronchial epithelial cells; HDAC, histone deacetylase; HIF-1α, hypoxia-inducible factor 1-alpha; ICS, inhaled corticosteroid; IFN-γ, interferon gamma; IL, interleukin; lncRNA, long-noncoding RNA; MAPK, mitogen-activated protein kinase; miRNAs, microRNAs; PBMCs, peripheral blood mononuclear cells; PGE2, prostaglandin E2; PI3K, phosphatidylinositol 3-kinase; ROS, reactive oxygen species; TGF, transforming growth factor; TLR, Toll-like receptor; TNF, tumor necrosis factor.

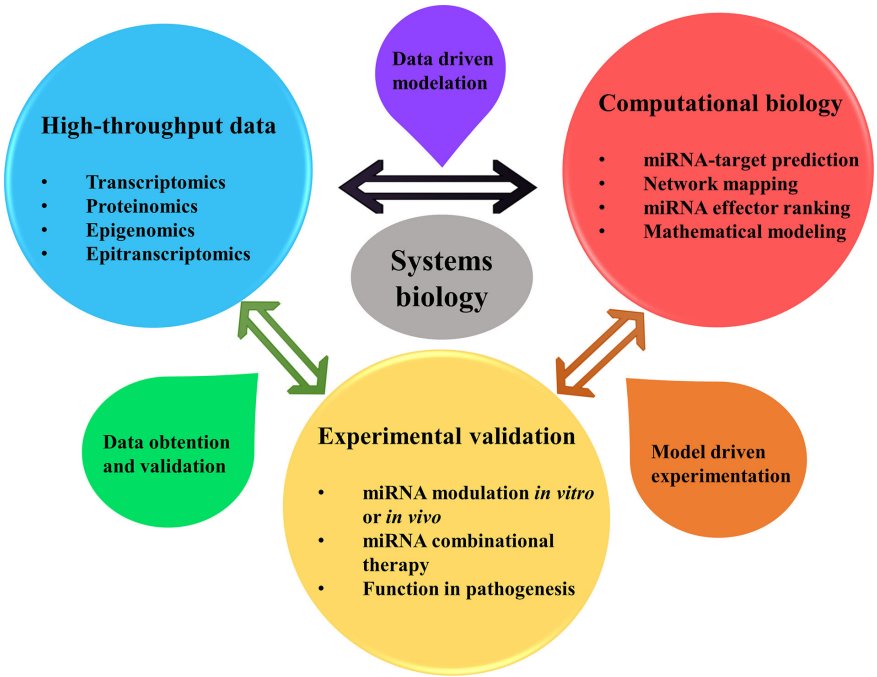

FIGURE 1 | Systems biology approaches allow for better understanding the roles of miRNAs in pathophysiology, diagnosis, and treatment of asthma and COPD. Being miRNAs regulators of multiple genes expression affecting thus several pathways simultaneously, a comprehension of the global picture of their regulation is in need. System biology approach helps in this matter, by using a data driven method for creating computational models from previous data of high-throughput experimentation (transcriptomics, proteomics, epigenomics and epitranscriptomics) that could be obtained from the literature. Network mapping modeling allows determining the interaction between miRNAs, genes (or proteins) and phenotype and clinical data. Besides, mathematical models can help finding key miRNAs with power to alter the core of cellular pathway regulation and performance. After this, model driven experimentation allows to confirm the predicted targeting by miRNAs in cooperation by their modulation *in vivo* or *in vitro*, uncovering their role in the disease and their use in therapy. Finally, this new data obtained and validated can be summed up to confirm previous high-throughput results, enlarging the available data of miRNA regulation in asthma or COPD.

be stratified into several phenotypes and endotypes. Phenotyping and endotyping of asthma with the use of induced sputum or peripheral blood cytology can facilitate responsiveness to treatment, specify the pathogenic mechanisms, and anticipate risks. These features attest to the complexity of asthmatic disease and the numerous factors involved in its pathophysiology, suggesting that systems biology can aid in understanding the key factors implicated in molecular networks.

COPD is a multifactorial and heterogeneous disease that affects millions of people worldwide (19). This pathology is a major cause of chronic morbidity and mortality, and many people bear the burden of this disease for years. COPD encompasses small airway obstruction, emphysema, and chronic bronchitis, and it is characterized by chronic inflammation of the airways and lung parenchyma with progressive and irreversible airflow limitation (20). Symptoms include dyspnea, cough, and sputum production (21). The phenotypic characterization of COPD patients may allow for better risk stratification and personalization of therapy (22). Airway damage in COPD is triggered by dust, fumes, vapors, or gas, but the primary factor is exposure to tobacco smoke (23). Cigarette smoke alters both innate and adaptive immunity by upregulating cytokines (IL-1, IL-6, IL-8, tumor necrosis factor [TNF]-α…) (24, 25), and modifying the physiological function of alveolar macrophages (26), dendritic cells (27), neutrophils (28), and natural killer cells (29). Smoking also modifies the behavior of the epithelium by increasing mucin production (MUC5AC) (30) and disrupting epithelial cell-cell junctions, thus increasing the permeability of the epithelial barrier (31).

It has been shown that besides altering the normal physiology of the airways, cigarette smoke may change the epigenetic landscape, and these changes can be passed on to future generations through inheritance (32). Several studies show that COPD causes certain epigenetic changes in the lungs (33, 34), and many of these changes are likely due to tobacco smoke exposure (35), such as *F2RL3* methylation, which is associated with smoking behavior and high mortality (7, 36). These epigenetic changes can be targeted as a possible therapy; current genetic editors like zinc-finger nucleases and CRISPR-Cas9 can be coupled to them and enzymes to rewrite epigenetic markers induced by tobacco smoke or related to COPD pathophysiology (37, 38).

MiRNAs IN LUNG DISEASES

The complex interplay between genetics, epigenetics, protein synthesis, and immune response in asthma and COPD is actually even more intricate when another layer of regulation is introduced:

miRNAs. These small molecules or noncoding RNAs are capable of regulating the gene-protein expression of immune system performance (39) and structural airway homeostasis and function (40). Moreover, miRNAs can regulate epigenetic modulators and be regulated by epigenetic changes as well (41). MiRNAs are therefore essential players in the physiopathology of both diseases, creating complex networks and interactions among diverse factors (genes, proteins, cells) that play a role in these pathologies (**Figure 2**).

It is important to differentiate between two kinds of miRNAs: intracellular and extracellular (found inside extracellular vesicles such as exosomes, microvesicles, and apoptotic bodies) (42). Intracellular miRNAs regulate several cellular pathways, and their expression is tissue- and disease-specific, so they have been widely used as prognostic and diagnostic biomarkers of different pathologies, including viral infections, cancer, cardiovascular and allergic diseases (43, 44). Also, circulating miRNAs have been studied and used as biomarkers due to their molecular properties (resistance to degradation and ubiquity) (45).

MiRNAs as Asthma Biomarkers

Circulating cell-free miRNAs can be found in serum or plasma incorporated into extracellular vesicles, such as exosomes, and in ribonucleoprotein complexes. There are many studies showing miRNA deregulation in asthmatic patients (**Table 1**). It is known that several miRNAs are increased in serum samples including miR-21, miR-145, miR-146a, and miR-338, among others (45, 70). Likewise, other authors have described downregulation of other serum miRNAs, such as miR-18a, miR-126, and miR-155 (71). However, due to the complex relation between miRNAs and genes (a single miRNA can regulate hundreds of genes), not all miRNAs qualify for use as biomarkers. One solution to this problem may be to use combinations of several miRNAs or a specific miRNA profile to achieve good sensitivity, specificity, and positive and negative predictive values.

In 2016, Panganiban et al. established a differential miRNA profile among asthmatic patients, non-asthmatic patients with allergic rhinitis, and non-asthmatic non-allergic subjects (45). In their study, the researchers found 30 miRNAs in plasma that were differentially expressed among three groups, showing six miRNAs (miR-125b, miR-16, miR-299-5p, miR-126, miR-206, and miR-133b) with a high predictive value when differentiating allergic and asthmatic status. Moreover, some of these circulating miRNAs grouped asthmatic patients into two clusters according to the number of peripheral blood eosinophils. Finally, they

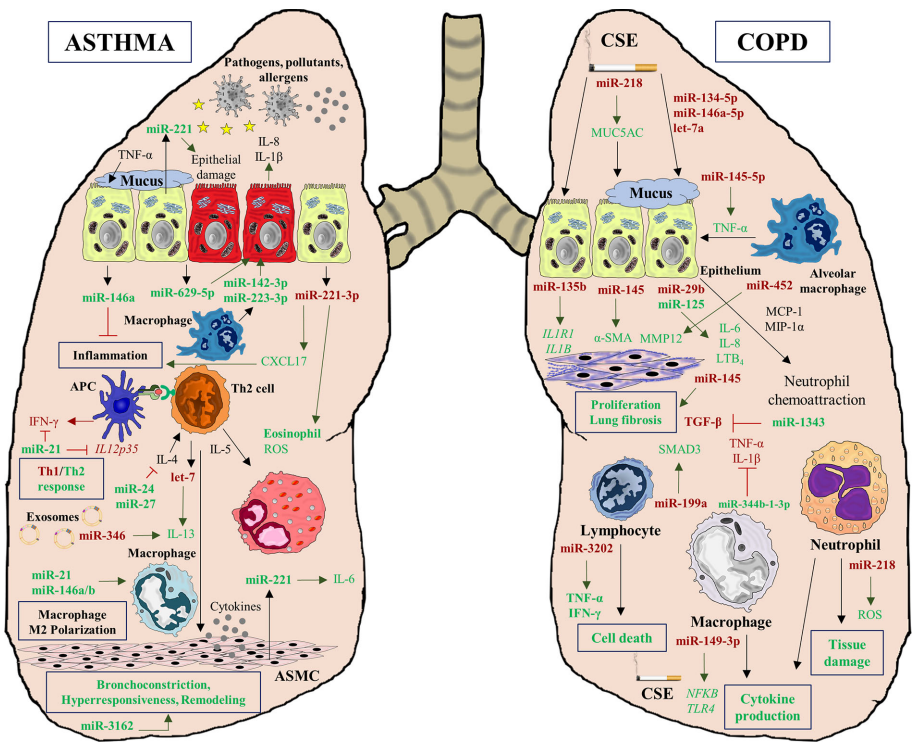

FIGURE 2 | MiRNA interactions in asthma and COPD diseases. MiRNAs play a crucial role, regulating multiples processes characteristics of both pathologies. In asthma, deregulation of multiples miRNAs affects to inflammatory processes (miR-221-3p), Th1/Th2 response imbalance (miR-21), cytokine production (miR-629-5p, miR-142-3p, and miR-223-3p), epithelial injury (miR-221), macrophage polarization to M2 phenotype (miR-146a/b, miR-21) and airway remodeling (miR-3162). However, miRNAs also can alleviate inflammation (miR-146a) and cytokine decrease production (miR-24 and miR-27). In COPD pathogenesis, miRNAs can be altered by CSE exposition and they are involved in mucus hypersecretion (miR-218) and cytokine production (miR-149-3p). Moreover, several deregulated miRNAs are implicated in lung fibrosis (miR-135b, miR-145, and miR-452), and in tissue damage (miR-218). Similarly to asthma, in COPD some miRNAs can act as regulators of inflammation decreasing the secretion of several cytokines such as TGF-β (miR-1343), TNF-α, and IL-1 β (miR-344b-1-3p).

TABLE 1 | List of miRNAs involved in asthma pathogenesis.

miRNA	Implication	Origin	Expression	Target Gene/Pathway	References
miR-140-3p	CD38 expression, chemokine regulation, inflammation and ASMC proliferation in asthma	ASMC	Downregulated	*CD38, CCL11, CXCL12, CXCL10, CCL5, CXCL8*	(46, 47)
miR-145	ASMC proliferation and migration		Upregulated	*KLF4*	(48)
miR-146a-5p	Mucus production		Downregulated	*UBD, CXCL10, CXCL8, CCL20, UCA1*	(49)
miR-638	ASMC proliferation and migration		Upregulated	*NR4A3, CCND1*	(50)
miR-708	CD38 expression, chemokine regulation, inflammation and ASMC proliferation in asthma		Downregulated	*CD38, CCL11, CXCL10, CCL2, CXCL8*, JNK, MAPK, PTEN/AKT signaling pathways	(47, 51)
miR-146a/b	Regulation of inflammation, macrophage M2 polarization	Epithelial cells, macrophages	Upregulated	*PTGS2, IL1B, NOTCH5*	(52–56)
let-7 family	Asthma biomarker	BALF-derived exosomes	Downregulated		(57)
miR-126	Asthma progression		Upregulated	*DNMT1*	(58)
miR-200 family	Asthma biomarker		Downregulated		(57)
miR-346	Airway inflammation, T helper cell differentiation		Downregulated	*IL13*	(59)
miR-574-5p			Downregulated	*IL5RA*	(59)
let-7	Regulation of asthmatic hyperresponse	Lung	Upregulated	*IL13*	(60)
miR-24	Cytokine regulation		Upregulated	IL-4 production pathway	(61)
miR-27			Upregulated	*GATA3*	(61)
miR-16	Asthma biomarker	Plasma	Upregulated		(45)
miR-125b			Upregulated		(45)
miR-133b			Downregulated		(45)
miR-206			Upregulated		(45)
miR-144-5p	Asthma biomarker	Serum	Upregulated		(43)
miR-155			Upregulated		(62)
miR-185-5p			Upregulated		(43)
miR-320a			Upregulated		(43)
miR-1246			Upregulated		(43)
miR-485-5p	Pediatric asthma		Upregulated	*SPRED2*	(63)
miR-3162-3p			Upregulated	*CTNNB1*	(64)
miR-221	Pediatric asthma, Epithelial cell injury	Serum, epithelial cells	Upregulated	*SPRED, SIRT1*	(63, 65)
miR-21	Imbalance Th1/Th2 response, macrophage M2 polarization	Serum, lung, macrophage	Upregulated	*IL12p3, IRF5, CSF1R*	(43, 52, 54, 62, 66, 67)
miR-142-3p	Neutrophilic asthma	Sputum	Upregulated	MAPK, NOD-like receptor, Toll-like receptor, JAK-STAT, and the TGF-β signaling pathways	(68)
miR-223-3p			Upregulated		(68)
miR-629-3p			Upregulated		(68)
miR-221-3p	Regulation of eosinophil counts and ROS production		Downregulated	*CXCL17*	(69)

demonstrated that circulating miRNAs could be used to diagnose both allergic rhinitis and asthmatic patients and characterize asthma subtypes. Milger et al., in 2017, identified some possible plasma miRNA candidates as biomarkers in a murine model of asthma (72). These miRNAs were validated in a different cohort of healthy subjects and asthmatic patients, using a regularized logistic regression model to identify five miRNA ratios that are able to differentiate allergic asthmatics from controls with an area under the curve (AUC) of 0.92. However, this miRNA signature did not differentiate asthma sub-phenotypes.

Our group recently described an eosinophil miRNA profile for asthma diagnosis based on statistical models (43). First, we described a miRNA signature from peripheral blood eosinophils, which is able to differentiate asthmatic subjects from healthy controls. Among deregulated miRNAs, we found upregulation of miR-21 and miR-146a/b, which have been associated with

asthma and allergic diseases (73). In addition, this molecular profile grouped the asthmatic population into two principal clusters, which are distinguishable by the number of peripheral blood eosinophils and serum periostin levels. Then, we evaluated these miRNAs in serum and found that miR-1246, miR-144-5p, miR-320a, miR-185-5p, and miR-21-5p were upregulated in asthmatic patients. Specifically, miR-185-5p was related to asthma severity. Combination of miR-185-5p, miR-144-5p, and miR-1246 in a logistic regression model distinguished healthy individuals from asthmatics with an AUC of 0.86, and a specificity and sensitivity of 0.89 and 0.77, respectively. Serum expression of miR-320a, miR-185-5p, and miR-144-5p was used to classify subjects into different asthma disease phenotypes (intermittent, mild persistent, moderate persistent, and severe persistent) in a random forest model, showing that miRNAs can be used for asthma diagnosis and severity classification. Unfortunately, to date no more studies about specific miRNAs of eosinophils have been conducted, making this is a field of potential research focus.

Elkashef et al. have reported the use of miR-21 and miR-155 as biomarkers in bronchial asthma (62). They showed that both miRNAs are higher in serum of individuals with eosinophilic asthma than healthy subjects. Through a receiver operating characteristic curve with both miRNAs, the authors obtained high values for sensitivity, specificity, and AUC. Thus, they proposed that these miRNAs could be used as non-invasive biomarkers in asthma diagnosis and response to therapy.

As mentioned previously, another important factor in asthma pathogenesis is the role that exosomes exert in the disease (74). These particles are nanovesicles, with a diameter of 30–150 nm, and their main role is linked to intercellular communication. It is worth highlighting that these small vesicles contain miRNAs in addition to DNA, proteins, and lipid mediators. Thus, some circulating miRNAs have been associated with exosomes and it has been observed that these exosomal miRNAs play a critical role in asthma pathogenesis (75, 76).

It is important to take into account that exosomes can be located in multiple biological fluids including serum, sputum, bronchoalveolar lavage fluid (BALF), urine, breast milk, etc., and that exosomes are associated with multiple pathological processes, including asthma (16). In 2013, Levänen et al. found significant differences in a set of exosomal miRNAs from BALF between mild asymptomatic asthmatic patients and healthy subjects, including miRNAs of the let-7 and miR-200 families (57). Later, Gon et al. showed 139 exosomal miRNAs from BALF deregulated in a house-dust mite murine model compared to control mice (59). Also, they observed that 54 altered miRNAs were common between exosomes and lung tissues. Using computational analysis, the authors then found that 31 genes were the targets of these miRNAs, including important genes in asthma pathogenesis such as *IL13* and *IL5RA*.

Different studies have been conducted in exosomes from serum (58, 77). These showed that several miRNAs, including miR-125b and miR-126, were altered in these nanovesicles between asthma condition and normal status. According to the authors, these results can be applied to the use of novel diagnostic strategies.

Sputum miRNAs Characterize the Inflammatory Focus

While it is clear that serum/plasma miRNAs are good non-invasive biomarkers, miRNAs from sputum samples could also be used as diagnostic tools. However, the number of studies in this field reduced drastically and only a few research articles address this topic (**Table 1**). One of them was performed in 2018, conducted by Zhang et al. (69). In this study, the authors found that sputum and plasma miR-221-3p levels were significantly decreased in asthmatics compared with healthy subjects. Furthermore, there was a positive correlation between plasma and induced sputum miR-221-3p levels and values of this miRNA in epithelial cells, just like a negative correlation with the eosinophil percentage in sputum, the number of eosinophils in bronchial biopsies, and fraction of exhaled nitric oxide levels. The study highlighted that sputum miR-221-3p levels were increased in asthmatic patients after 4 weeks of inhaled corticosteroid (ICS) treatment, compared with asthmatic patients at baseline. With these data, the researchers proposed that sputum miR-221-3p could be used as a biomarker for airway eosinophilic inflammation and response to treatment. In another study performed in 2016, Maes et al. showed a different miRNAs profile in sputum samples among healthy subjects, patients with mild-to-moderate asthma, and patients with severe asthma (68). They presented three miRNAs that were increased in sputum samples from patients with severe asthma, which are related to neutrophilic asthma phenotype (**Table 1**).

MiRNAs for Characterization of COPD

Study of miRNAs has been rapidly extended to respiratory diseases including COPD, likely due to research showing that cigarette smoke acts as a modulator of miRNA regulation in samples such as lung tissue (78, 79), serum (80) and sputum (81) (**Table 2**). Therefore, similarly to asthma, there are miRNAs that can serve as biomarkers for COPD against healthy conditions in different biofluids. MiRNAs also regulate the expression of genes in COPD. Several miRNAs have been implicated in the physiopathology of COPD (89, 149). However, it is also important to mention that some miRNAs are also related to protective functions in COPD pathology when induced by treatment (144).

Related to lung function, some miRNAs have shown correlation with worse pulmonary function values in COPD, some of them being directly correlated with forced expiratory volume in the first second (FEV_1) values (81, 104, 106, 130); while others, correlate negatively (96, 125); and even, in other cases, present a negative correlation with FEV1/FVC ratio (97, 113, 122) (**Table 2**).

Regarding characteristic processes of COPD, fibrosis is almost the main pathological event that occurs in this disease. MiR-1343 reduce transforming growth factor *(TGF)-β* receptors I and II, *SMAD2* and *SMAD3*, which are fibrotic factors (150), whereas miR-145 may have profibrotic effects, inducing differentiation of

TABLE 2 | List of miRNAs involved in COPD pathogenesis and diagnosis.

miRNA	Implication	Origin	Expression	Target Gene/Pathway	References
miR-452	Control of airway inflammation and remodeling	Alveolar macrophages	Downregulated	*MMP12*	(82)
miR-344b-1-3p	Modulator of the immune responses by CSE		Upregulated	*TLR2*	(83)
miR-637	Development of pulmonary hypertension	Artery smooth muscle cells	Downregulated	*CDK6*	(84)
miR-197	Vascular remodeling and contraction		Downregulated	*E2F1*	(85)
mir-106a-363 and -106b cluster	COPD diagnosis and severity	BALF, plasma, leukocytes	Upregulated/ downregulated	*AKT1, PTEN, MYD88, IRAK4, IL6, TGF-βR*	(86–88)
miR-146a	Inflammation and mucus secretion	BECs, fibroblasts, macrophages, plasma, lung tissue	Upregulated/ downregulated	*IRAK1/TRAF6, PGE2, COX2, PDE7A, IL-1R kinase-1*	(52, 89–95)
miR-195	Cytokine production and inflammation	BECs, lung tissue	Upregulated	*PHLPP2*	(96)
miR-132	Direct correlation to FEV1/FVC%	BECs, monocytes, serum	Upregulated	*SOCS5*	(97)
Profile of 9 miRNAs	Lung cancer prediction in COPD patients	Blood cells	Downregulated	*SRCAP, DCTN5, ULK1, and SEMA7A*	(98)
miR-183 (-5p)	Increases disease severity and pathogenesis	Blood, lungs, smooth muscle cells, leukocytes	Upregulated/ downregulated	*BKCaβ1, Autophagy, TLR, NSCLC, cardiomyopathy*	(88, 99)
Profile of 5 miRNAs	Differentiating healthy, asthma and COPD	Breath exhaled condensate	Downregulated in asthma	*IL-13, IL-5, GATA3, FcεR1 β, IL-1 β, MMP-1, Mucin-1*	(100)
miR-29b	Regulation of cytokine expression	Bronchial epithelial cells	Downregulated	*BRD4*	(101)
miR-10a-5p	Pathobiology of COPD and asthma		Upregulated	*FOXO3 and PDE7A*	(94)
miR-132-212, -17-92, -192-194 clusters	COPD diagnosis against lung cancer	BALF	Downregulated	*AKT1, ERBB2, KRAS, PTEN, MYD88*	(87)
miR-191	Endothelial injury and inflammation	Circulating endothelial microparticles released by CSE	Upregulated		(102)
miR-638	Regulation of oxidative stress response	Emphysematous lung tissue	Upregulated	*ADAM15, HDAC5, APBB1*	(103)
miR-126	Endothelial injury and inflammation	Endothelial microparticles, ECs, UVECs	Upregulated/ downregulated	*ATM protein kinase*	(102, 104)
miR-125a (-5p), 125b	Inflammation, severity and AECOPD	Endothelial microparticles, leukocytes, sputum, plasma	Upregulated	*Autophagy, TLR, NSCLC, cardiomyopathy*	(81, 88, 102, 105)
miR-503	Correlate with pulmonary function (FEV1)	Lung fibroblasts	Downregulated	*VEGF*	(106)
miR-335-5p	Modification of fibroblast behavior and function		Downregulated	*Rb1, CARF, and SGK3*	(107)
miR-31-5p	Regulator of mucus hypersecretion	Lung tissue	Upregulated	*ST3GAL2, PITPNM2, ARHGEF15*	(108)
miR-1274a, -424	Emphysema and fibrosis.	Lung tissue and bronchial epithelial cells	Upregulated	*IL-6, TEP1, CAT, TGFβ, and WNT pathway*	(79)
miR-134-5p	Chronic mucus hypersecretion homeostasis		Downregulated	*KRAS*	(90)
miR-150	Suppression of CSE-induced inflammation		Downregulated	*P53*	(109)
miR-223	Emphysema, fibrosis, immunity	Lung tissue, BECs	Upregulated	*IL-6, TEP1, CAT, TGFβ, WNT, HDAC2*	(79, 110)
let-7 family (a,c,d)	Mucus, inflammation, malignancy	Lung tissue, BECs, BEC, sputum, serum	Upregulated/ downregulated	*EDN1, IL-13, TGF- βR, TLR4, c-myc, TNFR-II*	(78, 81, 90, 100, 102, 111, 112)
miR-21	Lung function, inflammation, CRD differentiation	Lung tissue, BECs, exosomes, serum, plasma, BEC	Upregulated/ downregulated	*GF-β/Smad, PTEN, PI3K/HDAC2, Notch1, IL-13R, STAT3, IL-1 β*	(95, 100, 113–119)
miR-101	Mucus homeostasis and inflammation	Lung tissue, macrophages	Upregulated	*MKP-1*	(120)

(Continued)

TABLE 2 | Continued

miRNA	Implication	Origin	Expression	Target Gene/Pathway	References
miR-218 (-5p)	Malignant transformation, lung function	Lung tissue, BECs, serum	Downregulated/ upregulated	*BMI1, TNFR1*	(121–124)
miR-199a-5p	Negative correlation with pulmonary function	Lung tissue, PASMCs, Treg	Upregulated/ downregulated	*HIF-1α, SMAD3, TGF-β pathway*	(125–127)
miR-146b	Regulating innate macrophage responses	Macrophages	Upregulated	*STAT1*	(53)
profile of 8 miRNAs including miR-135b	Diagnosing AECOPD, inflammation	PBMCs, BECs	Upregulated	*IL-1R1 and IL-1β*	(128, 129)
miR-1273g-3p, -24-3p, -93-5p	Correlated with pulmonary function (FEV1)	Peripheral mononuclear cells	Downregulated	*IL18, IL1B, TNF, NFKBIA, CCL3, and CCL4*	(130)
Profile of 5 miRNAs	Differentiation of COPD and asthma	Plasma	Different expression between COPD and asthma	*Interferon-gamma inducible*	(131)
Profile of 9 miRNAs	Differentiation of COPD	Plasma and airway epithelial cell EVs	5 upregulated and 4 downregulated	*Inflammation, extracellular matrix and remodeling*	(132)
miR-206	Apoptosis, atrophy, inflammation	pvASMCs, limb tissue, fibroblasts	Upregulated	*Notch3, VEGF, HDAC3, HDAC4, IGF-1, SIRT-1, IRAK1*	(133–135)
miR-20a, -28-3p	COPD diagnosis	Serum	Downregulated		(136)
Profile of 9 miRNAs	Environmental factors in COPD subjects		Differentially expressed		(137)
miR-1	Atrophy	Serum / limb tissue	Downregulated / Upregulated	*pAKT, HDAC3, HDAC4, IGF-1, SIRT-1*	(133, 138)
miR-7	COPD diagnosis, inflammation	Serum, ASMCs	Upregulated	*Epac1*	(136, 139)
miR-100 (-5p)	COPD severity	Serum, leukocytes	Downregulated/ upregulated	*Autophagy, TLR, NSCLC, cardiomyopathy*	(88, 136)
miR-34 (a, b, c, c-5p)	Lung function, apoptosis, emphysema	Serum, lung tissue, pmvECs, BECs, sputum	Downregulated/ upregulated	*HIF-1α, Notch-1R, SIRT-1 and 6, SERPINE1*	(81, 125, 136, 140–142)
miR-181a, c	COPD development, inflammation, ROS	Serum, lung tissue, BECs	Downregulated	*MMP, cell growth, apoptosis, NKs, CCN1*	(118, 143)
miR320a, b,d	CRD differentiation, lung function, inflammation	Serum, PBMCs, BECs	Upregulated	*T-cellR, FoxO, TGF-β, MAPK, PI3K-AKT, IL1B*	(130, 144, 145)
miR-30a-3p	Correlate with pulmonary function (FEV1)	Sputum	Downregulated		(81)
miR-145	Differentiating CRDs, fibrosis and immunity	Sputum, serum, ASMCs, BECs, lung tissue, plasma	Upregulated/ downregulated	*SMAD3, KLF4 CFTR, KLF5*	(70, 111, 131, 146–148)
miR-338/(-3p)	Differentiation of asthma, COPD and ACO	Sputum, serum, plasma	Upregulated/ downregulated	*RAB14, IGF2R*	(70, 131)
miR-27a	Associated to muscle weakness and atrophy	Vastus lateralis from limb tissue	Upregulated	*HDAC3, HDAC4, IGF-1 and SIRT-1*	(133)

lung myofibroblasts, while also negatively regulating cytokine expression of airway smooth muscle cells (ASMCs) (146, 147). Mucus hypersecretion, is in turn regulated by several miRNAs in bronchial biopsies by targeting the mucin-related genes (90) (**Table 2**). Other miRNAs, such as miR-101 and miR-144, are upregulated in COPD lungs activating the ERK pathway (120, 151), while miR-15b is also increased in COPD lungs, and the expression of its target *SMAD7* is decreased (79).

MiRNAs are also important in COPD comorbidities like limb-muscle weakness, as it has been shown that miR-1, miR-206, and miR-27a are upregulated in limb tissues from weak muscle COPD (133). Decreased levels of miR-637 in COPD pulmonary artery smooth muscle cells (PASMCs) are related to pulmonary hypertension (84), while miR-197 is involved in ASMCs proliferation and phenotype (85), and miR-183 expression is augmented in blood from COPD and related to disease severity, targeting *KCNMB1* in lungs and smooth muscle cells (99).

Some miRNAs have been associated with emphysema, another COPD hallmark, like miR-638 (103); or miR-223 (110). On the contrary, others present protective effects on emphysema, like miR-452, appearing downregulated in alveolar macrophages from COPD (82), or miR-34c, that is also downregulated in moderate compared to mild emphysematous tissue (140).

Cigarette Smoke Induces Tissue miRNA Changes Associated With Malignancy

As previously said, miRNAs are profoundly implicated in the regulation of pathogenesis of respiratory diseases such as asthma and COPD. To begin with, miRNAs are affected by cigarette smoke exposure. Many researchers have studied the effect of cigarette smoke extract (CSE), both *in vivo* and *in vitro*, showing modulations in miRNA expression that are accompanied by the consequent functional effect.

In COPD, control of the inflammation induced by cigarette smoke is critical and is performed by miRNAs like miR-135b or

miR-29b, that regulates *IL1R1*, *IL1β*, and IL-8, respectively (128, 152). Indeed, in lung tissue and blood from COPD individuals, several cytokines such as IL-6 or TNF-α are found downregulated by the action of miR-203 (153). MiR-146a plays an important role in COPD as previously commented. It is upregulated in response to cigarette smoke and fine-tunes the immune response by controlling cyclooxygenase-2 (COX-2) expression in fibroblasts (91). MiR-146a is also upregulated in epithelial cells in response to particulate matter and acts as a negative feedback loop that involves IL-6 and IL-8 (NF-κβ signaling) (92). Nevertheless, the function of this miRNA might be more complex, as another study showed that fibroblasts from COPD stimulated with IL-1β and TNF-α produce less miR-146a, resulting in a high prostaglandin E_2 (PGE_2) expression (89). This can be supported by data that show that the minor allele of the rs2910164 polymorphism associates with less miR-146a expression and higher PGE_2 levels (154). This complexity might be explained by how this miRNA is expressed in a cell-specific manner as it seems to be downregulated in COPD sputum but overexpressed in lung tissue (79, 81).

This is not the only association of miRNA polymorphisms in COPD. Some polymorphisms provide resistance, as in rs3746444 (miR-499) and rs11614913 (miR-196a2), both associated with COPD protection, bronchodilator response and, to a lesser extent, COX-2 expression (miR-146 single nucleotide polymorphisms) (154–157).

Another study showed that miR-218-5p is reduced in lung tissue from COPD and healthy smokers and in mice and 16HBE exposed to CSE, and its expression correlates directly with FEV_1 values. This miRNA performs a protective role by reducing the inflammation in COPD lungs (122, 123), something that has been corroborated by other studies (101, 122–124). Similarly, miR-181c targets *CCN1* and reduces inflammation, reactive oxygen species (ROS), and neutrophil infiltration (143). MiR-483-5p is able to reduce Beas-2B proliferation and alpha-smooth muscle actin (α-SMA) and fibronectin production in fibroblasts (158) just like let-7c, which is decreased in COPD sputum and lungs from mice and rats exposed to CSE (78, 81, 159).

Other miRNAs exert similar effects, like miR-145-5p, which is able to reduce TNF-α, IL-8, and IL-6 (111). Nevertheless, the role of this miRNA is not clear, existing contradictory data about it (148).

In blood samples from smoking COPD patients, miR-149-3p was downregulated, and monocytes exposed to CSE diminished this miRNA expression and upregulated *TLR4* and *NF-κβ*, which increases inflammation (160). This is also observed for miR-3202, which suppresses the increase of TNF-α and interferon gamma (IFN-γ) induced by CSE in lymphocytes (161), and similarly for miR-150, who has a comparable role (109).

The methylation effect induced by CSE was observed in miRNAs from human bronchial epithelial cells (HBECs), where miR-218 and let-7c inhibition is related to HBE malignancy (112, 121, 162). MiRNAs are regulated by epigenetics, but they also regulate the epigenetic landscape, like miR-217. This miRNA is downregulated by CSE and, at the same time, CSE upregulates the long-noncoding RNA (lncRNA) *MALAT1*, which is a target of miR-217 inducing malignancy (163).

Some miRNAs are upregulated directly by CSE, like miR-21, which is induced by hypoxia-inducible factor 1-alpha (HIF-1α) (114, 164), or others, like miR-664a-3p (targets *FHL1*), which is raised in lung tissue and peripheral blood mononuclear cells (PBMCs) from COPD patients, and in Beas-2B cells exposed to CSE (165). Exosomes are also carriers for pathogenic miRNAs, as CSE-treated HBECs produce exosomes carrying miR-21, inducing myofibroblast differentiation and increasing α-SMA and collagen-I through HIF-1α. Interestingly, downregulation of miR-21 in mice prevented remodeling by CSE (113). This miRNA is also implicated in the autophagy and apoptosis produced by CSE in lung tissues of both mice and 16HBE cells, being associated with worse lung function, proving its potential as therapeutic target in COPD (115, 116).

It is known that CSE upregulates miR-34a expression in human pulmonary microvascular endothelial cells and increases their apoptosis by targeting *NOTCH1* receptor (141), although this relation seems to be the inverse in serum from women with COPD exposed to biomass smoke (117). MiR-34a upregulation is also induced by oxidative stress (related to CSE) *via* phosphatidylinositol 3-kinase (PI3K) signaling in HBECs, which downregulates the antiaging-related deacetylases *SIRT1* and *SIRT6* (166), being this result confirmed in another study (142).

In the same way, CSE upregulates miR-206 in human pulmonary microvascular endothelial cells and in COPD patients, inducing cell apoptosis (134). CSE exposure, in both mice and Beas-2B cells, increased miR-130a levels, inducing a decrease in *WNT1* and therefore causing cell injury, proliferation, and migration by regulation of Wnt/β-catenin signaling (167). Similarly, CSE upregulates miR-195 in Beas-2B cells, increasing phospho-AKT and IL-6 synthesis (96). To the contrary, other miRNAs, such as the anti-malignant miR-200c, are indirectly downregulated by CSE and IL-6 through NF-κβ signaling (168).

CSE exposure releases circulating endothelial microparticles that are miRNA-enriched and, when engulfed by macrophages, can inhibit their efferocytosis activity (102). Moreover, expression of *HIF-1α* is controlled by miR-34a and miR-199a-5p, both overexpressed in COPD lungs, and also by miR-186 in fibroblasts, showing the intricacy of miRNA regulation (125, 169). Confirming this complex interplay of miRNA master regulation, miR-199a-5p is downregulated in regulatory T cells from COPD. This miRNA targets the TGF-β pathway, and its aberrant expression may implicate adaptive immunity dysregulation (126). MiR-199a-5p downregulation is also present in monocytes from COPD patients, where the protein unfolding response is activated and involved in COPD pathology (170), while it also seems to regulate pulmonary artery hypertension through targeting of *SMAD3* (127). This account for the very different functions that miRNAs may perform depending on which tissues or cells are present, and how their expression is influenced by the pathological environments, performing a very specifically fine tuning of gene expressing that occurs in a systemic manner.

Monocytes exposed to CSE also upregulate miR-132 expression inducing an increase in epidermal growth factor

receptor, IL-1β, and TNF-α. Similar results were observed in 16HBE cells, and indeed this miRNA is upregulated in serum from COPD and smokers (97). In addition, ASMCs have deregulated miRNA expression due to the CSE effect, as seen by the upregulation of miR-7 and the consecutive reduction of its anti-inflammatory target Epac1 in ASMCs and COPD lungs (139, 171). Likewise, fibroblast behavior and function are altered by miRNAs modulated by CSE, adding another layer to the system regulation of miRNAs function in pathological status (93, 106, 107, 135, 172).

Finally, *in vitro* and *in vivo* CSE models showed that the increased DNA damage response due to CSE is also regulated by miR-126, whose downregulation in COPD causes *ATM* protein kinase activation promoting tissue dysfunction and aging (104).

Differential Expression of miRNAs in Asthma and COPD and Their Roles as Disease Mediators and Biomarkers

The implications of miRNAs in the human asthmatic response have been widely investigated in both pediatric and adult populations. In 2012, a study by Liu et al. showed differences in the miRNA profile between asthmatic children and healthy controls (63). They performed a miRNA microarray to screen for differential expression of miRNAs in the pediatric population and found upregulation of miR-221 and miR-485-3p in asthmatic children. Also, the authors identified a potential target of both miRNAs, *SPRED2*, a negative regulator of different mechanisms in asthma such as airway inflammation and hyperresponsiveness, by modulating IL-5 signaling pathway. These results were confirmed in a murine model of asthma, showing a significant reduction of Spred-2 in asthmatic mice. In the same context, miR-3162-3p was identified as upregulated in childhood asthma implicated in remodeling through β-catenin (64). Wang et al., in 2015, observed an altered miRNAs signature in peripheral blood from patients with childhood asthma, showing that the levels of plasma miR-let-7c, miR-486, and miR-1260a in children with asthma were significantly higher than in healthy individuals (173).

To ascertain how miRNAs are involved in adult response to asthma, several studies in adulthood population have also been performed. Most research compares the miRNAs profile between asthmatics and controls in a variety of sample types. Other studies on miRNAs in asthma in adult population have been reported, describing a number of miRNAs such as miR-20b, miR-138, miR-143, miR-145, and others and their role in adulthood asthma (174).

Examples of miRNA profiles that allow COPD diagnosis, development or differentiation against healthy conditions have been shown in serum (118, 136). Also, a set of nine miRNAs were found to be differentially expressed in serum between healthy, COPD, and a migrant population with COPD, showing that miRNAs may change with exposure to different environmental factors (137).

Plasma levels of miR-106b are associated with COPD patients versus normal smokers (86), and levels of seven miRNAs are distinctive COPD biomarkers distinguishing from healthy subjects and asthma patients, with miR-145-5p being related to severity and miR-338-3p related to smoking COPD (131). Also, in exhaled breath condensate has been described miRNA profiles that are differential between COPD, healthy patients, and asthmatics (100). Discriminating between COPD and similar diseases has also implemented miRNA studies. Blood cell miRNAs (a profile of 14 miRNAs) and clustered miRNAs from BALF can be used as biomarkers for discrimination of COPD against lung cancer (87, 175). Moreover, in blood, nine miRNAs including members of the miR-320 family, which target mitogen-activated protein kinase (MAPK) pathways, can be used for lung-cancer prediction in COPD subjects (98). Finally, the combined expression of hsa-miR-195 and hsa-miR-143, obtained from databases, is able to identify lung cancer compared to disease-free status, but cannot distinguish COPD from lung cancer (176). From peripheral leucocytes, differential expression of miR-106b-5p, miR-183-5p, miR-125a-5p, and miR-100-5p was found in COPD compared to healthy controls, and miR-106b-5p was directly correlated with disease severity alleviation (88). Several studies have focused their interest on miRNAs from specific immune system cells exploring the implication of these structures in processes linked to asthma or COPD. For example, miR-24 and miR-27 have implications for the type 2 response by regulating IL-4 production by T-cells (61). Other miRNAs such as miR-17 and miR-19 have regulatory functions on T cell proliferation and differentiation to Th1, Th17, and regulatory T cells or by modulating type 2 immune response by inducing PI3K, JAK-STAT, and NF-κβ signaling pathways (177). One of the most widely studied is miR-21. The first study that demonstrated the implication of miR-21 in allergic airway inflammation is by Lu et al. (66). The authors observed an upregulation of miR-21 in transgenic mice with allergic inflammation compared to controls. Through predictive algorithms, they identified potential target genes such as *IL-12p35*. This gene is implicated in type 1 immune response; thus, high levels of miR-21 repress the expression of *IL-12p35*, contributing to type 2 polarization characteristic of asthma and other allergic diseases. In another experimental *in vivo* model of asthma published in 2011, Lu et al. observed the preventive role of miR-21 in the expression of IL-3, IL-5, and IL-12 (178). In their study, the group observed that this miRNA may play a role as regulator in type 1/type 2 immune response balance, repressing cytokines of both types of response. In the same way, other miRNAs have been associated with asthma response in murine models, including miR-1, miR-145, miR-150, and miR-155 (179). Also, the let-7 family comprises the most abundant miRNAs in mouse lungs, playing a potent proinflammatory role in asthma (60). In particular, let-7a is an essential regulator of IL-13, which is a key cytokine that induces airway hyperresponsiveness in the lung tissue of asthmatics. Repression of this cytokine can alleviate allergic asthma symptoms. However, mmu-let-7a is markedly suppressed in Th2 cells, allowing IL-13 expression and stimulating the typical type 2 response of asthma pathology.

T lymphocytes are crucial in asthma pathogenesis, specifically orchestrating type 2 immune response. Naïve T cells turn into

Th2 cells, releasing a set of cytokines (IL-4, IL-5, and IL-13), which triggers the characteristic processes of asthma (180). In this case, miRNAs related to T cells play an important role in type 2 immune response and asthma pathology. One of these miRNAs is miR-29b, which is involved in the development of asthma. This miRNA indirectly affects to Th2 response by regulating T-box transcription factors and IFN-γ production in T helper cells (181), so a lower expression of this miRNA in asthmatic lung allows a higher production of IFN-γ in order to recover Th1/Th2 balance in asthmatic lungs (182). According to miR-19a, Simpson et al. in 2014 showed that this miRNA is expressed by T cells and promotes Th2 cytokine production by simultaneously targeting inhibitors of the NF-κB, JAK-STAT, and PI3K pathways (177). Also, they observed that miR-19a had higher expression in human airway-infiltrating T cells in asthma. MiR-19a promotes cytokine production, amplifying inflammatory signaling by inhibiting *PTEN*, the signaling inhibitor SOCS1, and the deubiquitinase A20. Another important miRNA linked to T cells is miR-34a. This miRNA has been found to be upregulated in lungs of ovalbumin-induced asthmatic mice (183), modulating *FOXP3*, a master regulator of regulatory T cells.

Macrophages are immune cells involved in a wide range of functions related to innate and adaptive response, including maintenance of tissues and homeostasis. An imbalance between macrophages M1 (classically activated) and M2 (alternatively activated) phenotypes exists, and M2 polarization has been associated with development of asthma (184). Macrophages play a dual role in this disease, contributing to the induction and progression of eosinophilic lung inflammation and airway remodeling, and protecting against both development of neutrophilic inflammation and more severe airway hyperresponsiveness (185). This phenotype is induced by Th2 cytokines (IL-4 and IL-13), upregulating several genes. The role played by several miRNAs in macrophage polarization and their influence in asthma have been established (186). Several studies have demonstrated that miR-146a, miR-146b, and miR-21 promote macrophage polarization toward the M2 phenotype or suppress M1 polarization (52, 53). According to previous research, these miRNAs are upregulated in asthma (54). They act by joining target genes (*NOTCH1*, *IRF5*, and *CSF1R*), inhibiting the inflammatory response (67, 187, 188). In macrophages from COPD patients, miR-344b-1-3p was upregulated and controlled *TLR2*, *TNF*, and *IL1β* expression (83).

In order to analyze the effects of miRNAs on mechanism associated to these pathologies, structural lung cells, including ASMCs and airway epithelial cells, are implicated in the pathologic mechanisms of asthma, and their miRNA content have been studied. On the one hand, ASMCs play a critical role in asthma pathogenesis due to their abilities related to hypercontractility, proliferation, and secretion of inflammatory mediators. Dileepan and collaborators showed that miR-708 and miR-140-3p regulate the MAPK and PI3K signaling pathways associated to asthma immune response in human ASMCs (46, 51, 189). Later, the same group showed that miR-708 and miR-140-3p exert different effects in other proinflammatory genes, including *CCL2*, *CCL5*, *CCL11*, *CXCL8*, *CXCL10*, and *CXCL12* (47). Moreover, other miRNAs from ASMCs have been described, such as miR-145, miR-146a-5p, and miR-638, altering the functions of airway muscle cells (48–50).

On the other hand, airway epithelial cells are another cell type implicated in several processes of asthmatic pathogenesis, including airway remodeling, epithelial barrier repair, and production of several proinflammatory mediators (190). In this context, a number of miRNAs have been described in this cell type, regulating their functions or other pathological processes of asthma. In 2018, Zhang et al. investigated the role of miR-221 in airway epithelial cell injury in asthma (65). This miRNA was significantly increased in bronchial epithelial cells from asthmatic subjects compared to healthy controls and was implicated in epithelial cell injury in asthma by inhibiting *SIRT1* expression. However, there are several miRNAs that mitigate inflammatory status. Lambert and co-workers showed that miR-146a is released by airway epithelial cells in response to inflammatory stimuli like TNF-α (55). This fact constitutes an anti-inflammatory mechanism to enhance glucocorticoid effects. In addition, this miRNA, in conjunction with miR-146b, has been described as a negative regulator of inflammatory gene expression (*PTGS2* and *IL1B*) in lung epithelial and smooth muscle cells (56).

Other studies set out to find miRNAs that can be used to predict comorbidities; for instance, in blood, miR-210 expression can differentiate subjects with COPD and ischemic stroke from those with COPD or ischemia alone (191). MiR-1 reduction has been related to quadriceps skeletal muscle dystrophy in COPD (138). Plasma miRNAs can be used to identify patients with acute exacerbations of COPD such as miR-125b (105). PBMC-derived miRNAs are also differentially expressed in acute exacerbations of COPD compared to stable COPD and can differentiate between both conditions (129).

As previously described, plasma and exhaled breath condensate present differential miRNA profiles between asthma and COPD, which may be used to differentiate these diseases (100, 131). Nevertheless, having one of these respiratory diseases does not protect an individual against the other, so they may be present concomitantly. Asthma-COPD overlapping (ACO) is a condition where subjects present characteristics of both COPD and asthma, and it has been described in the Global Initiative for Chronic Obstructive Lung Disease-ACO guidelines (192). These subjects are normally defined as COPD subjects with eosinophilia (blood eosinophil count ≥200 eosinophils/μL) or asthmatics with chronic airway obstruction and smoking habit (≥20 pack per year) (193). Some miRNAs have been described as differentially expressed for ACO and can distinguish between asthma, COPD, and ACO. MiR-619-5p is downregulated in eosinophilic COPD subject serum compared to smoking and non-smoking asthmatics and COPD, and miR-4486 is differentially expressed in eosinophilic COPD when compared to non-smoking asthmatics, showing that even within the ACO group differences in miRNA expression can be found. The targets of this set of miRNAs include epidermal growth factors belonging to the ErbB signaling pathway

associated to pathogenic inception of lung diseases and to the metabolism of xenobiotics by cytochrome P450 signaling pathways involved in ROS (194). Finally, our research group has showed that combined expression of miR-185-5p, miR-320a, and miR-21-5p was able to differentiate asthmatics from COPD and ACO with high sensitivity and specificity. Like in the previous article these deregulated miRNAs in asthma are able to regulated genes belonging to Erb2, MAPK, AMPK, and PI3K/AKT pathways that control cell proliferation and muscle contraction, alongside other targeted pathways as T-cell receptor, FoxO or TGF-β which are key in immune regulation. The regulation of those pathways by asthma specific miRNAs may account for the differences in asthma pathology compared to those other respiratory diseases (145).

In sputum, expression of miR-338 is higher in subjects with respiratory diseases (asthma, COPD, and ACO) compared to healthy subjects; similarly, miR-338 is higher in asthma than in COPD. The study by Lacedonia et al. also showed that miR-145 is increased in sputum supernatant of COPD and asthmatics *versus* controls, and that serum miR-338 levels are lower in ACO and COPD compared to healthy controls (70). Finally, miR-146a-5p, miR-10a-5p, and miR-31-5p have been shown to play a common role in both CRDs (94, 108).

Together, these works have demonstrated a variety of miRNAs dysregulated in asthma and COPD in relation to healthy subjects and promising results have been found, including the use of miRNAs as biomarkers. However, this is a broad field of research and many of the specific mechanisms and particular means of miRNA regulation in these respiratory diseases remain to be discovered, and systems biology can help to solve this enigma.

MiRNAs AND TREATMENTS IN LUNG DISEASES

MiRNAs and Asthma Treatment

Glucocorticoids (GCs) remain the cornerstone of therapy for treating the inflammatory component of asthma and preventing asthma exacerbations. However, clinical response to GCs is complex and varies among individuals, as well as within the same individual, and some patients are resistant to this therapy. Different factors belonging to microenvironment can alter the canonical GC-induced signaling pathways, leading to reduced efficacy, collectively termed as sub-sensitivity, which include the entire spectrum of steroid-insensitivity and -resistance (195). Steroid sensitivity has been associated with different mechanisms, including dysregulated expression of GC receptor isoforms, neutrophilic inflammation and TH17 cytokines, oxidative stress-induced factors, and the downstream effect on histone deacetylase (HDAC) activation and gene expression. Recently, a new factor has been added in order to explain this phenomenon: the alterations in the expression of key transcription elements like miRNAs. Several studies conducted in this area, suggesting that circulating miRNAs may be useful potential biomarkers of asthma status or response to therapy (179).

In this sense, miR-155 has been the focus of different studies. Zhou et al. proposed that GCs may affect the inflammatory response by suppressing miR-155; these authors found that GCs attenuate lipopolysaccharide-induced inflammation and sepsis *via* downregulation of miR-155 expression (196), and forced miR-155 expression reverts the anti-inflammatory role of GCs (197, 198). In addition, miR-155-5p and miR-532-5p were identified as significantly associated with changes in dexamethasone-induced transrepression of NF-κβ. Authors identified these two functional circulating miRNAs predictive of asthma ICS treatment response over time, with an AUC of 0.86 (199).

Another miRNA that has been widely studied is miR-21. The study of Hammad et al. revealed a negative association between miR-21 and FEV_1 post ICS treatment, which highlights the role in ICS treatment outcome as FEV_1 reflects the grade of airway obstruction after ICS treatment (95). Elbehidy et al. found that miR-21 could be a novel predictor of ICS response, which helps in decision-making and identifying patients who are likely or unlikely to benefit from ICS therapy reducing the risk of side effects and sparing patients from the disappointment of treatment failure. MiR-21 had a predictive value in differentiating steroid-sensitive from steroid-resistant patients with an AUC value of 0.99 (200). Similar results were described by Wu et al. in 2014, who found that miR-21 expression was up-regulated in asthmatic adult bronchial epithelial cells regardless of treatment (201), but expression levels were decreased following ICS therapy (202).

Also, Kim et al. found that miR-21 drives severe, steroid-insensitive experimental asthma by amplifying PI3K-mediated suppression of HDAC2; thus, inhibition of increased miR-21 or PI3K responses suppresses disease and restores steroid-sensitivity (119).

Other studies investigating the expression profiles of 579 miRNAs in transgenic mice revealed that miRNAs were differentially expressed upon induction of experimental asthma following treatment with doxycycline and additionally suggested that miR-21 was the most up-regulated miRNA (66, 203).

Other authors reported an increase in infection-induced miR-9 in the airways of a mouse model and a similar increase in miR-9 in the sputum of neutrophilic asthmatics. These researchers therefore propose that miR-9 regulates glucocorticoid receptor signaling and steroid-resistance by reducing protein phosphatase 2A activity. Thus, blocking miR-9 function restores steroid sensitivity and suggests that this might serve as a novel approach for the treatment of steroid-resistant AHR (204).

One of the most important challenges may be to find biomarkers predicting treatment outcomes, and for this reason McGeachie et al. in 2017 investigated serum expression of 738 miRNAs in 160 children with asthma aged 5–12 years in search of predictors of asthma remission at the age of 14. The model, which was based on 12 variables including different miRNAs (miR-146b-5p, miR-106a, miR-126, and miR-30a), allowed prediction of remission with a sensitivity of 84% and a specificity of 70%. Thus, they hypothesize that miRNAs are potentially predictive biomarkers for treatment outcome (205).

However, not all authors agree on the role of miRNAs as regulators of GC treatment. Williams et al. sustain that changes in miRNA expression do not appear to be involved in the anti-inflammatory action of the corticosteroid budesonide (206). This discrepancy may be explained by the fact that the inflammatory changes were too mild, and by the degree of cellular heterogeneity in airway biopsies.

MiRNAs and COPD Treatment

The main goal of pharmacologic COPD therapy is to treat the symptoms, reduce the frequency and severity of exacerbations, and improve tolerance and health status (207).

The main types of drugs normally used to treat COPD include long-acting β_2-agonists, long-acting muscarinic antagonists, and ICS, which are the most widely used treatment as anti-inflammatory agents in COPD. However, a high percentage of COPD patients show a poor response to this therapy (208). It has now been recognized that current COPD treatments such as corticosteroids work, in part, through epigenetic mechanisms (209) and miRNAs is one of them (37).

In a recent manuscript authored by Faiz et al. (144) four miRNAs with changed expression after 6- and 30-month treatment with ICS compared with basal status (without any treatment) were identified. MiR-708 and miR-155 were downregulated and miR-320d and miR-339-3p were upregulated in both periods of time after treatment (6 and 30 months). Moreover, three were also altered in the same direction by ICS plus long-acting β2-agonists compared to placebo at 6 months of therapy: miR-320d, miR-339-3p, and miR-708; *in vitro*, these data were confirmed for miR-320d. Overexpression of miR-320d significantly reduced the IL-1β-induced activation of NF-κB signaling compared to miRNA negative control. Thus, the negatively correlated predicted targets of miR-320d are diminished by ICS treatment. So, this study identified four miRNAs affected by short- and long-term treatment with ICS compared to placebo in patients with moderate to severe COPD (144) and miRNAs associated with ICS therapy and inflammation provide relevant candidates as potential therapeutic targets in chronic inflammatory diseases.

In addition, the increase of HDAC2 could reduce GC insensitivity in some patients. Leuenberger et al. (110) showed that HDAC2 is directly targeted by miR-223 by binding to seed matches located in the 3'UTR of this mRNA transcript; in addition, the activity of total HDAC and HDAC2 in pulmonary endothelial cells is repressed in response to miR-223 overexpression. The reduced activity of this histone has been classically described in COPD patients and a significant inverse correlation between HDAC2 and miR-223 level has been observed in this COPD population (110). Therefore, this miR-223, through regulation of another epigenetic factor as the HDAC2, could interfere with treatment efficacy in COPD disease.

As commented previously, miR-146a has been described as an enhancer of the anti-inflammatory effects of GCs (55) and is negatively correlated with inflammation and Global Initiative for Chronic Obstructive Lung Disease stage in both stable and acute exacerbation COPD patients (210). COPD patients show an increased secretion of PGE_2, which results in collagen overproduction and finally reduces lung capacity. In this sense, miR-146a expression is reduced in COPD patients and its target, COX-2, is simultaneously increased with a consequent increase of PGE_2 levels (89). As COX-2 is sensitive to steroids and miR-146a target, this miRNA could contribute to the anti-inflammatory effect of this drug to reduce the increase of mucus and worsening of COPD evolution.

Moreover, as we have previously commented, COPD could have different etiologies such as tobacco or biomass smoke exposure. A recent manuscript from Velasco-Torres et al. on COPD due to biomass smoke exposure reported downregulation of miR-34a which implicates an activation of Notch 1 signaling. This finding is relevant because Notch 1 could represent an important target for therapy in these phenotypes of COPD (117).

Though the list is still small, several miRNAs have been modified by classical COPD treatments and, likewise, these miRNAs act over therapy targets and could contribute in different ways to treatment response in this respiratory pathology.

CLINICAL ADVANCES IN THE USE OF MiRNAs

Finally, miRNA-based treatment has emerged as a potential approach for clinical intervention in some respiratory diseases such as asthma and COPD. It is based on miRNAs delivery in the specific site of action which constitutes one of the main aspects of development in relation to miRNA like therapeutic approach. A long list of miRNAs has been found to be linked to initiation, progression, or exacerbations in both respiratory diseases, especially in COPD. However, some have been studied more in depth, showing a high potential as future therapeutic tools through their up- or downregulation. In this sense, miR-146a (79, 89), miR-21 (113, 116), miR-150 (109), miR-145-5p (131, 148), miR-320d (132, 144), miR-155 (62) miR-223 (211), or miR-3162-3p (212) seem to hold promise as future elements in the therapeutic repertoire for COPD and asthma, respectively, some of which are common for both pathologies such as miR-146a (213–215) or miR-21 (54, 62).

All these examples show the never-ending list of miRNAs that, in the future, could potentially be a therapeutic approach in respiratory diseases. However, although the knowledge of miRNAs has grown exponentially in recent years, these data demonstrate that more studies are necessary before miRNAs can be employed as therapeutic tools. Currently, the idea of precision and personalized medicine is the objective for the near future, though this is a long and arduous path; thus, classical treatments continue to be the basis of therapy in asthma and COPD.

CONCLUDING REMARKS

This review summarizes the previous knowledge about miRNAs in chronic respiratory diseases as asthma and COPD, trying to be the first step forward for the compilation and application of systems biology approaches for understanding their roles. Many

miRNAs present differential expression in diverse samples, and are known for their capability of being biomarkers or for having a specific role in the pathogenesis of these diseases, but the current approaches are unsuited for giving a systemic level view for data interpretation.

For overcoming this issue, systems biology may be the optimal tool. By the combination of data-driven model elaboration and model-driven experimental design, researchers might be able to elucidate how miRNAs work together in disease pathogenesis and diagnosis, giving the full picture view of miRNA regulatory system.

AUTHOR CONTRIBUTIONS

JC, JR-M, BS, MG-M, NR, and VP conceived of the review and wrote the manuscript. JC, JR-M, and VP prepared the figures. The review was performed under the supervision of JC and VP. All authors contributed to the article and approved the submitted version.

FUNDING

This manuscript was supported by Fondo de Investigación Sanitaria – FIS and FEDER (Fondo Europeo de Desarrollo Regional) [PI15/00803, PI18/00044 and FI16/00036], CIBERES, Merck Health Foundation funds and RTC-2017-6501-1 (Ministerio de Ciencia, Innovación y Universidades).

ACKNOWLEDGMENTS

The authors recognize Oliver Shaw, PhD, English editor of IIS-FJD, for editing the manuscript for aspects of the English language.

REFERENCES

1. Sahu I, Hebalkar R, Kar S, TS SV, Gutti U, Gutti RK. Systems biology approach to study the role of miRNA in promoter targeting during megakaryopoiesis. *Exp Cell Res* (2018) 366:192–8. doi: 10.1016/j.yexcr.2018.03.022
2. Lee RC, Feinbaum RL, Ambros V. The C. elegans heterochronic gene lin-4 encodes small RNAs with antisense complementarity to lin-14. *Cell* (1993) 75:843–54. doi: 10.1016/0092-8674(93)90529-Y
3. Lai X, Eberhardt M, Schmitz U, Vera J. Systems biology-based investigation of cooperating microRNAs as monotherapy or adjuvant therapy in cancer. *Nucleic Acids Res* (2019) 47:7753–66. doi: 10.1093/nar/gkz638
4. Lai X, Bhattacharya A, Schmitz U, Kunz M, Vera J, Wolkenhauer O. A systems' biology approach to study microrna-mediated gene regulatory networks. *BioMed Res Int* (2013) 2013:703849. doi: 10.1155/2013/703849
5. Gomes CPC, Cho JH, Hood L, Franco OL, Pereira RW, Wang K. A review of computational tools in microRNA discovery. *Front Genet* (2013) 4:81:81. doi: 10.3389/fgene.2013.00081
6. Watanabe Y, Kanai A. Systems biology reveals microRNA-mediated gene regulation. *Front Genet* (2011) 2:29:29. doi: 10.3389/fgene.2011.00029
7. Breitling LP, Yang R, Korn B, Burwinkel B, Brenner H. Tobacco-smoking-related differential DNA methylation: 27K discovery and replication. *Am J Hum Genet* (2011) 88:450–7. doi: 10.1016/j.ajhg.2011.03.003
8. World Health Organization. *Chronic Respiratory Diseases* (2007). Available at: https://www.who.int/health-topics/chronic-respiratory-diseases#tab=tab_1 (Accessed Accesed April 23, 2020).
9. Beasley R, Semprini A, Mitchell EA. Risk factors for asthma: Is prevention possible? *Lancet* (2015) 386:1075–85. doi: 10.1016/S0140-6736(15)00156-7
10. Salvi SS, Barnes PJ. Chronic obstructive pulmonary disease in non-smokers. *Lancet* (2009) 374:733–43. doi: 10.1016/S0140-6736(09)61303-9
11. Agustí A, Hogg JC. Update on the pathogenesis of chronic obstructive pulmonary disease. *N Engl J Med* (2019) 381:1248–56. doi: 10.1056/NEJMra1900475
12. Kudo M, Ishigatsubo Y, Aoki I. Pathology of asthma. *Front Microbiol* (2013) 4:263. doi: 10.3389/fmicb.2013.00263
13. Macnee W. ABC of chronic obstructive pulmonary disease Pathology, pathogenesis, and pathophysiology. *BMJ* (2006) 332:1202–4. doi: 10.1136/bmj.3327551.1202
14. Fahy JV. Type 2 inflammation in asthma-present in most, absent in many. *Nat Rev Immunol* (2015) 15:57–65. doi: 10.1038/nri3786
15. Holgate ST. Innate and adaptive immune responses in asthma. *Nat Med* (2012) 18:673–83. doi: 10.1038/nm.2731
16. Cañas JA, Sastre B, Rodrigo-Muñoz JM, del Pozo V. Exosomes: A new approach to asthma pathology. *Clin Chim Acta* (2019) 495:139–47. doi: 10.1016/j.cca.2019.04.055
17. Global Initiative for Asthma Management and Prevention 2020. *Global Initiative for Asthma* (2020). Available at: www.ginasthma.org (Accessed April 8, 2020).
18. Anderson GP. Endotyping asthma: new insights into key pathogenic mechanisms in a complex, heterogeneous disease. *Lancet* (2008) 372:1107–19. doi: 10.1016/S0140-6736(08)61452-X
19. Brown DW, Croft JB, Greenlund KJ, Giles WH. Average age at death from COPD in the United States: 1980-85, 1990-95, 2000-05. *COPD J Chronic Obstr Pulm Dis* (2009) 6:152–4. doi: 10.1080/15412550902918428
20. Smith MC, Wrobel JP. Epidemiology and clinical impact of major comorbidities in patients with COPD. *Int J Chron Obstruct Pulmon Dis* (2014) 9:871–88. doi: 10.2147/COPD.S49621
21. Barnes PJ, Shapiro SD, Pauwels RA. Chronic obstructive pulmonary disease: Molecular and cellular mechanisms. *Eur Respir J* (2003) 22:672–88. doi: 10.1183/09031936.03.00040703
22. Miravitlles M, Calle M, Soler-Cataluña JJ. Fenotipos clínicos de la EPOC. Identificación, definición e implicaciones para las guías de tratamiento. *Arch Bronconeumol* (2012) 48:86–98. doi: 10.1016/j.arbres.2011.10.007
23. Trupin L, Earnest G, San Pedro M, Balmes JR, Eisner MD, Yelin E, et al. The occupational burden of chronic obstructive pulmonary disease. *Eur Respir J* (2003) 22:462–69. doi: 10.1183/09031936.03.00094203
24. Taylor JD. COPD and the response of the lung to tobacco smoke exposure. *Pulm Pharmacol Ther* (2010) 23:376–83. doi: 10.1016/j.pupt.2010.04.003
25. Strzelak A, Ratajczak A, Adamiec A, Feleszko W. Tobacco smoke induces and alters immune responses in the lung triggering inflammation, allergy, asthma and other lung diseases: A mechanistic review. *Int J Environ Res Public Health* (2018) 15:1033. doi: 10.3390/ijerph15051033
26. Dewhurst JA, Lea S, Hardaker E, Dungwa JV, Ravi AK, Singh D. Characterisation of lung macrophage subpopulations in COPD patients and controls. *Sci Rep* (2017) 7:7143. doi: 10.1038/s41598-017-07101-2
27. Tsoumakidou M, Demedts IK, Brusselle GG, Jeffery PK. Dendritic cells in chronic obstructive pulmonary disease: New players in an old game. *Am J Respir Crit Care Med* (2008) 177:1180–6. doi: 10.1164/rccm.200711-1727PP
28. Quint JK, Wedzicha JA. The neutrophil in chronic obstructive pulmonary disease. *J Allergy Clin Immunol* (2007) 119:1065–71. doi: 10.1016/j.jaci.2006.12.640
29. Eriksson-Ström J, Pourazar J, Linder R, Blomberg A, Lindberg A, Bucht A, et al. Cytotoxic lymphocytes in COPD airways: Increased NK cells associated with disease, iNKT and NKT-like cells with current smoking. *Respir Res* (2018) 19:244. doi: 10.1186/s12931-018-0940-7
30. Wang G, Xu Z, Wang R, Al-Hijji M, Salit J, Strulovici-Barel Y, et al. Genes associated with MUC5AC expression in small airway epithelium of human smokers and non-smokers. *BMC Med Genomics* (2012) 5:21. doi: 10.1186/1755-8794-5-21

31. Gangl K, Reininger R, Bernhard D, Campana R, Pree I, Reisinger J, et al. Cigarette smoke facilitates allergen penetration across respiratory epithelium. *Allergy Eur J Allergy Clin Immunol* (2009) 64:398–405. doi: 10.1111/j.1398-9995.2008.01861.x
32. Krauss-Etschmann S, Meyer KF, Dehmel S, Hylkema MN. Inter-and transgenerational epigenetic inheritance: Evidence in asthma and COPD? *Clin Epigenetics* (2015) 7:53. doi: 10.1186/s13148-015-0085-1
33. Vucic EA, Chari R, Thu KL, Wilson IM, Cotton AM, Kennett JY, et al. DNA methylation is globally disrupted and associated with expression changes in chronic obstructive pulmonary disease small airways. *Am J Respir Cell Mol Biol* (2014) 50:912–22. doi: 10.1165/rcmb.2013-0304OC
34. Meek PM, Sood A, Petersen H, Belinsky SA, Tesfaigzi Y. Epigenetic Change (GATA-4 Gene Methylation) Is Associated With Health Status in Chronic Obstructive Pulmonary Disease. *Biol Res Nurs* (2015) 17:191–8. doi: 10.1177/1099800414538113
35. Lee MK, Hong Y, Kim SY, Kim WJ, London SJ. Epigenome-wide association study of chronic obstructive pulmonary disease and lung function in Koreans. *Epigenomics* (2017) 9:971–84. doi: 10.2217/epi-2017-0002
36. Zhang Y, Yang R, Burwinkel B, Breitling LP, Holleczek B, Schöttker B, et al. F2RL3 Methylation in Blood DNA Is a Strong Predictor of Mortality. *Int J Epidemiol* (2014) 43:1215–25. doi: 10.1093/ije/dyu006
37. Wu DD, Song J, Bartel S, Krauss-Etschmann S, Rots MG, Hylkema MN. The potential for targeted rewriting of epigenetic marks in COPD as a new therapeutic approach. *Pharmacol Ther* (2018) 182:1–14. doi: 10.1016/j.pharmthera.2017.08.007
38. Song J, Cano-Rodriquez D, Winkle M, Gjaltema RAF, Goubert D, Jurkowski TP, et al. Targeted epigenetic editing of SPDEF reduces mucus production in lung epithelial cells. *Am J Physiol Lung Cell Mol Physiol* (2017) 312:L334–47. doi: 10.1152/ajplung.00059.2016
39. Mehta A, Baltimore D. MicroRNAs as regulatory elements in immune system logic. *Nat Rev Immunol* (2016) 16:279–94. doi: 10.1038/nri.2016.40
40. Sittka A, Schmeck B. MicroRNAs in the Lung. *Adv Exp Med Biol* (2013) 774:121–34. doi: 10.1007/978-94-007-5590-1_7
41. Iorio MV, Piovan C, Croce CM. Interplay between microRNAs and the epigenetic machinery: An intricate network. *Biochim Biophys Acta G* (2010) 1799:694–701. doi: 10.1016/j.bbagrm.2010.05.005
42. Papadopoulos NG, Taka S, Tzani-Tzanopoulou P, Wanstall H. MicroRNAs in asthma and respiratory infections: Identifying common pathways. *Allergy Asthma Immunol Res* (2020) 12:4–23. doi: 10.4168/aair.2020.12.1.4
43. Rodrigo-Muñoz JM, Cañas JA, Sastre B, Rego N, Greif G, Rial M, et al. Asthma diagnosis using integrated analysis of eosinophil microRNAs. *Allergy Eur J Allergy Clin Immunol* (2019) 74:507–17. doi: 10.1111/all.13570
44. Wang J, Chen J, Sen S. MicroRNA as Biomarkers and Diagnostics. *J Cell Physiol* (2016) 231:25–30. doi: 10.1002/jcp.25056
45. Panganiban RP, Wang Y, Howrylak J, Chinchilli VM, Craig TJ, August A, et al. Circulating microRNAs as biomarkers in patients with allergic rhinitis and asthma. *J Allergy Clin Immunol* (2016) 137:1423–32. doi: 10.1016/j.jaci.2016.01.029
46. Jude JA, Dileepan M, Subramanian S, Solway J, Panettieri RA Jr, Wasleth TF, et al. MiR-140-3p regulation of TNF-α-induced CD38 expression in human airway smooth muscle cells. *Am J Physiol Lung Cell Mol Physiol* (2012) 303: L460–8. doi: 10.1152/ajplung.00041.2012
47. Dileepan M, Sarver AE, Rao SP, Panettieri RA, Subramanian S, Kannan MS. MicroRNA mediated chemokine responses in human airway smooth muscle cells. *PloS One* (2016) 11:e0150842. doi: 10.1371/journal.pone.0150842
48. Liu Y, Sun X, Wu Y, Fang P, Shi H, Xu J, et al. Effects of miRNA-145 on airway smooth muscle cells function. *Mol Cell Biochem* (2015) 409:135–43. doi: 10.1007/s11010-015-2519-7
49. Faiz A, Weckmann M, Tasena H, Vermeulen CJ, Van Den Berge M, Ten Hacken NHT, et al. Profiling of healthy and asthmatic airway smooth muscle cells following interleukin-1β treatment: A novel role for CCL20 in chronic mucus hypersecretion. *Eur Respir J* (2018) 52:1800310. doi: 10.1183/13993003.00310-2018
50. Wang H, Yao H, Yi B, Kazama K, Liu Y, Deshpande D, et al. MicroRNA-638 inhibits human airway smooth muscle cell proliferation and migration through targeting cyclin D1 and NOR1. *J Cell Physiol* (2018) 234:369–81. doi: 10.1002/jcp.26930
51. Dileepan M, Jude JA, Rao SP, Walseth TF, Panettieri RA, Subramanian S, et al. MicroRNA-708 regulates CD38 expression through signaling pathways JNK MAP kinase and PTEN/AKT in human airway smooth muscle cells. *Respir Res* (2014) 15:107. doi: 10.1186/s12931-014-0107-0
52. Essandoh K, Li Y, Huo J, Fan GC. MiRNA-mediated macrophage polarization and its potential role in the regulation of inflammatory response. *Shock* (2016) 46:122–31. doi: 10.1097/SHK.0000000000000604
53. He X, Tang R, Sun Y, Wang YG, Zhen KY, Zhang DM, et al. MicroR-146 blocks the activation of M1 macrophage by targeting signal transducer and activator of transcription 1 in hepatic schistosomiasis. *EBioMedicine* (2016) 13:339–47. doi: 10.1016/j.ebiom.2016.10.024
54. Specjalski K, Niedoszytko M. MicroRNAs: future biomarkers and targets of therapy in asthma? *Curr Opin Pulm Med* (2020) 26:285–92. doi: 10.1097/MCP.0000000000000673
55. Lambert KA, Roff AN, Panganiban RP, Douglas S, Ishmael FT. MicroRNA-146a is induced by inflammatory stimuli in airway epithelial cells and augments the anti-inflammatory effects of glucocorticoids. *PloS One* (2018) 13:e0205434. doi: 10.1371/journal.pone.0205434
56. Comer BS, Camoretti-Mercado B, Kogut PC, Halayko AJ, Solway J, Gerthoffer WT. MicroRNA-146a and microRNA-146b expression and anti-inflammatory function in human airway smooth muscle. *Am J Physiol Lung Cell Mol Physiol* (2014) 307:L727–34. doi: 10.1152/ajplung.00174.2014
57. Levänen B, Bhakta NR, Torregrosa Paredes P, Barbeau R, Hiltbrunner S, Pollack JL, et al. Altered microRNA profiles in bronchoalveolar lavage fluid exosomes in asthmatic patients. *J Allergy Clin Immunol* (2013) 131:894–903. doi: 10.1016/j.jaci.2012.11.039
58. Zhao M, Li YP, Geng XR, Zhao M, Ma SB, Yang YH, et al. Expression Level of MiRNA-126 in Serum Exosomes of Allergic Asthma Patients and Lung Tissues of Asthmatic Mice. *Curr Drug Metab* (2019) 20:799–803. doi: 10.2174/1389200220666191011114452
59. Gon Y, Maruoka S, Inoue T, Kuroda K, Yamagishi K, Kozu Y, et al. Selective release of miRNAs via extracellular vesicles is associated with house-dust mite allergen-induced airway inflammation. *Clin Exp Allergy* (2017) 47:1586–98. doi: 10.1111/cea.13016
60. Polikepahad S, Knight JM, Naghavi AO, Oplt T, Creighton CJ, Shaw C, et al. Proinflammatory role for let-7 microRNAS in experimental asthma. *J Biol Chem* (2010) 285:30139–49. doi: 10.1074/jbc.M110.145698
61. Pua HH, Steiner DF, Patel S, Gonzalez JR, Ortiz-Carpena JF, Kageyama R, et al. MicroRNAs 24 and 27 Suppress Allergic Inflammation and Target a Network of Regulators of T Helper 2 Cell-Associated Cytokine Production. *Immunity* (2016) 44:821–32. doi: 10.1016/j.immuni.2016.01.003
62. ElKashef SMMAE, Ahmad SEA, Soliman YMA, Mostafa MS. Role of microRNA-21 and microRNA-155 as biomarkers for bronchial asthma. *Innate Immun* (2020) 1753425920901563:1–9. doi: 10.1177/1753425920901563
63. Liu F, Qin HB, Xu B, Zhou H, Zhao DY. Profiling of miRNAs in pediatric asthma: Upregulation of miRNA-221 and miRNA-485-3p. *Mol Med Rep* (2012) 6:1178–82. doi: 10.3892/mmr.2012.1030
64. Fang C, Lu W, Li C, Peng X, Wang Y, Huang X, et al. MiR-3162-3p is a novel MicroRNA that exacerbates asthma by regulating β-catenin. *PloS One* (2016) 11:e0149257. doi: 10.1371/journal.pone.0149257
65. Zhang H, Sun Y, Rong W, Fan L, Cai Y, Qu Q, et al. miR-221 participates in the airway epithelial cells injury in asthma via targeting SIRT1. *Exp Lung Res* (2018) 44:272–9. doi: 10.1080/01902148.2018.1533051
66. Lu TX, Munitz A, Rothenberg ME. MicroRNA-21 Is Up-Regulated in Allergic Airway Inflammation and Regulates IL-12p35 Expression. *J Immunol* (2009) 182:4994–5002. doi: 10.4049/jimmunol.0803560
67. Caescu CI, Guo X, Tesfa L, Bhagat TD, Verma A, Zheng D, et al. Colony stimulating factor-1 receptor signaling networks inhibit mouse macrophage inflammatory responses by induction of microRNA-21. *Blood* (2015) 125: e1–13. doi: 10.1182/blood-2014-10-608000
68. Maes T, Cobos FA, Schleich F, Sorbello V, Henket M, De Preter K, et al. Asthma inflammatory phenotypes show differential microRNA expression in sputum. *J Allergy Clin Immunol* (2016) 137:1433–46. doi: 10.1016/j.jaci.2016.02.018
69. Zhang K, Liang Y, Feng Y, Wu W, Zhang H, He J, et al. Decreased epithelial and sputum miR-221-3p associates with airway eosinophilic inflammation

and CXCL17 expression in asthma. *Am J Physiol Lung Cell Mol Physiol* (2018) 315:L253–64. doi: 10.1152/ajplung.00567.2017
70. Lacedonia D, Palladino GP, Foschino-Barbaro MP, Scioscia G, Elisiana G, Carpagnano EG. Expression profiling of miRNA-145 and miRNA-338 in serum and sputum of patients with COPD, asthma, and asthma–COPD overlap syndrome phenotype. *Int J Chron Obstruct Pulmon Dis* (2017) 12:1811–7. doi: 10.2147/COPD.S130616
71. Suojalehto H, Lindström I, Majuri ML, Mitts C, Karjalainen J, Wolff H, et al. Altered microRNA expression of nasal mucosa in long-term asthma and allergic rhinitis. *Int Arch Allergy Immunol* (2014) 163:168–78. doi: 10.1159/000358486
72. Milger K, Götschke J, Krause L, Nathan P, Alessandrini F, Tufman A, et al. Identification of a plasma miRNA biomarker signature for allergic asthma: A translational approach. *Allergy Eur J Allergy Clin Immunol* (2017) 72:1962–71. doi: 10.1111/all.13205
73. Baskara-Yhuellou I, Tost J. The impact of microRNAs on alterations of gene regulatory networks in allergic diseases. *Adv Protein Chem Struct Biol* (2020) 120:237–312. doi: 10.1016/bs.apcsb.2019.11.006
74. Nagano T, Katsurada M, Dokuni R, Hazama D, Kiriu T, Umezawa K, et al. Crucial Role of Extracellular Vesicles in Bronchial Asthma. *Int J Mol Sci* (2019) 20:2589. doi: 10.3390/ijms20102589
75. Fujita Y, Yoshioka Y, Ito S, Araya J, Kuwano K, Ochiya T. Intercellular communication by extracellular vesicles and their MicroRNAs in Asthma. *Clin Ther* (2014) 36:873–81. doi: 10.1016/j.clinthera.2014.05.006
76. Sastre B, Cañas JA, Rodrigo-Muñoz JM, del Pozo V. Novel modulators of asthma and allergy: Exosomes and microRNAs. *Front Immunol* (2017) 8:826. doi: 10.3389/fimmu.2017.00826
77. Zhao M, Juanjuan L, Weijia F, Jing X, Qiuhua H, Hua Z, et al. Expression Levels of MicroRNA-125b in Serum Exosomes of Patients with Asthma of Different Severity and its Diagnostic Significance. *Curr Drug Metab* (2019) 20:781–4. doi: 10.2174/1389200220666191021100001
78. Izzotti A, Calin GA, Arrigo P, Steele VE, Croce CM, De Flora S. Downregulation of microRNA expression in the lungs of rats exposed to cigarette smoke. *FASEB J* (2009) 23:806–12. doi: 10.1096/fj.08-121384
79. Ezzie ME, Crawford M, Cho JH, Orellana R, Zhang S, Gelinas R, et al. Gene expression networks in COPD: microRNA and mRNA regulation. *Thorax* (2012) 67:122–31. doi: 10.1136/thoraxjnl-2011-200089
80. Kara M, Kirkil G, Kalemci S. Differential Expression of MicroRNAs in Chronic Obstructive Pulmonary Disease. *Adv Clin Exp Med* (2016) 25:21–6. doi: 10.17219/ACEM/28343
81. Van Pottelberge GR, Mestdagh P, Bracke KR, Thas O, Van Durme YMTA, Joos GF, et al. MicroRNA expression in induced sputum of smokers and patients with chronic obstructive pulmonary disease. *Am J Respir Crit Care Med* (2011) 183:898–906. doi: 10.1164/rccm.201002-0304OC
82. Graff JW, Powers LS, Dickson AM, Kim J, Reisetter AC, Hassan IH, et al. Cigarette Smoking Decreases Global MicroRNA Expression in Human Alveolar Macrophages. *PloS One* (2012) 7:e44066. doi: 10.1371/journal.pone.0044066
83. Xu H, Wu Y, Li L, Yuan W, Zhang D, Yan Q, et al. MiR-344b-1-3p targets TLR2 and negatively regulates TLR2 signaling pathway. *Int J Chron Obstruct Pulmon Dis* (2017) 12:627–38. doi: 10.2147/COPD.S120415
84. Sang HY, Jin YL, Zhang WQ, Chen LB. Downregulation of microRNA-637 increases risk of hypoxia-induced pulmonary hypertension by modulating expression of cyclin dependent kinase 6 (CDK6) in pulmonary smooth muscle cells. *Med Sci Monit* (2016) 22:4066–72. doi: 10.12659/MSM.897254
85. Musri MM, Coll-Bonfill N, Maron BA, Peinado VI, Wang RS, Altirriba J, et al. MicroRNA dysregulation in pulmonary arteries from chronic obstructive pulmonary disease: Relationships with vascular remodeling. *Am J Respir Cell Mol Biol* (2018) 59:490–9. doi: 10.1165/rcmb.2017-0040OC
86. Soeda S, Ohyashiki JH, Ohtsuki K, Umezu T, Setoguchi Y, Ohyashiki K. Clinical relevance of plasma miR-106b levels in patients with chronic obstructive pulmonary disease. *Int J Mol Med* (2013) 31:533–9. doi: 10.3892/ijmm.2013.1251
87. Molina-Pinelo S, Pastor MD, Suarez R, Romero-Romero B, González De La Peña M, Salinas A, et al. MicroRNA clusters: Dysregulation in lung adenocarcinoma and COPD. *Eur Respir J* (2014) 43:1740–9. doi: 10.1183/09031936.00091513
88. Wang R, Xu J, Liu H, Zhao Z. Peripheral leukocyte microRNAs as novel biomarkers for COPD. *Int J Chron Obstruct Pulmon Dis* (2017) 12:1101–12. doi: 10.2147/COPD.S130416
89. Sato T, Liu X, Nelson A, Nakanishi M, Kanaji N, Wang X, et al. Reduced miR-146a increases prostaglandin E2 in chronic obstructive pulmonary disease fibroblasts. *Am J Respir Crit Care Med* (2010) 182:1020–9. doi: 10.1164/rccm.201001-0055OC
90. Tasena H, Faiz A, Timens W, Noordhoek J, Hylkema MN, Gosens R, et al. MicroRNA-mRNA regulatory networks underlying chronic mucus hypersecretion in COPD. *Eur Respir J* (2018) 52:1701556. doi: 10.1183/13993003.01556-2017
91. Zago M, Rico de Souza A, Hecht E, Rousseau S, Hamid Q, Eidelman DH, et al. The NF-κB family member RelB regulates microRNA miR-146a to suppress cigarette smoke-induced COX-2 protein expression in lung fibroblasts. *Toxicol Lett* (2014) 226:107–16. doi: 10.1016/j.toxlet.2014.01.020
92. Liu L, Wan C, Zhang W, Guan L, Tian G, Zhang F, et al. MiR-146a regulates PM1-induced inflammation via NF-κB signaling pathway in BEAS-2B cells. *Environ Toxicol* (2018) 33:743–51. doi: 10.1002/tox.22561
93. Osei ET, Florez-Sampedro L, Tasena H, Faiz A, Noordhoek JA, Timens W, et al. miR-146a-5p plays an essential role in the aberrant epithelial-fibroblast cross-talk in COPD. *Eur Respir J* (2017) 49:1602538. doi: 10.1183/13993003.02538-2016
94. Tsai MJ, Tsai YC, Chang WA, Lin YS, Tsai PH, Sheu CC, et al. Deducting microRNA-mediated changes common in bronchial epithelial cells of asthma and chronic obstructive pulmonary disease-a next-generation sequencing-guided bioinformatic approach. *Int J Mol Sci* (2019) 20:553. doi: 10.3390/ijms20030553
95. Hammad Mahmoud Hammad R, Hamed DHED, Eldosoky MAER, Ahmad AAES, Osman HM, Abd Elgalil HM, et al. Plasma microRNA-21, microRNA-146a and IL-13 expression in asthmatic children. *Innate Immun* (2018) 24:171–9. doi: 10.1177/1753425918763521
96. Gu W, Yuan Y, Yang H, Wu H, Wang L, Tang Z, et al. Role of miR-195 in cigarette smoke-induced chronic obstructive pulmonary disease. *Int Immunopharmacol* (2018) 55:49–54. doi: 10.1016/j.intimp.2017.11.030
97. Diao X, Zhou J, Wang S, Ma X. Upregulation of miR-132 contributes to the pathophysiology of COPD via targeting SOCS5. *Exp Mol Pathol* (2018) 105:285–92. doi: 10.1016/j.yexmp.2018.10.002
98. Keller A, Fehlmann T, Ludwig N, Kahraman M, Laufer T, Backes C, et al. Genome-wide MicroRNA Expression Profiles in COPD: Early Predictors for Cancer Development. *Genomics Proteomics Bioinformatics* (2018) 16:162–71. doi: 10.1016/j.gpb.2018.06.001
99. Cao Z, Zhang N, Lou T, Jin Y, Wu Y, Ye Z, et al. microRNA-183 down-regulates the expression of BKCaβ1 protein that is related to the severity of chronic obstructive pulmonary disease. *Hippokratia* (2014) 18:328.
100. Pinkerton M, Chinchilli V, Banta E, Craig T, August A, Bascom R, et al. Differential expression of microRNAs in exhaled breath condensates of patients with asthma, patients with chronic obstructive pulmonary disease, and healthy adults. *J Allergy Clin Immunol* (2013) 132:217–9. doi: 10.1016/j.jaci.2013.03.006
101. Schembri F, Sridhar S, Perdomo C, Gustafson AM, Zhang X, Ergun A, et al. MicroRNAs as modulators of smoking-induced gene expression changes in human airway epithelium. *Proc Natl Acad Sci USA* (2009) 106:2319–24. doi: 10.1073/pnas.0806383106
102. Serban KA, Rezania S, Petrusca DN, Poirier C, Cao D, Justice MJ, et al. Structural and functional characterization of endothelial microparticles released by cigarette smoke. *Sci Rep* (2016) 6:31596. doi: 10.1038/srep31596
103. Christenson SA, Brandsma CA, Campbell JD, Knight DA, Pechkovsky DV, Hogg JC, et al. MiR-638 regulates gene expression networks associated with emphysematous lung destruction. *Genome Med* (2013) 5:114. doi: 10.1186/gm519
104. Paschalaki KE, Zampetaki A, Baker JR, Birrell MA, Starke RD, Belvisi MG, et al. Downregulation of MicroRNA-126 Augments DNA Damage Response in Cigarette Smokers and Patients with Chronic Obstructive Pulmonary Disease. *Am J Respir Crit Care Med* (2018) 197:665–8. doi: 10.1164/rccm.201706-1304LE
105. Hu HL, Nie ZQ, Lu Y, Yang X, Song C, Chen H, et al. Circulating miR-125b but not miR-125a correlates with acute exacerbations of chronic obstructive pulmonary disease and the expressions of inflammatory cytokines. *Medicine (Baltimore)* (2017) 96:e9059. doi: 10.1097/MD.0000000000009059
106. Ikari J, Nelson AJ, Obaid J, Giron-Martinez A, Ikari K, Makino F, et al. Reduced microRNA-503 expression augments lung fibroblast VEGF

production in chronic obstructive pulmonary disease. *PloS One* (2017) 12: e0184039. doi: 10.1371/journal.pone.0184039
107. Ong J, van den Berg A, Faiz A, Boudewijn IM, Timens W, Vermeulen CJ, et al. Current smoking is associated with decreased expression of mir-335-5p in parenchymal lung fibroblasts. *Int J Mol Sci* (2019) 20:5176. doi: 10.3390/ijms20205176
108. Tasena H, Boudewijn IM, Faiz A, Timens W, Hylkema MN, Berg M, et al. MiR-31-5p: A shared regulator of chronic mucus hypersecretion in asthma and chronic obstructive pulmonary disease. *Allergy* (2020) 75:703–6. doi: 10.1111/all.14060
109. Xue H, Li MX. MicroRNA-150 protects against cigarette smoke-induced lung inflammation and airway epithelial cell apoptosis through repressing p53: MicroRNA-150 in CS-induced lung inflammation. *Hum Exp Toxicol* (2018) 37:920–8. doi: 10.1177/0960327117741749
110. Leuenberger C, Schuoler C, Bye H, Mignan C, Rechsteiner T, Hillinger S, et al. MicroRNA-223 controls the expression of histone deacetylase 2: a novel axis in COPD. *J Mol Med* (2016) 94:725–34. doi: 10.1007/s00109-016-1388-1
111. Dang X, Yang L, Guo J, Hu H, Li F, Liu Y, et al. miR-145-5p is associated with smoke-related chronic obstructive pulmonary disease via targeting KLF5. *Chem Biol Interact* (2019) 300:82–90. doi: 10.1016/j.cbi.2019.01.011
112. Lu L, Qi H, Luo F, Xu H, Ling M, Qin Y, et al. Feedback circuitry via let-7c between lncRNA CCAT1 and c-Myc is involved in cigarette smoke extract-induced malignant transformation of HBE cells. *Oncotarget* (2017) 8:19285–97. doi: 10.18632/oncotarget.15195
113. Xu H, Ling M, Xue J, Dai X, Sun Q, Chen C, et al. Exosomal microRNA-21 derived from bronchial epithelial cells is involved in aberrant epithelium-fibroblast cross-talk in COPD induced by cigarette smoking. *Theranostics* (2018) 8:5419–33. doi: 10.7150/thno.27876
114. Lu L, Xu H, Yang P, Xue J, Chen C, Sun Q, et al. Involvement of HIF-1α-regulated miR-21, acting via the Akt/NF-κB pathway, in malignant transformation of HBE cells induced by cigarette smoke extract. *Toxicol Lett* (2018) 289:14–21. doi: 10.1016/j.toxlet.2018.02.027
115. He S, Li L, Sun S, Zeng Z, Lu J, Xie L. A novel murine chronic obstructive pulmonary disease model and the pathogenic role of microRNA-21. *Front Physiol* (2018) 9:503. doi: 10.3389/fphys.2018.00503
116. Zeng Z, He SY, Lu JJ, Liu C, Lin H, Xu CQ, et al. MicroRNA-21 aggravates chronic obstructive pulmonary disease by promoting autophagy. *Exp Lung Res* (2018) 44:89–97. doi: 10.1080/01902148.2018.1439548
117. Velasco-Torres Y, López VR, Pérez-Bautista O, Buendía-Roldan I, Ramírez-Venegas A, Pérez-Ramos J, et al. MiR-34a in serum is involved in mild-to-moderate COPD in women exposed to biomass smoke. *BMC Pulm Med* (2019) 19:227. doi: 10.1186/s12890-019-0977-5
118. Xie L, Wu M, Lin H, Liu C, Yang H, Zhan J, et al. An increased ratio of serum miR-21 to miR-181a levels is associated with the early pathogenic process of chronic obstructive pulmonary disease in asymptomatic heavy smokers. *Mol Biosyst* (2014) 10:1072–81. doi: 10.1039/c3mb70564a
119. Kim RY, Horvat JC, Pinkerton JW, Starkey MR, Essilfie AT, Mayall JR, et al. MicroRNA-21 drives severe, steroid-insensitive experimental asthma by amplifying phosphoinositide 3-kinase–mediated suppression of histone deacetylase 2. *J Allergy Clin Immunol* (2017) 139:519–32. doi: 10.1016/j.jaci.2016.04.038
120. Zhu QY, Liu Q, Chen JX, Lan K, Ge BX. MicroRNA-101 Targets MAPK Phosphatase-1 To Regulate the Activation of MAPKs in Macrophages. *J Immunol* (2010) 185:7435–42. doi: 10.4049/jimmunol.1000798
121. Wang B, Liu Y, Luo F, Xu Y, Qin Y, Lu X, et al. Epigenetic silencing of microRNA-218 via EZH2-mediated H3K27 trimethylation is involved in malignant transformation of HBE cells induced by cigarette smoke extract. *Arch Toxicol* (2016) 90:449–61. doi: 10.1007/s00204-014-1435-z
122. Xu H, Sun Q, Lu L, Luo F, Zhou L, Liu J, et al. MicroRNA-218 acts by repressing TNFR1-mediated activation of NF-κB, which is involved in MUC5AC hyper-production and inflammation in smoking-induced bronchiolitis of COPD. *Toxicol Lett* (2017) 280:171–80. doi: 10.1016/j.toxlet.2017.08.079
123. Conickx G, Mestdagh P, Cobos FA, Verhamme FM, Maes T, Vanaudenaerde BM, et al. MicroRNA profiling reveals a role for MicroRNA-218-5p in the pathogenesis of chronic obstructive pulmonary disease. *Am J Respir Crit Care Med* (2017) 195:43–56. doi: 10.1164/rccm.201506-1182OC
124. Song J, Wang QH, Zou SC. Role of microRNA-218-5p in the pathogenesis of chronic obstructive pulmonary disease. *Eur Rev Med Pharmacol Sci* (2018) 22:4319–24. doi: 10.26355/eurrev_201807_15428
125. Mizuno S, Bogaard HJ, Gomez-Arroyo J, Alhussaini A, Kraskauskas D, Cool CD, et al. MicroRNA-199a-5p is associated with hypoxia-inducible factor-1α expression in lungs from patients with COPD. *Chest* (2012) 142:663–72. doi: 10.1378/chest.11-2746
126. Chatila WM, Criner GJ, Hancock WW, Akimova T, Moldover B, Chang JK, et al. Blunted expression of miR-199a-5p in regulatory T cells of patients with chronic obstructive pulmonary disease compared to unaffected smokers. *Clin Exp Immunol* (2014) 177:341–52. doi: 10.1111/cei.12325
127. Liu Y, Liu G, Zhang H, Wang J. MiRNA-199a-5p influences pulmonary artery hypertension via downregulating Smad3. *Biochem Biophys Res Commun* (2016) 473:859–66. doi: 10.1016/j.bbrc.2016.03.140
128. Halappanavar S, Nikota J, Wu D, Williams A, Yauk CL, Stampfli M. IL-1 Receptor Regulates microRNA-135b Expression in a Negative Feedback Mechanism during Cigarette Smoke–Induced Inflammation. *J Immunol* (2013) 190:3679–86. doi: 10.4049/jimmunol.1202456
129. Bertrams W, Griss K, Han M, Seidel K, Klemmer A, Sittka-Stark A, et al. Transcriptional analysis identifies potential biomarkers and molecular regulators in pneumonia and COPD exacerbation. *Sci Rep* (2020) 10:241. doi: 10.1038/s41598-019-57108-0
130. Dang X, Qu X, Wang W, Liao C, Li Y, Zhang X, et al. Bioinformatic analysis of microRNA and mRNA Regulation in peripheral blood mononuclear cells of patients with chronic obstructive pulmonary disease. *Respir Res* (2017) 18:4. doi: 10.1186/s12931-016-0486-5
131. Wang M, Huang Y, Liang Z, Liu D, Lu Y, Dai Y, et al. Plasma miRNAs might be promising biomarkers of chronic obstructive pulmonary disease. *Clin Respir J* (2016) 10:104–11. doi: 10.1111/crj.12194
132. Sundar IK, Li D, Rahman I. Small RNA-sequence analysis of plasma-derived extracellular vesicle miRNAs in smokers and patients with chronic obstructive pulmonary disease as circulating biomarkers. *J Extracell Vesicles* (2019) 8:1684816. doi: 10.1080/20013078.2019.1684816
133. Puig-Vilanova E, Martínez-Llorens J, Ausin P, Roca J, Gea J, Barreiro E. Quadriceps muscle weakness and atrophy are associated with a differential epigenetic profile in advanced COPD. *Clin Sci* (2015) 128:905–21. doi: 10.1042/CS20140428
134. Sun Y, An N, Li J, Xia J, Tian Y, Zhao P, et al. miRNA-206 regulates human pulmonary microvascular endothelial cell apoptosis via targeting in chronic obstructive pulmonary disease. *J Cell Biochem* (2019) 120:6223–36. doi: 10.1002/jcb.27910
135. Chu H, Qu X, Wang F, Chang J, Cheng R, Song X, et al. MicroRNA-206 promotes lipopolysaccharide-induced inflammation injury via regulation of IRAK1 in MRC-5 cells. *Int Immunopharmacol* (2019) 73:590–8. doi: 10.1016/j.intimp.2019.05.029
136. Akbas F, Coskunpinar E, Aynaci E, Müsteri-Oltulu Y, Yildiz P. Analysis of Serum Micro-RNAs as potential biomarker in chronic obstructive pulmonary disease. *Exp Lung Res* (2012) 38:286–94. doi: 10.3109/01902148.2012.689088
137. Liu PF, Yan P, Zhao DH, Shi WF, Meng S, Liu Y, et al. The effect of environmental factors on the differential expression of miRNAs in patients with chronic obstructive pulmonary disease: A pilot clinical study. *Int J Chron Obstruct Pulmon Dis* (2018) 13:741–51. doi: 10.2147/COPD.S156865
138. Lewis A, Riddoch-Contreras J, Natanek SA, Donaldson A, Man WDC, Moxham J, et al. Downregulation of the serum response factor/miR-1 axis in the quadriceps of patients with COPD. *Thorax* (2012) 67:26–34. doi: 10.1136/thoraxjnl-2011-200309
139. Oldenburger A, Van Basten B, Kooistra W, Meurs H, Maarsingh H, Krenning G, et al. Interaction between Epac1 and miRNA-7 in airway smooth muscle cells. *Naunyn Schmiedebergs Arch Pharmacol* (2014) 387:795–7. doi: 10.1007/s00210-014-1015-z
140. Savarimuthu-Francis SM, Davidson MR, Tan ME, Wright CM, Clarke BE, Duhig EE, et al. MicroRNA-34c is associated with emphysema severity and modulates SERPINE1 expression. *BMC Genomics* (2014) 15:88. doi: 10.1186/1471-2164-15-88
141. Long YJ, Liu XP, Chen SS, Zong DD, Chen Y, Chen P. miR-34a is involved in CSE-induced apoptosis of human pulmonary microvascular endothelial cells by targeting Notch-1 receptor protein. *Respir Res* (2018) 19:21. doi: 10.1186/s12931-018-0722-2
142. Kato R, Mizuno S, Kadowaki M, Shiozaki K, Akai M, Nakagawa K, et al. Sirt1 expression is associated with CD31 expression in blood cells from patients with chronic obstructive pulmonary disease. *Respir Res* (2016) 17:139. doi: 10.1186/s12931-016-0452-2

143. Du Y, Ding Y, Chen X, Mei Z, Ding H, Wu Y, et al. MicroRNA-181c inhibits cigarette smoke-induced chronic obstructive pulmonary disease by regulating CCN1 expression. *Respir Res* (2017) 18:155. doi: 10.1186/s12931-017-0639-1
144. Faiz A, Steiling K, Roffel MP, Postma DS, Spira A, Lenburg ME, et al. Effect of long-term corticosteroid treatment on microRNA and gene-expression profiles in COPD. *Eur Respir J* (2019) 53:1801202. doi: 10.1183/13993003.01202-2018
145. Rodrigo-Muñoz JM, Rial MJ, Sastre B, Cañas JA, Mahíllo-Fernández I, Quirce S, et al. Circulating miRNAs as diagnostic tool for discrimination of respiratory disease: Asthma, asthma-chronic obstructive pulmonary disease (COPD) overlap and COPD. *Allergy Eur J Allergy Clin Immunol* (2019) 74:2491–4. doi: 10.1111/all.13916
146. O'Leary L, Sevinç K, Papazoglou IM, Tildy B, Detillieux K, Halayko AJ, et al. Airway smooth muscle inflammation is regulated by microRNA-145 in COPD. *FEBS Lett* (2016) 590:1324–34. doi: 10.1002/1873-3468.12168
147. Yang S, Cui H, Xie N, Icyuz M, Banerjee S, Antony VB, et al. MiR-145 regulates myofibroblast differentiation and lung fibrosis. *FASEB J* (2013) 27:2382–91. doi: 10.1096/fj.12-219493
148. Dutta RK, Chinnapaiyan S, Rasmussen L, Raju SV, Unwalla HJ. A Neutralizing Aptamer to TGFBR2 and miR-145 Antagonism Rescue Cigarette Smoke- and TGF-β-Mediated CFTR Expression. *Mol Ther* (2019) 27:442–55. doi: 10.1016/j.ymthe.2018.11.017
149. Perry MM, Moschos SA, Williams AE, Shepherd NJ, Larner-Svensson HM, Lindsay MA. Rapid Changes in MicroRNA-146a Expression Negatively Regulate the IL-1β-Induced Inflammatory Response in Human Lung Alveolar Epithelial Cells. *J Immunol* (2008) 180:5689–98. doi: 10.4049/jimmunol.180.8.5689
150. Stolzenburg LR, Wachtel S, Dang H, Harris A. MIR-1343 attenuates pathways of fibrosis by targeting the TGF-ß receptors. *Biochem J* (2016) 473:245–56. doi: 10.1042/BJ20150821
151. Mercer BA, Kolesnikova N, Sonett J, D'Armiento J. Extracellular Regulated Kinase/Mitogen Activated Protein Kinase Is Up-regulated in Pulmonary Emphysema and Mediates Matrix Metalloproteinase-1 Induction by Cigarette Smoke. *J Biol Chem* (2004) 279:17690–6. doi: 10.1074/jbc.M313842200
152. Tang K, Zhao J, Xie J, Wang J. Decreased miR-29b expression is associated with airway inflammation in chronic obstructive pulmonary disease. *Am J Physiol Lung Cell Mol Physiol* (2019) 316:L621–9. doi: 10.1152/ajplung.00436.2018
153. Shi L, Xin Q, Chai R, Liu L, Ma Z. Ectopic expressed miR-203 contributes to chronic obstructive pulmonary disease via targeting TAK1 and PIK3CA. *Int J Clin Exp Pathol* (2015) 8:10662–70.
154. Wang R, Li M, Zhou S, Zeng D, Xu X, Xu R, et al. Effect of a single nucleotide polymorphism in miR-146a on COX-2 protein expression and lung function in smokers with chronic obstructive pulmonary disease. *Int J Chron Obstruct Pulmon Dis* (2015) 10:463–73. doi: 10.2147/COPD.S74345
155. Fawzy MS, Hussein MH, Abdelaziz EZ, Yamany HA, Ismail HM, Toraih EA. Association of microRNA-196a2 variant with response to short-acting β2-agonist in COPD: An Egyptian pilot study. *PloS One* (2016) 11:e0152834. doi: 10.1371/journal.pone.0152834
156. Li LJ, Gao LB, Lv ML, Dong W, Su XW, Liang WB, et al. Association between SNPs in pre-miRNA and risk of chronic obstructive pulmonary disease. *Clin Biochem* (2011) 44:813–6. doi: 10.1016/j.clinbiochem.2011.04.021
157. Zhou S, Liu Y, Li M, Wu P, Sun G, Fei G, et al. Combined effects of PVT1 and MiR-146a single nucleotide polymorphism on the lung function of smokers with chronic obstructive pulmonary disease. *Int J Biol Sci* (2018) 14:1153–62. doi: 10.7150/ijbs.25420
158. Shen Z, Tang W, Guo J, Sun S. MiR-483-5p plays a protective role in chronic obstructive pulmonary disease. *Int J Mol Med* (2017) 40:193–200. doi: 10.3892/ijmm.2017.2996
159. Izzotti A, Larghero P, Longobardi M, Cartiglia C, Camoirano A, Steele VE, et al. Dose-responsiveness and persistence of microRNA expression alterations induced by cigarette smoke in mouse lung. *Mutat Res* (2011) 717:9–16. doi: 10.1016/j.mrfmmm.2010.12.008
160. Shen W, Liu J, Zhao G, Fan M, Song G, Zhang Y, et al. Repression of toll-like receptor-4 by microRNA-149-3p is associated with smoking-related COPD. *Int J Chron Obstruct Pulmon Dis* (2017) 12:705–15. doi: 10.2147/COPD.S128031
161. Shen W, Liu J, Fan M, Wang S, Zhang Y, Wen L, et al. MiR-3202 protects smokers from chronic obstructive pulmonary disease through inhibiting FAIM2: An in vivo and in vitro study. *Exp Cell Res* (2018) 362:370–7. doi: 10.1016/j.yexcr.2017.11.038
162. Lewis CE, Harney AS, Pollard JW. The Multifaceted Role of Perivascular Macrophages in Tumors. *Cancer Cell* (2016) 30:18–25. doi: 10.1016/j.ccell.2016.05.017
163. Lu L, Luo F, Liu Y, Liu X, Shi L, Lu X, et al. Posttranscriptional silencing of the lncRNA MALAT1 by miR-217 inhibits the epithelial-mesenchymal transition via enhancer of zeste homolog 2 in the malignant transformation of HBE cells induced by cigarette smoke extract. *Toxicol Appl Pharmacol* (2015) 289:276–85. doi: 10.1016/j.taap.2015.09.016
164. Dino P, D'Anna C, Sangiorgi C, Di Sano C, Di Vincenzo S, Ferraro M, et al. Cigarette smoke extract modulates E-Cadherin, Claudin-1 and miR-21 and promotes cancer invasiveness in human colorectal adenocarcinoma cells. *Toxicol Lett* (2019) 317:102–9. doi: 10.1016/j.toxlet.2019.09.020
165. Zhong S, Chen C, Liu N, Yang L, Hu Z, Duan P, et al. Overexpression of hsa-miR-664a-3p is associated with cigarette smoke-induced chronic obstructive pulmonary disease via targeting FHL1. *Int J Chron Obstruct Pulmon Dis* (2019) 14:2319–29. doi: 10.2147/COPD.S224763
166. Baker JR, Vuppusetty C, Colley T, Papaioannou AI, Fenwick P, Donnelly L, et al. Oxidative stress dependent microRNA-34a activation via PI3Kα reduces the expression of sirtuin-1 and sirtuin-6 in epithelial cells. *Sci Rep* (2016) 6:35871. doi: 10.1038/srep35871
167. Wu Y, Guan S, Ge Y, Yang Y, Cao Y, Zhou J. Cigarette smoke promotes chronic obstructive pulmonary disease (COPD) through the miR-130a/Wnt1 axis. *Toxicol In Vitro* (2020) 65:104770. doi: 10.1016/j.tiv.2020.104770
168. Zhao Y, Xu Y, Li Y, Xu W, Luo F, Wang B, et al. NF-κB-mediated Inflammation Leading to EMT via miR-200c Is Involved in Cell Transformation Induced by Cigarette Smoke Extract. *Toxicol Sci* (2013) 135:265–76. doi: 10.1093/toxsci/kft150
169. Lin L, Sun J, Wu D, Lin D, Sun D, Li Q, et al. MicroRNA-186 is associated with hypoxia-inducible factor-1α expression in chronic obstructive pulmonary disease. *Mol Genet Genomic Med* (2019) 7:e531. doi: 10.1002/mgg3.531
170. Hassan T, Carroll TP, Buckley PG, Cummins R, O'Neill SJ, McElvaney NG, et al. MiR-199a-5p silencing regulates the unfolded protein response in chronic obstructive pulmonary disease and α1-antitrypsin deficiency. *Am J Respir Crit Care Med* (2014) 189:263–73. doi: 10.1164/rccm.201306-1151OC
171. Oldenburger A, Roscioni SS, Jansen E, Menzen MH, Halayko AJ, Timens W, et al. Anti-inflammatory role of the cAMP effectors Epac and PKA: Implications in chronic obstructive pulmonary disease. *PloS One* (2012) 7:e31574. doi: 10.1371/journal.pone.0031574
172. Ong J, Faiz A, Timens W, van den Berge M, Terpstra MM, Kok K, et al. Marked TGF-β-regulated miRNA expression changes in both COPD and control lung fibroblasts. *Sci Rep* (2019) 9:18214. doi: 10.1038/s41598-019-54728-4
173. Wang Y, Yang L, Li P, Huang H, Liu T, He H, et al. Circulating microRNA signatures associated with childhood asthma. *Clin Lab* (2015) 61:467–74. doi: 10.7754/Clin.Lab.2014.141020
174. Mousavi SR, Ahmadi A, Jamalkandi SA, Salimian J. Involvement of microRNAs in physiological and pathological processes in asthma. *J Cell Physiol* (2019) 234:21547–59. doi: 10.1002/jcp.28781
175. Leidinger P, Keller A, Borries A, Huwer H, Rohling M, Huebers J, et al. Specific peripheral miRNA profiles for distinguishing lung cancer from COPD. *Lung Cancer* (2011) 74:41–7. doi: 10.1016/j.lungcan.2011.02.003
176. Li L, Feng T, Zhang W, Gaon S, Wang R, Lv W. MicroRNA Biomarker hsa-miR-195-5p for Detecting the Risk of Lung Cancer. *Int J Genomics* (2020) 2020:7415909. doi: 10.1155/2020/7415909
177. Simpson LJ, Patel S, Bhakta NR, Choy DF, Brightbill HD, Ren X, et al. A microRNA upregulated in asthma airway T cells promotes T H 2 cytokine production. *Nat Immunol* (2014) 15:1162–70. doi: 10.1038/ni.3026
178. Lu TX, Hartner J, Lim EJ, Fabry V, Mingler MK, Cole ET, et al. MicroRNA-21 Limits In Vivo Immune Response-Mediated Activation of the IL-12/IFN-γ Pathway, Th1 Polarization, and the Severity of Delayed-Type Hypersensitivity. *J Immunol* (2011) 187:3362–73. doi: 10.4049/jimmunol.1101235
179. Perry MM, Adcock IM, Chung KF. Role of microRNAs in allergic asthma: Present and future. *Curr Opin Allergy Clin Immunol* (2015) 15:156–62. doi: 10.1097/ACI.0000000000000147
180. Walker JA, McKenzie ANJ. TH2 cell development and function. *Nat Rev Immunol* (2018) 18:121–33. doi: 10.1038/nri.2017.118
181. Steiner DF, Thomas MF, Hu JK, Yang Z, Babiarz JE, Allen CDC, et al. MicroRNA-29 Regulates T-Box Transcription Factors and Interferon-γ

Production in Helper T Cells. *Immunity* (2011) 35:169–81. doi: 10.1016/j.immuni.2011.07.009
182. Yan J, Zhang X, Sun S, Yang T, Yang J, Wu G, et al. MiR-29b Reverses T helper 1 cells/T helper 2 cells Imbalance and Alleviates Airway Eosinophils Recruitment in OVA-Induced Murine Asthma by Targeting Inducible Co-Stimulator. *Int Arch Allergy Immunol* (2019) 180:182–94. doi: 10.1159/000501686
183. Alharris E, Alghetaa H, Seth R, Chatterjee S, Singh NP, Nagarkatti M, et al. Resveratrol Attenuates Allergic Asthma and Associated Inflammation in the Lungs Through Regulation of miRNA-34a That Targets FoxP3 in Mice. *Front Immunol* (2018) 9:2992. doi: 10.3389/fimmu.2018.02992
184. Girodet PO, Nguyen D, Mancini JD, Hundal M, Zhou X, Israel E, et al. Alternative macrophage activation is increased in asthma. *Am J Respir Cell Mol Biol* (2016) 55:467–75. doi: 10.1165/rcmb.2015-0295OC
185. Draijer C, Robbe P, Boorsma CE, Hylkema MN, Melgert BN. Dual role of YM1+ M2 macrophages in allergic lung inflammation. *Sci Rep* (2018) 8:5105. doi: 10.1038/s41598-018-23269-7
186. Feketea G, Bocsan CI, Popescu C, Gaman M, Stanciu LA, Zdrenghea MT. A Review of Macrophage MicroRNAs' Role in Human Asthma. *Cells* (2019) 8:420. doi: 10.3390/cells8050420
187. Peng L, Zhang H, Hao Y, Xu F, Yang J, Zhang R, et al. Reprogramming macrophage orientation by microRNA 146b targeting transcription factor IRF5. *EBioMedicine* (2016) 14:83–96. doi: 10.1016/j.ebiom.2016.10.041
188. Huang C, Liu XJ, Qun Z, Xie J, Ma TT, Meng XM, et al. MiR-146a modulates macrophage polarization by inhibiting Notch1 pathway in RAW264.7 macrophages. *Int Immunopharmacol* (2016) 32:46–54. doi: 10.1016/j.intimp.2016.01.009
189. Athari SS. Targeting cell signaling in allergic asthma. *Signal Transduct Target Ther* (2019) 4:45. doi: 10.1038/s41392-019-0079-0
190. Davies DE. The role of the epithelium in airway remodeling in asthma. *Proc Am Thorac Soc* (2009) 6:678–82. doi: 10.1513/pats.200907-067DP
191. Wang LQ, Wang CL, Xu LN, Hua DF. The Expression Research of miR-210 in the Elderly Patients With COPD Combined With Ischemic Stroke. *Eur Rev MEd Pharmacol Sci* (2016) 20:4756–60.
192. Global Initiative For Chronic Obstructive Lung Disease. *Diagnosis of Diseases of Chronic Airflow Limitation: Asthma, COPD and Asthma-COPD Overlap Syndrome (ACOS)* (2015). Available at: www.ginasthma.orgwww.goldcopd.orghttp://www.ginasthma.orggoldreportsareavailableathttp//www.goldcopd.org (Accessed April 14, 2020).
193. Cosío BG, De Llano LP, Viña AL, Torrego A, Lopez-Campos JL, Soriano JB, et al. Th-2 signature in chronic airway diseases: Towards the extinction of asthma-COPD overlap syndrome? *Eur Respir J* (2017) 49:1602397. doi: 10.1183/13993003.02397-2016
194. Asensio VJ, Tomás A, Iglesias A, de Llano LP, del Pozo V, Cosío BG. Eosinophilic COPD Patients Display a Distinctive Serum miRNA Profile From Asthma and Non-eosinophilic COPD. *Arch Bronconeumol* (2019) 56:234–41. doi: 10.1016/j.arbres.2019.09.020
195. Mukherjee M, Svenningsen S, Nair P. Glucocortiosteroid subsensitivity and asthma severity. *Curr Opin Pulm Med* (2017) 23:78–88. doi: 10.1097/MCP.0000000000000337
196. Zhou H, Li J, Gao P, Wang Q, Zhang J. miR-155: A novel target in allergic asthma. *Int J Mol Sci* (2016) 17:1773. doi: 10.3390/ijms17101773
197. Wang ZH, Liang YB, Tang H, Chen ZB, Li ZY, Hu XC, et al. Dexamethasone down-regulates the expression of microRNA-155 in the livers of septic mice. *PloS One* (2013) 8:e80547. doi: 10.1371/journal.pone.0080547
198. Zheng Y, Xiong S, Jiang P, Liu R, Liu X, Qian J, et al. Glucocorticoids inhibit lipopolysaccharide-mediated inflammatory response by downregulating microRNA-155: A novel anti-inflammation mechanism. *Free Radic Biol Med* (2012) 52:1307–17. doi: 10.1016/j.freeradbiomed.2012.01.031
199. Li J, Panganiban R, Kho AT, McGeachie MJ, Farnam L, Chase RP, et al. Circulating MicroRNAs and Treatment Response in Childhood Asthma. *Am J Respir Crit Care Med* (2020) 202:65–72. doi: 10.1164/rccm.201907-1454oc
200. Elbehidy RM, Youssef DM, El-Shal AS, Shalaby SM, Sherbiny HS, Sherief LM, et al. MicroRNA-21 as a novel biomarker in diagnosis and response to therapy in asthmatic children. *Mol Immunol* (2016) 71:107–14. doi: 10.1016/j.molimm.2015.12.015
201. Wu SQ, Wang GL, Li LY, Ji J. Effects of microRNA-21 on the interleukin 12/signal transducer and activator of transcription 4 signaling pathway in asthmatic mice. *Cent Eur J Immunol* (2014) 39:40–5. doi: 10.5114/ceji.2014.42121
202. Sheedy FJ, Palsson-Mcdermott E, Hennessy EJ, Martin C, O'Leary JJ, Ruan Q, et al. Negative regulation of TLR4 via targeting of the proinflammatory tumor suppressor PDCD4 by the microRNA miR-21. *Nat Immunol* (2010) 11:141–7. doi: 10.1038/ni.1828
203. Lu LF, Liston A. MicroRNA in the immune system, microRNA as an immune system. *Immunology* (2009) 127:291–8. doi: 10.1111/j.1365-2567.2009.03092.x
204. Li JJ, Tay HL, Maltby S, Xiang Y, Eyers F, Hatchwell L, et al. MicroRNA-9 regulates steroid-resistant airway hyperresponsiveness by reducing protein phosphatase 2A activity. *J Allergy Clin Immunol* (2015) 136:462–73. doi: 10.1016/j.jaci.2014.11.044
205. McGeachie MJ, Davis JS, Kho AT, Dahlin A, Sordillo JE, Sun M, et al. Asthma remission: Predicting future airways responsiveness using an miRNA network. *J Allergy Clin Immunol* (2017) 140:598–600. doi: 10.1016/j.jaci.2017.01.023
206. Williams AE, Larner-Svensson H, Perry MM, Campbell GA, Herrick SE, Adcock IM, et al. MicroRNA expression profiling in mild asthmatic human airways and effect of corticosteroid therapy. *PloS One* (2009) 4:e5889. doi: 10.1371/journal.pone.0005889
207. World Health Organization. *COPD management* (2013). Available at: https://www.who.int/respiratory/copd/management/en/ (Accessed Accesed 18 April, 2020).
208. Lopez-Campos JL, Carrasco Hernández L, Muñoz X, Bustamante V, Barreiro E. Current controversies in the stepping up and stepping down of inhaled therapies for COPD at the patient level. *Respirology* (2018) 23:818–27. doi: 10.1111/resp.13341
209. Barnes PJ. Targeting the epigenome in the treatment of asthma and chronic obstructive pulmonary disease. *Proc Am Thorac Soc* (2009) 6:693–6. doi: 10.1513/pats.200907-071DP
210. Liu S, Liu M, Dong L. The clinical value of lncRNA MALAT1 and its targets miR-125b, miR-133, miR-146a, and miR-203 for predicting disease progression in chronic obstructive pulmonary disease patients. *J Clin Lab Anal* (2020) 34:e23410. doi: 10.1002/jcla.23410
211. Xu W, Wang Y, Ma Y, Yang J. MiR-223 plays a protecting role in neutrophilic asthmatic mice through the inhibition of NLRP3 inflammasome. *Respir Res* (2020) 21:116. doi: 10.1186/s12931-020-01374-4
212. Liu J, Chen Y, Zhang F, Peng X, Mao X, Lu W, et al. Divergent Roles of miR-3162-3p in Pulmonary Inflammation in Normal and Asthmatic Mice as well as Antagonism of miR-3162-3p in Asthma Treatment. *Int Arch Allergy Immunol* (2020) 181:594–605. doi: 10.1159/000507250
213. Cullinan P, Reid P. Pneumoconiosis. *Prim Care Respir J* (2013) 22:249–52. doi: 10.4104/pcrj.2013.00055
214. Wang X, Lu X, Ma C, Ma L, Han S. Combination of TLR agonist and miR146a mimics attenuates ovalbumin-induced asthma. *Mol Med* (2020) 26:65. doi: 10.1186/s10020-020-00191-1
215. Shi ZG, Sun Y, Wang KS, Jia JD, Yang J, Li YN. Effects of mir-26a/mir-146a/miR-31 on airway inflammation of asthma mice and asthma children. *Eur Rev Med Pharmacol Sci* (2019) 23:5432–40. doi: 10.26355/eurre

Conflict of Interest: VP has received honoraria (advisory board, speaker) and/or institutional grant/research support from Astra-Zeneca and GSK.

The remaining authors declare that the research was conducted in the absence of any commercial or financial relationships that could be construed as a potential conflict of interest.

Copyright © 2021 Cañas, Rodrigo-Muñoz, Sastre, Gil-Martinez, Redondo and del Pozo. This is an open-access article distributed under the terms of the Creative Commons Attribution License (CC BY). The use, distribution or reproduction in other forums is permitted, provided the original author(s) and the copyright owner(s) are credited and that the original publication in this journal is cited, in accordance with accepted academic practice. No use, distribution or reproduction is permitted which does not comply with these terms.

frontiers in Immunology

ORIGINAL RESEARCH
published: 11 February 2021
doi: 10.3389/fimmu.2020.595003

IL-4 and IL-17 Are Required for House Dust Mite-Driven Airway Hyperresponsiveness in Autoimmune Diabetes-Prone Non-Obese Diabetic Mice

Anne-Perrine Foray[1,2], *Céline Dietrich*[1,2], *Coralie Pecquet*[1,2], *François Machavoine*[1,2], *Lucienne Chatenoud*[1,2] *and Maria Leite-de-Moraes*[1,2*]

[1] Université de Paris, Paris, France, [2] Laboratory of Immunoregulation and Immunopathology, INEM (Institut Necker-Enfants Malades), CNRS UMR8253 and Inserm UMR1151, Paris, France

Allergic asthma is characterized by airway inflammation with a Th2-type cytokine profile, hyper-IgE production, mucus hypersecretion, and airway hyperreactivity (AHR). It is increasingly recognized that asthma is a heterogeneous disease implicating complex immune mechanisms resulting in distinct endotypes observed in patients. In this study, we showed that non-obese diabetic (NOD) mice, which spontaneously develop autoimmune diabetes, undergo more severe allergic asthma airway inflammation and AHR than pro-Th2 BALB/c mice upon house dust mite (HDM) sensitization and challenge. The use of IL-4-deficient NOD mice and the *in vivo* neutralization of IL-17 demonstrated that both IL-4 and IL-17 are responsible by the exacerbated airway inflammation and AHR observed in NOD mice. Overall, our findings indicate that autoimmune diabetes-prone NOD mice might become useful as a new HDM-induced asthma model to elucidate allergic dysimmune mechanisms involving Th2 and Th17 responses that could better mimic some asthmatic endoytpes.

Keywords: asthma, NOD mice, IL-17, iNKT cells, IL-4, house dust mite, iNKT cells, airway hyperreactivity

OPEN ACCESS

Edited by:
Girolamo Pelaia, University of Catanzaro, Italy

Reviewed by:
Ian Paul Lewkowich, Cincinnati Children's Hospital Medical Center, United States
Adam Collison, The University of Newcastle, Australia

***Correspondence:**
Maria Leite-de-Moraes
maria.leite-demoraes@inserm.fr

Specialty section:
This article was submitted to Inflammation, a section of the journal Frontiers in Immunology

Received: *14 August 2020*
Accepted: *29 December 2020*
Published: *11 February 2021*

Citation:
Foray A-P, Dietrich C, Pecquet C, Machavoine F, Chatenoud L and Leite-de-Moraes M (2021) IL-4 and IL-17 Are Required for House Dust Mite-Driven Airway Hyperresponsiveness in Autoimmune Diabetes-Prone Non-Obese Diabetic Mice. Front. Immunol. 11:595003. doi: 10.3389/fimmu.2020.595003

INTRODUCTION

Asthma is an heterogenous immune pathology characterized by wheeze, cough, shortness of breath, chest tightness, and variable degrees of airflow limitation. These symptoms are associated with different patterns of inflammation (1–5). Commonly, asthma is distinguished in two types: allergic and non-allergic. In the first case, inflammation is primarily caused by type 2 immune responses mediated through the Th2 cytokines IL-4, IL-5, and IL-13 and associated with increased Th2 cells and eosinophils in the airways (6, 7). By contrast, non-allergic asthma is mainly triggered by an inflammatory response to viral infections with a major neutrophilic component (7). There is

Abbreviations: AHR, airway hyperreactivity; BALF, bronchoalveolar lavage fluid; HDM, house dust mite; ILT, innate-like T cells; iNKT, invariant natural killer T cells; NOD, non-obese diabetic.

mounting evidence that neutrophilic forms of murine and human asthma are associated with IL-17A (hereafter referred to as IL-17) (8–10).

Th2 and Th17 inflammatory pathways in asthma are currently in investigation (11–13). It was reported that therapeutic targeting of Th2 and Th17 cytokines resulted in the amplification of activity of the opposing pathway (14). The cross-talk between these pathways is complex and further analysis are required to better understand this complexity.

We have previously reported using a classical asthma protocol induced by sensitization and challenge with ovalbumin (OVA) that non-obese diabetic (NOD) mice, which spontaneously develops insulin-dependent diabetes (15, 16), presented an exacerbated Th2-mediated airway inflammation and AHR (17). Further, we reported that NOD mice were prone to produce pro-Th17 cytokines and that IL-17-producing iNKT (iNKT17) cells (18, 19) were overrepresented in these mice (20). These observations led us to examine in more detail whether both Th2 and Th17 inflammatory pathways were implicated in the exacerbated airway inflammation in NOD mice. Here we used a more relevant allergic asthma allergen, the house dust mite (HDM) extracts, and analyzed the airway inflammation by comparing NOD and the Th2 prone BALB/c mice. We show that both IL-4 and IL-17 are critically implicated in the exacerbated AHR observed in NOD mice.

MATERIALS AND METHODS

Mice

Eight to 10-week-old specific pathogen-free NOD and BALB/c mice were bred in our facility. All animal experiments were carried out according to the guidelines for care and use of animals approved by the French Institutional Committee (*APAFIS#4105-201511171831592*).

Airway Allergen Sensitization and Challenge Model

Mice were immunized by intra nasal (i.n.) injection of 100 μg of HDM extracts (Greer Laboratories, USA) in 0.2 ml saline solution. Mice were then challenged on days 7, 11, and 17 with i.n. HDM (50 μg/mouse) or saline solution. Twenty-four hours after the last challenge, mice were anesthetized with a mixture of ketamine (150 mg/kg) and xylasine (400 μg/kg) and their tracheas were cannulated (tracheostomy with ligation). A flexiVent apparatus (SCIREQ) was used to measure airway-specific resistance (Rn, tidal volume of 10 ml/kg at a respiratory rate of 150 breaths/min in response to increasing doses of aerosolized acetyl-β-methylcholine chloride (methacholine; Sigma-Aldrich). Assessments were performed at least three times and the maximum R value obtained after each dose of methacholine was used for the measure.

Airway inflammation was assessed on cytospin preparations of cells from bronchoalveolar lavage fluid [BALF, 3 x 0.5 ml washes with phosphate-buffered saline (PBS)] that were stained with May-Grünwald/Giemsa (Merck). For some experiments, BALF cells were also analyzed by flow cytometry.

Serum was collected and total IgE and HDM-specific IgG1 were measured by ELISA.

Lung Histology

Lungs were fixed with 10% formalin *via* the trachea, removed, and stored in 10% formalin. Lung tissues were embedded into paraffin and 3 μm sections were stained with periodic acid Schiff (PAS) using standard protocols and examined with a light microscope.

Flow Cytometry

BALF or lung mononuclear cells were stained at 4°C in staining buffer (1X PBS, 2% FCS, 2mM EDTA), in the presence of Fc block (2.4G2; BD Biosciences) and analyzed by flow cytometry.

Cells were incubated with CD1d-PBS57-APC tetramers and/or the specific antibodies listed below. For intracellular staining, cells were further fixed with 4% PFA, washed, and permeabilized with 0.5% saponin (Sigma-Aldrich), and then incubated with the anti-cytokine antibodies. The cells were washed and fluorescence was detected using a LSRFortessa (Becton Dickinson). Data were analyzed using the FlowJo 10.4.1 software (Tree Star). **Figure S1** represents the gate strategy used.

Antibodies from BD Biosciences: anti-CD3-FITC (145-2C11), anti-CD45-APC-Cy7 (30F11). Antibodies from BioLegend: anti-CD4-Brilliant Violet 605 (RM4-5), anti-CD69-FITC (H1.2F3), anti-CD8a-Brilliant Violet 785 (53-6.7), anti-TCR Vγ1/Cr4-PE (2.11) [Tonegawa 1986 nomenclature, (21)]. Antibodies from eBioscience: anti-CD44-eFluor450 (IM7), anti-TCRb-AlexaFluor 700 (H57-598), anti-IL-13-PE-eFluor610 (eBio13A), anti-IL-17A-PerCP-Cy5.5 (eBio17B7), anti-IL-4-PE-Cy7 (BVD6-24G2), anti-TCRδ-eFluor450 and -PE-Cy7 (GL3), and Fixable Viability Dye eFluor 506.

Leucocytes From Lung Tissue

After measurement of airway resistance and collection of BALF, lungs were perfused with PBS, lung tissues were cut into pieces using a gentleMACS Dissociator (Miltenyi Biotec) and treated with collagenase type 4 (Thermo Fischer Scientific) plus DNAse I (Roche). The lymphocyte-enriched fraction was collected at the 35–70% interface of Percoll gradients (GE Healthcare). Cells were immediately stained or stimulated for 4 h with with 10^{-8} M PMA and 1 μg ml^{-1} ionomycin, in the presence of 10 μg ml^{-1} brefeldin A (all from Sigma-Aldrich).

Measurement of Total IgE and HDM-Specific IgG1 by ELISA

Total IgE was measured in the serum by using a mouse IgE ELISA set (BD Biosciences) according to supplier's recommendations. An indirect ELISA method was used to measure HDM-specific IgG1 levels in serum samples as previously described by Trompette et al. (22). Briefly, 96-well microtiter plates were coated overnight with 100 μl of HDM at 10 μg/ml in PBS. The next day, 200 μl of blocking solution (1% BSA in PBS) was added to the plate for 2 h at room temperature. Subsequently, 100 μl of serum sample diluted 1:100 and 1:500 in blocking buffer was added to the plate at 4°C overnight followed by goat-anti-mouse IgG1 (Southern Biotech) for 1 h. Then HRP-

donkey anti-goat IgG (Santa Cruz) was added to the plate for 1 h at room temperature, followed by the substract TMB. Absorbance was measured at 450 nm using a microplate reader (VersaMax microplate reader, Molecular Devices). No HDM-specific IgG1 was detected in control mice.

mRNA Expression

RNAs were extracted using the RNeasy Plus Mini Kit (Qiagen) including a DNase treatment. Then RNA was reverse transcribed using the High Capacity RNA-to-cDNA Kit (Thermo Fisher Scientific), according to the manufacturer's instructions. Primers and probes for real-time PCR were provided by Thermo Fisher Scientific under references: beta-2 microglobulin: Mm00437762_m1; interleukin 5: Mm00439646_m1; interleukin 13: Mm00434204_m1; interleukin 17A: Mm00439618_m1; Mucin 5b (Muc5b): Mm00466391_m1. All reactions were performed in triplicate with TaqMan® Fast Advanced Master Mix according to the supplier's instructions for a StepOnePlus apparatus (Thermo Fisher Scientific). All data were normalized to the internal standard, namely beta-2 microglobulin expression in each sample, and expressed as relative expression using the ΔΔCt method *versus* the reference sample.

Statistics

Data are expressed as means ± SEM. The AHR values were analyzed with 2-way repeated measures ANOVA followed by Bonferroni correction as a *post-hoc* test. All other values were analyzed with Mann-Whitney U test. Results were considered significant at a P value of 0.05 or less (*p<0.05; **p<0.01; ***p<0.001; ****p<0.0001). Data were analyzed using GraphPad Prism version 6 (GraphPad Software).

RESULTS

NOD Mice Display Exacerbated Airway Inflammation in Response to HDM Challenge

Here, we used a HDM-induced asthma model, consisting in intra-nasal (i.n.) immunization followed by three i.n. challenges on days 7, 11, and 17. No adjuvant was added. Mice were sacrificed 24h later. We found that total IgE tended to be higher in NOD compared to the Th2-prone BALB/c mice, but the difference was not statistically significant (1.55 ± 0.13 and 2.12 ± 0.62µg/ml mean ± s.e.m. for BALB/c and NOD, respectively). However, circulating HDM-specific IgG1 was enhanced in NOD compared to BALB/c mice (**Figure 1A**). Another cardinal feature of asthma, the percentage, and the numbers of airway eosinophils were also augmented in NOD mice (**Figure 1B**). No eosinophils, neutrophils, or lymphocytes were observed in BALF from BALB/c or NOD control mice treated with saline solution. Further, we found that NOD mice presented a higher airway hyperreactivity (AHR) as compared to BALB/c mice (**Figure 1C**). Of note, the HDM-induced asthma protocol used here barely induced AHR in BALB/c mice (**Figure 1C**) clearly showing that NOD mice strongly reacted to low doses of HDM sensitization and challenge.

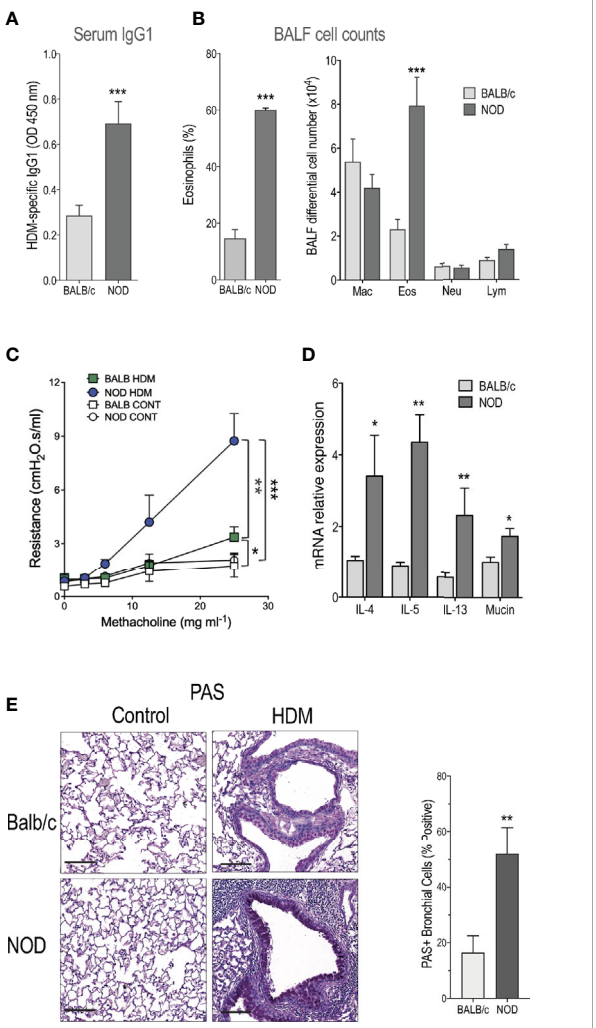

FIGURE 1 | Severe allergic-induced asthma phenotype in non-obese diabetic (NOD) mice. **(A)** Specific IgG1 in house dust mite (HDM)-treated BALB/c and NOD mice (n=9). **(B)** Percentage of eosinophils and macrophage (Mac), eosinophil (Eos), neutrophil (Neu), and lymphocyte (Lym) counts were determined in BALF of HDM-treated BALB/c and NOD mice (n=15). No eosinophils were detected in the lung of control mice. **(C)** Lung resistance was measured 24h after the last challenge with HDM or saline (n=10). **(D)** IL-4, IL-5, IL-13, and mucin messenger RNA (mRNA) expression assessed by quantitative RT-PCR in the lung of HDM-treated BALB/c and NOD mice (n=9). **(E)** Representative PAS-stained lung histology sections of saline controls and HDM-treated BALB/c and NOD mice (N=5). Statistical significance was determined between HDM-treated BALB/c and NOD mice. *p < 0.05, **p < 0.01, ***p < 0.001. Scale bars: 50µm.

HDM-sensitized and -challenged NOD (hereafter referred to as NOD HDM) mice expressed increased levels of IL-4, IL-5, IL-13, and mucin messenger RNA (mRNA) compared to HDM-sensitized and -challenged BALB/c (BALB/c HDM) mice (**Figure 1D**). In addition, HDM challenge in NOD mice led to increased PAS^+ goblet cell metaplasia (**Figure 1E**).

Activation and Cytokine Production by Lung ILT and Conventional T Cells in HDM-Treated BALB/c *Versus* NOD Mice

The distinct cytokine profiles generated during allergic asthma result from activation of both conventional and non-conventional T, also named innate-like T (ILT), cells, such as invariant natural killer T (iNKT) and γδ T. Our previous studies demonstrated that iNKT and γδ T cells contribute to the development of major asthma hallmarks in experimental models (23, 24). Here we provide evidence for reduced iNKT cell frequency in the lung of NOD HDM mice, relative to those recovered from BALB/c mice (**Figure 2A**). The few iNKT cells that did remain in the lung produced less IL-4 than their BALB/c counterpart, but promptly secreted IL-17) (**Figure 2B**), thereby revealing an overrepresentation of IL-17 producers (iNKT17) at the expense of IL-4 producers. These results confirm previous reports showing quantitative iNKT cell deficiency in thymus and spleen of NOD mice (25, 26). Further, our data also confirm that the remaining iNKT cells in NOD mice are mainly iNKT17 (20).

In contrast to iNKT cells, total γδ T cells as well as the Vγ1$^+$ γδ T subset, were increased in the lung of NOD HDM mice (**Figures 2C, D**). However, they were similarly biased in favor of a pro-Th17 profile, since total γδ T cells (**Figure 2C**) as well as the Vγ 1$^+$ γδ T subset (**Figure 2D**) generated low IL-4 and Vγ1$^+$ γδ T subset high IL-17 levels in the lung of NOD HDM compared to BALB/c HDM mice (**Figure 2D**).

Analysis of conventional TCRαβ$^+$CD4$^+$ T cells revealed that they were more activated in BALF from NOD HDM than from BALB/c HDM mice, as assessed by a higher expression of the CD69 marker (**Figure 2E**). In contrast to non-conventional iNKT and γδ T cells, both Th2 and Th17 profiles were increased among conventional TCRαβ$^+$CD4$^+$ T cells infiltrating the lung of NOD mice, as demonstrated by a higher proportion of IL-4$^+$, IL-13$^+$ as well as IL-17$^+$ subsets, by comparison with their BALB/c counterpart (**Figure 2F**). These findings indicated an inherent pro-Th2 and pro-Th17 potential in NOD HDM mice.

Reduced Airway Inflammation in NOD IL-4KO Mice

Knowing that HDM model is globally considered as IL-4 dependent in BALB/c mice (27–29), we first assessed the implication of this cytokine in the severe airway inflammation observed In NOD HDM mice. We addressed the role played by IL-4-producing cells in aggravating asthma, using NOD IL-4KO mice sensitized and challenged with HDM (NOD IL-4KO HDM). In the absence of IL-4, these mice were unable to mount high airway eosinophilia but presented a higher frequency of neutrophils in BALF (**Figures 3A, B**). Further, their expression of mucin mRNA and of PAS$^+$ goblet cells were decreased, compared to NOD HDM mice (**Figures 3C, D**). It is noteworthy that AHR was lower in NOD IL-4KO HDM than in NOD HDM mice (**Figure 3E**). However, AHR observed in NOD IL-4KO HDM remained higher than in control saline treated NOD or NOD IL-4KO mice, suggesting the implication of additional mechanisms.

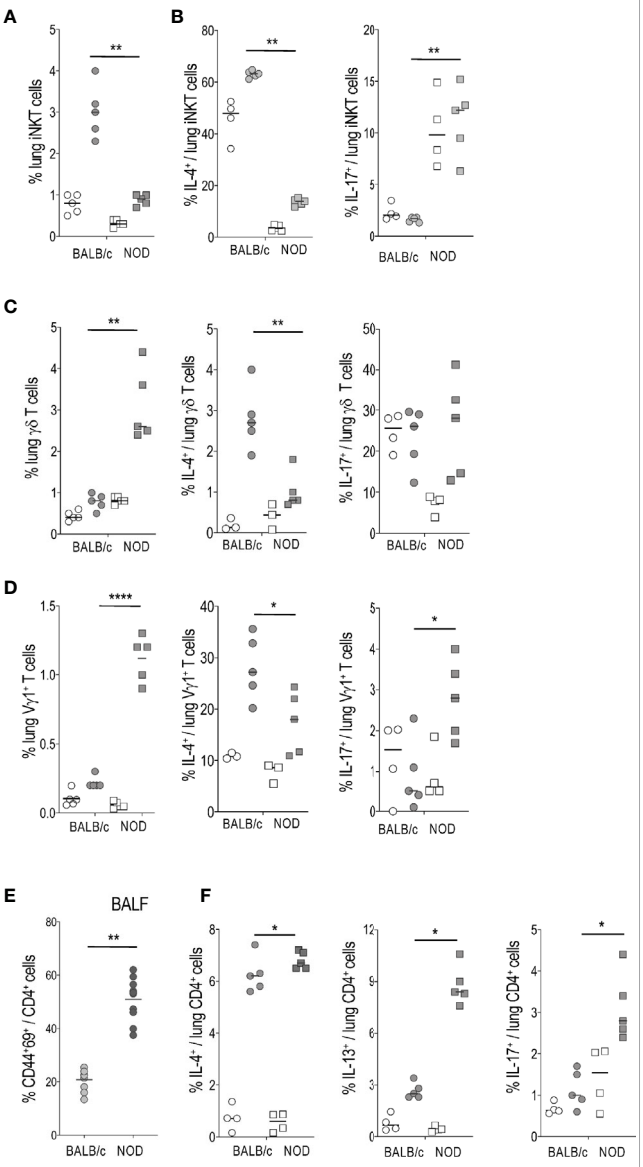

FIGURE 2 | Activation and cytokine production by lung ILT and conventional T cells in house dust mite (HDM)-treated BALB/c *versus* non-obese diabetic (NOD) mice. **(A, B)** Percentage of lung invariant natural killer T (iNKT) cells among gated T cells **(A)** and of IL-4$^+$ and IL-17$^+$ cells among gated iNKT cells **(B)**. **(C)** Percentage of lung γδ T or Vγ1$^+$ γδ T cells among gated T cells. **(D)** Percentage of lung IL-4$^+$ and IL-17$^+$ cells among gated Vγ1$^+$ γδ T cells. **(E)** Percentage of CD44$^+$CD69$^+$ among gated CD4$^+$ T cells in BALF from HDM-treated mice. No CD4+ T cells were observed in BALF from control mice. **(F)** Percentage of lung IL-4$^+$, IL-13$^+$, and IL-17$^+$ cells among gated CD4$^+$ T cells. Light circles and squares represent BALB/c and NOD control mice, respectively. Dark circles and squares represent BALB/c HDM and NOD HDM mice, respectively. *$p < 0.05$, **$p < 0.01$, ****$p < 0.0001$.

IL-4 and IL-17 Are Required for the Development of Airway Inflammation in NOD Mice

Figure 2B shows that the frequency of iNKT17 cells were higher in the lung of NOD compared with Balb/c mice even in the

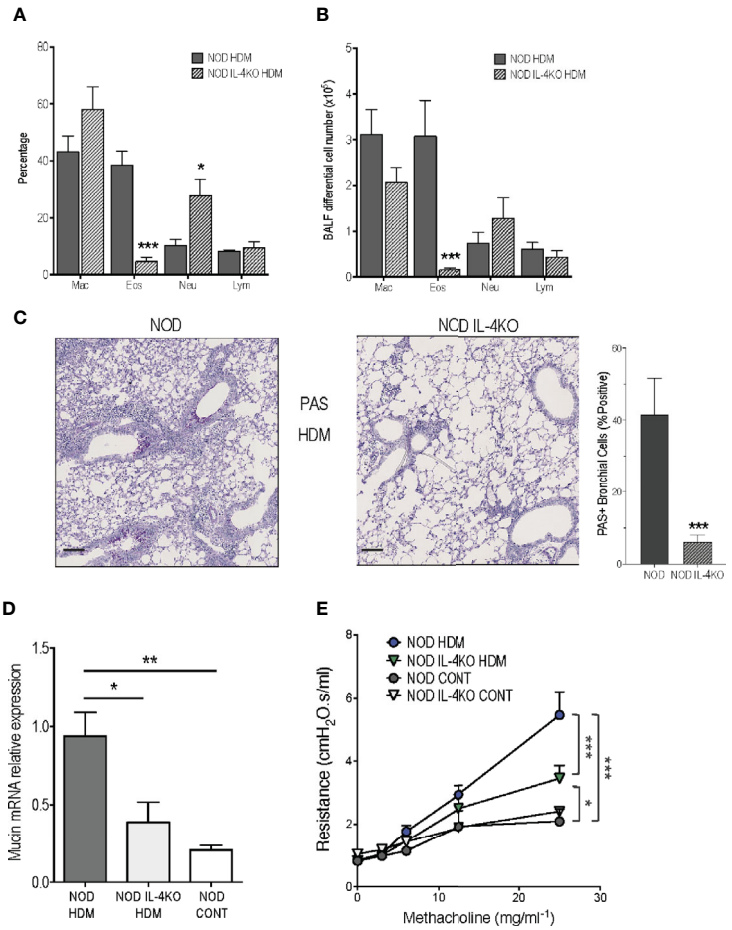

FIGURE 3 | Reduced airway inflammation in non-obese diabetic (NOD) IL-4KO mice. **(A, B)** Percentage and number of macrophages (Mac), eosinophils (Eos), neutrophils (Neu), and lymphocytes (Lym) in BALF of HDM-treated NOD and NOD IL-4KO mice (n=7). **(C)** Representative periodic acid Schiff (PAS)-stained lung histology sections of HDM-treated NOD and NOD IL-4KO mice (N=5). **(D)** Mucin mRNA expression assessed by quantitative RT-PCR in lung of HDM-treated NOD and NOD IL-4KO and NOD control mice (n=9). **(E)** Lung resistance was measured 24h after the last challenge with HDM challenge or saline (n=10). $*p < 0.05$, $**p < 0.01$, $***p < 0.001$. Scale bars: 50µm.

absence of HDM administration, supporting our previous observation that NOD mice are enriched in these cells (20). Bearing in mind that IL-17 is involved in certain severe cases of asthma likely by regulating neutrophilic inflammation (10) together with our present observation that $V\gamma1^+\gamma\delta$ and $CD4^+$ T cells from the lung of NOD HDM mice produced high levels of this cytokine (**Figure 2**), and that NOD IL-4KO HDM mice presented higher levels of neutrophils in the airway (**Figures 3A, B**), we further examined whether IL-17 contributed to the airway inflammation and AHR observed in NOD IL-4KO HDM mice. IL-17 mRNA expression was enhanced in the lung of NOD IL-4KO HDM compared to NOD HDM (**Figure 4A**) supporting the possible implication of IL-17 in the residual inflammation observed in NOD IL-4KO HDM mice. To assess IL-17 implication, NOD IL-4KO HDM mice were treated *in vivo* with a neutralizing anti-IL-17 mAb. These animals developed lower airway eosinophilia and neutrophilia compared to Ig treated NOD IL-4KO HDM mice (**Figure 4B**). Additionally, anti-IL-17 treatment significantly decreased IL-5 and tended to decrease IL-13 mRNA expression in the lung of NOD IL-4KO HDM mice (**Figure 4C**). Finally, AHR was decreased in NOD IL-4KO HDM mice when compared to both NOD IL-4KO HDM Ig and NOD HDM WT (**Figure 4D**). No significant difference was observed between NOD IL-4KO HDM treated with anti-IL-17 and NOD control, indicating that both IL-4 and IL-17 were required for increasing AHR. These results agree with previous observations showing that anti-IL-17 treatment could dampen neutrophil influx in BALF and airway hyperreactivity in mice (30).

DISCUSSION

Autoimmunity and allergy are two major examples of dysimmune diseases. They are both caused by an uncontrolled immune response against self or non-self-antigens involving Th1 or Th2 mechanisms, respectively. This notion has become more

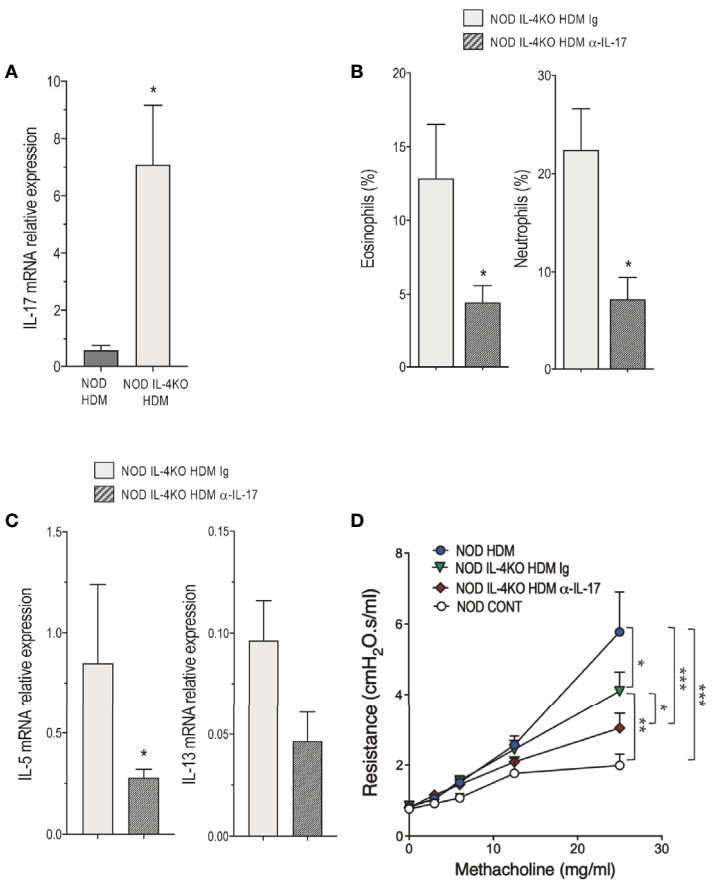

FIGURE 4 | IL-4 and IL-17 are required for the development of airway inflammation in non-obese diabetic (NOD) mice. **(A)** IL-17 messenger RNA (mRNA) expression assessed by quantitative RT-PCR in lung of HDM-treated NOD and NOD IL-4KO mice (n=4 to 6). **(B)** Percentage of eosinophils and neutrophils in bronchoalveolar lavage fluid (BALF) of house dust mite (HDM)-treated NOD IL-4KO mice treated with anti-IL-17 or Ig control (n=6 to 9). **(C)** IL-5 and IL-13 mRNA expression assessed by quantitative RT-PCR in lung of HDM-treated NOD IL-4KO mice treated with anti-IL-17 or Ig control (n=4 to 6). **(D)** Lung resistance was measured 24h after the last HDM challenge or controls (NaCl) (n=6 to 8). $^{*}p < 0.05$, $^{**}p < 0.01$, $^{***}p < 0.001$.

complex since it turned out that Th17 cells could also play a part in this process. NOD mouse spontaneously develops insulin-dependent diabetes, a prototypic Th1-mediated autoimmune disease (31, 32). These animals are also prone to produce pro-Th17 cytokines (20). These observations led us to examine in more detail the inflammatory response of NOD mice in a typical Th2-mediated disease.

Here we demonstrated that NOD mice presented enhanced airway inflammation and AHR in response to HDM sensitization and challenge when compared to the Th2-prone BALB/c mice. Both IL-4 and IL-17 were required for the severity of the symptoms. Our previous report showed that NOD mice developed a more pronounced Th2-mediated inflammatory response to OVA-alum sensitization and challenge compared to BALB/c mice (17). Using an HDM-induced asthma protocol, where HDM extracts were administrated intranasally and without adjuvants in mice, we could get inside the mechanisms implicated in the exacerbated airway inflammation and AHR observed in NOD mice. In fact, we demonstrated, by using NOD IL-4KO mice and by blocking IL-17 *in vivo*, that both Th2- and Th17-mediated immune responses were implicated.

Conventional $CD4^+$ T cells were the major source of Th2 cytokines while iNKT, $V\gamma1^+$, and $CD4^+$ produced IL-17 in the lung of NOD mice. We previously reported that iNKT cells were implicated in airway eosinophilia observed in NOD mice sensitized and challenged with OVA but the mechanisms remained to be determined (17). Here we showed that the frequency and the IL-4-producing capacity of iNKT cells in the lung of NOD mice were impaired. The ability of remaining iNKT cells to produce high levels of IL-17 suggest that iNKT17 cells could contribute to airway inflammation, as described (18), and AHR observed in NOD mice. It is noteworthy that both iNKT and $V\gamma1^+$ T cells, in contrast to conventional $CD4^+$ T cells, do not recognize peptides (33–35). These ILT cells can promptly produce cytokines following TCR-dependent or -independent activation (33–35). Taken these findings into account, we could consider that the exacerbated airway inflammation and AHR observed could result from a simultaneous and combined activation of conventional and ILT cells in the lung of NOD mice.

Previous studies reported that Th2 and Th17 inflammatory pathways are reciprocally regulated in asthma (14). Here we confirm these results since NOD IL-4KO HDM presented higher IL-17 mRNA expression and airway neutrophilia than NOD HDM animals indicating that in the absence of IL-4, IL-17 could induce a compensatory airway inflammation in NOD mice. Further, IL-17 blockage sufficed to reduce airway neutrophilia, IL-5 and IL-13 lung mRNA expression and AHR in NOD IL-4KO HDM mice. It was already described that IL-17 blockage could impair both neutrophilia and airway smooth muscle contraction in response to HDM sensitization and challenge in BALB/c mice (30). Our findings clearly indicate that Th2 and Th17 inflammatory responses contribute to asthmatic airway inflammation and AHR observed in NOD mice. However, further studies are required to better determine whether Th2 and Th17 responses act together or independently to induce huge airway inflammation and AHR in NOD mice.

Studies in patients indicated positive associations between asthma and type 1 diabetes (36, 37). However, the mechanisms implicated are still unclear. The co-occurrence of asthma and type 1 diabetes is in direct opposition to the proposed inhibitory model where Th1 and Th2-mediated immune responses could be exclusive. Our present findings support the idea that pathologies associated with pro-Th1, pro-Th2, and pro-Th17 immune responses could co-exist since NOD mice, which spontaneously develop autoimmune diabetes, presented high Th2 and Th17 airway inflammatory responses. Therefore, NOD mice could represent a unique model to better understand the key mechanisms implicated in the association between allergic airway inflammation and autoimmune diabetes. Future studies are required to determine for instance, as reported in humans (37), whether the asthma protocol using HDM sensitization and challenge could modify the incidence of diabetes in NOD mice.

CONCLUSION

In summary, we show that NOD mice, which spontaneously develop autoimmune diabetes, undergo more severe allergic asthma airway inflammation and hyperreactivity than pro-Th2 BALB/c mice upon HDM sensitization and challenge. Our data support the conclusion that increased secretion of both IL-4 and IL-17 by pulmonary conventional CD4+ and innate-like T lymphocytes is the major cause of this exacerbated airway inflammation leading to increased severity in NOD mice. We identified iNKT, $V\gamma1^+$, and $CD4^+$ T cells as sources of IL-17 and Th2 cells as IL-4 producers in the lung of HDM NOD mice. In our NOD HDM model, both eosinophils and neutrophils were recruited into the airways. It has already been reported that asthmatic patients whose airways are infiltrated with both eosinophils and neutrophils suffer from more severe symptoms than those recruiting either eosinophils or neutrophils (3, 4, 7). It is our belief that autoimmune diabetes-prone NOD mice might become useful as a new HDM-induced asthma model to elucidate allergic dysimmune mechanisms involving Th2 and Th17 responses that could better mimic some asthmatic endoytpes observed in patients in association or not with autoimmune diseases.

DATA AVAILABILITY STATEMENT

The raw data supporting the conclusions of this article will be made available by the authors, without undue reservation.

ETHICS STATEMENT

The animal study was reviewed and approved by French Institutional Committee (APAFIS#4105-201511171831592).

AUTHOR CONTRIBUTIONS

ML-d-M and LC designed the research. A-PF, FM, CD, and CP performed the research. A-PF and ML-d-M analyzed the data. A-PF, ML-d-M, and LC wrote the manuscript. All authors contributed to the article and approved the submitted version.

ACKNOWLEDGMENTS

This work was supported by grants from Fondation Day Solvay, Inserm (Institut National de la Santé et de la Recherche Médicale) and CNRS (Centre National de la Recherche Scientifique). We are grateful to the National Institutes of Health Tetramer Core Facility for providing CD1d tetramer reagents. We would like to thanks the staff of our animal house facilities and of the histology platform (SFR Necker).

SUPPLEMENTARY MATERIAL

The Supplementary Material for this article can be found online at: https://www.frontiersin.org/articles/10.3389/fimmu.2020.595003/full#supplementary-material

Supplementary Figure S1 | Flow cytometric gating strategy used to identify $Vg1^+$, iNKT ($TCRb^+$ CD1d-$PBS57^+$), $CD4^+$ ($CD4^+TCRb^+$ $iNKT^-$) cells from lung and their ability to produce IL-4, IL-13 or IL-17.

REFERENCES

1. Reddel HK, FitzGerald JM, Bateman ED, Bacharier LB, Becker A, Brusselle G, et al. GINA 2019: a fundamental change in asthma management: Treatment of asthma with short-acting bronchodilators alone is no longer recommended for adults and adolescents. *Eur Respir J* (2019) 53:1901046. doi: 10.1183/13993003.01046-2019
2. Victor JR, Lezmi G, Leite-de-Moraes M. New Insights into Asthma Inflammation: Focus on iNKT, MAIT, and gammadeltaT Cells. *Clin Rev Allergy Immunol* (2020) 59:371–81. doi: 10.1007/s12016-020-08784-8

3. Kaur R, Chupp G. Phenotypes and endotypes of adult asthma: Moving toward precision medicine. *J Allergy Clin Immunol* (2019) 144:1–12. doi: 10.1016/j.jaci.2019.05.031
4. Pavord ID, Beasley R, Agusti A, Anderson GP, Bel E, Brusselle G, et al. After asthma: redefining airways diseases. *Lancet* (2018) 391:350–400. doi: 10.1016/S0140-6736(17)30879-6
5. Lezmi G, Leite-de-Moraes M. Invariant Natural Killer T and Mucosal-Associated Invariant T Cells in Asthmatic Patients. *Front Immunol* (2018) 9:1766. doi: 10.3389/fimmu.2018.01766
6. Foster PS, Maltby S, Rosenberg HF, Tay HL, Hogan SP, Collison AM, et al. Modeling TH 2 responses and airway inflammation to understand fundamental mechanisms regulating the pathogenesis of asthma. *Immunol Rev* (2017) 278:20–40. doi: 10.1111/imr.12549
7. Wenzel SE. Asthma phenotypes: the evolution from clinical to molecular approaches. *Nat Med* (2012) 18:716–25. doi: 10.1038/nm.2678
8. Wilson RH, Whitehead GS, Nakano H, Free ME, Kolls JK, Cook DN. Allergic sensitization through the airway primes Th17-dependent neutrophilia and airway hyperresponsiveness. *Am J Respir Crit Care Med* (2009) 180:720–30. doi: 10.1164/rccm.200904-0573OC
9. Bullens DM, Truyen E, Coteur L, Dilissen E, Hellings PW, Dupont LJ, et al. IL-17 mRNA in sputum of asthmatic patients: linking T cell driven inflammation and granulocytic influx? *Respir Res* (2006) 7:135. doi: 10.1186/1465-9921-7-135
10. Chesne J, Braza F, Mahay G, Brouard S, Aronica M, Magnan A. IL-17 in severe asthma. Where do we stand? *Am J Respir Crit Care Med* (2014) 190:1094–101. doi: 10.1164/rccm.201405-0859PP
11. Leite-de-Moraes M, Belo R, Dietrich C, Soussan D, Aubier M, Pretolani M. Circulating IL-4, IFNgamma and IL-17 conventional and Innate-like T-cell producers in adult asthma. *Allergy* (2020). doi: 10.1111/all.14474
12. Hinks TS, Levine SJ, Brusselle GG. Treatment options in type-2 low asthma. *Eur Respir J* (2020) 57:2000528. doi: 10.1183/13993003.00528-2020
13. Svenningsen S, Nair P. Asthma Endotypes and an Overview of Targeted Therapy for Asthma. *Front Med (Lausanne)* (2017) 4:158. doi: 10.3389/fmed.2017.00158
14. Choy DF, Hart KM, Borthwick LA, Shikotra A, Nagarkar DR, Siddiqui S, et al. TH2 and TH17 inflammatory pathways are reciprocally regulated in asthma. *Sci Transl Med* (2015) 7:301ra129. doi: 10.1126/scitranslmed.aab3142
15. You S, Alyanakian MA, Segovia B, Damotte D, Bluestone J, Bach JF, et al. Immunoregulatory pathways controlling progression of autoimmunity in NOD mice. *Ann N Y Acad Sci* (2008) 1150:300–10. doi: 10.1196/annals.1447.046
16. Walker LS, von Herrath M. CD4 T cell differentiation in type 1 diabetes. *Clin Exp Immunol* (2016) 183:16–29. doi: 10.1111/cei.12672
17. Araujo LM, Lefort J, Nahori MA, Diem S, Zhu R, Dy M, et al. Exacerbated Th2-mediated airway inflammation and hyperresponsiveness in autoimmune diabetes-prone NOD mice: a critical role for CD1d-dependent NKT cells. *Eur J Immunol* (2004) 34:327–35. doi: 10.1002/eji.200324151
18. Michel ML, Keller AC, Paget C, Fujio M, Trottein F, Savage PB, et al. Identification of an IL-17-producing NK1.1(neg) iNKT cell population involved in airway neutrophilia. *J Exp Med* (2007) 204:995–1001. doi: 10.1084/jem.20061551
19. Michel ML, Mendes-da-Cruz D, Keller AC, Lochner M, Schneider E, Dy M, et al. Critical role of ROR-gammat in a new thymic pathway leading to IL-17-producing invariant NKT cell differentiation. *Proc Natl Acad Sci U S A* (2008) 105:19845–50. doi: 10.1073/pnas.0806472105
20. Simoni Y, Gautron AS, Beaudoin L, Bui LC, Michel ML, Coumoul X, et al. NOD mice contain an elevated frequency of iNKT17 cells that exacerbate diabetes. *Eur J Immunol* (2011) 41:3574–85. doi: 10.1002/eji.201141751
21. Heilig JS, Tonegawa S. Diversity of murine gamma genes and expression in fetal and adult T lymphocytes. *Nature* (1986) 322:836–40. doi: 10.1038/322836a0
22. Trompette A, Gollwitzer ES, Yadava K, Sichelstiel AK, Sprenger N, Ngom-Bru C, et al. Gut microbiota metabolism of dietary fiber influences allergic airway disease and hematopoiesis. *Nat Med* (2014) 20:159–66. doi: 10.1038/nm.3444
23. Lisbonne M, Diem S, de Castro Keller A, Lefort J, Araujo LM, Hachem P, et al. Cutting edge: invariant V alpha 14 NKT cells are required for allergen-induced airway inflammation and hyperreactivity in an experimental asthma model. *J Immunol* (2003) 171:1637–41. doi: 10.4049/jimmunol.171.4.1637
24. Belkadi A, Dietrich C, Machavoine F, Victor JR, Leite-de-Moraes M. gammadelta T cells amplify Blomia tropicalis-induced allergic airway disease. *Allergy* (2019) 74:395–8. doi: 10.1111/all.13618
25. Gombert JM, Herbelin A, Tancrede-Bohin E, Dy M, Carnaud C, Bach JF. Early quantitative and functional deficiency of NK1+-like thymocytes in the NOD mouse. *Eur J Immunol* (1996) 26:2989–98. doi: 10.1002/eji.1830261226
26. Sharif S, Arreaza GA, Zucker P, Mi QS, Sondhi J, Naidenko OV, et al. Activation of natural killer T cells by alpha-galactosylceramide treatment prevents the onset and recurrence of autoimmune Type 1 diabetes. *Nat Med* (2001) 7:1057–62. doi: 10.1038/nm0901-1057
27. Johnson JR, Wiley RE, Fattouh R, Swirski FK, Gajewska BU, Coyle AJ, et al. Continuous exposure to house dust mite elicits chronic airway inflammation and structural remodeling. *Am J Respir Crit Care Med* (2004) 169:378–85. doi: 10.1164/rccm.200308-1094OC
28. Johnson JR, Swirski FK, Gajewska BU, Wiley RE, Fattouh R, Pacitto SR, et al. Divergent immune responses to house dust mite lead to distinct structural-functional phenotypes. *Am J Physiol Lung Cell Mol Physiol* (2007) 293:L730–739. doi: 10.1152/ajplung.00056.2007
29. Hirota JA, Budelsky A, Smith D, Lipsky B, Ellis R, Xiang YY, et al. The role of interleukin-4Ralpha in the induction of glutamic acid decarboxylase in airway epithelium following acute house dust mite exposure. *Clin Exp Allergy* (2010) 40:820–30. doi: 10.1111/j.1365-2222.2010.03458.x
30. Chesne J, Braza F, Chadeuf G, Mahay G, Cheminant MA, Loy J, et al. Prime role of IL-17A in neutrophilia and airway smooth muscle contraction in a house dust mite-induced allergic asthma model. *J Allergy Clin Immunol* (2015) 135:1643–1643.e1643. doi: 10.1016/j.jaci.2014.12.1872
31. Debray-Sachs M, Carnaud C, Boitard C, Cohen H, Gresser I, Bedossa P, et al. Prevention of diabetes in NOD mice treated with antibody to murine IFN gamma. *J Autoimmun* (1991) 4:237–48. doi: 10.1016/0896-8411(91)90021-4
32. Trembleau S, Penna G, Gregori S, Gately MK, Adorini L. Deviation of pancreas-infiltrating cells to Th2 by interleukin-12 antagonist administration inhibits autoimmune diabetes. *Eur J Immunol* (1997) 27:2330–9. doi: 10.1002/eji.1830270930
33. Godfrey DI, Uldrich AP, McCluskey J, Rossjohn J, Moody DB. The burgeoning family of unconventional T cells. *Nat Immunol* (2015) 16:1114–23. doi: 10.1038/ni.3298
34. Cortesi F, Delfanti G, Casorati G, Dellabona P. The Pathophysiological Relevance of the iNKT Cell/Mononuclear Phagocyte Crosstalk in Tissues. *Front Immunol* (2018) 9:2375. doi: 10.3389/fimmu.2018.02375
35. Parker ME, Ciofani M. Regulation of gammadelta T Cell Effector Diversification in the Thymus. *Front Immunol* (2020) 11:42. doi: 10.3389/fimmu.2020.00042
36. Kero J, Gissler M, Hemminki E, Isolauri E. Could TH1 and TH2 diseases coexist? Evaluation of asthma incidence in children with coeliac disease, type 1 diabetes, or rheumatoid arthritis: a register study. *J Allergy Clin Immunol* (2001) 108:781–3. doi: 10.1067/mai.2001.119557
37. Smew AI, Lundholm C, Savendahl L, Lichtenstein P, Almqvist C. Familial Coaggregation of Asthma and Type 1 Diabetes in Children. *JAMA Netw Open* (2020) 3:e200834. doi: 10.1001/jamanetworkopen.2020.0834

Conflict of Interest: The authors declare that the research was conducted in the absence of any commercial or financial relationships that could be construed as a potential conflict of interest.

Copyright © 2021 Foray, Dietrich, Pecquet, Machavoine, Chatenoud and Leite-de-Moraes. This is an open-access article distributed under the terms of the Creative Commons Attribution License (CC BY). The use, distribution or reproduction in other forums is permitted, provided the original author(s) and the copyright owner(s) are credited and that the original publication in this journal is cited, in accordance with accepted academic practice. No use, distribution or reproduction is permitted which does not comply with these terms.

frontiers in Immunology

ORIGINAL RESEARCH
published: 16 March 2021
doi: 10.3389/fimmu.2021.596376

2-Methoxyestradiol Protects Against Lung Ischemia/Reperfusion Injury by Upregulating Annexin A1 Protein Expression

Wen-I Liao[1,2], *Shu-Yu Wu*[3], *Shih-Hung Tsai*[2,4], *Hsin-Ping Pao*[1], *Kun-Lun Huang*[1,3]* and *Shi-Jye Chu*[5]*

[1] The Graduate Institute of Medical Sciences, National Defense Medical Center, Taipei, Taiwan, [2] Department of Emergency Medicine, Tri-Service General Hospital, National Defense Medical Center, Taipei, Taiwan, [3] Institute of Aerospace and Undersea Medicine, National Defense Medical Center, Taipei, Taiwan, [4] Department of Physiology and Biophysics, Graduate Institute of Physiology, National Defense Medical Center, Taipei, Taiwan, [5] Department of Internal Medicine, Tri-Service General Hospital, National Defense Medical Center, Taipei, Taiwan

Background: 2-Methoxyestradiol (2ME), a natural 17-β estradiol metabolite, is a potent anti-inflammatory agent, but its effect on ischemia/reperfusion (IR)-induced acute lung inflammation remains unknown. Annexin A1 (AnxA1), a glucocorticoid-regulated protein, is effective at inhibiting neutrophil transendothelial migration by binding the formyl peptide receptors (FPRs). We aimed to investigate whether 2ME upregulates the expression of AnxA1 and protects against IR-induced lung damage.

Methods: IR-mediated acute lung inflammation was induced by ischemia for 40 min followed by reperfusion for 60 min in an isolated, perfused rat lung model. The rat lungs were randomly treated with vehicle or 2ME, and the functional relevance of AnxA1 was determined using an anti-AnxA1 antibody or BOC2 (a pan-receptor antagonist of the FPR). *In vitro*, human primary alveolar epithelial cells (HPAECs) and rat neutrophils were pretreated with 2ME and an AnxA1 siRNA or anti-AnxA1 antibody and subjected to hypoxia-reoxygenation (HR).

Results: 2ME significantly decreased all lung edema parameters, neutrophil infiltration, oxidative stress, proinflammatory cytokine production, lung cell apoptosis, tight junction protein disruption, and lung tissue injury in the IR-induced acute lung inflammation model. 2ME also increased the expression of the AnxA1 mRNA and protein and suppressed the activation of nuclear factor-κB (NF-κB). *In vitro*, 2ME attenuated HR-triggered NF-κB activation and interleukin-8 production in HPAECs, decreased transendothelial migration, tumor necrosis factor-α production, and increased apoptosis in neutrophils exposed to HR. These protective effects of 2ME were significantly abrogated by BOC2, the anti-AnxA1 antibody, or AnxA1 siRNA.

Conclusions: 2ME ameliorates IR-induced acute lung inflammation by increasing AnxA1 expression. Based on these results, 2ME may be a promising agent for attenuating IR-induced lung injury.

Keywords: 2-methoxyestradiol, acute lung injury, ischemia and reperfusion, epithelium, annexin A1

OPEN ACCESS

Edited by:
Girolamo Pelaia,
University of Catanzaro, Italy

Reviewed by:
Mihai Victor Podgoreanu,
Duke University, United States
Gareth S. D. Purvis,
University of Oxford, United Kingdom

***Correspondence:**
Kun-Lun Huang
kun@mail.ndmctsgh.edu.tw
Shi-Jye Chu
d1204812@mail.ndmctsgh.edu.tw

Specialty section:
This article was submitted to Inflammation, a section of the journal Frontiers in Immunology

Received: *19 August 2020*
Accepted: *22 February 2021*
Published: *16 March 2021*

Citation:
Liao W-I, Wu S-Y, Tsai S-H, Pao H-P, Huang K-L and Chu S-J (2021) 2-Methoxyestradiol Protects Against Lung Ischemia/Reperfusion Injury by Upregulating Annexin A1 Protein Expression. Front. Immunol. 12:596376. doi: 10.3389/fimmu.2021.596376

INTRODUCTION

Acute lung injury (ALI)/acute respiratory distress syndrome (ARDS) is a serious illness characterized by severe pulmonary edema and a profound inflammatory response in the lung. The mortality rate of patients with severe ARDS is as high as 46%, and the disease has a poor prognosis (1). Life-threatening acute lung inflammation can be induced by diverse ischemia/reperfusion (IR) injury conditions, including resuscitation for cardiac arrest, cardiopulmonary bypass, hemorrhagic shock, pulmonary embolism, and lung transplantation (2). Restoration of blood flow after ischemia is frequently associated with harmful effects that are characterized by epithelial and endothelial dysfunction, neutrophil infiltration, inflammatory cytokine release, and further recruitment of more neutrophils and macrophages into the alveoli (3). The exacerbation of inflammation initiated by lipid peroxidation and oxygen free radicals results in increased microvascular permeability and ultimately leads to acute lung edema (3). Currently, effective drugs are not available for treating IR-induced acute lung inflammation in the clinic, and the available treatment strategies are limited to supportive care (4).

2-Methoxyestradiol (2ME) is a natural endogenous metabolite of 17-β estradiol with low binding affinity for estrogen receptors and antitumor, antiangiogenic, and antiproliferative effects (5). In addition, 2ME has been shown to exert protective effects on several inflammation-associated diseases, such as rheumatoid arthritis and experimental autoimmune encephalomyelitis (6, 7). 2ME ameliorates multiple organ injury in mice with cecal ligation and puncture-induced sepsis by attenuating inflammatory cytokine production (8). 2ME reduces antigen-induced airway remodeling in a murine model of ovalbumin-induced inflammatory pulmonary disease (9). Furthermore, 2ME has been shown to protect against kidney and brain IR injury by reducing nuclear factor-κB (NF-κB) activity (10, 11).

The annexin A1 (AnxA1) protein is an important glucocorticoid-regulated endogenous inhibitor of inflammation that is expressed at high levels in lung, brain, kidney, and heart tissues, as well as various cells, such as neutrophils, fibroblasts, macrophages, and epithelial cells (12). AnxA1 exerts anti-inflammatory effect by interacting with formyl peptide receptors (FPRs) and reduces vascular inflammatory responses associated with IR injury (13, 14). Upon binding to the FPRs on neutrophils, AnxA1 limits neutrophil adhesion to the endothelium and transmigration, decreasing the production of proinflammatory mediators in the alveolar space (15). We recently reported a novel role for the exogenous AnxA1 N-terminal peptide in ameliorating IR-induced acute lung inflammation in rats by inhibiting the NF-κB pathway, and the protective effect was abrogated by BOC2 (a pan FPR antagonist) (16).

Currently, researchers have not clearly determined whether 2ME attenuates IR-induced acute lung inflammation. Studies have demonstrated that 17β-estradiol exhibited anti-inflammatory effects through upregulating expression of AnxA1 protein (17, 18). Since 2ME is a biologically active metabolite of 17β-estradiol, 2ME may exhibit anti-inflammatory effects through modulating the AnxA1 expression. Besides, 2ME has been shown similar anti-inflammatory properties to a glucocorticoid (dexamethasone) in acute lung inflammation (19). Further, AnxA1 is a glucocorticoid-regulated protein that mediates many of the anti-inflammatory effects of glucocorticoids (20). Based on these observations, we aimed to test whether 2ME would regulate, at least partially, AnxA1 protein expression that mediates the anti-inflammatory properties of 2ME. In our preliminary study, 2ME significantly increased the expression of endogenous AnxA1 in lung tissues (**Supplementary Figure 3A**), which may be related to the protective mechanism of 2ME. Although a possible protective role for AnxA1 has been extensively described in several models of IR injury, the modulation of this anti-inflammatory protein after the administration of pharmacological strategies, such as 2ME, remains unknown. Therefore, in this study, we investigated whether 2ME decreased IR-induced acute lung inflammation by upregulating the expression of endogenous AnxA1.

MATERIALS AND METHODS

Animals

All experiments were approved by the Institutional Animal Care and Use Committee of the National Defense Medical Center (approval number: IACUC-15-077, 19-March-2015). The care of male Sprague-Dawley rats (350 ± 20 g) was provided in accordance with the Guide for the Care and Use of Laboratory Animals. Rats were housed in a temperature-controlled room with a 12-h light-dark cycle.

Isolated Perfused Rat Lung Model

Briefly, the rats were ventilated with humidified 21% O_2 containing 5% CO_2 at a 1-cm H_2O positive end-expiratory pressure via a tracheostomy, and body temperature was maintained at 37°C with heating pads. The ventilator had a respiratory rate of 60 breaths per min and delivered a tidal volume of 3 ml. A median sternotomy was performed, the right ventricle was injected with 1 U of heparin/g body weight (BW), and 10 ml of blood was collected by cardiac puncture. Cardiac arrest developed immediately after the cardiac puncture. Then, a cannula was inserted into the pulmonary artery, and another wide-bore cannula was placed in the left ventricle and advanced into the left atrium through the mitral valve. The pulmonary venous pressure (PVP) and pulmonary artery pressure (PAP) were continuously recorded from the side arm of the cannula. The isolated lung was perfused with a "half-blood" perfusate containing 10 ml of a physiological salt solution (PSS) and a 10-ml sample of collected blood. The PSS contained 119 mM NaCl, 4.7 mM KCl, 1.17 mM $MgSO_4$, 22.6 mM $NaHCO_3$, 1.18 mM KH_2PO_4, 1.6 mM $CaCl_2$, 5.5 mM glucose, 50 mM sucrose, and 4% bovine serum albumin. The flow rate was constantly maintained at a rate of 8 ml/min by a roller pump. The real-time changes in the lung weight (LW) were recorded by an electronic balance, upon which the *in situ* isolated perfused lung was placed (21).

Design of the *in vivo* Experiment

We used the anti-AnxA1 antibody (Santa Cruz Biotechnology, USA) and N-Boc-Phe-Leu-Phe-Leu-Phe (BOC2, a non-selective FPR antagonist, ICN Pharmaceuticals, UK) to inhibit the action of AnxA1 and investigate whether AnxA1 was involved in the protective effects of 2ME. The neutralizing properties of the anti-AnxA1 antibody (Santa Cruz Biotechnology) were examined using immunoprecipitation and neutrophil transmigration assay (**Supplementary Figure 6**). The isolated rat lungs were randomly assigned to the control + dimethyl sulfoxide (DMSO), control + 2ME (20 mg/kg BW, intraperitoneal injection (i.p.), Sigma-Aldrich, USA), control + anti-AnxA1 antibody (60 μg/kg BW, i.p., Santa Cruz Biotechnology), IR + DMSO, IR + different dosages of 2ME (5, 10, 20 mg/kg BW), IR + anti-AnxA1 antibody, IR + BOC2 (50 μg per rat, i.p.), IR + anti-AnxA1 antibody + 2ME (20 mg/kg BW), or IR + BOC2 + 2ME (20 mg/kg BW) group ($n = 6$ rats per group). 2ME was dissolved in 0.5% DMSO in saline and injected intraperitoneally 60 min prior to IR. Rats were pretreated with the anti-AnxA1 antibody or BOC2 for 30 min before the 2ME injection in the IR + anti-AnxA1 antibody + 2ME or IR + BOC2 + 2ME group or prior to IR in the IR + anti-AnxA1 antibody, and IR + BOC2 groups. The doses of 2ME and BOC2 used in this study were determined based on previous studies and our preliminary investigations (10, 16) (**Supplementary Figure 3**). The dose of anti-AnxA1 antibody used in the present study (60 μg/kg BW) was selected according to the dose in our *in vitro* study that inhibited rat neutrophil migration (1 μg/ml). Lung ischemia was induced in rats in the IR group by stopping ventilation and perfusion for 40 min and then restoring them to allow reperfusion for another 60 min. The rats were ventilated with humidified 21% O_2 containing 5% CO_2 when ventilation and perfusion were restored after 40 min of ischemia. The $PaCO_2$, PaO_2, and pH levels in the perfusate were measured by an ABL 800FLEX blood gas analyzer (Radiometer, Denmark) before the start of ischemia and after the restoration of reperfusion for 60 min. The diagrams of the experimental design *in vivo* and *in vitro* are provided in **Supplementary Figures 1**, **2**, respectively.

Vascular Filtration Coefficient

The vascular filtration coefficient (K_f) was calculated from the elevation in the venous pressure-induced LW change, as previously described (22, 23). K_f was defined as the *y*-intercept of the plot (in $g \cdot min^{-1}$) divided by the PVP (10 cm H_2O) and LW and reported in whole units of $g \cdot min^{-1}$ cm $H_2O^{-1} \times 100$ g.

LW/BW and Wet/Dry (W/D) Weight Ratios

The right middle lobe was removed at the hilar region, weighed on an electronic balance, and recorded as the wet LW after the experiments. The LW/BW ratios were determined as the wet LW divided by BW. For the dry weight, the middle portion of the right lung was dried for 48 h at 60°C in an oven, and the W/D weight ratios were calculated.

Assessment of Protein Concentrations and Interleukin (IL)-6, Cytokine-Induced Neutrophil Chemoattractant (CINC)-1, Tumor Necrosis Factor (TNF)-α, and IL-8 Levels in Bronchoalveolar Lavage Fluid (BALF) and in Culture Supernatants

The BALF was obtained by rinsing the left lung with 2.5 ml of phosphate-buffered saline (PBS) twice and then centrifuging the sample at 200*g* for 10 min. A bicinchoninic acid test was used to measure the protein level in the supernatant. IL-6, CINC-1, and TNF-α levels in BALF and in rat neutrophil culture supernatants, and IL-8 levels in human primary alveolar epithelial cells (HPAECs) culture supernatants were quantified using commercial rat and human ELISA kits (R&D Systems, USA) according to the manufacturer's instructions.

Immunohistochemistry

Immunostaining for AnxA1, myeloperoxidase (MPO), CD45, Ly-6C, Ly-6G, Gal-3, FPR1, FPR2, and cleaved caspase-3 was performed on 5-μm-thick sections of rat lung tissue. Briefly, formalin-fixed paraffin lung tissue sections were deparaffinized before antigen retrieval. The endogenous peroxidases in lung tissue were quenched with 3% H_2O_2 and 100% methanol for 15 min. The sections were immunostained with a rabbit polyclonal antibody against AnxA1 (1:100, Bioss, USA), a rabbit polyclonal antibody against MPO (1:200, Thermo Fisher Scientific, USA), a mouse monoclonal antibody against CD45 (1:100, Merck KGaA, Germany), a mouse monoclonal antibody against Ly6C (1:200, Santa Cruz Biotechnology), a rabbit polyclonal antibody against Ly6G (1:300, Biorbyt, UK), a mouse monoclonal antibody against Gal-3 (1:100, Santa Cruz Biotechnology), and a rabbit polyclonal anti-cleaved caspase-3 antibody (1:200, CST, USA). Sections were washed twice with PBS containing 0.1% Tween-20 (PBST) and then incubated with a rat-specific horseradish peroxidase (HRP)-conjugated secondary antibody for 30 min. The HRP signal was visualized after a chromogenic reaction with diaminobenzidine for 5 min, and the lung tissue sections were counterstained with hematoxylin. Subsequently, the slides were dehydrated in a gradient of alcohol solutions (16).

Detection of the Protein Carbonyl Content and Malondialdehyde (MDA) Level in Lung Tissues

The methods for measuring the MDA level and protein carbonyl content were described previously (16). The protein carbonyl contents and MDA levels in the upper lobe of the right lung were determined using a Protein Carbonyl Content Assay Kit (Abcam, USA) and an MDA Assay Kit (Abcam), respectively, according to the manufacturer's instructions. The results of both assays are reported as nmol/mg protein.

Real-Time Quantitative PCR

Total RNA extraction and cDNA synthesis were performed using a Direct-zol RNA MiniPrep Kit (Zymo Research, USA) and MMLV Reverse Transcription Kit (Protech, Taiwan),

respectively, according to the manufacturer's instructions. Probes (AnxA1: Rn00563742_m1, FPR1: Rn01441684_s1, FPR2: Rn03037051_gH, and Actb: Rn00667869_m1) were purchased from Thermo Fisher Scientific. Thereafter, real-time PCR was performed using an Eco Real-Time PCR system (Illumina, USA) and 2X qPCRBIO Probe Blue Mix Lo-ROX (PCR Biosystems, USA). The real-time PCR mixture contained 1 μl of 20X TaqMan Gene Expression Assay, 10 μl of 2X qPCRBIO Probe Blue Mix, and 1 μl of cDNA templates in a total volume of 20 μl. The PCR cycling conditions were an initial incubation at 95°C for 2 min followed by 45 cycles of denaturation at 95°C for 5 s and annealing and extension at 60°C for 20 s.

Western Blotting

Lung tissues and protein lysates from cultured cells (30 μg/lane) were electrophoresed via 8–12% sodium dodecyl sulfate-polyacrylamide gel electrophoresis and transferred onto a polyvinylidene fluoride membrane. The membranes were blocked with 5% milk overnight to prevent non-specific binding. The blots were probed with one of the following primary antibodies: anti-AnxA1 (1:1,000, Bioss), anti-lamin B1 (1:100, Santa Cruz Biotechnology), anti-Bcl-2, anti-NF-κB p65, anti-phospho-NF-κB p65, anti-IκB-α, anti-IκB kinase (IKK)-β, anti-phospho-IKK-α/β, anti-ERK1/2, anti-phosho-ERK1/2, anti-p38, anti-phospho-p38 (1:1,000, CST), or β-actin (1:10,000, Sigma Chemical Company, USA). The blots were then washed with PBST for 10 min and incubated with HRP-conjugated goat anti-rabbit IgG (1:20,000) or goat anti-mouse IgG (1:20,000) secondary antibodies at room temperature for 1 h. After three washes with PBST for 10 min, the immunoreactive bands were visualized with an enhanced chemiluminescence kit and exposed using a UVP ChemiDoc-It Imaging System. The density of the immunoblots was calculated using image analysis software. The level of each protein was measured by repeating the Western blot analysis at least three times. The data are presented as the relative ratio of the target protein to the reference protein. The relative ratio of the target protein in the control group was arbitrarily set to 1.

Immunofluorescence Staining

Immunofluorescence staining was performed as previously described (16). Briefly, the primary antibodies rabbit polyclonal anti-claudin-3 and anti-occludin, mouse monoclonal anti-ZO-1 (1:200; Invitrogen, USA), rabbit polyclonal anti-AnxA1 (1:100, Bioss), rabbit polyclonal anti-Ly6G (1:200, Biorbyt), rabbit polyclonal anti-FPR-1(1:100, Santa Cruz Biotechnology), mouse monoclonal anti-FPR-2 (1:100, Santa Cruz Biotechnology), and rabbit polyclonal anti-cleaved-caspase-3 (1:400, CST) were used for immunofluorescence labeling. The ZO-1-labeled sections were incubated with a goat anti-mouse IgG-fluorescein isothiocyanate-labeled secondary antibody (green, diluted 1:200; Santa Cruz Biotechnology) for 30 min at room temperature. DyLight 633-labeled goat anti-rabbit IgG (red, diluted 1:200; Invitrogen) was used as the secondary antibody for the claudin-3 and occludin antibodies. Images were acquired using a fluorescence microscope (Leica DM 2500, Wetzlar, Germany).

Histopathological Analysis

Lung tissues were fixed with 10% formalin, embedded in paraffin, sliced into 4-μm sections, and stained with hematoxylin and eosin (H&E). Ten high-power fields at 400× magnification were used to count the numbers of polymorphonuclear leukocytes (PMN) and assign a lung injury score to each lung tissue sample. A light microscope (Olympus CKX41, Japan) was used to examine the morphological features. A minimum of 10 randomly selected fields was inspected for neutrophil infiltration in the airspace or vessel wall and thickening of the alveolar wall. A four-point scale was used to define the lung section score (16). In this classification, no (0), mild (1), moderate (2), or severe (3) lung injury was examined by two pathologists in a blinded manner. The two scores for each sample were summed for a total score ranging from 0 to 6 that represented the lung injury score.

Cell Viability Assays

Cell viability was determined using Premix WST-1 Cell Proliferation Reagent (Cayman Chemical, USA). HPAECs and rat neutrophils were plated in 96-well plates at a density of 6,000 cells per well and incubated overnight. 2ME was added at concentrations of 0, 0.1, 1, 10, and 100 μM or 0, 0.5, 1, 2, and 5 μM into three 96-well plates containing HPAECs or rat neutrophils, respectively. The HPAECs or rat neutrophils were then incubated with 10 μl of WST-1 per well for 0, 0.5, 1, 2, and 24 h or 0, 1, and 2 h, respectively. The final results were measured with a plate reader at 450 nm.

Cell Culture and Induction of HR

HPAECs (BCRC Cat# H6053) obtained from Cell Biologics were isolated from normal human lung tissue. Cells were routinely grown on plastic with Epithelial Cell Medium Kits (BCRC Cat# H6621) in a humidified atmosphere of 5% CO_2-95% room air. Neutrophils from adult male Sprague-Dawley rats (250–350 g) were freshly isolated using a previously described method (24). Before performing functional tests, neutrophils were allowed to recover for 30 min at 37°C in Roswell Park Memorial Institute (RPMI) 1640 medium (Gibco, USA) supplemented with 10% fetal bovine serum (FBS) (Thermo Fisher Scientific). Cells were resuspended in incubation buffer prior to functional assays. For AnxA1 knockdown, an AnxA1 small interfering RNA (siRNA) and empty vectors were purchased from Dharmacon (Lafayette, USA). The vectors were transfected into HPAECs with Lipofectamine RNAiMax (Thermo Fisher Scientific). The transfection efficiency was assessed using fluorescence microscopy and Western blot analysis. For hypoxia/reoxygenation (HR) induction, HPAECs or rat neutrophils were subjected to 24 or 2 h of hypoxia (1% O_2, 5% CO_2, and 94% N_2), respectively, followed by 1 h of reoxygenation (5% CO_2 and 95% room air) at 37°C. Before HR induction, HPAECs or rat neutrophils were pretreated with 2ME (1 μM) or 2ME (2 μM) and the anti-AnxA1 antibody (1 μg/ml), respectively. Normal mouse IgG (Santa Cruz Biotechnology) was used as the antibody control. Treatment conditions for rat neutrophils comprised (1) DMSO + IgG, (2) 2ME + IgG, and (3) 2ME + anti-AnxA1 antibody groups. The control group was maintained in the reoxygenated state without a hypoxic stimulus.

Rat Neutrophil Transmigration Assay

Neutrophil chemotaxis was evaluated using a Transwell system (3-μm pore size, Corning Costar, USA). First, 500 μl of RPMI 1640 medium containing 10% FBS were added to the lower well of the migration plate before the neutrophils were added. Then, 1.5×10^6 freshly isolated neutrophils in 150 μl of serum-free RPMI 1640 medium were added to the upper chamber. The agents, 2 μM 2ME and anti-AnxA1 antibody, were then added directly to the cell suspension in the upper chamber. After exposure to hypoxia for 2 h and reoxygenation for 1 h, neutrophils were harvested from the lower chamber and analyzed using an ADAM MC Auto Cell Counter or by adding BCECF-AM cell staining solution. The results are presented as the percentage of cells that had migrated to the lower chamber.

Immunocytochemistry/ Immunofluorescence Staining of HPAECs and Rat Neutrophils

After exposure to hypoxia for 24 h (HPAECs) or 2 h (neutrophils) followed by reoxygenation for 1 h, the cells were fixed and stained. Neutrophils were isolated using a Cytospin column (Thermo Shandon Cytospin 3) and centrifugation at 1,200 rpm for 5 min, and then the slides were air dried for 20 min at room temperature to increase cell adhesion and reduce loss during the subsequent staining procedure. Images were acquired using a fluorescence microscope (Leica DMi8, Germany).

Data and Statistical Analysis

Based on our previous report (23), the assumption of Cohen's *d* was defined as 3.98 [(1.097 – 0.207)/0.223607], which was decided to large effect size. Cohen's *d* was calculated by subtracting the population mean (Control group's post-reperfusion K_f) from the sample mean (IR group's post-reperfusion K_f). The two-tailed significant level and the expected power were set to 0.05 and 0.8, respectively. Six rats in each group were sufficient to distinguish the difference between the two groups calculated using GPower version 3.1.9.6. For the calculations of the expected animal attrition, the number per group was counted to be a maximum of eight per group, considering the potential animal loss due to possible complications during surgical interventions or anesthesia induction. All statistical calculations were performed using GraphPad Prism 6 statistical software (GraphPad Software, USA). Data are presented as the means ± standard deviation. Comparisons among groups were analyzed using one-way analysis of variance (ANOVA) followed by Bonferroni's *post-hoc* correction to evaluate the difference between each of the treatment and control groups. The increases in LW between groups were compared using two-way ANOVA followed by the Bonferroni *post-hoc* test. A value of $p < 0.05$ was defined as significant.

RESULTS

2ME Attenuated IR-Induced Lung Edema

When compared to the vehicle control, IR injury significantly increased the LW, K_f, LW/BW ratio, W/D weight ratio, and protein concentrations in the BALF. The anti-AnxA1 antibody and BOC2 showed a tendency to aggravate IR damage, which did not reach statistical significance (not shown). Compared to rats subjected to IR injury, rats pretreated with 2ME exhibited significantly attenuated IR-induced lung edema in a dose-dependent manner (**Figures 1A–E** and **Supplementary Figures 3B–F**). However, the addition of the anti-AnxA1 antibody or BOC2 significantly blocked the protective effects of 2ME on IR-induced lung edema. There was no statistically significant difference in the perfusate pH and $PaCO_2$ levels between groups. Compared with the vehicle control, IR injury significantly increased the difference between final PaO_2 and baseline PaO_2 levels. The 2ME pretreatment significantly reduced the PaO_2 difference in the IR group (**Supplementary Table 1**).

2ME Increased the Expression of the AnxA1 mRNA and Protein in Lung Tissues

Western blotting and qPCR were performed to quantify the AnxA1 content in lung tissue. Under unstimulated conditions, an intraperitoneal injection of 2ME induced a significant increase in AnxA1 expression at the mRNA and protein (intact and cleaved fragments) levels in the 2ME control group. Compared with the vehicle control group, the IR group exhibited a significant increase in the expression of the AnxA1 mRNA and protein. Furthermore, compared with the IR group, the 2ME pretreatment significantly decreased the expression of the AnxA1 mRNA and protein in the 2ME + IR group (**Figures 2A–D**). The addition of the anti-AnxA1 antibody or BOC2 reversed the effect of 2ME on IR injury. Immunohistochemical staining for AnxA1, FPR1, and FPR2 in lung tissues also produced similar results (**Figure 2C**, **Supplementary Figures 7A**, **8A**). To further determine whether increased AnxA1 expression was mainly attributed to neutrophils in IR-treated lungs, we performed double immunofluorescence staining of lung sections using antibodies for AnxA1 and the neutrophil marker Ly6G. We found that AnxA1 protein expression highly co-localized with infiltrated neutrophils in the lung sections (**Figure 2D**).

2ME Ameliorated IR-Induced Proinflammatory Cytokine Production in the BALF and Histopathological Changes

Compared with the control group, the IR group displayed significantly higher levels of proinflammatory cytokines, such as IL-6, CINC-1, and TNF-α, in the BALF. 2ME administration significantly attenuated these increases. Moreover, these protective effects of 2ME were abrogated by the addition of the anti-AnxA1 antibody or BOC2 (**Figures 3A–C**). CD45, Ly6C, Ly6G, and Gal-3 are markers of PMNs, monocytes, neutrophils, and macrophages, respectively. Morphological observations of the control group showed a normal thickness of the lung alveolar wall and neutrophil infiltration. Obvious thickening of the alveolar walls and increased neutrophil infiltrates and CD45, Ly6C, Ly6G, and Gal-3 staining were observed in the IR group. The 2ME pretreatment significantly decreased neutrophil infiltration into the lungs, CD45, Ly6C, Ly6G, and Gal-3 staining and the histological lung injury score in the IR group.

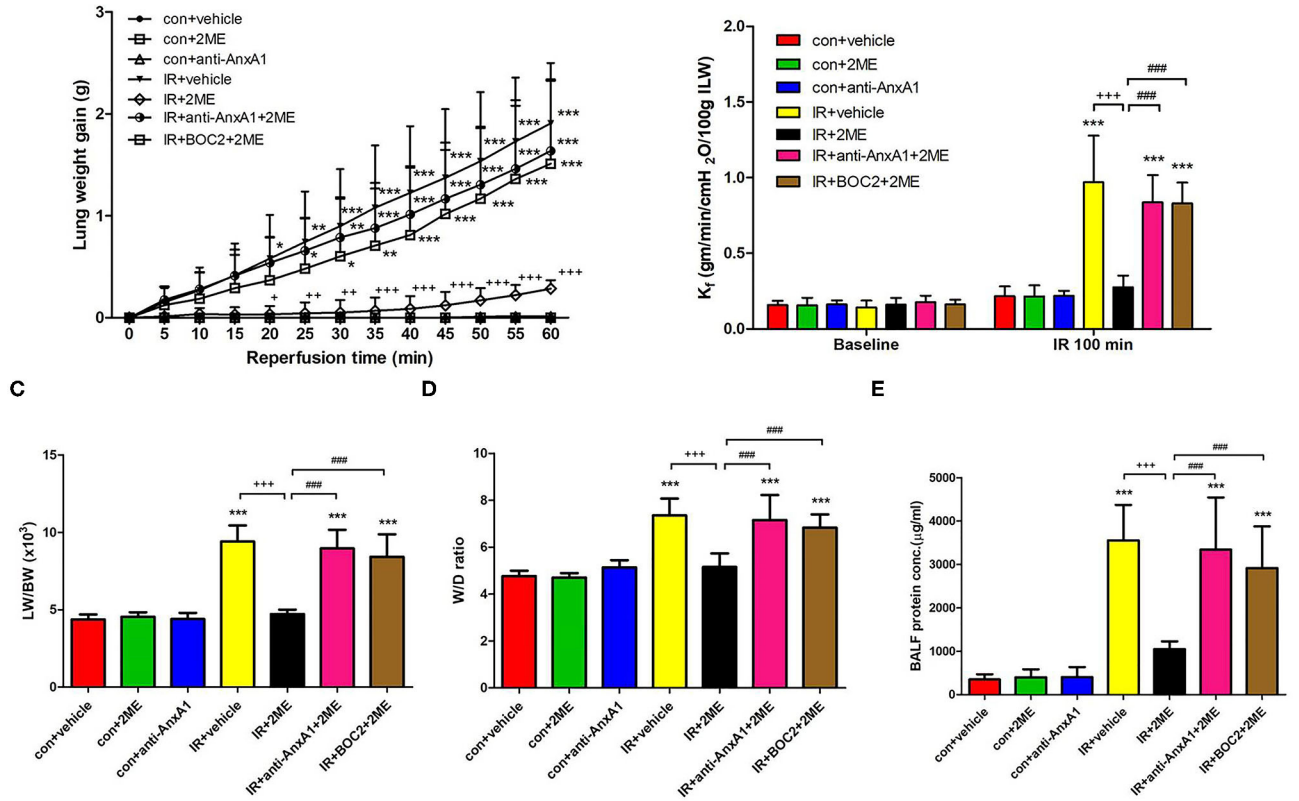

FIGURE 1 | 2ME alleviated IR-induced acute lung edema. **(A)** Lung weight gain, **(B)** K_f, **(C)** LW/BW, **(D)** W/D weight ratios, and **(E)** the protein concentration in BALF increased significantly in the IR group. The increases in these parameters were significantly ameliorated by 2ME administration. The protective effect of 2ME was abrogated by the addition of the anti-AnxA1 antibody or BOC2. Data are presented as the means ± SD ($n = 6$ rats per group). $^{*}p < 0.05$, $^{**}p < 0.01$, and $^{***}p < 0.001$ compared with the control group; $^{+}p < 0.05$, $^{++}p < 0.01$, and $^{+++}p < 0.001$ compared with the IR group; and $^{\#\#\#}p < 0.001$ compared with the IR + 2ME group.

However, the administration of the anti-AnxA1 antibody or BOC2 prevented the beneficial effect of the 2ME pretreatment (**Figures 3D–F** and **Supplementary Figure 4**).

2ME Decreased the Protein Carbonyl Content, MDA Level, and Number of MPO-Positive Cells in Lung Tissue Exposed to IR

Compared to rats subjected to IR injury, rats pretreated with 2ME prior to IR injury exhibited a significant attenuation of the IR-induced increases in the number of MPO-positive cells, protein carbonyl content, and MDA level in the lung tissue (**Figures 4A–C**). However, these antioxidant effects of 2ME were blocked by the administration of the anti-AnxA1 antibody.

2ME Increased Bcl-2 Levels but Reduced the Level of the Cleaved Caspase-3 Protein in Lung Tissues Exposed to IR

Compared to the IR group, the 2ME pretreatment significantly increased the level of the Bcl-2 protein and decreased the number of activated caspase-3-immunolabeled cells in the 2ME + IR group. The administration of the anti-AnxA1 antibody reversed these effects of 2ME (**Figures 5A,B**).

2ME Restored Claudin-3, Occludin, and ZO-1 Expression in the Lung Epithelium Exposed to IR

We evaluated the expression of the claudin-3, occludin, and ZO-1 proteins in lung tissues to assess the integrity of tight junction proteins. The lung epithelium in the control group exhibited strong linear staining for claudin-3, occludin, and ZO-1. The IR group showed fragmented and low-intensity staining in the alveolar walls. The 2ME pretreatment reversed the effects of IR, but the protective effects of 2ME were abolished by the addition of the anti-AnxA1 antibody (**Figures 6A,B**).

2ME Reduced the Activation of the NF-κB and Mitogen-Activated Protein Kinase (MAPK) Signaling Pathways in Lung Tissues Exposed to IR

Compared to the vehicle control, IR injury significantly increased the phosphorylation of IKK-β, degradation of IκB-α in the

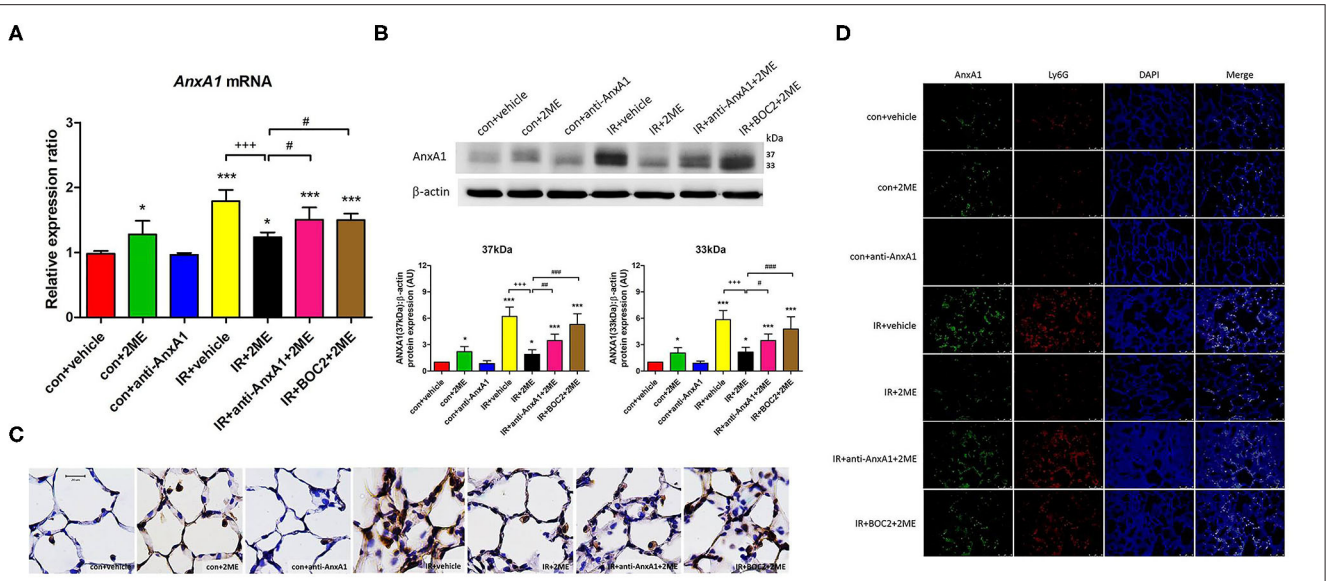

FIGURE 2 | 2ME increased AnxA1 mRNA and protein expression in normal lung tissues but decreased AnxA1 mRNA and protein expression in IR-injured lung tissues. Quantitative real-time PCR and Western blot analyses revealed that IR significantly increased the levels of the **(A)** AnxA1 mRNA and **(B)** both the intact and cleaved AnxA1 protein in the lung (as detected by the presence of the 37- or 33-kDa fragment) compared with the control group. Furthermore, the IR + 2ME group showed significantly decreased expression of the AnxA1 mRNA and protein in the lung compared with the IR group. Following anti-AnxA1 antibody or BOC2 pretreatment, the expression of the AnxA1 protein in the lung was significantly increased compared with the IR + 2ME group. **(C)** Serial paraffin-embedded sections of the rat lungs were immunohistochemically stained to assess AnxA1 expression (400× magnification). 2ME increased the number of AnxA1-stained epithelial cells compared with the vehicle alone in the control group. A large number of AnxA1-stained neutrophils infiltrated into the lung alveolar space upon IR injury, and the number was reduced after 2ME administration. The addition of the anti-AnxA1 antibody or BOC2 reversed the effect of 2ME. **(D)** Immunofluorescence analysis of AnxA1 protein in the lung sections after IR injury (400× magnification). Sections were co-stained for AnxA1 (green), Ly6G (red), and DAPI (blue). Images show co-localization of AnxA1 protein with Ly6G positive cells in the lung tissues of control or IR-challenged rats. $^{*}p < 0.05$ and $^{***}p < 0.001$ compared with the control group; $^{+++}p < 0.001$ compared with the IR group; and $^{\#}p < 0.05$, $^{\#\#}p < 0.01$, and $^{\#\#\#}p < 0.001$ compared with the IR + 2ME group.

cytoplasm, and nuclear translocation of NF-κB p65. Compared to rats subjected to IR injury, rats pretreated with 2ME prior to IR injury presented significantly decreased IKK-β phosphorylation, increased IκB-α levels, and the attenuated nuclear translocation of NF-κB p65 (**Figures 7A–E**). The levels of phosphorylated p38 and ERK were significantly increased by IR and reduced by the addition of 2ME compared to the vehicle control (**Figures 7F–H**). The administration of the anti-AnxA1 antibody or BOC2 attenuated these effects of 2ME.

2ME Upregulated AnxA1 Expression in HPAECs

We evaluated HPAECs using Western blotting (**Figure 8A**) and immunofluorescence staining (**Figure 8B**) to verify that AnxA1 was expressed in the lung. The viability of HPAECs was determined using WST-1 assays, and no cellular toxicity was detected when cells were treated with up to 1 μM 2ME (**Supplementary Figure 5A**). The level of the AnxA1 protein was obviously increased after pretreatment with 2ME at an optimal concentration of 1 μM under control condition (**Supplementary Figure 5B**). Compared with the vehicle control group, higher AnxA1 expression was detected in the HR group. However, no obvious differences in AnxA1 expression were observed between the HR group and the 2ME + HR group, despite the slight increase was observed after the 2ME pretreatment using Western blotting and immunofluorescence staining (**Figures 8A,B**).

2ME Attenuated NF-κB Activity and IL-8 Production and Increased ZO-1 Expression in HPAECs Subjected to HR

We established HR models in HPAECs to determine whether 2ME exerted its protective functions *in vitro*. Compared with vehicle control, the induction of HR in HPAECs led to increased phosphorylation of NF-κB p65, decreased expression of IκB-α and ZO-1, and increased levels of IL-8. 2ME (1 μM) significantly suppressed all of these effects of HR. However, these protective effects of 2ME were abrogated by the AnxA1 siRNA (**Figures 9A–D**).

2ME Increased AnxA1 and Cleaved Caspase-3 Levels, and Attenuated the Transmigration and TNF-α Production in Rat Neutrophils Subjected to HR

Rat neutrophils were cultured with 2ME and then subjected to HR and pretreated with the anti-AnxA1 antibody at concentrations of 0.5, 1, and 2 μg to investigate the anti-inflammatory effects of 2ME. WST-1 assays revealed that no cellular toxicity was detected upon the addition of up to

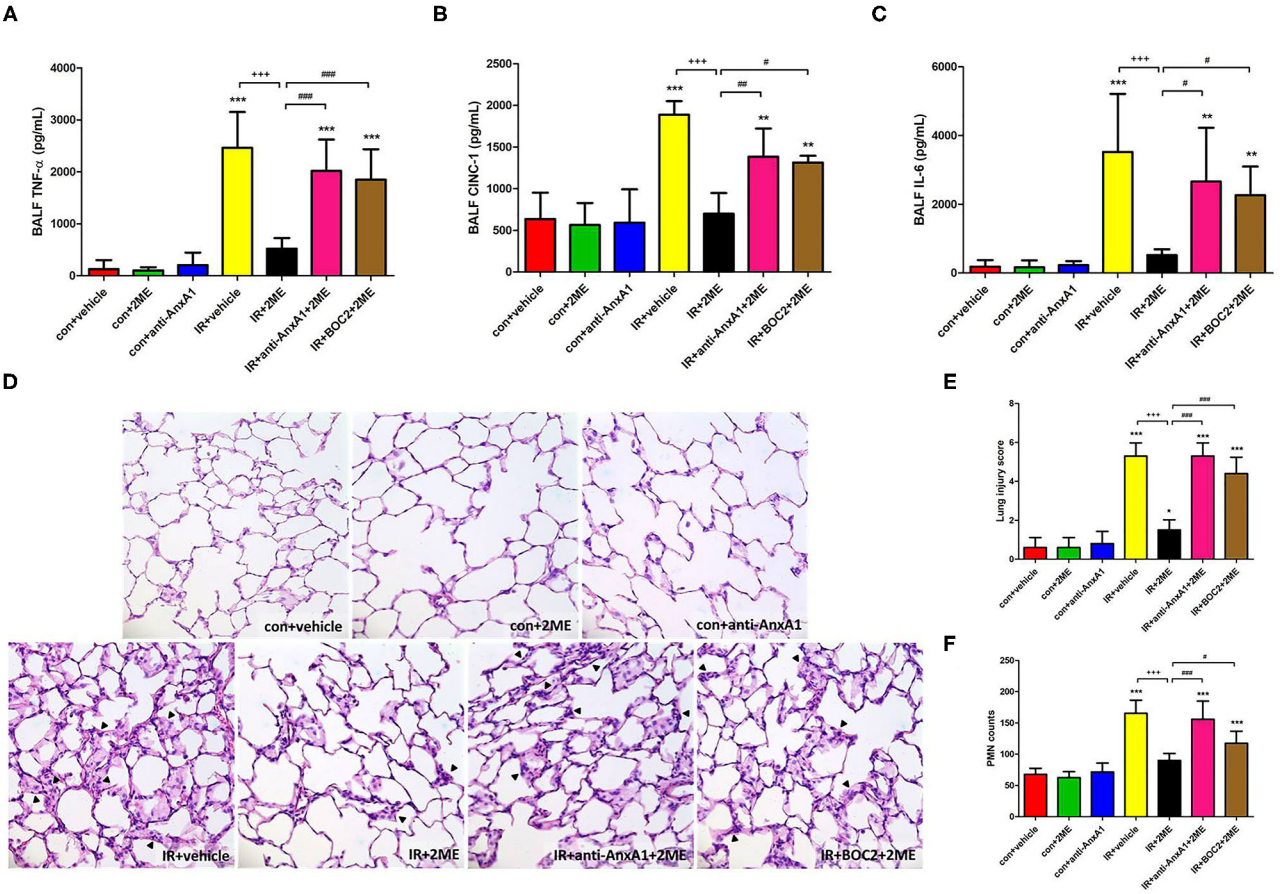

FIGURE 3 | 2ME reduced the IR-induced production of proinflammatory cytokines in the BALF and the severity of histological features in IR-injured lung tissue. 2ME significantly decreased IR-induced **(A)** TNF-α, **(B)** CINC-1, and **(C)** IL-6 levels in the BALF. The addition of the anti-AnxA1 antibody or BOC2 significantly abolished the anti-inflammatory effect of 2ME. **(D)** The lung tissue sections were stained with hematoxylin and eosin and examined under a light microscope (400× magnification). Lung injury was increased in the IR group, as evidenced by the increased neutrophil infiltration (arrowheads) and alveolar wall thickness. The 2ME pretreatment improved the histopathological changes. **(E)** Similar results were obtained by determining a histological lung injury score. **(F)** The numbers of infiltrated neutrophils per high power field (400× magnification) were elevated in the IR group, while the addition of 2ME significantly reduced the number of neutrophils, despite the IR injury. These improvements were all abrogated by the addition of the anti-AnxA1 antibody or BOC2. Data are presented as the means ± SD ($n = 6$ rats per group). $^{*}p < 0.05$, $^{**}p < 0.01$, and $^{***}p < 0.001$ compared with the control group; $^{+++}p < 0.001$ compared with the IR group; and $^{\#}p < 0.05$, $^{\#\#}p < 0.01$, and $^{\#\#\#}p < 0.001$ compared with the IR + 2ME group.

2 μM 2ME (**Supplementary Figure 5C**). The 2ME (2 μM) pretreatment increased AnxA1, FPR1&2, and cleaved caspase-3 levels in the unstimulated neutrophils. Compared to the vehicle control, the neutrophils subjected to HR injury expressed AnxA1, FPR1&2, and cleaved caspase-3 at higher levels. Higher levels of AnxA1 and cleaved caspase-3, and lower expression of FPR1&2 were observed in the 2ME + HR group than in HR only group (**Figures 10A,B** and **Supplementary Figures 7B,C, 8B,C**). In addition, 2ME reduced HR-induced neutrophil transmigration in a dose-dependent manner and TNF-α production (**Figures 10C,D** and **Supplementary Figure 6**). However, these effects of 2ME on the neutrophils were suppressed by the pretreatment with the anti-AnxA1 antibody (**Figures 10A,D** and **Supplementary Figure 6**).

DISCUSSION

In the present study, 2ME significantly upregulated AnxA1 expression and attenuated IR-induced lung edema, neutrophil infiltration, inflammatory cytokine production, oxidative stress, lung cell apoptosis, tight junction protein disruption, MAPK activation, and nuclear translocation of NF-κB in the lung tissue. In addition, the 2ME pretreatment exerted similar anti-inflammatory effects on HPAECs exposed to HR. Moreover, 2ME increased neutrophil apoptosis and decreased HR-induced neutrophil transmigration and TNF-α production. Finally, these protective effects of 2ME were abrogated by the anti-AnxA1 antibody or BOC2 in the animal model, by the AnxA1 siRNA in HPAECs, and by the anti-AnxA1 antibody in rat neutrophils.

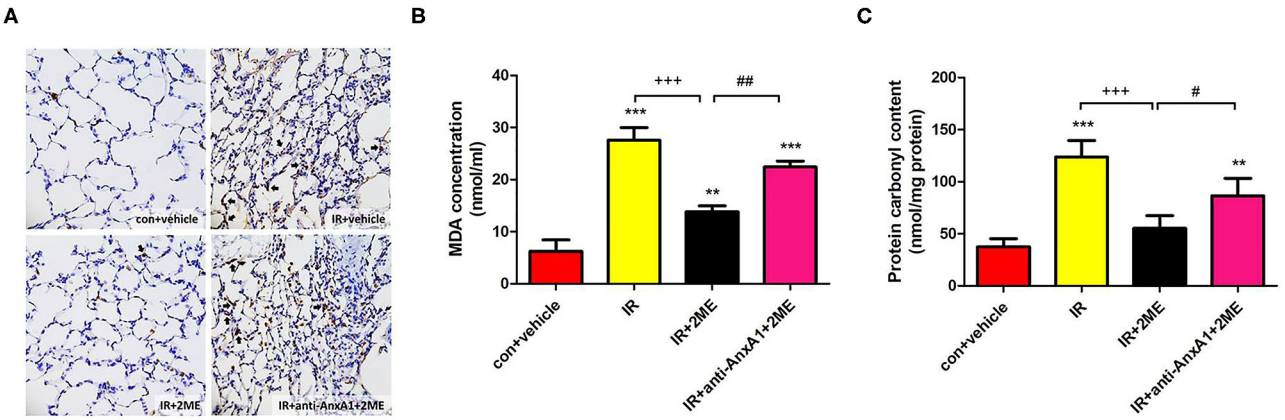

FIGURE 4 | 2ME decreased oxidative stress induced by IR injury in lung tissues. The number of **(A)** MPO-positive cells and the **(B)** MDA and **(C)** protein carbonyl levels in the rat lung tissues increased significantly after lung IR injury, whereas the 2ME pretreatment significantly attenuated these changes. The antioxidant effects of 2ME were blocked by the addition of the anti-AnxA1 antibody. **(A)** Immunohistochemistry for MPO in the lung (200× magnification). Black arrowheads indicate MPO-positive cells. Data are presented as the means ± SD ($n = 6$ rats per group). $^{**}p < 0.01$ and $^{***}p < 0.001$ compared with the control group; $^{+++}p < 0.001$ compared with the IR group; and $^{\#}p < 0.05$ and $^{\#\#}p < 0.01$ compared with the IR + 2ME group.

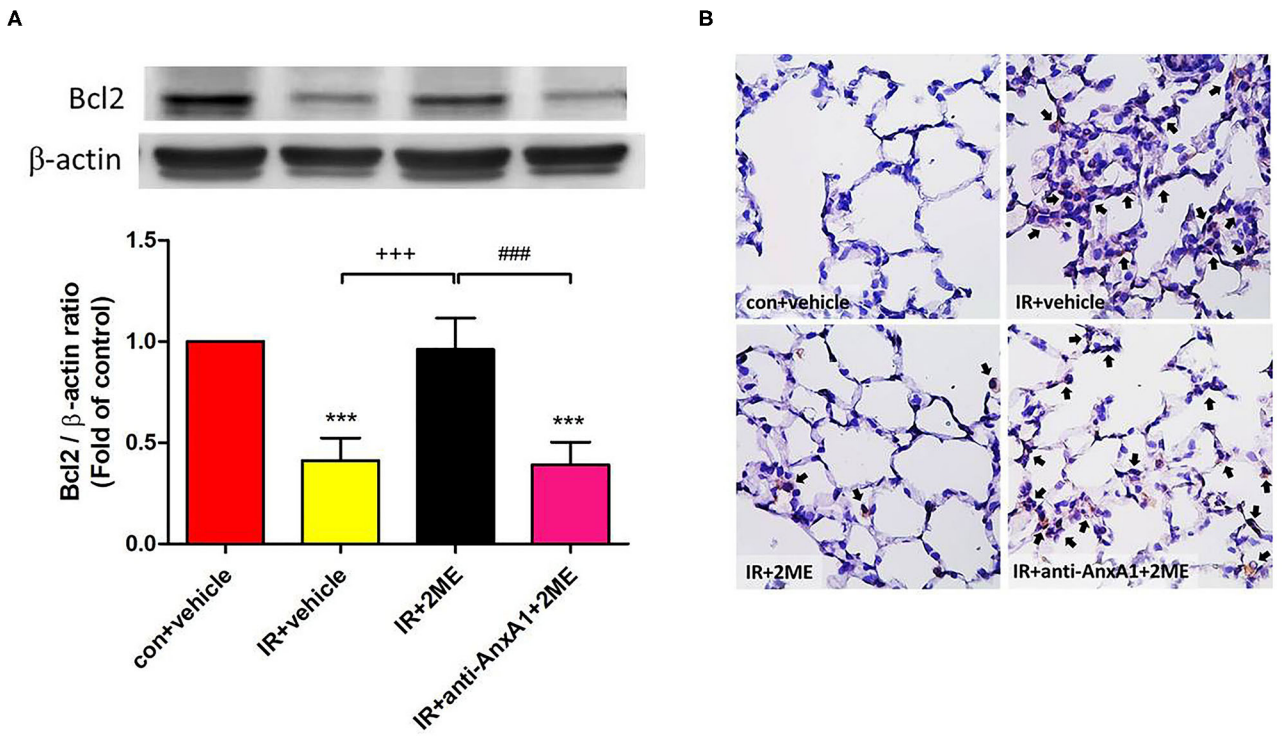

FIGURE 5 | 2ME attenuated IR-induced lung cell apoptosis. **(A)** Western blot showing the expression of Bcl-2 in the lung tissue. β-Actin served as a loading control for cytoplasmic proteins. Representative blots are shown. **(B)** Immunohistochemically staining (400× magnification) for cleaved caspase-3 expression in the lung tissue (indicated with black arrows). A large number of cleaved caspase-3-immunolabeled cells and significantly decreased expression of the Bcl-2 protein were observed in the IR group compared with the control group. The 2ME pretreatment significantly increased Bcl-2 protein expression and reduced the staining for cleaved caspase-3 in the IR group. Finally, when the anti-AnxA1 antibody was added, the antiapoptotic effects of 2ME on the lung tissue were abolished. $^{***}p < 0.001$ compared with the control group; $^{+++}p < 0.001$ compared with the IR group; and $^{\#\#\#}p < 0.001$ compared with the IR + 2ME group.

Based on these findings, 2ME ameliorates IR-induced acute lung inflammation by activating AnxA1-mediated anti-inflammatory effects.

Accumulating evidence has revealed a crucial role for 2ME in the immunomodulation of inflammatory diseases. Many studies have shown that 2ME reduces antigen-induced

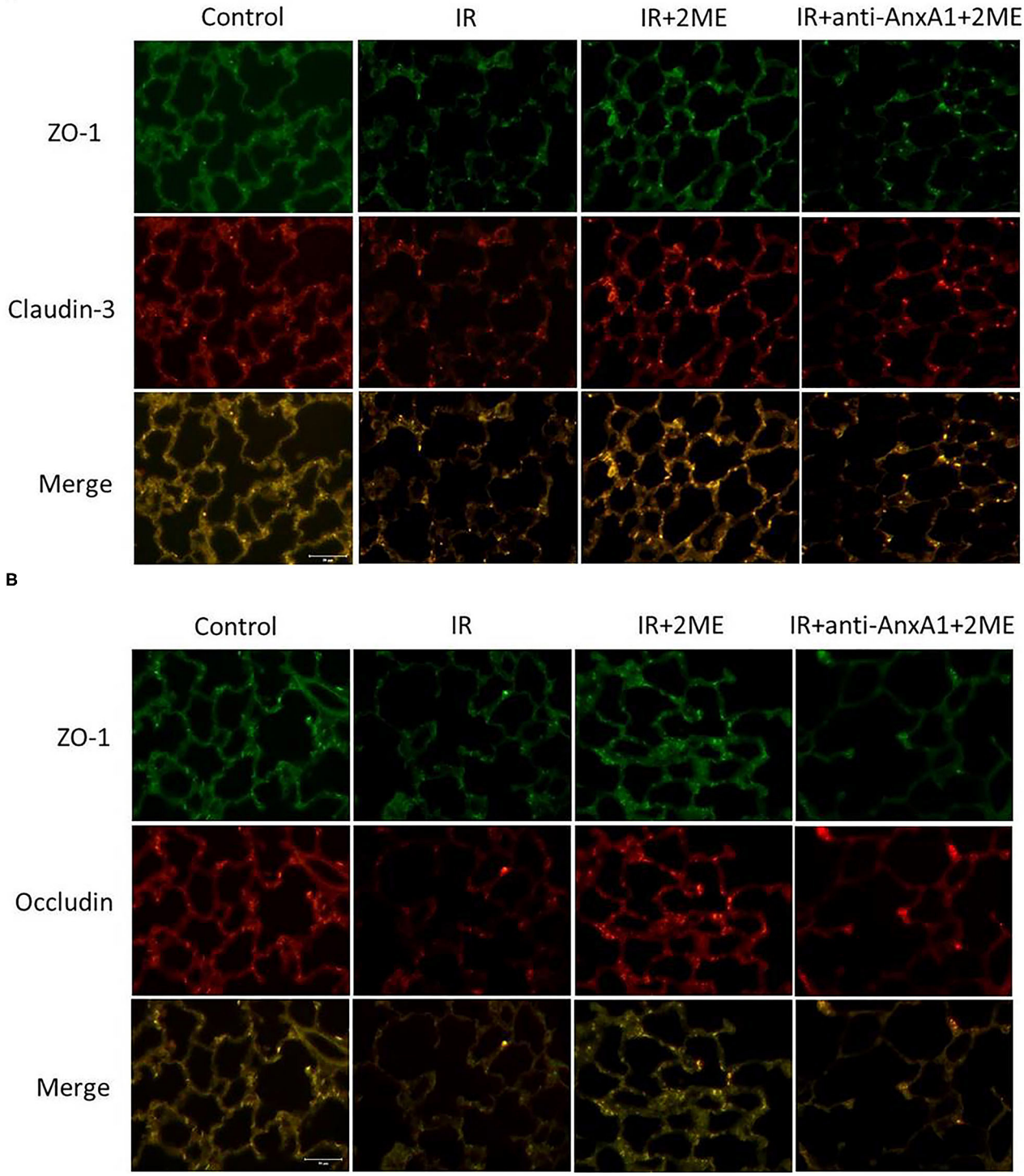

FIGURE 6 | 2ME suppressed IR-induced disruption of tight junction proteins. Lung sections were immunostained for claudin-3, occludin, and ZO-1 (400× magnification). The control group showed strong linear staining of tight junction proteins, including **(A)** claudin-3 (red), **(B)** occludin (red), and **(A,B)** ZO-1 (green). The IR injury group exhibited fragmented and low-intensity staining of these tight junction proteins in the alveolar septa. The 2ME pretreatment reversed the disruption of these tight junction proteins, but the protective effect of 2ME was abrogated by the addition of the anti-AnxA1 antibody.

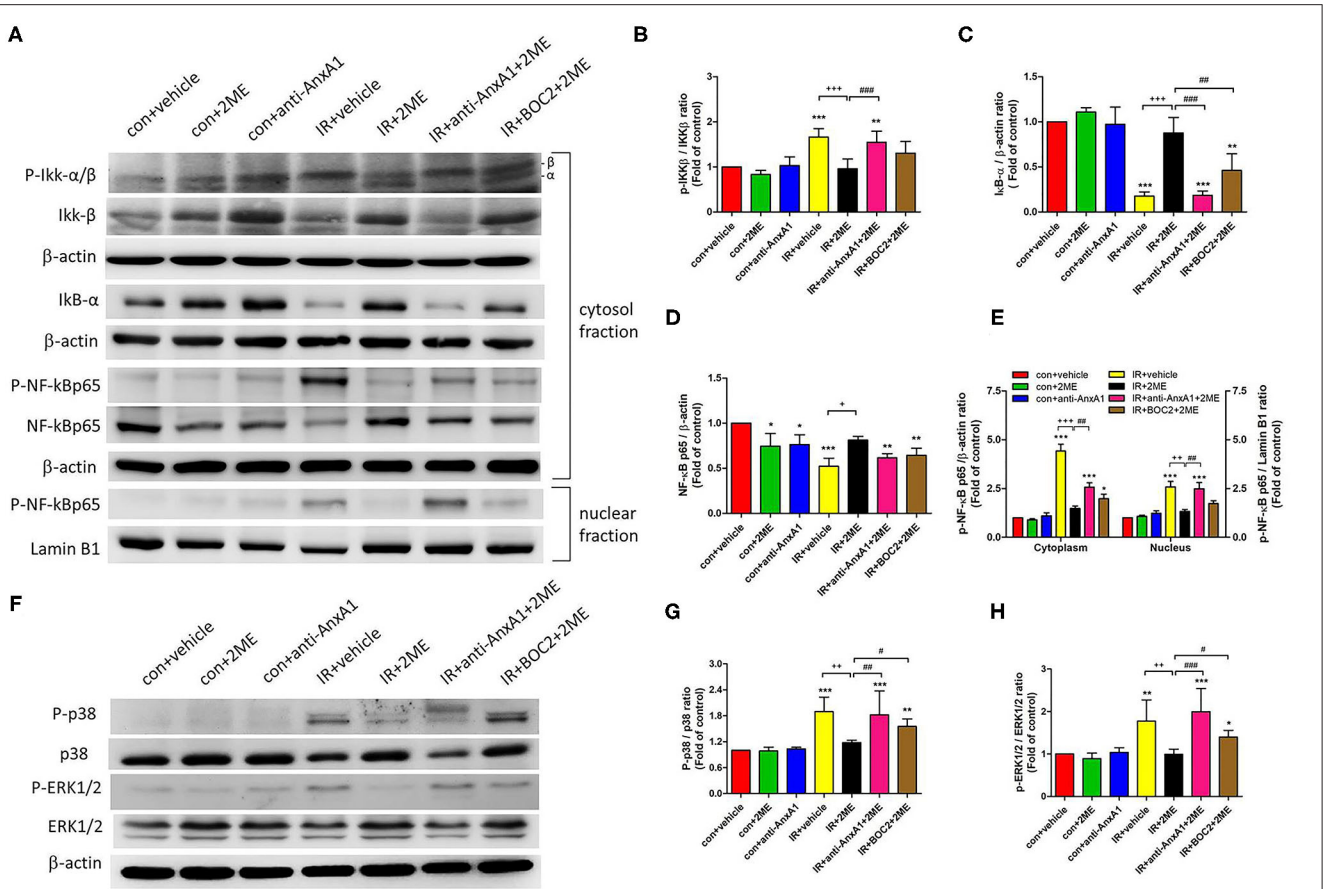

FIGURE 7 | 2ME repressed IR-induced NF-κB and MAPK activation in the lung tissue. **(A–E)** NF-κB and **(F–H)** MAPK signaling were detected in the lung tissue using Western blotting. 2ME reduced the **(B)** P-IKK-β, **(D,E)** nuclear and cytoplasmic P-NF-κB p65, **(G)** P-p38, and **(H)** P-ERK 1/2 levels, and increased the **(C)** IκB-α level in response to IR-induced lung injury. The addition of the anti-AnxA1 antibody or BOC2 significantly attenuated the inhibitory effects of 2ME on the NF-κB and MAPK signaling pathways. Lamin B1 and β-actin served as loading controls for nuclear and cytoplasmic proteins, respectively. $^{*}p < 0.05$, $^{**}p < 0.01$, and $^{***}p < 0.001$ compared with the control group; $^{+}p < 0.05$, $^{++}p < 0.01$, and $^{+++}p < 0.001$ compared with the IR group; and $^{\#}p < 0.05$, $^{\#\#}p < 0.01$, and $^{\#\#\#}p < 0.001$ compared with the IR + 2ME group.

airway inflammation (9, 25) and attenuates IgG immune complex-stimulated acute lung inflammation (26). In addition, 2ME decreases IR-induced hepatocellular damage (27), and ameliorates renal IR injury by inhibiting reactive oxygen species (ROS) and proinflammatory cytokine production (10). These studies suggest that 2ME may have potential value in protecting against lung IR injury. However, to date, no study has investigated the effect of 2ME on IR-induced acute lung inflammation, which is characterized by marked neutrophil infiltration in the lung interstitial and alveolar space. The migration of neutrophils from the pulmonary vasculature across the epithelium into the alveolar space has been shown to be a pathogenic factor during acute inflammatory lung injury (21, 28). As neutrophils are highly capable of producing ROS, they are responsible for a substantial proportion of the damage observed in IR-induced acute lung inflammation. In a previous study by Issekutz et al., 2ME significantly inhibited neutrophil migration to the joints in an adjuvant arthritis rat model (29). Here, we showed that 2ME suppressed IR-induced neutrophil infiltration and ameliorated oxidative damage in the lung tissue after a pretreatment. These observations were confirmed by the decreased numbers of MPO- and Ly6G-positive cells and decreased number of PMNs and MDA and protein carbonyl levels in the lung tissue.

Azevedo Loiola et al. have demonstrated that 17β-estradiol ameliorated LPS-induced brain inflammation through activation of AnxA1 (17). AnxA1 serves as an important anti-inflammatory regulatory factor in various animal models of inflammatory diseases, including multiple sclerosis, peritonitis, arthritis, and various types of IR injury (12, 16, 30). In addition, Purvis et al. reported that endogenous AnxA1 prevents insulin resistance and associated inflammatory complications in an experimental model type 2 diabetes (31). Under unstimulated conditions in the lung, the AnxA1 protein is localized to the cytoplasm of the epithelium, alveolar macrophages, and neutrophils (32). After exposure to various stimuli, the AnxA1 protein is trafficked to the plasma membrane and to be secreted, then it interacts with FPRs and mediates downstream cellular signaling in an autocrine and paracrine manner (33). FPRs are 7 transmembrane

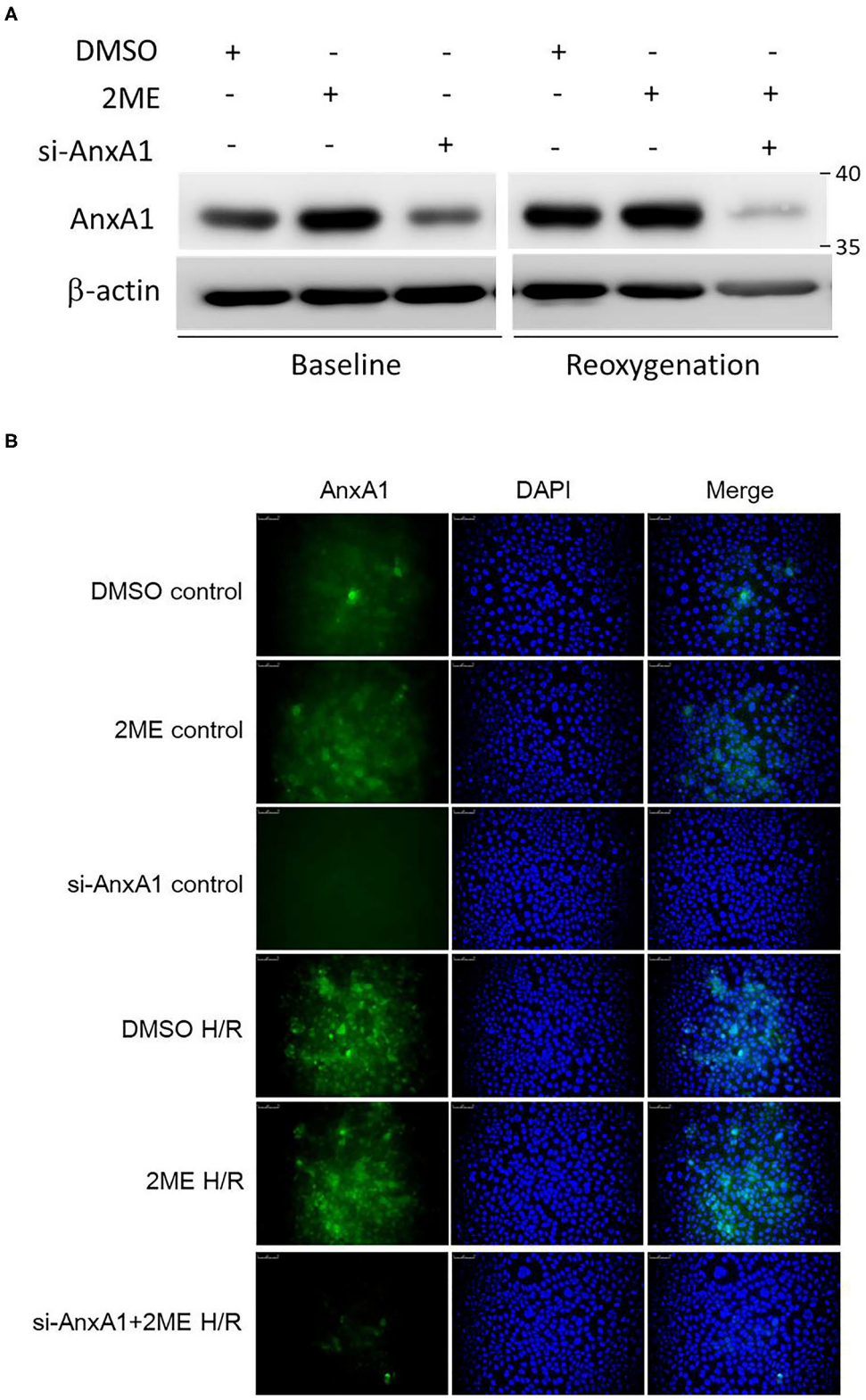

FIGURE 8 | 2ME increased AnxA1 expression in HPAECs. AnxA1 expression was detected using **(A)** Western blotting and **(B)** immunofluorescence staining. 2ME increased the expression level of AnxA1 in unstimulated cells. Compared to vehicle control, AnxA1 expression was substantially increased after HPAECs exposed to hypoxia for 24 h and reoxygenation for 1 h. No significant difference was observed between the HR and 2ME + HR groups.

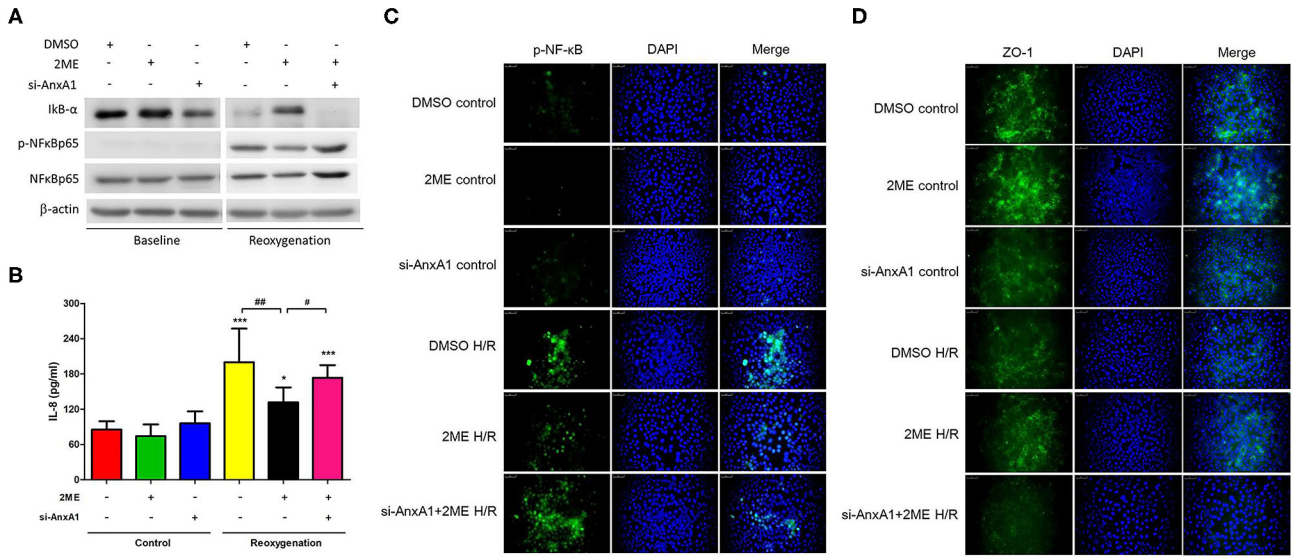

FIGURE 9 | 2ME suppressed NF-κB expression and IL-8 production, and enhanced ZO-1 activity in HPAECs upon HR injury. NF-κB and ZO-1 activity were detected using **(A)** Western blotting and/or **(C,D)** immunofluorescence staining. **(A,C)** 2ME increased the expression level of IκB-α, reduced the P-NF-κB and **(B)** IL-8 production, and increased **(D)** ZO-1 expression in HPAECs exposed to hypoxia for 24 h and reoxygenation for 1 h. Transfection with the AnxA1 siRNA reversed the 2ME-induced inhibition of NF-κB signaling, anti-inflammatory effects and increases in the levels of tight junction proteins in HPAECs. The results are representative of three independent experiments and presented as the means ± SD. $^{*}p < 0.05$ and $^{***}p < 0.001$ compared with the control group; and $^{\#}p < 0.05$ and $^{\#\#}p < 0.01$ compared with the HR + 2ME group.

G-protein coupled receptors, and three subtypes have been identified in humans, including FPR1, FPR2, and FPR3. FPR1 is predominantly expressed in neutrophils and rapidly upregulated in response to various inflammatory stimuli, including sepsis and autoimmune diseases (34). In contrast to the specific anti-inflammatory effect of FPR1, FPR2 is capable of interacting with numerous ligands, resulting in either anti-inflammatory or pro-inflammatory effects, depending on different ligand-specific interactions (35). An FPR2 agonist has been reported to ameliorate hyperoxia-induced lung injury in mice (36). AnxA1 binds FPR1&2 and subsequently inhibits neutrophil transmigration, promotes neutrophil apoptosis, and decreases the inflammatory response (13, 37). Our group and other researchers have shown that BOC2 (the FPR pan antagonist) abrogates the protective effects of Ac2-26 (exogenous AnxA1 peptide) on various types of IR injury (13, 16). Therefore, in the current study, we pretreated rats with BOC2 prior to 2ME administration to assess whether the protective effect of 2ME would be attenuated by an AnxA1 receptor antagonist, indirectly confirming that the effect of 2ME was mediated by AnxA1 signaling.

We and other investigators have shown that AnxA1 expression is upregulated during IR injury and accompanied by neutrophil infiltration (16, 38). In our study, 2ME increased endogenous AnxA1 expression in the lung tissue, HPAECs, and neutrophils under unstimulated conditions. However, a decreased AnxA1 expression in rat lungs was observed in the 2ME + IR group which was different from the 2ME + HR group in HPAECs or neutrophils. No significant difference was observed between the HR and 2ME + HR groups in HPAECs or neutrophils, despite the slight increase was observed after the 2ME pretreatment. We suggested that 2ME reduced AnxA1 expression after IR injury potentially by suppressing the infiltration of inflammatory neutrophils following an IR insult. *In vivo*, 2ME reduced the substantial influx of neutrophils expressing high levels of AnxA1 into the IR-injured lung, as evidenced by AnxA1, MPO, and Ly6G immunohistochemistry, immunoblotting, and double immunofluorescence staining of the lung tissue. *In vitro*, 2ME significantly suppressed HR-induced neutrophil transmigration and TNF-α production in rat neutrophils and increased ZO-1 expression in HPAECs, consistent with the *in vivo* results. Moreover, the anti-AnxA1 antibody, BOC2, or AnxA1 siRNA abolished the effects of 2ME on ameliorating IR injury *in vivo* or *in vitro*. These results further confirmed that the 2ME-induced anti-inflammatory effects were mediated by increasing the activity of the AnxA1 signaling pathway. Taken together, our study suggests that upregulating AnxA1 expression is mainly responsible for the protective effect of 2ME on IR-induced acute lung inflammation.

NF-κB, a regulatory transcription factor, is responsible for inducing the production of various cytokines and chemokines during inflammation. Under non-inflammatory conditions, IκB-α sequesters NF-κB dimers in the cytoplasm, which suppresses NF-κB nuclear translocation. IKK-β is an upstream regulator of NF-κB that regulates NF-κB activity by inhibiting IκB-α phosphorylation and degradation. IR causes IKK-β phosphorylation, subsequent IκB-α degradation, and NF-κB

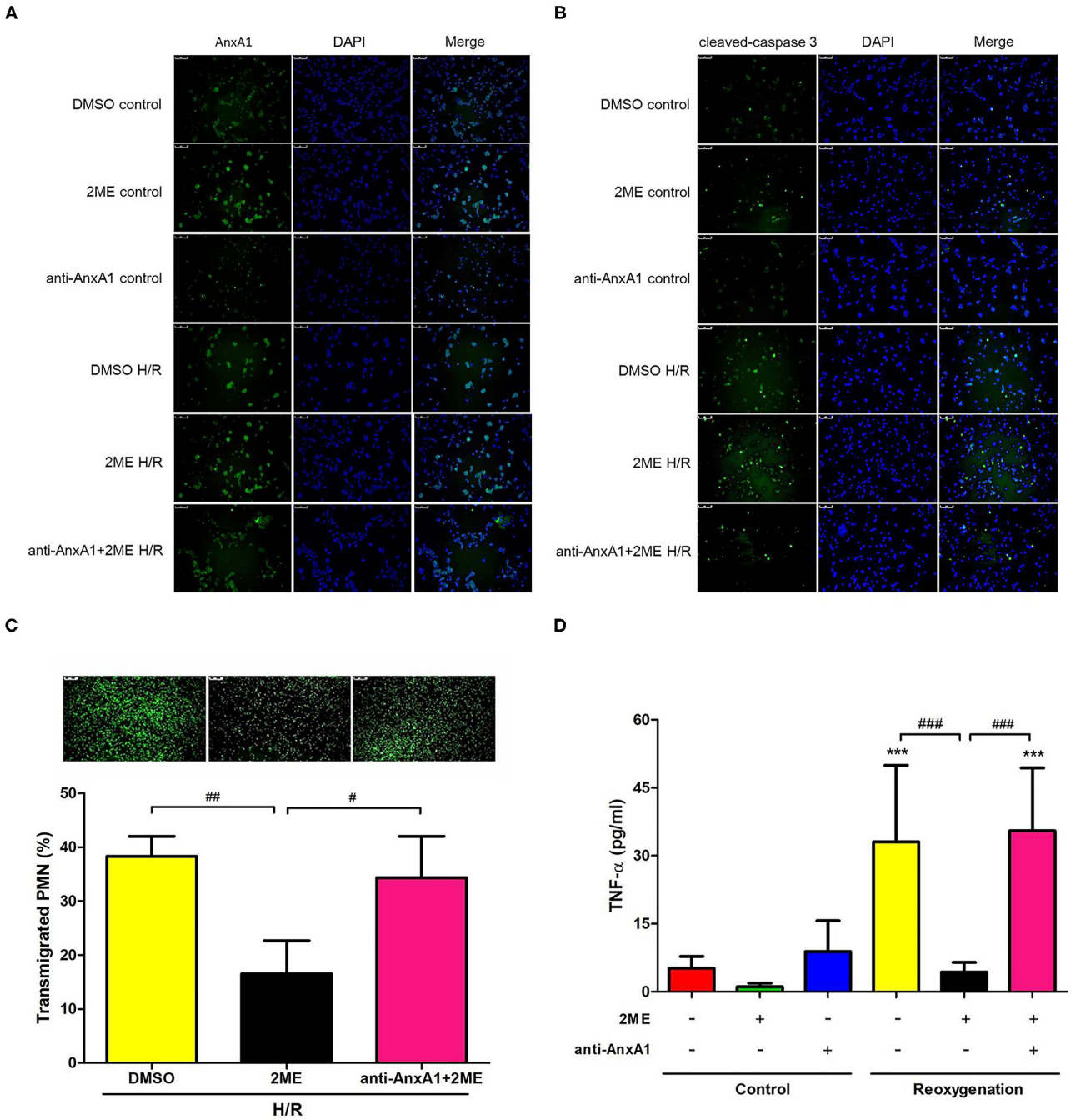

FIGURE 10 | 2ME increased AnxA1 and cleaved caspase-3 levels, and attenuated the transmigration and TNF-α production in rat neutrophils subjected to HR. AnxA1 and cleaved caspase-3 activity were evaluated using immunofluorescence staining **(A,B)**. Compared to the vehicle control group, 2ME increased AnxA1 and cleaved caspase-3 levels in the 2ME control group. Compared to the vehicle control group, the HR group presented higher AnxA1 and cleaved caspase-3 levels. 2ME administration further increased AnxA1 and cleaved caspase-3 levels in neutrophils exposed to HR. Rat neutrophils were stimulated with HR, induced to migrate across into the lower well of the migration chamber, and evaluated using a Leica DMi8 fluorescence microscope. 2ME attenuated **(C)** neutrophil transmigration and **(D)** TNF-α production after 2 h of hypoxia and 1 h of reoxygenation. These effects of 2ME were reversed by the anti-AnxA1 antibody. Normal mouse IgG was used as the control antibody in all experiments. $^{***}p < 0.001$ compared with the control group; $^{\#}p < 0.05$, $^{\#\#}p < 0.01$, and $^{\#\#\#}p < 0.001$ compared with the HR + 2ME group.

activation, which results in the production of proinflammatory cytokines, such as TNF-α and CINC-1 (16, 39). These increases in proinflammatory cytokine production further stimulate neutrophil recruitment and increase tissue injury. Our results was consistent with Liu et al. study showing that Ac2-26 decreases IKK-β activity and reduces oxygen-glucose

deprivation/reperfusion-induced proinflammatory cytokine production in microglia (40). AnxA1 has been shown to attenuate NF-κB activation and downstream proinflammatory cytokine production in acute lung inflammation (16). In addition, Yeh et al. found that 2ME reduced LPS-induced ALI by inhibiting NF-κB signaling (8). In the present study, 2ME effectively inhibited the activation of the NF-κB signaling pathway and proinflammatory cytokine production in the IR-injured lung and HPAECs exposed to HR, consistent with previous research (8, 26). Moreover, the anti-AnxA1 antibody, BOC2, or siRNA pretreatment abolished the inhibitory effect of 2ME on NF-κB. Therefore, the regulation of the NF-κB signaling pathway via the upregulation of AnxA1 might be a possible mechanism by which 2ME protects against acute lung inflammation induced by IR. However, further studies are necessary to clarify how AnxA1 inhibits NF-κB signaling.

Claudin-3 and occludin are tight junction proteins that form physical barriers restricting the diffusion of solutes through adjacent epithelial cell, and maintain the integrity of the permeability barrier of the alveolar wall (41, 42). ZO-1, a scaffolding protein, interacts with claudin-3 and occludin, which is critical for tight junction regulation (41, 42). Decreased levels of tight junction proteins in lung tissue are reliable indicators of the occurrence of ALI (43). IR injury may disrupt the integrity of the tight junction proteins and induce capillary leakage, which is a key component of the pathogenesis of pulmonary edema (28, 43). Further, exogenous recombinant AnxA1 upregulates occludin in brain endothelial cells and enhances tight junction formation to maintain blood-brain barrier integrity (33). The absence of AnxA1 disrupts occludin organization and increased blood-brain barrier permeability (33). As shown in our previous study, the expression levels of ZO-1, claudin-3, and occludin were significantly reduced upon IR injury but restored by an exogenous AnxA1 peptide (16). In the current study, 2ME significantly increased the integrity of these tight junction proteins in lung IR injury and HPAECs exposed to HR, but the effect was abolished by the anti-AnxA1 antibody or siRNA pretreatment. Therefore, the ability of 2ME to inhibit tight junction protein disruptions may be related to increased AnxA1 protein expression.

Significant increases in the apoptosis of lung epithelial and vascular endothelial cells are required for the development of acute lung inflammation (44). Bcl-2, an apoptotic regulator, possesses potent antiapoptotic activity to support the survival of cells and is implicated in the protective effect on IR injury (28, 44). Caspase-3 is a crucial effector caspase in the apoptotic pathway. Lung IR injury has been shown to decrease the levels of Bcl-2 and increase the levels of cleaved caspase-3 in the lung tissue to activate lung cell apoptosis (45, 46). Excessive lung cell apoptosis impairs the epithelial barrier and results in acute lung edema. Recent studies have reported that 2ME prevents apoptosis by increasing the expression of Bcl-2 in kidney IR injury (10) and by inhibiting the expression of caspase-3 in animal models of diabetic retinopathy and global ischemia (47, 48). In our study, 2ME significantly attenuated IR-induced apoptosis in the rat lung tissue, as evidenced by the decreased level of cleaved caspase-3 and increased level of Bcl-2 in the lung tissue. In addition, the antiapoptotic effect of 2ME was hampered by neutralizing AnxA1. Based on these findings, 2ME may increase AnxA1 expression to suppress IR-induced lung cell apoptosis.

Another interesting finding was that 2ME induced neutrophil apoptosis *in vitro*, as evidenced by the increase in cleaved caspase-3 levels, and this change was substantially attenuated in the presence of the AnxA1 antibody. Lung IR injury induces neutrophil infiltration into the alveoli and promotes high levels of inflammatory cytokine production (2, 16). Prolonged neutrophil survival may lead to an uncontrolled inflammatory response at local inflammatory sites, which can be opposed by pro-resolving mediators such as AnxA1 (49). Several investigations have revealed that AnxA1 promotes neutrophil apoptosis by activating caspase-3 to avoid the subsequent devastating inflammation (37, 50). Based on the results of the current study, 2ME may induce neutrophil apoptosis by upregulating AnxA1 expression following IR-induced lung injury.

2ME is an orally active and well-tolerated anticancer drug with low toxicity that has completed phase I and II clinical trials. We observed that 2ME reduced lung damage in rats exposed to IR injury, and the effects of 2ME on the resolution of IR-induced acute lung inflammation are associated with the modulation of AnxA1 expression in alveolar epithelial cells and neutrophils. However, our study has some limitations. First, sex-specific differences in survival have been reported in patients with ARDS (51). We only used male rats for the experiment which limits the opportunity to better understand the effect of 2ME in female animals. Second, Singh et al. demonstrated that 2ME protected against angiotensin II-induced hypertension in ovariectomized female mice (52). Whether pre- or post-menopausal status can alter the efficacy of 2ME in this experiment was not clear. Future studies specifically designed to answer these questions will be needed. Third, the isolated lung IR model with 40 min ischemia and 60 min reperfusion in our laboratory can produce significant lung injury (16, 53), however, this animal model may not completely translate to human in clinical condition according to the value of PaO_2/FiO_2 ratio in Berlin definition (54). It may be due to this reason that only the perfusate gas levels could be measured but a discrepancy between blood and perfusate gas levels may exist.

In conclusion, 2ME ameliorates IR-induced acute lung inflammation by upregulating the expression of endogenous AnxA1 in the lungs, alveolar epithelial cells, and neutrophils. Our study thus provides a molecular rationale for the use of 2ME as a possible treatment for IR-induced acute lung inflammation. Further studies of the potential clinical efficacy of 2ME are needed to determine whether it represents an attractive candidate as a drug that protects against pulmonary IR injury.

DATA AVAILABILITY STATEMENT

The original contributions presented in the study are included in the article/**Supplementary Material**, further inquiries can be directed to the corresponding author/s.

ETHICS STATEMENT

This animal study was reviewed and approved by the Institutional Animal Care and Use Committee of the National Defense Medical Center (approval number: IACUC-15-077, 19-March-2015).

AUTHOR CONTRIBUTIONS

W-IL, S-HT, K-LH, and S-JC participated in the research design. W-IL, H-PP, and S-YW conducted the experiments. S-YW and W-IL performed data analysis. W-IL and S-JC contributed to the writing of the manuscript. All authors contributed to the article and approved the submitted version.

FUNDING

This study was supported in part by the Ministry of Science and Technology, Taipei, Taiwan (grants MOST 106-2314-B-016-019-MY3 and MOST 107-2314-B-016-043); Tri-Service General Hospital, Taipei, Taiwan (grants TSGH-C105-055, TSGH-C108-065, TSGH-E-109217, TSGH-D-109078, TSGH-D-110045, and TSGH-1C109-106-2314-B-016-019-MY3); and Ministry of National Defense-Medical Affairs Bureau, Taiwan (grants MAB-107-012, MAB-108-016, MAB-108-017, MND-MAB-110-038, and MND-MAB-110-040).

ACKNOWLEDGMENTS

The authors thank Chung Yu Lai for consultation on the statistical analysis.

SUPPLEMENTARY MATERIAL

The Supplementary Material for this article can be found online at: https://www.frontiersin.org/articles/10.3389/fimmu.2021.596376/full#supplementary-material

Supplementary Figure 1 | Experimental design. **(A)** Experimental protocol showing the duration and time course of IR. **(B)** The experiment was designed to explore the roles of 2ME-related anti-inflammatory effects in IR lung injury.

Supplementary Figure 2 | Further study of the potential mechanisms of 2ME-mediated protection in **(A)** HPAECs or **(B)** rat neutrophils exposed to HR.

Supplementary Figure 3 | 2ME increased the expression of the AnxA1 mRNA and protein and ameliorated IR-induced acute lung edema in a dose-dependent manner. **(A)** Pretreatment with 2ME increased the expression of AnxA1 mRNA and protein compared to the vehicle control group. IR injury significantly increased the **(B)** lung weight gain, **(C)** K_f, **(D)** LW/BW, **(E)** W/D weight ratios, and **(F)** protein concentration in the BALF. Moreover, a significant decrease in these parameters was observed in the groups pretreated with 10 and 20 mg/kg BW 2ME prior to IR injury in a dose-dependent manner. $^{*}p < 0.05$, $^{**}p < 0.01$, and $^{***}p < 0.001$ compared with the control group; $^{+}p < 0.05$, $^{++}p < 0.01$, and $^{+++}p < 0.001$ compared with the IR group.

Supplementary Figure 4 | 2ME decreased polymorphonuclear leukocyte (PMN) infiltration induced by IR injury in the lung tissue. Lung tissues from each experimental group were immunostained with CD45, Ly6C, Ly6G, and Gal-3 antibodies and analyzed under a light microscope (200× magnification). The number of CD45-, Ly6C-, Ly6G-, and Gal-3-positive cells in the rat lung tissues were markedly increased after IR lung injury, particularly Ly6G-positive cells. Compared with IR injury alone, IR-challenged rats with 2-ME administration displayed a marked reduction in the infiltration of CD45-, Ly6C-, Ly6G-, and Gal-3-positive cells. The anti-inflammatory effects of 2ME were abolished by the addition of the anti-AnxA1 antibody.

Supplementary Figure 5 | The optimal 2ME concentration for inducing AnxA1 protein expression without cytotoxicity was 1 or 2 μM in HPAECs or rat neutrophils, respectively. Different concentrations of 2ME (0, 0.1, 1, 10, and 100 μM) or (0, 0.5, 1, 2, and 5 μM) were added to HPAECs or rat neutrophils for 24 or 2 h, respectively, prior to the detection of cell viability with WST-1 to define the cytotoxic concentration of 2ME. **(A,C)** No cellular toxicity was detected upon the addition of up to 1 μM 2ME in HPAECs and 2 μM 2ME in rat neutrophils. **(B)** Western blot showing differences in levels of the AnxA1 protein in unstimulated HPAECs were obtained from Western blotting after pretreated with 2ME at concentrations of 0, 0.1, 1, 10, and 100 μM. The optimal concentration of 2ME that induced AnxA1 protein expression was determined to be 1 μM among all investigated 2ME concentrations. **(D)** 2ME increased AnxA1 expression in unstimulated rat neutrophils, as detected using immunofluorescence staining. $^{*}p < 0.05$ compared with control group.

Supplementary Figure 6 | Rat neutrophils were cultured with 2ME (2 μM) and then subjected to HR and pretreated with the anti-AnxA1 antibody (Santa Cruz Biotechnology, sc-12740) at concentrations of 0.5, 1, and 2 μg. Besides, Ac2-26 (100 μg) was added to investigate the neutralizing effect of the anti-AnxA1 antibody. Compared to the vehicle + HR group, the number of transmigrated neutrophils was significantly reduced in the 2ME + HR group. The anti-inflammatory effects of 2ME were abrogated by the pretreatment with the anti-AnxA1 antibody in a dose-dependent manner. Compared to the vehicle + HR group, the level of neutrophil transmigration was similar to the Ac2-26 +anti-AnxA1 antibody (2 μg) + HR group. Compared to the Ac2-26 + anti-AnxA1 antibody (2 μg) + HR group, a lower level of neutrophil migration was observed in the Ac2-26 + anti-AnxA1 antibody (2 μg) + 2ME + HR group. These results indicated that the anti-AnxA1 antibody can neutralize the exogenous AnxA1 peptide and abrogated the anti-inflammatory effect of 2ME.

Supplementary Figure 7 | 2ME modulated FPR1 expression in the lung epithelium and neutrophils. FPR1 expression was examined using immunohistochemistry **(A)** in lung tissue and immunofluorescence staining **(C)** in neutrophils. **(B)** FPR1 transcript levels in the neutrophils were assessed using real-time quantitative PCR. Compared to the vehicle control, 2ME increased FPR1 expression in the lung epithelium and neutrophils. IR induced prominent epithelial FPR1 staining in rat lungs and HR induced a marked increase in FPR1 staining and mRNA levels in neutrophils. Compared to the IR or HR group, the 2ME pretreatment reduced FPR1 expression in lung tissue from the 2ME + IR group and in neutrophils from the 2ME + HR group.

Supplementary Figure 8 | 2ME modulated FPR2 expression in the lung epithelium and neutrophils. FPR2 expression was examined using immunohistochemistry **(A)** in lung tissue and immunofluorescence staining **(C)** in neutrophils. **(B)** FPR2 transcript levels in the neutrophils were assessed using real-time quantitative PCR. Compared to the vehicle control, 2ME increased FPR2 expression in the lung epithelium and neutrophils. IR induced prominent epithelial FPR2 staining in rat lungs and HR induced a marked increase in FPR2 staining and mRNA levels in neutrophils. Compared to the IR or HR group, the 2ME pretreatment reduced FPR2 expression in lung tissue from the 2ME + IR group and in neutrophils from the 2ME + HR group.

REFERENCES

1. Bellani G, Laffey JG, Pham T, Fan E, Brochard L, Esteban A, et al. Epidemiology, patterns of care, and mortality for patients with acute respiratory distress syndrome in intensive care units in 50 countries. *JAMA*. (2016) 315:788–800. doi: 10.1001/jama.2016.0291
2. Eltzschig HK, Eckle T. Ischemia and reperfusion–from mechanism to translation. *Nat Med*. (2011) 17:1391–401. doi: 10.1038/nm.2507

3. Ferrari RS, Andrade CF. Oxidative stress and lung ischemia-reperfusion injury. *Oxid Med Cell Longev.* (2015) 2015:590987. doi: 10.1155/2015/590987
4. Fan E, Brodie D, Slutsky AS. Acute respiratory distress syndrome: advances in diagnosis and treatment. *JAMA.* (2018) 319:698–710. doi: 10.1001/jama.2017.21907
5. Mueck AO, Seeger H. 2-Methoxyestradiol–biology and mechanism of action. *Steroids.* (2010) 75:625–31. doi: 10.1016/j.steroids.2010.02.016
6. Duncan GS, Brenner D, Tusche MW, Brustle A, Knobbe CB, Elia AJ, et al. 2-Methoxyestradiol inhibits experimental autoimmune encephalomyelitis through suppression of immune cell activation. *Proc Natl Acad Sci USA.* (2012) 109:21034–9. doi: 10.1073/pnas.1215558110
7. Stubelius A, Andreasson E, Karlsson A, Ohlsson C, Tivesten A, Islander U, et al. Role of 2-methoxyestradiol as inhibitor of arthritis and osteoporosis in a model of postmenopausal rheumatoid arthritis. *Clin Immunol.* (2011) 140:37–46. doi: 10.1016/j.clim.2011.03.006
8. Yeh CH, Chou W, Chu CC, So EC, Chang HC, Wang JJ, et al. Anticancer agent 2-methoxyestradiol improves survival in septic mice by reducing the production of cytokines and nitric oxide. *Shock.* (2011) 36:510–6. doi: 10.1097/SHK.0b013e318231866f
9. Huerta-Yepez S, Baay-Guzman GJ, Garcia-Zepeda R, Hernandez-Pando R, Vega MI, Gonzalez-Bonilla C, et al. 2-Methoxyestradiol (2-ME) reduces the airway inflammation and remodeling in an experimental mouse model. *Clin Immunol.* (2008) 129:313–24. doi: 10.1016/j.clim.2008.07.023
10. Chen YY, Yeh CH, So EC, Sun DP, Wang LY, Hsing CH. Anticancer drug 2-methoxyestradiol protects against renal ischemia/reperfusion injury by reducing inflammatory cytokines expression. *BioMed Res Int.* (2014) 2014:431524. doi: 10.1155/2014/431524
11. Yeh SH, Ou LC, Gean PW, Hung JJ, Chang WC. Selective inhibition of early–but not late–expressed HIF-1α is neuroprotective in rats after focal ischemic brain damage. *Brain Pathol.* (2011) 21:249–62. doi: 10.1111/j.1750-3639.2010.00443.x
12. Perretti M, Dalli J. Exploiting the annexin A1 pathway for the development of novel anti-inflammatory therapeutics. *Br J Pharmacol.* (2009) 158:936–46. doi: 10.1111/j.1476-5381.2009.00483.x
13. Vital SA, Becker F, Holloway PM, Russell J, Perretti M, Granger DN, et al. Formyl-peptide receptor 2/3/lipoxin A4 receptor regulates neutrophil-platelet aggregation and attenuates cerebral inflammation: impact for therapy in cardiovascular disease. *Circulation.* (2016) 133:2169–79. doi: 10.1161/CIRCULATIONAHA.115.020633
14. Smith HK, Gil CD, Oliani SM, Gavins FN. Targeting formyl peptide receptor 2 reduces leukocyte-endothelial interactions in a murine model of stroke. *FASEB J.* (2015) 29:2161–71. doi: 10.1096/fj.14-263160
15. Dalli J, Norling LV, Renshaw D, Cooper D, Leung KY, Perretti M. Annexin 1 mediates the rapid anti-inflammatory effects of neutrophil-derived microparticles. *Blood.* (2008) 112:2512–9. doi: 10.1182/blood-2008-02-140533
16. Liao WI, Wu SY, Wu GC, Pao HP, Tang SE, Huang KL, et al. Ac2-26, an annexin A1 peptide, attenuates ischemia-reperfusion-induced acute lung injury. *Int J Mol Sci.* (2017) 18:1771. doi: 10.3390/ijms18081771
17. Loiola RA, Wickstead ES, Solito E, McArthur S. Estrogen promotes pro-resolving microglial behavior and phagocytic cell clearance through the actions of annexin A1. *Front Endocrinol (Lausanne).* (2019) 10:420. doi: 10.3389/fendo.2019.00420
18. Davies E, Omer S, Morris JF, Christian HC. The influence of 17β-estradiol on annexin 1 expression in the anterior pituitary of the female rat and in a folliculo-stellate cell line. *J Endocrinol.* (2007) 192:429–42. doi: 10.1677/JOE-06-0132
19. Shand FH, Langenbach SY, Keenan CR, Ma SP, Wheaton BJ, Schuliga MJ, et al. *In vitro* and *in vivo* evidence for anti-inflammatory properties of 2-methoxyestradiol. *J Pharmacol Exp Ther.* (2011) 336:962–72. doi: 10.1124/jpet.110.174854
20. Yang YH, Morand E, Leech M. Annexin A1: potential for glucocorticoid sparing in RA. *Nat Rev Rheumatol.* (2013) 9:595–603. doi: 10.1038/nrrheum.2013.126
21. Li MH, Huang KL, Wu SY, Chen CW, Yan HC, Hsu K, et al. Baicalin attenuates air embolism-induced acute lung injury in rat isolated lungs. *Br J Pharmacol.* (2009) 157:244–51. doi: 10.1111/j.1476-5381.2009.00139.x
22. Chang H, Li MH, Chen CW, Yan HC, Huang KL, Chu SJ. Intravascular FC-77 attenuates phorbol myristate acetate-induced acute lung injury in isolated rat lungs. *Crit Care Med.* (2008) 36:1222–9. doi: 10.1097/CCM.0b013e31816a04d3
23. Wu SY, Tang SE, Ko FC, Wu GC, Huang KL, Chu SJ. Valproic acid attenuates acute lung injury induced by ischemia-reperfusion in rats. *Anesthesiology.* (2015) 122:1327–37. doi: 10.1097/ALN.0000000000000618
24. Oh H, Siano B, Diamond S. Neutrophil isolation protocol. *J Vis Exp.* (2008) 17:745. doi: 10.3791/745
25. Kim SR, Lee KS, Park HS, Park SJ, Min KH, Moon H, et al. HIF-1α inhibition ameliorates an allergic airway disease via VEGF suppression in bronchial epithelium. *Eur J Immunol.* (2010) 40:2858–69. doi: 10.1002/eji.200939948
26. Yan C, Shen Y, Sun Q, Yuan D, Tang H, Gao H. 2-Methoxyestradiol protects against IgG immune complex-induced acute lung injury by blocking NF-κB and CCAAT/enhancer-binding protein β activities. *Mol Immunol.* (2017) 85:89–99. doi: 10.1016/j.molimm.2017.02.007
27. Cho HI, Seo MJ, Lee SM. 2-Methoxyestradiol protects against ischemia/reperfusion injury in alcoholic fatty liver by enhancing sirtuin 1-mediated autophagy. *Biochem Pharmacol.* (2017) 131:40–51. doi: 10.1016/j.bcp.2017.02.008
28. Pao HP, Liao WI, Wu SY, Hung KY, Huang KL, Chu SJ. PG490-88, a derivative of triptolide, suppresses ischemia/reperfusion-induced lung damage by maintaining tight junction barriers and targeting multiple signaling pathways. *Int Immunopharmacol.* (2019) 68:17–29. doi: 10.1016/j.intimp.2018.12.058
29. Issekutz AC, Sapru K. Modulation of adjuvant arthritis in the rat by 2-methoxyestradiol: an effect independent of an anti-angiogenic action. *Int Immunopharmacol.* (2008) 8:708–16. doi: 10.1016/j.intimp.2008.01.016
30. Colamatteo A, Maggioli E, Azevedo Loiola R, Hamid Sheikh M, Cali G, Bruzzese D, et al. Reduced annexin A1 expression associates with disease severity and inflammation in multiple sclerosis patients. *J Immunol.* (2019) 203:1753–65. doi: 10.4049/jimmunol.1801683
31. Purvis GSD, Collino M, Loiola RA, Baragetti A, Chiazza F, Brovelli M, et al. Identification of annexinA1 as an endogenous regulator of RhoA, and its role in the pathophysiology and experimental therapy of type-2 diabetes. *Front Immunol.* (2019) 10:571. doi: 10.3389/fimmu.2019.00571
32. Senthilkumaran C, Hewson J, Ollivett TL, Bienzle D, Lillie BN, Clark M, et al. Localization of annexins A1 and A2 in the respiratory tract of healthy calves and those experimentally infected with *Mannheimia haemolytica*. *Vet Res.* (2015) 46:6. doi: 10.1186/s13567-014-0134-3
33. Cristante E, McArthur S, Mauro C, Maggioli E, Romero IA, Wylezinska-Arridge M, et al. Identification of an essential endogenous regulator of blood-brain barrier integrity, and its pathological and therapeutic implications. *Proc Natl Acad Sci USA.* (2013) 110:832–41. doi: 10.1073/pnas.1209362110
34. Dorward DA, Lucas CD, Chapman GB, Haslett C, Dhaliwal K, Rossi AG. The role of formylated peptides and formyl peptide receptor 1 in governing neutrophil function during acute inflammation. *Am J Pathol.* (2015) 185:1172–84. doi: 10.1016/j.ajpath.2015.01.020
35. Ansari J, Kaur G, Gavins FNE. Therapeutic potential of annexin A1 in ischemia reperfusion injury. *Int J Mol Sci.* (2018) 19:1211. doi: 10.3390/ijms19041211
36. Kim YE, Park WS, Ahn SY, Sung DK, Sung SI, Kim JH, et al. WKYMVm hexapeptide, a strong formyl peptide receptor 2 agonist, attenuates hyperoxia-induced lung injuries in newborn mice. *Sci Rep.* (2019) 9:6815. doi: 10.1038/s41598-019-43321-4
37. Vago JP, Nogueira CR, Tavares LP, Soriani FM, Lopes F, Russo RC, et al. Annexin A1 modulates natural and glucocorticoid-induced resolution of inflammation by enhancing neutrophil apoptosis. *J Leukoc Biol.* (2012) 92:249–58. doi: 10.1189/jlb.0112008
38. Zhao Y, Li X, Gong J, Li L, Chen L, Zheng L, et al. Annexin A1 nuclear translocation induces retinal ganglion cell apoptosis after ischemia-reperfusion injury through the p65/IL-1β pathway. *Biochim Biophys Acta Mol Basis Dis.* (2017) 1863:1350–8. doi: 10.1016/j.bbadis.2017.04.001
39. Beckers PAJ, Gielis JF, Van Schil PE, Adriaensen D. Lung ischemia reperfusion injury: the therapeutic role of dipeptidyl peptidase 4 inhibition. *Ann Transl Med.* (2017) 5:129. doi: 10.21037/atm.2017.01.41
40. Liu L, An D, Xu J, Shao B, Li X, Shi J. Ac2-26 induces IKKβ degradation through chaperone-mediated autophagy via HSPB1 in NCM-treated microglia. *Front Mol Neurosci.* (2018) 11:76. doi: 10.3389/fnmol.2018.00076
41. Gunzel D, Yu AS. Claudins and the modulation of tight junction permeability. *Physiol Rev.* (2013) 93:525–69. doi: 10.1152/physrev.00019.2012

42. Grailer JJ, Canning BA, Kalbitz M, Haggadone MD, Dhond RM, Andjelkovic AV, et al. Critical role for the NLRP3 inflammasome during acute lung injury. *J Immunol.* (2014) 192:5974–83. doi: 10.4049/jimmunol.1400368
43. Ohta H, Chiba S, Ebina M, Furuse M, Nukiwa T. Altered expression of tight junction molecules in alveolar septa in lung injury and fibrosis. *Am J Physiol Lung Cell Mol Physiol.* (2012) 302:L193–205. doi: 10.1152/ajplung.00349.2010
44. Ng CS, Wan S, Yim AP. Pulmonary ischaemia-reperfusion injury: role of apoptosis. *Eur Respir J.* (2005) 25:356–63. doi: 10.1183/09031936.05.00030304
45. Gao W, Jiang T, Liu YH, Ding WG, Guo CC, Cui XG. Endothelial progenitor cells attenuate the lung ischemia/reperfusion injury following lung transplantation via the endothelial nitric oxide synthase pathway. *J Thorac Cardiovasc Surg.* (2019) 157:803–14. doi: 10.1016/j.jtcvs.2018.08.092
46. Wu GC, Liao WI, Wu SY, Pao HP, Tang SE, Li MH, et al. Targeting of nicotinamide phosphoribosyltransferase enzymatic activity ameliorates lung damage induced by ischemia/reperfusion in rats. *Respir Res.* (2017) 18:71. doi: 10.1186/s12931-017-0557-2
47. Li Y, Xia ZL, Chen LB. HIF-1-α and survivin involved in the anti-apoptotic effect of 2ME2 after global ischemia in rats. *Neurol Res.* (2011) 33:583–92. doi: 10.1179/1743132810Y.0000000013
48. Gao X, Li Y, Wang H, Li C, Ding J. Inhibition of HIF-1α decreases expression of pro-inflammatory IL-6 and TNF-α in diabetic retinopathy. *Acta Ophthalmol.* (2017) 95:e746–50. doi: 10.1111/aos.13096
49. El Kebir D, Jozsef L, Filep JG. Opposing regulation of neutrophil apoptosis through the formyl peptide receptor-like 1/lipoxin A4 receptor: implications for resolution of inflammation. *J Leukoc Biol.* (2008) 84:600–6. doi: 10.1189/jlb.1107765
50. Dalli J, Consalvo AP, Ray V, Di Filippo C, D'Amico M, Mehta N, et al. Proresolving and tissue-protective actions of annexin A1-based cleavage-resistant peptides are mediated by formyl peptide receptor 2/lipoxin A4 receptor. *J Immunol.* (2013) 190:6478–87. doi: 10.4049/jimmunol.1203000
51. Moss M, Mannino DM. Race and gender differences in acute respiratory distress syndrome deaths in the United States: an analysis of multiple-cause mortality data (1979-1996). *Crit Care Med.* (2002) 30:1679–85. doi: 10.1097/00003246-200208000-00001
52. Singh P, Song CY, Dutta SR, Gonzalez FJ, Malik KU. Central CYP1B1 (cytochrome P450 1B1)-estradiol metabolite 2-methoxyestradiol protects from hypertension and neuroinflammation in female mice. *Hypertension.* (2020) 75:1054–62. doi: 10.1161/HYPERTENSIONAHA.119.14548
53. Hung KY, Liao WI, Pao HP, Wu SY, Huang KL, Chu SJ. Targeting F-box protein Fbxo3 attenuates lung injury induced by ischemia-reperfusion in rats. *Front Pharmacol.* (2019) 10:583. doi: 10.3389/fphar.2019.00583
54. Force ADT, Ranieri VM, Rubenfeld GD, Thompson BT, Ferguson ND, Caldwell E, et al. Acute respiratory distress syndrome: the Berlin Definition. *JAMA*. (2012) 307:2526–33. doi: 10.1001/jama.2012.5669

Conflict of Interest: The authors declare that the research was conducted in the absence of any commercial or financial relationships that could be construed as a potential conflict of interest.

Copyright © 2021 Liao, Wu, Tsai, Pao, Huang and Chu. This is an open-access article distributed under the terms of the Creative Commons Attribution License (CC BY). The use, distribution or reproduction in other forums is permitted, provided the original author(s) and the copyright owner(s) are credited and that the original publication in this journal is cited, in accordance with accepted academic practice. No use, distribution or reproduction is permitted which does not comply with these terms.

frontiers in Medicine

ORIGINAL RESEARCH
published: 18 March 2021
doi: 10.3389/fmed.2021.652824

Different Biological Pathways Between Good and Poor Inhaled Corticosteroid Responses in Asthma

*Byung-Keun Kim[1], Hyun-Seung Lee[2], Suh-Young Lee[3] and Heung-Woo Park[2,3,4]**

[1] Department of Internal Medicine, Korea University College of Medicine, Seoul, South Korea, [2] Institute of Allergy and Clinical Immunology, Seoul National University Medical Research Center, Seoul, South Korea, [3] Department of Internal Medicine, Seoul National University Hospital, Seoul, South Korea, [4] Department of Internal Medicine, Seoul National University College of Medicine, Seoul, South Korea

Gene regulatory networks address how transcription factors (TFs) and their regulatory roles in gene expression determine the responsiveness to anti-asthma therapy. The purpose of this study was to assess gene regulatory networks of adult patients with asthma who showed good or poor lung function improvements in response to inhaled corticosteroids (ICSs). A total of 47 patients with asthma were recruited and classified as good responders (GRs) and poor responders (PRs) based on their responses to ICSs. Genome-wide gene expression was measured using peripheral blood mononuclear cells obtained in a stable state. We used Passing Attributes between Networks for Data Assimilations to construct the gene regulatory networks associated with GRs and PRs to ICSs. We identified the top-10 TFs that showed large differences in high-confidence edges between the GR and PR aggregate networks. These top-10 TFs and their differentially-connected genes in the PR and GR aggregate networks were significantly enriched in distinct biological pathways, such as TGF-β signaling, cell cycle, and IL-4 and IL-13 signaling pathways. We identified multiple TFs and related biological pathways influencing ICS responses in asthma. Our results provide potential targets to overcome insensitivity to corticosteroids in patients with asthma.

Keywords: asthma, gene expression, gene regulatory networks, inhaled corticosteroid, transcription factor, pharmacogenomics, blood

OPEN ACCESS

Edited by:
Girolamo Pelaia,
University of Catanzaro, Italy

Reviewed by:
Bertrand De Meulder,
European Institute for Systems Biology and Medicine (EISBM), France
Feng-Ming Yang,
Taipei Medical University, Taiwan

***Correspondence:**
Heung-Woo Park
guinea71@snu.ac.kr
orcid.org/0000-0002-6970-3228

Specialty section:
This article was submitted to Pulmonary Medicine, a section of the journal Frontiers in Medicine

Received: *13 January 2021*
Accepted: *25 February 2021*
Published: *18 March 2021*

Citation:
Kim B-K, Lee H-S, Lee S-Y and Park H-W (2021) Different Biological Pathways Between Good and Poor Inhaled Corticosteroid Responses in Asthma. Front. Med. 8:652824. doi: 10.3389/fmed.2021.652824

INTRODUCTION

Blood contains many cells involved in immune responses, which explains why blood cell transcriptomics has been used for the study of asthma, an immune-mediated disease. For instance, it was reported that *MKP-1* and *IL-8* gene expression in peripheral blood mononuclear cells (PBMCs) of patients with asthma was useful in predicting clinical response to corticosteroids (1).

Recent transcriptomic studies have focused on the biological systems that are organized by various molecular entities such as genes, proteins and metabolites as well as the interactions between them. These systems can be visualized as networks, also interchangeably recognized as acyclic graphs, in which components (e.g., genes, proteins, or metabolites) are nodes that are connected by edges (relationships between nodes) (2). One good example is a gene co-expression network based on the similar, or correlated, gene expression patterns (3).

However, correlation does not necessarily imply causation. Gene regulatory networks attempt to identify the influencing patterns of transcription factors (TFs) on gene expression in a mechanistic fashion (4). As reviewed before, the activation or repression of different TFs and their regulatory roles in gene expression may determine the responsiveness to anti-asthma therapy, particularly to anti-inflammatory drugs (5). Qiu et al. found that TFs differentially affected gene expression in lymphoblastoid cell lines from children with asthma that included good and poor responders to inhaled corticosteroid (ICS) treatment by applying gene regulatory networks (6).

The purpose of this study was to assess gene regulatory networks of adult patients with asthma who showed good or poor lung function improvements in response to ICSs. To do this, we began by analyzing genome-wide gene expression levels in PBMCs from adult patients with asthma. Following this, we explored whether gene regulatory networks showed good or poor responder-specific regulatory patterns using the Passing Attributes between Networks for Data Assimilation (PANDA) algorithm. PANDA models information flow through networks under the assumption that both "transmitters" and "receivers" play active roles in modulating regulatory processes (7).

MATERIALS AND METHODS

This study was approved by the Institutional Review Board of the corresponding institution (H-1408-051-601 and 2019AN0240) and informed consent was obtained from all study participants.

Study Populations

We retrospectively reviewed the medical records of two institutes (Seoul National University Hospital and Korea University Anam Hospital, Seoul, Republic of Korea) and selected adult patients with asthma eligible for our study. The diagnosis of asthma was confirmed when forced expiratory volume in 1 s (FEV1) showed more than 12% (and 200 mL) increase after initiation of treatment. After diagnosis, all of patients were treated with medium dose ICSs (8) and regularly followed up; the pulmonary function measurement was performed every 4 weeks. Current or former smokers were excluded. We explained our study to eligible patients with asthma identified from medical records and enrolled them if they agreed to participate. We defined poor responders (PRs) or good responder (GRs) to ICSs, as patients who had less or more than 12% improvement in FEV1 compared to baseline values at 4 weeks after initiation of treatment, respectively (1). PRs eventually achieved more than 12% improvement in FEV1 responding to ICSs, but it took longer than 4 weeks. The overall study design is presented in **Figure 1**.

Gene Expression Arrays

Blood for gene expression analysis was drawn at a stable state, that is, no changes in anti-asthma medications and no acute exacerbations (short-term oral prednisone burst, unexpected clinic visit, and emergency room visit or hospitalization due to asthma symptom aggravation) within 4 weeks prior to blood sampling. PBMCs were isolated and genome-wide gene expression levels were measured using the Affymetrix GeneChip Human Gene 2.0 ST (Affymetrix, Santa Clara, CA, USA). We removed probes with bad chromosome annotations and probes in the X or Y chromosome. We then performed variance-stabilizing transformation and quantile-normalization to reduce technical noises and to make the distribution of expression level for each array closer to a normal distribution.

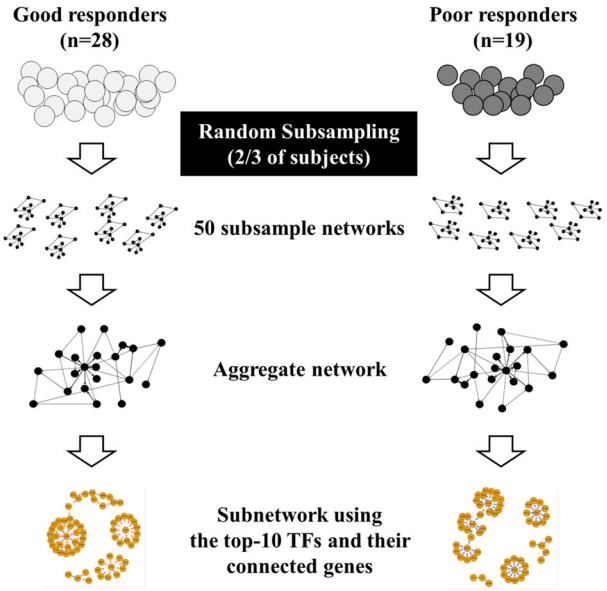

FIGURE 1 | Overall study design. Poor responders (PRs) or good responder (GRs) to inhaled corticosteroids was defined as patients who had less or more than 12% improvement in FEV1 compared to baseline values at 4 weeks after initiation of treatment, respectively, and genome-wide gene expression profiles were obtained from peripheral blood mononuclear cells of participants. Due to the small sample size, two-thirds of the participants were chosen from each GR and PR group at random (without replacement) to form subsamples. We constructed 50 gene regulatory networks in GRs and PRs using PANDA with these 50 subsamples. We then generated a single, aggregate gene regulatory network by averaging Z-scores of edges across the 50 networks identified from subsamples. Finally, we illustrated subnetworks using the top-10 transcription factors (TFs) identified and their differentially-connected genes in each aggregate GR and PR network.

Network Analysis

The analysis was performed with R version 4.0.2 (www.r-project.org). We performed PANDA analysis on gene expression profiles from GRs and PRs using the R package "pandaR" (9). network. To seed the PANDA algorithm, we used a mapping between TF motifs and target genes from the TRRUST database (10). This mapping file consists of 8,444 regulatory interactions for 800 TFs and 2,521 target genes. There are 796 TFs in both our gene expression data and the mapping file. These TFs correspond to 9,392 pairs of (TF, gene) and correspond to 2,490 genes in our expression data.

Abbreviations: EES, Edge Enrichment Score; FEV1, Forced expiratory volume in 1 second; GR, Good responder; ICS, Inhaled corticosteroid; PANDA, Passing Attributes between Networks for Data Assimilation; PBMCs, Peripheral blood mononuclear cells; PR, Poor responder; TF, Transcription factor.

To minimize the effect of outliers in our networks that were built on a smaller sample size, two-thirds of the participants were chosen from each GR and PR group at random (without replacement) to form subsamples. These 50 subsamples were used to construct 50 gene regulatory networks in GRs and PRs. PANDA reports the probability that a connection (edge) exists between a TF and gene in an estimated network as a Z-score (7). We generated a single, aggregate gene regulatory network by averaging Z-scores of edges across the 50 networks identified from subsamples, as described elsewhere (11). We then selected high-confidence edges that had an average edge Z-score >0 in the aggregate GR or PR networks. These edges can be interpreted as edges that are most likely to exist in each aggregate network.

To quantify differences in high-confidence edges, we calculated an edge enrichment score (EES) (11): $EES_i = log_2[(k^g{}_i/k^p{}_i)/(N^g/N^p)]$ where $k^g{}_i$ and $k^p{}_i$ are the (out-degree) number of high-confidence edges for TF i in the aggregate GR and PR networks, respectively, and N^g and N^p are the total number of high-confidence edges in each network. Note that the EES is positive for edge-enrichment from a particular TF in the aggregate GR network, and negative for edge-enrichment from a particular TF in the aggregate PR network.

Gene Set Enrichment Analysis

Based on EES, we selected the top-10 TFs from aggregate networks (5 of the highest ones and 5 of the lowest ones). We then identified genes connected to these 10 TFs differentially in the aggregate GR and PR networks by selecting genes whose differences in high-confidence edge Z-scores were >0.75. This means that these genes have at least a 75% chance of existing and being different in each aggregate network. As we assumed that these 10 TFs and their differentially-connected genes were the main drivers in each aggregate network, we constructed GR and PR subnetworks using them. To assign biological meaning to interpretability of each subnetwork, we performed pathway overrepresentation analysis (gene set enrichment analysis) of individual TF and its target genes in the GR and PR subnetworks using "g:Profiler" (database version: e100_eg47_p14_7733820) (12). g:Profiler (https://biit.cs.ut.ee/gprofiler/) provides an adjusted *P*-value calculated in a manner that accounts for the hierarchical relationships among the tested gene sets. g:Profiler utilizes 3 types of biological pathways; KEGG, Reactome, and WikiPathways. As Reactome provides more and diverse signaling pathways including immunological, developmental and kinase, signaling pathways, the drug- or target-based, stress activated, or lipid-mediated signaling pathways compared to the other databases (13), we selected Reactome database.

RESULTS

A total of 47 adult patients with asthma (28 GRs and 19 PRs) were enrolled. **Table 1** summarizes their baseline characteristics. There were no significant differences between GRs and PRs for age, sex, atopy, blood eosinophil counts, or pulmonary functions at baseline (before initiation of treatment). GRs showed significant improvement in FEV1 compared to PRs at 4 weeks after initiation of treatment [694.3 ± 410.9 mL (GR) vs. 78.4 ± 172.5 mL (PR), $P = 1.82 \times 10^{-7}$), as expected from the definition of 2 groups. Using PANDA, we created aggregate GR and PR networks and identified the top-10 TFs based on EES. **Table 2** lists top-5 TFs of those with the highest EES and top-5 TFs of those with the lowest EES. MXD1 has the highest EES, which means that high-confidence edges connecting MXD1 and genes are most greatly enriched in the aggregate GR network. Meanwhile SMAD7 with the lowest EES is positioned in the opposite end. **Table 2** also shows absolute numbers of high-confidence edges connecting top-10 TFs and genes in each aggregate GR or PR network and net differences between two aggregate networks. It was difficult to visualize the differential connectivity of TFs and connected genes in the aggregate GR and PR networks, if all TF-gene connections were considered. Hence, we illustrated subnetworks

TABLE 1 | Characteristics of enrolled patients with asthma.

	Good responder $n = 28$	Poor responder $n = 19$	*P*-value
Age (year)	51.9 (13.8)	52.8 (15.6)	0.83
Male	9 (32.1%)	8 (42.1%)	0.75
Atopy	15 (53.6%)	8 (42.1%)	0.64
Blood eosinophil (/μL)	541.7 (220.4)	605.3 (349.6)	0.48
FEV1 (ml)	1,897.1 (501.3)	2,323.1 (987.6)	0.057
FEV1 predicted (%)	67.5 (15.2)	71.9 (19.2)	0.092
FVC (mL)	2,770.3 (684.6)	3,178.4 (1,115.1)	0.12
FVC predicted (%)	79.1 (13.5)	86.2 (15.8)	0.11
FEV1/FVC ratio (%)	66.5 (11.5)	71.9 (10.3)	0.11
FEV1 increase (mL)[a]	694.3 (410.9)	78.4 (172.5)	1.82×10^{-7}
FEV1 increase (%)[a]	45.5 (42.7)	3.7 (8.1)	1.24×10^{-4}

FEV1, Forced expiratory volume in 1 second; FVC, Forced vital capacity.
[a]Differences between FEV1 measured at baseline and FEV1 measured at 4 weeks after initiation of treatment. Data are presented as "mean (standard deviation)" except for male and atopy which are presented as "number (%)."

TABLE 2 | Top-10 transcription factors identified from aggregate networks based on edge enrichment scores.

TF	*n*Edge(GR)	*n*Edge(PR)	*n*Diff	Log_2(EES)
MXD1	582	185	397	1.653
NFYB	430	142	288	1.598
E2F6	621	212	409	1.551
CREM	828	290	538	1.514
RFX2	590	209	381	1.497
ID3	235	662	−427	−1.494
HOXA1	279	818	−539	−1.552
JUNB	268	823	−555	−1.619
PROX1	205	678	−473	−1.726
SMAD7	57	323	−266	−2.503

TF, transcription factor; n, number; diff, difference; EES, edge enrichment score; GR, good responder; PR, poor responder.

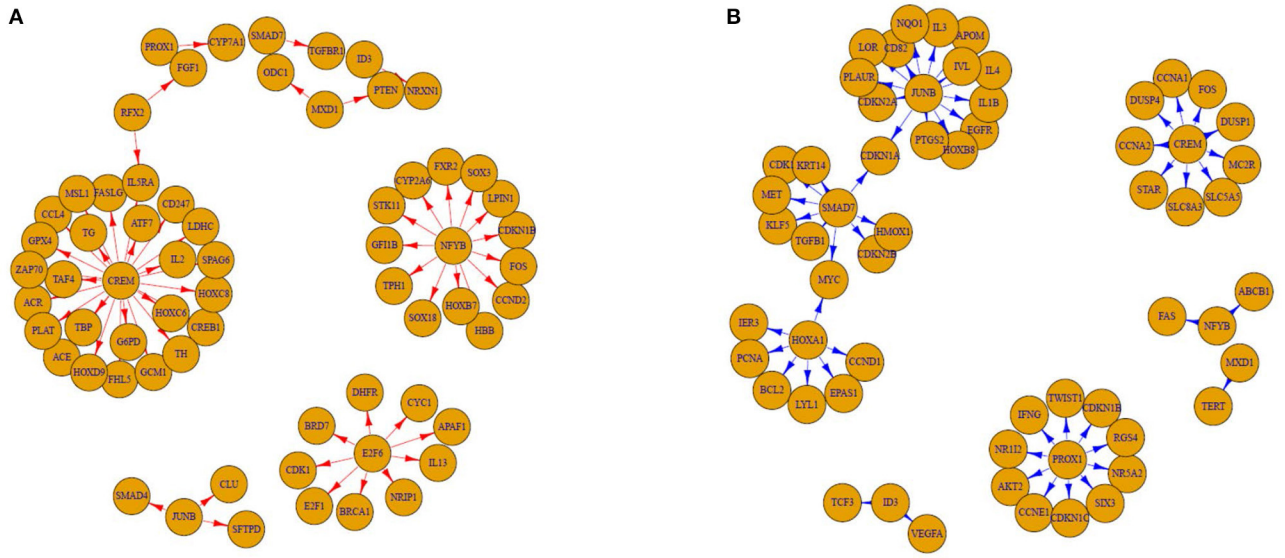

FIGURE 2 | Good (GR) and poor responder (PR) subnetwork made by the top-10 transcription factors and their differentially-connected genes. **(A)** GR and **(B)** PR. Based on edge enrichment score, we selected the top-10 TFs from aggregate networks (5 of the highest ones and 5 of the lowest ones). We then identified genes connected to these 10 TFs differentially in the aggregate GR and PR networks and illustrated subnetworks using them. The edges are directed from TFs to their targeting genes whose differences in high-confidence edge Z-scores are >0.75. This means that these genes have at least a 75% chance of existing and being different in each aggregate network.

using the top-10 TFs identified and their differentially-connected genes in each aggregate GR and PR network. **Figure 2** shows the differential connectivity of top-10 TFs to genes between aggregate GR and PR network. E2F6 and RFX2 are connected to genes with high-confidence in aggregate GR network only, whereas HOXA1 is connected to genes in aggregate PR network only. The other 7 TFs are differentially connected to genes between aggregate GR and PR networks. The name of genes connected to the top-10 TFs in each aggregate network is listed in **Table 3**. **Table 4** summarizes identified biological pathways in which TF and its connected genes in each aggregate network are enriched with adjusted P values less than 0.001. For example, E2F6 and its connected genes in aggregate GR network (APAF1, BRCA1, BRD7, CDK1, CYC1, DHFR, E2F1, IL13, and NRIP1) are significantly enriched in G1/S-Specific Transcription, Transcriptional Regulation by E2F6, G1/S Transition, Mitotic G1 phase and G1/S transition, and Transcriptional Regulation by TP53 pathways. The pathways that were identified helped us understand differences in regulatory control driven by Top-10 TFs between GR and PR. In the GR subnetwork, E2F6, and NFYB supposedly play important roles by regulating cell cycle-related and FOXO-mediated transcription pathways, respectively. Meanwhile, CREM, PROX1, and SMAD7 are crucial in the PR subnetwork controlling cell cycle-related, immune-mediated and TGF-β signaling pathways. Interestingly, JUNB is engaged in both GR and PR subnetworks. However, it differentially regulates biological pathways (TGF-β *vs.* IL-4 and IL-13 signaling pathways). The top-10 TFs identified in this study are not differentially expressed between GR and PR groups (data not shown).

DISCUSSION

In this study, we constructed gene regulatory networks associated with good or poor response to ICSs using gene expression profiles of PBMCs from 47 adult patients with asthma. We identified the top-10 TFs that showed large differences in EES in the aggregate GR and PR networks. We also identified subnetworks made by top-10 TFs and their differentially-connected genes in each aggregate GR and PR network. In addition, these TFs and genes were enriched in distinctly different biological pathways in GRs and PRs. Based on our results, we summarize that TGF-β signaling, cell cycle related, and IL-4 and IL-13 signaling pathways are important in determining responses to ICSs in patients with asthma.

Interestingly, the top-10 TFs and their differentially-connected genes in our regulatory networks showed no significant differences in expression between GRs and PRs (data not shown). It is possible that multiple TFs compete for the same binding site of a target gene, but which one primarily regulates that gene is dependent on the drug response phenotype. Gene regulatory networks provide us an opportunity to model biological processes as information flowing between genes and the potential to identify the underlying causes of the drug response that cannot be captured by differential gene expression networks. PANDA constructs networks based on differential connectivity by comparing differential expression of the TFs. Therefore, the same sets of TFs may regulate different sets of downstream genes between GRs and PRs, as we observed with JUNB in our analysis. Our results indicated that responses between good and poor responders to a certain drug does not

TABLE 3 | Top-10 transcription factors and their differentially-connected genes in the aggregate good and poor responder network.

Transcription factor	Connected genes
Good responder only	
E2F6	*APAF1; BRCA1; BRD7; CDK1; CYC1; DHFR; E2F1; IL13; NRIP1*
RFX2	*FGF1; IL5RA*
Poor responder only	
HOXA1	*BCL2; CCND1; EPAS1; IER3; LYL1; MYC; PCNA*
Common	
CREM	[Good responder] *ACE; ACR; ATF7; CCL4; CD247; CREB1; FASLG; FHL5; G6PD; GCM1; GPX4; HOXC6; HOXC8; HOXD9; IL2; IL5RA; LDHC; MSL1; PLAT; SPAG6; TAF4; TBP; TBP; TG; TH; ZAP70*
	[Poor responder] *CCNA1; CCNA2; DUSP1; DUSP4; FOS; MC2R; SLC5A5; SLC8A3; STAR*
ID3	[Good responder] *NRXN1*
	[Poor responder] *TCF3; VEGFA*
JUNB	[Good responder] *CLU; SMAD4; SFTPD*
	[Poor responder] *APOM; CD82; CDKN1A; CDKN2A; EGFR; HOXB8; IL1B; IL3; IL4; IVL; LOR; NQO1; PLAUR; PTGS2*
MXD1	[Good responder] *ODC1; PTEN*
	[Poor responder] *TERT*
NFYB	[Good responder] *CCND2; CDKN1B; CYP2A6; FOS; FXR2; GFI1B; HBB; HOXB7; LPIN1; SOX18; SOX3; STK11; TPH1*
	[Poor responder] *ABCB1; FAS*
PROX1	[Good responder] *CYP7A1*
	[Poor responder] *AKT2; CCNE1; CDKN1B; CDKN1C; IFNG; NR1I2; NR5A2; RGS4; SIX3; TWIST1*
SMAD7	[Good responder] *TGFBR1*
	[Poor responder] *CDK1; CDKN1A; CDKN2B; HMOX1; KLF5; KRT14; MET; MYC; TGFB1*

necessarily emanate from differential gene expression networks but may instead be from regulatory gene expression networks.

SMAD7 had the lowest EES, which suggests that it may play an important role in the aggregate PR network. Binding of TGF-β to its receptor triggers phosphorylation of SMAD2 and SMAD3 and phosphorylated SMAD2/3 proteins heterodimerize with SMAD4 to generate a complex that moves to the nucleus, where it regulates the expression of target genes (canonical TGF-β signaling) (14). This TGF-β-associated SMAD signaling is tightly controlled by SMAD7, another intracellular SMAD protein (15). Thus, SMAD 7 acts as a negative regulator of the canonical TGF-β signaling pathway. Previously, it was reported that TGF-β impairs therapeutic responses to corticosteroids in chronic airway diseases and the non-canonical signaling pathway is important in this process (16, 17). However, these reports were based on experiments using lung epithelial cells. TGF-β regulates pathologic CD4+ T cell responses by directly suppressing T-bet and GATA-3 expression and by downregulating both Th1 and Th2 cell differentiation (18, 19). In addition, TGF-β can promote the induction of regulatory T cells (20). For dendritic cells, TGF-β can downregulate the antigen-presenting function and expression of co-stimulatory molecules *in vitro* (21). Mice over-expressing Smad7 in T cells develop severe intestinal inflammation in various experimental models (22). In this study, we examined gene expression in PBMCs from adult patients with asthma, contrary to previous studies using lung epithelial cells. This would explain why Smad7 influence increases in the aggregate PR network in our study. In addition, we observed that JUNB is confidently connected with SMAD4 in the GR subnetwork (**Figure 2A**). A previous report showed that JUNB is a critical activator protein component mediating TGF-β signaling in human breast epithelium (23). Taken together, increased TGF-β signaling in blood cells may confer good response to ICSs in asthma. Although it was recently reported that knockdown of SMAD7 with a specific antisense oligonucleotide that restores endogenous TGF-β activity is not effective for patients with steroid-resistant/dependent Crohn disease (24), a SMAD7-targeting approach is worthy of being searched to treat patients with insensitivity to corticosteroids in asthma.

Corticosteroid possesses an anti-inflammatory action and inhibits various inflammatory chemokines and cytokines, including IL-4 and IL-13 (25). Unexpectedly, we found that JUNB and its related genes in the PR subnetwork were significantly enriched in the IL-4 and IL-13 signaling pathway. Moreover, we observed that E2F6 is connected to IL-13 in the GR subnetwork. Bruhn et al. have suggested an inhibitory role for E2F6 in the regulation of IL-13 and allergy based on gene expression analysis of CD4+ T cells (26). As participants in this study were treated with medium dose ICS, it was possible that the amount of corticosteroids was not enough to suppress IL-4 and IL-13 signaling pathway entirely. Another possible explanation is that corticosteroids in their conventional doses are not sufficient to suppress IL-4 and IL-13 signaling pathway completely in some patients. For example, the 1-week course of prednisone treatment did not show significant changes in bronchoalveolar lavage cells expressing IL-4 and IL-13 mRNA in patients with asthma who were recognized as PRs to corticosteroids (27). In this sense, the role of dupilumab, a monoclonal antibody blocking IL-4 and IL-13 signaling pathway by inhibiting IL-4R alpha, is promising for the management of patients with

TABLE 4 | Reactome pathways significantly enriched by the top-10 transcription factors and their differentially-connected genes in the good and poor responder subnetworks.

TF	Good responder		Poor responder	
	Pathway name	***P*-value***	**Pathway name**	***P*-value***
E2F6	G1/S-Specific Transcription	2.02E-06	None	
	Transcriptional Regulation by E2F6	4.57E-06		
	G1/S Transition	0.001104		
	Mitotic G1 phase and G1/S transition	0.001794		
	Transcriptional Regulation by TP53	0.002374		
CREM	None		Phosphorylation of proteins involved in the G2/M transition by Cyclin A:Cdc2 complexes	0.000465
			G2 Phase	0.001549
NFYB	FOXO-mediated transcription	0.006694	None	
JUNB	SMAD2/SMAD3:SMAD4 heterotrimer regulates transcription	0.007895	Interleukin-4 and interleukin-13 signaling	0.000039
			Signaling by interleukins	0.002486
			Cytokine signaling in immune system	0.005848
PROX1	None		Mitotic G1 phase and G1/S transition	0.000534
			PTK6 regulates cell cycle	0.001627
			Cyclin E associated events during G1/S transition	0.005497
			Cyclin A:Cdk2-associated events at S phase entry	0.005905
			AKT phosphorylates targets in the cytosol	0.009838
			TP53 regulates transcription of genes involved in G1 cell cycle arrest	0.009838
SMAD7	None		SMAD2/SMAD3:SMAD4 heterotrimer regulates transcription	0.000503
			Mitotic G1 phase and G1/S transition	0.001057
			Transcriptional activity of SMAD2/SMAD3:SMAD4 heterotrimer	0.001335
			TFAP2 (AP-2) family regulates transcription of cell cycle factors	0.001549
			Signaling by TGF-beta receptor complex	0.005696

**adjusted P-values.*

asthma with reduced response to corticosteroids, as reviewed recently (28). An interesting finding is that the cell cycle (G1/S transition) related pathways are significantly enriched in both GR and PR subnetworks. The accurate transition from G1 (Gap 1) phase of the cell cycle to S (Synthesis) phase is crucial for the control of eukaryotic cell proliferation (29). Since long time ago, we have known that dexamethasone induces irreversible G1 arrest and death of a human lymphoid cell line (30). An arrest of cell cycle progression in the G1/S phase also induced apoptosis of human eosinophils from patients with asthma (31). All these together imply a potential role of the G1/S transition in blood cells in response to corticosteroids. We found that E2F6 and its differentially-connected genes in the GR subnetwork and CREM and PROX1 and their differentially-connected genes in the PR subnetwork are enriched in the G1/S transition related pathways. E2F6 functions as a repressor of E2F-dependent transcription during S phase and thus is presumed to be a cell cycle transcriptional repressor (32). Meanwhile, CREM is implicated in the stimulation of cyclin A transcription at G1/S (33). PROX1, has conflicting roles in cell cycle regulation. PROX1 induces cell cycle arrest in liver hepatocellular carcinoma cells (34), but paradoxically increases proliferation in fetal hepatoblasts (35). These findings suggest that PROX1 regulates the cell cycle in a cell-type-dependent manner. Taken together, cell cycle arrest at G1/S may help to avoid steroid resistance. In addition, it was reported that dexamethasone can stimulate the G1/S transition in human airway fibroblasts in asthma, which may result in airway remodeling (36). In a study reported by Goleva E et al. (1), significantly more dexamethasone was required to suppress *in vitro* T cell proliferation in PBMC from steroid resistant than steroid sensitive asthmatics. Taken together, an intrinsic property related with PBMC proliferation in asthmatics may determine the susceptibility for corticosteroid treatment and thus a new approach focused on the G1/S transition is worthy of being investigated to overcome corticosteroid insensitivity.

RFX2 and HOXA1 may also play an important role in determining response to ICSs. Probably, the number of targeted genes with difference in high-confidence edge Z-scores greater than 0.75 between GR and PR groups is too small to be captured as a specific biologic pathway. As gene expression changes over time, the sampling time of PBMCs in this study may not be the

exact time representing the whole picture of RFX2- or HOXA1-related mechanisms.

A small number of participants in this study is a potential limitation. To minimize heterogeneity because of this, we constructed regulatory networks using random subsampling of participants and averaged these networks to identify aggregate GR and PR networks. By doing this, we removed the effect of changes in gene expression that are specific to only one individual (outliers) and focus on changes that are most likely a result of corticosteroid responses. We assumed that TFs with greater differences in high-confidence edges were the main drivers in each aggregate network. Moreover, it was difficult to visualize all the differential connectivity of TFs and their connected genes in the aggregate networks. For these reasons, we selected only the top-10 TFs with a quantified method (EES) focusing on the large-scale changes in edge numbers between two aggregate networks. However, it is possible that other TFs and their related genes excluded from our analysis would have their potential roles in determining ICS responses. Despite taking these precautions, we recognize that future studies are needed for the functional validation of our networks.

In addition, the statistical power and sample size should be considered before generalizing our observations. The performance of gene regulatory network inference algorithms with a genome-wide scale depends on the sample size. It is generally considered that the larger the sample size, the better the gene network inference performance. However, there has not been adequate information on determining the sample size for optimal performance of gene regulatory network inference. In one study using a pseudo gene regulatory network with 6 nodes which is generated from gene-gene associations based on the coefficient of intrinsic dependence, the false networks only appears $\leq$5 times in 100 simulations for the sample size $=$ 25, 50, and 100 (37). In other study based on the real world gene expression data sets, it was reported that the sample size around 64 is sufficient to obtain acceptable performance of the information-theory-based gene regulatory network inference algorithms (38). We cannot directly apply previous observations to ours, as inference algorithms are different with that of PANDA. However, considering previous reports, we may say that the chance of obtaining false positive gene regulatory networks in this study would not be too much.

In conclusion, we have identified gene regulatory networks to elucidate the differences between GRs and PRs to ICSs in patients with asthma. We identified the top-10 TFs showing different connections between GRs and PRs and found that these top-10 TFs and their differentially-connected genes were significantly enriched in distinct biological pathways, such as TGF-β signaling, cell cycle, and IL-4 and IL-13 signaling pathways. TFs and biological pathways that were identified in this study may be potential targets to overcome insensitivity to corticosteroids in patients with asthma.

CODE AVAILABILITY

Codes generated during the current study are available upon reasonable request.

DATA AVAILABILITY STATEMENT

Immediately following publication, individual participant data that underlie the results reported in this article will be able to be shared after de-identification with researchers who will provide a methodologically sound proposal. Proposals should be directed to guinea71@snu.ac.kr.

ETHICS STATEMENT

This study was approved by the Institutional Review Board of the corresponding institution (H-1408-051-601 and 2019AN0240) and informed consent was obtained from all study participants. The patients/participants provided their written informed consent to participate in this study.

AUTHOR CONTRIBUTIONS

B-KK, H-SL, S-YL, and H-WP were involved in study conception/design. B-KK, S-YL, and H-WP were involved in data acquisition. All authors were involved in data analysis and/or interpretation, involved in writing/critical review of draft versions of this manuscript and all approved the final version for submission for publication.

FUNDING

This research was supported by a grant from the Korea University Anam Hospital, Seoul, Republic of Korea (Grant No. K1922911 and O2000691).

REFERENCES

1. Goleva E, Jackson LP, Gleason M, Leung DY. Usefulness of PBMCs to predict clinical response to corticosteroids in asthmatic patients. *J Allergy Clin Immunol.* (2012) 129:687–93.e681. doi: 10.1016/j.jaci.2011.12.001
2. Sonawane AR, Weiss ST, Glass K, Sharma A. Network medicine in the age of biomedical big data. *Front Genet.* (2019) 10:294. doi: 10.3389/fgene.2019.00294
3. Roy S, Bhattacharyya DK, Kalita JK. Reconstruction of gene co-expression network from microarray data using local expression patterns. *BMC Bioinformatics.* (2014) 15 (Suppl. 7):S10. doi: 10.1186/1471-2105-15-S7-S10
4. Marbach D, Lamparter D, Quon G, Kellis M, Kutalik Z, Bergmann S. Tissue-specific regulatory circuits reveal variable modular perturbations across complex diseases. *Nat Methods.* (2016) 13:366–70. doi: 10.1038/nmeth.3799
5. Caramori G, Casolari P, Adcock I. Role of transcription factors in the pathogenesis of asthma and COPD. *Cell Commun Adhes.* (2013) 20:21–40. doi: 10.3109/15419061.2013.775257
6. Qiu W, Guo F, Glass K, Yuan GC, Quackenbush J, Zhou X, et al. Differential connectivity of gene regulatory networks distinguishes corticosteroid response in asthma. *J Allergy Clin Immunol.* (2018) 141:1250–8. doi: 10.1016/j.jaci.2017.05.052

7. Glass K, Huttenhower C, Quackenbush J, Yuan GC. Passing messages between biological networks to refine predicted interactions. *PLoS ONE*. (2013) 8:e64832. doi: 10.1371/journal.pone.0064832
8. Global Initiative for Asthma. *Global Strategy for Asthma Management and Prevention, 2020*. Global Initiative for Asthma (2020). Available online at: https://ginasthma.org/gina-reports/
9. Schlauch D, Paulson JN, Young A, Glass K, Quackenbush J. Estimating gene regulatory networks with pandaR. *Bioinformatics*. (2017) 33:2232–4. doi: 10.1093/bioinformatics/btx139
10. Han H, Cho JW, Lee S, Yun A, Kim H, Bae D, et al. TRRUST v2: an expanded reference database of human and mouse transcriptional regulatory interactions. *Nucleic Acids Res*. (2018) 46:D380–d386. doi: 10.1093/nar/gkx1013
11. Vargas AJ, Quackenbush J, Glass K. Diet-induced weight loss leads to a switch in gene regulatory network control in the rectal mucosa. *Genomics*. (2016) 108:126–33. doi: 10.1016/j.ygeno.2016.08.001
12. Reimand J, Arak T, Adler P, Kolberg L, Reisberg S, Peterson H, et al. g:Profiler-a web server for functional interpretation of gene lists (2016 update). *Nucleic Acids Res*. (2016) 44:W83–9. doi: 10.1093/nar/gkw199
13. Chowdhury S, Sarkar RR. Comparison of human cell signaling pathway databases–evolution, drawbacks and challenges. *Database*. (2015) 2015:bau126. doi: 10.1093/database/bau126
14. Piek E, Heldin CH, Ten Dijke P. Specificity, diversity, and regulation in TGF-beta superfamily signaling. *FASEB J*. (1999) 13:2105–24. doi: 10.1096/fasebj.13.15.2105
15. Massagué J, Seoane J, Wotton D. Smad transcription factors. *Genes Dev*. (2005) 19:2783–810. doi: 10.1101/gad.1350705
16. Keenan CR, Mok JS, Harris T, Xia Y, Salem S, Stewart AG. Bronchial epithelial cells are rendered insensitive to glucocorticoid transactivation by transforming growth factor-β1. *Respir Res*. (2014) 15:55. doi: 10.1186/1465-9921-15-55
17. Li M, Keenan CR, Lopez-Campos G, Mangum JE, Chen Q, Prodanovic D, et al. A non-canonical pathway with potential for safer modulation of transforming growth factor-β1 in steroid-resistant airway diseases. *iScience*. (2019) 12:232–46. doi: 10.1016/j.isci.2019.01.023
18. Li MO, Wan YY, Sanjabi S, Robertson AK, Flavell RA. Transforming growth factor-beta regulation of immune responses. *Annu Rev Immunol*. (2006) 24:99–146. doi: 10.1146/annurev.immunol.24.021605.090737
19. Marie JC, Liggitt D, Rudensky AY. Cellular mechanisms of fatal early-onset autoimmunity in mice with the T cell-specific targeting of transforming growth factor-beta receptor. *Immunity*. (2006) 25:441–54. doi: 10.1016/j.immuni.2006.07.012
20. Sakaguchi S, Powrie F. Emerging challenges in regulatory T cell function and biology. *Science*. (2007) 317:627–9. doi: 10.1126/science.1142331
21. Strobl H, Knapp W. TGF-beta1 regulation of dendritic cells. *Microbes Infect*. (1999) 1:1283–90. doi: 10.1016/S1286-4579(99)00256-7
22. Troncone E, Marafini I, Stolfi C, Monteleone G. Transforming growth factor-β1/Smad7 in intestinal immunity, inflammation, and cancer. *Front Immunol*. (2018) 9:1407. doi: 10.3389/fimmu.2018.01407
23. Sundqvist A, Morikawa M, Ren J, Vasilaki E, Kawasaki N, Kobayashi M, et al. JUNB governs a feed-forward network of TGFβ signaling that aggravates breast cancer invasion. *Nucleic Acids Res*. (2018) 46:1180–95. doi: 10.1093/nar/gkx1190
24. Sands BE, Feagan BG, Sandborn WJ, Schreiber S, Peyrin-Biroulet L, Frédéric Colombel J, et al. Mongersen (GED-0301) for active crohn's disease: results of a phase 3 study. *Am J Gastroenterol*. (2020) 115:738–45. doi: 10.14309/ajg.0000000000000493
25. Adcock IM, Lane SJ. Corticosteroid-insensitive asthma: molecular mechanisms. *J Endocrinol*. (2003) 178:347–55. doi: 10.1677/joe.0.1780347
26. Bruhn S, Katzenellenbogen M, Gustafsson M, Krönke A, Sönnichsen B, Zhang H, et al. Combining gene expression microarray- and cluster analysis with sequence-based predictions to identify regulators of IL-13 in allergy. *Cytokine*. (2012) 60:736–40. doi: 10.1016/j.cyto.2012.08.009
27. Leung DY, Martin RJ, Szefler SJ, Sher ER, Ying S, Kay AB, et al. Dysregulation of interleukin 4, interleukin 5, and interferon gamma gene expression in steroid-resistant asthma. *J Exp Med*. (1995) 181:33–40. doi: 10.1084/jem.181.1.33
28. Harb H, Chatila TA. Mechanisms of dupilumab. *Clin Exp Allergy*. (2020) 50:5–14. doi: 10.1111/cea.13491
29. Bertoli C, Skotheim JM, de Bruin RA. Control of cell cycle transcription during G1 and S phases. *Nat Rev Mol Cell Biol*. (2013) 14:518–28. doi: 10.1038/nrm3629
30. Harmon JM, Norman MR, Fowlkes BJ, Thompson EB. Dexamethasone induces irreversible G1 arrest and death of a human lymphoid cell line. *J Cell Physiol*. (1979) 98:267–78. doi: 10.1002/jcp.1040980203
31. Hu X, Wang J, Xia Y, Simayi M, Ikramullah S, He Y, et al. Resveratrol induces cell cycle arrest and apoptosis in human eosinophils from asthmatic individuals. *Mol Med Rep*. (2016) 14:5231–6. doi: 10.3892/mmr.2016.5884
32. Giangrande PH, Zhu W, Schlisio S, Sun X, Mori S, Gaubatz S, et al. A role for E2F6 in distinguishing G1/S- and G2/M-specific transcription. *Genes Dev*. (2004) 18:2941–51. doi: 10.1101/gad.1239304
33. Desdouets C, Matesic G, Molina CA, Foulkes NS, Sassone-Corsi P, Brechot C, et al. Cell cycle regulation of cyclin A gene expression by the cyclic AMP-responsive transcription factors CREB and CREM. *Mol Cell Biol*. (1995) 15:3301–9. doi: 10.1128/MCB.15.6.3301
34. Shimoda M, Takahashi M, Yoshimoto T, Kono T, Ikai I, Kubo H. A homeobox protein, prox1, is involved in the differentiation, proliferation, and prognosis in hepatocellular carcinoma. *Clin Cancer Res*. (2006) 12 (20 Pt. 1), 6005–11. doi: 10.1158/1078-0432.CCR-06-0712
35. Kamiya A, Kakinuma S, Onodera M, Miyajima A, Nakauchi H. Prospero-related homeobox 1 and liver receptor homolog 1 coordinately regulate long-term proliferation of murine fetal hepatoblasts. *Hepatology*. (2008) 48:252–64. doi: 10.1002/hep.22303
36. Fouty B, Moss T, Solodushko V, Kraft M. Dexamethasone can stimulate G1-S phase transition in human airway fibroblasts in asthma. *Eur Respir J*. (2006) 27:1160–7. doi: 10.1183/09031936.06.00078605
37. Liu LD, Hsiao YC, Chen HC, Yang YW, Chang MC. Construction of gene causal regulatory networks using microarray data with the coefficient of intrinsic dependence. *Bot Stud*. (2019) 60:22. doi: 10.1186/s40529-019-0268-8
38. Altay G. Empirically determining the sample size for large-scale gene network inference algorithms. *IET Syst Biol*. (2012) 6:35–43. doi: 10.1049/iet-syb.2010.0091

Conflict of Interest: The authors declare that the research was conducted in the absence of any commercial or financial relationships that could be construed as a potential conflict of interest.

Copyright © 2021 Kim, Lee, Lee and Park. This is an open-access article distributed under the terms of the Creative Commons Attribution License (CC BY). The use, distribution or reproduction in other forums is permitted, provided the original author(s) and the copyright owner(s) are credited and that the original publication in this journal is cited, in accordance with accepted academic practice. No use, distribution or reproduction is permitted which does not comply with these terms.

frontiers in Immunology

ORIGINAL RESEARCH
published: 15 April 2021
doi: 10.3389/fimmu.2021.640791

Prioritizing Molecular Biomarkers in Asthma and Respiratory Allergy Using Systems Biology

Lucía Cremades-Jimeno[1†], María Ángeles de Pedro[1†], María López-Ramos[1], Joaquín Sastre[2,3], Pablo Mínguez[4,5], Ignacio Mahillo Fernández[6], Selene Baos[1‡] and Blanca Cárdaba[1,3‡]*

[1] Immunology Department, IIS-Fundación Jiménez Díaz, Universidad Autónoma de Madrid (UAM), Madrid, Spain, [2] Allergy Department, Fundación Jiménez Díaz, Madrid, Spain, [3] Center for Biomedical Network of Respiratory Diseases (CIBERES), ISCIII, Madrid, Spain, [4] Department of Genetics, IIS-Fundación Jiménez Díaz, UAM, Madrid, Spain, [5] Center for Biomedical Network Research on Rare Diseases (CIBERER), ISCIII, Madrid, Spain, [6] Biostatistics and Epidemiology Unit, Fundación Jiménez Díaz, Madrid, Spain

OPEN ACCESS

Edited by:
Bo Li,
Chongqing Normal University, China

Reviewed by:
Ying Hong Li,
Chongqing University of Posts and Telecommunications, China
Yiyuan Duan,
Sichuan University, China

***Correspondence:**
Blanca Cárdaba
bcardaba@fjd.es

[†]These authors have contributed equally to this work

[‡]These authors share senior authorship

Specialty section:
This article was submitted to Inflammation, a section of the journal Frontiers in Immunology

Received: *12 December 2020*
Accepted: *15 March 2021*
Published: *15 April 2021*

Citation:
Cremades-Jimeno L, de Pedro MÁ, López-Ramos M, Sastre J, Mínguez P, Fernández IM, Baos S and Cárdaba B (2021) Prioritizing Molecular Biomarkers in Asthma and Respiratory Allergy Using Systems Biology. Front. Immunol. 12:640791. doi: 10.3389/fimmu.2021.640791

Highly prevalent respiratory diseases such as asthma and allergy remain a pressing health challenge. Currently, there is an unmet need for precise diagnostic tools capable of predicting the great heterogeneity of these illnesses. In a previous study of 94 asthma/respiratory allergy biomarker candidates, we defined a group of potential biomarkers to distinguish clinical phenotypes (i.e. nonallergic asthma, allergic asthma, respiratory allergy without asthma) and disease severity. Here, we analyze our experimental results using complex algorithmic approaches that establish holistic disease models (systems biology), combining these insights with information available in specialized databases developed worldwide. With this approach, we aim to prioritize the most relevant biomarkers according to their specificity and mechanistic implication with molecular motifs of the diseases. The Therapeutic Performance Mapping System (Anaxomics' TPMS technology) was used to generate one mathematical model per disease: allergic asthma (AA), non-allergic asthma (NA), and respiratory allergy (RA), defining specific molecular motifs for each. The relationship of our molecular biomarker candidates and each disease was analyzed by artificial neural networks (ANNs) scores. These analyses prioritized molecular biomarkers specific to the diseases and to particular molecular motifs. As a first step, molecular characterization of the pathophysiological processes of AA defined 16 molecular motifs: 2 specific for AA, 2 shared with RA, and 12 shared with NA. Mechanistic analysis showed 17 proteins that were strongly related to AA. Eleven proteins were associated with RA and 16 proteins with NA. Specificity analysis showed that 12 proteins were specific to AA, 7 were specific to RA, and 2 to NA. Finally, a triggering analysis revealed a relevant role for AKT1, STAT1, and MAPK13 in all three conditions and for TLR4 in asthmatic diseases (AA and NA). In conclusion, this study has enabled us to prioritize biomarkers depending on the functionality associated with each disease and with specific molecular motifs, which could improve the definition and usefulness of new molecular biomarkers.

Keywords: allergy, artificial intelligence, asthma, biomarker, respiratory diseases, systems biology

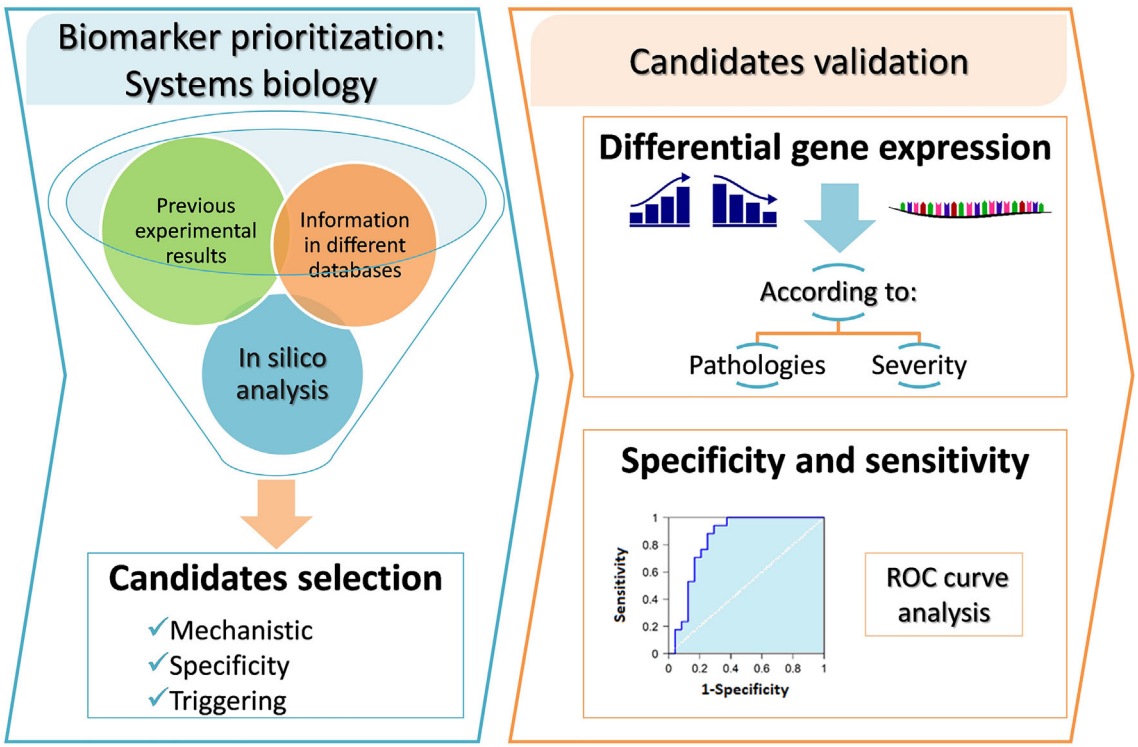

GRAPHICAL ABSTRACT |

INTRODUCTION

Chronic inflammatory respiratory diseases, including allergic diseases and asthma, are common, complex, and heterogeneous diseases in which the clinical course and treatment response are often challenging to predict. The high prevalence of these diseases and their impact on quality of life make them a serious public-health problem associated with a substantial economic burden.

The World Health Organization (WHO) defines asthma as the most common chronic disease in children, affecting more than 340 million people around the world (1). Approximately 10% of asthmatic patients develop severe clinical symptoms and have significant morbidity and mortality (2). Asthma is a disease that affects the airways, manifesting clinically as cough, dyspnea, chest tightness, shortness of breath, or mucus production. From a clinical point of view, asthma is associated with a progressive reduction in lung function and presence of inflammation. Asthma diagnoses span multiple clinical presentations (phenotypes), each with different pathophysiological mechanisms (endotypes) (3, 4). Allergic mechanisms have been implicated in 50 to 80% of asthmatic patients and in approximately 50% of those with severe disease. Allergic asthma, characterized by an early onset, is the most common asthma phenotype and is traditionally considered as an eosinophilic mediated disease characterized by overexpression and activation of T helper type 2 (Th-2) cells (5). As a result, asthma has been classically associated with type 2 respiratory inflammation, characterized by high levels of IgE, eosinophils, and some cytokines such as IL-4, IL-5, IL-13, and IL-9, canonically associated with allergic responses. However, there are also many clinical conditions where there is a combination of inflammatory cells (eosinophils/neutrophils) and no clear type of respiratory inflammation. Between 10 and 33% of subjects with asthma are not associated with allergy (non-allergic asthma) and exhibit non-type 2 inflammation (non-T2 or T2-low endotype) (6), in many cases with a prevalence of neutrophils; understanding of the immune mechanisms implicated is less developed (7–11).

Advances in our understanding of the immunologic mechanisms implicated in asthma disease have shown that there are many other important players, mainly those related to the innate immune response and its interrelation with tissue cells (derived from epithelial cells), and these are a frequent subject of review (12, 13). Especially relevant was the discovery that type 2 innate lymphoid cells (ILC-2), which have no antigen-specific receptors, could be crucial in mediating airway inflammation in eosinophilic phenotypes of asthma, whether or not these phenotypes are associated with atopic conditions (14). ILC-2 respond to epithelium-derived signals mediated by the so-called "alarmins" [IL-25, IL-33, and thymic stromal lymphopoietin (TSLP)] produced by epithelial cells after injury, through pattern-recognition receptors (15). In fact, allergic asthma, or type 2 immune response, is now considered as a complex network between type 2 cytokines (IL-4, IL-5, IL-9, and IL-13), which are mainly secreted from Th2 cells, IgE-producing B cells, group 2 innate lymphoid cells (ILC-2), and a small fraction of IL-4-producing NK cells and NK-T cells,

basophils, eosinophils, mast cells, and alarmins (IL-25, IL-33, and TSLP), which are released from tissue cells, particularly epithelial cells (12).

Despite the clinical complexity of asthma, most efforts to find new treatments have been centered on allergic asthma or asthma mediated by type 2 inflammation. Patients with allergic asthma would be classified under the T2-high endotype. Many targeted treatments (i.e. biological therapy against key elements of T2 inflammatory response such as anti-IL-4/IL-13, anti-IL-4, anti-IL-5, anti-IgE antibodies, anti-CRTH2) are in different stages of clinical development and have produced varying results (16). However, to understand the heterogeneity in T2 inflammation (17), patients with a higher likelihood to respond adequately to this kind of therapies must be identified.

Non-allergic or intrinsic asthma includes a subset of patients with non-T2 inflammation (18, 19). The pathophysiology and exact mechanisms of T2-low (Non-T2) asthma are less thoroughly understood and studied than other asthma types. In general, this type of asthma is characterized by a lack of eosinophilic inflammation/T2 markers and is occasionally associated with neutrophilic or pauci-granulocytic inflammation (20). The major mechanism leading to a non-type 2 response is thought to result from an irregular innate immune response, including intrinsic neutrophil abnormalities and activation of the IL-17-mediated pathway (12). T2-low asthma is common, accounts for one-third to 45% of patients with severe disease, and is associated with poor response to corticosteroid therapy (21). To date, no directed therapy has been found to be effective against this endotype (22).

Thus, there remains an unmet clinical need in the study of the mechanisms and biomarkers for both T2-high and T2-low endotypes as concerns their ability to predict response to targeted therapy (23). Better understanding of the complex immune network of asthma inflammation and key players of immunity are continuously subjected to study (12, 13, 18). Successful therapy of asthma requires better definition of underlying pathogenesis in order to find more precise therapy options or develop methods of precision medicine.

New techniques such as massive analysis or -omics have become important tools in the search for risk-related or protective biomarkers and the development of new drugs (24). Combined with multiple studies derived from -omics technologies, a systems biology approach, which treats disease as a holistic process without any targeted hypothesis, has been fruitfully used in other medical fields in recent years to develop a new molecular medicine (25).

Despite the many advances in this area, there are still large gaps that need to be understood in order to better manage this type of complex diseases, mainly related to the mechanisms involved in each clinical condition. Against this backdrop, many research groups are currently searching for new and complementary molecular biomarkers and respiratory disease endotypes (20, 26). Toward this purpose, we studied the differential gene-expression of 94 biomarker candidates in patients with different clinical respiratory diseases (i.e. respiratory allergy, allergic asthma, non-allergic asthma) (27, 28), defining molecular biomarkers that can discriminate between allergic (T2-high) and non-allergic asthma (T2-low or non-T2) and predict disease severity in non-invasive samples derived from peripheral blood. New genes and protein biomarkers, including CHI3L1, IL-8, IL-10, MSR1, PHLDA1, PI3, and SERPINB2, were proposed to discriminate healthy control subjects from non-allergic asthmatic patients (T2-low) and to determine asthma severity (29). The relevance of those potential biomarkers in asthma and allergy diseases has been discussed extensively (27). Later, we measured the ability of these biomarkers to discriminate between allergic (T2-high) and non-allergic asthma (T2-low or non T2) diseases and determine severity at the gene and protein levels. The results revealed panels of genes and proteins that can discriminate T2-high from T2-low asthma and measure disease severity (30) by using simple techniques and with very good discriminatory parameters. Though encouraging, our initial results showed limitations that should be addressed, and this is the primary motivation of this study. In particular, there were too many genes/proteins considered as "potentially useful," mainly those related to allergic phenotypes. This is why it was decided to prioritize the role played by these genes/proteins using new approaches as *in silico* studies, which make it possible to combine information from multiple databases with researchers' own experimental models, thus establishing a model thanks to the use of complex algorithms based on systems biology. With this aim, the three pathophysiological processes of interest (i.e. respiratory allergy, allergic asthma, non-allergic asthma) were defined at the molecular level. Next, the effector proteins of the manifestative and causative motifs of these three highly related processes were characterized at the molecular level, showing common and differential molecular motifs for these pathologies. This study aims to classify and define the usefulness of sets of biomarkers in order to provide additional diagnostic and therapeutic functional-targeted tools for these types of diseases.

MATERIALS AND METHODS

Molecular Characterization of Respiratory Allergy, Allergic Asthma, and Non-Allergic Asthma

Firstly, the molecular characterization of the three pathophysiological processes of interest (respiratory allergy, allergic asthma, and non-allergic asthma) was performed using the Therapeutic Performance Mapping System (TPMS) technology (Anaxomics Biotech, Barcelona, Catalonia, Spain) (31). Briefly, systems biology generates models that are able to reproduce the behavior of a disease in a patient, thus identifying the key genes, proteins, or metabolites in the development of the disease. A dictionary has been created to translate clinical and medical terms into molecular biology data, effectively linking the molecular and the clinical words. This dictionary, called the Biological Effectors Database (BED), relates biological processes (adverse events of drugs, drug indications, diseases, etc.) with the proteins most closely associated with them. Thus, the dictionary acts as a translator of clinical phenotypes into terms comprehensible for protein networks, and conversely allows for the translation of molecular measures toward clinical outcomes. The BED is

structured hierarchically, where the biggest level is the entire disease, which is divided into different pathophysiological molecular motifs, which in turn contain the proteins involved in the development of the disease. The motifs are classified into two levels depending on their respective implication, i.e. causal motifs, which are directly related to the onset or pathophysiology of the condition, and symptomatic (manifestative) motifs, which are a consequence of the disease.

In the present study, respiratory allergy, allergic asthma, and non-allergic asthma have been characterized at the molecular level. Therefore, the analysis of high throughput data by means of TPMS allows for identification of those proteins closely associated with the disease of interest and can provide a mechanistic rationale for their involvement. The effector proteins of the manifestative and causal molecular motifs of these three diseases have been identified through bibliographic review and curate data. **Figure 1** summarizes the workflow used for this study.

Artificial Neural Network (ANN) Analysis: Biomarker Prioritization

Mathematical Model Generation

To create mathematical models, it was builded a biological map around the key disease proteins defined during the characterization (**Figure 1**). The map was extended by adding knowledge-oriented connectivity layers, i.e., protein-to-protein interactions, including physical interactions and modulations, signaling, metabolic relationships, and gene expression regulation. Data were obtained from the following public and private external databases: KEGG (33), REACTOME (34), INTACT (35), BIOGRID (36), HDPR (37), and MINT (38) in addition to the scientific literature reviewed. At the same time, the network is embedded with all sorts of biological information derived from public sources (e.g. drug targets, tissue expression, biomarkers) about nodes (i.e. proteins) and edges (i.e. connections).

The 94 biomarker candidate proteins previously studied by our group (27, 28) were ranked according to their mechanistic relationship to each of the conditions of interest by means of artificial neural networks (ANNs) as indicated by TPMS technology (31).

Then, the models were trained with a proprietary Truth Table containing public and our list of candidates (28) related to each disease. This acts as a set of conditions that must be fulfilled to resemble the situation under study. Here, we have used artificial intelligence (AI) technologies to model complex network behavior, including graph theory and statistical pattern recognition technologies; genetic algorithms; artificial neural networks; dimensionality reduction techniques; and stochastic methods such as Monte Carlo simulated annealing, among others. ANNs identify relations among regions of the network (generalization).

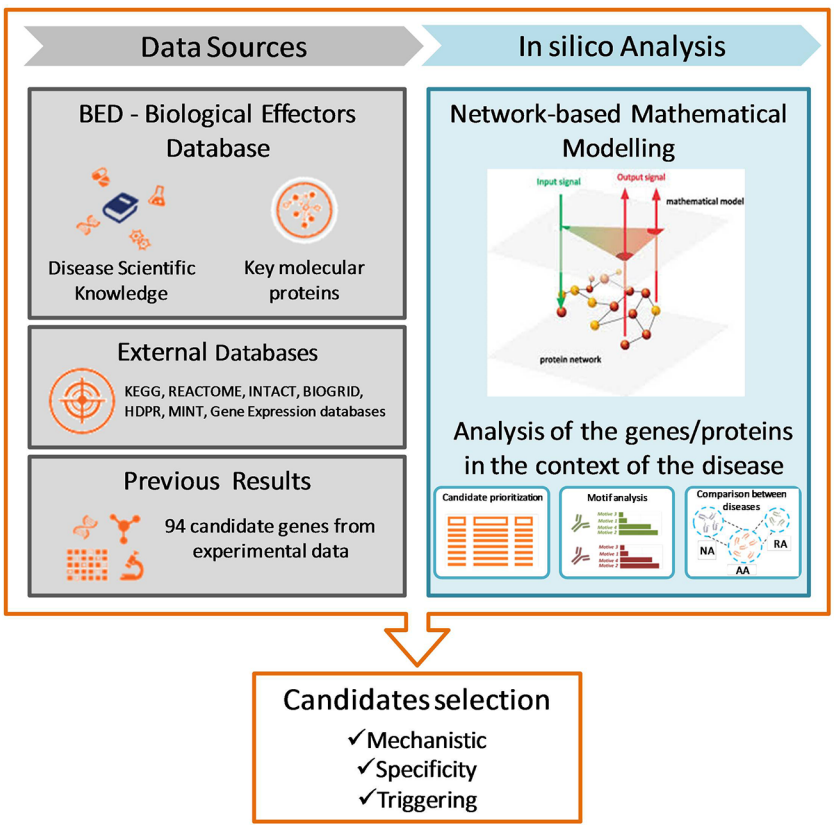

FIGURE 1 | Study design and workflow of systems biology study. NA, non-allergic Asthma; AA, Allergic Asthma; RA, Respiratory Allergy. [Based on Gimenez et al. (32)].

TPMS technology uses proprietary stochastic optimization algorithms based on ANNs to identify plausible protein interaction networks learning from those sets of prior knowledge. Specifically, the ANNs applied (39) use relationships between drug targets and clinical elements (BED) mapped onto the human proteome network compiled in a hand-screened truth table [based on the information contained in DrugBank about drugs and indications (40) for training a classifier]. The accuracy with which ANNs reproduce the indications of DrugBank is 98% for compounds with all targets in the human biological network after applying a cross-fold validation process (41–44). The models thus obtained reproduce the average behavior of patients under evaluation in agreement with current scientific understandings, allowing effective, mechanistically driven analyses.

Analysis of Proteomic Data in the Context of the Selected Disease

The 94 candidate genes proposed by our previous studies (27, 28) were compiled and processed in a format readable by TPMS technology. By means of artificial neural networks (ANN), the estimated effect of changes to these proteins on the selected disease was assessed. The system attempts to find the shortest distance between candidates and the effectors of the disease, thus generating a list of potential biomarkers ordered by their association with the selected disease. Finally, after checking the proteins that passed this automatic filter, the final candidates were selected in accordance with the published literature (**Figure 1**). ANN analyses score the proteins according to their predicted mechanistic relationships with the effector proteins of the molecular characterization of respiratory allergy, allergic asthma, and non-allergic asthma. ANN score is a numerical value that indicates the percentage of relationship between 2 sets of proteins (0–100%). Here, one set comprised each of our candidate proteins and the other was the set that defines the disease or its molecular motifs.

Two kinds of analyses were performed: the analysis of the relationship of each one of the candidate proteins with each of the entire disease or whole pathology (which provides an idea of how each protein relates to all the proteins involved in the disease); and analysis according to molecular motifs. The disease could be divided into several motifs that do not necessarily have to be closely related from a topological point of view. A protein could be topologically related to one motif with a low number of proteins that is not topologically related to the rest of proteins involved in the disease and, thus, the protein appears as weakly related to the characterization of the whole disease. Thus, a motif analysis can elucidate relationships between candidate proteins and the disease (considered as a group of motifs) that an analysis considering the entire disease would not reveal.

The use of ANNs permitted mechanistic ranking of the target proteins according to their relationship with each whole disease and with each molecular motif individually. Four categories were used to group the analyzed proteins according to the predicted relationship value: strongly related proteins ("*Very high*" group, ≥92% predicted ANN value, $p < 0.01$); highly related proteins ("*High*" group, with a predicted ANN value <92–≥78%, p values between 0.01 and 0.05); moderately related proteins ("*Medium*," with a predicted ANN value <78–≥38, *P* value between 0.05 and 0.25); and proteins with a mild relationship ("*Low*" group,<38% predicted ANN value, *P* value >0.25).

The final ranking was performed using two measures based on the relationship of each protein with whole diseases and the specific motifs:

- Relationship level: indicates the level of relationship of the proteins with each overall disease or any disease-specific motif.
- Specificity: indicates whether the protein presents a stronger relationship with the specific motifs of the disease than with the specific motifs of the other diseases.

Validation of Prioritized Biomarkers

The most useful (specific) biomarkers defined theoretically by systems biology were contrasted with our previous data of gene expression analyzed by RT-qPCR in RNA extracted from peripheral blood mononuclear cells (PBMCs) in a population of 114 subjects made up of healthy control subjects, respiratory allergic patients, allergic asthmatic subjects, and non-allergic asthmatic patients (27, 28). Significance of gene expression was defined by RQ (relative quantification) defined previously (27, 28).

The sensitivity and specificity of the best molecular biomarkers defined by systems biology was determined by ROC curve analysis in our study population (27, 28). A ROC curve was constructed for the candidate biomarkers common with our previous results and the defined by systems biology (biomarkers that showed high relationship to at least one of the studied condition). Eighteen kinds of comparisons were performed to determine the most effective biomarkers to distinguish among the different clinical conditions: healthy control group, non-allergic asthmatic patients, allergic asthmatic patients, and patients with respiratory allergy without asthma, as well as different severities in asthma groups. Details of the population studied were described previously (27). A guide for interpreting the ROC curves has been described previously (29). Only those results with a 95% confidence interval (95% CI) of between 0.70 and 1 were considered as statistically significant.

Triggering Analysis

Finally, this method based on systems biology was also used to analyze the ability of each biomarker candidate protein to cause the activation of the effector proteins that define respiratory allergy, allergic asthma, and non-allergic asthma. The objective of this strategy was to identify the proteins of interest whose modulation can promote the activation of the highest number of proteins involved (coverage) in these three diseases. It is an analysis that evaluates the ability of a set of genes to activate the disease. The results reflect which proteins, together, are capable of activating the highest percentage of disease-defining proteins. The possible role of the proteins of interest as respiratory allergy, allergic asthma, and non-allergic asthma triggers was also assessed.

Two types of scores were obtained:

Individual probability score: this value ranks the proteins of a given set according to their individual probability to act as triggers, that is, how likely a single protein is to act as a trigger.

The probability within each protein set ranges from 0 to 1. It is represented in an approximate asterisk scale, in which the proteins with the highest probability have up to five asterisks assigned, and the ones with the lowest probability have only one asterisk.

Cumulative score: indicates the percentage of effectors of the condition triggered by the alteration of a protein together with the rest of potential triggering, i.e. the cumulative score shows the added effect of combining the evaluated protein with all the previously evaluated proteins.

Statistical Analysis

The PPI network was visualized using Cytoscape V3.6.1 (https://cytoscape.org/). The relevant hub-genes were screened using the node degrees calculated in Cytoscape. Also, analyses of pathway interconnection between triggering and specific proteins and/or mechanistic proteins for each disease were analyzed by Pathlinkers application from Cytoscape.

The levels and relative expression of the proteins studied were compared between groups by unpaired t-test, using the GraphPad InStat 3 program. Statistical significance was established at a two-tailed P value <0.05. ROC curve analyses were performed using the R program.

RESULTS

Molecular Motifs of Diseases

Table 1 summarizes the common and differential molecular motifs that make up the diseases. A total number of 16 molecular motifs have been characterized, which, in combination, are representative of the three conditions of interest.

- Respiratory allergy: composed of two molecular motifs (*acute response* and *late-phase response*, highlighted in blue in **Table 1**), also present in allergic asthma.
- Allergic asthma: composed of 16 molecular motifs. All the motifs are shared with respiratory allergy or non-allergic asthma, with the exception of *Th2-mediated pulmonary inflammation* and *goblet cell hyperplasia* which are specific to allergic asthma, and *granulocyte (eosinophil) infiltration*, which show a stronger implication in allergic than in non-allergic asthma (in lilac in **Table 1**).
- Non-allergic asthma: composed of 12 molecular motifs, all shared with allergic asthma. However, some present higher specificity for nonallergic asthma than for allergic asthma (*Th17-mediated pulmonary inflammation*, and *neutrophil infiltration*, pink in **Table 1**), whereas one of them has a stronger implication in allergic than in non-allergic asthma [*granulocyte (eosinophil) infiltration*, in lilac in **Table 1**].

Biomarker Prioritization

To obtain the ranking of the best candidate proteins identified as relevant in respiratory allergy, allergic asthma, and non-allergic asthma according to their mechanistic relationship with each of these diseases, three kinds of analyses were performed: ranking of the proteins according to their mechanistic relationship to the diseases of interest, ranking according to their associated pathophysiological motifs, and assessment of the specificity of the candidate proteins to each disease (addressing, especially, the most specific motifs of each disease).

Proteins presenting many interactions, or proteins that do not have reported interactions, were not included in the network as they could disrupt the correct assessment of existing functional relationships. Therefore, one protein (C3AR1) out of the 94 proteins of interest was excluded from the analysis as it is not included in the network used.

TABLE 1 | Summary of the molecular motifs characterized for respiratory allergy, allergic asthma, and non-allergic asthma.

Specific Molecular Motif	Respiratory Allergy	Allergic Asthma	Non-allergic Asthma
Acute Response	•	•	X
Late-Phase Response	•	•	X
Th2-Mediated Pulmonary Inflammation	X	•	X
Goblet Cell Hyperplasia	X	•	X
Granulocyte (eosinophil) Infiltration	X	•	Δ
Th17-Mediated Pulmonary Inflammation	X	Δ	•
Neutrophil Infiltration	X	Δ	•
Dendritic Cell Activation	X	•	•
ECM Deposition	X	•	•
Angiogenesis Asthma	X	•	•
Airway Smooth Muscle Hypertrophy/Hyperplasia	X	•	•
Epithelial Dysfunction	X	•	•
Airway Smooth Muscle Hypercontractibility	X	•	•
Innervation And Hyper-Excitability	X	•	•
Bronchoconstriction	X	•	•
Mucus Production	X	•	•

• Strong implication of the molecular motif in the disease. Δ Weaker implication compared to the other variant of asthma, though still relevant. X No implication of the molecular motif in the disease. The strongest differential molecular motifs for each disease are indicated in color (Blue: respiratory allergy, Lilac: allergic asthma, Pink: non-allergic asthma).

Individual Evaluation

The mechanistic ranking by ANN analysis allows for classification of the list of 94 proteins based on their predicted functional or mechanistic relationship with a given condition. Here, 19 independent ANNs were carried out, one for each condition (respiratory allergy, allergic asthma, and non-allergic asthma) and one for each condition-specific molecular motif.

Protein Predicted Ranking to Entire Disease

The list of all proteins analyzed and the ANN score or relationship predicted values to the entire disease are presented in **Supplementary Table 1**. Whether the proteins are effectors of the disease is also displayed.

Table 2 summarizes the stronger predicted relationship for each disease. A total number of 11 proteins presented a "high" or stronger predicted relationship with respiratory allergy (**Table 2A**). All of them were effector proteins. For allergic asthma, 17 proteins reached a "high" relationship level (**Table 2B**), one of which (BAX) was not an effector of the disease. Finally,

TABLE 2 | Summary of proteins presenting a "HIGH" or stronger relationship level with each disease.

A. Respiratory Allergy

Uniprot ID	Gene name	Respiratory Allergy ANN score	Reference
P05113	***IL5***	**92.43**	Gani F et al. (45)
P35225	***IL13***	91.82	Gani F et al. (45)
P22301	***IL10***	90.26	Urry Z et al. (46)
P05231	***IL6***	90.15	Rose-John S et al. (47)
P15248	***IL9***	89.85	Urry Z et al. (46)
P01579	***IFNG***	88.99	Urry Z et al. (46)
P05112	***IL4***	88.49	Gani F et al. (45)
P43116	***PTGER2***	88.16	Nagai H (48)
P60568	***IL2***	88.13	Schwarz M et al. (49)
P24394	***IL4R***	85.21	Keegan AD et al. (50)
P14784	***IL2RB***	84.15	Mulloy JC et al. (51)

B. Allergic Asthma

Uniprot ID	Gene name	Allergic asthma ANN score	Reference
P98088	***MUC5AC***	88.43	Evans CM et al. (60)
P09917	***ALOX5***	87.92	Nagata M et al. (70)
P36222	***CHI3L1***	86.53	Pniewska E et al. (64)
Q8N138	***ORMDL3***	83.15	Loxham M et al. (63)
P12724	***RNASE3***	82.96	Lacy P et al. (62)
Q15063	***POSTN***	82.79	Heijink IH et al. (58)
A8K7I4	***CLCA1***	82.78	Woodruff PG et al. (57)
Q9HC84	***MUC5B***	82.64	Evans CM et al. (60)
P24394	***IL4R***	81.40	Evans CM et al. (60)
Q16552	***IL17A***	81.22	Chakir J et al. (54)
O95760	***IL33***	81.12	Davies DE (52)
P14151	***SELL***	81.04	Nadi E et al. (71)
Q9H293	***IL25***	80.90	Whelan T et al. (59)
P05120	***SERPINB2***	80.82	Woodruff PG et al. (57)
P27930	***IL1R2***	79.06	Knolle MD et al. (72)
Q07812	***BAX***	78.36	–
P01137	***TGFB1***	78.21	Yalcin AD et al. (73)

C. Non-allergic Asthma

Uniprot ID	Gene name	Nonallergic Asthma	Reference
P98088	***MUC5AC***	91.14	Evans CM et al. (60)
P36222	***CHI3L1***	89.91	Pniewska E et al. (64)
Q15063	***POSTN***	89.75	Heijink IH et al. (58)
O95760	***IL33***	89.01	Davies DE (52)
P12724	***RNASE3***	88.08	Lacy P et al. (62)
P14151	***SELL***	88.01	Nadi E et al. (71)
Q8N138	***ORMDL3***	87.70	Loxham M et al. (63)
Q9HC84	***MUC5B***	86.88	Evans CM et al. (60)
P09917	***ALOX5***	86.69	Nagata M et al. (70)
Q16552	***IL17A***	86.69	Chakir J et al. (54)
P43116	***PTGER2***	84.79	Nagai H (48)
P13501	***CCL5***	83.26	Isgrò M et al. (74)
Q9H293	***IL25***	82.81	Whelan T et al. (59)
A8K7I4	***CLCA1***	81.62	Woodruff PG et al. (57)
P05120	***SERPINB2***	79.93	Woodruff PG et al. (57)
P51671	***CCL11***	78.30	Isgrò M et al. (74)

ANN score is defined in methods. Four categories were used to group the analyzed proteins according to the predicted relationship value; here we represent the two main associated categories for each disease analyzed: Strongly related proteins ("Very high" group, ≥92% predicted ANN value, associated P-value <0.01) and Highly related proteins ("High" group, with a predicted ANN value <92–≥78%, associated P-value 0.01–0.05). References correspond to the definition of the respective protein as an effector protein. Strongly related proteins are labeled in bold. Blue: Respiratory Allergy, Lilac: Allergic Asthma, Pink: Non-Allergic Asthma.

for non-allergic asthma, 16 proteins reached a "high" relationship level with the disease (**Table 2C**) and all were identified as effectors of the disease.

Looking at the overlap of the proteins with a "high" or stronger relationship level (**Figure 2**), two results are worth mentioning: there were no proteins with a "high" or stronger relationship value with the three conditions at the same time, and the highest number of overlapping proteins (n = 13) was found between non-allergic and allergic asthma conditions, all of which were effectors of shared molecular motifs (**Table 3**).

Respiratory allergy and allergic asthma share 1 highly related protein, specifically IL-4R, which has been identified as an effector of the acute phase of allergy (60) and receptor of IL-4 and IL-13, molecules that have been proven to regulate IgE synthesis (45) and have been detected to be over-expressed in acute asthmatics.

Interestingly, PTGER2, a prostaglandin receptor with functions in both the acute phase allergy molecular motif (48) and bronchoconstriction asthma and allergic asthma molecular motif, although being reported as playing a role in the three diseases, presented a highly functional relationship to respiratory allergy and non-allergic asthma, but a moderate relationship to allergic asthma.

Individual Molecular Motifs Relationship Analysis

Next, to understand the implication of the proteins in the diseases studied, an independent ANN analysis was performed for each molecular motif defined for the three pathological conditions (respiratory allergy, allergic asthma, and non-allergic asthma) (**Table 4**). Two molecular motifs (*acute response* and *granulocyte infiltration*) presented proteins with a "very high" relationship level. All molecular motifs presented at least one protein with a "high" relationship level with the exception of *goblet cell hyperplasia*, *Th17-mediated pulmonary inflammation*, *ECM deposition*, and *innervation and hyper-excitability*. All the proteins predicted to have a "high" or stronger relationship level with a given molecular motif were identified as effectors of the molecular motif.

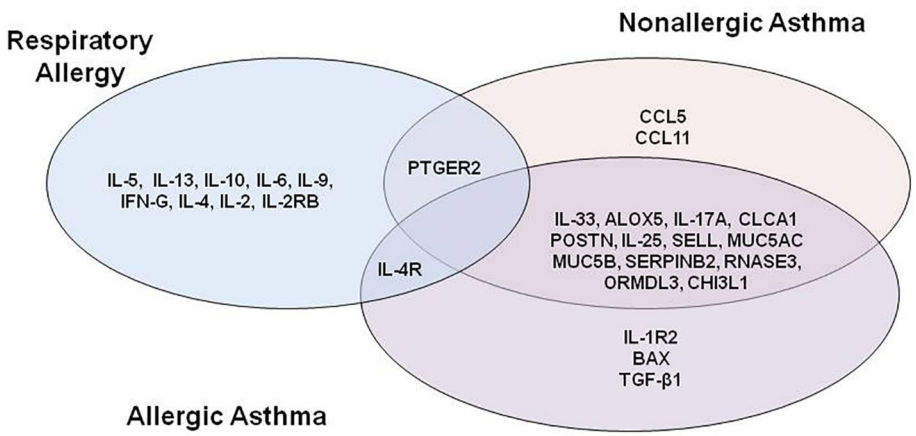

FIGURE 2 | Venn diagram of proteins with "high" or stronger relationship level with at least one disease.

TABLE 3 | Summary of commom proteins with a "high" or stronger relationship with allergic and non-allergic asthma.

Uniprot ID	Gene name	Molecular motif	Reference
O95760	***IL33***	Dendritic Cell Activation, Angiogenesis Asthma	Davies DE (52); Guo Z et al. (53)
P09917	***ALOX5***	Granulocyte Infiltration	Guo Z et al. (53)
Q16552	***IL17A***	Granulocyte Infiltration, Th17-Mediated Pulmonary Inflammation, Mucus Production	Chakir J et al. (54); Chesné J et al. (55); Barnes PJ (56)
A8K7I4	***CLCA1***	Airway Smooth Muscle Hypercontractibility	Woodruff PG et al. (57)
Q15063	***POSTN***	Granulocyte Infiltration, Angiogenesis Asthma	Heijink IH et al. (58); Woodruff PG et al. (57)
Q9H293	***IL25***	Angiogenesis Asthma	Woodruff PG et al. (57)
P14151	***SELL***	Granulocyte Infiltration	Whelan T et al. (59)
P98088	***MUC5AC***	Airway Smooth Muscle Hypercontractibility, Mucus Production	Evans CM et al. (60); Qi L et al. (61)
Q9HC84	***MUC5B***	Airway Smooth Muscle Hypercontractibility	Qi L et al. (61)
P05120	***SERPINB2***	Granulocyte Infiltration	Woodruff PG et al. (57)
P12724	***RNASE3***	Granulocyte Infiltration	Lacy P et al. (62)
Q8N138	***ORMDL3***	ECM Deposition	Loxham M et al. (63)
P36222	***CHI3L1***	Angiongenesis Asthma	Pniewska E et al. (64)

The molecular motifs for which these proteins act as effectors and the corresponding bibliographic reference are also displayed.

TABLE 4 | Ranking of Proteins classified by association with molecular motifs (Effectors proteins are underlined).

Specific Molecular Motif	Very High	HIGH	MEDIUM
Acute Response	IL-10, IL-4, IL-2, IL-9, IFNG, PTGER2	IL-4R, IL-2RB	IL-13, IL-5, FOXP3, IL-6, NFATC1, TLR4, IL-1R1, TNF, TGFB1, STAT1, MAPK13, IL-1R2, IL-33, ZAP70, TSLP, NFKBIZ, CD40, CD48, LYN, NLRP3, ADRB1.
Late-Phase Response	-	IL-13, IL-5, IL-6, TNF	IL-10, IL-4, FOXP3, NFATC1, IL-2, IL-4R, TNFAIL3, STAT1, MAPK13, IL-9, IFNG, TSLP, FPR3, ALOX5.
Th2-Mediated Pulmonary Inflammation	-	IL-10, IL-13, IL-4, IL-5, CCL17	FOXP3, IL-6, NFATC1, IL-2, IL-4R, TNFAIL3, TLR4, BAX, IL-1R1, CCL11, AKT1, TNF, TGFB1, STAT1, MAPK13, IL-9, IFNG, CCL5, IL-1R2, IL-33, ZAP70.
Goblet Cell Hyperplasia	-	-	IL-5, FOXP3, IL-6, NFATC1, IL-2, TNFAIP3, TLR4, TGFB1, MAPK13, IFNG, CCL5, ZAP70, IL-2RB, PTPRC, SPP1, SOS1, DUSP1, SVIL, LGALS3.
Granulocyte (eosinophil) Infiltration	INFG	IL-4R, CCL11, TGFB1, CCL5, CD40, RNASE3, ALOX5, SELL, IL-17A, ITGAL, POSTN, SERPINB2	IL-6, NFATC1, TLR4, TNF, STAT1, MAPK13, PTPRC, VCAN, SPP1, FPR3, NOS2, EIF5A, S1PR5, SMURF1, LYN, NCF2, ALOX15, GPX3.
Th17-Mediated Pulmonary Inflammation	-	-	IL-10, FOXP3, IL-6, NFATC1, TNF, TGFB1, STAT1, MAPK13, CD40, CD86, IL-17A, NLRP3, IL-25.
Neutrophil Infiltration	-	IL-6, LGALS3	FOXP3, NFATC1, TNFAIP3, TLR4, BAX, IL-1R1, AKT1, TNF, TGFB1, STAT1, MAPK13, CCL5, IL-1R2, IL-8, FPR3, CTSC, NFKBIZ, APAF1, NOS2, S100A9, S1PR5, NLRP3, NCF2
Dendritic Cell Activation	-	TLR4	NFATC1, IL-1R1, AKT1, TGFB1, MAPK13, IL-1R2, IL-33, TSLP, NFKBIZ, S100A9, HLA-DQB1, HLA-DRB1, IL-25.
ECM Deposition	-	-	NFATC1, TNFAIP3, TLR4, BAX, AKT1, TNF, TGFB1, STAT1, MAPK13, IFNG, CCL5, ZAP70, PTPRC, SPP1, FPR3, CD40, SOS1, NOS2, CD86, SVIL, RNASE3, ORMDL3, S100A9, LGALS3, NCF2, ITGB7, ITGB8.
Angiogenesis_Asthma	-	IL-33, ADAM33, CHI3L1, POSTN	NFATC1, TLR4, TNF, TGFB1, STAT1, MAPK13, VCAN, NOS2, NCF2.
Airway Smooth Muscle Hypertrophy/ Hyperplasia	-	TNF	IL-5, CCL17, FOXP3, IL-6, NFATC1, IL-2, TNFAIP3, TLR4, IL-1R1, CCL11, AKT1, TGFB1, STAT1, MAPK13, IFNG, CCL5, IL-1R2, ZAP70, IL-2RB, IL-8, VCAN, SPP1, FPR3, CTSC, NFKBIZ, DUSP1, NOS2, S100A9, IRAK3, NCF2.
Epithelial Dysfunction	-	CCL5	FOXP3, IL-6, NFATC1, TNFAIP3, TLR4, CCL11, TNF, TGFB1, STAT1, MAPK13, IFNG, VCAN, SPP1, FPR3, CD86, CTSG.
Airway Smooth Muscle Hypercontractibility	-	IL-4R, IL-1R2, MUC5AC	IL-10, IL-13, IL-4, IL-5, IL-6, IL-2, STAT1, IL-9, IFNG, TSLP, CD40, NOS2, CLCA1, MUC2, MUC5B.
Innervation And Hyper-Excitability	-	-	ZAP70, PTPRC, DUSP1, CD86.
Bronchoconstriction	-	PTGER2, ADRB1	IL-8, CLCA1.
Mucus Production	-	IL-8	IL-13, CCL17, NFATC1, CCL11, MAPK13, IL-9, CCL5, SPP1, FPR3, SOS1, S1PR5, IL-17A, MUC5AC.

These results classified the proteins by their specific relationship with molecular motifs. These results were taken into account for the final specificity analysis.

Specificity Analysis: Protein Ranking

Finally, to maximize the specificities of the proteins of interest, information from entire diseases and molecular motif analysis were combined taking into account the results obtained in the molecular motifs of differential weight for each disease:

- Respiratory Allergy: *allergy*, *acute response*, and *late-phase response* ANN results were combined.
- Allergic asthma: *Allergic asthma*, *Th2-mediated pulmonary inflammation*, *goblet cell hyperplasia*, and *granulocyte (eosinophil) infiltration* ANN results were combined.
- Non-allergic Asthma: *Asthma*, *Th-17 mediated pulmonary inflammation*, and *neutrophil inflammation* ANN results were combined.

Two different parameters (relationship level and specificity) were evaluated as explained in the methods section above. The results are summarized in **Table 5**.

The specificity ranking led to the identification of seven allergy specific proteins (**Table 5A**). The relationship found can be partially explained by the inflammatory component of the molecular motifs of allergy. In fact, the most strongly related proteins are directly involved in inflammatory processes (e.g. IL-2, IL-2RB, TNF, or PTGER2) or in the regulation of these processes (IL-10, IL-4, and IL-9).

A total number of 12 proteins have been identified to be specifically related to allergic asthma (**Table 5B**): ALOX5, RNASE3, TGFB1, CCL5, ITGAL CD40, SERPINB2, CCL11, POSTN, IL-17A, CCL17, and SELL. Among these, only CCL17 displayed a stronger non-specific relationship with allergic asthma when compared to the value obtained for the asthma evaluation.

Finally, two proteins were identified as more closely related to non-allergic asthma (**Table 5C**) according to specificity analysis,

TABLE 5 | Specificity ranking of the proteins with a high relationship to at least one of the studied conditions (overall disease and/or molecular motifs).

A. Respiratory Allergy

Protein information			Conditions				
			Respiratory Allergy				
Uniprot ID	Gene name	In topology	Respiratory Allergy ANN score	Specific Motifs ANN score		Relationship level	Specific motifs relationship
				Acute response	Late-phase response		
P24394	*IL4R*	✓	85.21	83.48	39.30	High	High
P05113	*IL5*	✓	92.43	72.65	81.36	Very high	High
P43116	***PTGER2***	✓	**88.16**	**92.44**	**5.58**	**Very high**	**Very high**
P35225	*IL13*	✓	91.82	72.16	81.03	High	High
P22301	***IL10***	✓	**90.26**	**94.51**	**75.18**	**Very high**	**Very high**
P05231	*IL6*	✓	90.15	70.66	83.91	High	High
P01375	***TNF***	✓	**75.99**	**76.33**	**83.71**	**High**	**High**
P15248	***IL9***	✓	**89.85**	**93.02**	**75.72**	**Very high**	**Very high**
P01579	*IFNG*	✓	88.99	94.00	71.68	Very high	Very high
P05112	***IL4***	✓	**88.49**	**93.03**	**75.72**	**Very high**	**Very high**
P60568	***IL2***	✓	**88.13**	**93.90**	**70.14**	**Very high**	**Very high**
P14784	***IL2RB***	✓	**84.15**	**87.59**	**29.56**	**High**	**High**

B. Allergic Asthma

Protein information			Conditions					
			Allergic Asthma					
Uniprot ID	Gene name	In topology	Allergic Asthma ANN score	Specific Motifs ANN score			Relationship level	Specific motifs relationship
				Th2-mediated inflammation	Goblet cell hyperplasia	Granulocyte infiltration		
P98088	*MUC5AC*	✓	88.43	9.46	10.10	8.51	High	Low
P36222	*CHI3L1*	✓	86.53	10.50	7.97	9.76	High	Low
Q15063	***POSTN***	✓	**82.79**	**10.33**	**9.32**	**85.87**	**High**	**High**
O95760	*IL33*	✓	81.12	39.98	9.77	10.24	High	Medium
P12724	***RNASE3***	✓	**82.96**	**15.95**	**8.81**	**83.89**	**High**	**High**
P14151	***SELL***	✓	**81.04**	**12.94**	**11.97**	**88.36**	**High**	**High**
Q8N138	*ORMDL3*	✓	83.15	15.95	12.64	7.61	High	Low
Q9HC84	*MUC5B*	✓	82.64	9.46	10.10	8.51	High	Low
P24394	*IL4R*	✓	81.40	64.45	33.49	83.51	High	High
P09917	***ALOX5***	✓	**87.92**	**15.19**	**13.17**	**91.42**	**High**	**High**
P05113	*IL5*	✓	71.80	80.56	49.32	19.41	High	High
Q16552	***IL17A***	✓	**81.22**	**11.68**	**8.86**	**85.81**	**High**	**High**
P13501	***CCL5***	✓	**77.01**	**41.77**	**45.46**	**89.83**	**High**	**High**

(Continued)

TABLE 5 | Continued

B. Allergic Asthma

Protein information			Conditions					
			Allergic Asthma					
Uniprot ID	Gene name	In topology	Allergic Asthma ANN score	Specific Motifs ANN score			Relationship level	Specific motifs relationship
				Th2-mediated inflammation	Goblet cell hyperplasia	Granulocyte infiltration		
Q9H293	*IL25*	✓	80.90	8.59	8.80	7.03	High	Low
A8K7I4	*CLCA1*	✓	82.78	14.41	9.99	15.48	High	Low
P25942	***CD40***	✓	**74.19**	**18.84**	**18.05**	**78.62**	**High**	**High**
P20701	***ITGAL***	✓	**77.00**	**11.30**	**10.84**	**81.65**	**High**	**High**
P05120	***SERPINB2***	✓	**80.82**	**7.98**	**22.20**	**90.37**	**High**	**High**
P35225	*IL13*	✓	71.19	85.95	9.02	26.72	High	High
P22301	*IL10*	✓	72.16	86.08	16.31	24.93	High	High
P27930	*IL1R2*	✓	79.06	40.74	29.16	12.68	High	Medium
P01579	*IFNG*	✓	71.11	42.66	49.77	92.43	Very high	Very high
P05112	*IL4*	✓	69.62	83.34	12.53	32.52	High	High
P51671	***CCL11***	✓	**75.25**	**56.74**	**10.05**	**88.73**	**High**	**High**
Q07812	*BAX*	✓	78.36	61.27	16.58	23.43	High	Medium
P01137	***TGFB1***	✓	**78.21**	**53.84**	**45.86**	**91.04**	**High**	**High**
Q92583	***CCL17***	✓	**77.87**	**79.66**	**11.87**	**37.72**	**High**	**High**

C. Non-allergic Asthma

Protein information			Conditions				
			Non-allergic Asthma				
Uniprot ID	Gene name	In topology	Non-allergic Asthma ANN score	Specific Motifs ANN score		Relationship level	Specific motifs relationship
				Th17-mediated inflammation	Neutrophil infiltration		
P98088	*MUC5AC*	✓	91.14	10.58	7.59	High	Low
P36222	*CHI3L1*	✓	89.91	16.37	10.88	High	Low
Q15063	*POSTN*	✓	89.75	12.03	11.19	High	Low
O95760	*IL33*	✓	89.01	9.40	13.22	High	Low
P12724	*RNASE3*	✓	88.08	12.22	13.19	High	Low
P14151	*SELL*	✓	88.01	15.73	10.55	High	Low
Q8N138	*ORMDL3*	✓	87.70	11.79	11.85	High	Low
Q9HC84	*MUC5B*	✓	86.88	10.58	7.59	High	Low
P09917	*ALOX5*	✓	86.69	7.91	14.47	High	Low

(Continued)

TABLE 5 | Continued

C. Non-allergic Asthma

Protein information			Conditions				
			Non-allergic Asthma				
Uniprot ID	Gene name	In topology	Non-allergic Asthma ANN score	Specific Motifs ANN score		Relationship level	Specific motifs relationship
				Th17-mediated inflammation	Neutrophil infiltration		
Q16552	*IL17A*	✓	86,69	75,50	10,62	High	Medium
P43116	*PTGER2*	✓	84,79	12,22	11,92	High	Low
P13501	*CCL5*	✓	83,26	17,66	45,33	High	Medium
Q9H293	***IL25***	✓	**82,81**	**69,62**	**8,22**	**High**	**Medium**
A8K7I4	*CLCA1*	✓	81,62	15,94	15,13	High	Low
P17931	***LGALS3***	✓	**77,78**	**16,32**	**80,96**	**High**	**High**
P05120	*SERPINB2*	✓	79,93	15,73	16,07	High	Low
P05231	*IL6*	✓	74,83	48,44	80,97	High	High
P51671	*CCL11*	✓	78,30	10,58	11,85	High	Low

Specific proteins according to the criteria defined in Methods *are remarked in bold. The final ranking was performed using two measures Relationship level and Specificity. Relationship level: indicates the level of relationship of the proteins with each overall disease or any disease-specific motif. Specificity: indicates whether the protein presents a stronger relationship with the specific motifs of the disease than with the specific motifs of the other diseases.*

namely IL-25 and LGALS3. Moreover, LGALS3 was the only one to display a stronger overall relationship with nonallergic than with allergic asthma.

In addition, some proteins that showed no specific relationship with any condition did present a distinct high overall relationship with them. Specifically, IFN-G, IL-13, IL-5, and IL-4R showed an especially high overall relationship with allergic conditions (respiratory allergy and allergic asthma).

MUC5B, ORMDL3, MUC5AC, CHI3L1, CLCA1, and IL-33 display a distinctly high non-specific relationship with allergic and non-allergic asthma.

Validation of Prioritized Results by Systems Biology

To validate the results of specificity obtained by systems biology, we compared our previous gene-expression data and constructed an ROC curve to analyze the experimental gene-expression data by disease condition. **Figure 3** summarizes the graphical overview of the three diseases combining the results of systems biology analysis of the total 94 biomarkers in each disease and our experimental data of gene-expression by clinical comparisons against healthy control subjects (RQ value), obtaining an overview of the diseases nodes interactions. This graph (**Figure 3**) combines the mathematical model results with our gene-expression results, showing differential and shared nodes for each disease with mechanistic information (effector proteins are indicated).

Next, the gene-expression analysis of each specific protein defined by systems biology was checked in order to compare the theoretical results and experimental data. **Table 6** summarizes the gene expression data for each specific protein defined per disease. Overall, there was a correlation between theoretical specificity and experimental results, although several of the "specific biomarkers" determined by systems biology were not classified as specific by our results despite the fact that these were relevant for the disease compared with healthy controls (because were relevant to more than one of the diseases). Several proteins were not compared due to a lack of experimental data, as indicated in the footnotes of each Table.

Finally, to determine the specificity and sensitivity of the biomarkers defined by systems biology (biomarkers that showed high relationship to at least one of the studied condition), ROC curve analysis was performed using our experimental results to establish their ability to determine diseases and severities. There were 13 common biomarkers (*ALOX5*, *CCL5*, *CHI3L1*, *IFNG*, *IL10*, *IL1R2*, *IL4R*, *IL8*, *SELL*, *SERPINB2*, *TGFB1*, *TLR4*, *TNF*) defined as potential good candidates by our previous experimental data (27, 28) and by the system biology analysis. The best biomarkers (AUC > 0.75) by clinical conditions are summarized in **Table 7**.

Triggering Analysis

The possible role of the proteins of interest in respiratory allergy, allergic asthma, and non-allergic asthma triggers has also been assessed. Two types of score, that is, individual probability score

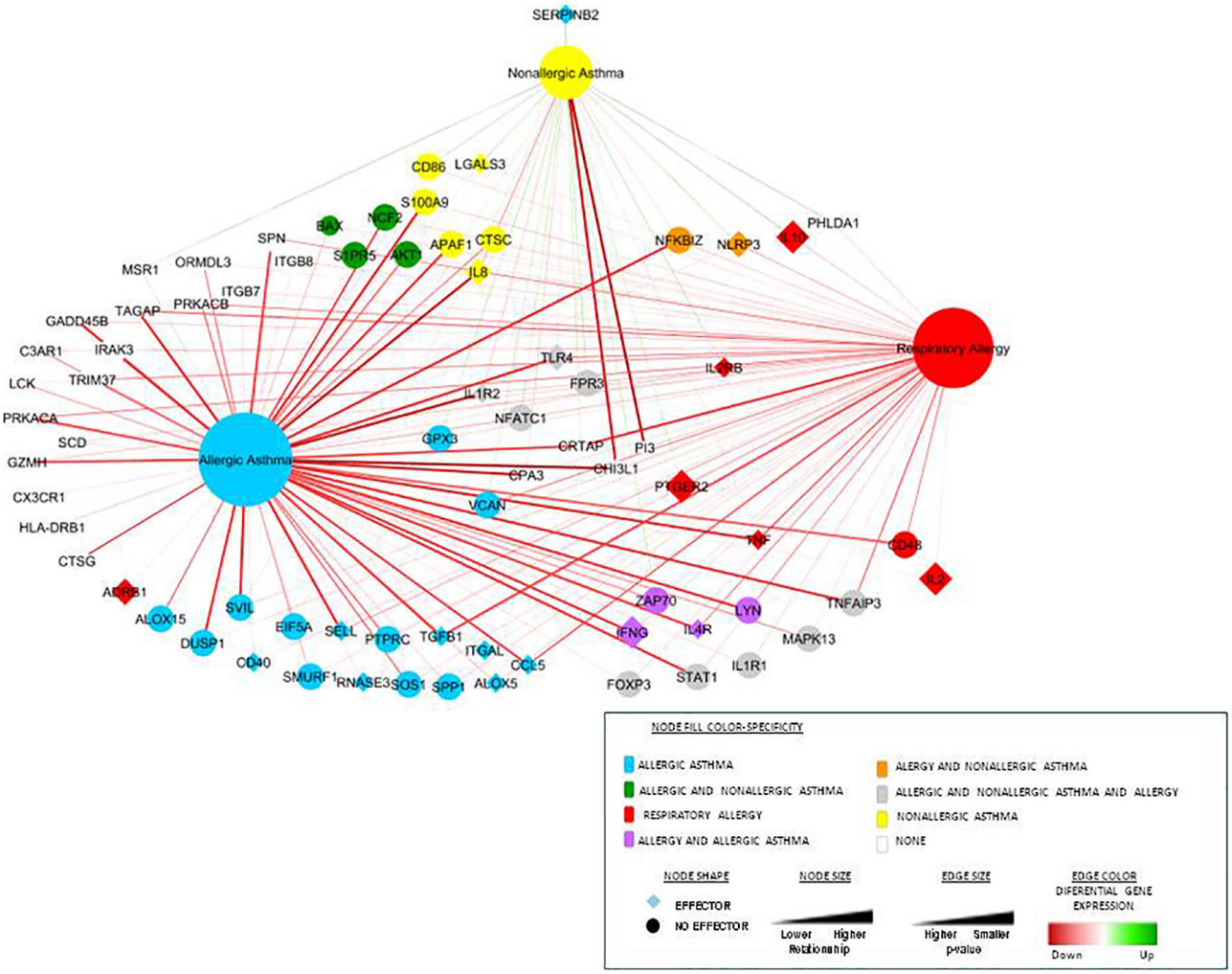

FIGURE 3 | Representation of the three diseases and their connections combined with the differential gene-expression proteins obtained from our experimental data. This network includes connections between the diseases (the three main nodes) and the most differential gene-expression proteins obtained from our experimental data (27, 28). The node shape illustrates whether the protein is an effector or not, color represents specificity and size and the level of relationship. Differential gene expression is represented by the edge color and the *p*-value by the size.

and accumulated score, were determined according to the indications appearing in the methods section above.

The results obtained from the triggering analysis of the 94 biomarker candidates are summarized in **Table 8**. According to the individual score, neither AKT1, MAPK13, nor STAT1 presented a high probability of promoting respiratory allergy on their own. However, looking at the cumulative triggering score of these proteins, nearly 90% of the effector proteins of respiratory allergy would be affected. Inclusion of the rest of proteins of interest would not increase the percentage of respiratory allergy effectors affected, i.e. they do not substantially influence effectors apart from the ones already affected by the aforementioned proteins. Therefore, the most promising protein combination as allergy triggers would be formed by AKT1, MAPK13, and STAT1 proteins.

Results of the triggering analysis performed over allergic asthma (**Table 8**) revealed that STAT1, MAPK13, and TLR4 are the top genes that play a trigger role according to the individual score. When considering the cumulative score, AKT1 appears to be the most probable promoter of allergic asthma, affecting 84.55% of the allergic asthma effectors. In addition, when taking into account AKT1 along with STAT1, MAPK13, and TLR4, nearly 90% of the effectors were affected and the consideration of the remaining proteins of interest would not significantly increase this percentage.

The triggering analysis performed on non-allergic asthma revealed that MAPK13 presents the highest individual triggering probability (**Table 8**). When looking at the cumulative score, the same combination of proteins (AKT1, STAT1, MAPK13, and TLR4) triggered 89.27% of the non-allergic asthma effector

TABLE 6 | Relative Quantification (RQ) values of gene expression in specific proteins defined by systems biology.

A. Respiratory Allergy (RA) specific proteins

Gene	RA *vs* Control		AA *vs* Control		NA *vs* Control	
	RQ	adjusted P	RQ	adjusted P	RQ	adjusted P
IL2RB	0.21	3.79E-8	0.38	9.24E-8	2.68	3.5E-4
TNF	0.13	3.5E-10	0.066	3.47E-21	0.41	0.011
PTGER2	0.30	7.3E-8	0.48	1.36E-6	1.86	0.003
IL10	0.15	5.06E-6	nd	nd	6.14	1.6E-6

No data for IL-4, IL-9, and IL-2. nd, not determined.

B. Allergic Asthma (AA) specific proteins

Gene	RA *vs* Control		AA *vs* Control		NA *vs* Control	
	RQ	adjusted P	RQ	adjusted P	RQ	adjusted P
ALOX5	0.25	2.8E-5	0.23	6.13E-8	nd	nd
RNASE3	0.41	8.9E-3	0.35	6.09E-4	nd	nd
TGFB1	0.20	3.5E-13	0.18	4.7E-20	nd	nd
CCL5	0.13	2.8E-10	0.14	3.18E-12	nd	nd
ITGAL	0.39	5.3E-6	0.45	2.58E-5	nd	nd
CD40	0.26	7.2E-5	0.35	3.48E-5	nd	nd
SERPINB2	nd	nd	1.67	nd	8.94	7.6E-5
SELL	0.14	4.25E-8	0.10	3.2E-15	0.53	0.039

No data for CCL11, POSTN, IL17A, CCL17.

C. Non-allergic Asthma (NA) specific proteins

Gene	RA *vs* Control		AA *vs* Control		NA *vs* Control	
	RQ	adjusted P	RQ	adjusted P	RQ	adjusted P
LGALS3	0.46	9.9E-4	0.46	1.9E-5	2.06	0.006

No data for IL-25.

proteins and inclusion of the rest of proteins of interest would not substantially increase this percentage.

Overall, the results of the triggering analysis reveal a relevant role for AKT1, STAT1, and MAPK13 proteins in the three conditions and point to the same set of genes as triggers of all three conditions. STAT1, AKT1, and MAPK13 appear as key mediators of the three diseases, with the addition of TRL4 only in asthmatic pathologies.

In order to determine possible mechanisms that connect the triggering proteins with prioritized proteins for each disease, we performed two types of analyses of Pathways (by Pantherlink) for each disease; we first used as a target of the triggering the highly related proteins with mechanistic implication in each disease, and secondly, using the specific proteins defined by the systems biology study as a target. **Supplementary Figures 1A–C** and **2A–C** show the network obtained with Pantherlink, including new proteins as link. A more graphic and functional scheme of these results is summarized in **Figures 4A–C** and **5A–C**, respectively.

DISCUSSION

The sheer volume of data generated nowadays by massive techniques makes interpretation and analysis a complicated task. Therefore, the use of new approaches that systematically bring together all this information alongside newly generated data is a revolutionary step in medicine, called precision medicine. At this respect, systems biology approaches are being considered as essential for moving along and implantation of new and relevant discoveries. The network-based approach established by systems biology enables elucidation of the underlying molecular mechanisms, mainly in terms of disease modules, disease phenotypes, and disease-disease associations (65, 66). These are conceptual models of disease mechanisms that include relevant signaling, metabolic and gene regulatory processes with evidence of their relationships to pathophysiological causes and outcomes (67). A number of studies have investigated the disease modules associated with specific phenotypes for diseases such as asthma, diabetes, and cancer, for which a disease module would mainly be detected (68, 69).

Systems biology is an integrative approach for modeling complex biologic systems and processes such as those occurring in asthma, through the use of multilevel multi-scale mathematical and computing methods in order to integrate the biologic networks and pathways involved. Such integration will allow for the discovery of new properties or mechanisms involved in asthma that have not been evident previously with the traditional reductionist approach (26).

TABLE 7 | ROC analysis of gene expression in the 13 common proteins defined by systems biology and experimental data.

A. Comparison between healthy controls and diseases

Control *vs.* Respiratory Allergy

Gene	N (C)	N (RA)	AUC (95% CI)	Threshold
IL1R2	27	14	0.82 (0.67–0.96)	8.91
IL4R	27	14	0.79 (0.65–0.94)	9.9
SELL	27	14	0.78 (0.63–0.93)	9.04
TLR4	27	14	0.86 (0.75–0.97)	9.9
CCL5	27	14	0.87 (0.75–0.98)	6.11
TGFB1	28	14	0.77 (0.59–0.96)	6.92

Control *vs.* Allergic asthma

Gene	N (C)	All severities			Severe asthma			Moderate-Mild asthma		
		N (AA)	AUC (95% CI)	Threshold	N (S-AA)	AUC (95% CI)	Threshold	N (MM-AA)	AUC (95% CI)	Threshold
ALOX5	27	30	0.79 (0.66–0.91)	8.28	15	0.78 (0.63–0.93)	7.96	15	0.79 (0.65–0.93)	8.3
CCL5	27	30	0.87 (0.77–0.97)	6.06	15	0.85 (0.70–1.00)	6.07	15	0.88 (0.77–1.00)	5.97
CHI3L1	27	**16**	**0.99 (0.96–1.00)**	**12.6**	**8**	**0.97 (0.93–1.00)**	**11**	**8**	**1.00 (1.00–1.00)**	**13.1**
IFNG	27	28	0.85 (0.76–0.95)	12.3	14	0.84 (0.71–0.98)	11.9	14	0.87 (0.75–0.98)	12.4
IL10	25	28	0.78 (0.65–0.91)	15.3	14	0.85 (0.72–0.98)	15.2			
IL1R2	27	**27**	**0.98 (0.94–1.00)**	**9.22**	**14**	**0.96 (0.91–1.00)**	**9.25**	**13**	**0.99 (0.96–1.00)**	**11.6**
IL4R	27	**30**	**0.92 (0.84–0.99)**	**10.4**	15	0.89 (0.78–1.00)	10.3	**15**	**0.94 (0.88–1.00)**	**9.8**
IL8	29	**30**	**0.94 (0.86–1.00)**	**2.94**	**15**	**0.92 (0.84–1.00)**	**2.94**	**15**	**0.95 (0.88–1.00)**	**4.77**
SELL	27	**30**	**0.92 (0.84–1.00)**	**8.61**	**15**	**0.90 (0.78–1.00)**	**8.68**	**15**	**0.94 (0.86–1.00)**	**8.38**
SERPINB2	24	29	0.82 (0.70–0.93)	13.9	15	0.88 (0.78–0.98)	13.5	14	0.75 (0.60–0.91)	13.9
TGFB1	28	**30**	**0.90 (0.81–0.99)**	**6.91**	15	0.83 (0.68–0.99)	6.84	**15**	**0.96 (0.89–1.00)**	**7.13**
TLR4	27	28	0.88 (0.78–0.97)	11	14	0.80 (0.66–0.94)	11	**14**	**0.95 (0.89–1.00)**	**11**
TNF	28	**30**	**0.92 (0.84–0.99)**	**5.11**	**15**	**0.91 (0.81–1.00)**	**5.16**	**15**	**0.92 (0.84–1.00)**	**5.11**

Control *vs.* Non-allergic asthma

Gene	N (C)	All severities			Severe asthma			Moderate-Mild asthma		
		N (NA)	AUC (95% CI)	Threshold	N(S-NA)	AUC (95% CI)	Threshold	N(MM-NA)	AUC (95% CI)	Threshold
CHI3L1	27	**19**	**0.95 (0.84–1.00)**	**11.8**	9	0.89 (0.67–1.00)	12.9	**10**	**1.00 (0.99–1.00)**	**11.8**
IL10	25	25	0.87 (0.75–0.98)	14.5	**13**	**0.94 (0.86–1.00)**	**14.8**	12	0.79 (0.59–1.00)	14.3
IL1R2	27	**25**	**0.93 (0.86–1.00)**	**8.97**	**13**	**0.93 (0.85–1.00)**	**9.29**	**12**	**0.93 (0.85–1.00)**	**8.97**
IL4R	27	26	0.77 (0.64–0.90)	9.6				13	0.88 (0.77–0.98)	10.2
IL8	29	**27**	**0.92 (0.83–1.00)**	**2.83**	**13**	**0.91 (0.81–1.00)**	**3.25**	**14**	**0.92 (0.84–1.00)**	**2.83**
SELL	27	27	0.84 (0.73–0.95)	8.21	13	0.82 (0.68–0.95)	8.44	14	0.86 (0.71–1.00)	8.21
SERPINB2	24	24	0.84 (0.72–0.95)	12.6	12	0.82 (0.65–0.98)	13.6	12	0.86 (0.73–0.98)	11.9
TLR4	27	25	0.83 (0.72–0.95)	10	13	0.80 (0.66–0.94)	9.8	12	0.87 (0.76–0.98)	10.4
TNF	28	28	0.83 (0.72–0.94)	4.52	15	0.82 (0.68–0.96)	4.57	13	0.85 (0.71–0.98)	4.96
IFNG	27							12	0.79 (0.63–0.95)	12.3

B. Comparison between diseases

Respiratory Allergy *vs.* Allergic asthma

Gene	N (RA)	All severities			Severe asthma			Moderate-Mild asthma		
		N (AA)	AUC (95% CI)	Threshold	N(S-AA)	AUC (95% CI)	Threshold	N(MM-AA)	AUC (95% CI)	Threshold
IL1R2	14	**27**	**0.90 (0.80–1.00)**	**10.5**	14	0.88 (0.75–1.00)	10.5	13	**0.92 (0.81–1.00)**	**11.3**
IL4R	14	30	0.80 (0.66–0.93)	10.6	**15**	0.78 (0.59–0.96)	10.7	**15**	0.82 (0.65–0.98)	10.6
TGFB1	14	30	0.76 (0.63–0.90)	7.27				15	**0.90 (0.77–1.00)**	**7.13**
CHI3L1	14	**16**	**0.95 (0.87–1.00)**	**12.6**	8	**0.92 (0.81–1.00)**	**12.6**	8	**0.97 (0.91–1.00)**	**13.1**
IL10	11	28	0.85 (0.73–0.97)	15	14	**0.94 (0.84–1.00)**	**14.7**	14	0.77 (0.59–0.96)	15.4

(Continued)

TABLE 7 | Continued

B. Comparison between diseases

Respiratory Allergy *vs.* Allergic asthma

Gene	N (RA)	All severities			Severe asthma			Moderate-Mild asthma		
		N (AA)	AUC (95% CI)	Threshold	N(S-AA)	AUC (95% CI)	Threshold	N(MM-AA)	AUC (95% CI)	Threshold
IL8	14	**30**	**0.92 (0.78–1.00)**	**3.41**	15	**0.90 (0.77–1.00)**	**3.41**	15	**0.93 (0.79–1.00)**	**4.6**
SERPINB2	13	30	0.82 (0.69–0.95)	5.27	15	0.78 (0.59–0.96)	13.5			
TNF	14				15	0.80 (0.63–0.96)	5.28	15	0.84 (0.70–0.99)	5.27

Respiratory Allergy *vs.* Non-allergic asthma

Gene	N (RA)	All severities			Severe asthma			Moderate-Mild asthma		
		N (NA)	AUC (95% CI)	Threshold	N(S-NA)	AUC (95% CI)	Threshold	N(MM-NA)	AUC (95% CI)	Threshold
CCL5	14	26	0.87 (0.75–0.98)	5.83	13	**0.91 (0.79–1.00)**	**5.65**	13	0.82 (0.65–1.00)	5.83
IL1R2	14	25	0.76 (0.60–0.92)	10.4	13	0.77 (0.59–0.96)	10.4			
CHI3L1	14	**19**	**0.91 (0.80–1.00)**	**12.4**	9	0.87 (0.65–1.00)	12.9	10	**0.96 (0.89–1.00)**	**12.4**
IL10	11	**25**	**0.90 (0.80–1.00)**	**14.6**	13	**0.97 (0.92–1.00)**	**14.6**	12	0.83 (0.63–1.00)	14.5
IL8	14	27	0.88 (0.73–1.00)	3.46	13	0.86 (0.69–1.00)	3.46	14	0.89 (0.75–1.00)	3.52
SERPINB2	13	24	0.77 (0.59–0.94)	11.9	12	0.76 (0.56–0.95)	13.5	12	0.78 (0.59–0.98)	11.9

Allergic asthma *vs.* Non-allergic asthma

Gene	All severities				Severe asthma				Moderate-Mild asthma			
	N(AA)	N(NA)	AUC (95% CI)	Threshold	N (S-AA)	N (S-NA)	AUC (95% CI)	Threshold	N (MM-AA)	N (MM-NA)	AUC (95% CI)	Threshold
CCL5	30	26	0.86 (0.76–0.96)	5.92	**15**	**13**	**0.90 (0.78–1.00)**	**5.77**	15	13	0.83 (0.66–1.00)	5.92
TGFB1	30	26	0.80 (0.68–0.92)	7.12	15	13	0.77 (0.59–0.96)	6.66	15	13	0.85 (0.70–1.00)	7.11
ALOX5	30	26	0.75 (0.62–0.89)	8.29	15	13	0.79 (0.61–0.97)	8.29				
SELL					15	13	0.82 (0.64–0.99)	8.98				
CHI3L1									8	10	0.74 (0.49–0.99)	15.3
IL8									15	14	0.87 (0.74–0.99)	5.81
SERPINB2									14	12	0.74 (0.53–0.95)	11.8
TLR4									14	12	0.76 (0.56–0.97)	11

C. Comparisons between asthma severities

Moderate-mild *vs.* Severe

Gene	Allergic Asthma			
	N(S-AA)	N(MM-AA)	AUC (95% CI)	Threshold
IL10	14	14	0.74 (0.55–0.94)	14.7
SERPINB2	15	14	0.73 (0.54–0.92)	11.6
TLR4	14	14	0.72 (0.53–0.92)	11.6

Moderate-mild *vs.* Severe

Gene	Non-allergic asthma			
	N(S-NA)	N(MM-NA)	AUC (95% CI)	Threshold
CCL5	13	13	0.76 (0.56–0.96)	5.53

Summary of the best biomarkers able to discriminate clinical conditions. ROC curve analysis was performed with the gene expression data from the 13 common genes between systems biology prediction and experimental data (27, 28). AUC value, area under the curve; 95% CI, 95% confidence interval. Threshold refers to the gene levels of each biomarker that distinguish each condition, with the AUC indicated. Options with the best statistical power (95% CI between 0.70 and 1) appear in bold. NA, non-allergic asthma; AA, allergic asthma; S, Severe; MM, Moderate-mild.

In this work, systems biology approaches have been used to evaluate and prioritize potential respiratory allergy, allergic asthma, and non-allergic asthma biomarker candidates based on their association with the disease and with mechanistic implications. Firstly, a molecular model of these three diseases was constructed mathematically using TPM's Anaxomic Technology (31). The effector proteins of the causal and symptomatic motifs of these three highly related processes

TABLE 8 | Results of triggering analysis of the three pathologies.

Uniprot ID	Gene name	Respiratory allergy		Allergic asthma		Non-allergic asthma	
		Individual probability	Accumulated score	Individual probability	Accumulated score	Individual probability	Accumulated score
P31749	***AKT1***	*	86.96	***	84.55	****	84.18
P42224	***STAT1***	**	91.30	****	89.27	****	88.27
O15264	***MAPK13***	**	89.13	****	89.27	*****	88.27
O00206	***TLR4***			****	90.12	****	89.28

*Individual and accumulated triggering score for each protein indicated. Probability ranking is indicated as one to five * (from lowest to highest probability).*

were characterized at the molecular level, revealing common and differential molecular motifs within the different diseases. A total number of 16 molecular motifs have been characterized; when combined, these were representative of the three conditions of interest (**Table 1**). Next, a mechanistic ranking of our 94 proteins of interest (27, 28) was performed by means of artificial neural networks (ANNs). This analysis enables prioritization of the proteins of interest and identification of the biomarker candidates with the highest level of specificity for each condition. A mechanistic analysis based on the relationship of each protein with the entire disease was performed, obtaining a ranking for the 94 genes analyzed (Supplementary **Table 1**). The best candidates or strongest predicted relationship with respiratory allergy (**Table 2A**) were IL-5, IL-2, IL-2RB, TNF, PTGER2, IL-6, IL-10, IL-4, and IL-9, all classified as effectors (45–51). These proteins are implicated mainly in inflammatory processes or their regulation.

Seventeen proteins (MUC5AC, ALOX5, CHI3L1, ORMDL3, RNASE3, POSTN, TGFB1, CCLA1, MUC5B, IL-4R, IL-17A, IL-33, SELL, IL-25, SERPINB2, IL-1R2, and BAX) were found to have a "high" relationship level with allergic asthma (**Table 2B**), and 16 proteins (MUC5AC, CHI3L1, POSTN, IL-33, RNASE3, SELL, ORMDL3, MUC5B, ALOX5, IL-17A, PTGER2, CCL5, IL-25, CCLA1, SERPINB2, CCL11) with non-allergic asthma (**Table 2C**). All of these proteins were identified as effectors (52, 54, 57–60, 62–64, 70–74), except BAX (pro-apoptotic member of the Bcl-2 family), which together Bcl-2 (anti-apoptotic molecule), has been described as an essential molecule to control immune cells and the chronicity of many inflammatory diseases, including asthma (75, 76) and with differences among allergic and non-allergic asthma (77). As shown in **Figure 2** and **Table 3**, allergic asthma and non-allergic asthma share 13 of these proteins. According to these analyses, IL-1R2, BAX, and TGFB1 were of particular interest due their "High" relationship level with allergic asthma and "Moderate" or weaker relationship value with allergy or nonallergic asthma. Also of interest is the fact that the classical T2 sign (CCLA1, POSTN, and SERPINB2) was associated with the two kinds of asthma analyzed, which is consistent with our previous published data (27–30).

Next, proteins were also analyzed according to each molecular motif defined to the three diseases, showing that all molecular motifs except 3 (*Goblet cell hyperplasia*, *Th17-mediated pulmonary inflammation*, *ECM deposition*, and *innervation and hyper-excitability*) presented at least one protein in the "High" relationship level and all the proteins predicted to have a "High" or stronger relationship level with a molecular motif were identified as effectors of the molecular motif (**Table 4**). These data are especially interesting in that they point to an ideal target to be checked in order to define the "real" mechanistic implication of each protein. "Moderate" relationships are also indicated in the Table to have a broader spectrum of protein implications and to try to reduce the possible bias towards under-studied proteins.

Finally, specificity was determined using the combination of the relationship of each protein with regard to the entire disease and the specific motifs. **Table 5** summarizes the strongest predicted relationships with respiratory allergy (**Table 5A**), that is, seven proteins (IL-2, IL-2RB, TNF, PTGER2, IL-10, IL-4, and IL-9) again related mainly with inflammatory response and regulation.

In total, 12 proteins were identified as being specifically related to allergic asthma (**Table 5B**): ALOX5, RNASE3, TGFB1, CCL5, ITGAL CD40, SERPINB2, CCL11, POSTN, IL-17A, CCL17, and SELL. Of these, only CCL17 (chemokine that specifically binds and induces chemotaxis in T cells *via* CCR4) displayed a higher non-specific relationship with allergic asthma when compared to the value obtained for non-allergic asthma. This finding is in agreement with the dominant role described for CCL17 in Th2-related diseases, such as atopic dermatitis and asthma (78, 79) and the recently reported relationship with TSLP induction (80). Finally, two proteins (IL-25 and LGALS3) were identified as being more related to non-allergic asthma (**Table 5C**) according to the specificity analysis performed. Moreover, LGALS3 or Galectin-3 was the only protein to display a higher general relationship with nonallergic than with allergic asthma. Galectin-3 is a member of the β-galactoside-binding animal lectins; interestingly, it has been described as one of the receptors of CHI3L1 (81). It is a pleiotropic protein with multiple cellular functions, including involvement in many aspects of allergic inflammation, such as eosinophil recruitment, airway remodeling, development of a Th2 phenotype, as well as increased expression of inflammatory mediators (82). Galectin-3 has also been involved in the recruitment, activation, and removal of neutrophils (83) and has been described as a potential biomarker and therapeutic target of asthma (82, 83).

In addition, some proteins that showed no specific relationship with any condition did present a distinctively high global relationship with these conditions. Specifically, IFNG, IL-

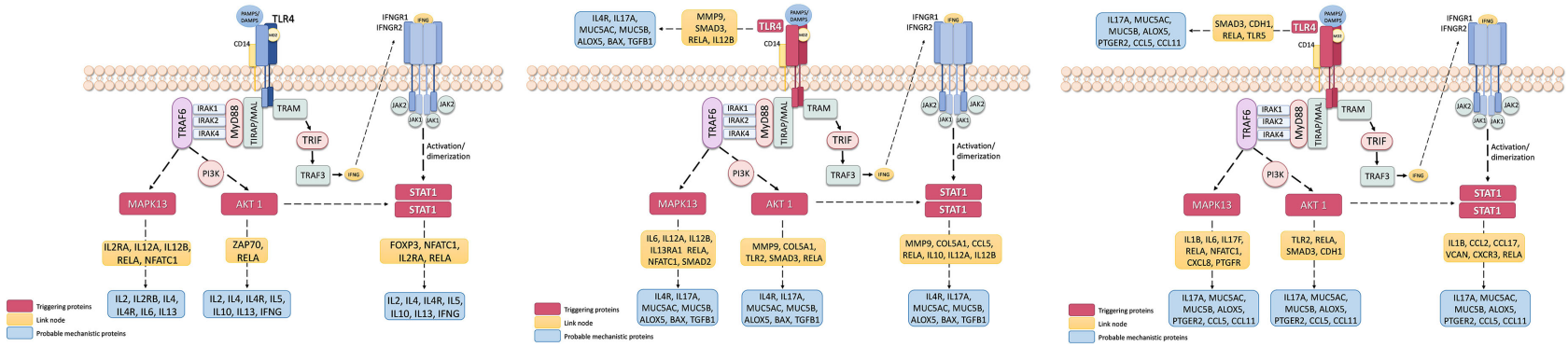

FIGURE 4 | Schematic representation of the triggering protein-activation pathway for each disease, using as a target the protein defined as mechanistically highly related to the disease. The proteins that link these pathways with proteins with high mechanistic value for this specific disease appear in yellow. **Supplementary Figure 1** represents the pathway scheme obtained by Pathlinker analysis using the Cytoscape V3.6.1 (https://cytoscape.org/) program. **(A)** Respiratory Allergy. **(B)** Allergic Asthma. **(C)** Non-allergic Asthma.

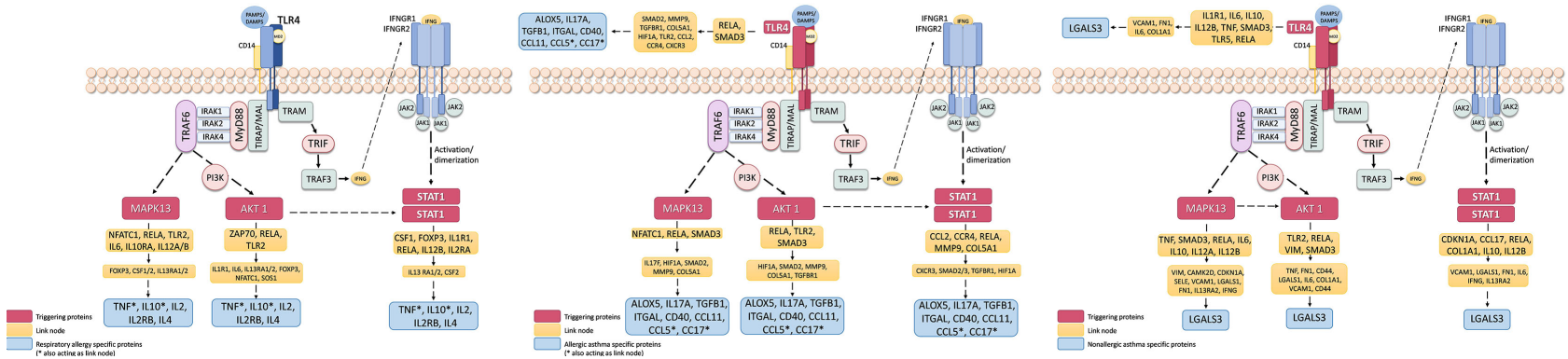

FIGURE 5 | Schematic representation of the triggering protein-activation pathway for each disease, using as a target the protein defined as highly specific for these diseases. The proteins that link these pathways with proteins with high mechanistic value for this specific disease are indicated in yellow. **Supplementary Figure 2** represents the pathway scheme obtained by Pathlinker analysis using the the Cytoscape V3.6.1 (https://cytoscape.org/) program. **(A)** Respiratory Allergy. **(B)** Allergic Asthma. **(C)** Non-allergic Asthma.

13, IL-5, and IL-4R showed an especially high overall relationship with allergic conditions (respiratory allergy and allergic asthma). MUC5B, ORMDL3, MUC5AC, CHI3L1, CLCA1, and IL-33 displayed a high non-specific relationship with allergic and nonallergic asthma.

All this information was combined with our previous gene-expression studies (27, 28), and **Figure 3** summarizes the network of interaction among these three diseases, highlighting effector proteins and relative gene-expression comparing healthy control subject *vs* patients.

The validation of ranking by systems biology is summarized in **Table 6**, which compares the experimental gene expression data analyzed in a population of 114 subjects with the three clinical conditions studied here and a healthy control population (27, 28). Overall, there was a correlation between theoretical specificity and experimental results, though several of the "specific biomarkers" indicated by systems biology, despite being relevant in the disease compared with healthy controls, could not be classified as specific by our results, as they are shared by more than one of the diseases.

The next step in validating and defining specificity and sensitivity was the ROC curve-based analysis of the "best" biomarkers defined by systems biology (high relationship to at least one of the studied conditions) according to our gene-expression data, comparing all the clinical conditions possible, according the number of groups studied. There were 13 common biomarkers (*ALOX5*, *CCL5*, *CHI3L1*, *IFNG*, *IL10*, *IL1R2*, *IL4R*, *IL8*, *SELL*, *SERPINB2*, *TGFB1*, *TLR4*, *TNF*) defined as potential good candidates by our previous experimental data (27, 28) and by the system biology analysis, that were analyzed. The results of this analysis are summarized in **Table 7**. These analyses confirmed that several of the previously defined biomarkers (29, 30) are theoretically corroborated as relevant in these diseases (*CHI3L1*, *IL-10*, *POSTN*, *SERPINB2*, *IL-8*) but others like *MSR1*, *PI3*, and *PHLDA1* were not included among the "best" biomarkers defined by systems biology. This could be due to the lower amount of information in the databases about several genes/proteins. This is an important aspect of this kind of approach and should be borne in mind. In contrast, other genes were prioritized thanks to this approach and should be analyzed in depth. Especially relevant are the *CCL5* results (**Table 7**). *CCL5/RANTES*, a member of the C-C chemokine family, is a potent eosinophil, monocyte, basophil, and lymphocyte chemo-attractant at the site of inflammation. Very recently, a meta-analysis study indicated that several RANTES polymorphisms may contribute to the development of childhood asthma, but without association by atopic status (84). In contrast, here we found a good biomarker that can discriminate between asthma (allergic and non-allergic) with a very good AUC (**Table 7B**), mainly between the most severe clinical phenotypes (severe AA *vs.* severe ANA, AUC: 0.90). Also was the only of the systems biology defined biomarkers able to discriminate severe *vs.* moderate/mild nonallergic asthma with a good AUC (0.76) (**Table 7C**).

Finally, another important use of systems biology seen here is the characterization of possible disease "triggering." The study results in this regard are summarized in **Table 8**. From our candidates, STAT1, AKT1, and MAPK13 appeared to act as key mediators of the three diseases, with the addition of TRL4 only in asthmatic pathologies. These four proteins have been related to the regulation of different aspect of asthma and allergic diseases (85–89), which is why their implication in the three pathologies should be studied more in depth. The possible mechanisms that connect these triggering to the prioritized proteins for each disease are summarized in **Supplementary Figures 1A–C** and **2A–C,** indicating several new proteins that could be interesting to analyze. The graphic and functional scheme of these results appears in **Figures 4A–C** and **Figures 5A–C** .

This report could be considered as a proof of concept in the sense that all the biomarker candidates analyzed here were previously defined by studies in samples derived from peripheral blood (27, 28) and not in samples from lung tissue or airways cells. As a result, several of the proteins to be validated, especially those related with asthma, may have been underestimated in terms of their implication as biomarkers (i.e. MUCINS). It will likely be of interest to analyze these same biomarkers in target organ-derived samples and to corroborate their correlations and relevance while increasing the size and clinical conditions of the population to be studied.

In summary, despite the limitations of this study and the limitations inherent to systems biology approaches, mainly related to the scarce information to several new biomarkers or poorly described (that could under bias, decreasing the accessibility to connection in network of new elements), this report shows the possibility of defining specific biomarkers associated with diseases and molecular motifs, confirmed by experimental data, opening the possibility of determining better implications of the candidates studied. This new information on potential biomarkers with a mechanistic implication provides new focus to find diagnostic and therapeutic tools for these types of diseases.

DATA AVAILABILITY STATEMENT

The original contributions presented in the study are included in the article/**Supplementary Material**. Further inquiries can be directed to the corresponding author.

ETHICS STATEMENT

The studies involving human participants were reviewed and approved by Research Ethics Committee of the IIS-FJD-UAM. The patients/participants provided their written informed consent to participate in this study.

AUTHOR CONTRIBUTIONS

LC-J and MD worked on the analysis, discussion, and drafting of the manuscript. ML-R and JS collaborated in drafting the manuscript. PM collaborated in the interpretation of

Bioinformatics analysis of results. IM collaborated in the statistical analysis. SB and BC worked on all the project steps, i.e., the design of the study, experimental work, analysis and discussion of the results, and drafting of the text. All authors contributed to the article and approved the submitted version.

FUNDING

Supported in part by research grant PI17/01682 and PI20/00903 cofunded by FEDER, CIBERES (ISCIII, 0013), and RETIC (RD09/0076/00101) from the *Fondo de Investigación Sanitaria* (*Ministerio de Sanidad y Consumo*, Spain) and in part by the research grant *Ayudas de la Sociedad Española de Alergia e Inmunología Clínica* (SEAIC). LC-J was supported by *Fundación Conchita Rábago*. MD was supported by a contract from *Comunidad de Madrid* (PEJ-2017-AI/SAL-5938, *Sistema de Garantía Juvenil*). ML-R was supported by a contract from *Comunidad de Madrid* (PEJD-2019-PRE/BMD-16537, *Sistema de Garantía Juvenil*). PM was supported by a Miguel Servet contract (CP16/00116) from *the Fondo de Investigación Sanitaria* (*Ministerio de Sanidad y Consumo*, Spain). SB was supported by PI17/01682.

ACKNOWLEDGMENTS

We are grateful to Oliver Shaw for revising the manuscript for English usage and style.
Thanks to employees of Anaxomics for their support in the analysis of data derived from a systems biology approach.

SUPPLEMENTARY MATERIAL

The Supplementary Material for this article can be found online at: https://www.frontiersin.org/articles/10.3389/fimmu.2021.640791/full#supplementary-material

REFERENCES

1. GINA. *Global Initiative for Asthma. Global Strategy for Asthma Management and Prevention*. (2019). Available at: https://ginasthma.org/.
2. McKeage K. Omalizumab: a review of its use in patients with severe persistent allergic asthma. *Drugs* (2013) 73(11):1197–212. doi: 10.1007/s40265-013-0085-4
3. Agache I, Akdis CA. Endotypes of allergic diseases and asthma: An important step in building blocks for the future of precision medicine. *Allergol Int* (2016) 65(3):243–52. doi: 10.1016/j.alit.2016.04.011
4. Tan HT, Hagner S, Ruchti F, Radzikowska U, Tan G, Altunbulakli C, et al. Tight junction, mucin, and inflammasome-related molecules are differentially expressed in eosinophilic, mixed, and neutrophilic experimental asthma in mice. *Allergy* (2019) 74(2):294–307. doi: 10.1111/all.13619
5. Kuruvilla ME, Lee FE, Lee GB. Understanding Asthma Phenotypes, Endotypes, and Mechanisms of Disease. *Clin Rev Allergy Immunol* (2019) 56(2):219–33. doi: 10.1007/s12016-018-8712-1
6. Peters SP. Asthma phenotypes: nonallergic (intrinsic) asthma. *J Allergy Clin Immunol Pract* (2014) 2(6):650–2. doi: 10.1016/j.jaip.2014.09.006
7. Peters MC, Mekonnen ZK, Yuan S, Bhakta NR, Woodruff PG, Fahy JV. Measures of gene expression in sputum cells can identify TH2-high and TH2-low subtypes of asthma. *J Allergy Clin Immunol* (2014) 133(2):388–94. doi: 10.1016/j.jaci.2013.07.036
8. Green RH, Brightling CE, Woltmann G, Parker D, Wardlaw AJ, Pavord ID. Analysis of induced sputum in adults with asthma: identification of subgroup with isolated sputum neutrophilia and poor response to inhaled corticosteroids. *Thorax* (2002) 57(10):875–9. doi: 10.1136/thorax.57.10.875
9. Bullens DM, Truyen E, Coteur L, Dilissen E, Hellings PW, Dupont LJ, et al. IL-17 mRNA in sputum of asthmatic patients: linking T cell driven inflammation and granulocytic influx? *Respir Res* (2006) 7(1):135. doi: 10.1186/1465-9921-7-135
10. Simpson JL, Gibson PG, Yang IA, Upham J, James A, Reynolds PN, et al. AMAZES Study Research Group. Impaired macrophage phagocytosis in non-eosinophilic asthma. *Clin Exp Allergy* (2013) 43(1):29–35. doi: 10.1111/j.1365-2222.2012.04075.x
11. Raedler D, Ballenberger N, Klucker E, Böck A, Otto R, Prazeres da Costa O, et al. Identification of novel immune phenotypes for allergic and nonallergic childhood asthma. *J Allergy Clin Immunol* (2015) 135(1):81–91. doi: 10.1016/j.jaci.2014.07.046
12. Boonpiyathad T, Sözener ZC, Satitsuksanoa P, Akdis CA. Immunologic mechanisms in asthma. *Semin Immunol* (2019) 46:101333. doi: 10.1016/j.smim.2019.101333
13. Khalaf K, Paoletti G, Puggioni F, Racca F, De Luca F, Giorgis V, et al. Asthma from immune pathogenesis to precision medicine. *Semin Immunol* (2019) 46:101294. doi: 10.1016/j.smim.2019.101294
14. Jonckheere AC, Bullens DMA, Seys SF. Innate lymphoid cells in asthma: pathophysiological insights from murine models to human asthma phenotypes. *Curr Opin Allergy Clin Immunol* (2019) 19(1):53–60. doi: 10.1097/ACI.0000000000000497
15. Roan F, Obata-Ninomiya K, Ziegler SF. Epithelial cell-derived cytokines: more than just signaling the alarm. *J Clin Invest* (2019) 129(4):1441–51. doi: 10.1172/JCI124606
16. Viswanathan RK, Busse WW. Biologic Therapy and Asthma. *Semin Respir Crit Care Med* (2018) 39(1):100–14. doi: 10.1055/s-0037-1606218
17. Peters MC, Ringel L, Dyjack N, Herrin R, Woodruff PG, Rios C, et al. A Transcriptomic Method to Determine Airway Immune Dysfunction in T2-High and T2-Low Asthma. *Am J Respir Crit Care Med* (2019) 199(4):465–77. doi: 10.1164/rccm.201807-1291OC
18. Dunn RM, Busse PJ, Wechsler ME. Asthma in the elderly and late-onset adult asthma. *Allergy* (2018) 73(2):284–94. doi: 10.1111/all.13258
19. Worth L, Michel S, Gaertner VD, Kabesch M, Schieck M. Asthma- and IgE-associated polymorphisms affect expression of TH 17 genes. *Allergy* (2018) 73 (6):1342–7. doi: 10.1111/all.13422
20. Narendra D, Blixt J, Hanania NA. Immunological biomarkers in severe asthma. *Semin Immunol* (2019) 46:101332. doi: 10.1016/j.smim.2019.101332
21. Peters SP, Busse WW. New and Anticipated Therapies for Severe Asthma. *J Allergy Clin Immunol Pract* (2017) 5(5S):S15–24. doi: 10.1016/j.jaip.2017.07.008
22. Muraro A, Lemanske RF Jr, Hellings PW, Akdis CA, Bieber T, Casale TB, et al. Precision medicine in patients with allergic diseases: Airway diseases and atopic dermatitis-PRACTALL document of the European Academy of Allergy and Clinical Immunology and the American Academy of Allergy, Asthma & Immunology. *J Allergy Clin Immunol* (2016) 137(5):1347–58. doi: 10.1016/j.jaci.2016.03.010
23. Richards LB, Neerincx AH, van Bragt JJMH, Sterk PJ, Bel EHD, Maitland-van der Zee AH. Biomarkers and asthma management: analysis and potential applications. *Curr Opin Allergy Clin Immunol* (2018) 18(2):96–108. doi: 10.1097/ACI.0000000000000426
24. Cárdaba B. Aspectos genéticos, ambientales y epigenéticos de las enfermedades alérgicas. In: IJ Dávila González, I Jauregui Presa, JM

Olaguibel Rivera y J.M. Zubeldía Ortuño, editors. *Tratado de Alergología, 2da Edición*. Madrid, Spain: Ergón (2015). p. 81–100.
25. Noell G, Faner R, Agustí A. From systems biology to P4 medicine: applications in respiratory medicine. *Eur Respir Rev* (2018) 27(147):170110. doi: 10.1183/16000617.0110-2017
26. Chung KF, Adcock IM. Precision medicine for the discovery of treatable mechanisms in severe asthma. *Allergy* (2019) 74(9):1649–59. doi: 10.1111/all.13771
27. Baos S, Calzada D, Cremades L, Sastre J, Quiralte J, Florido F, et al. Biomarkers associated with disease severity in allergic and nonallergic asthma. *Mol Immunol* (2017) 82:34–45. doi: 10.1016/j.molimm.2016.12.012
28. Baos S, Calzada D, Cremades L, Sastre J, Quiralte J, Florido F, et al. Data set on a study of gene expression in peripheral samples to identify biomarkers of severity of allergic and nonallergic asthma. *Data Brief* (2016) 10:505–10. doi: 10.1016/j.dib.2016.12.035
29. Baos S, Calzada D, Cremades-Jimeno L, Sastre J, Picado C, Quiralte J, et al. Nonallergic Asthma and Its Severity: Biomarkers for Its Discrimination in Peripheral Samples. *Front Immunol* (2018) 9:1416. doi: 10.3389/fimmu.2018.01416
30. Baos S, Calzada D, Cremades-Jimeno L, de Pedro M, Sastre J, Picado C, et al. Discriminatory Molecular Biomarkers of Allergic and Nonallergic Asthma and Its Severity. *Front Immunol* (2019) 10:1051. doi: 10.3389/fimmu.2019.01051
31. Valls R, Pujol A, Farrés J, Artigas L, Mas JM. *ANAXOMICS" Methodologies -Understanding the complexity of biological processes*. White paper (2013). Available at: http://www.anaxomics.com/white-papers.php.
32. Gimenez N, Tripathi R, Giró A, Rosich L, López-Guerra M, López-Oreja I. Systems biology drug screening identifies statins as enhancers of current therapies in chronic lymphocytic leukemia. *Sci Rep* (2020) 10(1):22153. doi: 10.1038/s41598-020-78315-0
33. Kanehisa M, Goto S, Kawashima S, Nakaya A. The KEGG databases at GenomeNet. *Nucleic Acids Res* (2002) 30(1):42–6. doi: 10.1093/nar/30.1.42
34. Croft D, Mundo AF, Haw R, Milacic M, Weiser J, Wu G, et al. The Reactome pathway knowledgebase. *Nucleic Acids Res* (2014) 42(Database issue):D472–7. doi: 10.1093/nar/gkt1102
35. Kerrien S, Aranda B, Breuza L, Bridge A, Broackes-Carter F, Chen C, et al. The IntAct molecular interaction database in 2012. *Nucleic Acids Res* (2012) 40 (Database issue):D841–6. doi: 10.1093/nar/gkr1088
36. Salwinski L, Licata L, Winter A, Thorneycroft D, Khadake J, Ceol A, et al. Recurated protein interaction datasets. *Nat Methods* (2009) 6(12):860–1. doi: 10.1038/nmeth1209-860
37. Keshava Prasad TS, Goel R, Kandasamy K, Keerthikumar S, Kumar S, Mathivanan S, et al. Human Protein Reference Database–2009 update. *Nucleic Acids Res* (2009) 37(Database issue):D767–72. doi: 10.1093/nar/gkn892
38. Licata L, Briganti L, Peluso D, Perfetto L, Iannuccelli M, Galeota E, et al. MINT, the molecular interaction database: 2012 update. *Nucleic Acids Res* (2012) 40(Database issue):D857–61. doi: 10.1093/nar/gkr930
39. Bishop CM. *Pattern Recognition and Machine Learning (Information Science and Statistics)*. M Jordan, J Kleinberg, B Schölkopf, editors. Berlin, Heidelberg: Springer-Verlag (2006).
40. Wishart DS, Feunang YD, Guo AC, Lo EJ, Marcu A, Grant JR, et al. DrugBank 5.0: a major update to the DrugBank database for 2018. *Nucleic Acids Res* (2018) 46(D1):D1074–82. doi: 10.1093/nar/gkx1037
41. Romeo-Guitart D, Forés J, Herrando-Grabulosa M, Valls R, Leiva-Rodríguez T, Galea E, et al. Neuroprotective Drug for Nerve Trauma Revealed Using Artificial Intelligence. *Sci Rep* (2018) 8(1):1879. doi: 10.1038/s41598-018-19767-3
42. Herrando-Grabulosa M, Mulet R, Pujol A, Mas JM, Navarro X, Aloy P, et al. Novel Neuroprotective Multicomponent Therapy for Amyotrophic Lateral Sclerosis Designed by Networked Systems. *PloS One* (2016) 11(1):e0147626. doi: 10.1371/journal.pone.0147626
43. Fiuza-Luces C, Santos-Lozano A, Llavero F, Campo R, Nogales-Gadea G, Díez-Bermejo J, et al. Muscle molecular adaptations to endurance exercise training are conditioned by glycogen availability: a proteomics-based analysis in the McArdle mouse model. *J Physiol* (2018) 596(6):1035–61. doi: 10.1113/JP275292
44. Lehár J, Zimmermann GR, Krueger AS, Molnar RA, Ledell JT, Heilbut AM, et al. Chemical combination effects predict connectivity in biological systems. *Mol Syst Biol* (2007) 3:80. doi: 10.1038/msb4100116
45. Gani F, Senna G, Piglia P, Grosso B, Mezzelani P, Pozzi E. Citochine ed asma [Cytokines and asthma]. *Recenti Prog Med* (1998) 89(10):520–8.
46. Urry Z, Xystrakis E, Hawrylowicz CM. Interleukin-10-secreting regulatory T cells in allergy and asthma. *Curr Allergy Asthma Rep* (2006) 6(5):363–71. doi: 10.1007/s11882-996-0005-8
47. Rose-John S, Waetzig GH, Scheller J, Grötzinger J, Seegert D. The IL-6/sIL-6R complex as a novel target for therapeutic approaches. *Expert Opin Ther Targets* (2007) 11(5):613–24. doi: 10.1517/14728222.11.5.613
48. Nagai H. Prostaglandin as a target molecule for pharmacotherapy of allergic inflammatory diseases. *Allergol Int* (2008) 57(3):187–96. doi: 10.2332/allergolint.R-08-161
49. Schwarz M, Sunder-Plassmann R, Cerwenka A, Pickl WF, Holter W. Regulation der Zytokinproduktion humaner T-Lymphozyten in der allergischen Immunantwort [Regulation of cytokine production by human T-lymphocytes in allergic immune response]. *Wien Klin Wochenschr* (1993) 105(23):672–6.
50. Keegan AD, Nelms K, White M, Wang LM, Pierce JH, Paul WE. An IL-4 receptor region containing an insulin receptor motif is important for IL-4-mediated IRS-1 phosphorylation and cell growth. *Cell* (1994) 76(5):811–20. doi: 10.1016/0092-8674(94)90356-5
51. Mulloy JC, Crownley RW, Fullen J, Leonard WJ, Franchini G. The human T-cell leukemia/lymphotropic virus type 1 p12I proteins bind the interleukin-2 receptor beta and gammac chains and affects their expression on the cell surface. *J Virol* (1996) 70(6):3599–605. doi: 10.1128/JVI.70.6.3599-3605.1996
52. Davies DE. Epithelial barrier function and immunity in asthma. *Ann Am Thorac Soc* (2014) 11 Suppl 5:S244–51. doi: 10.1513/AnnalsATS.201407-304AW
53. Guo Z, Wu J, Zhao J, Liu F, Chen Y, Bi L, et al. [IL-33/ST2 promotes airway remodeling in asthma by activating the expression of fibronectin 1 and type 1 collagen in human lung fibroblasts]. *Xi Bao Yu Fen Zi Mian Yi Xue Za Zhi (Chin J Cell Mol Immunol)* (2014) 30(9):975–9.
54. Chakir J, Shannon J, Molet S, Fukakusa M, Elias J, Laviolette M, et al. Airway remodeling-associated mediators in moderate to severe asthma: effect of steroids on TGF-beta, IL-11, IL-17, and type I and type III collagen expression. *J Allergy Clin Immunol* (2003) 111(6):1293–8. doi: 10.1067/mai.2003.1557
55. Chesné J, Braza F, Mahay G, Brouard S, Aronica M, Magnan A. IL-17 in severe asthma. Where do we stand? *Am J Respir Crit Care Med* (2014) 190 (10):1094–101. doi: 10.1164/rccm.201405-0859PP
56. Barnes PJ. The cytokine network in chronic obstructive pulmonary disease. *Am J Respir Cell Mol Biol* (2009) 41(6):631–8. doi: 10.1165/rcmb.2009-0220TR
57. Woodruff PG, Modrek B, Choy DF, Jia G, Abbas AR, Ellwanger A, et al. T-helper type 2-driven inflammation defines major subphenotypes of asthma. *Am J Respir Crit Care Med* (2009) 180(5):388–95. doi: 10.1164/rccm.200903-0392OC
58. Heijink IH, Nawijn MC, Hackett TL. Airway epithelial barrier function regulates the pathogenesis of allergic asthma. *Clin Exp Allergy* (2014) 44 (5):620–30. doi: 10.1111/cea.12296
59. Whelan T, Julian J, Levine M. Radiotherapy for breast cancer. *N Engl J Med* (2002) 346(11):862–4. doi: 10.1056/NEJM200203143461116
60. Evans CM, Kim K, Tuvim MJ, Dickey BF. Mucus hypersecretion in asthma: causes and effects. *Curr Opin Pulm Med* (2009) 15(1):4–11. doi: 10.1097/MCP.0b013e32831da8d3
61. Qi L, Xiangdong Z, Hongmei Y, Xiaohong N, Xiaoyan X. Regulation of neutrophil elastase-induced MUC5AC expression by nuclear factor erythroid-2 related factor 2 in human airway epithelial cells. *J Investig Med* (2010) 58 (5):730–6. doi: 10.231/JIM.0b013e3181d88fde
62. Lacy P, Weller PF, Moqbel R. A report from the International Eosinophil Society: eosinophils in a tug of war. *J Allergy Clin Immunol* (2001) 108(6):895–900. doi: 10.1067/mai.2001.120194
63. Loxham M, Davies DE, Blume C. Epithelial function and dysfunction in asthma. *Clin Exp Allergy* (2014) 44(11):1299–313. doi: 10.1111/cea.12309
64. Pniewska E, Sokolowska M, Kupryś-Lipińska I, Kacprzak D, Kuna P, Pawliczak R. Exacerbating factors induce different gene expression profiles in peripheral blood mononuclear cells from asthmatics, patients with chronic obstructive pulmonary disease and healthy subjects. *Int Arch Allergy Immunol* (2014) 165(4):229–43. doi: 10.1159/000370067
65. Chen B, Butte AJ. Network Medicine in Disease Analysis and Therapeutics. *Clin Pharmacol Ther* (2013) 94(6):627–9. doi: 10.1038/clpt.2013.181
66. Zhou X, Menche J, Barabási AL, Sharma A. Human symptoms–disease network. *Nat Commun* (2014) 26;5:4212. doi: 10.1038/ncomms5212

67. Mazein A, Ostaszewski M, Kuperstein I. Systems medicine disease maps: community-driven comprehensive representation of disease mechanisms. *NPJ Syst Biol Appl* (2018) 4:21. doi: 10.1038/s41540-018-0059-y
68. Ghiassian SD, Menche J, Barabási AL. A DiseAse MOdule Detection (DIAMOnD) algorithm derived from a systematic analysis of connectivity patterns of disease proteins in the human Interactome. *PloS Comput Biol* (2015) 11(4):e1004120. doi: 10.1371/journal.pcbi.1004120
69. Sharma A, Menche1 J, Huang CC, Ort T, Zhou X, Kitsak M, et al. A disease module in the interactome explains disease heterogeneity, drug response and captures novel pathways and genes in asthma. *Hum Mol Genet* (2015) 24 (11):3005–20. doi: 10.1093/hmg/ddv001
70. Nagata M, Saito K. The roles of cysteinyl leukotrienes in eosinophilic inflammation of asthmatic airways. *Int Arch Allergy Immunol* (2003) 131 Suppl 1:7–10. doi: 10.1159/000070474
71. Nadi E, Hajilooi M, Pajouhan S, Haidari M. Soluble L-Selectin as an Independent Biomarker of Bronchial Asthma. *J Clin Lab Anal* (2015) 29 (3):191–7. doi: 10.1002/jcla.21749
72. Knolle MD, Owen CA. ADAM8: a new therapeutic target for asthma. *Expert Opin Ther Targets* (2009) 13(5):523–40. doi: 10.1517/14728220902889788
73. Yalcin AD, Bisgin A, Gorczynski RM. IL-8, IL-10, TGF-β, and GCSF levels were increased in severe persistent allergic asthma patients with the anti-IgE treatment. *Mediators Inflammation* (2012) 2012:720976. doi: 10.1155/2012/720976
74. Isgrò M, Bianchetti L, Marini MA, Bellini A, Schmidt M, Mattoli S. The C-C motif chemokine ligands CCL5, CCL11, and CCL24 induce the migration of circulating fibrocytes from patients with severe asthma. *Mucosal Immunol* (2013) 6(4):718–27. doi: 10.1038/mi.2012.109
75. Taylor RC, Cullen SP, Martin SJ. Apoptosis: controlled demolition at the cellular level. *Nat Rev Mol Cell Biol* (2008) 9(3):231–41. doi: 10.1038/nrm2312
76. Abdulamir AS, Kadhim HS, Hafi RR, Ali MA, Faik I, Abubakar F, et al. Severity of asthma: the role of $CD25^+$, $CD30^+$, NF-κB, and apoptotic markers. *J Investig Allergol Clin Immunol* (2009) 19(3):218–24.
77. Mineev VN, Nesterovich II, Trofimov VI, Kashintseva TV, Rybakova MG, Grozov RV. Evaluating the activity of the apoptosis-regulating genes from Bcl-2, Bax expression, and caspase-3 activity in bronchial epithelial cells in patients with asthma. *Arkh Patol* (2011) 73(1):11–4. (in Russian).
78. Saeki H, Tamaki K. Thymus and activation regulated chemokine (TARC)/ CCL17 and skin diseases. *J Dermatol Sci* (2006) 43(2):75–84. doi: 10.1016/ j.jdermsci.2006.06.002
79. Romagnani S. Cytokines and chemoattractants in allergic inflammation. *Mol Immunol* (2002) 38: (12-13):881–5.
80. Chen YL, Chiang BL. Targeting TSLP with shRNA alleviates airway inflammation and decreases epithelial CCL17 in a murine model of asthma. *Mol Ther Nucleic Acids* (2016) 5(5):e316. doi: 10.1038/mtna.2016.29
81. Zhao T, Su Z, Li Y, Zhang X, You Q. Chitinase-3 like-protein-1 function and its role in diseases. *Signal Transduct Target Ther* (2020) 5(1):201. doi: 10.1038/ s41392-020-00303-7
82. Gao P, Simpson JL, Zhang J, Gibson PG. Galectin-3: its role in asthma and potential as an anti-inflammatory target. *Respir Res* (2013) 14(1):136. doi: 10.1186/1465-9921-14-136
83. Gao P, Gibson PG, Baines KJ, Yang IA, Upham JW, Reynolds PN, et al. Anti-inflammatory deficiencies in neutrophilic asthma: reduced galectin-3 and IL-1RA/IL-1β. *Respir Res* (2015) 16(1):5. doi: 10.1186/s12931-014-0163-5
84. Zhang YQ, Gao XX. Association of RANTES gene polymorphisms with susceptibility to childhood asthma: A meta-analysis. *Med (Baltimore)* (2020) 99(29):e20953. doi: 10.1097/MD.0000000000020953
85. Liu D, Pan J, Zhao D, Liu F. MicroRNA-223 inhibits deposition of the extracellular matrix by airway smooth muscle cells through targeting IGF-1R in the PI3K/Akt pathway. *Am J Transl Res* (2018) 10(3):744–52.
86. Ma L, Brown M, Kogut P, Serban K, Li X, McConville J, et al. Akt activation induces hypertrophy without contractile phenotypic maturation in airway smooth muscle. *Am J Physiol Lung Cell Mol Physiol* (2011) 300(5):L701–9. doi: 10.1152/ajplung.00119.2009
87. Xie M, Mustovich AT, Jang Y, Trudeau JB, Ray A, Ray P, et al. IL-27 and type 2 immunity in asthmatic patients: association with severity, CXCL9, and signal transducer and activator of transcription signaling. *J Allergy Clin Immunol* (2015) 135(2):386–94. doi: 10.1016/ j.jaci.2014.08.023
88. Alevy YG, Patel AC, Romero AG, Patel DA, Tucker J, Roswit WT, et al. IL-13-induced airway mucus production is attenuated by MAPK13 inhibition. *J Clin Invest* (2012) 122(12):4555–68. doi: 10.1172/JCI64896
89. Saik OV, Demenkov PS, Ivanisenko TV, Bragina EY, Freidin MB, Goncharova IA, et al. Novel candidate genes important for asthma and hypertension comorbidity revealed from associative gene networks. *BMC Med Genomics* (2018) 11(Suppl 1):15. doi: 10.1186/s12920-018-0331-4

Conflict of Interest: The authors declare that the research was conducted in the absence of any commercial or financial relationships that could be construed as a potential conflict of interest.

Copyright © 2021 Cremades-Jimeno, de Pedro, López-Ramos, Sastre, Mínguez, Fernández, Baos and Cárdaba. This is an open-access article distributed under the terms of the Creative Commons Attribution License (CC BY). The use, distribution or reproduction in other forums is permitted, provided the original author(s) and the copyright owner(s) are credited and that the original publication in this journal is cited, in accordance with accepted academic practice. No use, distribution or reproduction is permitted which does not comply with these terms.

frontiers in Medicine

ORIGINAL RESEARCH
published: 03 May 2021
doi: 10.3389/fmed.2021.617393

Tanshinone IIA Combined With Cyclosporine A Alleviates Lung Apoptosis Induced by Renal Ischemia-Reperfusion in Obese Rats

He Tai[1†], Xiao-lin Jiang[1,2†], Nan Song[1], Hong-he Xiao[3], Yue Li[1], Mei-jia Cheng[1], Xiao-mei Yin[1], Yi-ran Chen[1], Guan-lin Yang[1], Xiao-yu Jiang[4], Jin-song Kuang[5], Zhi-ming Lan[6*] and Lian-qun Jia[1*]*

[1] Key Laboratory of Ministry of Education for Traditional Chinese Medicine Viscera-State Theory and Applications, Liaoning University of Traditional Chinese Medicine, Shenyang, China, [2] Department of Nephrology, The Fourth of Affiliated Hospital of Guangzhou University of Traditional Chinese Medicine (Shenzhen Traditional Chinese Medicine Hospital), Guangzhou University of Traditional Chinese Medicine, Shenzhen, China, [3] School of Pharmacy, Liaoning University of Traditional Chinese Medicine, Dalian, China, [4] Department of Foreign Languages, Dalian Medical University, Dalian, China, [5] Department of Endocrinology and Metabolism, The Fourth People's Hospital of Shenyang, Shenyang, China, [6] Department of Medical Laboratory, The Fourth Affiliated Hospital of Guangzhou University of Traditional Chinese Medicine (Shenzhen Traditional Chinese Medicine Hospital), Guangzhou University of Traditional Chinese Medicine, Shenzhen, China

OPEN ACCESS

Edited by:
Girolamo Pelaia,
University of Catanzaro, Italy

Reviewed by:
Yanan Jiao,
China Medical University, China
Ming-yang Wang,
Shenyang Agricultural University, China

***Correspondence:**
Lian-qun Jia
jlq-8@163.com
Zhi-ming Lan
davidsson@126.com
Jin-song Kuang
270174194@qq.com

[†] These authors have contributed equally to this work

Specialty section:
This article was submitted to Pulmonary Medicine, a section of the journal Frontiers in Medicine

Received: 14 October 2020
Accepted: 19 March 2021
Published: 03 May 2021

Citation:
Tai H, Jiang X-l, Song N, Xiao H-h, Li Y, Cheng M-j, Yin X-m, Chen Y-r, Yang G-l, Jiang X-y, Kuang J-s, Lan Z-m and Jia L-q (2021) Tanshinone IIA Combined With Cyclosporine A Alleviates Lung Apoptosis Induced by Renal Ischemia-Reperfusion in Obese Rats. Front. Med. 8:617393. doi: 10.3389/fmed.2021.617393

Acute lung injury (ALI), which is induced by renal ischemia-reperfusion (IR), is one of the leading causes of acute renal IR-related death. Obesity raises the frequency and severity of acute kidney injury (AKI) and ALI. Tanshinone IIA (TIIA) combined with cyclosporine A (CsA) was employed to lessen the lung apoptosis led by renal IR and to evaluate whether TIIA combined with CsA could alleviate lung apoptosis by regulating mitochondrial function through the PI3K/Akt/Bad pathway in obese rats. Hematoxylin-eosin (HE) staining was used to assess the histology of the lung injury. Terminal deoxynucleotidyl transferase-mediated dUTP nick end-labeling (TUNEL) was used to assess apoptosis of the lung. Electron microscopy was used to assess mitochondrial morphology in lung cells. Arterial blood gas and pulmonary function were used to assess the external respiratory function. Mitochondrial function was used to assess the internal respiratory function and mitochondrial dynamics and biogenesis. Western blot (WB) was used to examine the PI3K/Akt/Bad pathway-related proteins. TIIA combined with CsA can alleviate lung apoptosis by regulating mitochondrial function through the PI3K/Akt/Bad pathway in obese rats.

Keywords: renal ischemia-reperfusion, obesity, mitochondrial dysfunction, acute lung injury, tanshinone IIA, cyclosporine A

INTRODUCTION

Acute kidney injury (AKI), as a common complication, is very serious, and even life-threatening (high mortality) in critically patients (1). The major cause of AKI is renal ischemia-reperfusion (IR) (2). Obesity is closely correlated with metabolic syndromes, including hyperuricemia, hyperlipidemia, and diabetes, and they can lead to hypertension and pathoglycemia and can all be seen as chronic hyperinflammatory conditions (3), which increase the severity and morbidity related to kidney disease (4). Ischemia AKI is often combined with multiple-organ dysfunction. It

is worth noting that respiratory failure rather than kidney failure is the main cause of death induced by AKI (5). The pathogenesis of acute lung injury (ALI) led by acute renal IR is ambiguous, which could be related to renal dysfunction-induced overload volume and hyperinflammatory state-induced lung injury (6). Lung endothelial cell inflammation and apoptosis induce ALI following AKI induced by renal IR (7, 8). As a potential mediator between lung and kidney injury, pulmonary microvascular endothelial cells (PMVECs) express proapoptosis and proinflammation genes, which can change after AKI is induced by renal IR (7, 8). Numerous studies have demonstrated that the occurrence of IR (especially in the nerves and heart) is closely related with mitochondrial dysfunction (9, 10). However, to our knowledge, no study has explored the change of mitochondrial function in the lung following renal IR in obese rats.

As the main active ingredient of the *Salvia miltiorrhiza* Bge, the main biological activities of tanshinone IIA (TIIA) are reducing the inflammatory response and resisting oxidant stress (11). Additionally, TIIA has a protective effect against myocardial ischemia (12). TIIA relieved acute lung injury induced by lipopolysaccharide *via* reducing proinflammatory factors and TRPM7 (13). In the meantime, TIIA performed a protective role in AKI induced by folic acid (14). Several studies have shown that TIIA can inhibit mitochondrial permeability transition pore (mPTP) and then achieve the aims of cardioprotection (15) and liver protection (16). With its anticalcineurin properties, cyclosporine A (CsA) can bind to cyclophilin D (CyP-D), preventing mPTP opening, and thereby decreasing the injury due to IR (17). CsA injection before ischemia can be used to preserve renal function (18). There are few studies available on TIIA and CsA lung protection through preventing mPTP opening.

Phosphoinositide-3 kinase (PI3K) transduces survival effects, which depend on the Akt kinase phosphorylation and activation, followed by proapoptotic Blc-2 family protein (Bad) phosphorylation and inhibition. PI3K plays a significant role in growth factor signal transduction. Under various cytokines and the activation of physiochemical factors, PI3K can produce myoinositol as a second messenger, and Akt performs crucial roles in many biological processes, including cell metabolism, cell cycle, cell growth, and apoptosis (19). The PI3K/Akt/Bad signaling pathway performs a significant function in inhibiting mitochondria-mediated apoptosis (20). However, there have been no studies on TIIA and CsA pulmonary protection with correcting mitochondrial dysfunction through the PI3K/Akt/Bad signal pathway in obese rats.

Given the increasing epidemic of obesity, especially in old people, the current study aimed to evaluate a method for AKI (induced by IR)-induced lung mitochondrial dysfunction using a combination of TIIA and CsA to cross the gap between mitochondrial dysfunction and lung injury, for the purpose of finding new therapeutic targets.

Abbreviations: IR, ischemia-reperfusion; AKI, acute kidney injury; ALI, acute lung injury; CsA, cyclosporine A; TIIA, tanshinone IIA; HE, hematoxylin-eosin; TUNEL, terminal deoxynucleotidyl transferase-mediated dUTP nick end-labeling; MMP, mitochondrial membrane potential; ATP, adenosine triphosphate; ROS, reactive oxygen species; RCR, respiration controlling rate; mPTP, mitochondrial permeability transition pore; OD, optical density; CyP-D, cyclophilin D; DMSO, dimethylsulfoxide; HFD, high-fat diet; NF-κB, nuclear translocation of the transcription factors; SD, Sprague-Dawley; PBS, phosphate-buffered saline; DAPI, 4′,6-diamidino-2-phenylindole; DCFH-DA, 2′,7′-dichlorofluorescein diacetate; RT-qPCR, real-time quantitative PCR; HE, hematoxylin-eosin; PaO_2, partial pressure of oxygen; $PaCO_2$, partial pressure of carbon dioxide; NAM, Non-invasive Airway Mechanics; TV, tidal volume; MV, minute ventilation; PIF, peak inspiratory force; PEF, peak expiratory force; EF50, exhale force metaphase; Sraw, specific resistance of airway; BCA, bicinchoninic acid; qPCR, quantitative polymerase chain reaction; mPTP, mitochondrial permeability transition pore; mtDNA, mitochondrial DNA; MPO, myeloperoxidase; IRI, ischemia-reperfusion injury; ANOVA, analysis of variance; PI3K, phosphoinositide-3 kinase; Cyt-c, cytochrome c; PARP, poly ADP-ribose polymerase.

RESULTS

Causes of Death During the Experiment

Ultimately, 66 rats [Sham group (13 rats), IR group (13 rats), IR (obese) group (10 rats), TIIA group (10 rats), CsA group (11 rats), and TIIA+CsA group (9 rats)] finished the study, and 54 rats died during the study (**Table 1**).

TIIA Combined With CsA Improved the Arterial Blood Gas and Pulmonary Function Led by Acute Renal IR in Obese Rats

We used arterial blood gas (**Figure 1A**) and pulmonary function (**Figure 1B**), which are external indicators of respiratory function. IR and IR (obese) can both decrease the blood pH, arterial partial pressure of carbon dioxide ($PaCO_2$), and arterial partial pressure of oxygen (PaO_2) especially IR (obese) ($p < 0.05$), and they can be increased by TIIA, CsA, and TIIA+CsA ($p < 0.05$), while pretreatment with TIIA+CsA was higher than TIIA and CsA ($p < 0.05$; **Figure 1A**). Rat pulmonary function was tested to further assess the lung injury. The TV, MV, PIF, PEF, and EF50 were decreased by IR and IR (obese), especially the IR (obese) ($p < 0.05$), which were decreased by TIIA, CsA, and TIIA+CsA ($p < 0.05$), and pretreatment with TIIA+CsA was higher than TIIA and CsA ($p < 0.05$). The Sraw was increased by IR and IR (obese), especially in the IR (obese) ($p < 0.05$), which were upregulated by TIIA, CsA, and TIIA+CsA ($p < 0.05$), and pretreatment with TIIA+CsA was lower than TIIA and CsA ($p < 0.05$; **Figure 1B**).

TIIA Combined With CsA Improved the Lungs Pathological Structure Led by Acute Renal IR in Obese Rats

We observed lung histology employing hematoxylin-eosin (HE) staining (**Figure 2A**). The alveoli only had slight exudation in the Sham group. Obviously, IR and IR (obese) can increase the numbers of disordered alveoli, especially IR (obese), with large numbers of inflammatory cells and blood cells in the alveolar cavity, combined with an obvious pulmonary interstitial edema. However, using TIIA, CsA, and TIIA+CsA could alleviate lung injury, shown as an improvement in interstitial edema and a reduction in inflammatory cells and red cells in the alveoli. All the changes associated with injury were evaluated through histological scores (**Figure 2B**). Statistical results showed that the IR and IR (obese) could increase the lung injury scores compared

TABLE 1 | The cause of death in the six groups rats.

Cause of death	Sham	IR (non)	IR (obese)	TIIA	CsA	TIIA+CsA
Infection after injection	00	0	0	1	0	0
Massive hemorrhage	1	1	2	2	3	3
Infection after surgery	2	2	3	3	2	3
Intestinal obstruction	4	4	5	4	4	5
Number of completed cases [*n* (%)]	13 (65.00%)	13 (65.00%)	10 (50.00%)	10 (50.00%)	11 (55.00%)	9 (45.00%)

with the Sham ($p < 0.05$), and TIIA, CsA, or TIIA+CsA could decrease the injury scores ($p < 0.05$; **Figure 2B**).

Lung Mitochondrial Morphological Changes Led by Acute Renal IR in Obese Rats

We detect the mitochondrial function, which can be thought as an internal indicator of respiratory function. First, we used electron microscopy to observe the lung mitochondrial morphological changes (**Figure 2**).

Electron microscopy images (×40,000) of rat lung tissue showed that the alveolar type II epithelial cells of the IR and IR (obese) groups showed the abnormal mitochondrial morphology in the form of swelling, even membrane rupture (paired black arrow) following renal IR, and most of mitochondria showed the normal morphology indicators (single black arrow) in the sham group. Renal IR and IR (obese) could increase the percentage of damaged mitochondria compared with the Sham group ($p < 0.05$), especially in the IR (obese), and giving TIIA, CsA, and TIIA+CsA could decrease the percentage of damaged mitochondria ($p < 0.05$), and pretreatment with TIIA+CsA was lower than TIIA and CsA ($p < 0.05$; **Figures 2C,D**).

TIIA Combined With CsA Reduced Lung Apoptosis Led by Acute Renal IR in Obese Rats

To research the effect of TIIA combined with CsA on lung cell apoptosis led by acute renal IR in obese rats, TUNEL assay was used to assess lung cell apoptosis (**Figure 3A**). The apoptotic cells of lung tissue in the two groups [IR (obese) and IR] were obviously increased, especially IR (obese) group ($p < 0.05$). However, giving CsA, TIIA, CsA, and TIIA+CsA alleviated lung cell apoptosis ($p < 0.05$), and pretreatment with TIIA+CsA was lower than TIIA and CsA ($p < 0.05$; **Figure 3B**). IR (obese) and IR could activate the caspase-3, especially IR (obese) ($p < 0.05$), while giving TIIA, CsA, and TIIA+CsA could decrease caspase-3 activity in lung cells ($p < 0.05$; **Figure 3C**). The method of western blot was used to detect the cleaved caspase-3 (**Figure 3D**), which was increased by IR (obese) and IR, especially IR (obese) ($p < 0.05$). However, giving TIIA and CsA could decrease the protein level of cleaved caspase-9/3, and pretreatment with TIIA+CsA was lower than TIIA and CsA ($p < 0.05$; $p < 0.05$; **Figure 3E**).

TIIA Combined With CsA Can Improve Mitochondrial Dysfunction Led by Acute Renal IR in Obese Rats

We detected the RCR, mitochondrial ROS, ATP, MMP (ratio of red/green), the opening of mPAP (%), and the mtDNA to evaluate the mitochondrial function in lung tissue. Mitochondria of lung tissues were separated from rat lung tissues. Acute renal IR can increase the ROS level and the opening of mPAP (%) dramatically, especially in the IR (obese) ($p < 0.05$), ROS level and the opening of mPAP (%) can be decreased by giving CsA, TIIA, and TIIA+CsA ($p < 0.05$), and pretreatment with TIIA+CsA was lower than TIIA and CsA ($p < 0.05$). Mitochondrial RCR, ATP level, and the MMP (ratio of red/green) could be decreased by acute renal IR dramatically, especially the IR (obese) ($p < 0.05$), which could be increased by giving CsA, TIIA, and TIIA+CsA ($p < 0.05$), and pretreatment with TIIA+CsA was higher than TIIA and CsA ($p < 0.05$). We used real-time qPCR to evaluate the levels of mtDNA damage. IR (obese) and IR decreased ratios of long/short fragments, especially IR (obese) ($p < 0.05$), which could be increased by giving CsA, TIIA, and TIIA+CsA ($p < 0.05$), and pretreatment with TIIA+CsA was higher than TIIA and CsA ($p < 0.05$; **Figure 4**).

TIIA Combined With CsA Can Improve the Abnormity of Mitochondrial Biogenesis and Dynamics Induced by Acute Renal IR in Obese Rats

Real-time qPCR and western blot were used to measure the mitochondrial dynamics and biogenesis, and we chose PGC-1α, Nrf1, and Tfam to represent mitochondrial biogenesis and Drp1 (fission), Mfn1 (fusion), and Mfn2 (fusion) to stand for mitochondrial dynamics (fission and fusion courses). In our study, the results showed that IR (obese) and IR could decrease the mRNA and protein levels of PGC-1α, Nrf1, Tfam, and Drp1, especially in the IR (obese) ($p < 0.05$), which were increased by giving with CsA, TIIA, and TIIA+CsA, and pretreatment with TIIA+CsA was higher than TIIA and CsA ($p < 0.05$; $p < 0.05$). IR (obese) and IR could increase the mRNA and protein expression levels of Mfn1 and Mfn2, especially IR (obese) ($p < 0.05$), which can be decreased by giving CsA, TIIA, and TIIA+CsA ($p < 0.05$), and pretreatment with TIIA+CsA was lower than TIIA and CsA ($p < 0.05$; **Figures 5A,B**).

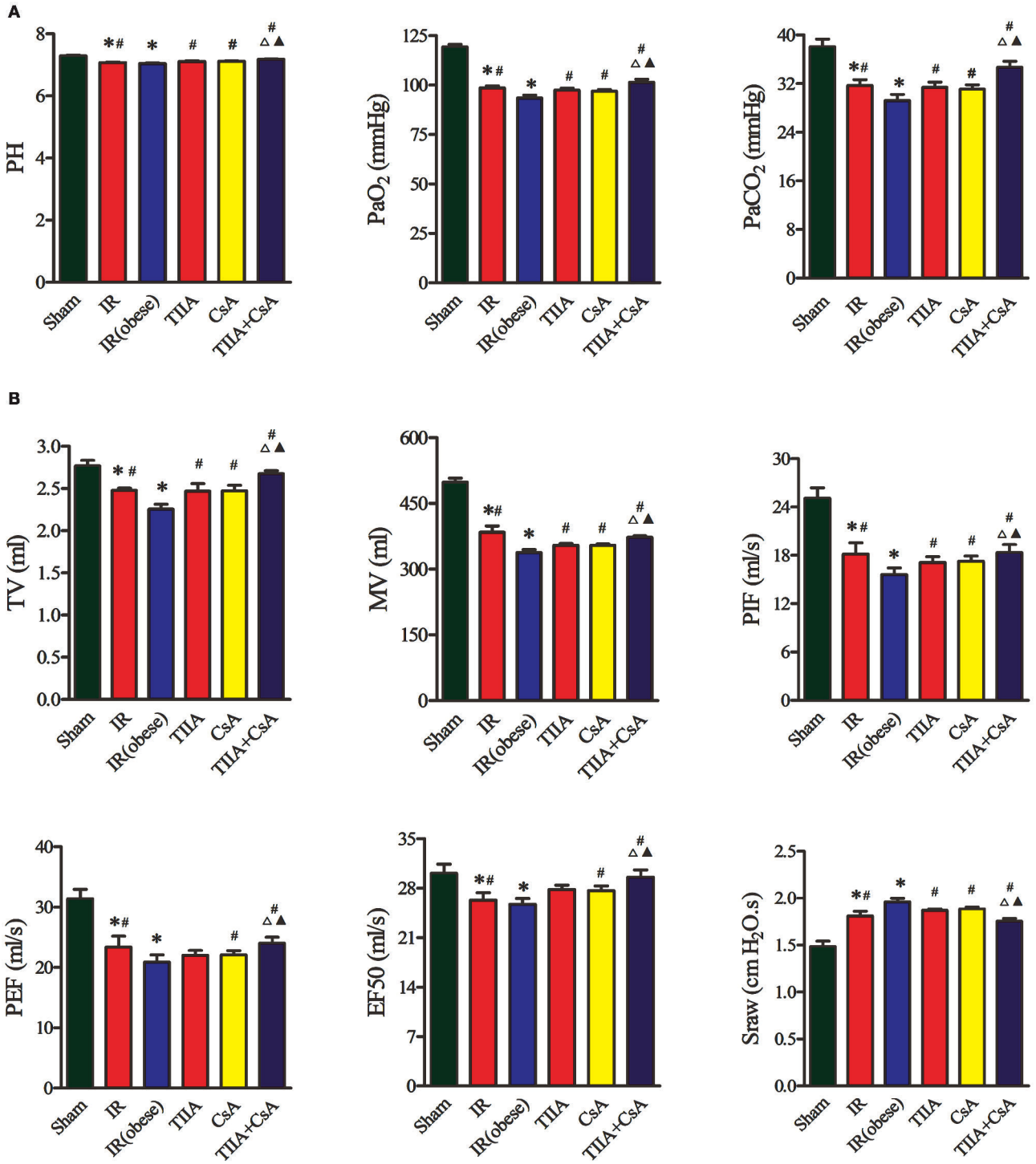

FIGURE 1 | Tanshinone IIA (TIIA)+ cyclosporine A (CsA) improved the arterial blood gas and pulmonary function induced by renal ischemia-reperfusion (IR). Rats were pretreated with TIIA alone or in combination with CsA followed by removing the right kidney and clamping of the left renal artery for 30 min and reperfusion for 24 h. Sham rats were used as control. Representative arterial blood gas **(A)** and pulmonary function **(B)** were evaluated under different conditions. The scale bars represent a length of 200 μm on histology. Data are shown as mean ± SD. $^{*}p < 0.05$ vs. sham group, $^{\#}p < 0.05$ vs. IR (obese) group, $^{\triangle}p < 0.05$ vs. TIIA group, $^{\blacktriangle}p < 0.05$ vs. CsA group.

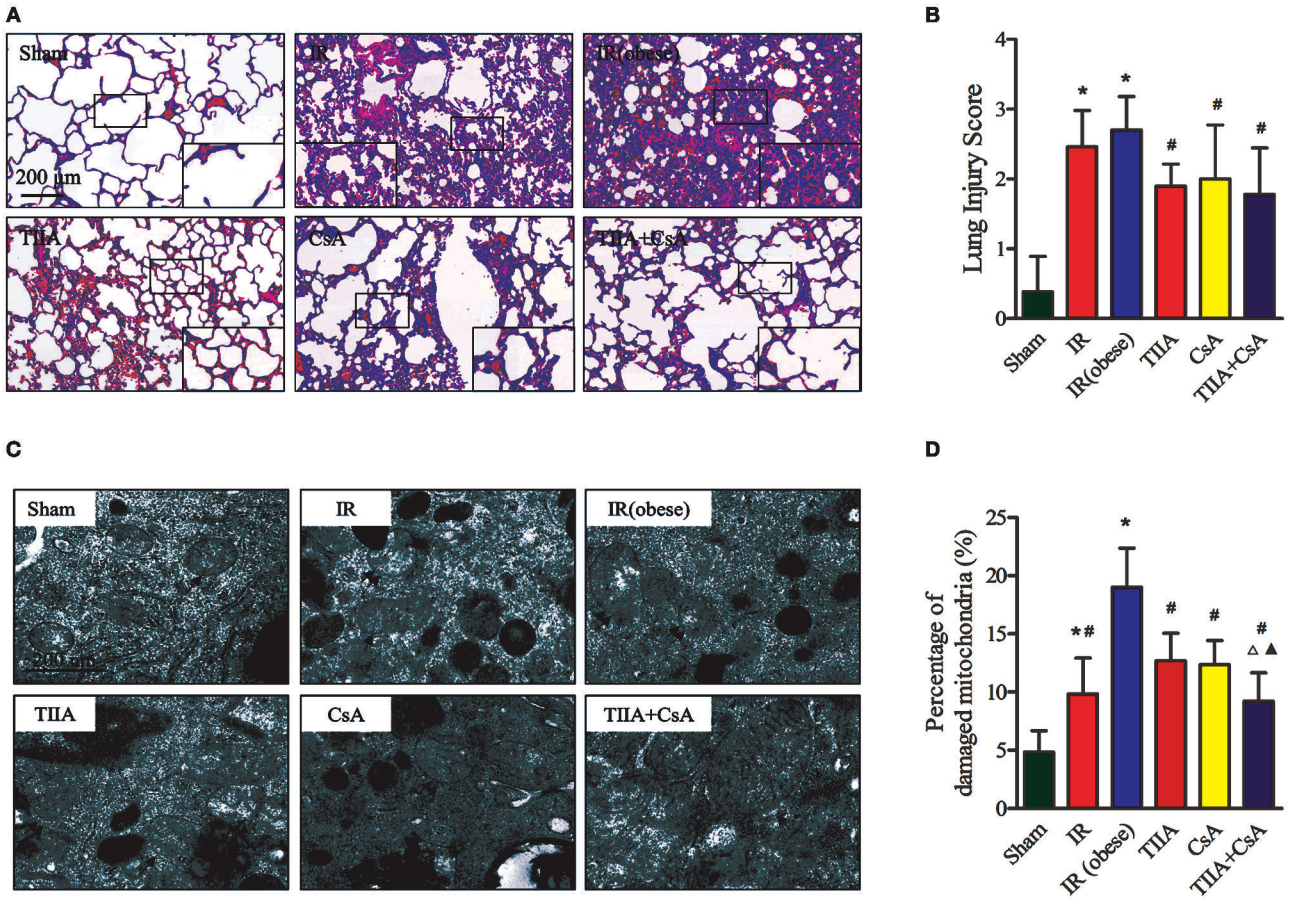

FIGURE 2 | Tanshinone IIA (TIIA)+ cyclosporine A (CsA) preserved lung architecture in renal ischemia-reperfusion (IR)-induced lung injury. Rats were pretreated with TIIA alone or in combination with CsA followed by removing the right kidney and clamping of the left renal artery for 30 min and reperfusion for 24 h. Sham rats were used as control. Representative photomicrographs of lung histology **(A)**, the scale bars represent a length of 200 μm on histology, and lung injury scores **(B)** were evaluated under different conditions. The scale bars represent a length of 200 μm on histology. Electron microscope pictures (×40,000) of rat lung tissue after renal ischemia-reperfusion (IR). Abnormal mitochondrial (paired black arrow) morphology showed mitochondrial membrane rupture or swellings; normal mitochondrial (single black arrow) morphology type showed smooth mitochondrial membrane and smooth and distinct inner carinulae **(C)**, and percentage of damaged mitochondria **(D)**. Data are shown as mean ± SD. $^{*}p < 0.05$ vs. sham group, $^{\#}p < 0.05$ vs. IR (obese) group, $^{\triangle}p < 0.05$ vs. TIIA group, $^{\blacktriangle}p < 0.05$ vs. CsA group.

TIIA Combined With CsA Modulated the PI3K/Akt/Bad Pathway

Finally, western blot was used to measure the target proteins of the PI3K/Akt/Bad pathway. We detected the PI3K, Akt, p-Akt, Bad, p-Bad, Bcl-2, Bax, Cyt-c, caspase-3, and PARP protein expression levels. The protein expression levels of Bax, Cyt-c, caspase-3, and PARP could be dramatically increased by acute renal IR, especially IR (obese) ($p < 0.05$), which could be decreased by giving CsA, TIIA, and TIIA+CsA ($p < 0.05$), and pretreatment with TIIA+CsA was lower than TIIA and CsA ($p < 0.05$). TIIA, CsA, and TIIA+CsA could induce Akt phosphorylation and enhance PI3K, p-Akt, p-Bad, and Bcl-2 expression and downregulate expression of p-Bad/Bad, Cyt-c, caspase-3, and PARP, especially TIIA+CsA ($p < 0.05$; **Figure 6**).

DISCUSSION

AKI often induces ALI in critically ill patients. When AKI is combined with ALI, the mortality is as high as ∼80% (21). As a clear risk factor for cardiovascular disease, hyperlipidemia can increase the risk of renal I/R injury by increasing ROS and inflammation (22, 23). In our study, we used high-fat diet (HFD) to feed rats to establish an obesity model. HFD cannot induce a significant injury in renal function and histological structure but can increase nuclear translocation of transcription factors (e.g., NF-κB) and their activity; these effects in turn could worsen the inflammatory damage in an autocrine-dependent manner (23). Renal IR triggers many complex changes that eventually induce apoptosis and necrosis in renal tissues. Inflammation and ROS can be increased by oxidative stress,

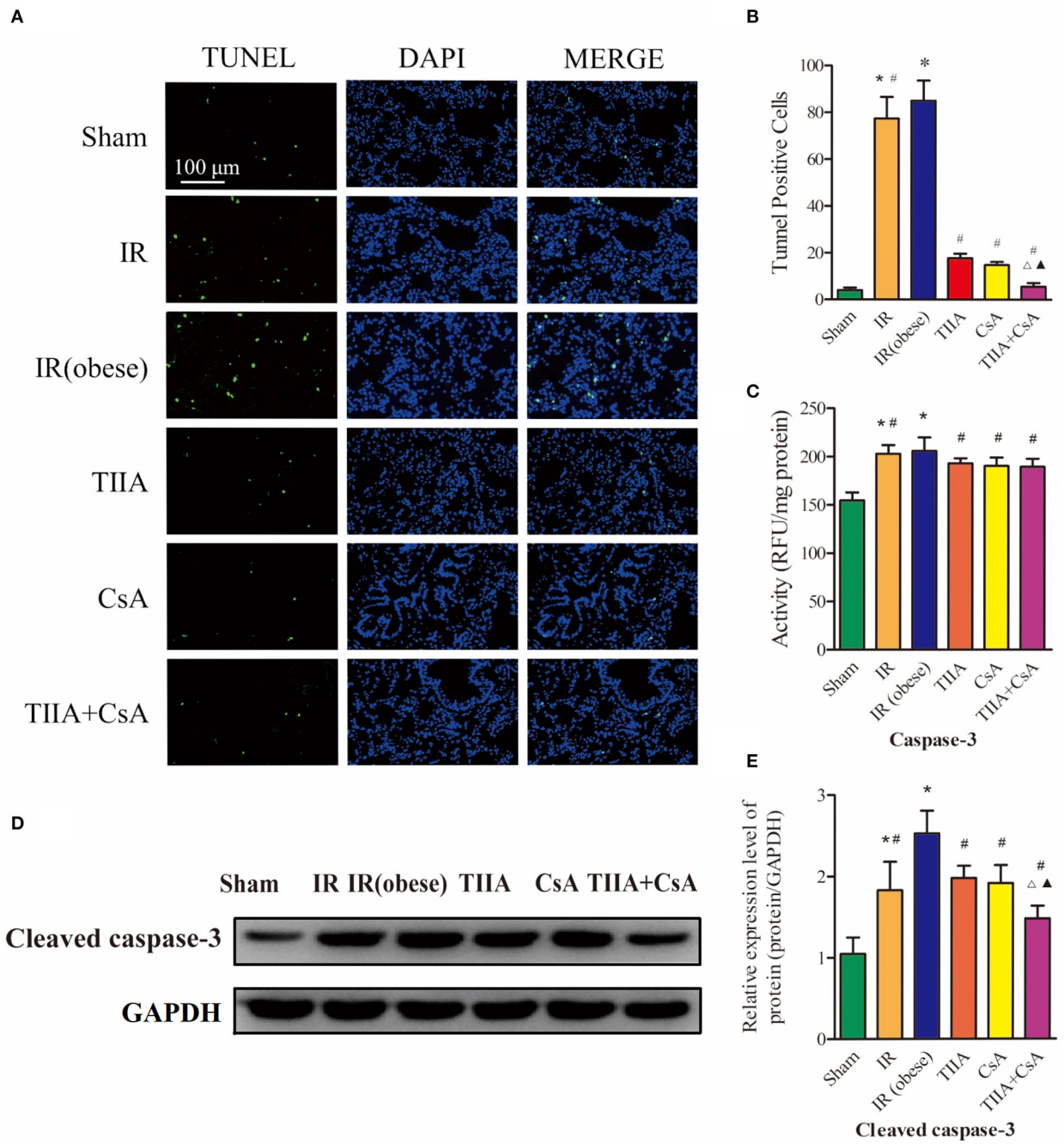

FIGURE 3 | Tanshinone IIA (TIIA)+ cyclosporine A (CsA) inhibited lung cells apoptosis after renal ischemia-reperfusion (IR). **(A)** Lung apoptosis with TUNEL; **(B)** TUNEL-positive cells in lung; **(C)** caspase-3 activity. Rats were pretreated with TIIA alone or in combination with CsA followed by removing the right kidney and clamping of the left renal artery for 30 min and reperfusion for 24 h. Sham rats were used as control. Representative apoptosis of lung cells **(A)** and TUNEL-positive cells **(B)** were evaluated under different conditions. The scale bars represent a length of 100 μm on histology. The activity of myocardial caspase-3 **(C)**, the protein expression of cleaved caspase-3 **(D)**, and the protein expression of cleaved caspase-3 **(E)** were evaluated in different groups. Data are shown as mean ± SD. $^{*}p < 0.05$ vs. sham group, $^{\#}p < 0.05$ vs. IR (obese) group, $^{\triangle}p < 0.05$ vs. TIIA group, $^{\blacktriangle}p < 0.05$ vs. CsA group.

inducing proinflammatory mediator release during the phase of reperfusion. For the mechanism of renal IR described above, several anti-inflammatory and antioxidant agents were discovered to play effective roles in reducing the injury of renal IR. They can raise the survivability of the kidney induced by IR injury (24). AKI often goes with ALI in critically ill patients, and

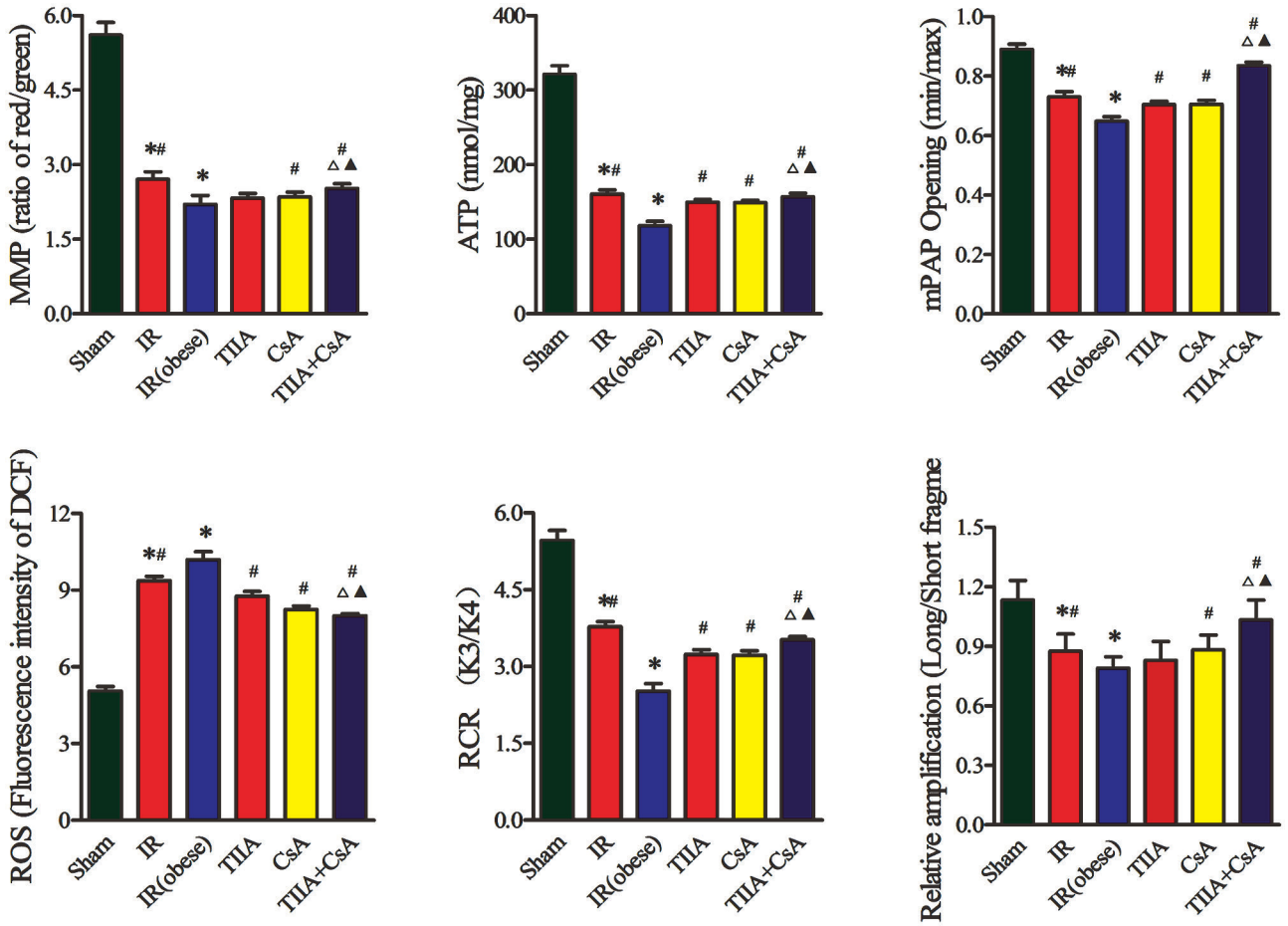

FIGURE 4 | Tanshinone IIA (TIIA)+ cyclosporine A (CsA) preserved lung mitochondrial function in renal ischemia-reperfusion (IR)-induced lung injury. The MMP (ratio of red/green), the mitochondrial ATP, the opening of mPAP (%), the mitochondrial ROS, the mitochondrial RCR, and the mtDNA damage (ratio of long/short fragments) were recorded above. Rats were pretreated with TIIA alone or in combination with CsA followed by removing the right kidney and clamping of the left renal artery for 30 min and reperfusion for 24 h. Sham rats were used as control. $^{*}p < 0.05$ vs. sham group, $^{\#}p < 0.05$ vs. IR (obese) group, $^{\triangle}p < 0.05$ vs. TIIA group, $^{\blacktriangle}p < 0.05$ vs. CsA group.

there is a clear relationship between AKI and ALI, but specific pathophysiological change between the kidney and the lungs remains unclear. This phenomenon has recently become a hot issue because of abnormal results; despite the use of dialysis, the mortality of AKI has remained at 50% (25), therefore, we must search for a new method to reduce the mortality of AKI combined with obesity. During 6 h of renal injury, pulmonary vascular permeability and associated lung diseases are increased due to oxidative stress and inflammation (5). Using multiple lines, White et al. found that apoptosis induced lung injury at 24 h (7). In our study, renal ischemia-reperfusion injury (IRI) induced ALI, and HE staining of lung histology for obese rats showed that renal IRI could notably induce disordered alveolar structure, large numbers of inflammatory cells and red blood cells in the alveolar cavity, and pulmonary interstitial edema, especially in the obesity model rats, and CsA, TIIA, and TIIA+CsA could alleviate lung injury (**Figure 2B**). In the meantime, the TUNEL results showed that acute renal IRI could induce lung cell apoptosis, and CsA, TIIA, and TIIA+CsA could decrease the quantity of apoptotic cells ($p < 0.05$; **Figure 3B**), pretreatment with TIIA+CsA was lower than TIIA and CsA. IR (obese) and IR could raise the activity of caspase-3 ($p < 0.05$; **Figure 3C**), and the cleaved caspase-3 in lung tissues could be raised by IR (obese) and IR (**Figure 3D**), and using CsA, TIIA, and TIIA+CsA could decrease them, especially in the TIIA+CsA ($p < 0.05$). ALI can induce lung cell apoptosis in a mechanism involving the α2AR/PI3K/Akt pathway in Li et al. (26). Structural damage of lung tissue decreases the external respiratory function; our results showed that the arterial blood pH value, PaO_2, and $PaCO_2$ were decreased in the two groups (IR (obese) and IR), especially in the IR (obese) group ($p < 0.05$; **Figure 1**). Our results are similar to those by Li et al. (26). The TV, MV, PIF, PEF, and EF50 can be decreased by IR and IR (obese). The Sraw can be raised by IR (obese) and IR ($p < 0.05$), and those index can be improved by giving CsA, TIIA, and TIIA+CsA, especially in the TIIA+CsA ($p < 0.05$; **Figure 1**).

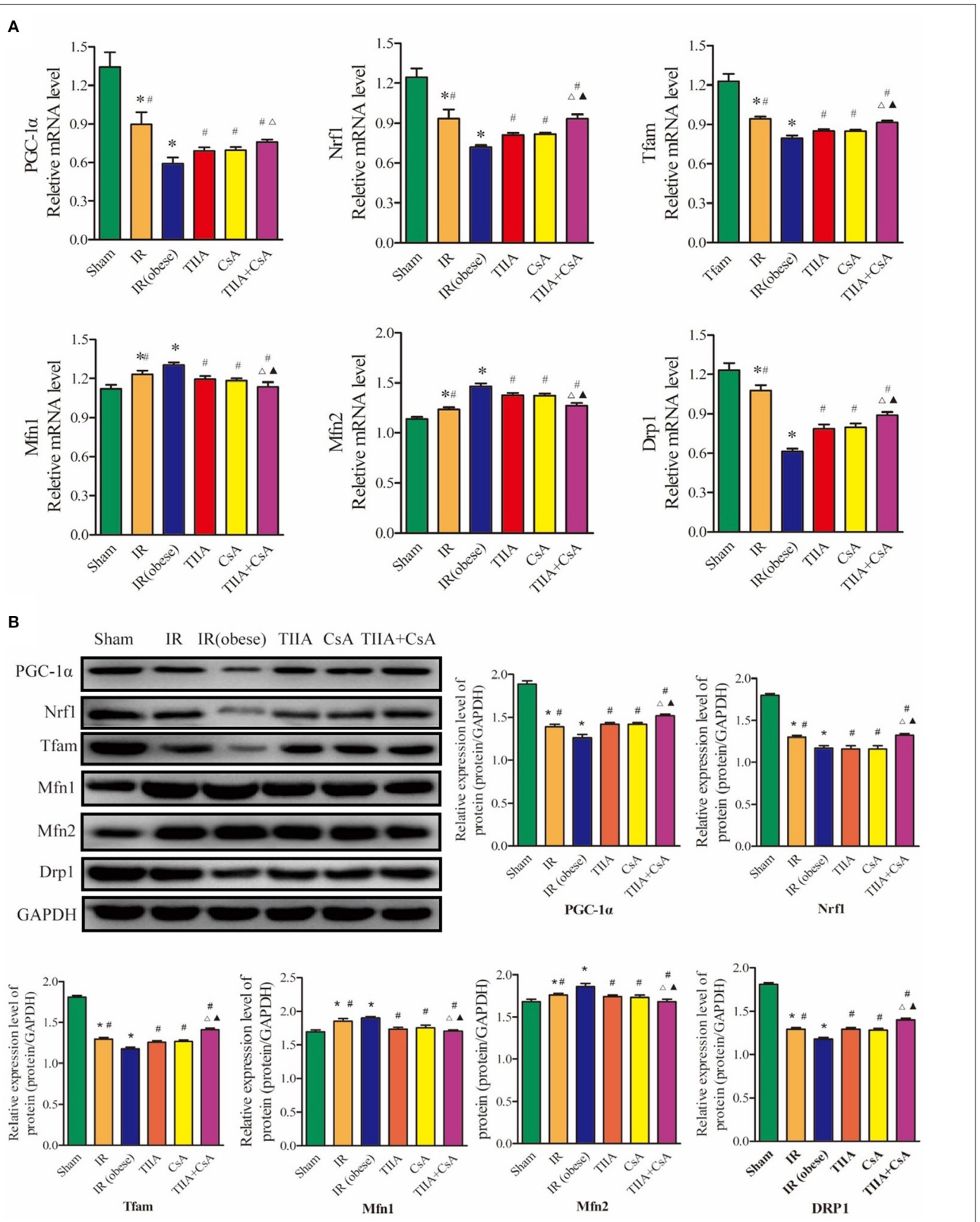

FIGURE 5 | Tanshinone IIA (TIIA)+ cyclosporine A (CsA) preserved lung mitochondrial biogenesis and dynamics in renal renal ischemia-reperfusion (IR)-induced lung injury. The expression of PGC-1α, Nrf1, and Tfam in mRNA **(A)** and protein **(B)** levels. The expression of Mfn1, Mfn2, and Drp1 in mRNA level. *$p < 0.05$ vs. sham group, #$p < 0.05$ vs. IR (obese) group, △$p < 0.05$ vs. TIIA group, ▲$p < 0.05$ vs. CsA group.

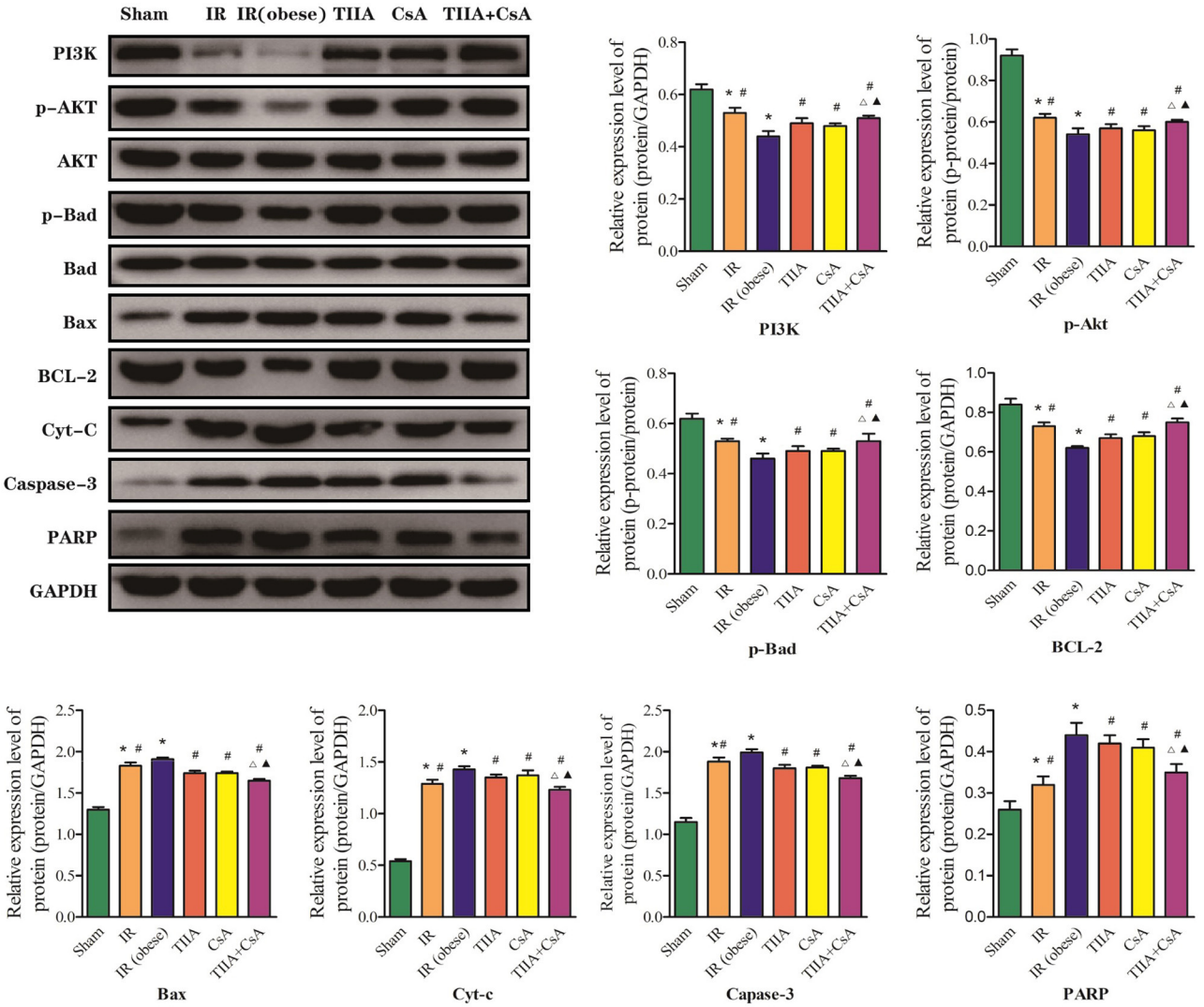

FIGURE 6 | Tanshinone IIA (TIIA)+ cyclosporine A (CsA) modulated myocardial PI3K/Akt/Bad pathway. The expression of PI3K, p-Akt, Akt, p-Bad, Bad, Bax, Bcl-2, Cyt-c, caspase-3, and PARP in protein level. $^{*}p < 0.05$ vs. sham group, $^{\#}p < 0.05$ vs. IR (obese) group, $^{\triangle}p < 0.05$ vs. TIIA group, $^{\blacktriangle}p < 0.05$ vs. CsA group.

To date, studies have shown that a variety of anti-inflammatory agents were discovered, including antiapoptotic agents (26), α-MSH (27), and IL-6 inhibitors (28). A previous research found that acute renal IR could induce lung mitochondrial dysfunction (only detected MMP) and that dexmedetomidine could attenuate lung inflammation, apoptosis, and MMP (26). However, using MMP alone to assess the mitochondrial dysfunction is too simple, and more methods and indexes can be used to assess the mitochondrial dysfunction. In our study, we detected MMP, opening of mPTP, mitochondrial ROS, mitochondrial ATP, mtDNA, and mitochondrial dynamics/biogenesis to assess the mitochondrial dysfunction comprehensively. However, no studies have explored the mitochondrial dysfunction in lungs induced by AKI, and no antimitochondrial dysfunction agents have been found to defend against ALI led by AKI in obese rats.

As a universal medicinal herb, modern technology has proved that *Salvia miltiorrhiza* Bge. can eliminate hazardous substances in the blood, promote thrombolysis and the activity of fibrinolytic enzymes, smooth blood vessels, reduce blood viscosity, and protect the cardiovascular system (29).

As the main active ingredient in *Salvia miltiorrhiza* Bge, TIIA can attenuate renal injury induced by renal IR through the downregulation of inflammation and the expression of myeloperoxidase (MPO) and caspase-3 (30). TIIA can decrease the release of cytochrome and the generation of ROS, prevent mPTP opening, reduce the percentage of apoptotic cells, and inactivate caspase-3 (31). Because CsA can inhibit the opening of the mPTP, it has been fundamental in implicating mPTP as a target for protective treatment, which can be improved at the initial stage of reperfusion (31). It is now widely believed that mitochondrial dysfunction (increasing the opening of mPTP

and decreasing MMP) plays an important role in raising injury induced by acute renal IRI (18). The opening of mPTP causes the membrane potential to inhibit oxidative phosphorylation and decrease and the swelling of mitochondria. The opening of the mPTP is operated by binding the CyP-D in the mitochondria membrane. Previous researches of the heart showed that CsA defended from IR by binding with CyP protein, independently of anticalcineurin properties, then inhibiting mPTP opening (32). However, to our knowledge, no study has explored whether CsA can be used to inhibit the opening of mPTP to protect renal IRI so as to protect lung mitochondria. Mitochondrial function can be conceptualized as the pathophysiological bridge between kidney-lung interactions during the clinical stage of renal IRI-induced ALI and AKI. Therefore, in this study, we hypothesized that the protective effect of TIIA and CsA on ALI was involved in improving the mitochondrial dysfunction.

As the energy center of cells, mitochondria supply more than 95% ATP (33). Therefore, mitochondria can be seen as a logical target in identifying pathophysiological processes and treatment target in various metabolic diseases. There are many methods for establishing ALI and AKI induced by renal IRI. To explore the mitochondrial relationship between the kidney and the lungs, renal IR rat model was established through removing the right kidney and clamping the left renal artery for 30 min, then reperfusing for 24 h, with pretreatment with TIIA combined with CsA, and then detecting the mitochondrial function. **Figure 2C** shows that acute renal IRI induced ALI, and using electron microscopy images (×40,000) of rat lung tissue, we could see the abnormal mitochondrial morphology typical of membrane rupture or mitochondrial swellings induced by renal IRI, especially in the obesity model rats, and we could decrease mitochondrial injury through pretreatment CsA, TIIA, and TIIA+CsA, especially with the TIIA+CsA ($p < 0.05$; **Figure 2C**). IR (obese) and IR could increase the percentage of damaged mitochondria in lung tissues ($p < 0.05$; **Figure 2D**). In the meantime, IR (obese) and IR could decrease the RCR, especially IR (obese), which could be relieved through pretreatment CsA, TIIA, and TIIA+CsA, especially with the TIIA+CsA ($p < 0.05$; **Figure 4**). The opening of mPAP (%) and ROS level could be increased by acute renal IR, and using TIIA and CsA could decrease the opening of mPAP (%) and ROS level ($p < 0.05$; **Figure 4**). MMP (ratio of red/green) and mitochondrial ATP level could be decreased by acute renal IR ($p < 0.05$), and using CsA, TIIA, and TIIA+CsA could decrease the MMP (ratio of red/green) and mitochondrial ATP level, especially with the TIIA+CsA ($p < 0.05$; **Figure 4**). Our results are similar to liver tissues reported by Luan et al. (34).

The mtDNA copy number in every mitochondria is constant; therefore, we can use the total copy number of mtDNA to evaluate mitochondria quantity in cells (35, 36). Although the mechanism of repairing mtDNA is unknown, mtDNA is adjacent to the respiratory chain, making it more fragile compared with nuclear DNA, because mtDNA is exposed to oxidative stress. In our study, we observed the injury effects of renal IR on mtDNA and CsA, TIIA, and TIIA+CsA had the protective effect. We used the ratio of long and short fragments to evaluate the degree of injury. Our results showed that IR (obese) and IR could decrease the ratio of long/short fragments, especially IR (obese) ($p < 0.05$), and pretreatment with CsA, TIIA, and TIIA+CsA could increase the ratio, especially with the TIIA+CsA ($p < 0.05$; **Figure 4**). Synthesis of electron transport chain proteins will be inhibited induced by damaged mtDNA, which will inhibit electron transport.

As an important adaptation of exposure to chronic energy deprivation, mitochondrial biogenesis may be modulated through multiple factors, such as Tfam and Nrf1. Nrf1 can facilitate the transcription of many nuclei-encoded mitochondrial proteins, including those involved in respiratory complexes and oxidative phosphorylation. Tfam can increase gene transcription and DNA replication in mitochondria through directly binding to the mitochondrial genome. PGC-1α is a critical transcriptional coactivator and can regulate key factors, including Nrf1 and Tfam and is thought to increase mitochondrial biogenesis (37). When the expression levels of the above genes change, mitochondrial biogenesis will become chaotic. **Figure 5** shows that acute renal IR could decrease the PGC-1α, Nrf1, and Tfam expression in the levels of mRNA and protein. TIIA+CsA markedly increased the mRNA and protein expression levels of PGC-1α, Nrf1, and Tfam. Pretreatment with, decreased ROS, a sufficient energy supply (ATP), and increased biogenesis factors may be operated synergistically to result in an improvement in the shortage of the intracellular energy supply (increasing ATP). Normally, harmful stimuli, including energy limitation, oxidative stress, and aging, can induce injury to mitochondria, which are then enclosed by autophagosomes, fused to lysosomes and finally degraded. Autophagy abnormalities in mitochondria can induce the increased levels of damaged mitochondria, resulting in mitochondrial dysfunction (34).

Normally, mitochondria undergo a fusion and fission dynamic process. This dynamic process plays a very important role in maintaining constant changes in the size, network of mitochondria, and shape; they are under the operation of Mfns and Drp1 proteins (38). Our results in **Figure 5** showed that the expression levels of Drp1 and Mfns (Mfn1 and Mfn2) changed in opposite directions after acute renal IR, indicating an imbalance of fission-fusion in mitochondria. Mfns and Drp1 were observed to play an important role in mitochondria fusion and mitochondria fission, respectively. We observed a decrease in Drp1 and an increase in Mfn1 and Mfn2 after acute renal IR in the lungs.

The PI3K/Akt/Bad signaling pathway performs an important function in inhibiting mitochondria-mediated apoptosis (20). Based on the close relationship between the PI3K/Akt/Bad pathway and apoptosis, we studied the effect of PI3K in our system. PI3K is a phosphatidylinositol kinase with activities as a serine/threonine-specific protein kinase and a phosphatidylinositol kinase (39). After activation, phosphatidylinositol family members on the cell membrane can be phosphorylated, and the downstream signal molecule Akt can be recruited and activated. Then, activated Akt phosphorylates Ser136/Ser112 residues of the Bad protein (40). Phosphorylated Bad separates from the apoptosis-promoting complex and forms a 14-3-3 protein complex, leading to the inactivation of its

apoptosis-promoting function and inhibiting apoptosis (41). Cytochrome c (Cyt-c) release from mitochondria into the cytosol can be induced by mitochondrial dysfunction, and Cyt-c can activate caspase-9 and caspase-3. Activation of either caspase can cleave poly ADP-ribose polymerase (PARP) and induce chromosomal DNA fragmentation (20). Our results showed that TIIA+CsA effectively regulated the expression of apoptotic PI3K/Akt/Bad pathway-related proteins, and CsA, TIIA, and TIIA+CsA could enhance PI3K and p-Akt expression and downregulate the expression of Cyt-c, cleaved caspase-3, and PARP. These results suggested that CsA, TIIA, and TIIA+CsA might improve mitochondrial function and inhibit the lung cells apoptosis induced by acute renal IRI through the PI3K/Akt/Bad signal pathway (**Figure 6**).

In our study, we separated mitochondria from lung tissues to demonstrate that renal IR promoted a large amount of ROS, which damaged proteins of the electron transport chain and mtDNA, ultimately damaging mitochondrial respiratory function, biogenesis and dynamic function and generating increasing amounts of ROS, especially in obese rats. The swelling of isolated mitochondria was led by the opening of the mPTP after IR. Opening the mPTP may cause a flow back of protons from the mitochondrial membrane space to the matrix, therefore, reducing MMP and ATP synthesis can induce metabolic abnormalities. The reductions in ATP synthesis and MMP were induced by the opening of the mPTP, resulting in the flow back of protons from the mitochondrial membrane space to the matrix, ultimately inducing the metabolic abnormalities and leading to lung cell apoptosis. However, pretreatment with TIIA+CsA can inhibit apoptosis by modulating mitochondrial function through activating the PI3K/Akt/Bad pathway in obese rats.

MATERIALS AND METHODS

Experimental Animals

Experiments were operated on male Sprague-Dawley (SD) rats)Liaoning Changsheng Biotechnology Co., Ltd. [Production License: SCXK(Liao) 2015-0001)], aged 8 weeks and weighing 180–220 g. The rats were housed in cages with controlled conditions of 45–65% humidity and 20 ± 3°C and with 12-h cycle of light/dark (lights on 06:00 h) and were fed with a pellet diet and water *ad libitum*.

Ethical Statement

Animal operating procedures and the experimental design were approved by the Ethical Committee of Animal Handling (2019019) of Liaoning University of Traditional Chinese Medicine, Shenyang, China and abided by the guidelines of the Care and Use of Laboratory Animals published by the US National Institutes of Health, and we made every effort to decrease the number of rats utilized and their suffering. In the meantime, we did our utmost to supply the better surroundings to the rats during research.

Drugs

TIIA (Injection of Sulfotanshinone Sodium, 10 mg each) was supplied by No. 1 Biochemical Pharmaceutical Co., Ltd in Shanghai. We used the deionized water to dissolve TIIA in order to obtain the 5-mg/ml stock solution. CsA (20 mg each) was obtained from Solarbio Science & Technology Co., Ltd, in Beijing. We used dimethylsulfoxide (DMSO) (0.1%) to dissolve CsA to obtain 2.5 mg/ml stock solution, which would be further diluted to obtain the appropriate concentration.

Animal Groupings and Methods of Drug Dosing

We randomly divided 120 rats into six groups, including the Sham operation, the IR, the IR (obese), the TIIA, the CsA, and the TIIA+ CsA group, with 20 rats in each group. All rats in the six groups were fed with general maintenance food for 2 weeks for the purpose of adapting to the environment. Then, the Sham group and the IR group were still fed with maintenance food for 8 weeks, but the other four groups were fed with HFD for 8 weeks. Sham group, the IR, and IR (obese) groups rats were given intraperitoneal injection of deionized water for 2 weeks. We gave 10 mg/(kg/day) TIIA (intraperitoneal injection) for 2 weeks before renal IR in the rats of TIIA group. We gave the 5-mg/kg CsA (intraperitoneal injection) 30 min before renal IR in the rats of CsA group, and the 10 mg/(kg/day) TIIA (intraperitoneal injection) for 2 weeks before renal IR+ 5 mg/kg CsA (intraperitoneal injection) 30 min before renal IR in the rats of TIIA+ CsA group. The components of the HFD included 25% total fat containing 18% protein, 11% unsaturated fat, 13% fiber, 44% carbohydrate, ash, and other ingredients (42). We chose the rats that increased 30% body weight for further research (43).

Surgical Procedure

We used the thiopental sodium (120 mg/kg) to anesthetize rats through intraperitoneal injection, and we pinched the rats paw and tail to evaluate the anesthetic effect. We opened the abdomen to expose the right kidney, and then dissected the renal pedicle to expose the renal vessels. 3–0 silk suture was used to ligate the blood vessel, and then we removed the right kidney. We exposed the left kidney, and used an arterial clamp to clamp off left renal artery for 30 min to build ischemia. With the 30-min ischemia, we removed the arterial clamp, and the tissue was reperfused for 24 h. The left kidneys were observed for 15 min to ensure normal blood reperfusion, which was shown by the color change of kidney to red again (44). The wound was closed with 3–0 silk suture. The rats were placed on a heating pad to maintain the 37°C body temperature throughout the whole experimental procedure. Sham-operated rats received the same surgical procedures without clamping off renal artery for 30 min (23).

Arterial Blood Gas Analysis

Arterial blood samples were used for arterial blood gas analysis. Arterial blood (0.5 ml) was obtained from the abdominal aorta, and the pH, partial pressure of oxygen (PaO_2), and partial pressure of carbon dioxide ($PaCO_2$) were measured with a blood gas analyzer (Beckman Coulter, Inc., USA).

Pulmonary Function Analysis

After the device [DSI's FinePointe Software and FinePointe Non-invasive Airway Mechanics (NAM) DSI, Inc., USA] was connected, rats were introduced into the double-lumen chamber and fixed to minimize the stress response. Data were collected after the double-lumen tube was stabilized. The data were collected and measured for 5 min each time. The rats were kept quiet before being measured. We chose tidal volume (TV), minute ventilation (MV), peak inspiratory force (PIF), peak expiratory force (PEF), exhale force Metaphase (EF50), and specific resistance of the airway (SRaw).

Histological Assessment of the Lung Using HE Staining

HE staining was performed as previously reported. After paraffin embedding, lung tissues were sectioned into 5-μm-thick sections (45). After immersion in paraformaldehyde (4%) for 24 h and then dehydration with ethanol (70%), we used H&E staining to stain the lung tissues and then visualized lung tissues with light microscopy. As previously reported, a scoring system was used to evaluate the histopathological injury (46). The injury degree of lung tissues was scored as follows (26): 0 grade, normal pulmonary tissues; 1 grade, mild or moderate infiltrations of leukocyte and neutrophil and interstitial congestion; 2 grade, formatting perivascular edema, partial leukocyte infiltration, and moderate infiltrations of neutrophils and leukocytes; and 3 grade, severe destruction in lung tissues and massive infiltration of neutrophils and leukocytes.

Apoptosis Assessment of the Lung Using TUNEL

We used the terminal deoxynucleotidyl transferase-mediated dUTP nick end-labeling (TUNEL) assay [*In Situ* Cell Death Detection Kit (Roche, Germany)] to detect apoptosis. As described in the HE staining section (45), we used 5-μm-thick sections to perform TUNEL staining. After deparaffinization and rehydration, protease K (10 μg/ml) was added to the sections for 15 min. The samples were supplemented with fresh TUNEL reaction mixture and were incubated at 37°C for 60 min with the dark. After washing, we used 0.1 μg/ml 4′,6-diamidino-2-phenylindole (DAPI) (Beyotime, China) to stain the cell nuclei. We used the fluorescence microscope (Canon, Japan) to analyze the samples in a drop of phosphate-buffered saline (PBS). We used a blinded manner to observe eight random visual fields per animal with ×200 magnification to calculate and analyze the number of TUNEL-positive cells per high-power field.

Caspase-3 Activity

We used the fluorescent caspase-specific substrate AcDEVD-7-pNA (Solarbio) to detect the caspase-3 activity. The lung tissue proteins (10 mg) were added to reaction buffer for incubation (37°C) for 2 h. We used the fluorimeter (405 nm) to quantify the enzyme-catalyzed release.

Using Electron Microscope to Observe Mitochondria

Lung tissues were obtained immediately after anesthesia and cut into small pieces (1 mm^3). After fixing the specimens with 2% glutaraldehyde at 4°C, we used phosphate buffer (0.1 mol/L) to wash the samples, which was then fixed with 1% osmium tetroxide and then stained with 1% aqueous uranyl acetate. We used capsules including embedding medium to place the specimens 70°C for approximately 48 h. Uranyl acetate and alkaline lead citrate were used to stain specimen sections then to observe under electron microscope (HITACHI H-7650, Tokyo, Japan).

Preparation of Lung Mitochondria Suspension

As previously studied in the liver (34), rats were anesthetized, and then the lung was harvested and placed in a pH 7.4 ice-cold isolated buffer (10 mM Tris-HCl, 250 mM sucrose, and 1 mM EDTA). After trimming, lung tissues were rinsed with a homogenizer in an isolation buffer, and 50–100 mg of tissue was weighed. For preserving mitochondria integrity, the whole isolation process was performed at 4°C. Following centrifugation at 700× *g* for 10 min, the supernatant was collected and the samples were centrifuged at 7,000× *g* for 10 min again. Then, we discarded the supernatant and washed the mitochondria pellet with 5 ml of isolation buffer, centrifuging twice in 7,000× *g* for 10 min. We obtained a clean mitochondria solution and preserved it in mitochondrial preservation solution (10 mM KH_2PO_4, 5 mM HEPES, 2 mM $MgCl_2$, 1 mM EDTA, 100 mM KCl, and 20 mM sucrose) to get a mitochondria suspension (5 mg/ml protein), which was placed on ice for immediate use. We measured the protein concentration of mitochondrial suspensions using the bicinchoninic acid (BCA) reagent box (Beyotime, Shanghai, China) and to ensure the protein concentrations were between 100 and 1,000 μg/ml. Mitochondria suspension was used to detect the mitochondrial membrane potential (MMP), the opening of the mPTP, reactive oxygen species (ROS), respiratory control rate (RCR), and adenosine triphosphate (ATP) synthesis.

Measurement of MMP

We detected the MMP using the mitochondrial membrane potential assay kit (Beyotime, Shanghai, China). (1) Diluting five times the JC-1 dyeing buffer into 1×; (2) then, we added five-diluted JC-1 working solution (0.9 ml) into purified mitochondria (0.1 ml) with the protein level 100–1,000 μg/ml; and (3) MMP was detected by fluoroenzyme-labeled reagent. We added mixed solution (1 ml) to fluoroenzyme-labeled assay, with the 530-nm emission wavelength and 490-nm excitation wavelength, and then the ratio of the red/green was calculated.

Measurement of ATP

We used the luciferase-based luminescence enhanced ATP assay kit (Beyotime, Shanghai, China) to measure the level of adenosine triphosphate (ATP) in the isolated mitochondria. We incubated isolated mitochondria (1 mg/ml) into the 0.5-mL respiration buffer (2.5 mM succinate, 2.5 mM malic acid, and 2.5 mM ADP)

for 10 min. We used the SpectraMax Paradigm Multi-Mode Microplate Reader (Molecular Devices, Sacramento, CA, USA) to detect the ATP concentrations.

The Opening of mPTP

The opening of the mPTP was measured by detecting the A540 absorbance of mitochondria exposed to 250 μM $CaCl_2$ ("+": treatment with Ca^+; "–": treatment without Ca^+). Purified Mitochondrial Membrane Pore Channel Colorimetric Assay kit (GENMED, Shanghai, China) was used for detection; 200 μmol/L $CaCl_2$ was used to induce mPTP opening. An ultramicro microporous plate spectrophotometer (Biotek, USA) was used to read the value of optical density (OD) from 0 to 10 min at 520 nm. The OD decrease reflected the mPTP opening. The OD value noted at the onset of the experiment (0 min) represented the minimum optical density (min OD); the OD value noted at the end of the experiment (10 min) represented the maximum optical density (min OD). The min/max OD was negatively associated with the extent of MPTP opening (34, 47).

Measurement of ROS

ROS was detected using a Multi-Mode Microplate Reader with a fluorescent probe of 2′,7′-dichlorodihydrofluorescein diacetate (DCFH-DA).

Measurement of RCR

We used the RCR (ratio of state III and state IV) to assess the integrity of isolated mitochondria, oxidative phosphorylation, and respiratory chain function. RCR was assessed using an Oxytherm Clark-type oxygen electrode (OXYT1/ED; Hansatech Instruments, Norfolk, UK). Sixty micrograms mitochondria (separated from the lung) were put into the oxytherm chamber containing pH 7.2 respiration buffer (0.1% BSA, 125 mM KCl, 20 mM HEPES, 2 mM $MgCl_2$, and 2.5 mM KH_2PO_4) and stirring respiration buffer at 37°C to ensure that all of the respiration buffer contained equal amounts of mitochondria. For each state of respiration, the slope of the response of mitochondria to consecutive administrations of respiration substrates was defined as rate of oxygen consumption, as previously reported (48).

Measurement of Damaged mtDNA

The injured mtDNA was calculated through the ratio of long and short fragments using real-time quantitative polymerase chain reaction (RT-qPCR). (1) DNA isolation: total lung DNA was extracted by the Genomic-tip 20/G kit (Qiagen, Valencia, CA, USA). The quantification of the PCR products or purified DNA was performed fluorometrically using the Picogreen dsDNA reagent (Invitrogen, Milan, Italy). (2) RT-qPCR was performed on lung DNA extracts as previously reported (35) using the following modification: the PCR amplification was performed using the Ranger DNA Polymerase with appropriate premixes (Bioline Ltd., London, UK). The two pairs (mtDNA long fragment and short fragment) of primers (General Biosystems, Anhui, China) are shown in **Table 2**. (3) For amplification of the mtDNA long fragment, the standard thermocycler program included an initial denaturation at 94°C (1 min), 94°C (15 s) for 18 cycles, 65°C (12 min), and a final extension at 72°C (10 min). The short fragment of the mtDNA was amplified by the same condition, except that the extension temperature was regulated to 60°C.

RNA Extraction and cDNA Synthesis

We isolated total genome RNA with TRIzol reagent (Invitrogen, Carlsbad, CA, USA). Spectrophotometry (260 nm) was used to assess the quality of isolated RNA. Reverse transcription was performed with 1 μg total RNA and an M-MLV Reverse Transcriptase Kit (Promega A3500; Promega, Madison, WI, USA). Briefly, the 40-μl total reaction volume was used in a Veriti 96 Well Thermal Cycler Long PCR system (Applied Biosystems, Foster City, CA, USA) according to the following reaction procedure: 72°C (3 min), 42°C (90 min), 70°C (15 min) and held at 4°C.

Real-Time qPCR

We used the RT-qPCR to detect the copy numbers of the transcription levels of specific genes with cDNA templates. PCR was performed on a Rotor-Gene Q Sequence Detection System (QIAGEN, Germany) using SYBR Premix Ex TaqII (TakaraBioINC) (49). The PCR was conducted in a 20-μl system (1 μl synthetic cDNA + 10 μl SYBR Premix Ex Taq II + 0.5 μM primers), with the following procedure: 95°C (10 min); 95°C (10 s), 40 cycles, 60 °C (15 s); 72 °C (20 s); and 72 °C (10 min). The values were calculated with GAPDH as the internal control (50). Two pairs of PCR primer sequences used in our study are shown in **Table 2**.

Protein Detection

Western blot was used to detect target protein. Total proteins were extracted from tissues using RIPA Lysis Buffer. Protein concentration was measured using a BCA Protein Assay Kit. To examine the expression of proteins, the same amount of total protein was loaded on an 8–12% sodium dodecyl sulfate-polyacrylamide gel electrophoresis (SDS-PAGE) gel. Separated proteins were then transferred onto PVDF membranes. After being blocked in skim milk solution, the membrane was incubated overnight separately with the antibodies anti-GAPDH, anti-PI3K, anti-p-Akt, anti-Akt, anti-p-Bad, anti-Bad, anti-Bax, anti-Bcl-2, anti-Cyt-c, anticaspase-3, anticleaved-caspase-3, anti-PARP, anti-Drp1, anti-Mfn1, anti-Mfn2, anti-PGC-1, anti-NRF1, and anti-TFam (antibodies are shown in **Table 3**). Subsequently, the membrane was incubated with secondary HRP-conjugated goat antirabbit antibodies (Santa Cruz Biotechnology). Proteins were visualized using an enhanced chemiluminescence kit from Thermo Fisher Scientific (Massachusetts, USA). ImageJ software (Alpha View SA) was used to perform densitometric analysis.

Statistical Analysis

Statistical analysis was operated by the SPSS statistical package (Version 17.0, SPSS Inc. Chicago, IL, USA). The mean ± standard deviation was used to express the data. The one-way analysis of variance (ANOVA) was used to compare among six independent groups. The two-to-two comparison among groups was used to analyze the variance, and Tukey's *t* test was used for

TABLE 2 | Sequence of primers for RT-PCR and long PCR.

Target gene	Primer sequence	Size (bp)	Tm (°C)
Mfn1	Forward: 5′-GGGAAGACCAAATCGACAGA-3′	152	57
	Reverse: 5′-CAAAACAGACAGGCGACAAA-3′		57
Mfn2	Forward: 5′-GAGAGGCGATTTGAGGAGTG-3′	165	58
	Reverse: 5′-CTCTTCCCGCATTTCAAGAC-3′		56
Drp1	Forward: 5′-GCCCGTGGATGATAAAAGTG-3′	215	56
	Reverse: 5′-TGGCGGTCAAGATGTCAATA-3′		56
PGC-1α	Forward: 5′-GGACGAATACCGCAGAGAGT-3′	201	59
	Reverse: 5′-CCATCATCCCGCAGATTTAC-3′		56
Nrf1	Forward: 5′-AAACCGAACACATGGCTACC-3′	168	58
	Reverse: 5′-CTGCCGTGGAGTTGAGTATG-3′		58
Tfam	Forward: 5′-TCACCTCAAGGGAAATTGAAG-3′	241	55
	Reverse: 5′-CCCAATCCCAATGACAACTC-3′		56
Long fragment	Forward:5′-AAAATCCCCGCAAACAATGACCACCC-3′	13,400	72
	Reverse: 5′-GGCAATTAAGAGTGGGATGGAGCCAA-3′		72
Shrot fragment	Forward: 5′-CCTCCCATTCATTATCGCCGCCCTGC-3′	235	60
	Reverse: 5′-GTCTGGGTCTCCTAGTAGGTCTGGGAA-3′		60
GAPDH	Forward: 5′- AGGTCGGTGTGAACGGATTTG—3′	20	58
	Reverse: 5′- GGGGTCGTTGATGGCAACA-3′		58

TABLE 3 | Antibodies used in the study.

Antibodies	Manufacturer	Catalog no.	Observed MW	Dilution
Anti-PI3K	Proteintech	67071-1-1g	110 KDa	1:10,000
Anti-p-Akt	Proteintech	66444-1-1g	62 KDa	1:10,000
Anti-Akt	Proteintech	10176-2-AP	56 KDa	1:5,000
Anti-p-Bad	Cell signaling technology	5284S	23 KDa	1:1,000
Anti-Bad	Proteintech	10435-1-AP	18 KDa	1:2,500
Anti-Bcl-2	Proteintech	26593-1-AP	26 KDa	1:2,500
Anti-Bax	Proteintech	50599-2-1g	26 KDa	1:10,000
Anti-Caspase-3	Proteintech	19677-1-AP	32 KDa	1:2,000
Anti-cleaved-Caspase-3	Abcam	ab49822	17 KDa	1:500
Anti-PARP1	Proteintech	13371-1-AP	89 KDa	1:2,000
Anti-Cyt-c	Proteintech	12245-1-AP	13 KDa	1:2,000
Anti-Mfn1	Proteintech	13798-1-AP	86 KDa	1:1,000
Anti-Mfn2	Proteintech	12186-1-AP	86 KDa	1:5,000
Anti-Drp1	Proteintech	10656-1-AP	27 KDa	1:4,000
Anti-PGC1a	Proteintech	66369-1-1 g	100 KDa	1:5,000
Anti-Nrf1	Proteintech	12482-1-AP	67 KDa	1:2,500
Anti-Tfam	Proteintech	22586-1-AP	25 KDa	1:5,000
Anti-GAPDH	Proteintech	60004-1-1g	36 KDa	1:10,000

multiple comparisons between six groups. We regarded $p < 0.05$ as having statistically significant difference.

CONCLUSIONS

Our results demonstrated that lung mitochondrial dysfunction was induced in the process of renal IR, especially in the obese rats. Mitochondrial dysfunction can be seen as the direct pathophysiological kidney-lung interactions during the stage of AKI and ALI induced by renal IR. During this process, lung mitochondrial function was impaired, dynamics was altered, and biogenesis was inhibited. ROS overproduction led to mtDNA damage and a significant decrease of MMP followed by a reduction of intracellular ATP. Thus, TIIA+CsA can be seen as a protective agent, which can attenuate lung apoptosis *via* modulating mitochondrial function by activating PI3K/Akt/Bad pathway in obese rats. But in our study, considering of the combination therapy, we did not use the PI3K/Akt/Bad pathway inhibitor, so the mechanism of drug intervention cannot be fully revealed. In the future, we will explore the other

protective mechanism of TIIA+CsA and the signaling pathway of apoptosis. These results may be a promising protective strategy for managing obesity-related AKI and ALI. However, this application needs further large-scale experimental and clinical studies.

DATA AVAILABILITY STATEMENT

The original contributions presented in the study are included in the article/supplementary material, further inquiries can be directed to the corresponding author/s.

ETHICS STATEMENT

The animal study was reviewed and approved by Animal operating procedures and the experimental design were approved by the Ethical Committee of Animal Handling (2019019) of Liaoning University of Traditional Chinese Medicine.

AUTHOR'S NOTE

We assess as a part of our study about heart apoptosis have been uploaded on a pre-print server which can be accessed at https://www.researchsquare.com/article/rs-77027/v1, and it has been submitted to another journal. Because our group have studied about the adjacent organs (the heart and lung) apoptosis induced by renal IR, and the materials and methods have many similarities which is hard to avoid, but the detection index are different from each other. In this manuscript we researched the lung apoptosis.

AUTHOR CONTRIBUTIONS

HT and X-lJ wrote the manuscript and researched data. YL, H-hX, and NS selected the rats and extracted blood. M-jC and X-mY dealed with the figures. Y-rC detected related index. G-lY and L-qJ contributed to the discussion and reviewed the manuscript. Rats model is builded by H-hX and M-jC. Editorial support (in the form of writing assistance, including development of the initial draft based on author input, assembling tables and figures, collating authors comments, grammatical editing, and referencing) was provided by HT, Z-mL, H-hX, and YL. The translator of English was provided by HT, X-lJ, and J-sK.

FUNDING

This study was supported by the National Natural Science Foundation of China to L-qJ (81774022), Fund Project of Innovation Team in Liaoning to L-qJ (LT2016012), Inheritance and Innovation Project of Traditional Chinese Medicine (Qihuang Project), and Xingliao Yingcai Project of Liaoning Province.

ACKNOWLEDGMENTS

The authors would like to thank all of the rats, the team of investigators, research partners, and operations staff involved in this study. Finally, I would like to thank my wife XJ for her support and understanding of my scientific research work.

REFERENCES

1. Koyner JL, Cerdá J, Goldstein SL, Jaber BL, Liu KD, Shea JA, et al. The daily burden of acute kidney injury: a survey of US nephrologists on world kidney day. *Am J Kidney Dis.* (2014) 64:394–401. doi: 10.1053/j.ajkd.2014.03.018
2. Oztay F, Kara-Kisla B, Orhan N, Yanardag R, Bolkent S. The protective effects of prostaglandin E1 on lung injury following renal ischemia-reperfusion in rats. *Toxicol Ind Health.* (2016) 32:1684–92. doi: 10.1177/0748233715576615
3. Hafner S, Hillenbrand A, Knippschild U, Radermacher P. The obesity paradox and acute kidney injury: beneficial effects of hyper-inflammation? *Crit Care.* (2013) 17:1023. doi: 10.1186/cc13152
4. Kelz RR, Reinke CE, Zubizarreta JR, Wang M, Saynisch P, Even-Shoshan O, et al. Acute kidney injury, renal function, and the elderly obese surgical patient: a matched case-control study. *Ann Surg.* (2013) 258:359–63. doi: 10.1097/SLA.0b013e31829654f3
5. Yeh JH, Yang YC, Wang JC, Wang D, Wang JJ. Curcumin attenuates renal ischemia and reperfusion injury-induced restrictive respiratory insufficiency. *Transplant Proc.* (2013) 45:3542–5. doi: 10.1016/j.transproceed.2013.09.004
6. Faubel S, Edelstein CL. Mechanisms and mediators of lung injury after acute kidney injury. *Nat Rev Nephrol.* (2016) 12:48–60. doi: 10.1038/nrneph.2015.158
7. White LE, Cui Y, Shelak CMF, Lie ML, Hassoun HT. Lung endothelial cell apoptosis during ischemic acute kidney injury. *Shock.* (2012) 38:320–7. doi: 10.1097/SHK.0b013e31826359d0
8. Feltes CM, Hassoun HT, Lie ML, Cheadle C, Rabb H. Pulmonary endothelial cell activation during experimental acute kidney injury. *Shock.* (2011) 36:170–6. doi: 10.1097/SHK.0b013e3182169c76
9. Kwong JQ, Molkentin JD. Physiological and pathological roles of the mitochondrial permeability transition pore in the heart. *Oxid Med Cell Longev Cell Metab.* (2015) 21:206–14. doi: 10.1016/j.cmet.2014.12.001
10. Sui S, Tian J, Gauba E, Wang Q, Guo L, Du H. Cyclophilin D regulates neuronal activity-induced filopodiagenesis by fine-tuning dendritic mitochondrial calcium dynamics. *J Neurochem.* (2018) 146:403–15. doi: 10.1111/jnc.14484
11. Yin X, Yin Y, Cao FL, Chen YF, Peng Y, Hou WG, et al. Tanshinone IIA attenuates the inflammatory response and apoptosis after traumatic injury of the spinal cord in adult rats. *PLoS ONE.* (2012) 7:e38381. doi: 10.1371/journal.pone.0038381
12. Xu W, Yang J, Wu L M. Cardioprotective effects of tanshinone IIA on myocardial ischemia injury in rats. *Die Pharmazie.* (2009) 64:332–6.
13. Li J, Zheng Y, Li MX, Yang CW, Liu YF. Tanshinone IIA alleviates lipopolysaccharide-induced acute lung injury by downregulating TRPM7 and pro-inflammatory factors. *J Cell Mol Med.* (2018) 22:646–54. doi: 10.1111/jcmm.13350
14. Jiang C, Zhu W, Shao Q, Yan X, Jin B, Zhang M, et al. Tanshinone IIA protects against folic acid-induced acute kidney injury. *Am J Chin Med.* (2016) 44:737–53. doi: 10.1142/S0192415X16500403
15. Zhang SZ, Ye ZG, Xia Q, Zhang W, Bruce I. Inhibition of mitochondrial permeability transition pore: a possible mechanism for cardioprotection conferred by pretreatment with tanshinone IIA. *Conf Proc IEEE Eng Med Biol Soc.* (2005) 3:2276–9. doi: 10.1109/IEMBS.2005.1616918
16. Zhu B, Zhai Q, Yu B. Tanshinone IIA protects rat primary hepatocytes against carbon tetrachloride toxicity viainhibiting mitochondria permeability transition. *Pharm Biol.* (2010) 48:484–7. doi: 10.3109/13880200903179699

17. Baines CP, Kaiser RA, Purcell NH, Blair NS, Osinska H, Hambleton MA, et al. Loss of cyclophilin D reveals a critical role for mitochondrial permeability transition in cell death. *Nature.* (2005) 434:658–62. doi: 10.1038/nature03434
18. Lemoine S, Pillot B, Augeul L, Rabeyrin M, Varennes A, Normand G, et al. Dose and timing of injections for effective cyclosporine A pretreatment before renal ischemia reperfusion in mice. *PLoS ONE.* (2017) 12:e0182358. doi: 10.1371/journal.pone.0182358
19. Rodgers SJ, Ferguson DT, Mitchell CA, Ooms LM. Regulation of PI3K effector signalling in cancer by the phosphoinositide phosphatases. *Biosci Rep.* (2017) 37:BSR20160432. doi: 10.1042/BSR20160432
20. Zeng KW, Wang XM, Ko H, Kwon HC, Cha JW, Yang HO. Hyperoside protects primary rat cortical neurons from neurotoxicity induced by amyloid β-protein via the PI3K/Akt/Bad/Bcl(XL)-regulated mitochondrial apoptotic pathway. *Eur J Pharmacol.* (2011) 672:45–55. doi: 10.1016/j.ejphar.2011.09.177
21. Doi K, Ishizu T, Fujita T, Noiri E. Lung injury following acute kidney injury: kidney-lung crosstalk. *Clin Exp Nephrol.* (2011) 15:464–70. doi: 10.1007/s10157-011-0459-4
22. Satoru S, Kazuyoshi K, Naoko YI, Katsuaki I, Masahiro I. Amelioration of renal ischemia-reperfusion injury by inhibition of IL-6 production in the hyperlipidemia. *J Pharmacol Sci.* (2009) 110:47–54. doi: 10.1254/jphs.08283FP
23. Ali SI, Alhusseini NF, Atteia HH, Idris RA, Hasan RA. Renoprotective effect of a combination of garlic and telmisartan against ischemin/reperfusion-induced kidney injury in obese rats. *Free Radic Res.* (2016) 50:966–86. doi: 10.1080/10715762.2016.1211644
24. Agarwal KC. Therapeutic actions of garlic constituents. *Med Res Rev.* (1996) 16:111–24. doi: 10.1002/(SICI)1098-1128(199601)16:1<111::AID-MED4>3.0.CO;2-5
25. Hassoun HT, Lie ML, Grigoryev DN, Liu M, Tuder RM, Rabb H. Kidney ischemia-reperfusion injury induces caspase-dependent pulmonary apoptosis. *Am J Physiol Renal Physiol.* (2009) 297:F125–37. doi: 10.1152/ajprenal.90666.2008
26. Li JJ, Chen Q, He XH, Azeem A, NingJL, Bin Y, et al. Dexmedetomidine attenuates lung apoptosis induced by renal ischemia-reperfusion injury through α2AR/PI3K/Akt pathway. *J Transl Med.* (2018) 16:78. doi: 10.1186/s12967-018-1455-1
27. Deng J, Hu X, Yuen PST, Star RA. α-Melanocyte-stimulating hormone inhibits lung injury after renal ischemia/reperfusion. *Am J Respir Crit Care.* (2004) 169:749–56. doi: 10.1164/rccm.200303-372OC
28. Klein CL, Hoke TS, Fang W, Altmann CJ, Douglas IS, Faubel S. Interleukin-6 mediates lung injury following ischemic acute kidney injury or bilateral nephrectomy. *Kidney Int.* (2008) 74:901–9. doi: 10.1038/ki.2008.314
29. Song M, Hang TJ, Zhang ZX. Pharmacokinetic interactions between the main components in the extracts of salvia miltiorrhiza bge. In rat. *Yao Xue Xue Bao.* (2007) 42:301–7.
30. Xu YM, Ding GH, Huang J, Xiong Y. Tanshinone IIA pretreatment attenuates ischemia/reperfusion-induced renal injury. *Exp Ther Med.* (2016) 12:2741–6. doi: 10.3892/etm.2016.3674
31. Zhang Z, He H, Qiao Y, Huang J, Wu Z, Xu P, et al. Tanshinone IIA pretreatment protects H9c2 cells against anoxia/reoxygenation injury: involvement of the translocation of Bcl-2 to mitochondria mediated by 14-3-3 η. *Oxid Med Cell Longev.* (2018) 2018:3583921. doi: 10.1155/2018/3583921
32. Lemoine S, Pillot B, Rognant N, Augeul L, Rayberin M, Varennes A, et al. Postconditioning with cyclosporine a reduces early renal dysfunction by inhibiting mitochondrial permeability transition. *Transplantation.* (2015) 99:717–23. doi: 10.1097/TP.0000000000000530
33. Kaaman M, Sparks LM, van Harmelen V, Smith SR, Sjölin E, Dahlman I, et al. Strong association between mitochondrial DNA copy number and lipogenesis in human white adipose tissue. *Diabetologia.* (2007) 50:2526–33. doi: 10.1007/s00125-007-0818-6
34. Luan G, Li G, Ma X, Jin Y, Hu N, Li J, et al. Dexamethasone-Induced mitochondrial dysfunction and insulin resistance-study in 3T3-L1 adipocytes and mitochondria isolated from mouse liver. *Molecules.* (2019) 24: pii: E1982. doi: 10.3390/molecules24101982
35. Federica C, Rosalba S, Pasquale L, Angela Z, Arianna M, Raffaella C, et al. Fructose-Rich diet affects mitochondrial DNA damage and repair in rats. *Nutrients.* (2017) 9:323. doi: 10.3390/nu9040323
36. Clay Montier LL, Deng JJ, Bai Y. **N**umber matters: control of mammalian mitochondrial DNA copy number. *J Genet Genomics.* (2009) 36:125–31. doi: 10.1016/S1673-8527(08)60099-5
37. Kelly DP, Scarpulla RC. Transcriptional regulatory circuits controlling mitochondrial biogenesis and function. *Genes Dev.* (2004) 15; 18:357–68. doi: 10.1101/gad.1177604
38. de Brito OM, Scorrano L. Mitofusin 2 tethers endoplasmic reticulum to mitochondria. *Nature.* (2008) 456:605–10. doi: 10.1038/nature07534
39. Wang YL, Yuan YT, Gao YT, Li X, Tian F, Liu F, et al. MicroRNA-31 regulating apoptosis by mediating the phosphatidylinositol-3kinase/protein kinase B signaling pathway in treatment of spinal cord injury. *Brain Dev.* (2019) 41:649–61. doi: 10.1016/j.braindev.2019.04.010
40. Fang X, Yu S, Eder A, Mao M, Bast RC Jr, Boyd D, et al. Regulationof BAD phosphorylation at serine 112 by the Ras-mitogen-activated protein kinase pathway. *Oncogene.* (1999) 18:6635–40. doi: 10.1038/sj.onc.1203076
41. Sakamaki J, Daitoku H, Katsuya U, Ayano H, Kazuyuki Y, Akiyoshi F. Arginine methylation of BCL-2 antagonist of cell death (BAD) counteracts its phosphorylation and inactivation by Akt. *Proc Natl Acad Sci USA.* (2011) 108:6085–90. doi: 10.1073/pnas.1015328108
42. Neto JS, Nakao A, Kimizuka K, Romanosky AJ, Stolz DB, Uchiyama T, et al. Protection of transplantinduced renal ischemia-reperfusion injury with carbon monoxide. *Am Physiol J Renal Physiol.* (2004) 287:F979–89. doi: 10.1152/ajprenal.00158.2004
43. Alzoubi KH, Abdul-Razzak KK, Khabour OF, Al-Tuweiq GM, Alzubi MA, Alkadhi KA. Adverse effect of combination of chronic psychosocial stress and high fat diet on hippocampus-dependent memory in rats. *Behav Brain Res.* (2009) 204:117–23. doi: 10.1016/j.bbr.2009.05.025
44. Tawfik MK. Renoprotective activity of telmisartan versus pioglitazone on ischemia/reperfusion induced renal damage in diabetic rats. *Eur Rev Med Pharmacol Sci.* (2012) 16:600–9.
45. Tang FC, Wang HY, Ma MM, Guan TW, Pan L, Yao DC, et al. Simvastain attenuated rat thoracic aorta remodeling by decreasing ROCK2-mediated CyPA secretion and CD147-ERK1/2-cyclin pathway. *Mol Med Rep.* (2017) 16:8123–9. doi: 10.3892/mmr.2017.7640
46. Pan L, Yao DC, Yu YZ, Li SJ, Chen BJ, Hu GH, et al. Necrostatin-1 protects against oleic acid-induced acute respiratory distress syndrome in rats. *Biochem Biophys Res Commun.* (2016) 478:1602–8. doi: 10.1016/j.bbrc.2016.08.163
47. Li X, Jia P, Huang Z, Liu S, Miao J, Guo Y, et al. Lycopene protects against myocardial ischemia-reperfusion injury by inhibiting mitochondrial permeability transition pore opening. *Drug Des Devel Ther.* (2019) 13:2331–42. doi: 10.2147/DDDT.S194753
48. Gilmer LK, Ansari MA, Roberts KN, Scheff SW. Age-Related mitochondrial changes after traumatic brain injury. *J Neurotrauma.* (2010) 27:939–50. doi: 10.1089/neu.2009.1181
49. Wagner EM. Monitoring gene expression: quantitative real-time rt-PCR. *Methods Mol Biol.* (2013) 1027:19–45. doi: 10.1007/978-1-60327-369-5_2
50. Livak KJ, Schmittgen TD. Analysis of relative gene expression data using real-time quantitative PCR and the 2(-Delta DeltaC(T)) method. *Methods.* (2001) 25:402–8. doi: 10.1006/meth.2001.1262

Conflict of Interest: The authors declare that the research was conducted in the absence of any commercial or financial relationships that could be construed as a potential conflict of interest.

Copyright © 2021 Tai, Jiang, Song, Xiao, Li, Cheng, Yin, Chen, Yang, Jiang, Kuang, Lan and Jia. This is an open-access article distributed under the terms of the Creative Commons Attribution License (CC BY). The use, distribution or reproduction in other forums is permitted, provided the original author(s) and the copyright owner(s) are credited and that the original publication in this journal is cited, in accordance with accepted academic practice. No use, distribution or reproduction is permitted which does not comply with these terms.

frontiers in Immunology

ORIGINAL RESEARCH
published: 20 May 2021
doi: 10.3389/fimmu.2021.585595

Safranal Alleviated OVA-Induced Asthma Model and Inhibits Mast Cell Activation

Peeraphong Lertnimitphun[1,2†], Wenhui Zhang[1†], Wenwei Fu[1], Baican Yang[1], Changwu Zheng[1], Man Yuan[1], Hua Zhou[3], Xue Zhang[4], Weizhong Pei[4], Yue Lu[1] and Hongxi Xu[1,3*]*

[1] School of Pharmacy, Shanghai University of Traditional Chinese Medicine, Shanghai, China, [2] Department of Acupuncture and Moxibustion, Huachiew TCM Hospital, Bangkok, Thailand, [3] Shuguang Hospital, Shanghai University of Traditional Chinese Medicine, Shanghai, China, [4] Saffron Department and International Trade Department, Shanghai Traditional Chinese Medicine Co., Ltd., Shanghai, China

OPEN ACCESS

Edited by:
Girolamo Pelaia,
University of Catanzaro, Italy

Reviewed by:
Rui Li,
University of Pennsylvania, United States
Guanghai Yan,
Yanbian University Medical College, China

***Correspondence:**
Hongxi Xu
xuhongxi88@gmail.com
Yue Lu
lvyue126@hotmail.com

[†]These authors have contributed equally to this work

Specialty section:
This article was submitted to Inflammation, a section of the journal Frontiers in Immunology

Received: 21 July 2020
Accepted: 19 April 2021
Published: 20 May 2021

Citation:
Lertnimitphun P, Zhang W, Fu W, Yang B, Zheng C, Yuan M, Zhou H, Zhang X, Pei W, Lu Y and Xu H (2021) Safranal Alleviated OVA-Induced Asthma Model and Inhibits Mast Cell Activation. Front. Immunol. 12:585595. doi: 10.3389/fimmu.2021.585595

Introduction: Asthma is a chronic and recurring airway disease, which related to mast cell activation. Many compounds derived from Chinese herbal medicine has promising effects on stabilizing mast cells and decreasing inflammatory mediator production. Safranal, one of the active compounds from *Crocus sativus*, shows many anti-inflammatory properties. In this study, we evaluated the effect of safranal in ovalbumin (OVA)-induced asthma model. Furthermore, we investigate the effectiveness of safranal on stabilizing mast cell and inhibiting the production of inflammatory mediators in passive systemic anaphylaxis (PSA) model.

Methods: OVA-induced asthma and PSA model were used to evaluate the effect of safranal *in vivo.* Lung tissues were collected for H&E, TB, IHC, and PAS staining. ELISA were used to determine level of IgE and chemokines (IL-4, IL-5, TNF-α, and IFN-γ). RNA sequencing was used to uncovers genes that safranal regulate. Bone marrow-derived mast cells (BMMCs) were used to investigate the inhibitory effect and mechanism of safranal. Cytokine production (IL-6, TNF-α, and LTC_4) and NF-κB and MAPKs signaling pathway were assessed.

Results: Safranal reduced the level of serum IgE, the number of mast cells in lung tissue were decreased and Th1/Th2 cytokine levels were normalized in OVA-induced asthma model. Furthermore, safranal inhibited BMMCs degranulation and inhibited the production of LTC_4, IL-6, and TNF-α. Safranal inhibits NF-κB and MAPKs pathway protein phosphorylation and decreases NF-κB p65, AP-1 nuclear translocation. In the PSA model, safranal reduced the levels of histamine and LTC_4 in serum.

Conclusions: Safranal alleviates OVA-induced asthma, inhibits mast cell activation and PSA reaction. The possible mechanism occurs through the inhibition of the MAPKs and NF-κB pathways.

Keywords: *Crocus sativus*, Safranal, BMMCs, asthma, passive systemic anaphylaxis

INTRODUCTION

Asthma is a chronic and recurring airway disease characterized by shortness of breath and a tight feeling in the chest. In severe cases asthma attack could lead to death. Asthma is induced by the sensitization process from repeated exposure to allergens, which increased airway responsiveness. In clinical practice, first-line drugs, such as corticosteroids and bronchodilators, are used. However, more than half of the patients receiving first-line drug therapy do not respond to the treatment (1). Thus, finding new treatments for asthma is crucial. The histological integrity of asthma includes an increase in the number of goblet cells and thickening of the airway smooth muscle (2). With repeated exposure to allergen, the number of mast cells in the bronchial tissue significantly increases (3). Therefore, mast cells are well known instigators of the asthma reaction.

Mast cells are innate immune cells that are implicated in many allergic diseases, such as allergic dermatitis (4), allergic asthma (5) and systemic anaphylaxis (6). Mast cells express various cell receptors, one of which is FcεRI. In the early phase, mast cells are activated by a specific pathogen IgE binding to an FcεRI receptor when the mast cell interacts with specific allergens, it degranulates to release its preformed contents, which contain substances such as histamine and proteases. The activation of mast cells also initiates signaling pathways, such as the NF-κB and MAPKs pathways. These pathways lead to the transcription and production of inflammatory cytokines, i.e., IL-6, TNF-α, and LTC_4 via the 5-LO and $cPLA_2$ pathways. These inflammatory mediators increase inflammatory reactions by inducing microvascular dilation and muscular contraction, which are the cause of edema and airway narrowing during an asthma episode. If left untreated, chronic allergic inflammation can lead to remodeling in the airway (7). Therefore, it is important to control allergic inflammation in its early phase.

Mast cells also contribute to systemic anaphylaxis, which are acute and could be lethal in severe cases. Studies have shown the relationship of mast cells, which is believed to be responsible for the elevated level of histamine in anaphylaxis patients (8). While first-line treatments, such as corticosteroid and antihistamine drugs are effective in treating asthma and anaphylactic reactions, some patients do not respond to the treatments, and some patients have a high rate of recurrence. Long-term usage of these drugs produces severe side effects. However, the side effect of these drugs remained high.

Recent investigations have focused on finding new mast cell stabilizers derived from Chinese herbal medicine. Compounds from Chinese herbal medicine showed potential efficacy in stabilizing mast cells. Saffron (*Crocus sativus.*), one of the commonly used Chinese herbal medicines, has shown many promising effects for treating anxiety and cardiovascular-related diseases. However, its active ingredients and its mechanism need further examination. Safranal is one of the main active compounds derived from saffron. It has shown therapeutic effects in the treatment of Alzheimer's disease (9) and antioxidant (10). A previous study has shown that safranal decreased airway responsiveness in the OVA-induced asthma model (11). In this study, we investigated this effect *in vivo via* the PSA model and evaluated the effect of safranal on OVA-induced asthma in mice. Furthermore, we used primary mast cells (BMMCs) to investigate the effectiveness of safranal on stabilizing mast cell degranulation and inhibiting the production of inflammatory mediators.

Abbreviations: PSA, passive systemic anaphylaxis; OVA, ovalbumin; BMMCs, bone marrow-derived mast cells; LTC_4, leukotriene C4; IL, interleukin; TNF-α, tumor necrosis factor alpha; IFN-γ, interferon gamma; NF-κB, nuclear factor-kappa B; MAPKs, a mitogen-activated protein kinase; ERK, extracellular signal-regulated kinase 1/2; JNK, c-Jun N-terminal kinase; IKK, I kappa B kinase; AP-1, activator protein 1; 5-LO, 5-lipoxygenase; $cPLA_2$, cytosolic phospholipase A2; AA, arachidonic acid; HSA, human serum albumin; PWM-SCM, Pokeweed mitogen-spleen cell conditioned medium.

MATERIALS AND METHODS

Drug and Reagents

Safranal, OVA, DNP-IgE, and DNP-HSA was purchased from Sigma Aldrich (MO, USA), purity of Safranal is ≥90.0%. RMPI-1640, fetal bovine serum (FBS), penicillin, and streptomycin were purchased from Gibco (Grand Island, NY/Carlsbad, CA, USA). Milli-Q water was supplied from a water purification system (Millipore, MA, USA). The horseradish peroxidase (HRP)-conjugated goat anti-rabbit IgG was purchased from Invitrogen (Carlsbad, CA, USA), Alum Adjuvant (Thermo Scientific, USA).

Animal Grouping

Female BALB/c mice (18-20 g) were purchased from the Shanghai SLAC Laboratory (Shanghai, China) and housed in an SPF (specific pathogen-free) and controlled temperature (25 ± 2°C) environment with a 12-h light/dark cycle in the Shanghai University of Traditional Chinese Medicine. The animal ethics committee of Shanghai University of Traditional Chinese Medicine approved the animal experimental procedures and welfare (No. SZY201807007). Mice were provided a normal diet and drinking water and acclimated to the new environment for at least one week before the beginning of the experiment.

Induction of OVA-Induced Asthma

Mice were randomly divided into five groups: a control group, an ovalbumin (OVA) model group, a low-dose safranal (200 mg/kg) group, a high-dose safranal (500 mg/kg) group, and a dexamethasone (DEX) group (0.5 mg/kg). Mice were sensitized by injection with OVA i.p (20 μg in PBS and alum) on day 0 and day 14 with a total volume of 200 μl. On days 15 to 21, mice were treated with vehicle, safranal or DEX p.o. q.d. On days 22, 23, and 24, mice were treated with OVA (1% in PBS) aerosolized in an airtight box for 30 min. On day 25, the mice were anesthetized with 1% pentobarbital sodium before cardiac puncture for blood collection. The lung and spleen were collected for further analysis.

Induction of Passive Systemic Anaphylaxis

To induce PSA, mice were randomly divided into 4 groups: a normal control group, a positive control group (administered

anti-DNP-IgE and vehicle), a low-concentration safranal group (administered anti-DNP-IgE, vehicle and 200 mg/kg, p.o.) and a high-concentration safranal group (administered anti-DNP-IgE, vehicle and 500 mg/kg, p.o). On the first day, we injected anti-DNP-IgE (2 μg in 100 μl PBS) i.v., and after 24 h, the mice were given safranal or vehicle for 1 h before i.v injection with DNP-HSA (2 mg in 200 μl PBS). After 5 min, the mice were anesthetized with 1% pentobarbital sodium and euthanized by cardiac puncture. Blood was collected and kept at 4°C for 4 h before centrifugation, at 3,000 rpm for 15 min. Serum was collected for further analysis.

Culture and Activation of BMMCs

Female BALB/c mice (18–20 g) were euthanized, and the hind legs were dissected. Bone marrow was flushed with serum-free RPMI-1640, and 30% Pokeweed Mitogen-Spleen Cell Conditioned Medium (PWM-SCM) was used to culture the bone marrow cells. The medium was changed every other day. After 5 to 6 weeks, the BMMCs were mature and confirmed according to previously described procedures (12). Prior to the experiment, BMMCs were changed from culture medium to RPMI-1640 and sensitized overnight with DNP-IgE (500 ng/ml). Cells were washed with PBS and pretreated with or without safranal for 1 h before stimulation with DNP-HSA (100 ng/ml).

Cell Viability Assay

Cell viability was determined using the MTT assay. BMMCs were seeded in 96-well plates at a concentration of 1×10^5 cells/ml overnight. Cells were treated with various concentrations of safranal for 4 h before the addition of MTT (0.5 mg/ml) and incubated for 4 h. The supernatant was removed, and hydrochloride-isopropanol was added to the precipitate and mixed until fully dissolved. The OD was measured at 570 nm.

Measurement of β-Hexosaminidase

To measure the percentage of degranulation in mast cells, BMMCs were pretreated with DNP-IgE (500 ng/ml) in HBSS medium overnight before performing the assays. Cells were washed with PBS for three times, then diluted to 1×10^6 cells/ml, seeded in 96-well plates and treated with or without safranal for 30 min before stimulation with DNP-HSA (100 ng/ml) for 15 min. The percentage of β-hexosaminidase (β-hex) released was determined by adding substrate containing P-nitrophenyl-N-acetyl-β-D-glucosaminide (Sigma-Aldrich, MO, USA) and citric acid (pH 4.5) to the supernatant as previously described (5).

Measurement of Inflammatory Mediators

BMMCs were seeded at 1×10^6 cells/ml and incubated overnight. Safranal (10 μM or 100 μM) was added for 1 h, and the cells were stimulated with DNP-HSA for 24 h at 37°C and 5% CO_2 in an incubator. The supernatants were collected and centrifuged at 3000 rpm for 5 min at 4°C for analysis of IFN-γ, IL-6, and TNF-α concentrations using ELISA (R&D Systems, Minneapolis, MN, USA). IgE and IL-5 levels were measured by ELISA (BD Bioscience, NJ, USA). The levels of LTC_4 and histamine were measured using an EIA kit (Cayman Chemical, MI, USA). IL-13 and IL-4 levels were measured by an ELISA kit (Thermo Scientific, USA) according to the manufacturer's instructions.

Western Blot Analysis

BMMCs were homogenized, and protein levels were quantified using BCA reagent (Beyotime, Shanghai, China). Nuclear and cytoplasmic extractions were performed as instructed by the manufacturer (Beyotime, Shanghai, China). Samples were loaded and electrophoresed by 10% to 12% SDS-PAGE and transferred to nitrocellulose membranes. The membranes were blocked in 5% nonfat milk and diluted in TBS-T for 2 h, followed by incubation with primary antibodies. The following primary antibodies were used in this experiment, iNOS, COX-2, phospho-IKKα/β, IKKα/β, phospho-IκBα, IκBα, phospho-ERK½, ERK½, phospho-p38, p38, p65, phospho-c-Jun, c-Jun, c-fos, β-tubulin, lamin A/C, phospho-JNK, JNK, phospho-$cPLA_2$, 5-LO, and β-actin, at a 1:1000 dilution (Cell Signaling Technology, Danvers, MA, USA). Secondary antibodies included horseradish peroxide-conjugated goat anti-rabbit antibody and anti-mouse IgG at a 1:2500 dilution.

RNA Sequencing

BMMCs were collected after treatment with DNP-HSA with or without treatment with safranal. Total RNA was extracted using the Qiagen RNeasy Kit (Qiagen, Hombrechtikon, Switzerland), according to the manufacturer's instructions. RNA-seq data was filtered with SOAPnuke (v1.5.2) (13). The clean reads were mapped to the reference genome using HISAT2 (v2.0.4) (14). Bowtie2 (v.2.2.5) (15) was applied to align clean reads to the reference coding gene set, and then the expression level of the gene was calculated by RSEM (v1.2.12) (16). Differential expression analysis was performed using PossionDis with false discovery rate (FDR) ≤ 0.05 and $|\text{Log2Ratio}| \geq 1$. KEGG enrichment analysis of annotated differentially expressed genes was performed by Phyper based on the hypergeometric test. The sequence data were deposited in the BioSample database under the SRA accession number PRJNA639182

Statistical Analysis

Data and statistic results are presented as the mean ± S.E.M., and all results were derived from at least three independent experiments. Statistical analyses were performed using GraphPad Prism Software 8.0 (San Diego, CA, USA). Differences between two groups were analyzed using an unpaired Student's t test, and multiple comparisons were assessed using one-way analysis of variance (ANOVA) with Tukey's multiple comparison test. $P<0.05$ was considered statistically significant.

RESULTS

Safranal Alleviated OVA-Induced Asthma

To investigate the effect of safranal on anti-allergic reactions, we established an OVA-induced asthma model (**Figure 1A**). After challenging with OVA, the serum IgE levels were measured. The

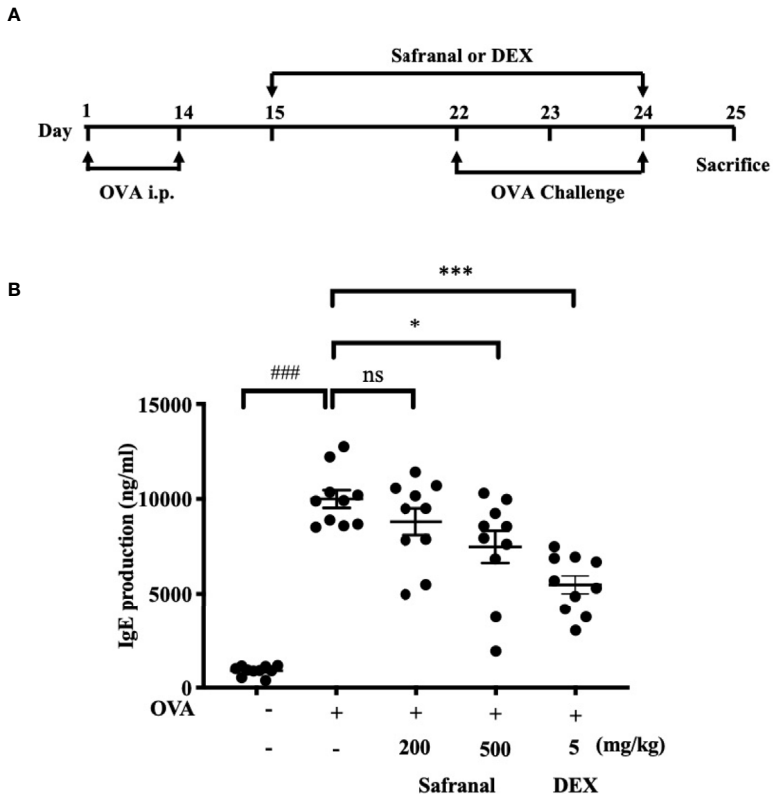

FIGURE 1 | Safranal alleviates OVA-induced asthma. **(A)** OVA-induced asthma model. Mice were sensitized with OVA on days 1 and 14 before oral administration of vehicle, Safranal or Dexamethasone. On days 22, 23, and 24 Mice were challenged with OVA. Blood samples were collected by cardiac puncture and level of serum IgE was determined **(B)**. The data are presented as the means ± S.E.M. of n=10. Ns=no significance $^{###}p < 0.001$ compared to nontreated group, $^{*}p < 0.05$, $^{***}p < 0.001$ compared to OVA treated group.

results showed that safranal significantly reduced the IgE levels in serum (**Figure 1B**). Next, the histology of the lung tissue was evaluated *via* H&E, PAS and toluidine blue staining. We found that the infiltration of inflammatory cells and the amount of mucus secretion in the OVA-treated group were increased, while safranal suppressed the infiltration of inflammatory cells and the amount of mucus secretion (**Figures 2A, B**). The number of mast cells in the lung tissue was determined by toluidine blue staining and immunohistochemistry of c-kit. The results showed that mast cell infiltration increased significantly in the OVA-treated mice. Safranal-treated mice showed less mast cell infiltration in lung tissue than the OVA-treated mice (**Figures 2C–F**). Since Th1/Th2 cytokines are crucial in asthma, an imbalance of these cytokines can cause allergic asthma (17). We analyzed Th1/Th2 cytokine levels in lung tissue and found that the levels of IL-4, IL-5, IL-13 significantly increased, while the IFN-γ level decreased in the OVA-treated group. Safranal significantly decreased the IL-4, IL-5, and IL-13 levels (**Figures 3A–C**) and increased the IFN-γ levels in lung tissue (**Figure 3D**). This finding is consistent with the previous study (11). The production of Th1/Th2 cytokines is related to T cells. To further investigate the effect of safranal on T cells, lung tissue was stained for CD4 and Foxp3, which are markers for T cells. The results showed an increase in CD4 and Foxp3, which are $CD4^+$ T cell markers in the OVA-treated group, and safranal decreased the infiltration of $CD4^+$ T cells (**Figures 3E, F**). Since the spleen is an important peripheral immune organ, and it contains many types of immune cells, we further stimulated splenocyte with OVA and collected the cells for western blot analysis. We investigated whether safranal decreased the activation of the NF-κB and MAPKs pathways in splenocyte. The results showed that a high dose of safranal suppressed the activation of the NF-κB and MAPKs pathways in splenocyte (**Figures 4A–E**).

RNA-Sequencing of Safranal and DNP-HSA–Treated BMMCs

To alternatively uncover the genes that safranal might regulate and investigate the new potential properties of safranal, we performed RNA sequencing on antigen-activated and safranal-treated BMMCs. As the heatmap shows, the differentially expressed genes are presented in **Figure 5A** and **Supplementary 1**. We analyzed the results using the KEGG pathway database and found 13 differentially expressed genes that were related to the immune systems (**Figure 5B**). The protein interactions of these

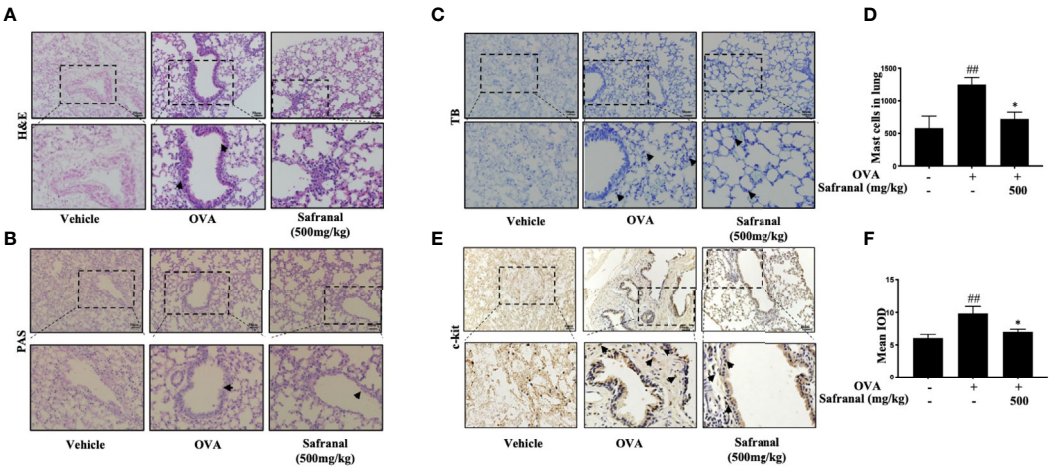

FIGURE 2 | Histological of lung tissue. **(A, B)** H&E and PAS staining showed safranal suppressed infiltration of inflammatory cells, amount of mucus secretion. **(C, D)** Toluidine blue staining of lung tissue showed the number of mast cell in lung tissue. Numbers of mast cells within the lung were quantified in 200×200μm. **(E, F)** IHC staining of c-kit showed marker of the mast cells. The data are presented as the means ± S.E.M. of n=10. $^{\#\#}p<0.01$ compared to nontreated group. $^{*}p<0.05$ compared to OVA treated group. The scale labels shown are 50 μm.

genes were evaluated, and we found that Ccl7 and Cxcl10 were highly related among the differentially expressed genes, as shown in **Figure 5C**. We also found that safranal regulated genes that are related to transient neonatal diabetes, postaxial polydactyly and allergic rhinitis (**Supplementary 2**). As result suggested that safranal regulated Cxcl10 gene, this gene is related to occurrence of asthma (18), we found that safranal decrease the level of Cxcl10 in lung tissue of OVA-treated mice (**Supplementary 3**). These chemokines may be potential target for asthma treatment and needs to be further investigated.

Safranal Inhibited Degranulation and Decreased Inflammatory Mediator Production in BMMCs

Since safranal showed effect on reducing mast cell infiltration in OVA-induced asthma model and RNA sequencing reveals

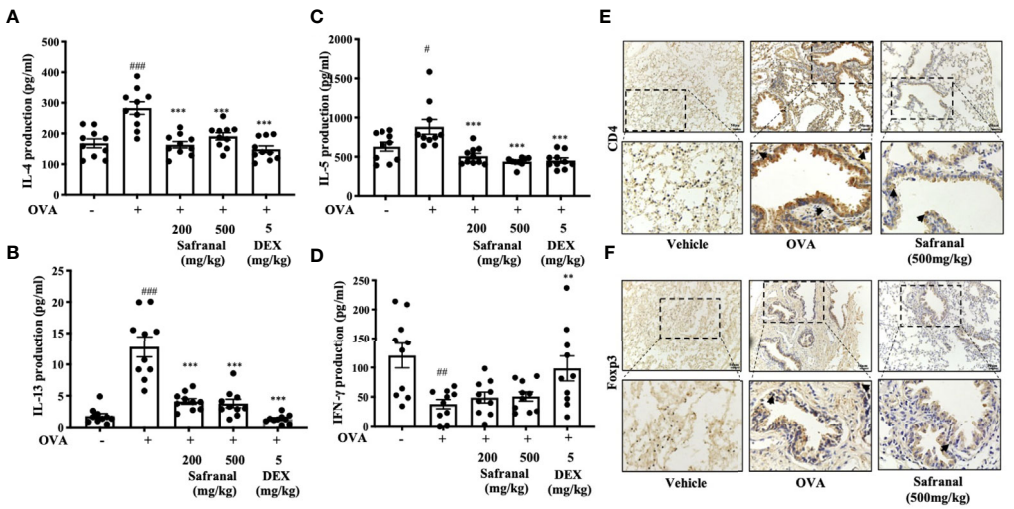

FIGURE 3 | Effect of Safranal on Th1/Th2 cytokines and T cells in lung tissues. Safranal decrease the level of IL-4, IL-5, IL-13 **(A–C)** in lung tissues, while IFN-γ level increased **(D)**. Effect of safranal on T cell in lung tissues. **(E, F)** IHC staining of CD4 and Foxp3. The result showed decreased of CD4 and Foxp3 in safranal treated group. The data are presented as the means ± S.E.M. of n = 10. $^{\#}p<0.05$, $^{\#\#}p<0.01$, $^{\#\#\#}p<0.001$ compared to nontreated group. $^{**}p<0.01$, $^{***}p<0.001$ compared to OVA treated group. The scale labels shown are 50μm.

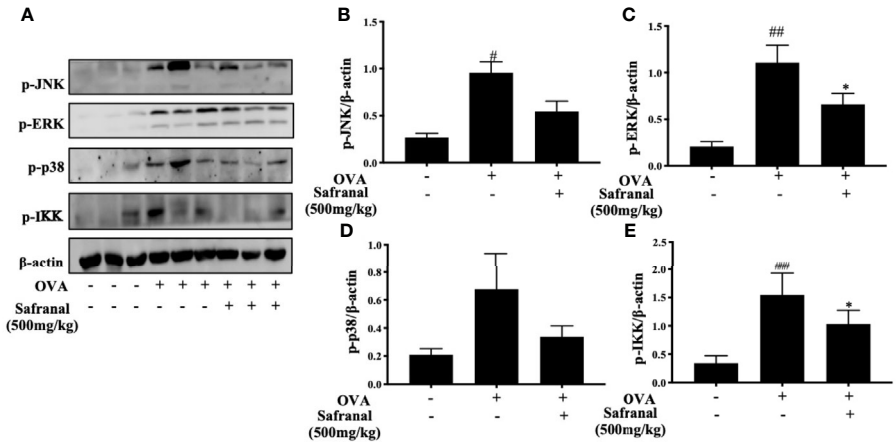

FIGURE 4 | Effect of Safranal on NF-κB and MAPKs pathways in splenocyte. Safranal suppressed the activation of the NF-κB and MAPKs pathways proteins in splenocyte **(A–E)**. The data are presented as the means ± S.E.M. of n = 10. $^{\#}p$ <0.05, $^{\#\#}p$ <0.01, $^{\#\#\#}p$ <0.001 compared to nontreated group. $^{*}p$ <0.05 compared to OVA treated group.

regulation of Cxcl10 and Ccl7, we proceed with the *in vitro* experiment. First, we evaluated the cytotoxicity of safranal in BMMCs by MTT assay. BMMCs were treated with various concentrations of safranal, and we found no significant cell toxicity at 100 μM (**Figure 6A**). The highest concentration of 100 μM was used in the *in vivo* experiment. Next, the degranulation of BMMCs was detected by β-hex assay. After DNP-HSA activation, mast cells released β-hex by 40% compared to that from nontreated BMMCs. We found that safranal significantly reduced the percentage of β-hex released (**Figure 6B**). While the activation of BMMCs also released cytokines, such as IL-6 and TNF-α, our results suggested that safranal significantly inhibited the production of TNF-α and IL-6 (**Figures 6C, D**). LTC_4 is a potent cytokine released by mast cells and is related to many allergic diseases. Our results showed that safranal treatment dose-dependently decreased the production of LTC_4 (**Figure 6E**). When activated, $cPLA_2$ is phosphorylated to release arachidonic acid (AA) from the

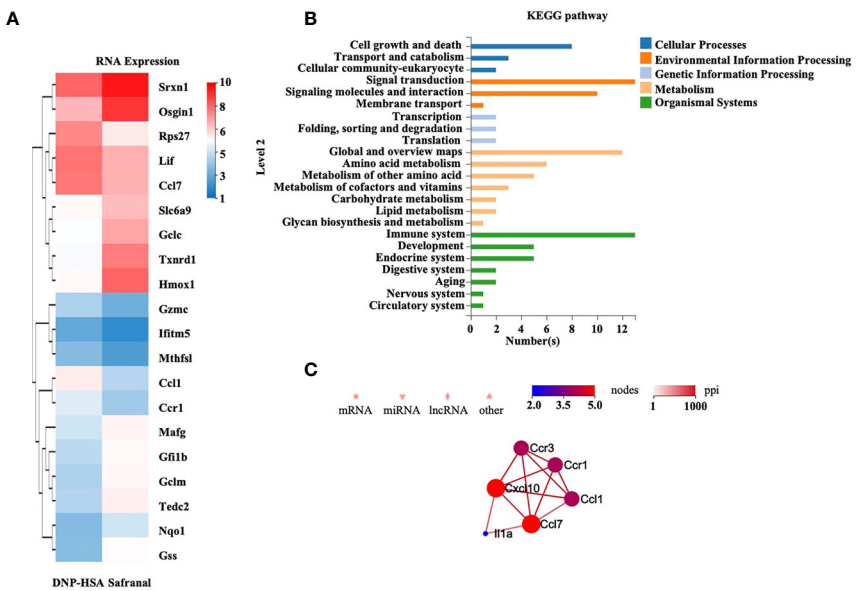

FIGURE 5 | RNA-sequencing of safranal and DNP-HSA treated BMMCs. BMMCs were treated with safranal before stimulating with DNP-HSA. **(A)** Heatmap of genes expression shows effect of safranal treated BMMC on representative differentially expressed genes comparing to DNP-HSA treated. False Discovery Rate (FDR) ≤ 0.05 and |Log2Ratio| ≥ 1. **(B)** KEGG pathway database analysis found 13 differentially expressed genes that were related to the immune systems. **(C)** The protein interactions of these genes were evaluated, Ccl7 and Cxcl10 were found to be most related among the differentially expressed genes.

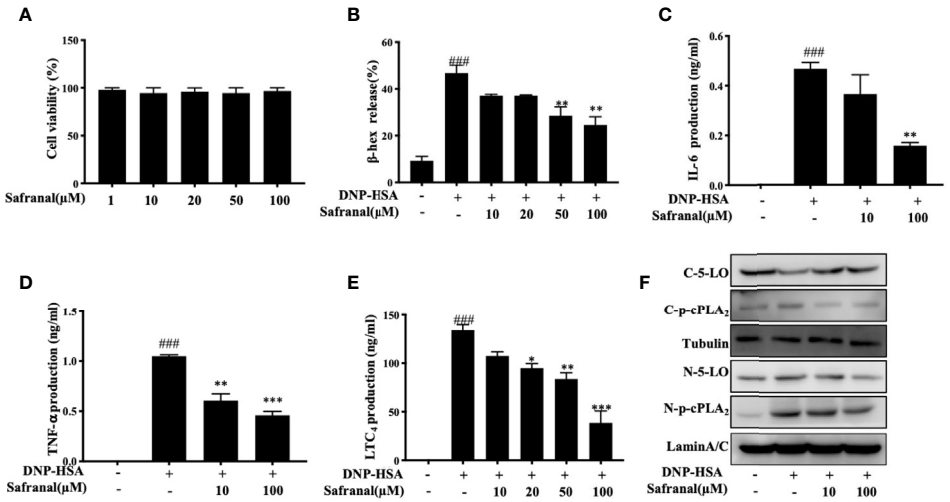

FIGURE 6 | Safranal inhibited degranulation and decreased inflammatory mediator production in BMMCs. **(A)** Cytotoxicity of safranal in BMMC. Cells were treated with various concentrations of safranal, cell viability was measured using the MTT assay. **(B–E)** BMMCs were incubated with safranal and stimulation with DNP-HSA. Supernatant were collected and analyzed for β-hexosaminidase, IL-6, TNF-α, and LTC_4 production. **(F)** Level of 5-LO and p-$cPLA_2$ in cytosol and nucleus were analyzed by western blot analysis. The data shown are representative of three independent experiments. Data are the means ± S.E.M. of three independent experiments. $^{###}p$ <0.001 compared to nontreated group, $^{*}p$ <0.05, $^{**}p$ <0.01, $^{***}p$ <0.001 compared to DNP-HSA.

nuclear membrane, and this molecule is converted to LTC_4 by 5-LO. We found that safranal inhibited the phosphorylation of $cPLA_2$ and nuclear translocation of 5-LO (**Figure 6F**).

Safranal Inhibited the MAPKs and NF-κB Signaling Pathways

Whereas the MAPKs and NF-κB signaling pathways play a great role in inflammatory responses, our RNA-seq data showed differentially expressed genes that were related to the immune systems such as Ccl7 and Cxcl10 are related to MAPKs and NF-κB signaling pathways (19). As we previously reported, safranal inhibited the MAPKs and NF-κB signaling pathways in macrophages (20). We investigated whether safranal also inhibited these signaling pathways in BMMCs. As expected, the phosphorylation of proteins in MAPKs pathways, such as ERK, JNK, and p38, were inhibited (**Figures 7A–D**), as well as the phosphorylation of IKK and IκBα in the NF-κB pathway (**Figures 7E–G**). When both signaling pathways are activated, the transcription factors NF-κB and AP-1 are translocated into the nucleus. The transcription factors then bind to DNA and produce inflammatory mediators. We investigated whether safranal inhibited their nuclear translocation. Western blot analysis showed that the nuclear translocation of p-65 and AP-1 was inhibited (**Figure 8A**). Furthermore, we also measured the transcription factor activity *via* TransAM assay and found similar results (**Figures 8B, C**).

Safranal Alleviated the PSA Reaction

The systemic allergic reaction is acute and deadly, and this effect is mainly due to the activation of mast cells (21). Since safranal has inhibitory effects against mast cell activation, a passive systemic anaphylaxis (PSA) model was used to investigate the anti-allergic effects of safranal *in vivo*. The levels of LTC_4 and histamine in serum from the PSA model were analyzed. We found that the levels of LTC_4 and histamine significantly increased in the vehicle group and decreased in the safranal-treated group (**Figures 9A, B**).

DISCUSSION

Research has suggested that Chinese herbal medicine has potential anti-allergic effect by inhibiting different allergic mechanisms, such as stabilizing mast cells (5), regulating eosinophils (22), balancing Treg/Th2 cells (23), and regulating the gut microbial flora (24). Saffron is commonly used in Chinese herbal medicine and has shown potential in treating diseases. Recent clinical trials suggested that saffron could be used for treating depression (25), macular degeneration (26) and asthma (27). However, its active compounds that take part in this effect are not well characterized. Active compounds derived from saffron include crocin, crocetin, picrocrocin, and safranal. Studies have reported that safranal has the potential to treat diseases such as Parkinson's disease (28) and gastric ulcers (29). In this study, we further investigated the mechanisms involved in the anti-asthma effect of safranal.

The early asthmatic reaction is highly IgE dependent (30). Therapeutic approaches for refractory asthma include the reduction in bronchial mucosal IgE levels, and this can improve patients' lung function (31). Since mast cells are highly associated with allergic diseases, including asthma, mast cell inhibitor showed promising results in controlling corticosteroid-dependent asthma (32). The results of this study showed that the number of mast cells increased in lung tissue and showed improvement in the integrity of lung histology. This finding suggests that safranal can reduce the migration of mast cells, thus reduce the inflammation in lung tissue.

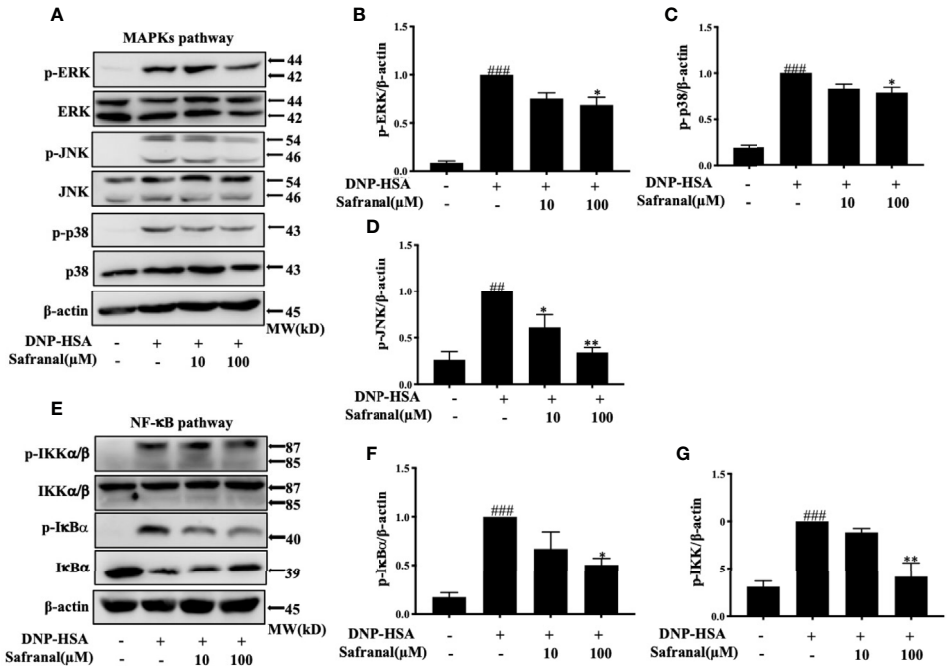

FIGURE 7 | Safranal inhibited the MAPKs and NF-κB signaling pathways. Cells were pretreated with Safranal for 1 h prior to DNP-HSA treatment. The levels of phosphorylation of proteins in MAPKs pathways ERK, JNK and p38 **(A–D)** and NF-κB pathway IKK and IκBα **(E–G)** were measured by western blot and normalized to β-actin. The data shown are representative of three independent experiments and indicate the means ± S.E.M. $^{\#\#}p < 0.01$, $^{\#\#\#}p < 0.001$ compared to nontreated group, $^{*}p < 0.05$, $^{**}p < 0.01$compared to DNP-HSA.

Another approach for the treatment of asthma is keeping a balance of Th2 cytokines (33). A previous report demonstrated that safranal alleviated asthma in mice by reducing iNOS levels and balancing Th2 cytokines (11). In this study, we showed safranal could reduce the production of IL-4, IL-5, and IL-13, the finding is comparable with dexamethasone. Since these cytokines are mainly produced by T cells, we further investigated the amounts of Foxp3 and CD4 in lung tissue, which are markers of T cells. These proteins were reduced in safranal-treated mice, suggested that safranal reduces the number of T cells in lung tissue. Since activation of mast cells can recruit T cells to the inflammation site (34), we suspected that safranal may decrease the number of mast cells and stabilize them to decrease the recruitment of T cells in lung tissue.

Mast cells are known to be related to allergy-related diseases, such as atopic dermatitis, asthma, systemic anaphylactic, etc. During the sensitization process, allergen specific IgE antibody is produced by B cells and binds to the FcεRI receptor on mast cells. In the early-phase allergic reaction, specific pathogens bind to the sensitized mast cells, resulting in the degranulation and production of inflammatory mediators. Preformed substances that are deposited in mast cell granules include histamine and proteases which can cause edema and vasodilation. While the activation of pathogens also initiates the NF-κB signaling pathway, the signaling begins with phosphorylation of IKK, which leads to IκBα degradation into NF-κB p65 and p50 dimers (35). NF-κB dimers then translocate into the nucleus, the translation of dimers leads to the production of inflammatory mediators, such as IL-6 and TNF-α. Activation of specific pathogens *via* IgE-mediated reactions also leads to the phosphorylation of MAPKs, such as p38, ERK, and JNK. These MAPKs lead to nuclear translocation of AP-1, which transcribes and produces cytokines, such as IL-6 and TNF-α. Furthermore, phosphorylation of MAPKs, especially ERK (36), increases LTC_4 biosynthesis from AA *via* the cytoplasmic $cPLA_2$ and 5-LO pathway. When activated by phosphorylated ERK, $cPLA_2$ frees AA from plasmid membranes. Free AA then is synthesized into LTA_4 by 5-LO, followed by the conjugation with glutathione, which converts LTA_4 to LTC_4. As reported, histamine and LTC_4 are potent mediators of anaphylactic diseases, such as asthma and systemic anaphylaxis. Studies have suggested that patients with anaphylactic shock have high levels of LTC_4 and histamine. These mediators increase microvascular permeability, induce bronchoconstriction, etc. These are the cause of death in anaphylactic shock patients. This phenomenon is highly related to mast cell activation and degranulation. Some findings have suggested that anaphylactic reaction can be reduced by inhibiting mast cell activation (37). Several approaches have been reported to stabilized mast cells by targeting KIT (38), Fyn and Lyn (39), reducing IgE (40), etc. This study showed that safranal stabilized mast cells by decreasing degranulation and production of inflammatory mediators IL-6, TNF-α, and LTC_4. The mechanism occurred *via* the inhibition of NF-κB and MAPKs and the inhibition of nuclear transcriptional factors. However, phosphorylated p38 and JNK protein expression in lung tissue has no statistically significant difference between model group and

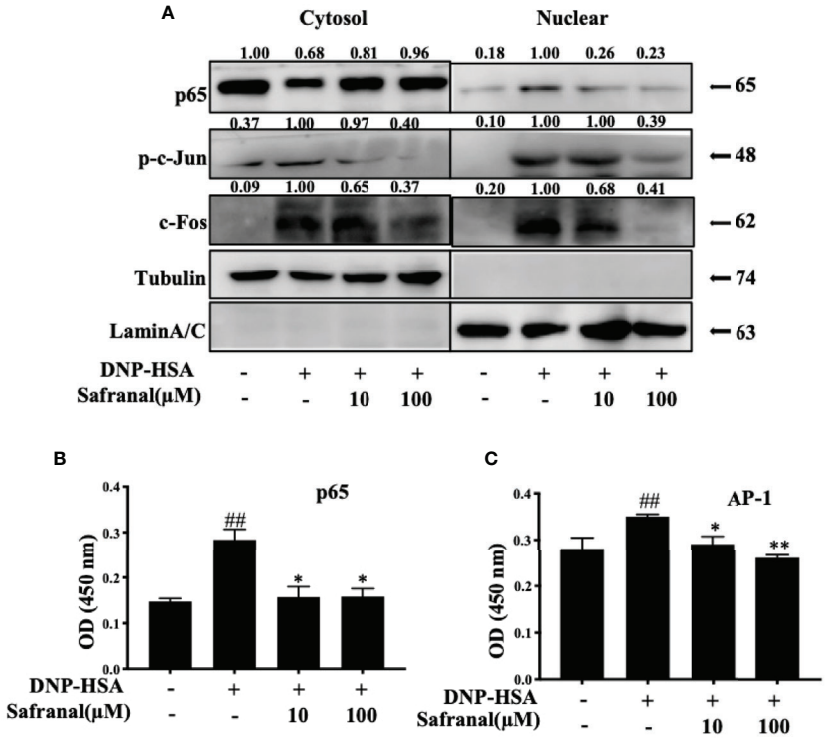

FIGURE 8 | Safranal inhibited the nuclear translocation of NF-κB, AP-1. **(A)** BMMCs were collected after incubation with safranal and stimulation of DNP-HSA. Transcriptional factors p65, p-c-jun, and c-Fos in cytoplasmic or nuclear extracts were determined using western blot. **(B, C)** Nuclear transcriptional factors binding activity of p65, and AP-1 were determined by Trans AM kit, the result present in OD value. The data shown are representative of three independent experiments and indicate the means ± S.E.M. $^{\#\#}p$ <0.01 compared to nontreated group, $^{*}p$ <0.05, $^{**}p$ <0.01 compared to DNP-HSA.

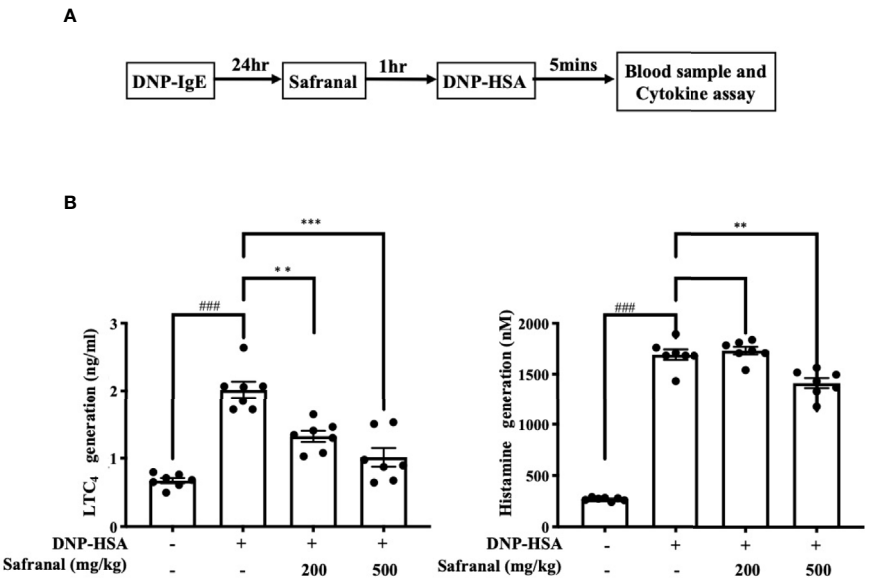

FIGURE 9 | Safranal alleviated PSA reaction. **(A)** Mice were sensitized with DNP-IgE 24 h before oral administration of PBS or safranal. After 1 h mice were i.v. injected with DNP-HSA for 5 min. Blood samples were collected by cardiac puncture. **(B)** Serum was collected and analyzed for LTC_4 and histamine production. All data shown are the means ± S.E.M. of n=7. $^{\#\#\#}p$ <0.001 compared to nontreated group, $^{**}p$ <0.01, $^{***}p$ <0.001 compared to DNP-HSA treated group.

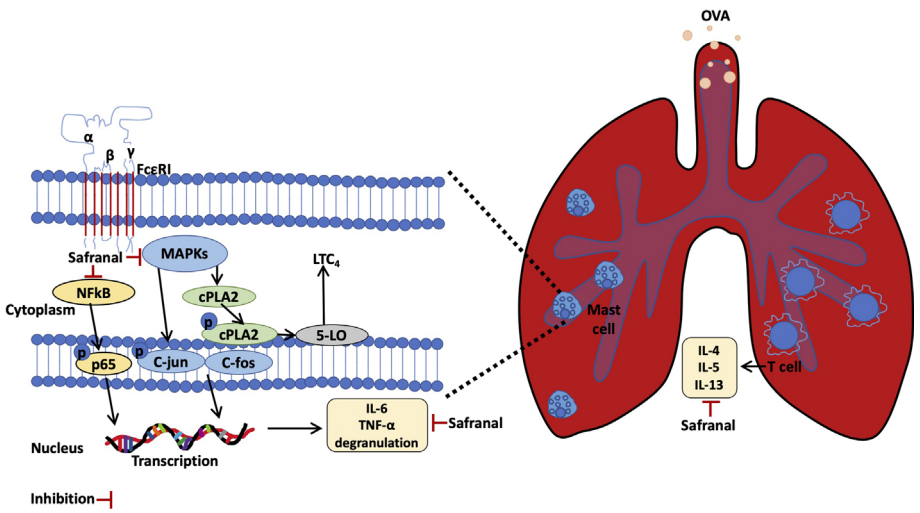

FIGURE 10 | Safranal alleviated OVA-induced asthma model and inhibits mast cell activation.

high dose safranal group. The results showed decreasing trend of the two proteins. Thus, further studies should be conducted to verify with greater sample size. We also found that the inhibition of MAPKs decreased LTC_4 production by decreasing the activation and nuclear translocation of 5-LO and $cPLA_2$. Since the effect of safranal on stabilizing mast cells was shown, we further investigated whether safranal could alleviate mast cell-related anaphylactic reactions. By using the PSA model, which passively stimulates mast cells *in vivo*, we found that the levels of histamine and LTC_4 in serum were decreased.

As RNA-seq results revealed the effect of safranal on decreasing Ccl7 and Cxcl10 expression. These chemokines are related to asthma (18). Ccl7 is a chemoattractant for mast cells. By inhibiting Ccl7, the number of mast cells in lung tissue decreased (41). While 50% of asthma patients who are not responsive to corticosteroid treatments have elevated levels of Cxcl10, a study suggested that Cxcl10 could reduce steroid resistance (42). The production of Cxcl10 is related to JNK and NF-κB p65 activation (43), thus safranal could reduce Cxcl10 by the inhibition of JNK and NF-κB p65. In allergic conjunctivitis, Ccl7 promotes FcεRI-mediated allergic reaction (44). Therefore, Ccl7 and Cxcl10 are potential targets to overcome allergic diseases. Further investigation of this mechanism should be conducted.

Here, we report that safranal, an active compound derived from *Crocus sativus*, has the potential to treat allergic diseases such as systemic anaphylaxis and asthma. Safranal also has potential to stabilizing mast cells and inhibiting cytokine production. The possible mechanism occurs through the inhibition of the MAPKs and NF-κB pathways. As summarised in **Figure 10**.

DATA AVAILABILITY STATEMENT

The RNA-sequencing data sets presented in this study can be found in online repositories. The names of the repository/repositories and accession number(s) can be found in the article/**Supplementary Material**.

ETHICS STATEMENT

The animal ethics committee of Shanghai University of Traditional Chinese Medicine approved the animal experimental procedures and welfare (no. SZY201807007).

AUTHOR CONTRIBUTIONS

HX, HZ, XZ, WP, and YL supervised the project and acquired funding. PL collected and analyzed data and investigated the results. PL and WZ collected specimens. MY, CZ, WF, and BY reviewed the data and drafts of the manuscript. All authors contributed to the article and approved the submitted version.

FUNDING

This work was financially sponsored by the National Natural Science Foundation of China (NSFC) 81803545; Fok Ying-Tong Education Foundation (161039); Guangdong Province Key Area R&D Program of China (No.2020B1111110003); China-Morocco Traditional Chinese Medicine Center construction project (ZY (2018-2020)-GJHZ-1005).

SUPPLEMENTARY MATERIAL

The Supplementary Material for this article can be found online at: https://www.frontiersin.org/articles/10.3389/fimmu.2021.585595/full#supplementary-material

REFERENCES

1. Partridge MR, van der Molen T, Myrseth SE, Busse WW. Attitudes and Actions of Asthma Patients on Regular Maintenance Therapy: The INSPIRE Study. *BMC Pulm Med* (2006) 6:13. doi: 10.1186/1471-2466-6-13
2. Yang SJ, Allahverdian S, Saunders ADR, Liu E, Dorscheid DR. Il-13 Signaling Through IL-13 Receptor Alpha2 Mediates Airway Epithelial Wound Repair. *FASEB J* (2019) 33(3):3746–57. doi: 10.1096/fj.201801285R
3. Kassel O, de Blay F, Duvernelle C, Olgart C, Israel-Biet D, Krieger P, et al. Local Increase in the Number of Mast Cells and Expression of Nerve Growth Factor in the Bronchus of Asthmatic Patients After Repeated Inhalation of Allergen At Low-Dose. *Clin Exp Allergy* (2001) 31(9):1432–40. doi: 10.1046/j.1365-2222.2001.01177.x
4. Kawana S, Kato Y, Omi T. Efficacy of a 5-HT1a Receptor Agonist in Atopic Dermatitis. *Clin Exp Dermatol* (2010) 35(8):835–40. doi: 10.1111/j.1365-2230.2009.03771.x
5. Shou Q, Lang J, Jin L, Fang M, Cao B, Cai Y, et al. Total Glucosides of Peony Improve Ovalbumin-Induced Allergic Asthma by Inhibiting Mast Cell Degranulation. *J Ethnopharmacol* (2019) 244:112136. doi: 10.1016/j.jep.2019.112136
6. Bryce PJ, Falahati R, Kenney LL, Leung J, Bebbington C, Tomasevic N, et al. Humanized Mouse Model of Mast Cell-Mediated Passive Cutaneous Anaphylaxis and Passive Systemic Anaphylaxis. *J Allergy Clin Immunol* (2016) 138(3):769–79. doi: 10.1016/j.jaci.2016.01.049
7. Chen ZY, Zhou SH, Zhou QF, Tang HB. Inflammation and Airway Remodeling of the Lung in Guinea Pigs With Allergic Rhinitis. *Exp Ther Med* (2017) 14(4):3485–90. doi: 10.3892/etm.2017.4937
8. Boehm T, Reiter B, Ristl R, Petroczi K, Sperr W, Stimpfl T, et al. Massive Release of the Histamine-Degrading Enzyme Diamine Oxidase During Severe Anaphylaxis in Mastocytosis Patients. *Allergy* (2019) 74(3):583–93. doi: 10.1111/all.13663
9. Rafieipour F, Hadipour E, Emami SA, Asili J, Tayarani-Najaran Z. Safranal Protects Against Beta-Amyloid Peptide-Induced Cell Toxicity in PC12 Cells Via MAPK and PI3 K Pathways. *Metab Brain Dis* (2019) 34(1):165–72. doi: 10.1007/s11011-018-0329-9
10. Samarghandian S, Samini F, Azimi-Nezhad M, Farkhondeh T. Anti-Oxidative Effects of Safranal on Immobilization-Induced Oxidative Damage in Rat Brain. *Neurosci Lett* (2017) 659:26–32. doi: 10.1016/j.neulet.2017.08.065
11. Bukhari SI, Pattnaik B, Rayees S, Kaul S, Dhar MK. Safranal of Crocus Sativus L. Inhibits Inducible Nitric Oxide Synthase and Attenuates Asthma in a Mouse Model of Asthma. *Phytother Res* (2015) 29(4):617–27. doi: 10.1002/ptr.5315
12. Li X, Kwon O, Kim DY, Taketomi Y, Murakami M, Chang HW. NecroX-5 Suppresses IgE/Ag-stimulated Anaphylaxis and Mast Cell Activation by Regulating the SHP-1-Syk Signaling Module. *Allergy* (2016) 71(2):198–209. doi: 10.1111/all.12786
13. Li R, Li Y, Kristiansen K, Wang J. SOAP: Short Oligonucleotide Alignment Program. *Bioinformatics* (2008) 24(5):713–4. doi: 10.1093/bioinformatics/btn025
14. Kim D, Langmead B, Salzberg SL. HISAT: A Fast Spliced Aligner With Low Memory Requirements. *Nat Methods* (2015) 12(4):357–60. doi: 10.1038/nmeth.3317
15. Langmead B, Salzberg SL. Fast Gapped-Read Alignment With Bowtie 2. *Nat Methods* (2012) 9(4):357–9. doi: 10.1038/nmeth.1923
16. Li B, Dewey CN. RSEM: Accurate Transcript Quantification From RNA-Seq Data With or Without a Reference Genome. *BMC Bioinformatics* (2011) 12:323. doi: 10.1186/1471-2105-12-323
17. Park HJ, Lee CM, Jung ID, Lee JS, Jeong YI, Chang JH, et al. Quercetin Regulates Th1/Th2 Balance in a Murine Model of Asthma. *Int Immunopharmacol* (2009) 9(3):261–7. doi: 10.1016/j.intimp.2008.10.021
18. APennings JLA, Kimman TG, Janssen R. Identification of a Common Gene Expression Response in Different Lung Inflammatory Diseases in Rodents and Macaques. *PLoS One* (2008) 3(7):2596. doi: 10.1371/journal.pone.0002596
19. AThompson WL, Van Eldik LJ. Inflammatory Cytokines Stimulate the Chemokines CCL2/MCP-1 and CCL7/MCP-3 Through NFkB and MAPK Dependent Pathways in Rat Astrocytes [Corrected]. *Brain Res* (2009) 1287:47–57. doi: 10.1016/j.brainres.2009.06.081
20. Lertnimitphun P, Jiang Y, Kim N, Fu W, Zheng C, Tan H, et al. Safranal Alleviates Dextran Sulfate Sodium-Induced Colitis and Suppresses Macrophage-Mediated Inflammation. *Front Pharmacol* (2019) 10:1281–. doi: 10.3389/fphar.2019.01281
21. Xia X, Wan W, Chen Q, Liu K, Majaz S, Mo P, et al. Deficiency in Steroid Receptor Coactivator 3 Enhances Cytokine Production in IgE-stimulated Mast Cells and Passive Systemic Anaphylaxis in Mice. *Cell Biosci* (2014) 4:21. doi: 10.1186/2045-3701-4-21
22. Shin NR, Kwon HJ, Ko JW, Kim JS, Lee IC, Kim JC, et al. S-Allyl Cysteine Reduces Eosinophilic Airway Inflammation and Mucus Overproduction on Ovalbumin-Induced Allergic Asthma Model. *Int Immunopharmacol* (2019) 68:124–30. doi: 10.1016/j.intimp.2019.01.001
23. Cheng BH, Hu TY, Mo LH, Ma L, Hu WH, Li YS, et al. Yan-Hou-Qing Formula Attenuates Allergic Airway Inflammation Via Up-Regulation of Treg and Suppressing Th2 Responses in Ovalbumin-induced Asthmatic Mice. *J Ethnopharmacol* (2019) 231:275–82. doi: 10.1016/j.jep.2018.11.038
24. Tsang MS, Cheng SW, Zhu J, Atli K, Chan BC, Liu D, et al. Anti-Inflammatory Activities of Pentaherbs Formula and Its Influence on Gut Microbiota in Allergic Asthma. *Molecules* (2018) 23(11):2776. doi: 10.3390/molecules23112776
25. Hausenblas HA, Saha D, Dubyak PJ, Anton SD. Saffron (Crocus Sativus L.) and Major Depressive Disorder: A Meta-Analysis of Randomized Clinical Trials. *J Integr Med* (2013) 11(6):377–83. doi: 10.3736/jintegrmed2013056
26. Broadhead GK, Grigg JR, McCluskey P, Hong T, Schlub TE, Chang AA. Saffron Therapy for the Treatment of Mild/Moderate Age-Related Macular Degeneration: A Randomised Clinical Trial. *Graefes Arch Clin Exp Ophthalmol* (2019) 257(1):31–40. doi: 10.1007/s00417-018-4163-x
27. Zilaee M, Hosseini SA, Jafarirad S, Abolnezhadian F, Cheraghian B, Namjoyan F, et al. An Evaluation of the Effects of Saffron Supplementation on the Asthma Clinical Symptoms and Asthma Severity in Patients With Mild and Moderate Persistent Allergic Asthma: A Double-Blind, Randomized Placebo-Controlled Trial. *Respir Res* (2019) 20(1):39. doi: 10.1186/s12931-019-0998-x
28. Save SS, Rachineni K, Hosur RV, Choudhary S. Natural Compound Safranal Driven Inhibition and Dis-Aggregation of Alpha-Synuclein Fibrils. *Int J Biol Macromol* (2019) 141:585–95. doi: 10.1016/j.ijbiomac.2019.09.053
29. Tamaddonfard E, Erfanparast A, Farshid AA, Imani M, Mirzakhani N, Salighedar R, et al. Safranal, a Constituent of Saffron, Exerts Gastro-Protective Effects Against Indomethacin-Induced Gastric Ulcer. *Life Sci* (2019) 224:88–94. doi: 10.1016/j.lfs.2019.03.054
30. Hatzivlassiou M, Grainge C, Kehagia V, Lau L, Howarth PH. The Allergen Specificity of the Late Asthmatic Reaction. *Allergy* (2010) 65(3):355–8. doi: 10.1111/j.1398-9995.2009.02184.x
31. Pillai P, Chan YC, Wu SY, Ohm-Laursen L, Thomas C, Durham SR, et al. Omalizumab Reduces Bronchial Mucosal IgE and Improves Lung Function in non-Atopic Asthma. *Eur Respir J* (2016) 48(6):1593–601. doi: 10.1183/13993003.01501-2015
32. Humbert M, de Blay F, Garcia G, Prud'homme A, Leroyer C, Magnan A, et al. Masitinib, a C-Kit/PDGF Receptor Tyrosine Kinase Inhibitor, Improves Disease Control in Severe Corticosteroid-Dependent Asthmatics. *Allergy* (2009) 64(8):1194–201. doi: 10.1111/j.1398-9995.2009.02122.x
33. Choy DF, Hart KM, Borthwick LA, Shikotra A, Nagarkar DR, Siddiqui S, et al. TH2 and TH17 Inflammatory Pathways are Reciprocally Regulated in Asthma. *Sci Trans Med* (2015) 7(301):301ra129. doi: 10.1126/scitranslmed.aab3142
34. McLachlan JB, Hart JP, Pizzo SV, Shelburne CP, Staats HF, Gunn MD, et al. Mast Cell-Derived Tumor Necrosis Factor Induces Hypertrophy of Draining Lymph Nodes During Infection. *Nat Immunol* (2003) 4(12):1199–205. doi: 10.1038/ni1005
35. Mathes E, O'Dea EL, Hoffmann A, Ghosh G. NF-Kappab Dictates the Degradation Pathway of IkappaBalpha. *EMBO J* (2008) 27(9):1357–67. doi: 10.1038/emboj.2008.73
36. Berenbaum F, Humbert L, Bereziat G, Thirion S. Concomitant Recruitment of ERK1/2 and P38 MAPK Signalling Pathway is Required for Activation of Cytoplasmic Phospholipase A2 Via ATP in Articular Chondrocytes. *J Biol Chem* (2003) 278(16):13680–7. doi: 10.1074/jbc.M211570200
37. Ye J, Piao H, Jiang J, Jin G, Zheng M, Yang J, et al. Polydatin Inhibits Mast Cell-Mediated Allergic Inflammation by Targeting PI3K/Akt, Mapk, Nf-κb and Nrf2/HO-1 Pathways. *Sci Rep* (2017) 7(1):11895. doi: 10.1038/s41598-017-12252-3

38. Cahill KN, Katz HR, Cui J, Lai J, Kazani S, Crosby-Thompson A, et al. Kit Inhibition by Imatinib in Patients With Severe Refractory Asthma. *N Engl J Med* (2017) 376(20):1911–20. doi: 10.1056/NEJMoa1613125
39. Park YH, Kim DK, Kim HS, Lee D, Lee MB, Min KY, et al. WZ3146 Inhibits Mast Cell Lyn and Fyn to Reduce IgE-mediated Allergic Responses In Vitro and In Vivo. *Toxicol Appl Pharmacol* (2019) 383:114763. doi: 10.1016/j.taap.2019.114763
40. Vigl B, Salhat N, Parth M, Pankevych H, Mairhofer A, Bartl S, et al. Quantitative In Vitro and In Vivo Models to Assess Human Ige B Cell Receptor Crosslinking by IgE and EMPD Ige Targeting Antibodies. *J Immunol Methods* (2017) 449:28–36. doi: 10.1016/j.jim.2017.06.006
41. Kuo C-H, Collins AM, Boettner DR, Yang Y, Ono SJ. Role of CCL7 in Type I Hypersensitivity Reactions in Murine Experimental Allergic Conjunctivitis. *J Immunol* (2017) 198(2):645–56. doi: 10.4049/jimmunol.1502416
42. Gauthier M, Chakraborty K, Oriss TB, Raundhal M, Das S, Chen J, et al. Severe Asthma in Humans and Mouse Model Suggests a CXCL10 Signature Underlies Corticosteroid-Resistant Th1 Bias. *JCI Insight* (2017) 2(13):94580. doi: 10.1172/jci.insight.94580
43. Alrashdan YA, Alkhouri H, Chen E, Lalor DJ, Poniris M, Henness S, et al. Asthmatic Airway Smooth Muscle CXCL10 Production: Mitogen-Activated Protein Kinase JNK Involvement. *Am J Physiol Lung Cell Mol Physiol* (2012) 302(10):L1118–27. doi: 10.1152/ajplung.00232.2011
44. BMéndez-Samperio P, Pérez A, Rivera L. Mycobacterium Bovis Bacillus Calmette-Guérin (BCG)-Induced Activation of PI3K/Akt and NF-kB Signaling Pathways Regulates Expression of CXCL10 in Epithelial Cells. *Cell Immunol* (2009) 256(1-2):12–8. doi: 10.1016/j.cellimm.2008.12.002

Conflict of Interest: Authors XZ and WP were employed by company Shanghai Traditional Chinese Medicine Co., Ltd.

The remaining authors declare that the research was conducted in the absence of any commercial or financial relationships that could be construed as a potential conflict of interest.

Copyright © 2021 Lertnimitphun, Zhang, Fu, Yang, Zheng, Yuan, Zhou, Zhang, Pei, Lu and Xu. This is an open-access article distributed under the terms of the Creative Commons Attribution License (CC BY). The use, distribution or reproduction in other forums is permitted, provided the original author(s) and the copyright owner(s) are credited and that the original publication in this journal is cited, in accordance with accepted academic practice. No use, distribution or reproduction is permitted which does not comply with these terms.

frontiers in Immunology

ORIGINAL RESEARCH
published: 28 May 2021
doi: 10.3389/fimmu.2021.674316

Suppression of Endoplasmic Reticulum Stress by 4-PBA Protects Against Hyperoxia-Induced Acute Lung Injury *via* Up-Regulating Claudin-4 Expression

Hsin-Ping Pao[1], *Wen-I. Liao*[2], *Shih-En Tang*[3,4], *Shu-Yu Wu*[4], *Kun-Lun Huang*[1] *and Shi-Jye Chu*[5*]

[1] The Graduate Institute of Medical Sciences, National Defense Medical Center, Taipei, Taiwan, [2] Department of Emergency Medicine, Tri-Service General Hospital, National Defense Medical Center, Taipei, Taiwan, [3] Division of Pulmonary and Critical Care Medicine, Department of Internal Medicine, Tri-Service General Hospital, National Defense Medical Center, Taipei, Taiwan, [4] Institute of Aerospace and Undersea Medicine, National Defense Medical Center, Taipei, Taiwan, [5] Department of Internal Medicine, Tri-Service General Hospital, National Defense Medical Center, Taipei, Taiwan

OPEN ACCESS

Edited by:
Girolamo Pelaia,
University of Catanzaro, Italy

Reviewed by:
Lei Yang,
Shenzhen University, China
Juerg Hamacher,
Lindenhofspital, Switzerland

***Correspondence:**
Shi-Jye Chu
d1204812@mail.ndmctsgh.edu.tw

Specialty section:
This article was submitted to Inflammation, a section of the journal Frontiers in Immunology

Received: 01 March 2021
Accepted: 10 May 2021
Published: 28 May 2021

Citation:
Pao H-P, Liao W-I, Tang S-E, Wu S-Y, Huang K-L and Chu S-J (2021) Suppression of Endoplasmic Reticulum Stress by 4-PBA Protects Against Hyperoxia-Induced Acute Lung Injury via Up-Regulating Claudin-4 Expression. Front. Immunol. 12:674316. doi: 10.3389/fimmu.2021.674316

Endoplasmic reticulum (ER) stress that disrupts ER function can occur in response to a wide variety of cellular stress factors leads to the accumulation of unfolded and misfolded proteins in the ER. Many studies have shown that ER stress amplified inflammatory reactions and was involved in various inflammatory diseases. However, little is known regarding the role of ER stress in hyperoxia-induced acute lung injury (HALI). This study investigated the influence of ER stress inhibitor, 4-phenyl butyric acid (4-PBA), in mice with HALI. Treatment with 4-PBA in the hyperoxia groups significantly prolonged the survival, decreased lung edema, and reduced the levels of inflammatory mediators, lactate dehydrogenase, and protein in bronchoalveolar lavage fluid, and increased claudin-4 protein expression in lung tissue. Moreover, 4-PBA reduced the ER stress-related protein expression, NF-κB activation, and apoptosis in the lung tissue. In *in vitro* study, 4-PBA also exerted a similar effect in hyperoxia-exposed mouse lung epithelial cells (MLE-12). However, when claudin-4 siRNA was administrated in mice and MLE-12 cells, the protective effect of 4-PBA was abrogated. These results suggested that 4-PBA protected against hyperoxia-induced ALI *via* enhancing claudin-4 expression.

Keywords: 4-phenyl butyric acid, hyperoxia, acute lung injury, endoplasmic reticulum stress, claudin-4, oxidative stress

INTRODUCTION

In critical pulmonary and cardiorespiratory disease, the delivery of oxygen to peripheral tissues is increased with supplemental oxygen treatment. However, prolonged exposure to very high concentrations of oxygen (≥ 50%) leads to an acute lung injury and acute respiratoryIntroduction distress syndrome (ALI/ARDS), and eventually death (1). ALI induced by exposure to supraphysiological concentrations of oxygen (hyperoxia) is characterized by

capillary endothelial and alveolar epithelial cell damage, inflammatory cell infiltration, and non-cardiogenic pulmonary edema (2). Hyperoxia-induced acute lung injury (HALI) is caused by reactive oxygen species and the release of pro-inflammatory mediators that induces lung epithelial cell death *via* apoptosis or necrosis (3, 4). However, the molecular mechanisms behind HALI in this disease process have not been adequately understood.

The endoplasmic reticulum (ER) stress originates as a cascade of reactions called the unfolded protein response (UPR), which is activated in response to an accumulation of unfolded or misfolded proteins in the ER lumen (5). Three specialized ER-localized protein sensors are involved in UPR initiation: inositol-requiring enzyme 1α (IRE1α), double-stranded RNA-dependent protein kinase (PKR)-like ER kinase (PERK), and activating transcription factor 6 (ATF6), which are released from binding immunoglobulin protein (BiP; also known as glucose-regulated protein–78, or GRP78) during ER stress. GRP78 is an ER-resident chaperone, which associates with these three ER stress sensors and represses their activity (6, 7). During ER stress, GRP78 was released from these three proteins to activate UPR and modified downstream effectors, including phosphorylation α subunit of eukaryotic initiation factor-2 (eIF-2α), activating transcription factor 4 (ATF4), ATF6, and increasing CCAAT/enhancer-binding protein (C/EBP) homologous protein (CHOP) levels (8–10). In addition, ER stress can activate the NF-κB signaling, thereby promoting the production of various inflammatory mediators (11). ER stress has been contributed to the progression of the disease involving inflammation including respiratory diseases, diabetes, obesity, neurodegenerative diseases, inflammatory bowel diseases, and many metabolic diseases (5, 11–14). 4-Phenyl butyric acid (4-PBA) is commonly thought an "ER stress inhibitor" primarily as a chemical chaperone. The major mechanism for the action of 4-PBA is that the hydrophobic regions of the chaperone interact with exposed hydrophobic segments of the unfolded protein. This interaction protects the protein from aggregation, promotes the folding of proteins, and reduces ER stress. 4-PBA is an orally bioavailable, and low molecular weight fatty acid that has been approved by the Food and Drug Administration for clinical use to treat urea cycle disorders and hyperammonemia (15). 4-PBA has potential benefit for a wide variety of diseases like cancer, cystic fibrosis, thalassemia, spinal muscular atrophy as well as protein folding diseases such as type 2 diabetes mellitus, amyotrophic lateral sclerosis, Huntington disease, Alzheimer's disease, and Parkinson disease (15–20). Moreover, ER stress has a role in developing HALI (21). However, the pathophysiology of ER stress in HALI is still elusive.

Claudins belong to a large family of integral membrane proteins that are essential components in the tight junction (TJ) formation and function. Different claudins with distinct roles modulated paracellular solutes transportation through adjacent epithelial cells. Claudin-3, claudin-4, and claudin-18 are predominantly expressed in the alveolar epithelium (22). Expression of claudin-4 protein well correlates with an alveolar barrier function in mice and human lungs (23, 24). Kage et al. reported that claudin-4 deficient mice had been shown to increase susceptibility to HALI (25). One study reported that *dermatophagoides farinae*-sensitized mice had increased ER stress and impaired airway epithelial barrier function which was associated with an exaggerated decrease of TJ proteins. In contrast, 4-PBA (an inhibitor of ER stress) inhibited the increase of ER stress and subsequently reversed the decrease of TJ proteins (26). Besides, 4-PBA prevented the loss of TJ proteins by suppressing ER stress after spinal cord injury (27). Although it has been demonstrated that hyperoxia exposure decreases the protein expression of claudin-4 in the pulmonary epithelial barrier (28), the contribution of ER stress in HALI to pulmonary TJ barrier dysfunction is still not conclusive.

Therefore, the present study investigated whether 4-PBA reduced ER stress and enhanced the expression of the claudin-4 protein in a mouse model of HALI and then determined the role of claudin-4 protein in the beneficial effects of 4-PBA using small interfering RNA (siRNA). Similar studies were also performed in mouse lung epithelial cells exposed to hyperoxia.

METHODS

Animal Model of Hyperoxia Exposure

Male C57BL/6J mice (8-10 weeks of age) were housed according to the National Institutes of Health Guidelines. All experiments were approved by the Animal Review Committee of National Defense Medical Center (approval number: IACUC-17-258). The room was regulated with 12 hours day/night cycle. Food and water were provided *ad libitum*. The mice were randomly assigned to the control group, hyperoxia group, and hyperoxia + 4-PBA group. 4-PBA (10 mg/kg per day; Sigma-Aldrich, St Louis, MO, USA) or saline was intraperitoneally administrated to mice at 0, 24, 48 and 72 h. The dose of 4-PBA in the present study was selected based on previous studies and our preliminary studies (20) (**Supplementary Figure 1**). The hyperoxia mice were exposed to more than 99% oxygen in an airproof chamber for 24, 48, and 72 hours, respectively, as described previously (3). The control mice were exposed only to room air.

Survival Study

Mice treated with saline, or 4-PBA were continuously exposed to hyperoxia for evaluation of survival. The number of surviving mice was determined at 5-hours intervals until the last mouse died.

Wet/Dry Lung Weight Ratio

The right upper lung lobe was excised at the end of the experiment. After the wet lung weight was determined, and then a part of the right upper lung lobe was dried in an oven at 60°C for 48 hours. The W/D weight ratio was calculated.

Alveolar Fluid Clearance (AFC)

AFC was determined *in vivo* using an *in situ* model of mouse lung as previously described (29, 30). In brief, anesthetized mice were maintained at 37°C using a heating pad and lamp. During the experiment, the trachea was exposed and cannulated with an 18-gauge intravenous catheter. The lungs were inflated with

100% oxygen at continuous positive airway pressure of 7 cm H_2O. Then, the instillate containing fluorescein isothiocyanate (FITC)-labeled albumin (Sigma-Aldrich, St. Louis, MO) was delivered to the lungs within 1 minute at a dose of 12.5 mL/kg. Alveolar fluid samples (100 μL) were collected 1 minute after instillation and at the end of the experiment (15 minutes later). The collected fluids were centrifuged at 3,000×g for 10 minutes, and the fluorescence activity in the supernatant was counted in duplicate. AFC was computed from the increase in alveolar fluid albumin concentration as follows:

$$AFC = (C_f - C_i)/C_f \times 100,$$

where C_i and C_f represented the initial and final concentrations of FITC-albumin in the aspirate at 1 and 15 minutes, respectively, as assessed by the fluorescence activity measurements.

Bronchoalveolar Lavage Analysis of Protein, Lactate Dehydrogenase (LDH), and Cytokine Contents

The left lung was lavaged twice with 0.5 mL of saline after the experiment. The bronchoalveolar lavage fluid (BALF) was centrifuged at 200×*g* for 10 minutes. The concentration of proteins in the supernatant was measured using a bicinchoninic acid protein assay kit (Pierce, Rockford, IL). Lactate dehydrogenase (LDH) activity in BALF was measured using the method as previously described (31). BALF tumor necrosis factor-α (TNF-α, catalog number: RTA00), Monocyte Chemoattractant Protein-1 (MCP-1, catalog number: RCN100), interleukin-6 (IL-6, catalog number: R6000B), and keratinocyte-derived chemokine (KC, catalog number: R6000B) levels were determined using a commercial mouse ELISA kit (R&D Systems Inc., Minneapolis, MN, USA).

Malondialdehyde (MDA) and Protein Carbonyl Content in the Lung Tissue

MDA and protein carbonyl content were estimated as previously described (32). Briefly, the MDA of the supernatant was measured by absorbance at 532 nm and was expressed as nmol/mg protein. The protein carbonyl content was measured by the reaction with dinitrophenylhydrazine and was expressed as the concentration of carbonyl derivatives in the protein (nmol carbonyl/mg protein).

Immunohistochemical Analysis of Lung Myeloperoxidase

Immunohistochemical staining to evaluate myeloperoxidase (MPO) was performed as described previously (33). Briefly, paraffin-embedded lung tissue sections were deparaffinized before antigen retrieval. The lung sections were incubated with a solution of 3% H_2O_2 in methanol for 15 min to block endogenous peroxidase. The slides were exposed to rabbit polyclonal antibody (anti-MPO, 1:100, Cell Signaling Technology, Danvers, MA, USA). The slides were then washed and incubated for 30 min with rat-specific horseradish peroxidase polymer anti-rabbit antibody (Nichirei Biosciences, Tokyo, Japan), and then horseradish peroxidase substrate was added for 3 min. The lung sections were then counterstained with hematoxylin.

Western Blotting Analysis

The right lung samples and cell protein lysates were separated by 10% SDS polyacrylamide gel electrophoresis and immunoblots were developed as previously described (34). The membranes were blocked for 1 hours at room temperature with 5% nonfat milk and then incubated overnight at 4°C with the following antibodies: claudin-3 (Invitrogen, Carlsbad, CA, USA), claudin-4 (OriGene Technologies, Inc., Rockville, MD, USA), claudin-18 (Invitrogen), GRP78 (Abcam, Cambridge, MA, USA), phospho PERK (Taiclone, Taipei, Taiwan), phospho IRE1 (Abcam), ATF6 (Bioss Antibodies, Woburn, MA, USA), ATF4 (Bioss), GADD153 (CHOP, Santa Cruz Biotechnology, Dallas, TX, USA), B-cell lymphoma (Bcl)-2 (Santa Cruz Biotechnology), NF-κB p65, phospho-NF-κB p65, inhibitor of NF-κB (Iκ B)-α, cleaved caspase-3 and proliferating cell nuclear antigen (PCNA, Cell Signaling Technology), and β-actin (Sigma-Aldrich). All results were normalized to β-actin and expressed as the relative values to those for the control group.

Immunofluorescence Detections for Claudin-4

Immunofluorescence staining for claudin-4 was performed as previously described (34). Lung tissue sections were deparaffinized, permeabilized using 0.1% Triton X-100, and blocked with 5% BSA before incubation with anti-claudin-4 (1:200, OriGene Technologies, Inc.) antibody overnight at 4°C. Fluorescein isothiocyanate-conjugated goat anti-rabbit IgG (1:200; Santa Cruz Biotechnology) was used as the secondary antibody for counterstaining. After washing in PBS and DAPI staining, slides were observed and images were captured using a fluorescence microscope (Leica DM 2500; Leica Microsystems GmbH, Wentzler, Germany).

Cell Culture and Treatments

Mouse lung epithelial (MLE)-12 cells were cultured in DMEM/F-12 medium (Invitrogen) supplemented with 10% fetal bovine serum, penicillin (100 U/mL), and streptomycin (10 μg/mL) at 37°C and 5% CO_2 in humidified air as described previously (34). These cells were exposed to hyperoxia (95% O_2 and 5% CO_2) for 72 hours. The cells were pretreated with vehicle, 4-PBA (0.3 mM), or claudin-4 siRNA (25 nM). The dose of 25 nM claudin-4 siRNA used in MLE-12 cell was determined by Western blot (**Supplementary Figure 2**). For claudin-4 siRNA transfection, MLE-12 cells were incubated for 24 hours and transfected with claudin-4 siRNA, using DharmaFECT^{TM} 1 siRNA Transfection Reagent (Dharmacon Inc. Chicago, IL, USA). MLE-12 cells with non-targeting control siRNA treatment were used as negative controls. After 24 hours, the culture medium was replaced with the recommended medium. Forty-eight hours after claudin-4 siRNA treatment, MLE-12 cells were exposed to hyperoxia for 72 hours. Next, cells were lysed for protein extraction subjected to the western blot procedure. The supernatant was collected and

assayed for KC using a mouse KC ELISA kit (R&D, Inc.). The experiments were performed in triplicates.

siRNA Transfection *In Vivo*

100 μg of claudin-4 siRNA per mouse was administrated intratracheally in 50 μl. The intratracheal dose of 100 μg claudin-4 siRNA was determined by Western blot in the lung tissue (**Supplementary Figure 3**). Claudin-4 siRNA was sprayed directly into the mice lungs *via* the endotracheal route using a MicroSprayere aerolizer (Penn-Century, Philadelphia, PA, USA) as described previously (35). Forty-eight hours after injection, 4-PBA or saline was given intraperitoneally and then mice were exposed to hyperoxia for 72 hours. All the mice were sacrificed 72 hours after anesthesia, and the lung samples were collected.

Electric Cell-Substrate Impedance Sensing (ECIS)

Epithelial barrier function was determined as previously described (36) using an ECIS system (Applied Biophysics, Troy, NY, USA). The ECIS with two 8W1E array plates (ibidi GmbH, Martinsried, Germany) served as a platform. The array holder was placed in a standard cell culture incubator (37°C, 100% humidity and 5% CO_2). The array plates were equilibrated overnight with 400 μl of DMEM/F12 at cell culture conditions. Then 6×10^5 MLE-12 cells were seeded on ECIS electrode arrays. After 20 hours of adherence, the arrays were affixed to the ECIS system and recorded with ECMS 1.0 software (CET, IA, USA). ECIS tracings expressed as transepithelial electric resistance (TER) are normalized to plateaued resistance values (subsequent values divided by initial values), and comparisons were made between 4-PBA (0.3 mM), claudin-4 siRNA (25 nM), and vehicle control-treated MLE-12 cells.

Data Analysis

Statistical analyses were performed using GraphPad Prism 5 statistical software (GraphPad Software, San Diego, CA, USA). The data were presented as means ± SD, and multiple groups were evaluated using one-way ANOVA followed by a *post-hoc* Bonferroni test. Differences in survival were conducted using the Kaplan–Meier method with a log-rank test. p-value < 0.05 was considered statistically significant differences.

RESULTS

4-PBA Ameliorated HALI in Mice

To investigate the protective effect of 4-PBA in mice with exposure to 100% O_2, the survival was compared between the hyperoxia + 4-PBA group and the saline + hyperoxia group. All mice exposed to hyperoxia died within 105 h hours, whereas treatment with 4-PBA significantly prolonged survival in mice exposed to hyperoxia (**Figure 1A**). The protein and LDH levels in the BALF in mice with exposure to hyperoxia for 24, 48, and 72 hours were time-dependently increased (**Figures 1B, C**). The W/D ratio was significantly increased but AFC was significantly decreased in mice with exposure to hyperoxia for 72 hours when compared with the room air group (**Figures 1D, E**). Histologic evaluation of lung tissues in mice with exposure to hyperoxia for 72 hours showed distinct alveolar wall thickening and increased neutrophil infiltration in the interstitium and alveoli (**Figure 1F**). In contrast, treatment with 4-PBA significantly decreased protein and LDH levels in the BALF, and W/D ratio, increased AFC, and improved pathological change in lung tissue (**Figures 1B–F**).

4-PBA Suppressed Hyperoxia-Induced Increase of Inflammatory Mediator Production in BALF

To assess the anti-inflammatory effects of 4-PBA on HALI, TNF-α, IL-6, KC, and MCP-1 production in BALF were detected. The levels of TNF-α, IL-6, MCP-1 and KC were significantly increased after exposure to hyperoxia for 72 hours compared with the room air group (**Figures 2A–D**). However, 4-PBA-treated mice markedly reduced the level of these inflammatory mediators in BALF. These results indicate that 4-PBA may attenuate HALI by suppressing the inflammatory response.

4-PBA Attenuated Hyperoxia-Induced ROS Production

The index for oxidative stress including MPO, MDA, and protein carbonyl was examined to evaluate the anti-oxidative activity of 4-PBA in mice with HALI. Hyperoxia induced significant increases in the numbers of MPO-positive cells, and the levels of MDA and protein carbonyl contents in the lung tissue (**Figures 3A–C**). However, 4-PBA significantly suppressed these increases.

4-PBA Inhibited NF-κB Signaling Pathway and Apoptosis in Mice With HALI

To investigate whether 4-PBA treatment can inhibit the NF-κB signaling pathway and apoptosis in HALI, the protein expressions of NF-κB, IκB-α, cleaved caspase-3, and Bcl-2 were measured by Western blotting. The reduction in cytoplasmic IκB-α after 72 hours of exposure to hyperoxia corresponded with an increase in nuclear p65, indicating activation of the NF-κB pathway (**Figures 4A–C**). The level of cleaved caspase-3 was significantly increased (**Figures 4A, E**), whereas the Bcl-2 was significantly decreased in the hyperoxia group compared to the room air group (**Figures 4A, D**). In contrast, 4-PBA treatment significantly increased IκB-α and Bcl-2 levels, and decreased NF-κB p65 and cleaved caspase-3 levels.

4-PBA Reduced ER Stress-Related Protein Expressions in Mice With HALI

To evaluate whether ER stress-related proteins are activated upon HALI, the protein levels of GRP78, p-PERK, p-IRE1, ATF-6, CHOP, ATF-4, and p-eIF2α were measured in lung tissues. Western blot analyses demonstrated that the levels of GRP78, p-PERK, p-IRE1, ATF-6, CHOP, ATF-4, and p-eIF2α in lung tissues were significantly increased after 72 hours hyperoxia exposure, compared with the room air group. The increase of ER stress-related proteins after 72hours hyperoxia exposure were markedly reduced by administration of 4-PBA (**Figures 5A–H**).

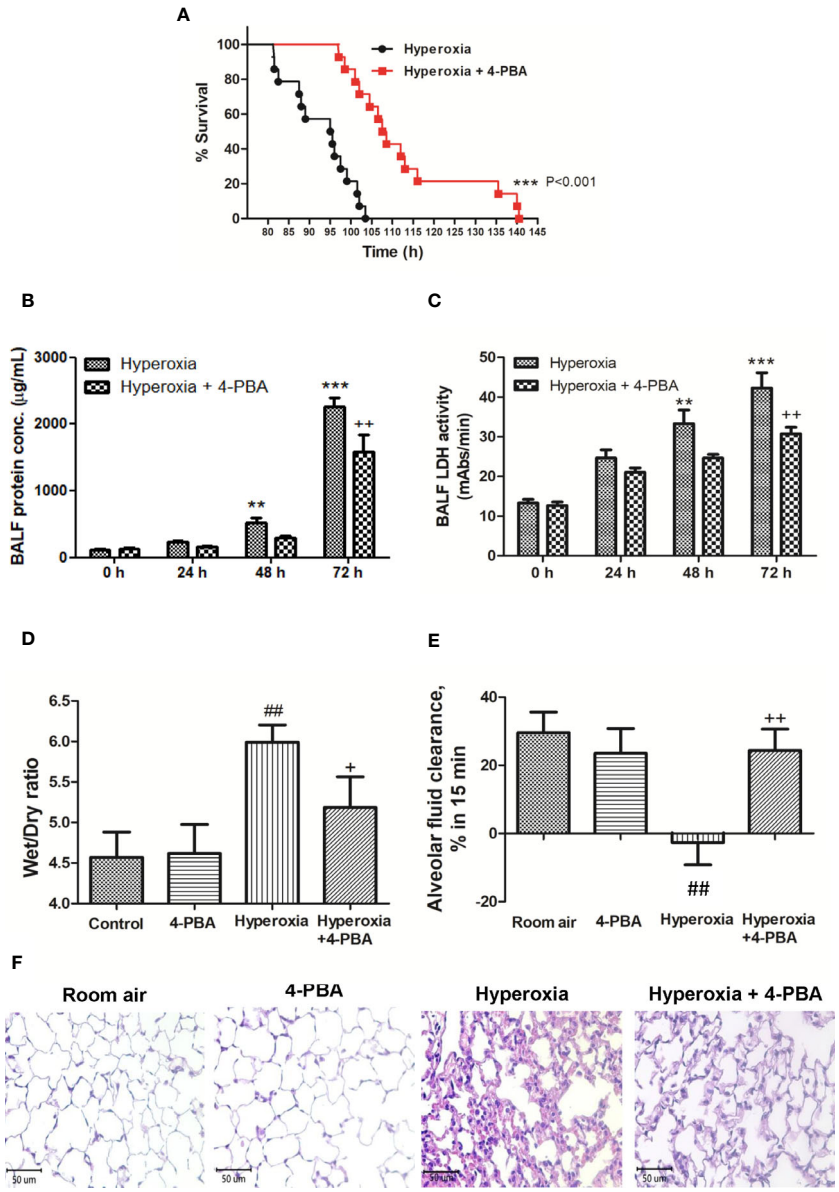

FIGURE 1 | 4-PBA prolonged survival rate, and improved lung edema and lung histopathology in mice with hyperoxia-induced lung injury. Survival was determined every 5 hours. The Kaplan–Meier survival curve was plotted and the difference in survival between the groups was significant ($p < 0.001$, log-rank test) **(A)**. Protein concentration in bronchoalveolar lavage fluid (BALF) **(B)**, BALF lactate dehydrogenase (LDH) activity **(C)**, and lung wet/dry ratio (W/D) **(D)** significantly increased in the hyperoxia group. Treatment with 4-PBA significantly attenuated the increase in these parameters. In addition, the 4-PBA increased AFC in mice exposed to hyperoxia 72 hours **(E)**. 4-PBA treatment significantly reduced thickening of the alveolar walls and neutrophil infiltration in the hyperoxia group. (representative results, Bar = 50 μm, hematoxylin, and eosin staining) **(F)**. Data are expressed as mean ± SD (6 mice per group). $^{**}p < 0.01$, $^{***}p < 0.001$, compared with the 0 hour group; $^{+}p < 0.05$, $^{++}p < 0.01$, compared with the hyperoxia (72h) group; $^{\#\#}p < 0.01$ compared with the room air group.

4-PBA Restored the Hyperoxia-Induced Disruption of Tight Junctions in Lung Tissue

To understand whether 4-PBA can regulate the expression of various claudin proteins in mice with HALI, claudin-3, claudin-4, and claudin-18 in the lung were determined. The result demonstrated that the levels of claudin-3, claudin-4, and claudin-18 in lung tissues were significantly decreased at 72 hours exposed to hyperoxia, compared with the room air group. The decrease of claudin-4 protein after hyperoxia exposure was significantly increased by administration of 4-PBA but not for claudin-3 and claudin-18 (**Figures 6A, B**). Immunofluorescence images from the room air group indicated that claudin-4 was localized in the alveolar epithelium cells showing continuous distribution. After 72 hours exposure to hyperoxia, claudin-4 showed discontinuous and decreased expression. Treatment with 4-PBA increased the staining intensity compared with the

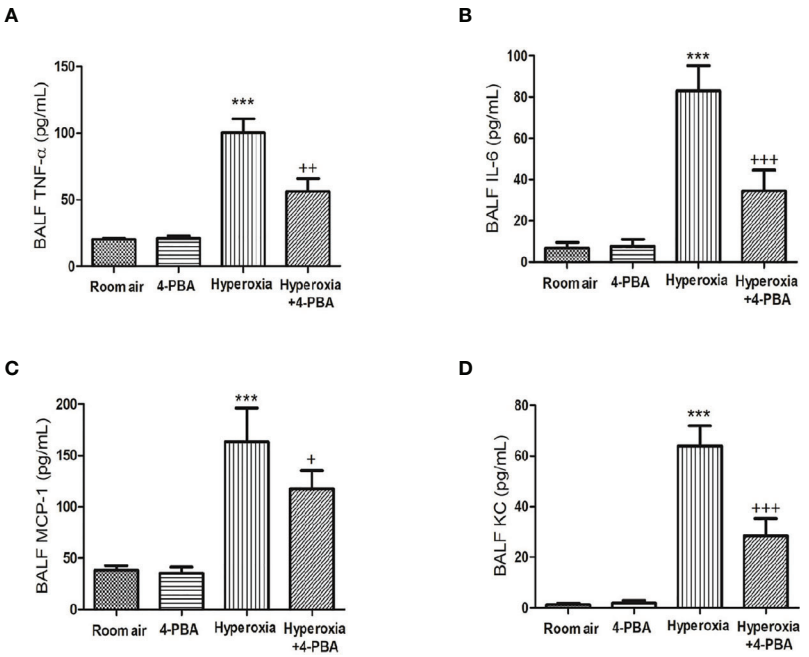

FIGURE 2 | 4-PBA alleviates hyperoxia-induced inflammatory mediator production in the bronchoalveolar lavage fluid (BALF). TNF-α **(A)**, IL-6 **(B)**, MCP-1 **(C)**, and KC **(D)** levels were analyzed by ELISA in the BALF. Data are expressed as mean ± SD (6 mice per group). ***p < 0.001, compared with the room air group; $^{+}$p < 0.05, $^{++}$p < 0.01, $^{+++}$p < 0.001 compared with the hyperoxia group.

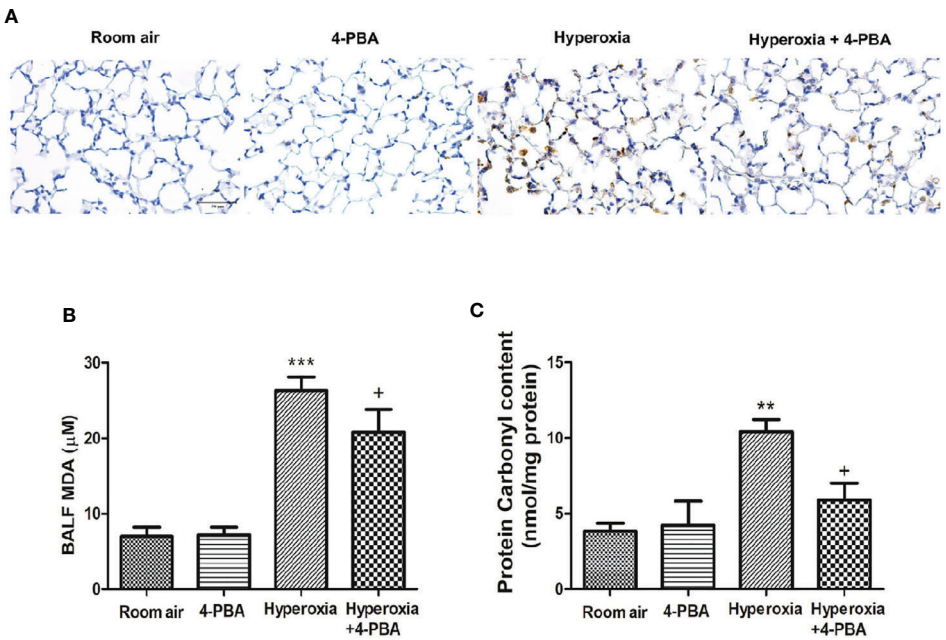

FIGURE 3 | 4-PBA attenuates hyperoxia-induced oxidative stress in lung tissue. Immunohistochemical staining (×200) of MPO in 72 hours after hyperoxia **(A)**. The MDA levels in the BALF **(B)**, and protein carbonyl contents **(C)** in lung tissues were analyzed by ELISA. Data are expressed as mean ± SD (6 mice per group). **p < 0.01, ***p < 0.001, compared with the room air group; $^{+}$p < 0.05 compared with the hyperoxia group.

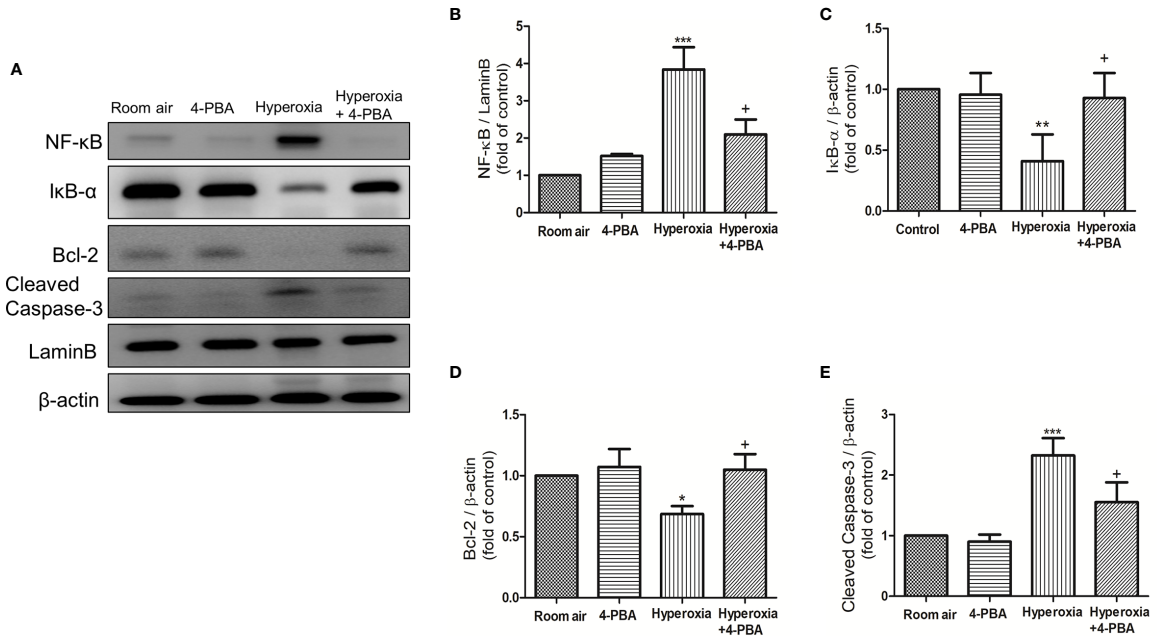

FIGURE 4 | 4-PBA suppresses NF-κB signaling pathway and apoptosis in mice with HALI. **(A)** Western blot analysis of NF-κB, IκB-α, Bcl-2 and cleaved caspase-3 expression in lung tissues. Relative expressions of NF-κB **(B)**, IκB-α **(C)**, Bcl-2 **(D)**, and cleaved caspase-3 **(E)** in lung tissues were shown. Data are expressed as mean ± SD (3 mice per group). *p < 0.05, **p < 0.01, ***p < 0.001, compared with the room air group; $^{+}$p < 0.05 compared with the hyperoxia group.

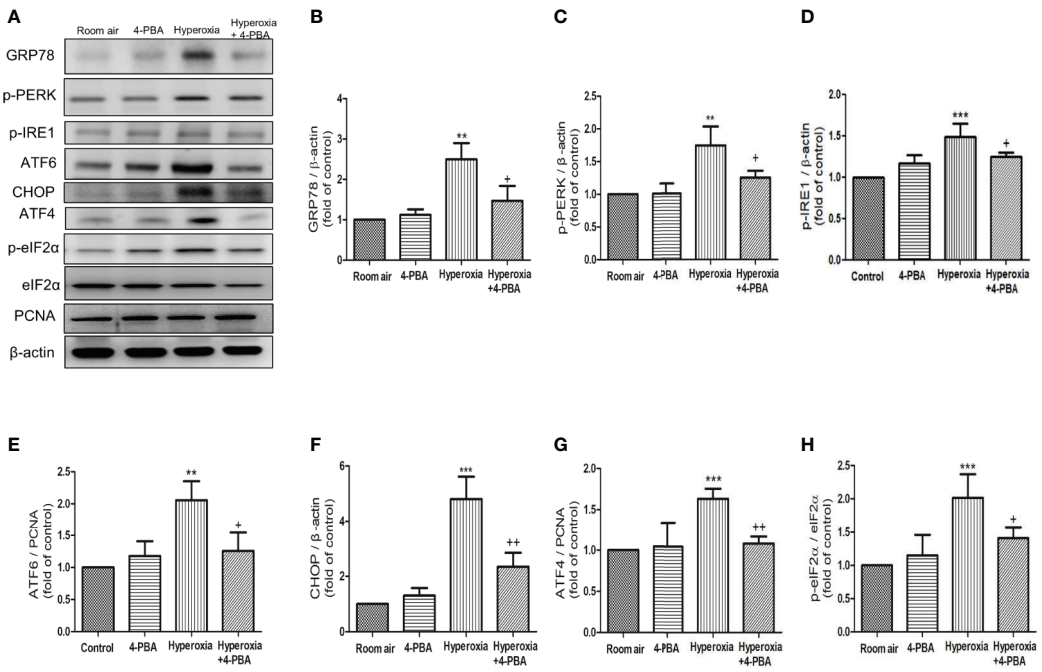

FIGURE 5 | 4-PBA alleviates hyperoxia-induced ER stress-related proteins in lung tissues. **(A)** Western blot analysis of GRP78, p-PERK, p-IRE1, ATF6, CHOP, ATF4, and p-eIF-2 expression in lung tissues. Relative expressions of GRP78 **(B)**, p-PERK **(C)**, p-IRE1 **(D)**, ATF6 **(E)**, CHOP **(F)**, ATF4 **(G)**, and p-eIF-2 **(H)** in lung tissues were shown. Data are expressed as mean ± SD (3 mice per group). **p < 0.01, ***p < 0.001, compared with the room air group; $^{+}$p < 0.05, $^{++}$p < 0.01 compared with the hyperoxia group.

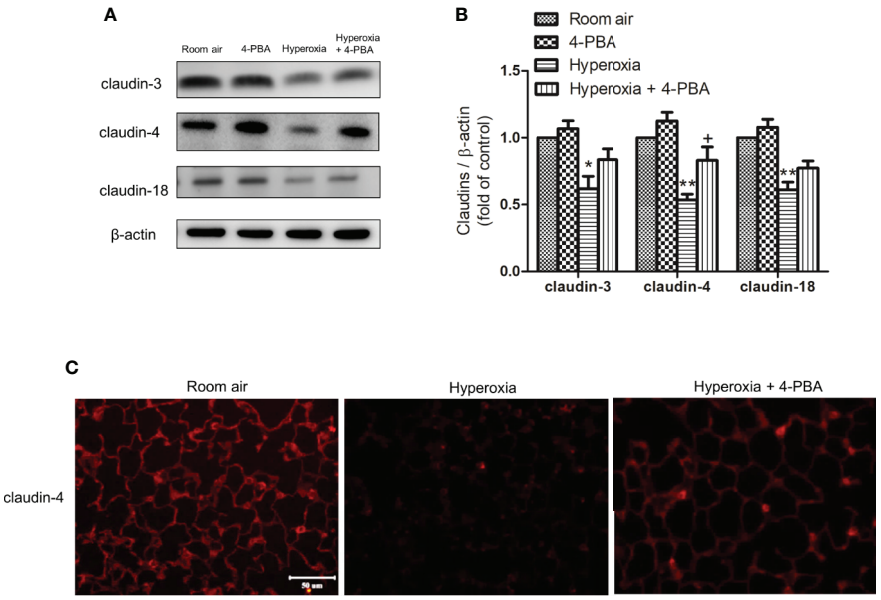

FIGURE 6 | 4-PBA enhances claudin-4 protein expression in mice with HALI. **(A)** Western blot analysis of claudin-3, claudin-4, and claudin-18 expression in lung tissues. **(B)** Relative expressions of claudins in lung tissues were shown. **(C)** Representative immunofluorescence staining of claudin-4 (red fluorescence). The results are expressed as the mean ± SD; n= 3. *p < 0.05 and **p < 0.01, compared with the room air group, $^{+}$p < 0.05 compared with the hyperoxia group.

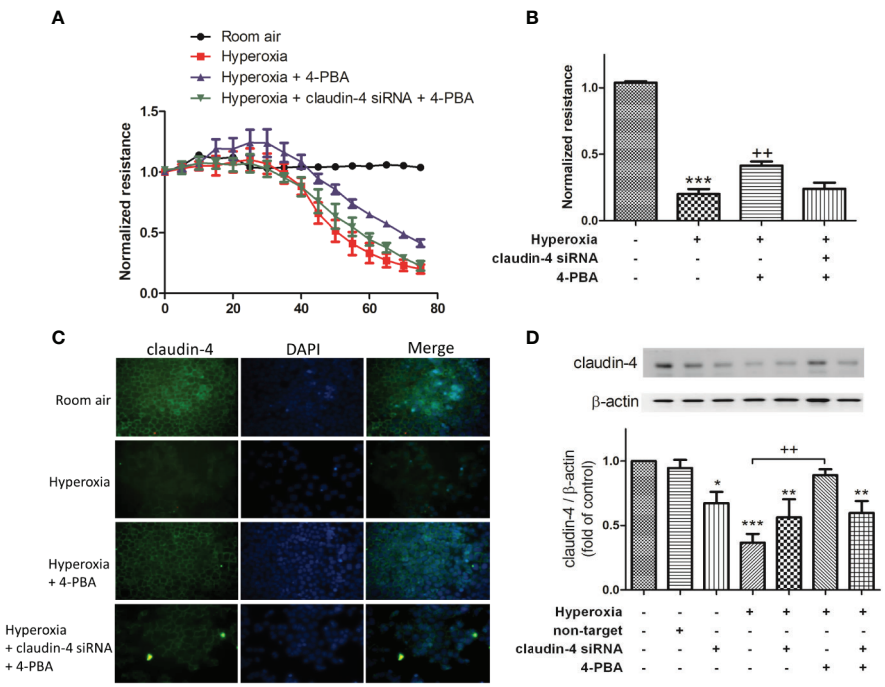

FIGURE 7 | Claudin-4 knockdown abrogates the beneficial effects of 4-PBA on barrier function of MLE-12 cells. **(A)** Dynamic measurement of barrier function in MLE-12 cells subjected to room air, hyperoxia, hyperoxia + 4-PBA, and hyperoxia + claudin-4 siRNA + 4-PBA. Depicted plots were mean normalized resistance values with standard error from 3 repeated measures in each condition **(B)** Quantitation of normalized resistance 72 hours in each condition in MLE-12 cells **(C)** Representative immunofluorescence staining of claudin-4 (green fluorescence). **(D)** Representative Western blot and densitometry analysis of claudin-4. Data are mean ± SD, each experiment was performed at least independently in triplicate, *p < 0.05, **p < 0.01, ***p < 0.001 compared with the room air group, $^{++}$p < 0.01, compared with the hyperoxia group.

hyperoxia group, demonstrating retrieval of claudin-4 protein expression (**Figure 6C**).

4-PBA Protected Against Hyperoxia-Induced Epithelial Barrier Dysfunction in MLE-12 Cells *via* Enhancing Claudin-4 Expression

To verify the role of claudin-4 in the protective effect of 4-PBA, cells were transfected with siRNA targeting claudin-4. As shown in **Figures 7A, B**, MLE-12 decreased resistance after exposed to hyperoxia, as using ECIS assessment compared with the room air group. 4-PBA-treated MLE-12 significantly increased resistance after exposed to hyperoxia. But the protective effect of 4-PBA was blunted when claudin-4 was knockdown. The immunofluorescence staining showed that the decreased fluorescence intensity and disrupted distribution of claudin-4 was noted in the MLE-12 cells exposed to hyperoxia when compared with room air. 4-PBA failed to restore barrier function in claudin-4 siRNA -treated MLE12 exposed to hyperoxia (**Figure 7C**). Treatment with 4-PBA in MLE-12 increased claudin-4 protein expression in the hyperoxia group. But the increased claudin-4 protein expression induced by 4-PBA was abolished by claudin-4 knockdown (**Figure 7D**).

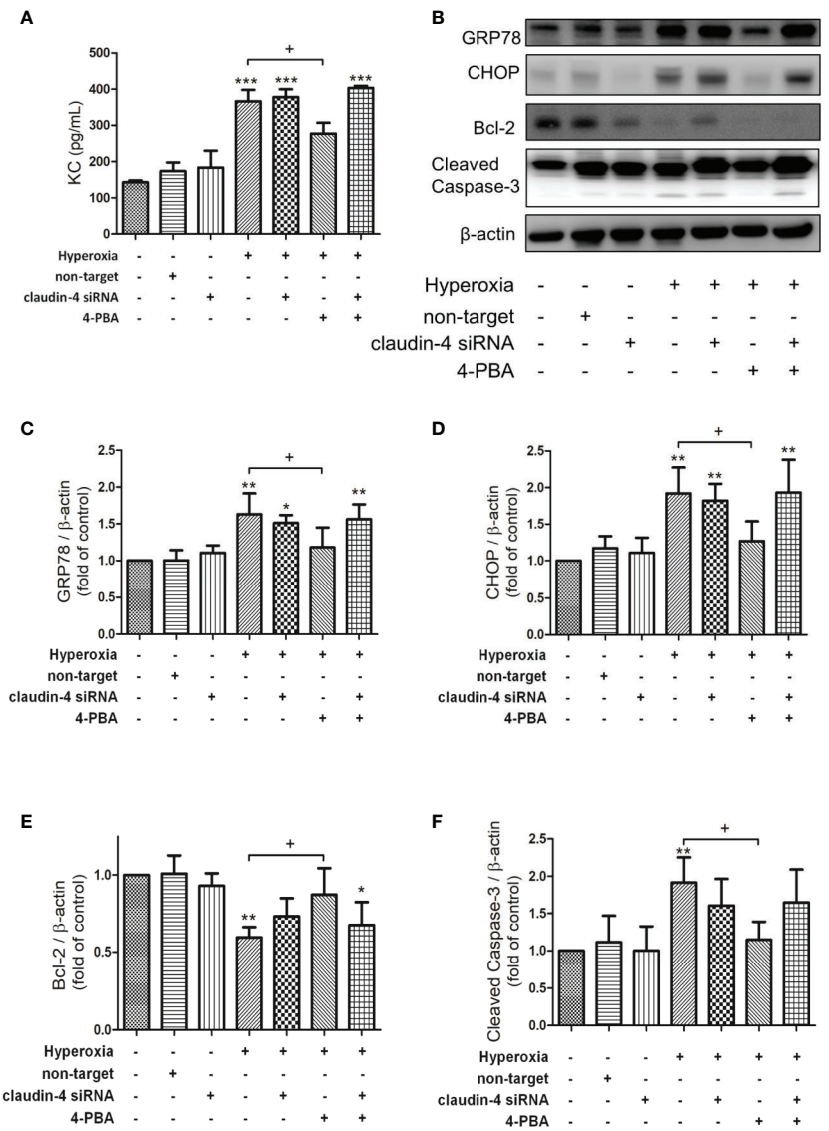

FIGURE 8 | Claudin-4 knockdown blunts the beneficial effects of 4-PBA in KC production, GRP78 and CHOP protein expression, and apoptosis in hyperoxia-exposed MLE-12 cells. **(A)** KC in BALF was measured by ELISA. **(B)** Western blot analysis of GRP78, CHOP, Bcl-2, and cleaved caspase-3 expression in MLE-12 cells. Relative expressions of GRP78 **(C)**, CHOP **(D)**, Bcl-2 **(E)**, and cleaved caspase-3 **(F)** in MLE-12 cells were shown. Data are mean ± SDs, each experiment was performed at least independently in triplicate, *$p < 0.05$, **$p < 0.01$, ***$p < 0.001$ compared with the control group, $^{+}p < 0.05$, compared with the hyperoxia group.

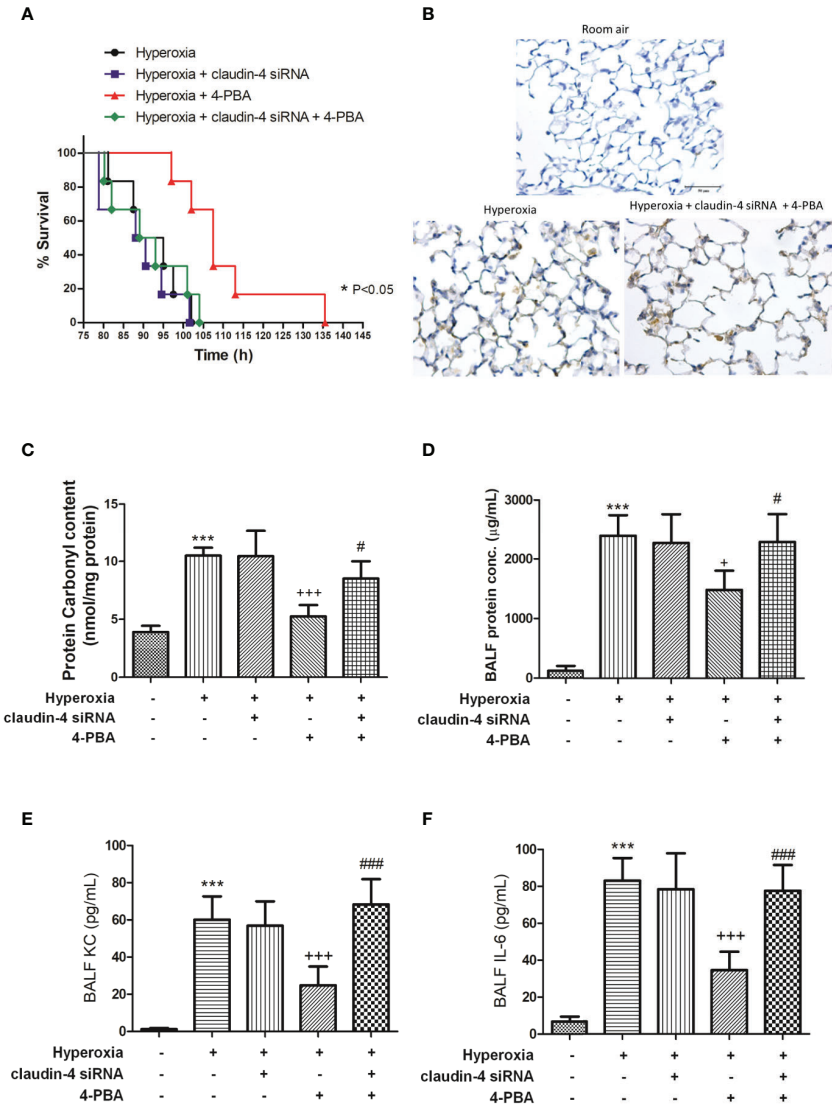

FIGURE 9 | The beneficial effects of 4-PBA in mice with hyperoxia-induced lung injury were abolished by claudin-4 siRNA. Survival for each group was monitored during the observation period and plotted as Kaplan-Meier survival curves. The difference in survival between hyperoxia + 4-PBA and hyperoxia + claudin-4 siRNA + 4-PBA groups was significant ($p < 0.05$, log-rank test) **(A)**. Representative immunohistochemical staining images of MPO **(B)**. Protein carbonyl contents **(C)** in lung tissue and protein **(D)**, KC **(E)**, and IL-6 **(F)** levels in the BALF were measured by ELISA. The results are expressed as the mean ± SD; n=6. $^{***}p < 0.001$, compared with the control group; $^{+}p < 0.05$, $^{+++}p < 0.001$ compared with the hyperoxia group. $^{\#}p < 0.05$, $^{\#\#\#}p < 0.001$ compared with the hyperoxia + 4-PBA group.

The Protective Effects of 4-PBA in Attenuating KC Production, GRP78 and CHOP Protein Expression, and Apoptosis in Hyperoxia-Exposed MLE-12 Cells Were Blocked by Claudin-4 Knockdown

In MLE-12 cells, 4PBA significantly attenuated the hyperoxia-induced increase in the level of KC, GRP78, and CHOP protein expression, and cleaved caspase-3 protein expression but decreased Bcl-2 protein expression. These beneficial effects of 4PBA were abolished in cells transfected with claudin-4 siRNA (**Figures 8A–F**).

Claudin-4 Knockdown Abolishes the Beneficial Effect of 4-PBA in Mice With HALI

When mice were treated with claudin-4 siRNA, the beneficial effect of 4-PBA in the survival of hyperoxia mice was abrogated (**Figure 9A**). Further, mice treated claudin-4 siRNA also abolished the effect of 4-PBA in decreasing pathological changes, carbonyl content in lung tissue, and protein, IL-6, and KC concentrations in BALF in hyperoxia-exposed mice (**Figures 9B–F**).

Claudin-4 Knockdown Blocked the Effect of 4-PBA in ER Stress, NF-κB Signaling Pathway, and Apoptosis in Mice With HALI

As shown in **Figure 10**, 4-PBA decreased GRP78, CHOP, NF-κB, and cleaved caspase-3 protein expressions, and increased IκB-α and Bcl-2 protein expressions. However, these beneficial effects of 4PBA disappeared when claudin-4 siRNA was employed in the mice (**Figures 10A–G**).

DISCUSSION

This study demonstrated that 4-PBA, a chemical chaperone, significantly improved multiple indices of HALI, such as prolonging survival, and decreasing AFC, lung edema, and disruption of tight junction proteins, production of pro-inflammatory cytokines, oxidative stress, the pulmonary neutrophil influx, and lung tissue damage. Furthermore, 4-PBA also inhibited hyperoxia-induced ER stress protein expressions,

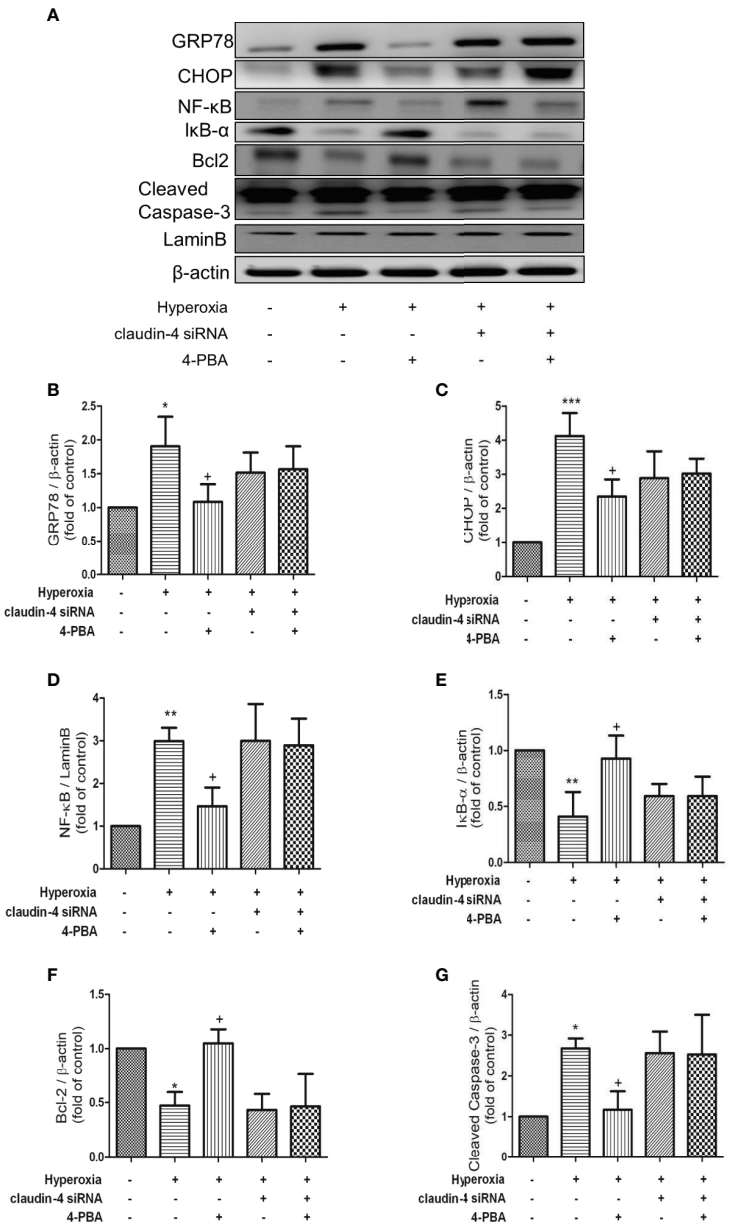

FIGURE 10 | Claudin-4 knockdown attenuates the effect of 4-PBA in GRP78 and CHOP protein expression, NF-κB signaling pathway, and apoptosis in mice with hyperoxia-induced lung injury. **(A)** Western blot analysis of GRP78, CHOP, NF-κB, IκB-α, Bcl-2, and cleaved caspase-3 expression in lung tissues. Relative expressions of GRP78 **(B)**, CHOP **(C)**, NF-κB **(D)**, IκB-α **(E)**, Bcl-2 **(F),** and cleaved caspase-3 **(G)** in lung tissues were shown. The results are expressed as the mean ± SD; n=3. *$p < 0.05$, **$p < 0.01$, ***$p < 0.001$, compared with the control group; $^{+}p < 0.05$, compared with the hyperoxia group.

apoptosis, and NF-κB signaling pathways. Consistent with *in vivo* findings, 4-PBA treatment had a similar advantageous effect on MLE-12 epithelial cells exposed to hyperoxia. Importantly, 4-PBA enhanced claudin-4 protein expression in mice and MLE-12 cells exposed to hyperoxia. However, these protective effects of 4-PBA were abolished when claudin-4 was knockdown. These experiments indicate that 4-PBA may have potential benefits as adjuvant therapy for HALI and the protective mechanism was *via* enhancing claudin-4 expression.

The involvement of ER stress in pulmonary disorders including lung cancer, pulmonary fibrosis, pulmonary infection, cigarette smoke exposure, and asthma have been reported (37–41). ER stress contributes to impair hyperoxia-induced lung injury in the rat (42, 43). 4-PBA attenuates unfold protein aggregation and ER stress in LPS-induced lung inflammation (44). In this study, 4-PBA reduced the hyperoxia-induced up-regulation of GRP78, PERK, IRE1α, ATF4, ATF6, eIF2, and CHOP in both mice and MLE12. The results showed that 4-PBA was able to attenuate the pathologic changes associated with HALI. These findings suggest that ER stress is one of the crucial players during inducing and maintaining HALI.

Transmembrane and cytosolic proteins create a primary barrier to maintain lung fluid balance. The barrier function of all epithelia and endothelia is mainly provided by tight junction proteins. Claudins were integral membrane proteins found in tight junction that mainly provided the barrier function of all epithelia and endothelia (45). Hyperoxia exposure decreased claudin-4 protein expression that resulted in alveolar epithelial barrier dysfunction (18). Vyas-Read et al. (46) demonstrated that the claudin composition of tight junctions in the pulmonary epithelium was affected by hyperoxia that increased rat sensibility to pulmonary edema and respiratory distresses. The results showed that hyperoxia impaired the expression of claudin-4 proteins and thereby increased the vascular permeability, and 4-PBA treatment significantly increased claudin-4 protein expression but not claudin-3 and claudin-18, which reduced the severity of lung injury. Moreover, in *in vitro* studies using MLE-12 epithelial cells exposed to hyperoxia, 4-PBA significantly attenuated the hyperoxia-induced epithelial barrier dysfunction and increased claudin-4 protein expression. However, the beneficial effect of 4-PBA was diminished by claudin-4 siRNA administration in mice and MLE-12 cells. These data suggested that the beneficial effect of 4-PBA in HALI was mediated by enhancing claudin-4 protein expression. Further study is needed to understand how 4-PBA increases the expression of claudin-4 in HALI.

It is clear that ER and oxidative stress are highly inter-related biological processes of exacerbating the inflammation which leads to pathophysiology in HALI (4). When ER protein folding is severely impaired in HALI, a large amount of ROS will be produced (4). High ROS levels can activate injured signaling pathways that aggravate inflammation, modify cellular signaling and function, leading to cell death. ER stress was also an important feature in epithelial cell dysfunction and death, both of which contributed to inflammation and disease. Harding et al. (47) have reported that the production of ROS has been linked to ER stress and the UPR. Further, ROS generation and ER stress are closely linked events of apoptosis (48). When the ER stress is lessened, cells will survive due to UPR-activated pro-survival signaling (48). Blocking ER stress with 4-PBA significantly decreased intracellular ROS generation and apoptosis (49–51). Therefore, ROS generation and ER stress accentuated each other through a positive feed-forward loop (48, 52). In the present study, administration of 4-PBA effectively reduced ER stress, MDA, protein carbonyl, and inflammatory response in HALI. Our results were also comparable with previous reports (50, 51). However, the exact mechanism needs further clarification.

A lot of evidence has demonstrated that ROS can disrupt epithelial and endothelial TJ proteins (53). Compromised tight junction barrier increases paracellular permeability and triggers a series of events including apoptosis and inflammatory response in the gastrointestinal tract, liver, kidney, lung, and brain (35, 53, 54). TJ barrier dysfunction and inflammation are closely related with each other, and proinflammatory cytokines contributes to the inflammatory cascade, TJ dysregulation, and apoptosis. Further, ROS can disturb ER protein folding, induce ER stress, and decrease the expression of TJs (49, 55). Subsequently, it can stimulate the UPR to cause apoptosis (49, 56). Previous studies also demonstrated the complex links between TJ proteins, cell death pathways, and inflammatory responses (56). In this study, 4-PBA effectively reduced oxidative and ER stress, the level of proinflammatory cytokines, and apoptosis but increased claudin 4 protein expression in HALI. Therefore, the integration of the TJ proteins, inflammatory signaling pathways, ROS, ER stress and apoptosis is important to the pathogenesis of a variety of diseases. However, the detailed molecular mechanisms in the complex network of interactions are still not elucidated. Further study will be required to understand the interplay.

NF-kB signaling pathway is critical for inflammatory response and associated with the production of various cytokines and chemokines (57). Under physiological conditions, NF-κB proteins are normally sequestered in the cytoplasm by its endogenous inhibitor, IκB. Upon activation, IκB phosphorylation triggers ubiquitin-dependent degradation and subsequently releases NF-κB which translocates to the nucleus and induces transcription of target genes (58). Previous studies have previously demonstrated that HALI promoted IκB degradation and NF-κB activation (29, 46). It had been previously shown that inhibition of NF-κB attenuated the stretch-induced increase in alveolar epithelial cell permeability (59). Kim et al. (45) showed that 4-PBA attenuated LPS-mediated NF-κB activation in the lungs. In this study, 4-PBA significantly suppressed IκB degradation and NF-κB activation that led to decreased production of proinflammatory cytokines and chemokines, such as TNF-α, IL-6, MCP-1, and KC, and reduced leukocyte infiltration in lung tissue. Moreover, in *in vitro* studies, 4-PBA also significantly inhibited NF-κB activation and the production of KC in MLE-12. Therefore, the anti-inflammatory effect of 4-PBA could be partly explained by its inhibition of NF-κB signaling and the consequent production of pro-inflammatory cytokines. However, these protective effects of 4-PBA were canceled by claudin-4 gene knockdown.

The present study focused on changes in the protein levels of claudin-4 by 4-PBA. Other types of intercellular junctions, such as occludin and zonula occludens (ZO) proteins also regulate tight junction assembly. Occludin-deficient mice are viable, indicating that occludin is not required for epithelia to form functional tight junctions. Further, barrier function in ZO-1/ZO-2-deficient Madin-Darby canine kidney cells is comparable to that of wild-type

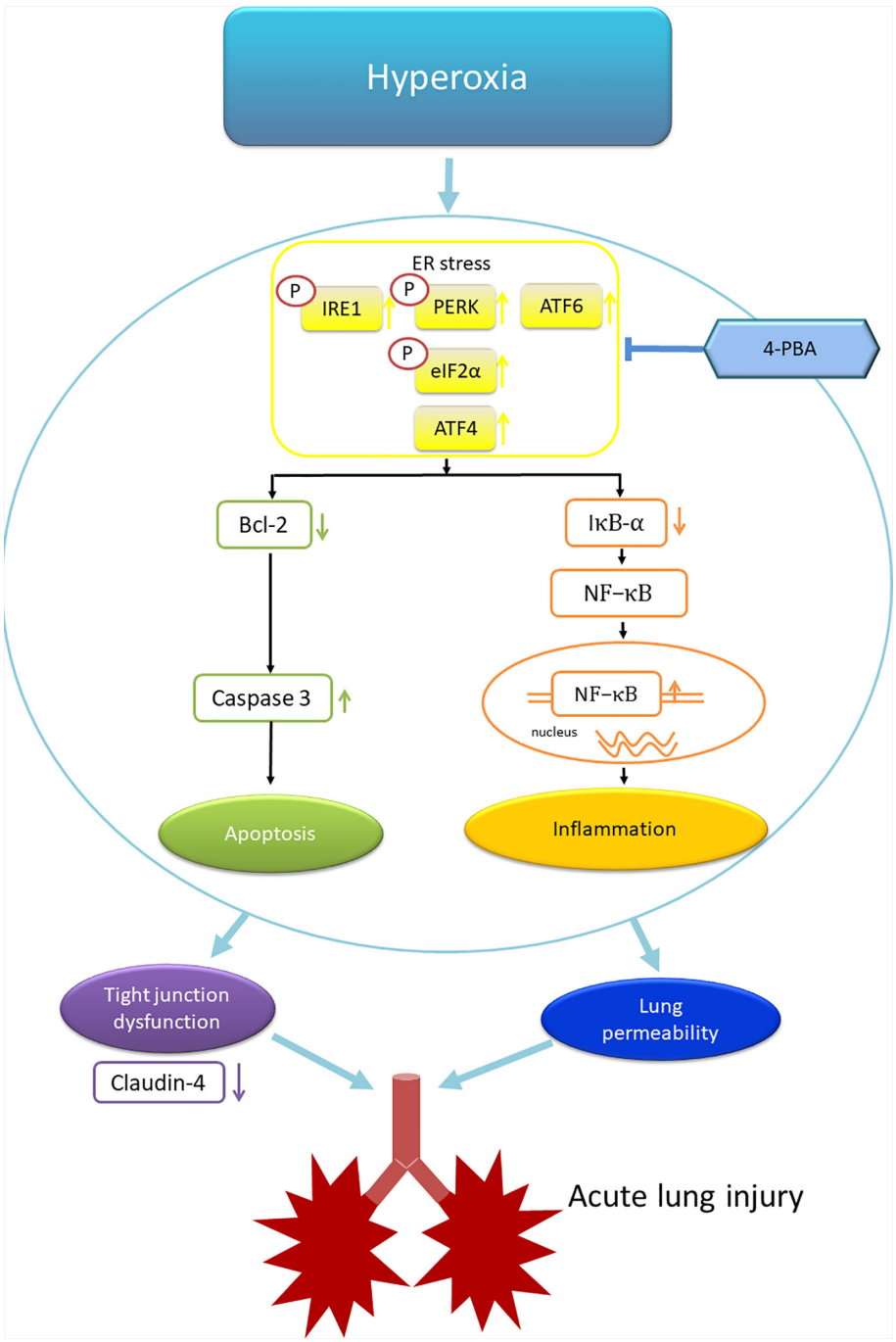

FIGURE 11 | Schematic shows that hyperoxia triggers endoplasmic reticulum (ER) stress responses that lead to inflammation and apoptosis. The inflammation and apoptosis impair tight junction function and lung vascular permeability that induce acute lung injury. 4-PBA administration improves these phenomena. ATF4, activating transcription factor 4; ATF6, activating transcription factor 6; IRE1, inositol-requiring enzyme 1; PERK, protein kinase-like ER kinase. p-eIF-2α, eukaryotic translation initiation factor 2α.

controls (60). All claudin family members have their various roles in modulating paracellular solutes transportation through adjacent epithelial cells. The effects of combinations of other claudins with claudin-4 in HALI were not clear (61). Further, the possibility that ER stress is involved in the oligomerization of these proteins under hyperoxia condition should be further investigated.

In summary, this study demonstrated that 4-PBA, an ER stress inhibitor, attenuated HALI by prolonging survival, decreasing lung edema, production of inflammatory cytokines, reactive oxygen species, apoptosis, and the activation of NF-κB and ER stress signaling (**Figure 11**). In addition, 4-PBA increased the TJ protein expression of claudin-4. The results of *in vitro* experiments with 4-PBA and MLE-12 cells exposed to hyperoxia confirmed the *in vivo* experiments. But these beneficial effects of 4-PBA were abolished when claudin-4 was knocked down. Further understanding of the physiological action of 4-PBA for tight junction protein is needed before being considered as a therapeutic option in HALI.

DATA AVAILABILITY STATEMENT

The raw data supporting the conclusions of this article will be made available by the authors, without undue reservation.

ETHICS STATEMENT

The animal study was reviewed and approved by the Animal Review Committee of National Defense Medical Center (approval number: IACUC-17-258).

AUTHOR CONTRIBUTIONS

H-PP, K-LH and S-ET participated in research design. H-PP and S-YW conducted experiments. W-IL and S-YW performed data analysis. H-PP and S-JC contributed to the writing of the manuscript. All authors contributed to the article and approved the submitted version.

FUNDING

This study was supported, in part, by grants MOST 106-2314-B-016-019 -MY3 and MOST 109-2314-B-016-028- from Ministry of Science and Technology, Taiwan, TSGH-D-110045, TSGH-D-109078, and TSGH-C107-054 from Tri-Service General Hospital, and MND-MAB-110-038, MAB-109-021, MAB-108-016, and MAB-107-011 from Ministry of National Defense-Medical Affairs Bureau, Taiwan.

SUPPLEMENTARY MATERIAL

The Supplementary Material for this article can be found online at: https://www.frontiersin.org/articles/10.3389/fimmu.2021.674316/full#supplementary-material

Supplementary Figure 1 | Survival was determined every 5 hours. The Kaplan–Meier survival curve was plotted. Mice administered 4-PBA 10 mg/kg had a higher survival rate versus the other three groups ($p < 0.001$, log-rank test).

Supplementary Figure 2 | MLE-12 cells were transfected with varying doses of claudin-4 siRNA and immunoblotted against claudin-4 or β-actin (loading control).

Supplementary Figure 3 | Two doses of claudin-4 siRNA were administrated intratracheally. These lung lysates were immunoblotted against claudin-4 or β-actin (loading control).

REFERENCES

1. Kallet RH, Matthay MA. Hyperoxic Acute Lung Injury. *Respir Care* (2013) 58:123–41. doi: 10.4187/respcare.01963
2. Gore A, Muralidhar M, Espey MG, Degenhardt K, Mantell LL. Hyperoxia Sensing: From Molecular Mechanisms to Significance in Disease. *J Immunotoxicol* (2010) 7:239–54. doi: 10.3109/1547691X.2010.492254
3. Perng WC, Huang KL, Li MH, Hsu CW, Tsai SH, Chu SJ, et al. Glutamine Attenuates Hyperoxia-Induced Acute Lung Injury in Mice. *Clin Exp Pharmacol Physiol* (2010) 37:56–61. doi: 10.1111/j.1440-1681.2009.05239.x
4. Altemeier WA, Sinclair SE. Hyperoxia in the Intensive Care Unit: Why More Is Not Always Better. *Curr Opin Crit Care* (2007) 13:73–8. doi: 10.1097/MCC.0b013e32801162cb
5. Zhang K, Kaufman RJ. From Endoplasmic-Reticulum Stress to the Inflammatory Response. *Nature* (2008) 454:455–62. doi: 10.1038/nature07203
6. Rutkowski DT, Kaufman RJ. That Which Does Not Kill Me Makes Me Stronger: Adapting to Chronic ER Stress. *Trends Biochem Sci* (2007) 32:469–76. doi: 10.1016/j.tibs.2007.09.003
7. Oslowski CM, Urano F. Measuring ER Stress and the Unfolded Protein Response Using Mammalian Tissue Culture System. *Methods Enzymol* (2011) 490:71–92. doi: 10.1016/B978-0-12-385114-7.00004-0
8. Rozpedek W, Pytel D, Mucha B, Leszczynska H, Diehl JA, Majsterek I. The Role of the PERK/eIF2α/ATF4/CHOP Signaling Pathway in Tumor Progression During Endoplasmic Reticulum Stress. *Curr Mol Med* (2016) 16:533–44. doi: 10.2174/1566524016666160523143937
9. Pakos-Zebrucka K, Koryga I, Mnich K, Ljujic M, Samali A, Gorman AM. The Integrated Stress Response. *EMBO Rep* (2016) 17:1374–95. doi: 10.15252/embr.201642195
10. Wu R, Zhang Q-H, Lu Y-J, Ren K, Yi G-H. Involvement of the IRE1α-XBP1 Pathway and XBP1s-Dependent Transcriptional Reprogramming in Metabolic Diseases. *DNA Cell Biol* (2015) 34:6–18. doi: 10.1089/dna.2014.2552
11. Hotamisligil GS. Endoplasmic Reticulum Stress and the Inflammatory Basis of Metabolic Disease. *Cell* (2010) 140:900–17. doi: 10.1016/j.cell.2010.02.034
12. Matus S, Glimcher LH, Hetz C. Protein Folding Stress in Neurodegenerative Diseases: A Glimpse Into the ER. *Curr Opin Cell Biol* (2011) 23:239–52. doi: 10.1016/j.ceb.2011.01.003
13. McGuckin MA, Eri RD, Das I, Lourie R, Florin TH. ER Stress and the Unfolded Protein Response in Intestinal Inflammation. *Am J Physiol Gastrointest Liver Physiol* (2010) 298:G820–32. doi: 10.1152/ajpgi.00063.2010
14. Marciniak SJ. Endoplasmic Reticulum Stress in Lung Disease. *Eur Respir Rev* (2017) 26:170018. doi: 10.1183/16000617.0018-2017
15. Tommaso I, Beniamino P. Clinical and Experimental Applications of Sodium Phenylbutyrate. *Drugs R D* (2011) 11(3):227–49. doi: 10.2165/11591280-000000000-00000
16. Ceylan-Isik AF, Sreejayan N, Ren J. Endoplasmic Reticulum Chaperon Tauroursodeoxycholic Acid Alleviates Obesity-Induced Myocardial Contractile Dysfunction. *J Mol Cell Cardiol* (2011) 50:107–16. doi: 10.1016/j.yjmcc.2010.10.023
17. Özcan U, Yilmaz E, Özcan L, Furuhashi M, Vaillancourt E, Smith RO, et al. Chemical Chaperones Reduce ER Stress and Restore Glucose Homeostasis in

a Mouse Model of Type 2 Diabetes. *Science* (2006) 313:1137–40. doi: 10.1126/science.1128294
18. Qi X, Hosoi T, Okuma Y, Kaneko M, Nomura Y. Sodium 4-Phenylbutyrate Protects Against Cerebral Ischemic Injury. *Mol Pharmacol* (2004) 66:899–908. doi: 10.1124/mol.104.001339
19. Ricobaraza A, Cuadrado-Tejedor M, Marco S, Pérez-Otaño I, García-Osta A. Phenylbutyrate Rescues Dendritic Spine Loss Associated With Memory Deficits in a Mouse Model of Alzheimer Disease. *Hippocampus* (2012) 22:1040–50. doi: 10.1002/hipo.20883
20. Zeng M, Sang W, Chen S, Chen R, Zhang H, Xue F, et al. 4-PBA Inhibits LPS-Induced Inflammation Through Regulating ER Stress and Autophagy in Acute Lung Injury Models. *Toxicol Lett* (2017) 271:26–37. doi: 10.1016/j.toxlet.2017.02.023
21. Teng R-J, Jing X, Michalkiewicz T, Afolayan AJ, Wu T-J, Konduri GG. Attenuation of Endoplasmic Reticulum Stress by Caffeine Ameliorates Hyperoxia-Induced Lung Injury. *Am J Physiol Lung Cell Mol Physiol* (2017) 312:L586–L98. doi: 10.1152/ajplung.00405.2016
22. Schlingmann B, Molina SA, Koval M. Claudins: Gatekeepers of Lung Epithelial Function. *Semin Cell Dev Biol* (2015) 42:47–57. doi: 10.1016/j.semcdb.2015.04.009
23. Frank JA. Claudins and Alveolar Epithelial Barrier Function in the Lung. *Ann N Y Acad Sci* (2012) 1257:175–83. doi: 10.1111/j.1749-6632.2012.06533.x
24. Rokkam D, LaFemina MJ, Lee JW, Matthay MA, Frank JA. Claudin-4 Levels are Associated With Intact Alveolar Fluid Clearance in Human Lungs. *Am J Pathol* (2011) 179:1081–87. doi: 10.1016/j.ajpath.2011.05.017
25. Kage H, Flodby P, Gao D, Kim YH, Marconett CN, DeMaio L, et al. Claudin 4 Knockout Mice: Normal Physiological Phenotype With Increased Susceptibility to Lung Injury. *Am J Physiol Lung Cell Mol Physiol* (2014) 307:L524–L36. doi: 10.1152/ajplung.00077.2014
26. Yuan X, Wang J, Li Y, He X, Niu B, Wu D, et al. Allergy Immunotherapy Restores Airway Epithelial Barrier Dysfunction Through Suppressing IL-25-induced Endoplasmic Reticulum Stress in Asthma. *Sci Rep* (2018) 8:1–11. doi: 10.1038/s41598-018-26221-x
27. Zhou Y, Ye L, Zheng B, Zhu S, Shi H, Zhang H, et al. Phenylbutyrate Prevents Disruption of Blood-Spinal Cord Barrier by Inhibiting Endoplasmic Reticulum Stress After Spinal Cord Injury. *Am J Transl Res* (2016) 8(4):1864–75.
28. Xu S, Xue X, You K, Fu J. Caveolin-1 Regulates the Expression of Tight Junction Proteins During Hyperoxia-Induced Pulmonary Epithelial Barrier Breakdown. *Respir Res* (2016) 17:50. doi: 10.1186/s12931-016-0364-1
29. Lin H-J, Wu C-P, Peng C-K, Lin S-H, Uchida S, Yang S-S, et al. With-No-Lysine Kinase 4 Mediates Alveolar Fluid Regulation in Hyperoxia-Induced Lung Injury. *Crit Care Med* (2015) 43:e412–9. doi: 10.1097/CCM.0000000000001144
30. Nadia R, Brigitte E, Chrystophe F, Alexandre F, Nicole F-J, Ci C, et al. β-Liddle Mutation of the Epithelial Sodium Channel Increases Alveolar Fluid Clearance and Reduces the Severity of Hydrostatic Pulmonary Oedema in Mice. *J Physiol* (2007) 582(Pt 2):777–88. doi: 10.1113/jphysiol.2007.131078
31. Wu G-C, Liao W-I, Wu S-Y, Pao H-P, Tang S-E, Li M-H, et al. Targeting of Nicotinamide Phosphoribosyltransferase Enzymatic Activity Ameliorates Lung Damage Induced by Ischemia/Reperfusion in Rats. *Respir Res* (2017) 18:71. doi: 10.1186/s12931-017-0557-2
32. Liao W-I, Wu S-Y, Wu G-C, Pao H-P, Tang S-E, Huang K-L, et al. Ac2-26, an Annexin A1 Peptide, Attenuates Ischemia-Reperfusion-Induced Acute Lung Injury. *Int J Mol Sci* (2017) 18:1771. doi: 10.3390/ijms18081771
33. Wu S-Y, Tang S-E, Ko F-C, Wu G-C, Huang K-L, Chu S-J. Valproic Acid Attenuates Acute Lung Injury Induced by Ischemia–Reperfusion in Rats. *Anesthesiology* (2015) 122:1327–37. doi: 10.1097/ALN.0000000000000618
34. Hung K-Y, Liao W-I, Pao H-P, Wu S-Y, Huang K-L, Chu S-J. Targeting F-Box Protein Fbxo3 Attenuates Lung Injury Induced by Ischemia-Reperfusion in Rats. *Front Pharmacol* (2019) 10:583. doi: 10.3389/fphar.2019.00583
35. Pao H-P, Liao W-I, Wu S-Y, Hung K-Y, Huang K-L, Chu S-J. PG490-88, a Derivative of Triptolide, Suppresses Ischemia/Reperfusion-Induced Lung Damage by Maintaining Tight Junction Barriers and Targeting Multiple Signaling Pathways. *Int Immunopharmacol* (2019) 68:17–29. doi: 10.1016/j.intimp.2018.12.058
36. Bivas-Benita M, Zwier R, Junginger HE, Borchard G. Non-Invasive Pulmonary Aerosol Delivery in Mice by the Endotracheal Route. *Eur J Pharm Biopharm* (2005) 61:214–18. doi: 10.1016/j.ejpb.2005.04.009
37. Heijink IH, Brandenburg SM, Noordhoek JA, Postma DS, Slebos DJ, Oosterhout AJM. Characterisation of Cell Adhesion in Airway Epithelial Cell Types Using Electric Cell-Substrate Impedance Sensing. *Eur Respir J* (2010) 35:894–903. doi: 10.1183/09031936.00065809
38. Zhang J, Liang Y, Lin Y, Liu Y, Yin W. IRE1α-TRAF2-ASK1 Pathway Is Involved in CSTMP-induced Apoptosis and ER Stress in Human Non-Small Cell Lung Cancer A549 Cells. *BioMed Pharmacother* (2016) 82:281–89. doi: 10.1016/j.biopha.2016.04.050
39. Ayaub EA, Kolb PS, Mohammed-Ali Z, Tat V, Murphy J, Bellaye PS, et al. GRP78 and CHOP Modulate Macrophage Apoptosis and the Development of Bleomycin-Induced Pulmonary Fibrosis. *J Pathol* (2016) 239:411–25. doi: 10.1002/path.4738
40. van't Wout EF, van Schadewijk A, van Boxtel R, Dalton LE, Clarke HJ, Tommassen J, et al. Virulence Factors of Pseudomonas Aeruginosa Induce Both the Unfolded Protein and Integrated Stress Responses in Airway Epithelial Cells. *PloS Pathog* (2015) 11:e1004946. doi: 10.1371/journal.ppat.1004946
41. Kenche H, Baty CJ, Vedagiri K, Shapiro SD, Blumental-Perry A. Cigarette Smoking Affects Oxidative Protein Folding in Endoplasmic Reticulum by Modifying Protein Disulfide Isomerase. *FASEB J* (2013) 27:965–77. doi: 10.1096/fj.12-216234
42. Lee KS, Jeong JS, Kim SR, Cho SH, Kolliputi N, Ko YH, et al. Phosphoinositide 3-Kinase-δ Regulates Fungus-Induced Allergic Lung Inflammation Through Endoplasmic Reticulum Stress. *Thorax* (2016) 71:52–63. doi: 10.1136/thoraxjnl-2015-207096
43. Choo-Wing R, Syed MA, Harijith A, Bowen B, Pryhuber G, Janér C, et al. Hyperoxia and Interferon-γ–Induced Injury in Developing Lungs Occur Via Cyclooxygenase-2 and the Endoplasmic Reticulum Stress–Dependent Pathway. *Am J Respir Cell Mol Biol* (2013) 48:749–57. doi: 10.1165/rcmb.2012-381OC
44. Lu HY, Zhang J, Wang QX, Tang W, Zhang LJ. Activation of the Endoplasmic Reticulum Stress Pathway Involving CHOP in the Lungs of Rats With Hyperoxia–Induced Bronchopulmonary Dysplasia. *Mol Med Rep* (2015) 12:4494–500. doi: 10.3892/mmr.2015.3979
45. Kim HJ, Jeong JS, Kim SR, Park SY, Chae HJ, Lee YC. Inhibition of Endoplasmic Reticulum Stress Alleviates Lipopolysaccharide-Induced Lung Inflammation Through Modulation of NF-κb/Hif-1α Signaling Pathway. *Sci Rep* (2013) 3:1–10. doi: 10.1038/srep01142
46. Narala VR, Fukumoto J, Hernández-Cuervo H, Patil SS, Krishnamurthy S, Breitzig M, et al. Akap1 Genetic Deletion Increases the Severity of Hyperoxia-Induced Acute Lung Injury in Mice. *Am J Physiol Lung Cell Mol Physiol* (2018) 314:L860–L70. doi: 10.1152/ajplung.00365.2017
47. Vyas-Read S, Vance RJ, Wang W, Colvocoresses-Dodds J, Brown LA, Koval M. Hyperoxia Induces Paracellular Leak and Alters Claudin Expression by Neonatal Alveolar Epithelial Cells. *Pediatr Pulmonol* (2018) 53:17–27. doi: 10.1002/ppul.23681
48. Li PC, Wang BR, Li CC, Lu X, Qian WS, Li YJ, et al. Seawater Inhalation Induces Acute Lung Injury Via ROS Generation and the Endoplasmic Reticulum Stress Pathway. *Int J Mol Med* (2018) 41:2505–16. doi: 10.3892/ijmm.2018.3486
49. Harding HP, Zhang Y, Zeng H, Novoa I, Lu PD, Calfon M, et al. An Integrated Stress Response Regulates Amino Acid Metabolism and Resistance to Oxidative Stress. *Mol Cell* (2003) 11:619–33. doi: 10.1016/s1097-2765(03)00105-9
50. Yang L, Guan GP, Lei LJ, Liu JN, Cao LL, Wang XG. Oxidative and Endoplasmic Reticulum Stresses Are Involved in Palmitic Acid-Induced H9c2 Cell Apoptosis. *Biosci Rep* (2019) 39(5):BSR20190225. doi: 10.1042/BSR20190225
51. Lei LJ, Ge JB, Zhao H, Wang XG, Yan L. Role of Endoplasmic Reticulum Stress in Lipopolysaccharide-Inhibited Mouse Granulosa Cell Estradiol Production. *J Reprod Dev* (2019) 65(5):459–65. doi: 10.1262/jrd.2019-052
52. Malhotra JD, Kaufman RJ. Endoplasmic Reticulum Stress and Oxidative Stress: A Vicious Cycle or a Double-Edged Sword? *Antioxid Redox Signal* (2007) 9:2277–94. doi: 10.1089/ars.2007.1782
53. Rao R. Oxidative Stress-Induced Disruption of Epithelial and Endothelial Tight Junctions. *Front Biosci* (2008) 13:7210–26. doi: 10.2741/3223
54. Fukui A, Naito Y, Handa O, Kugai M, Tsuji T, Yoriki H. Acetyl Salicylic Acid Induces Damage to Intestinal Epithelial Cells by Oxidation-Related

Modifications of ZO-1. *Am J Physiol Gastrointest Liver Physiol* (2012) 303: G927–36. doi: 10.1152/ajpgi.00236.2012
55. Song MJ, Davidovich N, Lawrence GG, Margulies SS. Superoxide Mediates Tight Junction Complex Dissociation in Cyclically Stretched Lung Slices. *J Biomech* (2016) 49:1330–5. doi: 10.1016/j.jbiomech.2015.10.032
56. Ajaz AB, Srijayaprakash U, Iman WA, Sheema H, Santosh KY, Muralitharan S, et al. Tight Junction Proteins and Signaling Pathways in Cancer and Inflammation: A Functional Crosstalk. *Front Physiol* (2019) 9:1942. doi: 10.3389/fphys.2018.01942
57. Shih VF-S, Tsui R, Caldwell A, Hoffmann A. A Single NFκB System for Both Canonical and Non-Canonical Signaling. *Cell Res* (2011) 21:86–102. doi: 10.1038/cr.2010.161
58. Hayden MS, Ghosh S. NF-κB, the First Quarter-Century: Remarkable Progress and Outstanding Questions. *Genes Dev* (2012) 26:203–34. doi: 10.1101/gad.183434.111
59. Davidovich N, DiPaolo BC, Lawrence GG, Chhour P, Yehya N, Margulies SS. Cyclic Stretch-Induced Oxidative Stress Increases Pulmonary Alveolar Epithelial Permeability. *Am J Respir Cell Mol Biol* (2013) 49:156–64. doi: 10.1165/rcmb.2012-0252OC
60. McNeil E, Capaldo CT, Macara IG. Zonula Occludens-1 Function in the Assembly of Tight Junctions in Madin-Darby Canine Kidney Epithelial Cells. *Mol Biol Cell* (2006) 17(4):1922–32. doi: 10.1091/mbc.E05-07-0650
61. Tsukita S, Tanaka H, Tamura A. The Claudins: From Tight Junctions to Biological Systems. *Trends Biochem Sci* (2019) 44:141–52. doi: 10.1016/j.tibs.2018.09.008

Conflict of Interest: The authors declare that the research was conducted in the absence of any commercial or financial relationships that could be construed as a potential conflict of interest.

Copyright © 2021 Pao, Liao, Tang, Wu, Huang and Chu. This is an open-access article distributed under the terms of the Creative Commons Attribution License (CC BY). The use, distribution or reproduction in other forums is permitted, provided the original author(s) and the copyright owner(s) are credited and that the original publication in this journal is cited, in accordance with accepted academic practice. No use, distribution or reproduction is permitted which does not comply with these terms.

frontiers in Medicine

REVIEW
published: 30 June 2021
doi: 10.3389/fmed.2021.640636

Interrelationship Between Obstructive Sleep Apnea Syndrome and Severe Asthma: From Endo-Phenotype to Clinical Aspects

Beatrice Ragnoli[1], *Patrizia Pochetti*[1], *Alberto Raie*[1] *and Mario Malerba*[1,2]*

[1] Respiratory Unit, Sant'Andrea Hospital, Vercelli, Italy, [2] Traslational Medicine Department, University of Eastern Piedmont, Novara, Italy

Sleep-related breathing disorders (SBDs) are characterized by abnormal respiration during sleep. Obstructive sleep apnea (OSA), a common SBD increasingly recognized by physicians, is characterized by recurrent episodes of partial or complete closure of the upper airway resulting in disturbed breathing during sleep. OSA syndrome (OSAS) is associated with decreased patients' quality of life (QoL) and the presence of significant comorbidities, such as daytime sleepiness. Similarly to what seen for OSAS, the prevalence of asthma has been steadily rising in recent years. Interestingly, severe asthma (SA) patients are also affected by poor sleep quality—often attributed to nocturnal worsening of their asthma—and increased daytime sleepiness and snoring compared to the general population. The fact that such symptoms are also found in OSAS, and that these two conditions share common risk factors, such as obesity, rhinitis, and gastroesophageal reflux, has led many to postulate an association between these two conditions. Specifically, it has been proposed a bidirectional correlation between SA and OSAS, with a mutual negative effect in term of disease severity. According to this model, OSAS not only acts as an independent risk factor of asthma exacerbations, but its co-existence can also worsen asthma symptoms, and the same is true for asthma with respect to OSAS. In this comprehensive review, we summarize past and present studies on the interrelationship between OSAS and SA, from endo-phenotype to clinical aspects, highlighting possible implications for clinical practice and future research directions.

Keywords: sleep-reated breathing disorders, obstructive sleep apnea syndrome, severe asthma, airway inflammation, obesity

OPEN ACCESS

Edited by:
Girolamo Pelaia,
University of Catanzaro, Italy

Reviewed by:
Donato Lacedonia,
University of Foggia, Italy
Anna Brzecka,
Wroclaw Medical University, Poland

***Correspondence:**
Mario Malerba
mario.malerba@uniupo.it

Specialty section:
This article was submitted to Pulmonary Medicine, a section of the journal Frontiers in Medicine

Received: *11 December 2020*
Accepted: *27 May 2021*
Published: *30 June 2021*

Citation:
Ragnoli B, Pochetti P, Raie A and Malerba M (2021) Interrelationship Between Obstructive Sleep Apnea Syndrome and Severe Asthma: From Endo-Phenotype to Clinical Aspects. Front. Med. 8:640636. doi: 10.3389/fmed.2021.640636

INTRODUCTION

While sleep-related breathing disorders (SBDs) and asthma, two of the most widespread respiratory diseases, have been increasingly well-characterized, their mutual comorbidity and potential bidirectional relationship still need to be fully addressed. Obstructive sleep apnea syndrome (OSAS) is the most common—albeit currently underdiagnosed—form of SBD, with a prevalence of up to 30% in Western populations (1). In the last 20–30 years, there has been growing evidence that OSAS is associated with increased bronchial hyperresponsiveness (2) and inflammation (3) and that may represent an independent risk factor for asthma exacerbations (4). Similarly, the prevalence of asthma has been steadily rising, affecting up to 22% of the population in many countries (5).

Many patients suffering from asthma report poor sleep conditions, often attributed to nocturnal worsening of their asthma (6–8), increased daytime sleepiness (6), and a higher prevalence of snoring as compared to the general population (9). Such symptoms are commonly found in OSAS patients, suggesting an association between these two conditions (10). Moreover, these two diseases share common risk factors, such as obesity, rhinitis, and gastroesophageal reflux (GER) (11). However, it still remains to be determined whether—and to what extent—OSAS and asthma are just two distinct diseases with similar symptoms, or they are pathophysiologically associated (10).

DEFINITIONS AND EPIDEMIOLOGY

Over the last decade, growing attention has been paid to sleep and SBDs, the latter characterized by abnormal respiration during sleep. According to the International Classification of Sleep Disorders (3rd edition), they can be classified in into four major groups: (i) obstructive sleep apnea (OSA); (ii) central sleep apnea (CSA); (iii) sleep-related hypoventilation; and (iv) sleep-related hypoxemia disorder (12, 13). The most common sleep-related breathing disorder is OSAS, which is increasingly being recognized due to the obesity epidemic and a greater public and physician awareness (14). OSAS is a syndrome characterized by recurrent episodes of partial or complete closure of the upper airway, resulting in disturbed breathing during sleep. The recurrent collapse of the pharyngeal airway during sleep is associated with decreased quality of life (QoL) and significant medical comorbidities (14), leading to apnea or hypopnea and, thus, to intermittent hypoxia and sleep segmentation throughout the night (15–17). Abnormal fluctuations of cardiac rhythm, blood pressure, and intrathoracic pressure are also frequently observed (16, 18). These acute disturbances evolve into mid- and long-term sequelae, such as chronic inflammation, endothelial dysfunction, and metabolic dysregulation (17, 19, 20), followed by hypertension, cardiovascular morbidities (16, 18–20), obesity, insulin resistance (17, 19, 20), impaired cognitive function (16, 20–22), mood, and QoL (16, 20, 22, 23), and premature death (16, 20, 24–26). In recent years, the prevalence of SBDs among the general population has been constantly growing probably due to the availability of more sophisticated and reliable diagnostic devices alongside the aforementioned increased physician awareness. However, these estimates are often biased by methodological issues, such as the different criteria used to define OSAS and the type of technology being employed.

In-laboratory attended diagnostic polysomnography or portable home sleep testing can be used to diagnose sleep apnea (14). In the 80's, an average estimate of prevalence in the general population was set at around 5–30%, with higher rates being more common males (1, 20). In the early 90's, Young and colleagues published the results of the Wisconsin Cohort study (WSCS) (27), the first study on SDB prevalence, confirming that these conditions generally affect more men than women (24 vs. 9%, respectively). The authors also estimated that 2% of women and 4% of men belonging to the middle-aged workforce met the diagnostic criteria for sleep apnea syndrome—i.e., an individual with an apnea-hypopnea score of 5 or higher and co-existing daytime hypersomnolence. These estimates were subsequently revised upwards in a follow-up study (16).

In the following years, new criteria for case definition and revised recommendations for recording and scoring were issued by the American Academy of Sleep Medicine. Furthermore, the combined use of nasal pressure technology and pulse oximeters led to a substantial improvement of the sensitivity of breath recording during sleep hours (20). Thanks to these advances, a large population-based study (HypnoLaus) was able to report a significantly higher prevalence of moderate-to-severe sleep-disordered breathing ($\geq$15 events per h) in men compared to women (49.7 vs. 23.4%, respectively) (20), potentially linked to risk factors such as smoking habits, hormonal influences, and different patterns of fat deposition and responsiveness to inspiratory loading.

Continuous positive airway pressure (C-PAP) therapy is the first-line treatment for OSAS in adults (14). Other modalities include mandibular advancement devices, surgery, or upper airway stimulation therapy. Adjunctive therapy should include weight loss in overweight patients, avoidance of sedatives and alcohol before sleep, and possibly positional therapy (14).

Similarly to what seen for OSAS, also the prevalence of asthma has been steadily rising in recent years, now affecting around 22% of the population in several countries across the globe (5, 28, 29). Indeed, asthma affects more than 330 million people worldwide, and it is likely that by 2025 100 million more people could suffer from it (30, 31). Even though asthma prevalence is higher in developed countries, it continues to rise in low- to middle-income countries where it is associated with a higher mortality rate (31, 32). In the US, the prevalence of asthma in 2017 was 7.9%, with higher rates in children ($<$18 years; 8.4%) and lower rates in adults ($\geq$18 years; 7.7%) (32). In 2010, nearly 1.8 million emergency room visits were attributed to asthma, and in 2013 this disease accounted for an estimated 10.1 million lost work days among employed adults (33).

To make matter worse, over nine million children in the US have been diagnosed with asthma, of whom 75% have active disease (28, 29). While asthma is more common in males during childhood, it becomes more prevalent in adult women. This gender gap narrows down in the 5th decade, suggesting that sex hormones may play a role in the development of some forms of asthma (31).

Asthma is a multifactorial chronic respiratory disease, usually associated with airway hyperresponsiveness to direct or indirect stimuli, and with persistent airway inflammation. These features may lead to variable expiratory airflow limitation and to the common symptoms of wheeze, shortness of breath, chest tightness, and/or cough (5).

Asthma may have different underlying causes and processes. Indeed, its etiology has been increasingly attributed to interactions between environmental factors (e.g., air pollution, aeroallergens, and weather), host factors (e.g., obesity, nutritional factors, infections, and allergic sensitization), and genetic factors (e.g., asthma susceptibility genes, sex) (31). Interestingly enough,

asthma shares a common background of chronic inflammation—and thus statistical association—with other health issues, for example psoriasis and vitiligo (34, 35) or food anaphylaxis (36).

Based on diverse recognizable clusters of demographic elements, clinical features, and pathophysiological characteristics, it is possible to recognize several different "asthma phenotypes." Some of the common phenotypes indicated by the Global Initiative for Asthma (GINA) 2020 guidelines are summarized in **Table 1** (5). Moreover, nearly 3–5% of the total asthma population can be classified as having severe asthma (SA): the small group of SA patients accounts for most of the cost for asthma care (40). The current definition of SA is based on the 2014 ERS/ATS guidelines (41, 42). The diagnostic criteria of SA in patients aged ≥6 years and those of uncontrolled asthma are shown in **Table 2**.

A large number of patients suffering from asthma report poor sleep, often attributed to nocturnal worsening of their asthma (6–8), increased daytime sleepiness (6), and a higher prevalence of snoring than that of the general population (9).

UNDERLYING PATHWAYS

Symptoms present in both OSAS and asthma suggest a possible association between the two conditions. The first demonstration that asthma is associated with an increased risk of developing OSAS came from the Wisconsin Sleep Cohort Study, a randomized population-based prospective study started in 1988, where 547 adult subjects (52% females, mean age 50 years) were subjected to polysomnography every 4 years. Asthma data were recorded by general practitioners or through the administration of questionnaires. Subsequently, the relationship between the incidence of asthma and OSAS and excessive daytime sleepiness (EDS) was examined by regression analysis. The results showed that the relative risk for asthma patients—adjusted by sex, age, and body mass index (BMI)—of developing OSAS during a 4-year observational period was quite high (RR = 1.39). The observation that asthma was significantly related to the development of new OSAS (RR = 2.72, $P = 0.045$) led the authors to conclude that asthma is related to the development of OSAS with EDS (43–45). Further studies suggested a bidirectional correlation between asthma and OSAS, with a mutual negative effect in term of severity. Specifically, OSAS was shown to not just be an independent risk factor for asthma exacerbations (4) but also to worsen asthma (46). Likewise, asthma was shown to exacerbate OSAS in the same study (46). Lastly, the Berlin Questionnaire survey study recorded a more frequent occurrence of daytime sleepiness and apnea in asthmatic patients compared to the general population (10).

The first evidence of a higher frequency of roncopathy in atopic women (47) was described by a 14-year prospective study, showing a pathogenetic role of asthma in sleep respiratory disorder development (48). Other authors evaluated the effect of OSAS on asthma control, reporting that the presence of OSAS was associated with poor asthma control (3) both at daytime and night (11). In addition, OSAS treatment ameliorated asthma symptoms, morning peak flow values, and QoL (12). Further confirmation of the interplay between asthma and OSAS came from a series of polysomnographic studies showing a high OSAS prevalence (up to 90%) in patients suffering from SA (49, 50). Fittingly, findings from an SA cohort study demonstrated that a higher proportion of patients with SA were at high risk of developing OSAS compared to controls (26 vs. 3%, respectively) (51).

TABLE 1 | Most common phenotypes of asthma (5).

Allergic asthma: Associated with a personal history of a respiratory allergen sensitization and, less commonly, with a food, drug, or contact allergy, this phenotype reveals how much dysregulated immunity seems to be important in the development of asthma, with elevated serum immunoglobulin E (IgE) levels, release of mediators from mast cells, skewed T helper 1 (Th1) and Th2 responses and eosinophilic airway inflammation (28), recognizable by the examination of the induced sputum or the evaluation of its surrogate biomarker, the fractional exhaled nitric oxide (FeNO) (37, 38). Often this phenotype responds well to inhaled corticosteroid (ICS) treatment.

Non-allergic asthma: The other cluster of patients that do not suffer from allergy; in these patients, the cellular profile of sputum may be neutrophilic, eosinophilic or paucigranulocytic, containing only a few inflammatory cells. ICS therapy has less response in this subgroup of patients.

Late-onset asthma: Some patients, women in particular, develop asthma signs and symptoms in adult life for the very first time. Often, this subgroup of patients is non-allergic and requires higher doses of ICS for the correct treatment.

Asthma with persistent airflow limitation: This phenotype can develop in adults with long-standing asthma, probably following airway wall remodeling (39).

Asthma with obesity: Patients may display strong respiratory symptoms but little eosinophilic airway inflammation.

TABLE 2 | Definition of severe asthma (2014 ERS/ATS guidelines).

Asthma is defined as severe if it was treated with:

Asthma which requires treatment with guidelines suggested medications for GINA steps 4–5 asthma (high dose ICS[#] and LABA or leukotriene modifier/theophylline) for the previous year or systemic CS for ≥50% of the previous year to prevent it from becoming "uncontrolled" or which remains "uncontrolled" despite this therapy

Asthma is defined as uncontrolled when it has the following signs and symptoms:

a) Poor symptom control:
ACQ consistently ≥ 1.5, ACT < 20 (or "not well-controlled" by NAEPP/GINA guidelines)
b) Frequent severe exacerbations:
Two or more bursts of systemic CS (≥3 days each) in the previous year
c) Serious exacerbations:
At least one hospitalization, ICU stay or mechanical ventilation in the previous year
d) Airflow limitation:
After appropriate bronchodilator withhold FEV1 < 80% predicted (despite reduced FEV1/FVC, defined as less than the lower limit of normal)

[#] *The definition of high dose inhaled corticosteroids (ICS) is age-specific.*
GINA, Global Initiative for Asthma; LABA, long-acting β_2-agonists; CS, corticosteroids; ACQ, Asthma Control Questionnaire; ACT, Asthma Control Test; ICU, Intensive Care unit; NAEPP, National Asthma Education and Prevention Program; FEV1, forced expiratory volume in 1 s.

According to the results of the Severe Asthma Research Program, SA patients experienced poorer sleep quality, were sleepier, and had a worse QoL than their healthy counterparts. A significant association between the Sleep Apnea Scale of the Sleep Disorders Questionnaire (SA-SDQ) and the count of polymorphonuclear cells in sputum was recorded as well. In particular, each increase in SA-SDQ score by its standard deviation (6.85 units) was associated with a rise in percentage of sputum neutrophils of 7.78 (95% CI 2.33–13.22, $P = 0.0006$), independent of obesity and other confounders (51). Thus, the authors concluded that OSAS symptoms are more prevalent among asthmatics, where they tend to associate with higher disease burden. Finally, among asthma patients, the increased risk of OSAS was associated with the occurrence of neutrophilic airway inflammation, suggesting that OSAS may be an important contributor to neutrophilic asthma (51).

PATOPHYSIOLOGICAL CORRELATION BETWEEN OBSTRUCTIVE SLEEP APNEA SYNDROME AND SEVERE ASTHMA

The observation that OSAS is an independent risk factor of asthma exacerbation and that each condition can worsen the other (51) suggests a bidirectional correlation between asthma and OSAS with a reciprocal negative effect in term of severity. Congruently, SA, SA treatment, and comorbidities can all lead to pharynx alterations, favoring OSAS development. Furthermore, in asthma patients, prolonged inhaled corticosteroid (ICS) therapy in the presence of gastroesophageal reflux is associated with chronic snoring and higher risk of OSAS (52) independently from classical risk factors such as obesity or rhinitis. Finally, long-term ICS therapy can modulate hormones secretion, especially growth hormone release (53, 54), which may cause metabolic and cardiovascular complications (55), thereby worsening the effects of OSAS. The hypothesized mechanism underlying the interrelationship between OSAS and SA is shown in **Table 3**. More recently, researchers have proposed that OSAS and asthma patients may be more susceptible to SA attacks induced by systemic inflammation (71, 72). These findings strongly suggest that all asthmatic patients should be evaluated for OSAS-associated risk factors, such as gastroesophageal reflux and rhinitis, in order to detect—and eventually treat—sleep apneas. Overall, in light of the higher incidence of respiratory sleep disorders in SA patients, OSAS treatment may reduce the number of asthma attacks, lead to a better control of asthma, and improve the patients' QoL.

TABLE 3 | Mechanisms underlying the relationship between asthma and OSAS.

OSAS (effects on asthma)
OSAS is linked to increased bronchial hyperresponsiveness (2, 56) and may be an independent risk factor for asthma exacerbations (4).
The presence of OSAS is associated with poor asthma control (43) both at daytime and night (57).
OSAS treatment improves asthma symptoms, morning peak flow values, and QoL (46).
Asthma (effects on OSAS)
A higher frequency of roncopathy in atopic women (47) was first reported by a 14-year prospective study showing a pathogenetic role of asthma in sleep respiratory disorder development (48).
Asthma may modify the pharynx collapsibility (58).
During asthma attacks, increased negative intrathoracic pressure may lead to higher pharynx collapsibility (59), which can also arise from decreased respiratory volumes (as in asthma patients) (60).
As asthma is also associated with respiratory muscles weakness and upper ways instability, sleep fragmentation due to asthma with nocturnal symptoms may also induce a loss of slow-waves sleep and cognitive impairment (61).
An additional way from asthma to OSAS is systemic inflammation and use of systemic and inhaled corticosteroids (62, 63). Corticosteroids, frequently prescribed in asthma patients, may lead to a pharyngeal structures remodeling and fatty tissue redistribution (54, 55, 64).
Study on dogs showed that dexamethasone may lead to instability of pharyngeal muscles ("floppy") reducing their protective effect on upper airways during sleep (65).
Asthma and obesity
Major risk factor and a disease modifier of asthma both in children and adults. Obese subjects have increased risk of asthma.
Obese asthmatics have more symptoms, more frequent and severe exacerbations, a reduced response to medications and an overall decreased quality of life (66).
Different phenotypes within the obese asthma syndrome: those seen in lean individuals complicated by obesity, disease newly arising in obese individuals and phenotypes worsens by increased environmental pollutants response (67).
Different factors contributing to the syndrome of obesity-related asthma: Diet, microbiome, genetic factors, metabolic and immune function, environmental exposures, and mechanical effects (68).
Other conditions and comorbidities
Toxic effect on the pharyngeal mucosa by gastroesophageal reflux, a frequent condition in asthma (69), associated with laryngospasm and neurogenic inflammation (64).
OSAS patients display a higher frequency of acid reflux along with micro-aspiration phenomenon of gastric acid and nocturnal bronchoconstriction (70), thereby establishing a bidirectional relationship.

OSAS, Obstructive Sleep Disorder Syndrome; QoL, Quality of Life.

ASTHMA INVOLVMENT IN THE PATHOGENESIS OF OBSTRUCTIVE SLEEP APNEA SYNDROME

Different observations highlighted a relationship between asthma symptoms and their impact on sleep quality revealing often a coexistence of asthma and obstructive sleep apnea syndrome. Risk factors common to the two diseases include obesity, rhinitis and gastroesophageal reflux. Airway and systemic inflammation, neuromechanical effects of recurrent upper airways collapse and asthma medications are additional explanatory factors. Recent evidences demonstrated the underlying mechanisms to the development of OSAS in asthma patients. An interesting research by Kalra et al. in a large population-based cohort of young atopic women found 20.5% prevalence of habitual snoring ($\geq$3 nights per week), moreover they also reported a significant association between asthma and snoring. This effect was independent of upper respiratory tract symptoms (e.g., rhinitis), cigarette smoking, and race (47). Another longitudinal 14-year prospective study on risk factors for habitual snoring in a general adult

population indicated the presence of asthma as a risk factor for snoring, showing its pathogenetic role for sleep-disordered breathing development (48). It was previously observed how asthma may modify the pharynx collapsibility (58), in particular during asthma attacks, increased negative intrathoracic pressure may lead to higher pharynx collapsibility (59), which can also arise from decreased respiratory volumes (the same happens in asthma patients) (60). As asthma is also associated with respiratory muscles weakness and upper ways instability, sleep fragmentation caused by asthma nocturnal symptoms may also induce a loss of slow-waves sleep and cognitive impairment (61) An additional link between asthma and OSAS is sustained by systemic inflammation and the use of systemic and inhaled corticosteroids (62, 63). Corticosteroids, frequently prescribed in asthma patients, may lead to a pharyngeal structures remodeling (64). Study on dogs showed that dexamethasone may lead to instability of pharyngeal muscles ("floppy") reducing their protective effect on upper airways during sleep (65). Lastly it is important to underline the toxic effect on the pharyngeal mucosa by gastroesophageal reflux, a frequent condition in asthma (69), associated with laryngospasm and neurogenic inflammation (64). OSAS patients display a higher frequency of acid reflux along with micro-aspiration phenomenon of gastric acid and nocturnal bronchoconstriction, thereby establishing a bidirectional relationship (70).

RELATIONSHIP BETWEEN ASTHMA AND OBESITY

Obesity represents a major risk factor and a disease modifier of asthma both in children and adults (66). It was found that obese subjects have increased risk of asthma and obese asthmatics have more symptoms, more frequent and severe exacerbations, a reduced response to medications and an overall decreased quality of life highlighting a bidirectional correlation between these two entities. There are likely different phenotypes within the obese asthma syndrome: those seen in lean individuals complicated by obesity, disease newly arising in obese individuals and phenotypes worsens by increased environmental pollutants response (67). Different factors contributing to the syndrome of obesity-related asthma have been hypothesized such as diet, the microbiome, genetic factors, metabolic and immune function (oxidative stress, cytokines, innate, and adaptive immunity), environmental exposures and mechanical effects: reduction in functional residual capacity (FRC) and expiratory reserve volume (ERV) (68). As obese asthma syndrome is a complex and multifactorial entity which is just beginning to be understood further studies should better characterize this disease to understand, in particular, mechanisms conducting to the phenotype of severe and uncontrolled asthma.

CLINICAL IMPLICATIONS

It remains unclear whether OSAS in asthmatic subjects is merely a comorbidity or a specific "subphenotype" of asthma. On the one hand, patients with allergic asthma are often characterized by T2-driven inflammation and over-production of IL-5—resulting in airway eosinophilia—and IL-13—leading to airway smooth muscle hyperresponsiveness and mucus hypersecretion—, complicated by the development of obesity and OSAS (40, 73). On the other hand, in obese female patients with later onset of non-allergic asthma, mechanical changes affecting the lung function (i.e., restrictive pattern) may favor obstructive apnea development. In these patients, adipose tissue are known to secret several cytokines and adipokines that can have a direct effects on the airway epithelium and trigger bronchial hyperreactivity (**Figure 1**) (66, 74).

The relationship between OSAS, obesity, and asthma may be even more complex and may involve other players, including mechanical, dietary, and genetic factors (75). A plausible explanation to this interplay comes from the "integrated airway" hypothesis, according to which an inflammatory process within a continuous upper airway obstruction results in intrathoracic pressure swings, frequent arousals, and intermittent hypoxia, all contributing to an inflammatory milieu, as demonstrated by the association of OSAS with cardiovascular and cerebrovascular diseases (40, 76). The result of the association of OSAS with SA is an increased risk of comorbidities, such as cardiovascular sequelae (51).

For the reasons above mentioned polysomnography is recommended in asthmatics with inadequate control of nocturnal symptoms despite adequate treatment (77).

HOW OSAS THERAPY CAN AFFECT ASTHMA AND VICEVERSA

A recent research has investigated the relationship between OSAS, asthma and quality of life, going deeply on the prevalence of sleep impairment and predictors of sleep quality among asthmatic patients (78). The results of this study highlight that sleep disturbance is a common problem among these patients and suggest that sleep quality can be predicted considering the level of asthma control and the presence of comorbid conditions. The results of this study suggest the need for clinicians to detect poor sleep quality in these subjects to better address the correct and targeted treatment for each condition. Previous studies have shown, for example, that PAP treatment is beneficial to control sleep disturbances either in OSAS and asthmatic patients. In asthmatic patients with OSAS, C-PAP treatment may lead to a significant improvement in asthma symptoms, morning peak expiratory flow, and quality of life (QoL) (79). Fittingly, C-PAP treatment reduced asthma symptoms and bronchodilator use while improving lung function tests and QoL (40). CPAP in this context represent a valid tool to integrate with the corticosteroid treatment considering that corticosteroids, may have side effects like leading to a pharyngeal structures remodeling, fatty tissue redistribution, impairment of growth hormone (GH)-insulin-like growth factor (IGF)-1 axis conducting to a negative role in bone metabolism (54, 55, 64). Moreover, studies on animals demonstrated that corticosteroids may enhance force fluctuation-induced relengthening in contracted airway smooth muscle leading to instability of pharyngeal muscles reducing

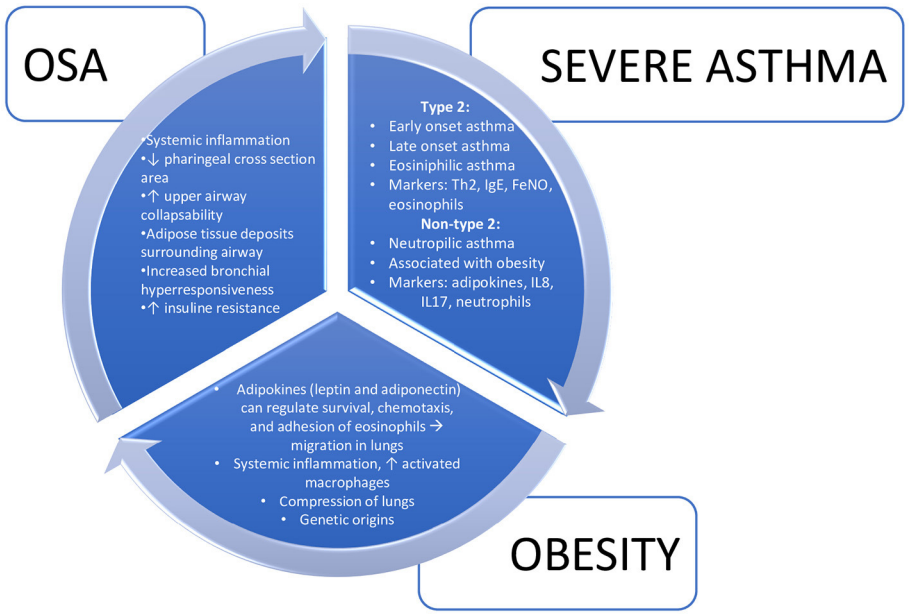

FIGURE 1 | Interrelationships between severe asthma, obesity, and obstructive sleep apnea.

their protective effect on upper airways during sleep (65) and conducting to a worsening of OSAS.

A prospective trial by Serrano-Pariente et al. has shown that the proportion of adult asthmatic patients suffering from uncontrolled asthma decreased from 41.4 to 17.2% in response to C-PAP therapy. Likewise, the percentage of patients experiencing asthma attacks during the course of 6 months decreased from 35.4 to 17.2% following C-PAP treatment (80).

In good agreement, OSAS treatment in SA patients has been shown to influence the cardiovascular risk. Oxidative stress and systemic inflammation may, in fact, lead to metabolic dysregulation in OSAS patients (44, 46).

The fact that OSAS patients, regardless of their weight, display increased oxidative stress with vascular endothelial dysfunction has led to the hypothesis that continuous positive airway pressure therapy (C-PAP) and anti-oxidant treatment (vitamin C) may improve endothelial function (68). Moreover, in OSAS patients, atherosclerosis symptoms can be ameliorated through mandibular advancement devices (MADs) or C-PAP (81), suggesting that OSAS treatment, primitive or comorbid, may prevent cardiovascular sequelae, such as acute myocardial infarction, stroke, and acute fatal cardiovascular events.

CONCLUSIONS AND FUTURE DIRECTIONS

In conclusion, mounting evidence appear to indicate that there exists a relationship between OSAS and SA based on shared pathophysiological factors and bidirectional interactions (40). Similarly to asthma, OSAS promotes inflammatory responses by means of hypoxia, hypercapnia, and sleep fragmentation, resulting in a reversible increase in C-reactive protein (CRP). Production of TNF-α, a pro-inflammatory cytokine, is elevated in OSAS patients and plays an important role in collapse and re-opening of the airways. Both pro-inflammatory factors tend to decrease following C-PAP treatment (77), thereby improving asthma symptoms and QoL (40). In our experience, C-PAP therapy can also improve lung function tests in adult asthmatic patients (unpublished data).

Taken all together, the results from the literature highlight the importance of assessing the co-existence of asthma, chiefly SA—a condition with poor prognosis and higher managements cost—, in OSAS patients as well as the presence of other sleep-related breathing disorders and apneas, especially when asthma is difficult to control or comorbid.

Overall, the key observation that OSAS treatment reduces cardiovascular sequelae while improving the QoL (11) points to the urgent need to fill critical gaps in our knowledge about endotypes, phenotypes, and comorbidities in OSAS.

AUTHOR CONTRIBUTIONS

MM conceived the idea of the manuscript. BR, AR, and PP contributed to various parts of the text, wrote the manuscript, and prepared the tables and bibliography. All the authors edited, revised, commented on the manuscript, and approved the submitted version of the article.

FUNDING

This study was (partially) funded by the AGING Project—Department of Excellence—DIMET, Università del Piemonte Orientale.

REFERENCES

1. Young T, Peppard PE, Gottlieb DJ. Epidemiology of obstructive sleep apnea: a population health perspective. *Am J Respirat Crit Care Med.* (2002). 165:1217–39. doi: 10.1164/rccm.2109080
2. Lin C-C, Lin C-Y. Obstructive sleep apnea syndrome and bronchial hyperreactivity. *Lung.* (1995) 173:117–26. doi: 10.1007/BF02981471
3. Kheirandish-Gozal L, Gozal D. Obstructive sleep apnea and inflammation: proof of concept based on two illustrative cytokines. *Int J Mol Sci.* (2019) 20:310. doi: 10.3390/ijms20030459
4. ten Brinke A. Risk factors of frequent exacerbations in difficult-to-treat asthma. *Eur Respirat J.* (2005) 26:812–8. doi: 10.1183/09031936.05.00037905
5. Global Initiative for Asthma. *Global Strategy for Asthma Management and Prevention: Online Appendix 2020.* (2020) Available online at: www.ginasthma.org (accessed September 8, 2020).
6. Janson C, De Backer W, Gislason T, Plaschke P, Björnsson E, Hetta J, et al. Increased prevalence of sleep disturbances and daytime sleepiness in subjects with bronchial asthma: a population study of young adults in three European countries. *Eur Respirat J.* (1996) 9:2132–8. doi: 10.1183/09031936.96.09102132
7. Khan WH, Mohsenin V, D'Ambrosio CM. Sleep in asthma. *Clin Chest Med.* (2014) 35:483–93. doi: 10.1016/j.ccm.2014.06.004
8. D'Ambrosio CM, Mohsenin V. Sleep in asthma. *Clin Chest Med.* (1998) 19:127–37. doi: 10.1016/S0272-5231(05)70437-8
9. Fitzpatrick MF, Martin K, Fossey E, Shapiro CM, Elton RA, Douglas NJ. Snoring, asthma and sleep disturbance in Britian: a community-based survey. *Eur Respirat J.* (1993) 6:531–5.
10. Auckley D, Moallem M, Shaman Z, Mustafa M. Findings of a Berlin Questionnaire survey: comparison between patients seen in an asthma clinic versus internal medicine clinic. *Sleep Med.* (2008) 9:494–9. doi: 10.1016/j.sleep.2007.06.010
11. Prasad B, Nyenhuis SM, Weaver TE. Obstructive sleep apnea and asthma: associations and treatment implications. *Sleep Med Rev.* (2014) 18:165–71. doi: 10.1016/j.smrv.2013.04.004
12. American Academy of Sleep Medicine. *International Classification of Sleep Disorders*. 3rd ed. Darien, IL: American Academy of Sleep Medicine (2014).
13. Sateia MJ. International classification of sleep disorders-third edition highlights and modifications. *Chest.* (2014) 146:1387–94. doi: 10.1378/chest.14-0970
14. Burman D. Sleep disorders: sleep-related breathing disorders. *FP Essentials.* (2017) 460:11–21.
15. Matsumoto T, Chin K. Prevalence of sleep disturbances: sleep disordered breathing, short sleep duration, and non-restorative sleep. *Respirat Investig.* (2019) 57:227–37. doi: 10.1016/j.resinv.2019.01.008
16. Peppard PE, Young T, Barnet JH, Palta M, Hagen EW, Hla KM. Increased prevalence of sleep-disordered breathing in adults. *Am J Epidemiol.* (2013) 177:1006–14. doi: 10.1093/aje/kws342
17. Dempsey JA, Veasey SC, Morgan BJ, O'Donnell CP. Pathophysiology of sleep apnea. *Physiol Rev.* (2010) 90:47–112. doi: 10.1152/physrev.00043.2008
18. Somers VK, White DP, Amin R, Abraham WT, Costa F, Culebras A, et al. Sleep apnea and cardiovascular disease: an American Heart Association/American College of Cardiology Foundation scientific statement from the American Heart Association Council for High Blood Pressure Research Professional Education Committee, Council. *Circulation.* (2008) 118:1080–111. doi: 10.1161/CIRCULATIONAHA.107.189420
19. Shamsuzzaman ASM, Gersh BJ, Somers VK. Obstructive sleep apnea: implications for cardiac and vascular disease. *JAMA.* (2003) 290:1906. doi: 10.1001/jama.290.14.1906
20. Heinzer R, Vat S, Marques-Vidal P, Marti-Soler H, Andries D, Tobback N, et al. Prevalence of sleep-disordered breathing in the general population: the HypnoLaus study. *Lancet Respirat Med.* (2015) 3:310–8. doi: 10.1016/S2213-2600(15)00043-0
21. Kim HC, Young T, Matthews CG, Weber SM, Woodard AR, Palta M. Sleep-disordered breathing and neuropsychological deficits: a population-based study. *Am J Respirat Crit Care Med.* (1997) 156:1813–9. doi: 10.1164/ajrccm.156.6.9610026
22. Sforza E, Roche F. Sleep apnea syndrome and cognition. *Front. Neurol.* (2012) 3:1–7. doi: 10.3389/fneur.2012.00087
23. Baldwin CM, Griffith KA, Nieto FJ, O'Connor GT, Walsleben JA, Redline S. The association of sleep-disordered breathing and sleep symptoms with quality of life in the sleep heart health study. *Sleep.* (2001) 24:96–105. doi: 10.1093/sleep/24.1.96
24. Young T, Finn L, Peppard PE, Szklo-coxe M, Austin D, Nieto FJ, et al. Sleep disordered breathing and mortality: eighteen-year follow-up of the Wisconsin Sleep Cohort. *Sleep.* (2008) 31:1071–8.
25. Marshall NS, Wong KKH, Liu PY, Cullen SRJ, Knuiman MW, Grunstein RR. Sleep apnea as an independent risk factor for all-cause mortality: the Busselton Health Study. *Sleep.* (2008) 31:1079–85. doi: 10.5665/sleep/31.8.1079
26. Gami AS, Olson EJ, Shen WK, Wright RS, Ballman KV, Hodge DO, et al. Obstructive sleep apnea and the risk of sudden cardiac death: a longitudinal study of 10,701 adults. *J Am Coll Cardiol.* (2013) 62:610–6. doi: 10.1016/j.jacc.2013.04.080
27. Young T, Palta M, Dempsey J, Skatrud J, Weber S, Badr S. The occurrence of sleep- disordered breathing among middle-aged adults. *N Engl J Med.* (1993) 328:1230–5. doi: 10.1056/NEJM199304293281704
28. Toskala E, Kennedy DW. Asthma risk factors. *Int For Allergy Rhinol.* (2015) 5:S11–6. doi: 10.1002/alr.21557
29. American Lung Association. *Asthma and Children Fact Sheet.* (2020). Available online at: https://www.lung.org/lung-health-diseases/lung-disease-lookup/asthma/learn-about-asthma/asthma-children-facts-sheet (accessed September 8, 2020).
30. Global Asthma Network. *The Global Asthma Report 2018*. (2018). Available online at: www.globalasthmanetwork.org (accessed September 8, 2020).
31. Dharmage SC, Perret JL, Custovic A. Epidemiology of asthma in children and adults. *Front Pediatr.* (2019) 7:1–15. doi: 10.3389/fped.2019.00246
32. Stern J, Pier J, Litonjua AA. Asthma epidemiology and risk factors. *Semin Immunopathol.* (2020) 42:5–15. doi: 10.1007/s00281-020-00785-1
33. American Lung Association. *Asthma in Adults Fact Sheet.* (2020). Available online at: https://www.lung.org/lung-health-diseases/lung-disease-lookup/asthma/learn-about-asthma/asthma-adults-facts-sheet (accessed September 8, 2020).
34. Damiani G, Radaeli A, Olivini A, Calvara-Pinton P, Malerba M. Increased airway inflammation in patients with psoriasis. *Br J Dermatol.* (2016) 175:797–9. doi: 10.1111/bjd.14546
35. Malerba M, Damiani G, Radaeli A, Ragnoli B, Olivini A, Calzavara-Pinton PG. Narrowband ultraviolet B phototherapy in psoriasis reduces pro-inflammatory cytokine levels and improves vitiligo and neutrophilic asthma. *Br J Dermatol.* (2015) 173:1544–5. doi: 10.1111/bjd.13988
36. Rolla G, Mietta S, Raie A, Bussolino C, Nebiolo F, Galimberti M, et al. Incidence of food anaphylaxis in Piemonte region (Italy): data from registry of Center for Severe Allergic Reactions. *Intern Emerg Med.* (2013) 8:615–20. doi: 10.1007/s11739-013-0978-y
37. Malerba M, Ragnoli B, Radaeli A, Tantucci C. Usefulness of exhaled nitric oxide and sputum eosinophils in the long-term control of eosinophilic asthma. *Chest.* (2008) 134:733–9. doi: 10.1378/chest.08-0763
38. Malerba M, Radaeli A, Olivini A, Ragnoli B, Ricciardolo F, Montuschi P. The combined impact of exhaled nitric oxide and sputum eosinophils monitoring in asthma treatment: a prospective cohort study. *Curr Pharmaceut Design.* (2015) 21:4752–62. doi: 10.2174/1871524915666150710123415
39. Ten Brinke A, Zwinderman AH, Sterk PJ, Rabe KF, Bel EH. Factors associated with persistent airflow limitation in severe asthma. *Am J Respirat Crit Care Med.* (2001) 164:744–8. doi: 10.1164/ajrccm.164.5.2011026
40. Deslypere G, Dupont L. Principal comorbidities in severe asthma: how to manage and what is their influence on asthma endpoints. *EC Pulmonol Respirat Med.* (2017) 3:162–174.
41. Chung KF, Wenzel SE, Brozek JL, Bush A, Castro M, Sterk PJ, et al. International ERS/ATS guidelines on definition, evaluation and treatment of severe asthma. *Eur Respirat J.* (2014) 43:343–73. doi: 10.1183/09031936.00202013
42. Holguin F, Cardet JC, Chung KF, Diver S, Ferreira DS, Fitzpatrick A, et al. Management of severe asthma: a European Respiratory Society/American Thoracic Society guideline. *Eur Respirat J.* (2020) 43155:1900588. doi: 10.1183/13993003.00588-2019
43. Teodorescu M, Polomis DA, Hall SV, Teodorescu MC, Gangnon RE, Peterson AG, et al. Association of obstructive sleep apnea risk with asthma control in adults. *Chest.* (2010) 138:543–50. doi: 10.1378/chest.09-3066
44. Teodorescu M, Barnet JH, Hagen EW, Palta M, Young TB, Peppard PE. Association between asthma and risk of developing obstructive sleep apnea. *J Am Med Assoc.* (2015) 2014:17822. doi: 10.1001/jama.2014.17822

45. Teodorescu M, Barnet JH, Hagen EW, Palta M, Young TB, Peppard PE. Association between asthma and risk of developing obstructive sleep apnea—comment by Kathryn E. McGoldrick. *Survey Anesthesiol.* (2016) 60:91–2. doi: 10.1097/SA.0000000000000216
46. Alkhalil M, Schulman E, Getsy J. Obstructive sleep apnea syndrome and asthma: what are the links? *J Clin Sleep Med.* (2009) 2009:27397. doi: 10.5664/jcsm.27397
47. Kalra M, Biagini J, Bernstein D, Stanforth S, Burkle J, Cohen A, et al. Effect of asthma on the risk of obstructive sleep apnea syndrome in atopic women. *Ann Allergy Asthma Immunol.* (2006) 97:231–5. doi: 10.1016/S1081-1206(10)60019-1
48. Knuiman M, James A, Divitini M, Bartholomew H. Longitudinal study of risk factors for habitual snoring in a general adult population: the Busselton Health Study. *Chest.* (2006) 130:1779–83. doi: 10.1378/chest.130.6.1779
49. Julien JY, Martin JG, Ernst P, Olivenstein R, Hamid Q, Lemière C, et al. Prevalence of obstructive sleep apnea-hypopnea in severe versus moderate asthma. *J Allergy Clin Immunol.* (2009) 124:371–6. doi: 10.1016/j.jaci.2009.05.016
50. Yigla M, Tov N, Solomonov A, Rubin AE, Harlev D. Difficult-to-control asthma and obstructive sleep apnea. *J Asthma.* (2003) 40:865–71. doi: 10.1081/JAS-120023577
51. Teodorescu M, Broytman O, Curran-Everett D, Sorkness RL, Crisafi G, Bleecker ER, et al. Obstructive sleep apnea risk, asthma burden, and lower airway inflammation in adults in the severe asthma research program (SARP) II. *J Allergy Clin Immunol Pract.* (2015) 3:566–75.e1. doi: 10.1016/j.jaip.2015.04.002
52. Teodorescu M, Consens FB, Bria WF, Coffey MJ, McMorris MS, Weatherwax KJ, et al. Predictors of habitual snoring and obstructive sleep apnea risk in patients with asthma. *Chest.* (2009) 135:1125–32. doi: 10.1378/chest.08-1273
53. Malerba M, Bossoni S, Radaeli A, Mori E, Romanelli G, Tantucci C, et al. Bone ultrasonometric features and growth hormone secretion in asthmatic patients during chronic inhaled corticosteroid therapy. *Bone.* (2006) 38:119–24. doi: 10.1016/j.bone.2005.07.002
54. Malerba M, Bossoni S, Radaeli A, Mori E, Bonadonna S, Giustina A, et al. Growth hormone response to growth hormone-releasing hormone is reduced in adult asthmatic patients receiving long-term inhaled corticosteroid treatment. *Chest.* (2005) 127:515–21. doi: 10.1378/chest.127.2.515
55. Mazziotti G, Giustina A. Glucocorticoids and the regulation of growth hormone secretion. *Nat Rev Endocrinol.* (2013) 9:265–76. doi: 10.1038/nrendo.2013.5
56. Bulcun E, Ekici M, Ekici A, Tireli G, Karakoç T, Sentürk E, et al. Bronchial hyperresponsiveness in patients with obstructive sleep apnea syndrome. *Tuberkuloz ve toraks.* (2013) 61:221–6. doi: 10.5578/tt.5791
57. Teodorescu M, Polomis DA, Teodorescu MC, Gangnon RE, Peterson AG, Consens FB, et al. Association of obstructive sleep apnea risk or diagnosis with daytime asthma in adults. *J Asthma.* (2012) 49:620–8. doi: 10.3109/02770903.2012.689408
58. White DP. Pathogenesis of obstructive and central sleep apnea. *Am J Respirat Crit Care Med.* (2005) 172:1363–70. doi: 10.1164/rccm.200412-1631SO
59. Van de Graaff WB. Thoracic influence on upper airway patency. *J Appl Physiol.* (1988) 65:2124–31. doi: 10.1152/jappl.1988.65.5.2124
60. Ballard RD, Clover CW, White DP. Influence of non-REM sleep on inspiratory muscle activity and lung volume in asthmatic patients. *Am Rev Respirat Dis.* (1993) 147:880–6. doi: 10.1164/ajrccm/147.4.880
61. Sériès F, Roy N, Marc I. Effects of sleep deprivation and sleep fragmentation on upper airway collapsibility in normal subjects. *Am J Respirat Crit Care Med.* (1994) 150:481–5. doi: 10.1164/ajrccm.150.2.8049833
62. Bjermer L. Time for a paradigm shift in asthma treatment: from relieving bronchospasm to controlling systemic inflammation. *J Allergy Clin Immunol.* (2007) 120:1269–75. doi: 10.1016/j.jaci.2007.09.017
63. Teodorescu M, Xie A, Sorkness CA, Robbins JA, Reeder S, Gong Y, et al. Effects of inhaled fluticasone on upper airway during sleep and wakefulness in asthma: a pilot study. *J Clin Sleep Med.* (2014) 10:183–93. doi: 10.5664/jcsm.3450
64. Orr WC, Elsenbruch S, Harnish MJ, Johnson LF. Proximal migration of esophageal acid perfusions during waking and sleep. *Am J Gastroenterol.* (2000) 95:37–42. doi: 10.1111/j.1572-0241.2000.01669.x
65. Lakser OJ, Dowell ML, Hoyte FL, Chen B, Lavoie TL, Ferreira C, et al. Steroids augment relengthening of contracted airway smooth muscle: potential additional mechanism of benefit in asthma. *Eur Respirat J.* (2008) 32:1224–30. doi: 10.1183/09031936.00092908
66. Sideleva O, Suratt BT, Black KE, Tharp WG, Pratley RE, Forgione P, et al. Obesity and asthma: an inflammatory disease of adipose tissue not the airway. *Am J Respirat Crit Care Med.* (2012) 186:598–605. doi: 10.1164/rccm.201203-0573OC
67. Peters U, Dixon A, Forno E. Obesity and Asthma. *J Allergy Clin Immunol.* (2018) 141:1169–79. doi: 10.1016/j.jaci.2018.02.004
68. Jelic S, Lederer DJ, Adams T, Padeletti M, Colombo PC, Factor PH, et al. Vascular inflammation in obesity and sleep apnea. *Circulation.* (2010) 121:1014–21. doi: 10.1161/CIRCULATIONAHA.109.900357
69. Emilsson ÖI, Bengtsson A, Franklin KA, Torén K, Benediktsdóttir B, Farkhooye A, et al. Nocturnal gastro-oesophageal reflux, asthma and symptoms of OSA: a longitudinal, general population study. *Eur Respirat J.* (2013) 41:1347–54. doi: 10.1183/09031936.00052512
70. Demeter P, Pap A. The relationship between gastroesophageal reflux disease and obstructive sleep apnea. *J Gastroenterol.* (2004) 39:815–20. doi: 10.1007/s00535-004-1416-8
71. Wang Y, Liu K, Hu K, Yang J, Li Z, Nie M, et al. Impact of obstructive sleep apnea on severe asthma exacerbations. *Sleep Med.* (2016) 26:1–5. doi: 10.1016/j.sleep.2016.06.013
72. Sheludko EG, Naumov DE, Perelman YM, Kolosov VP. The problem of obstructive sleep apnea syndrome in asthmatic patients. *Terapevticheskii Arkhiv.* (2017) 89:107–11. doi: 10.17116/terarkh2017891107-111
73. Nystad W, Meyer HE, Nafstad P, Tverdal A, Engeland A. Body mass index in relation to adult asthma among 135,000 Norwegian men and women. *Am J Epidemiol.* (2004) 160:969–76. doi: 10.1093/aje/kwh303
74. Malerba M, Radaeli A, Olivini A, Damiani G, Ragnoli B, Sorbello V, et al. Association of FEF25-75% impairment with bronchial hyperresponsiveness and airway inflammation in subjects with asthma-like symptoms. *Respiration.* (2016) 91:206–14. doi: 10.1159/000443797
75. Boudreau M, Bacon SL, Ouellet K, Jacob A, Lavoie KL. Mediator effect of depressive symptoms on the association between BMI and asthma control in adults. *Chest.* (2014) 146:348–54. doi: 10.1378/chest.13-1796
76. Teodorescu M, Polomis DA, Gangnon RE, Fedie JE, Consens FB, Chervin RD, et al. Asthma control and its relationship with obstructive sleep apnea (OSA) in older adults. *Sleep Disord.* (2013) 2013:1–11. doi: 10.1155/2013/251567
77. Razak MRA, Chirakalwasan N. Obstructive sleep apnea and asthma. *Asian Pacific J Allergy Immunol.* (2016) 34:265–71. doi: 10.12932/AP0828
78. Braido F, Baiardini I, Ferrando M, Scichilone N, Santus P, Petrone A, et al. The prevalence of sleep impairments and predictors of sleep quality among patients with asthma. *J Asthma.* (2020) 58:481–7. doi: 10.1080/02770903.2019.1711391
79. Alkhalil M, Schulman ES, Getsy J. Obstructive sleep apnea syndrome and asthma: the role of continuous positive airway pressure treatment. *Ann Allergy Asthma Immunol.* (2008) 101:350–7. doi: 10.1016/S1081-1206(10)60309-2
80. Serrano-Pariente J, Plaza V, Soriano JB, Mayos M, López-Viña A, Picado C, et al. Asthma outcomes improve with continuous positive airway pressure for obstructive sleep apnea. *Allergy Eur J Allergy Clin Immunol.* (2017) 72:802–12. doi: 10.1111/all.13070
81. Drager LF, Bortolotto LA, Figueiredo AC, Krieger EM, Lorenzi-Filho G. Effects of continuous positive airway pressure on early signs of atherosclerosis in obstructive sleep apnea. *Am J Respirat Crit Care Med.* (2007) 176:706–12. doi: 10.1164/rccm.200703-500OC

Conflict of Interest: The authors declare that the research was conducted in the absence of any commercial or financial relationships that could be construed as a potential conflict of interest.

Copyright © 2021 Ragnoli, Pochetti, Raie and Malerba. This is an open-access article distributed under the terms of the Creative Commons Attribution License (CC BY). The use, distribution or reproduction in other forums is permitted, provided the original author(s) and the copyright owner(s) are credited and that the original publication in this journal is cited, in accordance with accepted academic practice. No use, distribution or reproduction is permitted which does not comply with these terms.

frontiers in Medicine

ORIGINAL RESEARCH
published: 05 August 2021
doi: 10.3389/fmed.2021.645356

Clinical Evaluation for Sublingual Immunotherapy With *Dermatophagoides farinae* in Polysensitized Allergic Asthma Patients

*Ai-zhi Zhang[1], Mei-e Liang[2], Xiao-xue Chen[2], Yan-fen Wang[2], Ke Ma[2], Zhi Lin[3], Kuan-kuan Xue[4], Li-ru Cao[4], Rong Yang[4] and Huan-ping Zhang[2]**

[1] Department of Pulmonary and Critical Care Medicine, Second Hospital Affiliated to Shanxi Medical University, Taiyuan, China, [2] Department of Allergy Medicine, Shanxi Bethune Hospital, Shanxi Academy of Medical Sciences, Tongji Shanxi Hospital, Third Hospital of Shanxi Medical University, Taiyuan, China, [3] Department of Pulmonary and Critical Care Medicine, First Hospital Affiliated to Shanxi Medical University, Taiyuan, China, [4] Department of Internal Medicine, Shanxi Medical University, Taiyuan, China

OPEN ACCESS

Edited by:
Girolamo Pelaia,
University of Catanzaro, Italy

Reviewed by:
Petra Ursula Zieglmayer,
Karl Landsteiner University of Health Sciences, Austria
Nerin Bahceciler,
Near East University, Cyprus

***Correspondence:**
Huan-ping Zhang
zhp326@163.com

Specialty section:
This article was submitted to Pulmonary Medicine, a section of the journal Frontiers in Medicine

Received: 23 December 2020
Accepted: 05 July 2021
Published: 05 August 2021

Citation:
Zhang A-z, Liang M-e, Chen X-x, Wang Y-f, Ma K, Lin Z, Xue K-k, Cao L-r, Yang R and Zhang H-p (2021) Clinical Evaluation for Sublingual Immunotherapy With Dermatophagoides farinae in Polysensitized Allergic Asthma Patients. Front. Med. 8:645356. doi: 10.3389/fmed.2021.645356

Background: Many studies have demonstrated the efficacy of single-allergen sublingual immunotherapy (SLIT) in polysensitized patients with allergic rhinitis (AR), but less is reported in polysensitized patients with allergic asthma (AS).

Method: Data of 133 adult patients with house dust mite (HDM)-induced AS who had been treated for 3 years were collected. These patients were divided into the control group (treated with low to moderate dose of inhaled glucocorticoids and long-acting β2 agonists, $n = 37$) and the SLIT group (further treated with *Dermatophagoides farinae* drops, $n = 96$). The SLIT group contained three subgroups: the single-allergen group (only sensitized to HDM, $n = 35$), the 1- to 2-allergen group (HDM combined with one to two other allergens, $n = 32$), and the 3-or-more-allergen group (HDM combined with three or more other allergens, $n = 29$). The total asthma symptom score (TASS), total asthma medicine score (TAMS), and asthma control test (ACT) were assessed before treatment and at yearly visits. Forced expiratory volume in 1 s/forced vital capacity (FEV1/FVC) was assessed before treatment and at the end of SLIT.

Results: TASS and ACT scores in the control group were significantly higher than that in the single-allergen group and the 1- to 2-allergen group after 1, 2, and 3 years of SLIT and significantly higher than that in the 3-or-more-allergen group after 3-year SLIT (all $p < 0.05$). TAMS of the control group was significantly higher than that of the other three groups after 0.5, 1, 2, and 3 years of SLIT (all $p < 0.05$). FEV1/FVC in the control group was significantly higher than baseline after 3 years of immunotherapy ($p < 0.05$).

Conclusion: Patients sensitized to HDM with/without other allergens showed similar efficacy after 3 years of SLIT. However, the initial response of patients with three or more allergens was slower during immunotherapy process.

Keywords: allergic asthma, sublingual immunotherapy, monosensitization, polysensitization, efficacy

INTRODUCTION

Asthma is a common chronic airway disease worldwide, affecting 18% of the populations in different countries (1). It has been recently proposed that asthma is a heterogeneous disease with different clinical phenotypes, and allergic asthma (AS) is one of the most important phenotypes, accounting for more than three-fifths of adult asthma (2). The World Allergy Organization Position Paper estimated that the global prevalence of allergic diseases was 10–40%, including 300 million patients with AS (3). In China, house dust mite (HDM) is the main allergen for patients with allergic diseases and the prevalence of sensitization was ∼48% (4). HDM served as the main allergen in southern places while pollen might be the main allergen in the northern area in China. Kewu Huang and his colleagues reported in the *Lancet* that the prevalence of asthma in people aged over 20 was 4.2% in China, and the total number of patients had reached 45.7 million in 2019. However, 71.2% of 2,032 asthma patients had been never diagnosed by a physician in China and only 5.6% of them had received formal treatment (5).

Allergen immunotherapy (AIT) was born in 1,911 and has a history of more than 100 years. AIT is considered as the only option that may alter the natural course of allergic diseases (6). The latest international consensus on AIT has clearly stated that it has significant effect on allergic rhinitis (AR) and AS (7, 8). Sublingual immunotherapy (SLIT) and subcutaneous immunotherapy (SCIT) are the most common approaches for AIT. Considering the potential risks of AIT-associated adverse events (AEs), SLIT has been the preferred route of allergen administration compared to SCIT because of its better safety profile and the convenience of self-administration without medical supervision (9).

Polysensitization is a highly prevalent clinical phenomenon (10). Recent meta-analyses and systematic reviews showed that SLIT with a single allergen is efficacious in both monosensitized and polysensitized patients with AR (11, 12), while the effect of SLIT for AS is less complete. The purpose of this study was to evaluate the efficacy of single-allergen SLIT in polysensitized AS patients and provide an important reference for the specific immunotherapy in clinical practice.

METHODS

Ethics Statement

The clinical trial was approved by the Medical Ethics Committee of Shanxi Medical University. All patients were informed of the trial details, and all patients signed written informed consent prior to performing any procedures.

Study Design

This clinical trial was carried out in the Second Hospital Affiliated to Shanxi Medical University, Shanxi Bethune Hospital, Shanxi Academy of Medical Sciences, Tongji Shanxi Hospital, Third Hospital of Shanxi Medical University, and First Hospital Affiliated to Shanxi Medical University. Subjects aged 18–60 years were recruited from the outpatients that visited the departments between, March 15, 2016, and September 15, 2016. Patients' asthma symptoms and medication scores were recorded in our database; besides, suspected patients with bronchial asthma required the asthma control test (ACT). The number of samples collected is based on the actual number of patients who finished the treatment in each group.

Recruitment criteria included patients sensitized to aeroallergens aged 18–60 years, all of whom have been diagnosed with mild-to-moderate bronchial asthma; pulmonary function test FEV1 >70% of the predicted value; patients without previous AIT and with single allergen of HDM or HDM combined with other one to three or more allergens were recruited; other allergens are limited to inhaled allergens, but there is no limit to the types of allergens (including *Humulus scandens*, *Ragweed*, *Alternaria alternata*, *Cladosporium cladosporium*, *Aspergillus fumigatus*, cat hair, dog hairs, pillow material, Mulberry silk, and cockroach). The allergen protein homology between *Dermatophagoides farinae* (*D. farinae*) and *Dermatophagoides pteronyssinusanf* (*D. pteronyssinusanf*) is as high as 80% (13); therefore, both are included in the HDM allergen group. Sensitization to *D. farinae* and/or *D. pteronyssinusanf* and other inhaled allergens were confirmed by the presence of specific immunoglobulin E (sIgE) $\geq$ 0.70 KU/L (grade 2 and above) using the UniCAP system (Phadia, Uppsala, Sweden). Patients were excluded from the study if they had one of the following conditions: severe or uncontrolled asthma; uncontrolled or acute allergic diseases (anaphylactic shock); taking Angiotensin-Converting Enzyme (ACE) or β-blockers; serious psychological or mental illness; severe acute or chronic heart failure, kidney failure; pregnancy; and malignant tumors.

Demographic and clinical data were collected at each phase. According to the treatment method selected by the patients themselves rather than random grouping, eligible participants were divided into the control group (treated with low to moderate dose of inhaled glucocorticoid and long-acting β2 agonists) and SLIT group (treated with low to moderate dose of inhaled glucocorticoids and long-acting β2 agonists further treated with *D. farinae* drops); both the control group and the SLIT group were divided into single-HDM SLIT subgroup, HDM combining with other 1–2 allergen SLIT subgroup, and HDM combining with other 3 or more allergen SLIT subgroup, respectively. Patients were treated using standardized allergen *D. farinae* drops (Chanllergen; Zhejiang Wolwo Bio-Pharmaceutical Co., Ltd., Zhejiang, China) labeled from 1 to 5 containing proteins of 1, 10, 100, 333, and 1,000 μg/ml, respectively. The main components of vials 1–5 are the same, but the concentrations of protein are different. Information regarding normal drug dosage is shown in **Table 1**. The drug was self-administered daily at the same time and administered sublingually for 1–3 min before swallowing.

Clinical Efficacy

During the treatment, patients were required to keep a diary recording of symptom and medication use. The investigators calculated the weekly average scores at every visit. The total asthma symptom score (TASS), total asthma medicine score (TAMS), ACT, and forced expiratory volume in 1 s/forced vital capacity (FEV1/FVC) were recorded. TASS was the sum of daytime asthma symptoms scores and nocturnal asthma

TABLE 1 | SLIT drops dosing for patients.

Week	Vial no.	Dose (drops)						
		1 d	2 d	3 d	4 d	5 d	6 d	7 d
1	1	1	2	3	4	6	8	10
2	2	1	2	3	4	6	8	10
3	3	1	2	3	4	6	8	10
4–5	4	3	3	3	3	3	3	3
≥6	5	2	2	2	2	2	2	2

symptoms scores. The daytime asthma symptoms were scored from 0 to 5 points according to the general severity of wheeze, shortness of breath, dyspnea, and cough and its impact on daily life. The nocturnal symptoms were scored from 0 to 4 points according to the frequency of nocturnal and early morning awakening by asthma (14). TAMS was calculated as follows (per day): one point for long-acting β2 agonists and two points for inhaled glucocorticoids; TAMS is the sum of all the recorded medicine scores (15). ACT is an effective tool to assess the degree of asthma control. Twenty-five points mean well-controlled, 20–24 points mean partially controlled, and it is uncontrolled when the points are below 20 (16). In addition, FEV1/FVC were measured to evaluate the pulmonary function of patients at the beginning and the end of immunotherapy by a pulmonary function tester.

Safety Assessment

Safety profile was assessed according to AEs recorded in daily cards. All AEs were addressed under the instruction of the physicians.

Patient Management

Initial clinical education and follow-up education were carried out for all the patients. The patient files were established to record symptoms, medication use, and AEs of patients at the beginning of the treatment. Telephone follow-ups were provided to patients to solve problems that occurred in the treatment process and to arrange the next follow-up visit.

Statistical Analysis

Statistical analyses were performed using the SPSS 21.0 software (IBM Corp., Armonk, New York, USA). Data were assessed for normality and equal variation and results were expressed as mean ± standard deviation (SD). Kolmogorov–Smirnov test was performed to assess the normality of the distribution in continuous variables. Two-way analysis of variance (ANOVA) was used when the variables distributed normally. Otherwise, Kruskal–Wallis H test or Mann-Whitney U-test was performed. The two-tailed level of statistical significance was set at $p = 0.05$. Figures were plotted using GraphPad Prism 7.0 (Software Inc. La Jolla, CA, USA), and $p < 0.05$ was considered statistically significant.

RESULTS

Subjects

A total of 230 participants [mean age, 41.19 ± 11.02 years; 33.91% female ($n = 78$), 66.09% male ($n = 152$)] were screened, of whom 133 completed the entire study in the control group ($n = 37$), single-allergen group ($n = 35$), 1- to 2-allergen group ($n = 32$), and 3-or-more-allergen group ($n = 29$). All groups were comparable with respect to gender, age, TASS, TAMS, and ACT, and there were no statistical differences in all items except the single-allergen group vs. the control group and the 1- to 2-allergen group in the FEV1/FVC% item (**Table 2**). The reasons for the patients' dropout included incomplete study ($n = 20$), withdrew consent ($n = 9$), lost to follow-up ($n = 36$), undetermined FEV1/FVC at the end of SLIT ($n = 29$), and others ($n = 3$).

TASS Evaluation

There was no statistical difference of TASS between the control group, single-allergen group, 1- to 2-allergen group, and 3-or-more-allergen group at baseline and 0.5 years (all $p > 0.05$), while there was a significant difference between the control group and the single-allergen group and 1- to 2-allergen group after immunotherapy after 1 and 2 years (all $p < 0.05$). The TASS score of the control group was significantly higher than that of the single-allergen group, the 1- to 2-allergen group, and the 3-or-more-allergen group at 3 years ($p < 0.05$, **Figure 1A**).

TAMS Evaluation

As shown in **Figure 1B**, there was no statistical difference of TAMS between the control group, the single-allergen group, the 1- to 2-allergen group, and the 3-or-more-allergen group at baseline (all $p > 0.05$). However, TAMS in the control group was significantly higher than that in the single-allergen group, 1- to 2-allergen group and 3-or-more-allergen group after immunotherapy for 0.5 ($p < 0.001$), 1 ($p < 0.05$), 2 ($p < 0.05$), and 3 ($p < 0.001$) years.

ACT Evaluation

Similar to the trend of TASS, there was no significant difference between all groups at baseline and 0.5 years (all $p > 0.05$). The values of ACT in the single-allergen group and 1- to 2-allergen group were significantly higher than that in the control group at 1 and 2 years (all $p < 0.05$), and the ACT score of the control group was significantly higher than that of the single-allergen group, 1- to 2-allergen group and 3-or-more-allergen group at 3 years ($p < 0.05$, **Figure 2A**).

FEV1/FVC Evaluation

FEV1/FVC was directly assessed at baseline and after 3 years of immunotherapy. In the single-allergen group, the FEV1/FVC was significantly lower than the control group ($p < 0.001$) and 1- to 2-allergen group ($p < 0.05$) at baseline. Although there was no significant difference between the single-allergen group, 1- to 2-allergen group, and 3-or-more-allergen group (all $p > 0.05$) after immunotherapy for 3 years, there were significant differences between them and the control group (all $p < 0.05$, **Figure 2B**).

TABLE 2 | The demographic and clinical characteristics before treatment in the four groups.

Character	Control group	Single-allergen group	1- to 2-allergen group	≥3 allergen group	*p*-value
Case No.	37	35	32	29	$p > 0.05$
Male	10	16	8	13	$p > 0.05$
Female	27	19	24	16	$p > 0.05$
Age (years)	42.16 ± 11.10	39.49 ± 11.60	41.88 ± 11.29	36.97 ± 10.25	All $p > 0.05$
TASS	5.35 ± 1.21	5.06 ± 1.37	4.78 ± 1.29	5.03 ± 1.35	All $p > 0.05$
TAMS	7.60 ± 1.01	7.86 ± 1.42	7.31 ± 1.89	7.55 ± 1.64	All $p > 0.05$
ACT	14.73 ± 2.24	15.37±2.37	14.97 ± 2.44	14.00 ± 2.02	All $p > 0.05$
FEV1/FVC%	76.80 ± 5.54	73.65 ± 5.64	76.23 ± 4.95	75.13 ± 3.85	$p < 0.05$ (Single vs. Control/1–2)

TASS, total asthma symptom score; TAMS, total asthma medicine score; ACT, asthma control test; FEV1/FVC%, forced expiratory volume in 1 s/forced vital capacity.

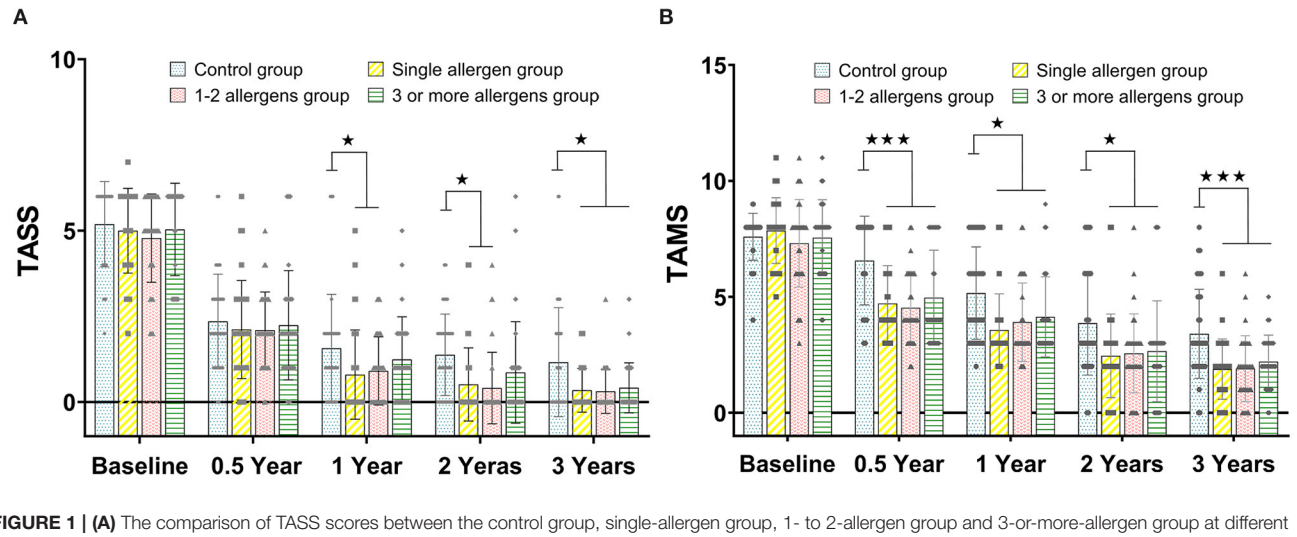

FIGURE 1 | (A) The comparison of TASS scores between the control group, single-allergen group, 1- to 2-allergen group and 3-or-more-allergen group at different time points (mean ± SD). **(B)** The comparison of TAMS scores between the control group, single-allergen group, 1- to 2-allergen group and 3-or-more-allergen group at different time points (mean ± SD). *$p < 0.05$, ***$p < 0.001$.

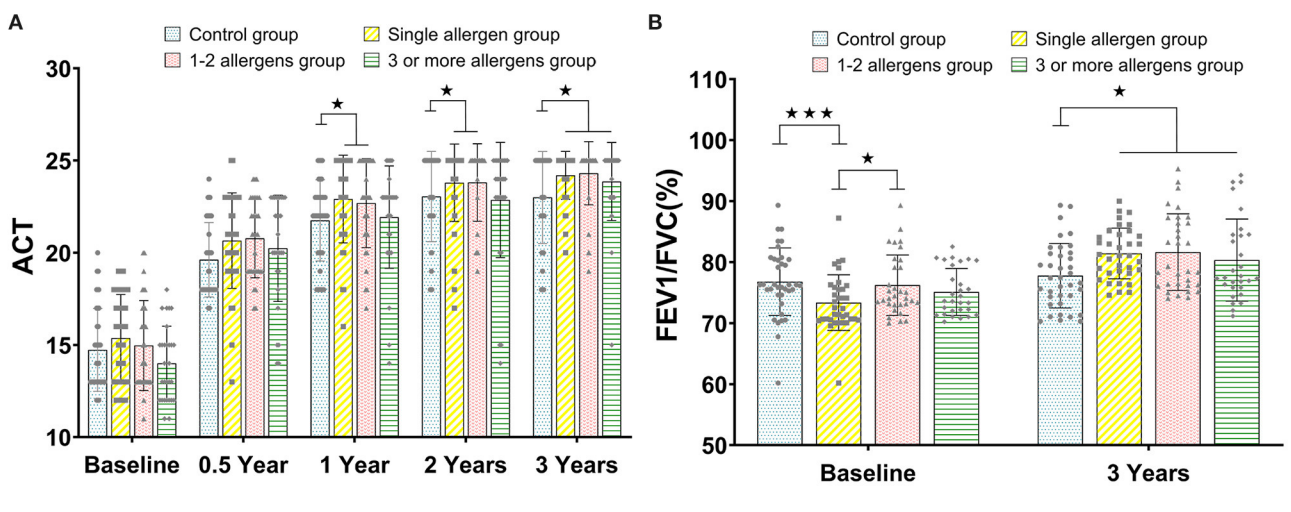

FIGURE 2 | (A) The comparison of ACT between the control group, single-allergen group, 1- to 2-allergen group and 3-or-more-allergen group at different time points (mean ± SD). **(B)** The comparison of FEV1/FVC(%) between the control group, single-allergen group, 1- to 2-allergen group and 3-or-more-allergen group at different time points (mean ± SD). *$p < 0.05$, ***$p < 0.001$.

Safety

No severe systemic adverse effects (AEs), anaphylaxis, asthma acute attack, or use of adrenaline were reported during the entire treatment period. Overall, 10 AEs occurred in the control group: 5 oral or sublingual itching, 3 swelling, and 2 diarrhea; 23 AEs occurred in the single-allergen group: 11 oral numbness or pruritus, 8 mild gastrointestinal reaction, and 4 aggravation of allergic symptoms; 9 numbness of tongue and 5 mouth ulcer make up all the AEs of the 1- to 2-allergen group, and there were 15 AEs in the 3-or-more-allergen group involving 7 oral numbness or pruritus and 8 mild gastrointestinal reaction. All AEs were relieved without any treatment within a week.

DISCUSSION

AS is one of the most common chronic diseases in all age population with high incidence and prevalence. As a disease-modifying therapy, SLIT is strongly recommended for treatment of AS patients, which has the potential to prevent the onset of new allergen sensitizations and the progression of respiratory allergies (7). Although SLIT has been widely studied, it mainly focuses on the area of single-allergen efficacy (17), objective indicators (18), and immune response pathway (19). Meanwhile, we found that most patients are not limited to a single allergen but multiple allergies in the actual clinical diagnosis and treatment process. What we are really concerned about is the efficacy of single-allergen SLIT for polysensitized patients. In this study, we selected patients allergic to *D. farinae* as the main body, as the research drug is specifically designed for HDM. In addition, other allergens are restricted to inhalation allergens, because inhalation allergens are more difficult to avoid in life. The number and types of allergens in each patient are also different in clinical treatment and the diagnosis and treatment ability of each hospital is different; therefore, this classification method is more conducive to guiding clinical practice for doctors.

In our study, there was a significant difference in FEV1/FVC between the single-allergen group, the control group, and the 1- to 2-allergen group, which indicated that FEV1/FVC in the single-allergen group is significantly lower than that in the other groups. The results of TASS and TAMS scores showed that efficacy of SLIT was consistent for patients in the single-allergen group and the 1- to 2-allergen group. Although patients in the 3-or-more-allergen group had slower onset of initial immunotherapy, they eventually achieved the same effect as the single-allergen group and the 1- to 2-allergen group. ACT identified as an effective tool for monitoring and assessing asthma (20). In present study, ACT was similar to the trend of TASS, although the response of patients in the 3-or-more-allergen group was slower than that in the single-allergen group and the 1- to 2-allergen group; the same effect as these two groups could be achieved in the end. The ACT results of patients were all above 20, and asthma symptoms were partially controlled after SLIT for 0.5, 1, 2, and 3 years. At baseline, FEV1/FVC in the single-allergen group was significantly lower than that in the control group and the 1- to 2-allergen group, which indicated that the lung function of patients in the single-allergen group was worse than that of patients in other groups. Additionally, the FVE1/FVC of patients in all three SLIT subgroups were significantly higher than that in the control group for the 3-year treatment, suggesting that lung function has been significantly improved whether patients have one or more allergens after 3-year SLIT.

However, there was no difference after treatment between the control group and some SLIT groups at certain time points, like the 0.5-year group of the TASS (**Figure 1A**) and ACT (**Figure 2A**). For this, we speculated that both the SLIT group and the control group were treated with symptomatic drugs at the early beginning. Therefore, the consistency in the symptoms of patients might be attributed to the role of inhaled glucocorticoids and long-acting β2 agonists in this process. After that, with the withdrawal of symptomatic drugs, the actual therapeutic effect has been shown.

The safety of SLIT has been demonstrated in multiple reviews of a large number of clinical trials (5, 21). No severe systemic AEs were reported in this trial. All the AEs were mainly local AEs such as transient oral itching and swelling. All the AEs were relieved within a week, with or without therapy. In addition, our study had relatively high compliance with 133/230 people completing the study; this was inseparable from the regular follow-up of medical staff. We also found that the total number of dropouts gradually increased as the follow-up time prolonged. Most patients quit SLIT mainly because their symptoms were under control. The period of dropout among these patients was mainly distributed during the follow-up period of 4–6 months. This might be related to the serious lack of knowledge of AS and SLIT treatment, the insufficient medical propaganda, and insufficient attention to asthma patients in China.

In this study, it was not easy for more than 100 patients to complete the treatment for 3 years; this was mainly due to our management of patients. We presented the information of patients at different time points; these data mainly came from our follow-up and collection of patients. The actual frequency of follow-up was much higher than the data we displayed. We believed that without our close contact with patients, these data could not be obtained. So, we look forward to sharing our follow-up methods with you in the future. However, the absence of a placebo control group was the main limitation in this study. Besides, we lacked the analysis of objective indicators of curative effect, and only the most important antibody component sIgE was partially introduced. Although there is no final conclusion on predictors, we expect to make our own voice in further research.

In conclusion, patients sensitized to HDM with/without other allergens showed similar efficacy after 3 years of SLIT. However, the initial response of patients with 3 or more allergens was slower during the immunotherapy process.

DATA AVAILABILITY STATEMENT

The raw data supporting the conclusions of this article will be made available by the authors, without undue reservation.

ETHICS STATEMENT

The studies involving human participants were reviewed and approved by the raw data supporting the conclusions

of this article will be made available by the authors, without undue reservation. The patients/participants provided their written informed consent to participate in this study.

AUTHOR CONTRIBUTIONS

A-zZ, X-xC, Y-fW, KM, K-kX, L-rC, and RY performed experiments, analyzed data, and reviewed the manuscript. M-eL organized the study and supervised experiments. H-pZ designed the project and prepared the manuscript. All authors contributed to the article and approved the submitted version.

FUNDING

This study was supported by a Grant from the Shanxi Province Oversea Research Personnel Initiative Fund (2016-116) and the Scientific Research Initiative Funds of Shanxi Bethune Hospital (2020RC004).

REFERENCES

1. Bateman ED, Hurd SS, Barnes PJ, Bousquet J, Drazen JM, FitzGerald JM, et al. Global strategy for asthma management and prevention: gina executive summary. *Eur Respir J.* (2008) 31:143–78. doi: 10.1183/09031936.00138707
2. Knudsen TB, Thomsen SF, Nolte H, Backer V. A population-based clinical study of allergic and non-allergic asthma. *J Asthma.* (2009) 46:91–4. doi: 10.1080/02770900802524657
3. Backman H, Raisanen P, Hedman L, Stridsman C, Andersson M, Lindberg A, et al. Increased prevalence of allergic asthma from 1996 to 2006 and further to 2016-results from three population surveys. *Clin Exp Allergy.* (2017) 47:1426–35. doi: 10.1111/cea.12963
4. Zureik M, Neukirch C, Leynaert B, Liard R, Bousquet J, Neukirch F, et al. Sensitisation to airborne moulds and severity of asthma: cross sectional study from European community respiratory health survey. *BMJ.* (2002) 325:411–4. doi: 10.1136/bmj.325.7361.411
5. Huang K, Yang T, Xu J, Yang L, Zhao J, Zhang X, et al. Prevalence, risk factors, and management of Asthma in China: a national cross-sectional study. *Lancet.* (2019) 394:407–18. doi: 10.1016/S0140-6736(19)31147-X
6. Hrubisko M, Spicak V. Allergen immunotherapy in polysensitized patient. *Eur Ann Allergy Clin Immunol.* (2016) 48:69–76.
7. Jutel M, Agache I, Bonini S, Burks AW, Calderon M, Canonica W, et al. International consensus on allergy immunotherapy. *J Allergy Clin Immunol.* (2015) 136:556–68. doi: 10.1016/j.jaci.2015.04.047
8. Marogna M, Tomassetti D, Bernasconi A, Colombo F, Massolo A, Businco AD, et al. Preventive effects of sublingual immunotherapy in childhood: an open randomized controlled study. *Ann Allergy Asthma Immunol.* (2008) 101:206–11. doi: 10.1016/S1081-1206(10)60211-6
9. Pfaar O, Lou H, Zhang Y, Klimek L, Zhang L. Recent developments and highlights in allergen immunotherapy. *Allergy.* (2018) 73:2274–89. doi: 10.1111/all.13652
10. Kuperstock JE, Brook CD, Ryan MW, Platt MP. Correlation between the number of allergen sensitizations and immunoglobulin E: monosensitization vs polysensitization. *Int Forum Allergy Rhinol.* (2017) 7:385–8. doi: 10.1002/alr.21890
11. Ciprandi G, Cirillo I. Monosensitization and polysensitization in allergic rhinitis. *Eur J Intern Med.* (2011) 22:e75–9. doi: 10.1016/j.ejim.2011.05.009
12. Gao Y, Lin X, Ma J, Wei X, Wang Q, Wang M. Enhanced efficacy of dust mite sublingual immunotherapy in low-response allergic rhinitis patients after dose increment at 6 months: a prospective study. *Int Arch Allergy Immunol.* (2020) 181:311–9. doi: 10.1159/000505746
13. Thomas WR, Smith WA, Hales BJ, Mills KL, O'Brien RM. Characterization and immunobiology of house dust mite allergens. *Int Arch Allergy Immunol.* (2002) 129:1–18. doi: 10.1159/000065179
14. Wang H, Lin X, Hao C, Zhang C, Sun B, Zheng J, et al. A double-blind, placebo-controlled study of house dust mite immunotherapy in chinese asthmatic patients. *Allergy.* (2006) 61:191–7. doi: 10.1111/j.1398-9995.2005.00913.x
15. Pfaar O, Demoly P, Gerth van Wijk R, Bonini S, Bousquet J, Canonica GW, et al. Recommendations for the standardization of clinical outcomes used in allergen immunotherapy trials for allergic rhinoconjunctivitis: an eaaci position paper. *Allergy.* (2014) 69:854–67. doi: 10.1111/all.12383
16. Schlosser RJ, Smith TL, Mace J, Soler ZM. Asthma quality of life and control after sinus surgery in patients with chronic rhinosinusitis. *Allergy.* (2017) 72:483–91. doi: 10.1111/all.13048
17. Zhong C, Yang W, Li Y, Zou L, Deng Z, Liu M, et al. Clinical evaluation for sublingual immunotherapy with *Dermatophagoides farinae* drops in adult patients with allergic asthma. *Irish J Med Sci.* (2018) 187:441–6. doi: 10.1007/s11845-017-1685-x
18. Wang Z, Li W, Chen H, Zhang W. Effect of sublingual immunotherapy on level of cytokines in PBMCs of patients with allergic asthma. *J Huazhong Univ Sci Technolog Med Sci.* (2011) 31:376–8. doi: 10.1007/s11596-011-0384-5
19. Tian M, Wang Y, Lu Y, Jiang YH, Zhao DY. Effects of sublingual immunotherapy for dermatophagoides farinae on Th17 cells and CD4(+) CD25(+) regulatory T cells in peripheral blood of children with allergic asthma. *Int Forum Allergy Rhinol.* (2014) 4:371–5. doi: 10.1002/alr.21305
20. Nguyen VN, Chavannes N, Le LT, Price D. The asthma control test (Act) as an alternative tool to global initiative for asthma (Gina) guideline criteria for assessing asthma control in vietnamese outpatients. *Prim Care Respir J.* (2012) 21:85–9. doi: 10.4104/pcrj.2011.00093
21. Cheng L, Zhou WC. Sublingual immunotherapy of house dust mite respiratory allergy in China. *Allergol Immunopathol (Madr).* (2019) 47:85–9. doi: 10.1016/j.aller.2018.02.008

Conflict of Interest: The authors declare that the research was conducted in the absence of any commercial or financial relationships that could be construed as a potential conflict of interest.

Publisher's Note: All claims expressed in this article are solely those of the authors and do not necessarily represent those of their affiliated organizations, or those of the publisher, the editors and the reviewers. Any product that may be evaluated in this article, or claim that may be made by its manufacturer, is not guaranteed or endorsed by the publisher.

Copyright © 2021 Zhang, Liang, Chen, Wang, Ma, Lin, Xue, Cao, Yang and Zhang. This is an open-access article distributed under the terms of the Creative Commons Attribution License (CC BY). The use, distribution or reproduction in other forums is permitted, provided the original author(s) and the copyright owner(s) are credited and that the original publication in this journal is cited, in accordance with accepted academic practice. No use, distribution or reproduction is permitted which does not comply with these terms.

Advantages of publishing in Frontiers

OPEN ACCESS
Articles are free to read for greatest visibility and readership

FAST PUBLICATION
Around 90 days from submission to decision

HIGH QUALITY PEER-REVIEW
Rigorous, collaborative, and constructive peer-review

TRANSPARENT PEER-REVIEW
Editors and reviewers acknowledged by name on published articles

Frontiers
Avenue du Tribunal-Fédéral 34
1005 Lausanne | Switzerland

Visit us: www.frontiersin.org
Contact us: frontiersin.org/about/contact

REPRODUCIBILITY OF RESEARCH
Support open data and methods to enhance research reproducibility

DIGITAL PUBLISHING
Articles designed for optimal readership across devices

FOLLOW US
@frontiersin

IMPACT METRICS
Advanced article metrics track visibility across digital media

EXTENSIVE PROMOTION
Marketing and promotion of impactful research

LOOP RESEARCH NETWORK
Our network increases your article's readership